

THE
American Journal of
ANATOMY

MANAGING EDITOR
DONALD DUNCAN
THE UNIVERSITY OF TEXAS
MEDICAL BRANCH
GALVESTON TEXAS

ASSOCIATE EDITORS

BURTON L BAKER
UNIVERSITY OF MICHIGAN

SAM L CLARK JR
WASHINGTON UNIVERSITY

C P LEBLOND
MCGILL UNIVERSITY

RICHARD J BLANDAU
UNIVERSITY OF WASHINGTON

DON W FAWCETT
HARVARD UNIVERSITY

HARLAND W MOSSMAN
UNIVERSITY OF WISCONSIN

VOLUME 119
JULY, SEPTEMBER, NOVEMBER 1966

PUBLISHED BY
THE WISTAR INSTITUTE OF ANATOMY AND BIOLOGY
PHILADELPHIA PA

CONTENTS

No 1 JULY 1966

LOIS JEAN SMITH The Changing Pattern of Basophilia in the Mouse Uterus from Mating through Implantation	1
LOIS JEAN SMITH Metrial Gland and Other Glycogen Containing Cells in the Mouse Uterus Following Mating and Through Implantation of the Embryo	15
WILLIAM A WIMSATT PHILIP H KRUTZSCH AND LEONARD NAPOLITANO Studies on Sperm Survival Mechanisms in the Female Reproductive Tract of Hibernating Bats I Cytology and Ultra structure of Intra uterine Spermatozoa in <i>Myotis lucifugus</i>	25
G DALLENBACH HELLWEG A B DAWSON AND F L HISAW The Effect of Relaxin on the Endometrium of Monkeys Histological and Histochemical Studies	61
ROBERT E HABEL The Topographic Anatomy of the Muscles Nerves and Arteries of the Bovine Female Perineum	79
TREVOR HEATH AND STEVEN L WISSIG Fine Structure of the Surface of Mouse Hepatic Cells	97
DON W FAWCETT On the Occurrence of a Fibrous Lamina on the Inner Aspect of the Nuclear Envelope in Certain Cells of Vertebrates	129
MAX A LISTGARTEN Electron Microscopic Study of the Gingivo-dental Junction of Man	147

No 2 SEPTEMBER 1966

- GERALD F WINKLER AND MERRILL K WOLF The Development and Maintenance of Myelinated Tissue Cultures of Rat Trigeminal Ganglion 17
- PHYLLIS W SCHULTZ JAMES F REGER AND RICHARD L SCHULTZ Effects of Triton WR 1339 on the Rat Yolk Sac Placenta 19
- EL SAYED H H HEGAB AND VICTOR J FERRANS A Histochemical Study of the Esterases of the Rat Heart 23
- JOHN H VENABLE Constant Cell Populations in Normal Testosterone deprived and Testosterone stimulated Levator Ani Muscles 26
- JOHN H VENABLE Morphology of the Cells of Normal Testosterone deprived and Testosterone stimulated Levator Ani Muscles 27
- ELEANOR C ADAMS ARTHUR T HERTIG AND SUSANNE FOSTER Studies on Guinea Pig Oocytes II Histochemical Observations on Some Phosphatases and Lipid in Developing and in Atretic Oocytes and Follicles 303

No 3 NOVEMBER 1966

- EMMA SHELTON Differentiation of Mouse Thymus Cultured in Diffusion Chambers 341
- * ROBERT J MERKLIN Suprarenal Gland Lymphatic Drainage 359
- SAM L CLARK JR The Synthesis and Storage of Protein by Isolated Lymphoid Cells Examined by Autoradiography with the Electron Microscope 375
- AHMAD EL BADAWI AND ERIC A SCHENK Dual Innervation of the Mammalian Urinary Bladder A Histochemical Study of the Distribution of Cholinergic and Adrenergic Nerves 405

CONTENTS

v

ROBERT M BRENNER Fine Structure of Adrenocortical Cells in Adult Male Rhesus Monkeys	429
ROBERT S McCUSKEY A Dynamic and Static Study of Hepatic Arterioles and Hepatic Sphincters	455
LAWRENCE KRUGER AND DAVID S MAXWELL The Fine Structure of Ependymal Processes in the Teleost Optic Tectum	479
THOMAS K SHIRES An Evaluation of Possible Intracellular Nucleic Acid Quenching of Carcinogenic Hydrocarbon Fluorescence	499
AKHOURI A SINHA AND H W MOSSMAN Placentation of the Sea Otter	521
ROBERT L BRENT The Production of Congenital Malformations Using Tissue Antisera IV Evaluation of the Mechanism of Teratogenesis by Varying the Route and Time of Administration of Anti Rat Kidney Antiserum	555
INDEX TO VOLUME 119	563

ERRATUM

VENABLE JOHN H Morphology of the Cells of Normal Testosterone-deprived and Testosterone stimulated Levator Ani Muscles Am J Anat 119 271-302

Line 13 page 283 the word *hagfish* should be corrected to *axolotl*

Correct line is printed below and should be cut out and pasted over the incorrect line

5% reported herein In the axolotl they

The Changing Pattern of Basophilia in the Mouse Uterus from Mating through Implantation

LOIS JEAN SMITH¹

Department of Anatomy Albert Einstein College of Medicine
New York New York

ABSTRACT Changes in RNA localization and concentration in mouse uteri taken from one-half to seven and one-quarter days after mating were visualized as changes in basophilia following staining by a histochemical method specific for RNA. The basophilia of the luminal epithelium falls abruptly between one half and two days and is still lower at two and three-quarter days. By 2 and three-quarter days however that of the stroma and especially that of the subepithelial endothelial cells is increasing. A further slight increase is found at three and three-quarter days and by four days a band of subepithelial stromal cells wider in the antimesometrial than in the mesometrial portion of the uterus is highly basophilic. At four and one-quarter days when a distinct decidual reaction is evident cells in the primary decidual zone are less basophilic than at four days. During the remaining period of observation cells in different regions of the uterus show increased and often later decreased basophilia. It was concluded that these results are in complete accord with those from a recent biochemical study of changes in RNA in the intact rat uterus during the interval from induction of pseudopregnancy through decidualoma formation if the difference in timing in the two species is taken into account.

Although Jeener reported in 1948 that estrogen administration leads to increased RNA synthesis in the rodent uterus it was not until the function of the various RNAs in the chain from DNA to specific protein was uncovered that the possible significance of this finding was fully appreciated. Numerous recent data from many laboratories now strongly support the view that the cyclic differentiation of the adult uterus may be based on cyclic activation of specific genes by estrogen. These findings include information on the time sequence of new syntheses of RNA, DNA and protein after estrogen administration, on the effects of concurrent administration of actinomycin D and puromycin on RNA and protein synthesis, and on the demonstration that estrogen administration results in differential protein synthesis in a variety of tissues.

As a consequence of these studies the role of estrogen during pregnancy and of other factors involved in uterine differentiation are being investigated with renewed interest. Most of the newer data on the sequence of syntheses of RNA, DNA and protein in the interval from mating to decidua formation have been obtained from biochemical analyses of whole rodent

uteri, however, and there appears to be a paucity of information on localized changes in concentration during this period of differentiation. This is particularly so with respect to RNA since data based on the affinity of nucleoproteins for basic dyes under controlled staining conditions seem to consist of a report on three rats of unstated stages of pregnancy (Wislocki and Dempsey '45) and a study devoted principally to the trophoblast giant cells in which methylene blue of unspecified pH was used (Alden '48). There is also an account of the differentiation of the metrial gland in which passing reference is made to the stainability of the endometrium (Baker '48) and a description of basophilia in the uterus at a stage just prior to the time of attachment of the allantois (Bulmer and Dickson '61).

In the present paper are to be found the results of a histochemical study of RNA in the endometrium of the pregnant mouse from one half to seven and one quarter days after mating. For the study the method of Flax and Himes ('52) involving the use of the metachromatic dye Azure B

¹ Present address: Department of Biology, Queens College of the City University of New York, Flushing, New York 11367.

The Changing Pattern of Basophilia in the Mouse Uterus from Mating through Implantation

LOIS JEAN SMITH*

Department of Anatomy Albert Einstein College of Medicine
New York New York

ABSTRACT Changes in RNA localization and concentration in mouse uteri taken from one half to seven and one-quarter days after mating were visualized as changes in basophilia following staining by a histochemical method specific for RNA. The basophilia of the luminal epithelium falls abruptly between one half and two days and is still lower at two and three-quarter days. By 2 and three-quarter days however that of the stroma and especially that of the subepithelial endothelial cells is increasing. A further slight increase is found at three and three-quarter days and by four days a band of subepithelial stromal cells wider in the antimesometrial than in the mesometrial portion of the uterus is highly basophilic. At four and one-quarter days when a distinct decidual reaction is evident cells in the primary decidual zone are less basophilic than at four days. During the remaining period of observation cells in different regions of the uterus show increased and often later decreased basophilia. It was concluded that these results are in complete accord with those from a recent biochemical study of changes in RNA in the intact rat uterus during the interval from induction of pseudopregnancy through deciduoma formation if the difference in timing in the two species is taken into account.

Although Jeener reported in 1948 that estrogen administration leads to increased RNA synthesis in the rodent uterus it was not until the function of the various RNAs in the chain from DNA to specific protein was uncovered that the possible significance of this finding was fully appreciated. Numerous recent data from many laboratories now strongly support the view that the cyclic differentiation of the adult uterus may be based on cyclic activation of specific genes by estrogen. These findings include information on the time sequence of new syntheses of RNA, DNA and protein after estrogen administration on the effects of concurrent administration of actinomycin D and puromycin on RNA and protein synthesis and on the demonstration that estrogen administration results in differential protein synthesis in a variety of tissues.

As a consequence of these studies the role of estrogen during pregnancy and of other factors involved in uterine differentiation are being investigated with renewed interest. Most of the newer data on the sequence of syntheses of RNA, DNA and protein in the interval from mating to decidua formation have been obtained from biochemical analyses of whole rodent

uteri however and there appears to be a paucity of information on localized changes in concentration during this period of differentiation. This is particularly so with respect to RNA since data based on the affinity of nucleoproteins for basic dyes under controlled staining conditions seem to consist of a report on three rats of unstated stages of pregnancy (Wislocki and Dempsey '45) and a study devoted principally to the trophoblast giant cells in which methylene blue of unspecified pH was used (Alden '48). There is also an account of the differentiation of the metrial gland in which passing reference is made to the stainability of the endometrium (Baker '48) and a description of basophilia in the uterus at a stage just prior to the time of attachment of the allantois (Bulmer and Dickson '61).

In the present paper are to be found the results of a histochemical study of RNA in the endometrium of the pregnant mouse from one half to seven and one quarter days after mating. For the study the method of Flax and Humes ('52) involving the use of the metachromatic dye Azure B

*Present address: Department of Biology, Queens College of the City University of New York, Flushing, New York 11367.

was chosen. Their results indicate that this method distinguishes between RNA, DNA and acid mucopolysaccharides and is semi-quantitative with respect to RNA. During the course of the study, basophilic cells which seem to be precursors of metrial gland cells were found at younger stages than previously reported. A full discussion of these observations and those of a parallel study of glycogen distribution are to be found in Smith (66).

MATERIALS AND METHODS

F1 females from several different types of crosses were exposed to males from the same crosses between 5 P.M. and 10 A.M. to obtain uteri four and one half to seven and one quarter days post coitum and between 9 P.M. and 2 A.M. to get earlier stages. Mating was arbitrarily assumed to have occurred at 1 A.M. of the day a vaginal plug was found and the females were sacrificed from one half to seven and one quarter days later. Uteri from two pregnant females only were examined at one half and two days for each of the other times at least five were available. All females had had one or two previous litters before being used in this study.

Uteri to be stained for basophilia were fixed in Carnoy's fluid, sectioned serially either transversely or longitudinally and stained by the Azure B method of Flax and Himes (52). Ribonuclease digestion was performed at some stages. Examples stained with Delafield's and iron hematoxylin and by the Feulgen method were available for many of the stages up to seven and one quarter days and for eight and one half and nine day stages as well.

RESULTS

The following account of uterine differentiation during early pregnancy includes what appear to be significant stages in trophoblast development with respect to uterine trophoblast interactions. For current stages in embryo development see Flax (53) and Smith (56) for the interval from mating through the third day of pregnancy and Snell (41) for the remaining period investigated. These embryonic stages are also illustrated diagrammatically in figures 1-10.

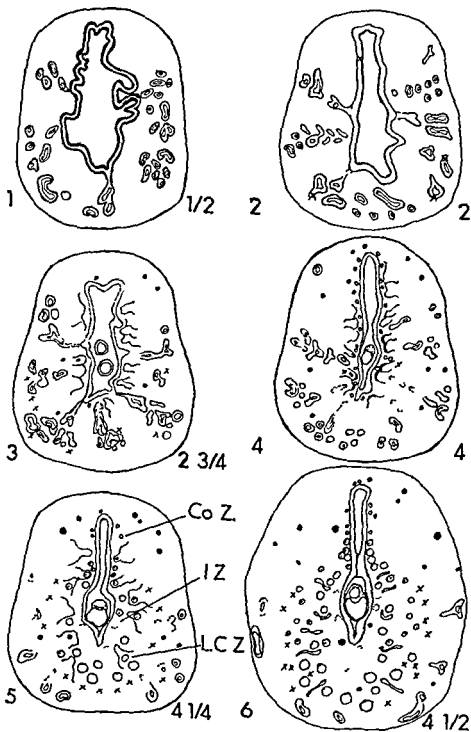
One half day after mating

At 12 hours after mating almost no glands empty into the mesometrial one quarter to one fifth of the uterine lumen and because of this the endometrium appears to be divided more or less distinctly into mesometrial and antimesometrial portions (fig 1). In addition in the mesometrial region and in particular around the lumen the stromal cells are more tightly packed than they are elsewhere in the mucosa and tend to have rounder nuclei and more cytoplasm than do the antimesometrial cells. The basal layer contains no glands. In it the spindle shaped cells have oval nuclei and are widely spaced.

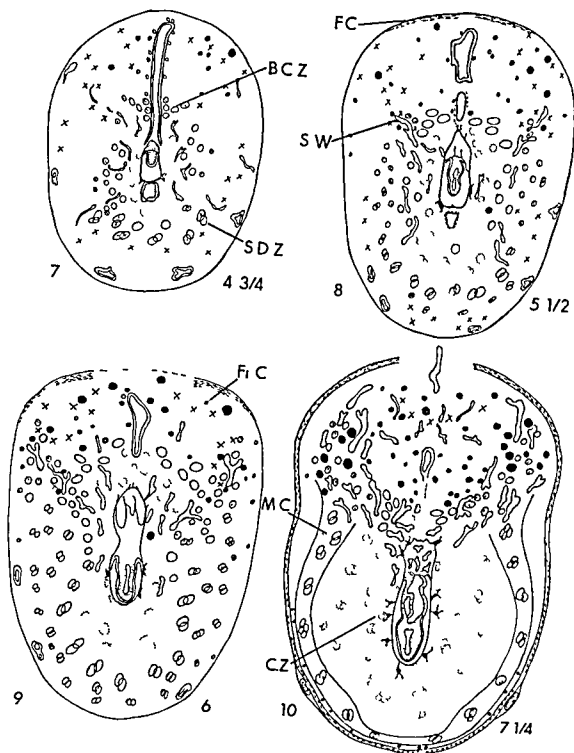
Neutrophilic polymorphonuclear leukocytes, lymphocytes, macrophages and reticular cells are present throughout the endometrium. The neutrophils appear to be almost as plentiful as the stromal cells and like them decrease in concentration from lumen to periphery. The lymphocytes are found mainly in the lymph spaces at the periphery. The cytoplasm of these cells of the macrophages which contain a light sprinkling of yellow granules and of the stromal cells show very little affinity for Azure B while cells which seem to be reticular cells or immature plasma cells stain intensely. The latter are found in highest concentration around the glands.

The high columnar cells of the luminal epithelium show greater basophilia of both apical and basal cytoplasm at this time than at any other stage studied and probably greater basophilia than is shown by any other uterine cell examined. The basophilic material which is removed by ribonuclease also stains much more meta-chromatically than does the approximately equally heavily stained material of the em-

Figures 1-6 Diagrammatic cross sections of pregnant uteri from one half to four and one half days after mating. The mesometrial region is uppermost. Luminal and glandular epithelium are indicated by double lines, capillaries by single lines. Mitotic figures are symbolized by (x) dark and metrial gland cells by (●) compact zone cells by (○) other mononuclear cells increasing in size and with 2 to 3 basophilic nucleoli by (⊙). Further increase in cell size is shown by the increased size of the symbols. Degeneration or loss of basophilia is indicated by broken out lines. Zones indicated on the drawings on the day they first appear are: compact zone Co 7 implantation zone IZ large cell zone LC 7



Figures 1-6



Figs 7-10 Diagrammatic cross sections of pregnant uteri from four and one fourth days after mating. At two-thirds the magnification of figures 1-6. Additional cell types seen during this period are binuclear cells (∞) and multinuclear cells (\odot). Additional zones found are basophilic cell zone BCZ, central zone CZ, fibrous capsule FC, fibrinoid capsule FiC, multinuclear cell zone MC, sinusoid wings SW, secondary decidal zone SD.

bryonic cells of later stages Hall (60) noted similar differences in metachromasy in stromal and epithelial cells after staining with toluidine blue. The cytoplasm of the glandular epithelium is also highly basophilic and more so basally than apically. No neutrophils are found in the glandular epithelium but there are large numbers often in patches between the luminal epithelial cells.

Two days

The principal change to be seen in the non-epithelial cells of the mucosa at this age is a marked decrease in the number of neutrophils; those present often have a pyknotic nucleus.

The luminal epithelium however is very much changed (fig 2). The massive folding found at 12 hours has disappeared; the height of individual cells is less and cytoplasmic basophilia has dropped sharply especially in the basal portion of the cells. In places the orderly arrangement of the centrally located nuclei is disrupted and the epithelial surface generally shows a rough and irregular outline. In addition large basally located vacuoles containing pyknotic nuclei are present between apparently normal epithelial cells. There are occasional mitotic figures in the luminal epithelium and many in the distal portion of the glandular epithelium.

Two and three quarter days

Of the six uteri taken at this interval after mating the four in which the morulae are most dispersed show the most intense basophilia.

In all these uteri the size and basophilia of the cells of the capillaries adjacent to the uterine lumen are markedly greater than at two days; the capillaries tending to stand out against a background of palely staining stromal cells (fig 3). The latter also seem to show slightly increased amounts of cytoplasm and increased basophilia. Peripherally the diameter but not the basophilia of the capillaries has increased. Throughout the endothelium mitotic figures are common and they are also frequent around the glands. In the latter location however it is impossible to determine what cell types are involved.

The number of polymorphs now present in the stroma has fallen sharply but lymphocytes flood some areas around large capillaries. In addition around the glands there are both mature plasma cells and a new type of basophilic cell usually distinct from the plasma cell on the basis of nuclear stainability and cell shape. This new type of cell described more fully in Smith (66) varies continuously in size from that of a large lymphocyte with a narrow rim of basophilic cytoplasm to a cell with a wide band of distinctively striated cytoplasm. Cells with such striated cytoplasm seem to be small metrial gland cells and will be so designated henceforth to distinguish them from the smaller "dark" cells of the new type.

The luminal epithelium at two and three quarter days is more highly columnar than at 48 hours and the vacuoles present at the earlier stages are rare. In addition increased numbers of mitotic figures are present in the epithelium. Basophilia however is even more reduced. Finally the epithelium of the neck of some of the glands is now disorganized and shows very reduced cytoplasmic basophilia. Such glands often appear occluded adjacent to the uterine lumen. Distally however the lumens of all glands are enlarged and basophilia is confined to the basal cytoplasm. Mitotic figures are fairly frequent distally.

Three and one half to four days

Both the basophilia and the size of the cells in three and one half day old pregnant uteri are very similar to those in two and three-quarter day old uteri. In uteri taken between three and one half and three and three-quarter days post coitum however and containing blastocysts whose blastocoel is slightly larger than the inner cell mass the luminal epithelial cells next to the blastocysts are lower and show less basophilia than those only a short distance away and a few contain shrunken nuclei. This portion of the epithelium can often be seen to be connected to the plump basophilic trophoblast cells of the blastocysts by fine protoplasmic strands. Parenthetically in sections fixed for staining by the PAS technique the zona pellucida around blastocysts of this size appears cracked.

The zona is apparently lost very soon after this for in uteri taken between three and three quarter and four days after mating and containing embryos with a somewhat larger blastocoel it is clear that the embryos are firmly fixed to the epithelium by three or four enlarged and vacuolated trophoblast cells. At this stage of nidation the uterine epithelial and stromal cells are separated in the region immediately around the embryos. Interestingly, there also seems to be a minor mobilization of lymphocytes beneath the epithelium. Some of the nuclei of these lymphocytes are irregular lobulated or fragmented.

Four days

In uteri taken at four days the blastocysts are pressed tightly against the epithelium into which blunt processes from the trophoblast extend. In the region of such blastocysts the organization of the epithelium as a single layer of cells has clearly been lost and some of the epithelial nuclei are pycnotic. In addition there are a few spherical bodies which stain heavily for DNA with both Azure B and the Feulgen reagent in the basal portion of the epithelium while under the epithelium there are large numbers of cells with irregularly shaped nuclei and similar pycnotic bodies. It is assumed that both are the remains of the invading lymphocytes.

At this stage a subepithelial strip slightly wider in the vicinity of the implanting embryo than elsewhere is sharply delimited from the remainder of the stroma by its greater Azure B stainability (fig 4). The stromal cells in this strip particularly those in the antimesometrial area are clearly larger than those in earlier stages are more tightly packed and are now as basophilic as the cells lining the capillaries. The latter cells have also enlarged and so much so that some of the capillaries adjacent to the epithelium lateral and antimesometrial to the embryos appear occluded. There are also a few mitotic figures in the stroma at the level of the embryo

Four and one quarter days

Both the inner cell mass and the blastocoel of embryos of this age have enlarged. The blastocoel is often collapsed however and the much flattened trophoblast cells

surrounding such a blastocoel are separated from the epithelium. Basophilic processes from these trophoblast cells can nevertheless be seen deep within the less basophilic epithelium. Such processes frequently contain elongate, pycnotic nuclei and similar nuclei lie between the blastocyst and the epithelium.

At this stage the size of the cells in a wide strip of mucosa lateral and antimesometrial to even the least developmentally advanced of the embryos is clearly greater than that of the cells in the same region at four days. Furthermore this strip can be divided, roughly into a subepithelial and a vascular layer since the capillaries immediately beneath the luminal epithelium no longer seem patent while those located more distally are open and are larger in diameter than any found elsewhere in the endometrium (fig 5). The subepithelial layer seems to correspond to the primary decidual zone of Krehbiel (37) and in more advanced four and one quarter day uteri the stromal cells of this region are less basophilic than are those in the vascular layer. This loss of basophilia seems to be the first sign of the formation of the implantation zone (Krehbiel 37).

Immediately external to the vascular layer where the cells are less tightly packed there are large numbers of mitotic figures. These figures are especially frequent in a cup-shaped area antimesometrial to the embryo and in the least advanced of the four and one quarter day uteri the largest cells of the uterus are found here and in the vascular layer just mesometrial to it. These cells are uni-nuclear and have 2 to 3 very large nucleoli. In older four and one quarter day uteri all of the cells of the vascular layer are like this and are clearly larger than those elsewhere in the uterus. The vascular layer will hereafter be called the large cell zone.

Immediately mesometrial to the embryo the capillaries are still open adjacent to the luminal epithelium so that in this region there is no primary decidual zone only a large cell zone. Still more mesometrially around the mesometrial portion of the lumen, the subepithelial cells decrease in size rather abruptly and are more closely packed than are cells in other regions. This

region will henceforth be called the compact zone

By this stage also the luminal epithelium can be divided into the four regions mesometrial transitional implantational and antimesometrial described by Krehbiel (37) at the start of the sixth day in the rat Basophilia is lowest in the implantational epithelium which is detached from the underlying stroma Finally in the region of implantation normal appearing glandular epithelium is present only in the basal layer closer to the lumen nothing but pale cords remain

Four and one half days

By this time as the result of the hyperplasia and hypertrophy of the stromal cells immediately mesometrial to the embryo the epithelial sac surrounding the embryonic crypt is almost completely cut off from the main portion of the lumen (fig 6) Furthermore the organization of the epithelium forming the sac has broken down and the cells are either jumbled together or missing When missing their place is taken by the enlarging vacuolated trophoblast cells which now encircle the blastocoel The latter often contain fragmented epithelial cells Finally the width of the zone of cells showing reduced basophilia (the implantation zone) has increased considerably and now completely surrounds the embryo

Four and three quarter days

Four trends which presage the future direction of the decidual reaction and the formation of the definitive placenta are present at this time (fig 7) First some of the cells in the cup-shaped area of the large cell zone antimesometrial to the embryo are now binuclear Krehbiel (37) called the zone in which the binuclear cells appeared the secondary decidual zone Second although mitotic figures are still frequent at the periphery of the mucosa lateral to the embryo for the first time a very large number is present mesometrial to the embryo Some are in endothelial cells in the region of sinusoid development (see below) and others may be in stromal cells around the enlarging capillaries Still others are in the compact zone but whether in endothelial or stromal cells could not be

determined Third a polarization of enlarging capillaries suggests the beginning stages of the sinusoid wings described by Krehbiel (37) Fourth since the enlarged capillaries are not found within the portion of the large cell zone mesometrial to the embryo and adjacent to the transitional epithelium this area as a whole appears to be the most basophilic in the uterus This portion of the large cell zone will be called the basophilic cell zone henceforth

At this time the dissolution of the luminal epithelium has progressed to the point where the trophoblast is in direct contact with the stroma everywhere except mesometrially in the region of the inner cell mass and antimesometrially where the embryo still rests on a shelf of compressed epithelium In addition the trophoblast cells surrounding the blastocoel are becoming transformed into giant cells and a few processes from them have penetrated between the decidual cells of the implantation zone

Five and one half days

Thin cords of cells projecting from the ectoplacental cone have by now grown up the narrow channel still connecting the embryonic crypt with the uterine lumen almost as far mesometrially as the basophilic cell zone (fig 8) The cells at the periphery of the trophoblast cords also seem to have eroded some of the sinusoids formed from the enlarged capillaries seen at four and three-quarter days because maternal red blood cells are now present between the trophoblast cords Large trophoblast cells are easily distinguishable from the large decidual cells by virtue of their greater basophilia and large extremely lobulate nuclei See Alden (48) also

At this time after staining by the PAS technique the basophilic cell zone can be seen to correspond to the glycogenic area of Krehbiel (37)

Six days

The degree of basophilia and the cell types characterizing each region of the preplacental pregnant uterus are sharply distinct at this time (fig 9) External to the sinusoid wings and mesometrial to the compact zone some of the fibroblasts of the basal layer now appear compressed and

highly basophilic. These compressed cells are apparently what Bridgman (48a) described as a fibrous layer. The compact zone which will form the mid portion of the decidua basalis contains two types of stromal cells: small tightly packed mononuclear cells which seem to differ from those seen at 12 hours only by a slight increase in size and a great increase in basophilia and many medium sized metrial gland cells. The latter stand out from the fusiform stromal cells by virtue of their shape: vacuolization, kidney shaped nucleus and large nucleoli. This zone now also contains many mitotic figures.

There is a sharp discontinuity in size between the cells of the compact zone and of the basophilic cell zone immediately antimesometrial to it. The basophilic cell zone is made up of cells of giant size: high basophilia and a single nucleus with 2 or 3 very large, compact and basophilic nucleoli. The area of the sinusoid wings contains smaller cells similar to those in the basophilic cell zone with respect to their basophilia and nuclear morphology and some metrial gland cells.

In the widening implantation zone the poorly basophilic cells have shrunken nuclei and pale nucleoli. Processes from trophoblast cells seem to be lying within the eroded capillaries of this region. External to the implantation zone and lateral and antimesometrial to the embryo the cells are moderately basophilic and usually binuclear. They are also easily distinguished by their multiple small pale nucleoli.

Seven and one quarter days

The compact zone has increased in size conspicuously if the remnant of lumen still remaining at this time is used as a marker (fig 10). Here the sinusoids have become much more plentiful although they remain relatively small as compared to those in the sinusoid wings and stromal cell number is greatly increased. The number of dark and medium sized metrial gland cells now present is striking. Even larger metrial gland cells and very many dark cells are present throughout the region of the sinusoid wings. The latter contain large numbers of leucocytes.

A few of the now giant cells of the basophilic cell zone and of the smaller cells in the sinusoid wings are binuclear at this stage, the nucleus of others being irregular in shape. All have remained highly basophilic however and still have only 2 to 3 large basophilic nucleoli. A small number of metrial gland cells is now seen in this zone.

Almost all of the cells of the endometrium lateral and antimesometrial to the embryo except those immediately beneath the basal layer are also greatly enlarged at this stage and most contain multiple small pale nucleoli. The largest of these maternal giant cells are located at the periphery of this area and some are tri- or tetranuclear while many have irregular or lobulate nuclei. Basophilia is highest here also. The small cells next to the basal layer are mononuclear and contain 2 to 3 nucleoli. These small cells have vacuolated cytoplasm as do the small mononuclear cells immediately external to the sinusoid wings and beneath the fibrous layer. These cells probably make up the fibrinoid capsule of Bulmer and Dickson (61).

At this time the cells forming the mesometrial roof of the ectoplacental cavity (the cytotrophoblast or the lamina of Everett 35) are highly basophilic as are the peripherally located giant cells. Both are in sharp contrast to the pale vacuolated spongiotrophoblast cells internal to these regions and to the adjacent maternal cells which the giant cells often appear to be surrounding. The beginning of central zone formation (Everett 35) is thus evident.

Eight and one half days

The allantois has made contact with the lamina of the ectoplacental cone by now and the central zone is several cells wide. Polymorphs and metrial gland cells are present in the maternal blood spaces of the mesometrial portion of the zone.

Nine and one half days

By nine and one half days after mating the ectoplacental cone extends in the form of a wedge up the original uterine lumen almost to the level of the compact zone and most of the cells in the basophilic cell zone have either been pushed laterally or phagocytized. The giant cells of the

trophoblast about therefore mesometrially on the compact zone with its many large metrial gland cells and laterally on the sinusoid area which also contains very large metrial gland cells. Some of the latter appear to be free in the maternal sinuses. Enlarged endothelial cells encircled by a cuff of metrial gland cells such as was described by Dickson and Bulmer (61) and Bridgman (48b) are present in the compact zone at this time.

Summary of the changing pattern of basophilia

Mature plasma cells are present around the uterine glands in fairly high numbers

by two and three-quarter days after mating and some are still found at seven and one quarter days. Since it seems reasonable to assume that the basophilia of these cells remains rather constant during this period the intensity of their staining was used as a standard of comparison for estimating relative changes in the basophilia of other uterine cells (table 1). It must be stressed however that the values in the table are arbitrary and are intended to show only the direction of the change i.e. either increases or decreases in basophilia. It should also be noted that the values in the table are for the cytoplasmic basophilia of individual cells within a particular area.

TABLE 1

A summary and rough estimate of the changes in basophilia of individual cells within the pregnant uterus from one half to seven and one-quarter days after mating. The basophilia of the mature plasma cell was taken as a constant and given the value 4. Less basophilic cells received lower numbers. Areas within the uterus have been identified both by number on the drawing and in terms of their prospective fate. Where values are shown as 1-0 the first figure is for more medially located cells.

Dysmating	1	2	3	4	5	6	7	8	9
	Luminal epithelium	Glandular epithelium	Primordial zone	Large cell zone	Multi-nuclear cell zone	Basal zone	Basophilic cell zone	Compact zone	Trophoblast
½	7	3	2	2	1	0	2	2	
2	4*	4	2	2	1	0	2	2	
2¾	2	2-4	+3 2	+3 2	+3 1	0	+3 2	+3 2	
3½	x2 2½	0-4	+4 3	+4 2½	+3 1½	0	+4 3-2	+4 3-2	4
4	x2 2½	0-4	+4 4	+4 3	2	0	+4 4-2	+4 4-2	4 or 2
4¼	x1 2	0-4	4 or 2	4	2	1	4-2	4-2	4 or 2
4½	x0 2	0-4	2	4	2½	1½	4-2	4-2	5
4¾	x0 2	3	1	3-4	3	2	5-2	4-2	5
5	x† 2	3	0	2-4	3½	2	5-2	4-2	5
5½	2	2½	0	1-4	4	2½	4-5-3	4-2	5
6	2	†	†	3	4½	3	3-6-4	5	6
7¼	1	†	†	1-3	5-6	xx7	6	5	6

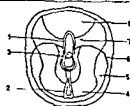
† mitosing

apical, in degenerating cells
normal cell

+ capillary only

x near embryo

xx fibroblastic pulp only



one allows for the difference in the rate of development in the two species. The marked similarity in the decidual morphology of the two species would appear to make this a valid comparison in spite of some evidence that hormonal differences exist between them. Furthermore Shelesnyak and co-workers (Marcus et al. 64) found that the histamine content of the early pregnant uterus was different from that of pseudopregnant uterus at comparable times and concluded that the hormonal influences on the two types of uterus were also different. Atkinson and Hooker (45) however came to the opposite conclusion in their study of the mouse.

In the present histochemical study the basophilia of the epithelium particularly of the luminal epithelium was found to fall abruptly between 12 and 48 hours after mating (although the low point had probably not been reached by 48 hours) while that of the remaining cells of the endometrium remained fairly constant. The drop in basophilia in the luminal epithelium was so great that it seems likely that a decided drop in RNA content might well be found to have occurred between 12 and 48 hours if biochemical analyses of entire uterus were done at these two times. An additional reduction would probably come about as a consequence of the morphological changes during this interval since they were similar to those seen between estrus and late metestrus (Allen 22) and Drasher (52) reported a sharp drop in RNA P/DNA P ratios between estrus and diestrus in the mouse. Except for a difference in timing therefore these results agree with those of Shelesnyak and Tic who found a drop in RNA content of entire uterus immediately after inducing pseudopregnancy at proestrus with the lowest value being reached at what would be the time of diestrus in the normal cycle. Moreover their data for this period seem identical to those they obtained at comparable times in the normal cycle.

The two sets of data on RNA content in uterus undergoing "sensitization" to the stimulus for decidualization also seem to agree except that this process appears to begin earlier in the mouse than in the rat. In the histochemical study the intensity of endometrial basophilia (excluding that

of the epithelium) was found to be visibly greater at two and three-quarter days than at two days and it rose slowly until the fourth day. The intensity of basophilia in the luminal epithelium on the other hand was still lower at two and three quarter days than at two days after mating but it had risen somewhat by three and one half days although in the region of the embryo it continued to rise only until about three and three-quarter days. As the detailed description of the situation during these hours indicated this pattern of increase in intensity of basophilia is quite different from that seen in a normal cycle. That is the increase is not one of increasing basophilia in multiplying luminal and glandular epithelium but is primarily one of an intensifying basophilia in endothelial cells which are also increasing in size and number and secondly one of an intensifying basophilia in stromal cells which are increasing in size and number too but more slowly. In addition the basophilic metrial gland cells are beginning to differentiate at two and three-quarter days. It is these changes then together with an increase in capillary size which is also found at two and three-quarter days which results in a uterus competent to respond "sensitized" to the stimulus for decidualization.

With respect to the level of RNA in the rat uterus during the period of sensitization from the data of Shelesnyak and Tic RNA concentration seems to remain very low between Day 1 and Day 3 or until approximately three and one half days after the induction of pseudopregnancy by the timing used in this mouse study. After that there appears to be a slow rise which seems to correspond to that seen between two and three-quarter and four days in the mouse. Before the decidualization stimulus was given at four and one half days there had been an "elevation of the content and concentration of protein RNA and DNA over the basal level of dioestrus".

Since it is currently proposed that the buildup of RNA is mediated by estrogen (Ui and Mueller 63 and Frieden 64 for additional references) the hormonal state during the period from mating or from the time pseudopregnancy is induced to the time the stimulus for decidualization is given is of course of interest. Shelesnyak

and are not for the area as a whole. The scores therefore, reflect only imperfectly the major changes in the amount of RNA which occur in the pregnant uterus during the period covered by this study.

DISCUSSION

General uterine organization

From the results reported here, it is apparent that the endometrium even at 12 hours after a successful mating is not homogeneous. Even at this time the mesometrial portion differs from the antimesometrial in the relationship of glands to lumen and to stromal cells and probably also in the state of the stromal cells around the lumen. In addition both Williams (48) and Young (51) found differences in vascularization in the two regions in the rat.

Examination of successively older stages reveals that it is the fusiform stromal cells together with the endothelial cells adjacent to the degenerating gland necks which early become basophilic and enlarged when the uterus is becoming sensitized to decidualization and that it is these same stromal cells in which the decidual reaction is first localized following the stimulation of trophoblast attachment. In other words only the stromal cells in the region containing glands seem to differentiate into maternal giant cells. These large cells are also the shortest lived of the decidual cells and many have disappeared by the time placental circulation begins.

The stromal cells around the mesometrial lumen on the other hand never get very large and show few morphological signs of differentiation at least in the interval studied. Unlike the large antimesometrial multinucleolate stromal cells however it seems reasonable to suppose they provide an environment suitable for the differentiation of the precursors of the metrial gland cells which are so plentiful in this area in later stages of uterine development. It should be noted here that a possible origin of metrial gland cells from cells other than *in situ* mesometrial stromal cells is suggested in Smith (66).

Cytology of the decidual cells

In Krehbiel's (37) now classic study of the pregnant rat uterus it was reported

that glycogen bearing cells are found almost exclusively in the mesometrial portion of the decidua while cells containing large amounts of lipid are characteristic of the antimesometrial decidua. The present work discloses what appears to be a further and functionally significant difference between the two areas in the mouse. This is that the multinuclear antimesometrial cells which possess 2 to 3 highly basophilic nucleoli per nucleus in early stages of differentiation in later stages contain many small pale nucleoli and as cell size increases in this area basophilia tends to decrease. The mesometrial decidual cells of the basophilic cell zone and sinusoid wings on the other hand are characterized by the presence of only 2 to 3 large basophilic nucleoli per nucleus all during differentiation and cytoplasmic basophilia tends to remain constant as cell size increases. Vacuoles however are evident in the cytoplasm when glycogen makes its appearance in these cells at five and one half days.

The recent electron microscopic study of Jollie and Bencosme (65) in which the fate of the glycogen containing cells of the primary decidual zone in the rat was followed appears to offer no contradictions to these findings although it is difficult to determine corresponding cell types and timing in the two studies. Subepithelial cells in the primary decidual zone in the mouse however lose their basophilia as soon as they begin to enlarge then become glycogen laden and finally are phagocytized by five and one half days after mating (Smith 66).

Pattern of basophilia in the uterus

The changes in basophilia observed in the endometrium of the mouse between 12 hours and seven and one quarter days after mating are on the whole what would be expected on the basis of the association between the basophilia seen after Azure B staining and RNA (Flax and Himes 52) and the present ideas on the relationship of RNA to protein synthesis during differentiation and growth.

The changes also parallel in striking fashion the changes in RNA content during artificial decidualization of the pregestational rat uterus as determined biochemically by Shelesnyak and Tic (63) if

subepithelial stromal cells with respect to size is evident. As the data indicate from four and one quarter days on the increase in cell size and number and in differentiation continues unchecked in the implantation site as some cells gain basophilia while others are losing it.

It seems necessary to emphasize that an interaction between the embryo and the uterus is most probably the stimulus for decidualization in view of the hypothesis of Shelesnyak (Marcus et al 64) that it is the estrogen surge which releases histamine from mast cells which is the stimulus rather than the trauma of implantation or an exogenous trauma in the case of deciduoma induction (See Noyes et al 63 for a discussion of the active role of the rat egg in implantation). Nevertheless in Shelesnyak and Tics study an exogenous trauma was given at four and one half days and following this there was a second and rapid rise in RNA concentration and deciduoma formation. As was previously indicated it was impossible to so accurately pinpoint the time of onset of the sharp rise in basophilia seen in this mouse study.

With respect to a later stage an apparent difference in the pattern of basophilia between the rat and the mouse must be mentioned. Bulmer and Dickson (61) report greater basophilia just outside the implantation zone of the antimesometrial decidua of the nine day rat than more peripherally. This is the reverse of the finding in the mouse at a similar stage (i.e. at seven and one-quarter days). Their material however was preserved in formalin containing fixatives while the mouse material was not. It is also possible that their description of this stage was taken from material stained with a stain other than Azure B.

ACKNOWLEDGMENTS

This investigation was supported by Research Career Development Award 8K3-HD-4334 from the National Institutes of Health and by a National Science Foundation Research grant GB 646.

LITERATURE CITED

- Alden R H 1948 Implantation of the rat egg
III. Origin and development of primary trophoblast giant cells. *Am J Anat* 83 143-181
- Allen E 1922 The oestrous cycle in the mouse. *Am J Anat* 30 297-371
- Atkinson W B and C W Hooker 1945 The day to day level of estrogen and progesterone throughout pregnancy and pseudopregnancy in the mouse. *Anat Rec* 93 75-95
- Baker B L 1948 Histochemical variations in the metrial gland of the rat during pregnancy and lactation. *Proc Soc Exp Biol and Med* 68 492-496
- Bloch S 1958 Experimentelle Untersuchungen über die hormonalen Grundlagen der Implantation des Säugetieres. *Experientia* 14 447-449
- Bridgman J 1948a A morphological study of the development of the placenta of the rat. I. An outline of the development of the placenta of the white rat. *J Morph* 83 61-85
- 1948b A morphological study of the development of the placenta of the rat. II. An histological and cytological study of the development of the chorioallantoic placenta of the white rat. *J Morph* 83 195-223
- Bulmer D and A D Dickson 1961 The fibrioid capsule of the rat placenta and the disappearance of the decidua. *J Anat* 95 300-310
- Dickson A D and D Bulmer 1961 Observations on the origin of metrial gland cells in the rat placenta. *J Anat* 95 262-273
- Drasler M L 1952 Morphological and chemical observations on the mouse uterus during the estrous cycle and under hormonal treatment. *J Exp Zool* 119 333-353
- Everett J W 1935 Morphological and physiological studies on the placenta in the albino rat. *J Exp Zool* 70 243-285
- Flax M H 1953 Ribose nucleic acid and protein during oogenesis and early embryonic development in the mouse. Ph.D. Dissertation. Columbia University 46 pp
- Flax M H and M H Himes 1952 Microspectrophotometric analysis of metachromatic staining of nucleic acids. *Physiol Zool* 25 297-311
- Frieden E H 1964 Sex hormones and the metabolism of amino acids and proteins. In: *Action of Hormones on Molecular Processes*, edited by G Litwack and D Kritchevsky. John Wiley and Sons, New York, pp 509-559
- Hall K 1960 Modification by relaxin of the response of the reproductive tract of mice to oestradiol and progesterone. *J Endocr* 20 355-364
- Jeener R 1948 Acides nucléiques et phosphatases au cours de phénomènes de croissance provoqués par l'oestradiol et la prolactine. *Biochim Biophys Acta* 2 439-453
- Jollie W P and S A Benscosme 1965 Electron microscopic observations on primary decidua formation in the rat. *Am J Anat* 116 217-235
- Krehbiel R H 1937 Cytological studies of the decidual reaction in the rat during early pregnancy and in the production of deciduomata. *Physiol Zool* 10 212-234
- Marcus C J M C Shelesnyak and P F Kraicer 1964 Studies on the mechanism of nidation

has proposed that a brief estrogen surge during the period of progesterone domination and different from that required for priming the uterus for proliferation is responsible for the transient sensitization of the rat uterus to decidual induction (Shelesnyak et al., 63). Furthermore they suggest that their data indicate that the surge occurs in their strain at about 12 noon of Day 3 (or at three and one half days by my timing). Zeilmaker (63) who ovariectomized pregnant rats obtained similar results. This is about the time of the beginning of the transient elevation in RNA seen in Shelesnyak and Tics study. In addition Mayer (63) was able to induce nidation at will within 48 hours after the injection of estradiol into pregnant rats ovariectomized on Day 3 (same timing as Shelesnyak) and maintained on progesterone. Finally Yochim and DeFeo (63) have shown that exceeding the optimal level of estrogen results in a failure of deciduoma formation in rats.

Unfortunately no similar data are available for the mouse that will allow as clear cut a correlation to be made between the time of the estrogen surge and the time basophilia begins to increase in the endometrial cells (at approximately two and three quarter days in the mice used in this study). That estrogen is necessary for implantation in the mouse was shown by Bloch (58) and Smithberg and Runner (60). Furthermore the latter authors were also able to induce nidation with progesterone alone if the ovaries were removed one or two days post coitum (Smithberg and Runner 56) which suggested to them that estrogen is needed at least 1 or 2 days earlier in the mouse than it is in the rat (Smithberg and Runner 60). This agrees with the morphological data of Atkinson and Hooker (45) who concluded that estrogen is at its highest at the time of mating falls to a low level on the next day and has almost disappeared by the third day of pregnancy.

Until more exact endocrinological data are available for the mouse therefore the time of entrance of the morulae into the uterus may be the best indication that the same stages of embryo and uterine differentiation have been reached in the two rodents. Morulae had entered the mouse

uterus slightly before two and three quarter days post coitum and an increase in endometrial basophilia was evident at two and three quarter days. According to most investigators morulae enter the rat uterus around three and one half days after mating and Shelesnyak and Tics data suggest RNA concentration begins to increase by this time.

The corresponding times at which the stimuli for decidualization were given the mouse and the rat resulting in a second and very sharp rise in basophilia in the mouse and in RNA in the rat are even more difficult to determine. This is partly because it is impossible to be sure on purely morphological grounds what constituted the stimulus in the present study. The sequence of changes in the blastocyst in the epithelium next to the blastocyst and in the subepithelial stromal cells between three and one half and four days after mating however suggests that the stimulus for decidualization in the present study was received slightly before the fourth day. These changes also suggest that the stimulus was the contact between a blastocyst differentiated to the extent of being able to adhere to the epithelium and the epithelium overlying a competent stroma. With respect to this interpretation of what constitutes the stimulus for decidualization it is most important to stress that localized changes in the epithelium in the underlying basement membrane and in the lymphocytes are evident before the subepithelial stromal cells attain maximum basophilia. These cells have reached this state by the time blunt processes from the trophoblast can be seen within the epithelium (at 4 days) and at this time stromal cell volume and number are very obviously increasing. Unless this increase in stromal cell volume and number constitutes sensitization of the uterus to decidualization rather than the beginning stages of decidualization therefore the shallow penetration of the epithelium by the trophoblast cells at four days and the presence of the invasive cells (Wilson 63) at four and one quarter days seem to follow the stimulus. It must be pointed out however that it is not until four and one quarter days after mating that a clear difference between mesometrial and antimesometrial

subepithelial stromal cells with respect to size is evident. As the data indicate from four and one quarter days on the increase in cell size and number and in differentiation continues unchecked in the implantation site as some cells gain basophilia while others are losing it.

It seems necessary to emphasize that an interaction between the embryo and the uterus is most probably the stimulus for decidualization in view of the hypothesis of Shelesnyak (Marcus et al 64) that it is the estrogen surge which releases histamine from mast cells which is the stimulus rather than the trauma of implantation or an exogenous trauma in the case of deciduoma induction (See Noyes et al 63 for a discussion of the active role of the rat egg in implantation). Nevertheless in Shelesnyak and Tics study an exogenous trauma was given at four and one half days and following this there was a second and rapid rise in RNA concentration and deciduoma formation. As was previously indicated it was impossible to so accurately pinpoint the time of onset of the sharp rise in basophilia seen in this mouse study.

With respect to a later stage an apparent difference in the pattern of basophilia between the rat and the mouse must be mentioned. Bulmer and Dickson (61) report greater basophilia just outside the implantation zone of the antimesometrial decidua of the nine day rat than more peripherally. This is the reverse of the finding in the mouse at a similar stage i.e. at seven and one-quarter days. Their material however was preserved in formalin containing fixatives while the mouse material was not. It is also possible that their description of this stage was taken from material stained with a stain other than Azure B.

ACKNOWLEDGMENTS

This investigation was supported by Research Career Development Award 8 K3-HD 4334 from the National Institutes of Health and by a National Science Foundation Research grant GB 646.

LITERATURE CITED

- Alden R H 1948 Implantation of the rat egg III. Origin and development of primary trophoblast giant cells. *Am J Anat* 83 143-181.
- Allen E 1922 The oestrous cycle in the mouse. *Am J Anat* 30 297-371.
- Atkinson W B and C W Hooker 1945 The day to day level of estrogen and progesterin throughout pregnancy and pseudopregnancy in the mouse. *Anat Rec* 93 75-95.
- Baker B L 1948 Histochemical variations in the metrial gland of the rat during pregnancy and lactation. *Proc Soc Exp Biol and Med* 68 492-496.
- Bloch S 1958 Experimentelle Untersuchungen über die hormonalen Grundlagen der Implantation des Säugetierkeimes. *Experientia* 14 447-449.
- Bridgman J 1948a A morphological study of the development of the placenta of the rat I. An outline of the development of the placenta of the white rat. *J Morph* 83 61-85.
- 1948b A morphological study of the development of the placenta of the rat II. An histological and cytological study of the development of the chorioallantoic placenta of the white rat. *J Morph* 83 195-223.
- Bulmer D and A D Dickson 1961 The fibrinoid capsule of the rat placenta and the disappearance of the decidua. *J Anat* 95 300-310.
- Dickson A D and D Bulmer 1961 Observations on the origin of metrial gland cells in the rat placenta. *J Anat* 95 262-273.
- Drasler M L 1952 Morphological and chemical observations on the mouse uterus during the estrous cycle and under hormonal treatment. *J Exp Zool* 119 333-353.
- Everett J W 1935 Morphological and physiological studies on the placenta in the albino rat. *J Exp Zool* 70 243-285.
- Flax M H 1953 Ribose nucleic acid and protein during oogenesis and early embryonic development in the mouse. Ph.D. Dissertation, Columbia University 46 pp.
- Flax M H and M H Himes 1952 Microspectrophotometric analysis of metachromatic staining of nucleic acids. *Physiol Zool* 25 297-311.
- Frieden E H 1964 Sex hormones and the metabolism of amino acids and proteins. In: *Action of Hormones on Molecular Processes*, edited by G Litwack and D Kravitsky. John Wiley and Sons, New York pp 509-559.
- Hall K 1960 Modification by relaxin of the response of the reproductive tract of mice to oestradiol and progesterone. *J Endocr* 20 355-364.
- Jeener R 1948 Acides nucléiques et phosphates au cours de phénomènes de croissance provoqués par l'oestradiol et la prolactine. *Biochim Biophys Acta* 2 439-453.
- Jollie W P and S A Benscosme 1965 Electron microscopic observations on primary decidua formation in the rat. *Am J Anat* 116 217-235.
- Krehbiel R H 1937 Cytological studies of the decidual reaction in the rat during early pregnancy and in the production of deciduomata. *Physiol Zool* 10 212-234.
- Marcus C J, M C Shelesnyak and P F Traicer 1964 Studies on the mechanism of nidation.

- X The oestrogen surge histamine release and decidual induction in the rat *Acta Endocr* 47 255-264
- Mayer G 1963 Delayed nidation in rats: a method of exploring the mechanism of ova implantation In *Delayed Implantation* A C Enders ed Univ Chicago Press Chicago pp 213-231
- Noyes R W Z Dickmann L L Doyle and A H Gates 1963 Ovum transfers synchronous and asynchronous in the study of implantation In *Delayed Implantation* A C Enders ed Univ Chicago Press Chicago pp 197-211
- Shelesnyak M C P F Kraicer and G H Zeilmaker 1963 Studies on the mechanism of decidualization I The oestrogen surge of pseudopregnancy and progravity and its role in the process of decidualization *Acta Endocr* 42 225-232
- Shelesnyak M C and L Tic 1963 Studies on the mechanism of decidualization IV Synthetic processes in the decidualizing uterus *Acta Endocr* 42 465-472
- Smith L J 1956 A morphological and histochemical investigation of a preimplantation lethal (t^{11}) in the house mouse *J Exp Zool* 132 51-84
- 1966 Metrial gland and other glycogen containing cells in the mouse uterus following mating and through implantation of the embryo *Am J Anat* 119 15-24
- Smithberg M and M N Runner 1956 The induction and maintenance of pregnancy in prepuberal mice *J Exp Zool* 133 411-457
- 1960 Retention of blastocysts in non progestational uteri of mice *J Exp Zool* 143 21-31
- Snell G D (Ed) 1941 *Biology of the Laboratory Mouse* Blakiston Company Philadelphia pp 1-54
- Ul H and G C Mueller 1963 The role of RNA synthesis in early estrogen action *Proc Nat Acad Sci* 50 256-260
- Williams M F 1948 The vascular architecture of the rat uterus as influenced by estrogen and progesterone *Am J Anat* 83 247-307
- Wilson I B 1963 A new factor associated with the implantation of the mouse egg *J Reprod Fertil* 5 281-282
- Wislocki G B and E W Dempsey 1945 Histochemical reactions of the endometrium in pregnancy *Am J Anat* 77 365-403
- Yochim J M and V J DeFco 1963 Hormonal control of the onset magnitude and duration of uterine sensitivity in the rat by steroid hormones of the ovary *Endocr* 72 317-326
- Young A 1951 The vascular architecture of the rat uterus during pregnancy *Proc Royal Soc (Edinb)* Sec B 64 292-311
- Zeilmaker G H 1963 Experimental studies on the effects of ovariectomy and hypophysectomy on blastocyst implantation in the rat *Acta Endocr* 44 355-366

Metrial Gland and Other Glycogen Containing Cells in the Mouse Uterus Following Mating and Through Implantation of the Embryo

LOIS JEAN SMITH

Department of Anatomy Albert Einstein College of Medicine
New York New York

ABSTRACT Mouse uteri and embryos from 12 hours to seven days after mating were examined for RNA and glycogen following specific histochemical staining. Because of their greater basophilia cells present throughout the endometrium which seem to be metrial gland cell precursors could be distinguished as early as two and three-quarter days. At this time the uterus is just beginning to undergo "sensitization to decidualization." By seven days these precursor cells and metrial gland cells proper have disappeared from all regions of the endometrium except that of the future decidua basalis. Glycogen is present in cells which may be the metrial gland cell precursors, plasma cells and polymorphonuclear leucocytes as well as in the lumens and cells of the uterine glands at three and one-half days. Between four and one-fourth and five and one-half days glycogen is found in the primary decidual zone. By six days there is a heavy deposit in the "glycogenic areas." At seven days many of the metrial gland cells in the future decidua basalis are PAS-positive. These findings are discussed and the possible origin of the metrial gland cells from a cell of the lymphocytic series is suggested.

Differences in the basophilia of several cell types in the uterus made possible the discovery that cells which seem to be metrial gland cell precursors are present in small numbers throughout the endometrium of the mouse at 65 hours after mating (Smith '66). At this time the conceptuses have just entered the uterus which itself is just beginning to transform into an organ into which the embryos can implant. Metrial gland cells and their precursors have not previously been reported anywhere in the mouse or rat uterus at such an early stage of pregnancy. At later stages these cells are concentrated around blood vessels in the decidua basalis and in the metrial gland proper.

Mature metrial gland cells are characterized by a distinctively striated cytoplasm and contain both glycogen and PAS-positive diastase resistant granules. The function of these cells and whether or not the metrial gland is in fact a gland is still being debated. Investigators from Jenkinson ('02) through Padykula and Richardson ('63) have discussed the possible contribution of the intracellular glycogen to the nourishment of the embryo but have been unable to agree on any one hypothesis.

Wislocki et al ('57) have suggested that the diastase resistant granules are relaxin and Velardo et al ('53) while speculating that the metrial gland might furnish such a factor have associated the gland with a continuation of luteal function in the ovaries. Dickson and Bulmer ('61) have also attributed a possible luteotropic function to metrial gland cells.

The present paper reports the localization and describes the differentiation of metrial gland cells and their precursors in the mouse uterus from two and three quarters to seven and one quarter days post coitum. The time of acquisition of glycogen by the metrial gland cells and other glycogen-containing cells of the mouse uterus and of the embryo is also given. A detailed account of concomitant changes in other endometrial cells may be found in Smith ('66).

MATERIALS AND METHODS

F1 females from crosses of mice of either the Balb or J strain to animals of various mutant stocks were exposed to

Present address: Department of Biology, Queens College of the City University of New York, Flushing New York 11367

- X The oestrogen surge histamine release and decidual induction in the rat *Acta Endocr* 47 255-264
- Mayer G 1963 Delayed nidation in rats a method of exploring the mechanism of ova implantation In *Delayed Implantation* A C Enders ed Univ Chicago Press Chicago pp 213-231
- Noyes R W Z Dickmann L L Doyle and A H Gates 1963 Ovum transfers synchronous and asynchronous in the study of implantation In *Delayed Implantation* A C Enders ed Univ Chicago Press Chicago pp 197-211
- Shelesnyak M C P F Kralcer and G H Zellmaker 1963 Studies on the mechanism of decidualization I The oestrogen surge of pseudopregnancy and progravity and its role in the process of decidualization *Acta Endocr* 42 225-232
- Shelesnyak M C and L Tic 1963 Studies on the mechanism of decidualization IV Synthetic processes in the decidualizing uterus *Acta Endocr* 42 465-472
- Smith L J 1956 A morphological and histochemical investigation of a preimplantation lethal (t^H) in the house mouse *J Exp Zool* 132 51-84
- 1966 Metrial gland and other glycogen containing cells in the mouse uterus following mating and through implantation of the embryo *Am J Anat* 119 15-24
- Smithberg M and M N Runner 1956 The induction and maintenance of pregnancy in prepuberal mice *J Exp Zool* 133 441-45
- 1960 Retention of blastocysts in non-pregestational uteri of mice *J Exp Zool* 143 21-31
- Snell G D (Ed) 1941 *Biology of the Laboratory Mouse* Blackiston Company Philadelphia pp 1-54
- Ui H and G C Mueller 1963 The role of RNA synthesis in early estrogen action *Proc Nat Acad Sci* 50 256-260
- Williams M F 1948 The vascular architecture of the rat uterus as influenced by estrogen and progesterone *Am J Anat* 83 247-307
- Wilson I B 1963 A new factor associated with the implantation of the mouse egg *J Reprod Fertil* 5 281-282
- Wislocki G B and E W Dempsey 1945 Histochemical reactions of the endometrium in pregnancy *Am J Anat* 77 365-403
- Yochim J M and V J DeFco 1963 Hormonal control of the onset magnitude and duration of uterine sensitivity in the rat by steroid hormones of the ovary *Endocr* 72 317-326
- Young A 1951 The vascular architecture of the rat uterus during pregnancy *Proc Roy Soc (Edinb)* Sec B 64 292-311
- Zellmaker G H 1963 Experimental studies on the effects of ovariectomy and hypophysectomy on blastocyst implantation in the rat *Acta Endocr* 44 355-366

Metrial Gland and Other Glycogen Containing Cells in the Mouse Uterus Following Mating and Through Implantation of the Embryo

LOIS JEAN SMITH¹

Department of Anatomy Albert Einstein College of Medicine
New York New York

ABSTRACT Mouse uteri and embryos from 12 hours to seven days after mating were examined for RNA and glycogen following specific histochemical staining. Because of their greater basophilia cells present throughout the endometrium which seem to be metrial gland cell precursors could be distinguished as early as two and three-quarter days. At this time the uterus is just beginning to undergo "sensitization to decidualization." By seven days these precursor cells and metrial gland cells proper have disappeared from all regions of the endometrium except that of the future decidua basalis. Glycogen is present in cells which may be the metrial gland cell precursors, plasma cells and polymorphonuclear leucocytes as well as in the lumens and cells of the uterine glands at three and one half days. Between four and one fourth and five and one half days glycogen is found in the primary decidual zone. By six days there is a heavy deposit in the "glycogenic areas." At seven days many of the metrial gland cells in the future decidua basalis are PAS-positive. These findings are discussed and the possible origin of the metrial gland cells from a cell of the lymphocytic series is suggested.

Differences in the basophilia of several cell types in the uterus made possible the discovery that cells which seem to be metrial gland cell precursors are present in small numbers throughout the endometrium of the mouse at 65 hours after mating (Smith '66). At this time the conceptuses have just entered the uterus which itself is just beginning to transform into an organ into which the embryos can implant. Metrial gland cells and their precursors have not previously been reported anywhere in the mouse or rat uterus at such an early stage of pregnancy. At later stages these cells are concentrated around blood vessels in the decidua basalis and in the metrial gland proper.

Mature metrial gland cells are characterized by a distinctively striated cytoplasm and contain both glycogen and PAS positive diastase resistant granules. The function of these cells and whether or not the metrial gland is in fact a gland is still being debated. Investigators from Jenkinson ('02) through Padykula and Richardson ('63) have discussed the possible contribution of the intracellular glycogen to the nourishment of the embryo but have been unable to agree on any one hypoth-

esis. Wislocki et al. ('57) have suggested that the diastase resistant granules are relaxin and Velardo et al. ('53) while speculating that the metrial gland might furnish such a factor have associated the gland with a continuation of luteal function in the ovaries. Dickson and Bulmer ('61) have also attributed a possible luteotropic function to metrial gland cells.

The present paper reports the localization and describes the differentiation of metrial gland cells and their precursors in the mouse uterus from two and three quarters to seven and one quarter days post coitum. The time of acquisition of glycogen by the metrial gland cells and other glycogen-containing cells of the mouse uterus and of the embryo is also given. A detailed account of concomitant changes in other endometrial cells may be found in Smith ('66).

MATERIALS AND METHODS

F1 females from crosses of mice of either the Balb or J strain to animals of various mutant stocks were exposed to

¹ Present address: Department of Biology, Queens College of the City University of New York, Flushing New York 11367.

F1 males from the same cross in the evening and checked for vaginal plugs the following morning. Mating was arbitrarily assumed to have occurred at 1 00 AM of the day the plug was found and the females were killed at intervals from one half to seven and one-quarter days afterwards. Each female had produced one or two litters before being sacrificed. The rate of embryonic development was in complete accord with that reported by Snell (41).

To demonstrate basophilia the uteri were fixed in Carnoy's fluid and stained with Azure B (Flax and Humes 52). Glycogen was determined by the PAS method. All uteri for the latter study with the exception of those of the three and one half day stage were fixed in Lison's Gendre fluid, cooled in an acetone CO₂ mixture. Those for the three and one half day stage were fixed in Carnoy's fluid. Control sections were subjected to amylase digestion prior to the PAS procedure.

RESULTS

Metrial gland cells

As early as two and three fourths days after mating in uteri stained with Azure B scattered cells with basophilic cytoplasm stand out against a background of palely stained stellate endometrial stromal cells. The basophilic cells are of two usually distinct types: one plasma cells, the other cells thought to be the precursors of the metrial gland cells. The supposed precursor cell, unlike the plasma cell, is round and its cytoplasm shows no lightly stained patch or halo. In addition its diffusely stained nucleus contains 1 or 2 strongly basophilic irregularly shaped nucleoli often attached to one side of the nuclear membrane, a feature which further distinguishes this cell from the plasma cell (fig 2). As shown in figure 1 the size of the round cells seen at 65 hours varies considerably. The smallest is the size of a large lymphocyte while the largest has both a larger nucleus (frequently kidney shaped) and a wider rim of cytoplasm. The nucleoli enlarge as cell size increases. Much of the basophilic material in the cytoplasm of the largest of these round cells, even at 65 hours, is in

the form of thick filaments and in later stages of pregnancy when still larger cells of this type are present the filaments in them are more widely separated giving these cells a very distinctive appearance. The larger round cells with basophilic filaments will henceforth be called metrial gland cells, the smaller round cells dark cells. Both dark and metrial gland cells are found in small numbers throughout the stroma under the luminal epithelium and around the glands at 65 hours after mating. They are often concentrated near the enlarging endometrial capillaries characteristic of this stage of pregnancy.

From 65 to 96 hours after mating the total number of metrial gland and dark cells, the proportion of metrial gland to dark cells, and the maximum size of the metrial gland cells increases steadily. It is at 96 hours that blunt processes from the trophoblast are first seen within the uterine epithelium in the mice used in this study.

At four and one quarter days after mating the dark and metrial gland cells are found principally in the mesometrial region of the implantation site although there are a few in the antimesometrial decidua. Surprisingly there are also many large vacuolated metrial gland cells present around the lumen in the area between implantation sites (fig 3).

As late as six days after mating or when the embryo is well implanted extremely vacuolated metrial gland cells are still seen occasionally between the very large antimesometrial stromal cells. The number in this region is negligible though when compared to that in the mesometrial decidua where medium sized metrial gland cells and large dark cells are particularly numerous around the mesometrial end of the remaining lumen and in the region of the sinusoid wings. A few large metrial gland cells can still be found in the interdecidual regions.

By seven and one quarter days the region around the mesometrial lumen and destined to form the mid portion of the decidua basalis has increased in size markedly. At this time it contains very large numbers of medium sized metrial gland cells (fig 4) many of which in sections stained with hematoxylin can be

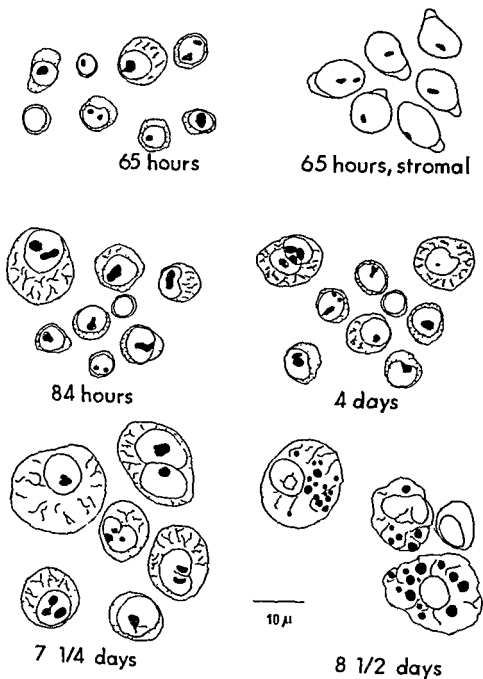


Fig 1 Representative metrial gland and dark cells found in the mouse endometrium from two and three-quarters to eight and one half days after mating. Also representative stromal cells from around the mesometrial lumen at two and three-quarter days. Camera lucida drawings made at 3,200 \times and reduced to 1,280 \times .

seen to be lying on the basement membrane of the swollen capillaries. The endothelial lining cells of the latter are now basophilic and enlarged. A few very large metrial gland cells and very many of the smaller ones surround the highly developed sinusoids laterally. At seven and one quarter days metrial gland cells have disappeared from between the implantation sites.

In hematoxylin stained sections of eight and one half day pregnant uteri large metrial gland cells with large cytoplasmic granules are found in the decidua basalis and occasionally one lies free in the maternal blood spaces between the giant trophoblast cells. It is at eight to eight and one half days that the allantois first makes contact with the ectoplacental cone in the mice used in this study.

In summary small round basophilic cells which seem to be related to large lymphocytes through a series of transitional forms are present in the endometrium at 65 hours after mating. Similar round basophilic cells are found at all subsequent stages examined and a continuous series of transitional forms links them to mature metrial gland cells in the oldest stage examined (fig 1).

General glycogen localization

At three and one half days after mating much glycogen is present in the lumens of the uterine glands and small granules of glycogen are found in the apical cytoplasm of cells of the uterine glands near the periphery of the endometrium. No glycogen is demonstrable in the cells of the luminal epithelium or in the fusiform stromal cells. However an occasional round cell in the stroma having a spherical or kidney shaped nucleus contains a few cytoplasmic granules adjacent to the area where the nucleolus apposes the nuclear membrane (a metrial gland cell?). Some oval cells (plasma cells?) and what appear to be polymorphonuclear leucocytes are also PAS positive. In the three and one half day blastocyst PAS stainability is high in the trophoblast and somewhat less intense in the inner cell mass.

In the most developmentally advanced four and one quarter day stages embryonic glycogen has disappeared but cells in a

cup shaped area of decidua antimesometrial to the embryo (part of the primary decidual zone of Krehbiel '37) contain small granules. By four and three quarter days cells in the lateral primary decidual zone are also reactive.

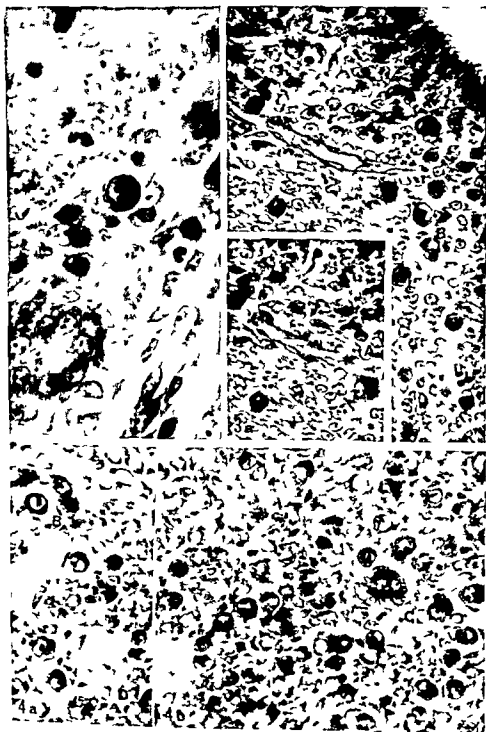
At five and one half days cells in the antimesometrial and lateral primary decidual zone are no longer PAS positive while those in the primary decidual zone adjacent to the disintegrating luminal epithelium mesometrial to the embryo are. This is the area called glycogenic area by Krehbiel ('37) and the basophilic cell zone by Smith ('66). By six days an extremely heavy deposit of glycogen is present in the basophilic cell zone. In addition glycogen begins to reappear in the embryo at this time for 2 or 3 PAS positive cells are found within the ectoplacental cone of some of the embryos. Other structures also PAS positive are the apices of the vacuolated endoderm cells covering the egg cylinder, Reichert's membrane and a few giant trophoblast cells. In all these however the reaction is not eliminated by amylase digestion.

At six and three quarter to seven days after mating the glycogen reaction has spread to the fusiform cells of the sinusoid region lateral and mesometrial to the basophilic cell zone. Many of the metrial gland cells in this region and in the area of small cells surrounding the mesometrial lumen also contain glycogen. The granules in them however are fewer and much smaller than those in other glycogen bearing cells. Glycogen is now also present in small mononuclear cells located between

Fig 2 The large round cell in the center of the field is a "dark" cell. To the left of it are three plasma cells. From a uterus taken three and one half days after mating. Azure B 10 μ 1000 \times .

Fig 3 Dark and small metrial gland cells in the interdecidual region at four and one half days. Note the height of the luminal epithelium in this region at this stage. a and b are two levels of the same section. Azure B 10 μ 500 \times .

Fig 4 Dark and metrial gland cells in the compact zone at seven and one quarter days after mating. a and b are two levels of the same section. Azure B 10 μ 500 \times . A a small dark cell. B large dark cells. C cells with basophilic filaments. D a highly vacuolated cell.



seen to be lying on the basement membrane of the swollen capillaries. The endothelial lining cells of the latter are now basophilic and enlarged. A few very large metrial gland cells and very many of the smaller ones surround the highly developed sinusoids laterally. At seven and one quarter days metrial gland cells have disappeared from between the implantation sites.

In hematoxylin stained sections of eight and one half day pregnant uteri large metrial gland cells with large cytoplasmic granules are found in the decidua basalis and occasionally one lies free in the maternal blood spaces between the giant trophoblast cells. It is at eight to eight and one half days that the allantois first makes contact with the ectoplacental cone in the mice used in this study.

In summary small round basophilic cells which seem to be related to large lymphocytes through a series of transitional forms are present in the endometrium at 65 hours after mating. Similar round basophilic cells are found at all subsequent stages examined and a continuous series of transitional forms links them to mature metrial gland cells in the oldest stage examined (fig 1).

General glycogen localization

At three and one half days after mating much glycogen is present in the lumens of the uterine glands and small granules of glycogen are found in the apical cytoplasm of cells of the uterine glands near the periphery of the endometrium. No glycogen is demonstrable in the cells of the luminal epithelium or in the fusiform stromal cells. However an occasional round cell in the stroma having a spherical or kidney shaped nucleus contains a few cytoplasmic granules adjacent to the area where the nucleolus apposes the nuclear membrane (a metrial gland cell?). Some oval cells (plasma cells?) and what appear to be polymorphonuclear leucocytes are also PAS positive. In the three and one half day blastocyst PAS stainability is high in the trophoblast and somewhat less intense in the inner cell mass.

In the most developmentally advanced four and one quarter day stages embryonic glycogen has disappeared but cells in a

cup shaped area of decidua antimesometrial to the embryo (part of the primary decidual zone of Krehbiel '37) contain small granules. By four and three quarter days cells in the lateral primary decidual zone are also reactive.

At five and one half days cells in the antimesometrial and lateral primary decidual zone are no longer PAS positive while those in the primary decidual zone adjacent to the disintegrating luminal epithelium mesometrial to the embryo are. This is the area called glycogenic area by Krehbiel ('37) and the basophilic cell zone by Smith ('66). By six days an extremely heavy deposit of glycogen is present in the basophilic cell zone. In addition glycogen begins to reappear in the embryo at this time for 2 or 3 PAS positive cells are found within the ectoplacental cone of some of the embryos. Other structures also PAS positive are the apices of the vacuolated endoderm cells covering the egg cylinder Reichert's membrane and a few giant trophoblast cells. In all these however, the reaction is not eliminated by amylase digestion.

At six and three quarter to seven days after mating the glycogen reaction has spread to the fusiform cells of the sinusoid region lateral and mesometrial to the basophilic cell zone. Many of the metrial gland cells in this region and in the area of small cells surrounding the mesometrial lumen also contain glycogen the granules in them however are fewer and much smaller than those in other glycogen bearing cells. Glycogen is now also present in small mononuclear cells located between

Fig 2 The large round cell in the center of the field is a dark cell. To the left of it are three plasma cells. From a uterus taken three and one half days after mating. Azure B 10 μ 1000 \times .

Fig 3 Dark and small metrial gland cells in the interdecidual region at four and one half days. Note the height of the luminal epithelium in this region at this stage. a and b are two levels of the same section. Azure B 10 μ 500 \times .

Fig 4 Dark and metrial gland cells in the compact zone at seven and one quarter days after mating. a and b are two levels of the same section. Azure B 10 μ 500 \times . A a small dark cell. B large dark cells. C cells with basophilic filaments. D a highly vacuolated cell.

treated with estrogen and relaxin or estrogen alone

Function of metrial gland cells

It is of course frequently the case that pattern formation during differentiation is the result of loss of cells in some regions and their continued differentiation in others and this may account for the presence of metrial gland cells throughout the endometrium as early as 65 hours after mating in the inter-decidual sites up until six and one half days in the decidua basalis until about 14 days and in the metrial gland until term. Nevertheless their continuous presence in some portion of the uterus from 65 hours until term and their localization around the vascular channels may indicate that they subserve some long term function other than supplying glycogen to the embryo. Several such long term functions can be and have been suggested. For example if metrial gland cells do indeed arise from lymphocytes or thymocytes a possible role in the suppression of the maternal immune reaction might be looked for. Both Summons and Russell (62) and Edidin (64) have data which suggest that the mouse trophoblast is immunologically competent in very early stages perhaps even as early as seven days after mating.

Long term relaxin like activity is another possibility (Velardo et al 53 and Wislocki et al 57). The data of Bloom et al (58) however argue against the idea that relaxin is found in the metrial gland cells since their extract of metrial glands taken at 21 days of pregnancy did not affect myometrial motility of the rat uterus while an ovarian extract did. Kroc et al (59) also found a high level of relaxin activity only in ovaries of pregnant rats and mice and not in placentae or uteri.

A luteotropic function must also be considered and the acidophilic granules have been linked to this hormone by Dickson and Bulmer (61). Furthermore both Velardo et al (53) and Melampy et al (64) have presented evidence that the greater the amount of decidual tissue in rats with induced deciduomata the longer the duration of pseudopregnancy. Melampy et al however suggest that the "transformation

of endometrium into decidual tissue reduced luteolytic activity" rather than increased luteotropic activity. They also report that "prolactin injected daily with decidual tissue in one horn was sufficient to override the luteolytic activity of the non traumatized horn".

Glycogen localization

The changing pattern in decidual glycogen localization found in this study in cells other than metrial gland cells seems identical in the main to that described by Krehbiel (37) for the rat although the timing differs in the two species. Glycogen is present only in the antimesometrial cells of the primary decidual zone at four and one-quarter days after mating in the mouse at six days in the rat. The glycogen reaction has spread to the cells of the lateral primary decidual zone by four and three-quarter days in the mouse and by six and one half days in the rat. Glycogen has disappeared from these regions and is present in the glycogenic area only by five and one half days in the mouse and by seven and one half days in the rat. In the implanting mouse blastocyst glycogen disappears shortly before glycogen is visible in the decidua and it reappears in the central portion of the ectoplacental cone when the sinusoid regions of the mesometrial decidua are acquiring large amounts. Bridgman (48a) says that glycogen can be found in the cone of rat embryos by the sixth day.

In the mouse in the subepithelial antimesometrial and lateral primary decidual zone cells and in the mesometrial decidual cells next to the degenerating epithelium lining the decidual crypt the acquisition of glycogen is preceded by a sharp diminution in basophilia (Smith 66). The latter apparently follows the occlusion of the subepithelial capillaries as the result of the great increase in size of the endothelial cells in this region. The cells with reduced basophilia then become compressed and flattened and disappear by about the 6th day. Presumably they are phagocytized by the differentiating trophoblast giant cells although occlusion of the capillaries must play a part in their breakdown. It seems reasonable to assume that the glycogen of these glycogen containing cells

the basal layer of the uterus and the sinusoid wings and between the basal layer and the most mesometrial cells of the anti-mesometrial decidua. From their location this new type of glycogen containing cell appears to be in a portion of the fibrinoid capsule of Bulmer and Dickson (61). Many cells within the ectoplacental cone are now reactive.

DISCUSSION

Origin of metrial gland cells

Almost as many types of cells have been proposed as metrial gland cell precursors as there have been investigators describing them. Jenkinson (52) and Gérard (27) who studied metrial gland cells in the mouse suggested that they were derived from the fusiform stromal cells. Baker (48) and Velardo et al. (53) proposed an origin from mesometrial mesenchymal cells in the rat. Selye and McKeown (35) stated that almost any mesenchymal cell in the rat endometrium, myometrium or the region of the mesometrial triangle might be able to dedifferentiate to resemble a small fibroblast then redifferentiate into a typical metrial gland cell. Lewis (24) who studied Hofbauer cells in the early human villosus said there were transitional forms between them and mesenchymal cells. On the other hand the variation in size of the round and oval ones down almost to the size of white blood cells suggests the possibility that they may arise from white blood cells that have wandered in the tissue spaces. Hofbauer cells appear to be morphologically identical to metrial gland cells. They too contain glycogen, show a residual reaction with the PAS technique after digestion or contain occasional droplets which stain with hematoxylin (Wislocki and Padykula 61). It was similarities such as these which led Dickson and Bulmer (61) to suggest that some metrial gland cells of the decidua basalis of the rat might be derived from the trophoblast.

Several of the observations reported here suggest the possibility that a cell of the lymphocytic series may be the precursor cell. First there appears to be a continuous series of transitional forms from

the larger lymphocytes to the smallest basophilic dark cells and from the dark cells to mature metrial gland cells. Second both lymphocytes and the smaller dark cells are found together in the tissues near the enlarging capillaries at 65 hours and at later stages the basophilic cells are particularly numerous near the sinusoids of the decidua basalis and metrial gland. Finally the great developmental potentiality of lymphocytes or thymocytes is suggested by their recently demonstrated polymorphism (Murray and Woods 64 for example). Fortunately the method used by these authors provides a way of testing this hypothesis.

The present study does not exclude any of the other proposed hypotheses of the origin of metrial gland cells but lends more weight to some than to others. For example as is evident from figure 1 the nucleus of the stellate mesometrial stromal cells at 65 hours is larger and the nucleoli are smaller than those of the smallest basophilic cells suggesting that the smallest basophilic cells are not merely rounded up stromal cells. It is less easy to reject the possibility that metrial gland cells may be escaped endothelial cells or perhaps primitive reticular cells from the capillary walls. There does seem to be an association in time between the enlargement and appearance of basophilia in the endothelial cells and the presence of metrial gland cell precursors. This association is especially evident at 65 hours when metrial gland cell precursors are first seen and at seven days when they increase in number markedly in the central portion of the decidua basalis.

No matter what their origin however on the basis of the time of their first appearance it seems reasonable to assume that the stimulus which sets off the differentiation of the metrial gland cells may be the same stimulus which triggers differentiation of the uterus into an organ responsive to the stimulus for decidualization. In this regard it is interesting that Hall (60) found large vacuolated cells containing both glycogen and PAS positive diastase resistant granules in the stroma of ovariectomized virgin mice treated with progesterone and estrogen and not in those

treated with estrogen and relaxin or estrogen alone

Function of metrial gland cells

It is of course frequently the case that pattern formation during differentiation is the result of loss of cells in some regions and their continued differentiation in others and thus may account for the presence of metrial gland cells throughout the endometrium as early as 65 hours after mating in the inner-decidual sites up until six and one half days in the decidua basalis until about 14 days and in the metrial gland until term. Nevertheless their continuous presence in some portion of the uterus from 65 hours until term and their localization around the vascular channels may indicate that they subserve some long term function other than supplying glycogen to the embryo. Several such long term functions can be and have been suggested. For example if metrial gland cells do indeed arise from lymphocytes or thymocytes a possible role in the suppression of the maternal immune reaction might be looked for. Both Simmons and Russell (62) and Edidin (64) have data which suggest that the mouse trophoblast is immunologically competent in very early stages perhaps even as early as seven days after mating.

Long term relaxin like activity is another possibility (Velardo et al '53 and Wislocki et al '57). The data of Bloom et al (58) however argue against the idea that relaxin is found in the metrial gland cells since their extract of metrial glands taken at 21 days of pregnancy did not affect myometrial motility of the rat uterus while an ovarian extract did. Kroc et al (59) also found a high level of relaxin activity only in ovaries of pregnant rats and mice and not in placentae or uteri.

A luteotropic function must also be considered and the acidophilic granules have been linked to this hormone by Dickson and Bulmer (61). Furthermore both Velardo et al (53) and Melampy et al (64) have presented evidence that the greater the amount of decidual tissue in rats with induced deciduomata the longer the duration of pseudopregnancy. Melampy et al however suggest that the transformation

of endometrium into decidual tissue produces "luteotropic activity" rather than increased "gonadotropic activity". They also report that "maternal injected duff" with decidual tissue in one horn was sufficient to override the "luteotropic activity" of the non-injected horn."

Glycogen localization

The changing pattern in decidual glycogen localization found in this study in cells other than metrial gland cells seems identical, in the main, to that described by Krehbiel (37) for the rat although the timing differs in the two species. Glycogen is present only in the antimesometrial cells at the primary decidual zone at four and one-quarter days after mating in the mouse at six days in the rat. The glycogen reaction has spread to the cells of the lateral primary decidual zone by four and three-quarter days in the mouse and by six and one-half days in the rat. Glycogen has disappeared from these regions and is present in the glycogenic area only by five and one half days in the mouse and by seven and one-half days in the rat. In the implanting mouse blastocyst glycogen disappears shortly before glycogen is visible in the decidua and it reappears in the central portion of the ectoplacental cone when the sinusoid regions of the mesometrial decidua are acquiring large amounts. Bridgman (48a) says that glycogen can be found in the cone of rat embryos by the sixth day.

In the mouse in the subepithelial anti mesometrial and lateral primary decidual zone cells and in the mesometrial decidua cells next to the degenerating epithelium lining the decidual crypt the acquisition of glycogen is preceded by a sharp diminution in basophilia (Smith 66). The latter apparently follows the occlusion of the subepithelial capillaries as the result of the great increase in size of the endothelial cells in this region. The cells with reduced basophilia then become compressed and flattened and disappear by about the 6th day. Presumably they are phagocytized by the differentiating trophoblast giant cells although occlusion of the capillaries must play a part in their breakdown. It seems reasonable to assume that the glycogen of these glycogen containing cells

the basal layer of the uterus and the sinusoid wings and between the basal layer and the most mesometrial cells of the antimesometrial decidua. From their location this new type of glycogen containing cell appears to be in a portion of the fibrinoid capsule of Bulmer and Dickson (61). Many cells within the ectoplacental cone are now reactive.

DISCUSSION

Origin of metrial gland cells

Almost as many types of cells have been proposed as metrial gland cell precursors as there have been investigators describing them. Jenkinson (52) and Gerard (27) who studied metrial gland cells in the mouse suggested that they were derived from the fusiform stromal cells. Baker (48) and Velardo et al (53) proposed an origin from mesometrial mesenchymal cells in the rat. Selye and McKeown (35) stated that almost any mesenchymal cell in the rat endometrium, myometrium or the region of the mesometrial triangle might be able to dedifferentiate and come to resemble a small fibroblast then redifferentiate into a typical metrial gland cell. Lewis (24) who studied Hofbauer cells in the early human villosus said there were transitional forms between them and mesenchymal cells. On the other hand the variation in size of the round and oval ones down almost to the size of white blood cells suggests the possibility that they may arise from white blood cells that have wandered in the tissue spaces. Hofbauer cells appear to be morphologically identical to metrial gland cells. They too contain glycogen, show a residual reaction with the PAS technique after digestion or contain occasional droplets which stain with hematoxylin (Wislocki and Padykula 61). It was similarities such as these which led Dickson and Bulmer (61) to suggest that some metrial gland cells of the decidua basalis of the rat might be derived from the trophoblast.

Several of the observations reported here suggest the possibility that a cell of the lymphocytic series may be the precursor cell. First there appears to be a continuous series of transitional forms from

the larger lymphocytes to the smallest basophilic dark cells and from the dark cells to mature metrial gland cells. Second both lymphocytes and the smaller dark cells are found together in the tissues near the enlarging capillaries at 60 hours and at later stages the basophilic cells are particularly numerous near the sinusoids of the decidua basalis and metrial gland. Finally the great developmental potentiality of lymphocytes or thymocytes is suggested by their recently demonstrated polymorphism (Murray and Woods 61 for example). Fortunately the method used by these authors provides a way of testing this hypothesis.

The present study does not exclude any of the other proposed hypotheses of the origin of metrial gland cells but lends more weight to some than to others. For example it is evident from figure 1 the nucleus of the stellate mesometrial stromal cells at 65 hours is larger and the nucleolus are smaller than those of the smallest basophilic cells suggesting that the smallest basophilic cells are not merely rounded up stromal cells. It is less easy to reject the possibility that metrial gland cells may be escaped endothelial cells or perhaps primitive reticular cells from the capillary walls. There does seem to be an association in time between the enlargement and appearance of basophilic in the endothelial cells and the presence of metrial gland cell precursors. This association is especially evident at 65 hours when metrial gland cell precursors are first seen and a seven days when they increase in number markedly in the central portion of the decidua basalis.

No matter what their origin however on the basis of the time of their first appearance it seems reasonable to assume that the stimulus which sets off the differentiation of the metrial gland cells may be the same stimulus which triggers differentiation of the uterus into an organ responsive to the stimulus for decidualization. In this regard it is interesting that Hall (60) found large vacuolated cells containing both glycogen and PAS positive diastase resistant granules in the stroma of ovariectomized virgin mice treated with progesterone and estrogen and not in those

- the mouse *Tijdschr Nederl Dierk Vereen* 2nd Series 124-198
- Jollie W P and S A Bencosme 1965 Electron microscopic observations on primary decidua formation in the rat *Am J Anat* 116 217-235
- Krehbiel R H 1937 Cytological studies of the decidual reaction in the rat during early pregnancy and in the production of deciduomata *Physiol Zool* 10 212-234
- Kroc R L B G Steinetz and V L Beach 1959 The effects of estrogens, progestagens and relaxin in pregnant and non pregnant laboratory rodents *Ann NY Acad Sci* 75 942-980
- Lewis W H 1924 Hofbauer cells (clasmato-cytes) of the human chorionic villus *Johns Hopkins Hosp Bull* 35 183-185
- Melampy R M L L Anderson and C L Kragt 1964 Uterus and life span of rat corpora lutea *Endocr* 74 501-504
- Murray R G and P A Woods 1964 Studies on the fate of lymphocytes. III The migration and metamorphosis of in situ labeled thymic lymphocytes *Anat. Rec* 150 113-128
- Padykula H A and D Richardson 1963 A correlated histochemical and biochemical study of glycogen storage in the rat placenta *Am J Anat* 112 215-241
- Selye H and I M Keown 1935 Studies on the physiology of the maternal placenta in the rat *Proc Royal Soc London (B)* 119 1-31
- Simmons R L and P S Russell 1962 The antigenicity of mouse trophoblast *Ann. NY Acad Sci* 99 717-732
- Smith L J 1966 The changing pattern of basophilia in the mouse uterus from mating through implantation *Am J Anat* 119 1-14
- Snell G D (Ed) 1941 *Biology of the laboratory mouse* Blakiston Co Philadelphia pp 1-54
- Velardo J T A B Dawson A G Olsen and F L Hisaw 1953 Sequence of histological changes in the uterus and vagina of the rat during prolongation of pseudopregnancy associated with the presence of deciduomata *Am J Anat* 93 273-305
- Wislocki G B and H A Padykula 1961 Histochemistry and electron microscopy of the placenta. In *Sex and Internal Secretions* edited by W C Young The Williams and Wilkins Co Baltimore pp 883-957
- Wislocki G B L P Weiss M H Burgos and R A Ellis 1957 The cytology histochemistry and electron microscopy of the granular cells of the metrial gland of the gravid rat *J Anat* 91 130-140

serves as a source of energy for the developing embryo although PAS positive saliva-digestible material is not found in the trophoblast cells or in the endoderm covering the egg cylinder at this stage

Jollie and Bencosme (65) followed the fate of what appear to be similar glycogen containing cells in the rat from just before the induction of decidualization (day 0) until five days after trauma. They report that lysosomes first appear at day 2 and are present until day 5. However they also report that glycogen granules were not identified in the cells they examined before day 4. Day 4 would seem to correspond to the 8th day post coitum in a typical implantation.

In contrast to the situation with respect to the primary decidual zone cells the glycogen containing cells in the sinusoid regions and in the basophilic cell zone (the glycogenic area) just outside the mesometrial portion of the implantation zone do not lose their basophilia before acquiring glycogen (Smith 66). The reason for this difference is unclear but the capillaries in the latter two regions do not become occluded and these glycogen bearing cells are much longer lived (Jenkinson 02).

Finally although there are many similarities in glycogen localization in rats and mice there are also differences. One of the latter may help explain why there has been little doubt expressed concerning the origin of some of the glycogen-containing cells of the mouse ectoplacental cone and placenta (Jenkinson 02) although this has not been the case for the rat (Bridgman 48b, Bulmer and Dickson 60). For instance plate 1 figure 1 of Padykula and Richardson (63) and their description of glycogen in the 8 day ectoplacental cone and adjacent decidual cells indicates that these glycogen areas are closer to each other in the rat than they are in the mouse. A comparison of the glycogenic area of the decidua and of the cone in Krehbiel's (37) diagrams for Day 8 and 9 and in Smith's (66) figures 9 and 10 shows this also. The existence of a wider band of maternal cells free of glycogen between the maternal and fetal glycogenic areas in the mouse at the time the cone is acquiring glycogen may be one reason the separate

origins of the glycogen bearing cells in the maternal and fetal glycogenic areas of the mouse seems quite clear. Perhaps the proximity of these same areas in the rat has also contributed to the uncertainty over the relationship between the metrial gland cells of the decidua basalis and similar cells in the trophoblast in older stages of pregnancy (Dickson and Bulmer 61).

ACKNOWLEDGMENTS

This investigation was supported by Research Career Development Award 8k3 HD 4334 from the National Institutes of Health and by National Science Foundation Research grant GB 646.

LITERATURE CITED

- Baker B L 1948 Histochemical variations in the metrial gland of the rat during pregnancy and lactation *Proc Soc Exp Biol and Med* 68 492-496
- Bloom G K G Paul and N Wqvist 1958 A uterine relaxing factor in the pregnant rat *Acta Endocr* 28 112-118
- Bridgman J 1948a A morphological study of the development of the placenta of the rat I An outline of the development of the placenta of the white rat *J Morph* 83 61-85
- 1948b A morphological study of the development of the placenta of the rat II An histological and cytological study of the development of the chorioallantoic placenta of the white rat *J Morph* 83 195-223
- Bulmer D and A D Dickson 1960 Observations on carbohydrate materials in the rat placenta *J Anat* 94 46-58
- 1961 The fibrinoid capsule of the rat placenta and the disappearance of the decidua *J Anat* 95 300-310
- Dickson A D and D Bulmer 1961 Observations on the origin of metrial gland cells in the rat placenta *J Anat* 95 262-273
- Eddin M 1964 Transplantation antigens in the mouse embryo. The fate of early embryo tissues transplanted to adult hosts *J Emb Exp Morph* 12 309-316
- Flax M H and M H Himes 1952 Micro spectrophotometric analysis of metachromatic staining of nucleic acids *Physiol Zool* 25 297-311
- Gérard P 1927 Recherches morphologiques et expérimentales. Contribution à l'étude du placenta maternel des rongeurs *Arch de Biol* 37 407-454
- Hall K 1960 Modification by relaxin of the response of the reproductive tract of mice to oestradiol and progesterone *J Endocr* 20 355-364
- Jenkinson J W 1902 Observations on the histology and physiology of the placenta of

Studies on Sperm Survival Mechanisms in the Female Reproductive Tract of Hibernating Bats

I CYTOLOGY AND ULTRA STRUCTURE OF INTRA UTERINE SPERMATOZOA IN MYOTIS LUCIFUGUS^{1,2}

WILLIAM A WIMSATT PHILIP H KRUTZSCH³ AND
LEONARD NAPOLITANO⁴

Division of Biological Sciences Cornell University Ithaca New York and
Department of Anatomy University of Pittsburgh School of Medicine
Pittsburgh Pennsylvania

ABSTRACT Among mammals prolonged survival of spermatozoa in the reproductive tract of the female (circa 7 ± months) is known in only a few species of hibernating bats but its physiological basis remains obscure. Presumably survival involves special physiological adaptations of the spermatozoa the uterus or both. We have initiated studies of sperm survival mechanisms in the hibernating bat *Myotis lucifugus* involving analysis of the cytology and fine structure of intra uterine sperm the morphology and histochemistry of sperm uterus interactions and selected biochemical parameters of the reproductive tract. This paper summarizes our findings concerning the morphology of epididymal and intra uterine spermatozoa and emphasizes those aspects not detailed by others. The microscopic organization of epididymal sperm is described in detail with particular attention to peculiarities of the head middle piece and cytoplasmic droplet. The latter contains amylase resistant PAS+ granules and acid phosphatase both possibly of lysosomal origin. Most ultrastructural features elucidated by Fawcett and collaborators are confirmed but additional details concerning the head post nuclear sheath origin of axial filament complex and the outer coarse fibrils are provided. A functional interrelationship between coarse fibrils 3 and 8 and the longitudinal columns of the fibrous sheath is also postulated.

Structural differences between epididymal and uterine sperm are minor suggesting that uterine environmental factors are most important for sperm survival.

A new basis is suggested for the apparent helical arrangement of mitochondria in the middle piece. In *Myotis* sperm the configuration is illusory being the result of an orderly alternation in the staining of the serially arranged mitochondrial pairs. We suggest that the "patterned" staining of mitochondria may reflect sequential cyclic functional alterations of significance in the initiation and/or coordination of the geometrically oriented tail movements.

The unusual reproductive habits of hibernating vespertilionid and rhinolophid bats have long been known but many aspects of their physiological regulation remain obscure. A major unsolved problem concerns the mechanism of sperm storage and survival in the female reproductive tract where the cells may retain their viability for as long as 5-7 months (Matthews 37 Wimsatt 44). Prolonged storage of viable spermatozoa within the female tract is by no means novel among invertebrates or even lower vertebrates but among mammals the phenomenon observed in bats is unique and is therefore of great theoretical interest. Earlier workers have variously proposed with scarcely any direct evidence that lowering of body temperature mechanical or chemical inhibition of motility elevated CO₂ levels secretion of nutrients and other

¹ Supported by research grants from the National Science Foundation and the National Institute of Health. H. H. H. flows NSF G-24043 (W.A.W.) NIH RG 6592 C-5 (P.H.K.) NIH AM 09432-01 (L.N.).

² Shortly after an original draft of this article had been completed, the splendid study of Fawcett and Ito (65) on the fine structure of bat sperm was published. The overlap between their observations and ours was substantial and we have felt obliged to revise our fine structure section to avoid publishing frankly repetitive material. The present section on ultrastructure is a substantially shortened version of the original. We obviously could not eliminate all redundancy in observations and still achieve a coherent account, but those retained for the most part complement differ from or confirm where they seemed desirable the observations of Fawcett and Ito. Furthermore our primary objective has been and is to determine the bases of sperm longevity in the uterus and our observations of fine structure are focused mainly on intra uterine sperm, whereas those of Fawcett and Ito dealt wholly with unjacketed sperm from the epididymis. Characterization of the fine structure of surviving sperm *in utero* as compared with those still within the epididymis is essential to the achievement of our main objective. The section summarizing our microscopic and histochemical observations has not been altered from the original since these observations are not duplicated in the study of Fawcett and Ito.

³ Present address: Department of Anatomy University of Arizona College of Medicine Tucson Arizona.

⁴ Present address: Department of Anatomy University of New Mexico School of Medicine Albuquerque New Mexico.



derson (63) Control Sections (cryostat following cold formalin fixation) of prostate and liver were run simultaneously with the sperm preparations as were also comparable preparations in which enzymic activity had been inhibited by sodium fluoride. All tests of sperm were carried out on fresh cell suspensions from the epididymis. Thick sperm suspensions were activated in Locke's fluid for 15 minutes. The sperm were then smeared on slides rapidly dried and fixed briefly in cold formal-calcium. They were then quickly rinsed in distilled water and immersed in the incubating medium. The control slides were treated similarly except they were exposed to a 0.1% NaFl solution for 20 minutes at 60 C before being placed in the incubating medium. In other instances the fresh sperm suspensions were introduced directly into the incubating media (or in fluoride solution followed by incubating medium) and only after their removal from the latter were spotted on slides, dried, fixed, dehydrated and mounted. Comparable results were obtained with both procedures.

We have adopted here the terminology for sperm cell components recommended by Fawcett (66) and are grateful to Dr Fawcett for his kindness in allowing us to examine his paper in proof.

The expert technical assistance of Mr Anthony Guerniere and Dr Mona L Coetzee in the careful execution of these procedures is also gratefully acknowledged.

MICROSCOPIC OBSERVATIONS

Pre-ejaculatory spermatozoa

In order to establish base lines for delineation of possible morphological changes in surviving intra uterine spermatozoa we have examined cell suspensions and smears of sperm expressed from the caudae epididymidis of male bats killed directly from the hibernating state in the months December through April. Most of the structural details to be reviewed are observable in figures 3 to 8 inclusive.

The only variable observed in sperm samples collected on different dates involved the cytoplasmic droplet. Droplets were an obvious component of the majority of sperm from two males killed in mid

December a single specimen each in January and February and in three April specimens. On the other hand droplets were scarce in four December specimens and were absent in approximately 20 additional bats killed in January, February, March and April. In *Myotis* spermatogenic activity ceases in September so epididymal sperm in hibernating animals are products of the previous summer's activity. Loss of the cytoplasmic droplet attends sperm maturation and the tendency for the droplets to disappear in late winter animals is perhaps not surprising. Why they should persist in sperm from April animals when they were already lost in others killed earlier in the season is not clear. Dormancy (as in hibernation) is characterized by a drastic reduction of metabolic functions and body temperature with an attendant curtailment of cellular activities of all sorts including probably sperm maturation in the caudae epididymidis (Wimsatt 60). But hibernation in bats is not a continuous process; spontaneous arousals do occur and probably with individual variations in frequency. During these periods metabolic activity and body temperature return to normal activity levels and cell metabolism is increased. The chronological rate of sperm maturation in the epididymis would likely be influenced by the total elapsed time the individual animal had been active during the winter months. Presumably the April specimens whose sperm retained cytoplasmic droplets were those whose arousals (spontaneous or induced by disturbance) had been of minimal frequency and duration.

In most epididymal sperm regardless of the month of collection the droplet when present was attached distally on the middle piece just cephalad of its junction with the principal piece. Typically it is eccentric, globular and rarely constricted at its attachment. Less frequently it is annular, forming an obtuse spindle like swelling about the end of the middle piece which passes through its center (figs 3-9). In a small proportion of spermatozoa examined especially from the first two December specimens mentioned above droplet material was located at higher levels in the middle piece even as far forward as the neck region in some instances. Often in

factors singly or in combination somehow support sperm longevity. The alternatives that bat spermatozoa may be inherently specialized or that the adaptive capability may have evolved on both sides during evolution of the hibernating habit have been scarcely considered.

The more dynamic aspects of the sperm survival mechanism can presumably only be resolved through application of appropriate physiological and biochemical procedures but delineation of any special morphological adaptations or interrelations between stored sperm and the tissues of the female tract may be indispensable for a complete understanding of the phenomenon. The morphology of stored spermatozoa and of sperm uterus relationships has not been systematically explored in any hibernating bat. A study has been undertaken principally in *Myotis lucifugus*, a common hibernating vespertilionid bat of the eastern and central United States. Observations will be presented here on the microscopic and ultrastructural organization of epididymal and intra uterine sperm. The sperm uterus relationship and certain biochemical findings will be analyzed in later reports.

MATERIAL AND METHODS

Specimens of the little brown bat (*Myotis lucifugus lucifugus*) were collected from natural populations hibernating in caverns in New York, Pennsylvania, New Jersey and West Virginia throughout the natural hibernating period. In the laboratory all specimens were maintained in an artificial hibernaculum under controlled temperature and humidity until sacrificed. The bats were killed by cervical fracture while still torpid and the cauda epididymides and uteri were immediately removed for fixation. Materials intended for analysis by electron microscopy were handled as follows: the fresh tissues were cut into blocks of approximately 1 mm³ and immersed in cold phosphate buffered osmium tetroxide (1%) for 1 to 2 hours. Following rapid dehydration in increasing concentrations of cold ethanol the tissue blocks were embedded in Vestapol W. Sections were cut on a Huxley microtome and those displaying gold interference colors were mounted on grids and stained by the

lead hydroxide technique of Karnovsky (61). Electron micrographs were obtained in a Phillips EM 200 at initial magnifications of 2 000 to 34 000.

Materials intended for light microscopy were variously fixed in 10% neutral formalin Bouin Helly and chilled Zenker's and Rossman's fluids. For the most part fixation was accomplished by immersing the small organs in toto but in several instances the cornual extremities of the uterus or the oviducts were separated and fixed independently in cold reagents. By using torpid animals and chilled fixing solutions it was hoped to minimize sperm mobilization and displacement within the organs. Following dehydration in ethanol and clearing in cedar oil, dioxane or chloroform the tissues were embedded in paraffin cut at 5 to 10 μ on a rotary microtome and mounted on glass slides. Staining procedures routinely applied included Harris hematoxylin and eosin, iron hematoxylin, Masson trichrome, eosin and methylene blue (methylene blue in buffered solution at pH 6.0-6.5) and the periodic acid-Schiff (PAS) procedure with or without hematoxylin counterstain.

Preparations of whole epididymal and uterine sperm were made by opening and stripping the organs in a small drop of distilled water or saline. The resultant sperm suspensions were diluted to the desired density with additional water taken up in a Wintrobe pipette and spotted on glass slides resting on a warm plate. The preparations were fixed immediately after drying in 10% formalin, cold Rossman, Carnoy, Regaud Helly, formal calcium Bodian or absolute ethanol and ether rinsed and again dried. They were then variously stained in hematoxylin and eosin, iron hematoxylin, PAS and hematoxylin Bodian, protargol, Holmes (43) silver stain, Feulgen, Masson trichrome and Baker's acid hematein. Those fixed in Regaud were postchromed in 3% potassium dichromate for 3 to 8 days at 37°C and stained in Altmann's aniline acid fuchsin, methyl green, phosphotungstic acid, hematoxylin and Sudan black B.

Sites of acid phosphatase activity were visualized by the modified Gomori lead sulphide and Burstone azo-coupling procedures recommended by Barka and An

erson (63) Control Sections (cryostat following cold formalin fixation) of prostate and liver were run simultaneously with the sperm preparations as were also comparable preparations in which enzymic activity had been inhibited by sodium fluoride. All tests of sperm were carried out on fresh cell suspensions from the epididymis. Thick sperm suspensions were activated in Locke's fluid for 15 minutes. The sperm were then smeared on slides rapidly dried and fixed briefly in cold formal-calcium. They were then quickly rinsed in distilled water and immersed in the incubating medium. The control slides were treated similarly except they were exposed to a 0.1% NaFl solution for 20 minutes at 60°C before being placed in the incubating medium. In other instances the fresh sperm suspensions were introduced directly into the incubating media (or in fluoride solution followed by incubating medium) and only after their removal from the latter were spotted on slides, dried, fixed, dehydrated and mounted. Comparable results were obtained with both procedures.

We have adopted here the terminology for sperm cell components recommended by Fawcett (66) and are grateful to Dr Fawcett for his kindness in allowing us to examine his paper in proof.

The expert technical assistance of Mr Anthony Guerriere and Dr Mona L. Coetzee in the careful execution of these procedures is also gratefully acknowledged.

MICROSCOPIC OBSERVATIONS

Pre-ejaculatory spermatozoa

In order to establish base lines for delineation of possible morphological changes in surviving intra uterine spermatozoa we have examined cell suspensions and smears of sperm expressed from the caudae epididymidis of male bats killed directly from the hibernating state in the months December through April. Most of the structural details to be reviewed are observable in figures 3 to 8 inclusive.

The only variable observed in sperm samples collected on different dates involved the cytoplasmic droplet. Droplets were an obvious component of the majority of sperm from two males killed in mid

December, a single specimen each in January and February and in three April specimens. On the other hand droplets were scarce in four December specimens and were absent in approximately 20 additional bats killed in January, February, March and April. In *Myotis* spermatogenic activity ceases in September, so epididymal sperm in hibernating animals are products of the previous summer's activity. Loss of the cytoplasmic droplet attends sperm maturation and the tendency for the droplets to disappear in late winter animals is perhaps not surprising. Why they should persist in sperm from April animals when they were already lost in others killed earlier in the season is not clear. Dormancy (as in hibernation) is characterized by a drastic reduction of metabolic functions and body temperature with an attendant curtailment of cellular activities of all sorts including probably sperm maturation in the caudae epididymidis (Wimsatt 60). But hibernation in bats is not a continuous process; spontaneous arousals do occur and probably with individual variations in frequency. During these periods metabolic activity and body temperature return to normal activity levels and cell metabolism is increased. The chronological rate of sperm maturation in the epididymis would likely be influenced by the total elapsed time the individual animal had been active during the winter months. Presumably the April specimens whose sperm retained cytoplasmic droplets were those whose arousals (spontaneous or induced by disturbance) had been of minimal frequency and duration.

In most epididymal sperm regardless of the month of collection the droplet when present was attached distally on the middle piece just cephalad of its junction with the principal piece. Typically it is eccentric, globular and rarely constricted at its attachment. Less frequently it is annular, forming an obtuse spindle-like swelling about the end of the middle piece which passes through its center (figs 3-9). In a small proportion of spermatozoa examined especially from the first two December specimens mentioned above droplet material was located at higher levels in the middle piece even as far forward as the neck region in some instances. Often in

such cases the droplet was flattened and spread out along one side of the middle piece, being the more flattened nearer the head. Only a special staining characteristic (described below) enabled this extremely flattened droplet material to be identified with certainty.

The cytoplasmic droplets are generally resistant to staining. They are usually more easily observed with phase-contrast optics than in stained light microscope preparations. They do demonstrate a feeble acidophilia similar to that of the general cytoplasm of the middle piece but basophilic components were not demonstrable. In one respect, however, the staining of the droplets is unique: they react intensely and selectively to PAS and the staining is unaffected by the previous action of salivary amylase so it is not attributable to glycogen. In the more flattened droplets of younger spermatozoa the reactive material is discrete and granular, and serves as a selective marker for the identification of presumptive droplet cytoplasm in the younger cells. In older spermatozoa with distal globular or annular droplets the PAS reaction is more homogeneous permeating the cytoplasm of the droplets except centrally, where a clear area surrounds the mitochondrial sheath (fig 3). The situation in younger sperm suggests that PAS reactivity is associated with discrete but exceedingly minute cytoplasmic organelles: a discrete morphological basis for the denser more homogeneous reaction in droplets of older sperm was not discernible at the microscopic level. The PAS reactivity of the cytoplasmic droplet in *Myotis* sperm is the more striking in that no other constituent is stained not even the acrosomal cap (see below). It is not unique: however for Bishop and Walton (60) cite an observation by Hancock that droplets in other mammalian sperm (not identified in citation) are PAS positive and Cavazos and Melampy (54) call attention to PAS reactive materials in the droplets of bull ram and boar sperm. Possibly the phenomenon is general in mammals.

Another histochemical peculiarity of many cytoplasmic droplets was the presence of acid phosphatase as revealed by the Gomori lead sulphide method (fig 13).

The staining was never uniform, for in any given preparation seldom more than a third of the droplets present showed a positive reaction: a result which is at least consistent with the well known vagaries of the Gomori procedure. In reactive droplets the reaction product tended to be concentrated peripherally, while the central area surrounding the mitochondrial sheath remained unstained. A positive reaction was also observed in many of the flattened non-terminal droplets of presumably younger sperm. It is thus seen that the distribution of enzymic activity coincides with that of the PAS reactive materials previously mentioned. Control slides treated with NaFl which inhibits acid phosphatase activity were always uniformly negative. We were unable to demonstrate acid phosphatase unequivocally in sperm by means of the Burstone azo coupling procedure, even though simultaneously processed control sections of prostate and liver gave strong positive reactions. Possibly the explanation lies in the lower contrast or optical transparency of the reaction product where present in minute quantities, or perhaps to a lower sensitivity of the azo-coupling procedure.

The head of the spermatozoon in *Myotis* is somewhat elongate, the length being slightly greater than twice the width (figs 3-6). The overall length is less, however than it appears to be in the sperm of the greater horseshoe bat (*Rhinolophus ferrum-equinum*) depicted in phase contrast and ultraviolet micrographs by Bishop and Walton (60). The principal difference resides in a greater elongation of the acrosomal cap in *Rhinolophus*. In other respects the heads of the spermatozoa of these two hibernating (although not closely related) bats are more or less similar. At cursory glance the head of an unsectioned *Myotis* sperm resembles a cylinder with straight sides which converge ever so slightly posteriorly. In reality it is flattened only slightly at the base but progressively more so anteriorly so that when viewed on edge it presents a triangular or wedge shape (figs 1-17). In normal (flat) aspect the anterior end of the nucleus is rounded and we have determined by Feulgen staining and phase-contrast microscopy that it extends nearly to the tip

of the acrosomal cap This appears not to be so in *Rhinolophus* sperm (cf figs of Bishop and Walton '60) where the cap extends substantially beyond the nuclear apex In *Myotis* the base of the nucleus which is slightly ellipsoidal in section profile is deeply invaginated and into this oval depression or implantation fossa inserts the short and apparently constricted neck piece (figs 1 4 17) The region above the curvilinear margin of the fossa shows up in smear preparations as a dense basophilic band it is selectively stained by silver in the Bodian protargol technique (fig 7) and less conspicuously by the Holmes procedure (fig 8)

The detailed morphology of the acrosomal cap in *Myotis* spermatozoa is not easily visualized microscopically for it is simple in form extends only slightly beyond the nuclear apex and is both optically transparent and remarkably resistant to staining Fortunately these difficulties are circumvented in electron micrographs to which we shall allude shortly Nevertheless the presence of the cap is indicated microscopically by a progressive "fading out of the stained nucleus anteriorly beginning about two thirds of the way back from the nuclear apex (figs 3-6) This point coincides with the posterior margin of the acrosomal cap and is frequently indicated by a stainable but usually diffuse band which extends across the nucleus at right angles to its long axis this band was most consistently revealed by iron hematoxylin but is also apparent in acid phosphatase (Gomori procedure) preparations (fig 13) These observations suggest that the acrosomal cap is thin posteriorly and thickens progressively nearer its apex There are no lateral extensions or wings and the smooth anterior margin of the cap reproduces the uniformly curved profile of the nuclear tip It is at present unknown whether the acrosomal materials of transforming spermatids in the testis of *Myotis* are PAS reactive (as in rat and other rodents Clermont and Leblond '55 Leblond and Clermont '52) but the acrosomal cap material itself was totally unreactive in smears of epididymal and intrauterine sperm regardless of the fixation employed

The middle piece is perhaps the most diagnostic segment in *Myotis* spermatozoa for it is unusually thick and prominent (figs 3 4) Constituents easily recognized in stained smears include a central filament passing through the length of the segment a conspicuous mitochondrial sheath having the apparent form of a helix and a prominent cytoplasmic sheath and limiting membrane An undulant or twisted profile of the middle piece which we have occasionally seen and which has been mentioned or figured by others (e.g. Hirth '60 Fawcett and Ito '65) is presumably a shrinkage artifact for it is not observed in well fixed material The mitochondrial component was generally apparent in Masson or iron hematoxylin preparations and even in sperm stained solely with eosin but was always revealed with greatest clarity by special mitochondrial stains such as Altmann's aniline acid fuchsin methyl green or phosphotungstic acid hematoxylin after Regaud fixation and prolonged post-chromatization (fig 4) It is also demonstrated effectively by Baker's acid hematein and Sudan black Typically at lower magnifications and even under oil immersion in less than perfect preparations the mitochondria collectively display the continuous coil like arrangement so often referred to in the classical descriptions of mammalian spermatozoa it can readily be appreciated how cytologists may have been misled into believing that the mitochondria fuse end to end to form a single or double helically wound strand within the middle piece That fusion does not actually occur at least in the sperm of higher mammals has now been well demonstrated by electron microscopy and *Myotis* sperm are no exception

While the length of the middle piece is only slightly greater than three times the head length the principal piece is appreciably longer being approximately eight times the head length Hirth ('60) gives the following average figures for *Myotis lucifugus* sperm head 4.3 μ middle piece 12.7 μ principal and end pieces together 38 μ for a total cell length of approximately 55 μ There is no abrupt reduction in girth at the transition between middle piece and principal piece but the latter does begin here to taper gradually and uni-

formly to its end (figs 3 4 5 8) In stained preparations however the transition appears abrupt for among the stained elements of the middle piece only the central filament continues on into the principal piece In most stained microscopic preparations the boundary between principal and end pieces was not visualized although they are readily separable by use of phase contrast optics The principal piece is further distinguished from the middle piece by its greater apparent density and enhanced acidophilicity (fig 5) These features in combination with the greater difficulty encountered in visualizing the central filament within the principal piece are presumably related to the presence of the fibrous sheath which is restricted to this segment of the flagellum It was found that the Holmes (13) silver nitrate procedure (for nerve fibers) stained the axial complex of the middle piece and the fibrous sheath of the principal piece in a highly selective manner (fig 8) An unusual feature observed only in the Holmes preparations was an intense blackening of a short spatulate segment at the distal end of the principal piece The reaction was consistent and characteristic A morphological or other basis for it was not discernible in other types of preparations and its significance is unknown Its constancy in the Holmes preparations suggests however that it is not an artifact

The so-called annulus (end ring ring centriole) and proximal centriolar bodies were not resolved in the stained smears The centriolar complex lies within the implantation fossa at the nuclear base and is not easily seen in stained whole spermatozoa The annulus situated at the end of the middle piece either resembles the mitochondria in its staining reactions or remains unstained for it is not clearly distinguished in these microscopic preparations

Abnormal epididymal spermatozoa

Abnormal spermatozoa were observed occasionally in the epididymal smears and resembled for the most part common abnormalities described in other species Most of them involved larger than normal heads with accompanying grossness of the middle piece and anterior or posterior du-

plication of parts (fig 6) Decapitate sperm were also noted, but they could have been casualties of the technical procedures employed In most of the abnormal sperm terminalization of the cytoplasmic droplet had not occurred most often the droplet cytoplasm was flattened and situated proximally on the middle piece but was easily discernible in PAS preparations because of its content of reactive granules

Intra uterine spermatozoa

The study of uterine sections and of sperm suspensions and smears from the uterus of hibernating animals failed to reveal any striking alterations in sperm morphology over the organization of epididymal sperm just described except for the absence of the cytoplasmic droplet In no case was a droplet found on intra uterine sperm nor is this surprising for it is normally jettisoned by the sperm of other mammals at ejaculation if not sooner There was perhaps a slight tendency for the mitochondrial helix of intra uterine sperm to be less easily stained than in those from the epididymis but its general organization and that of the other head and tail components were not obviously altered over the epididymal condition If there are subtle morphological changes in bat sperm associated with their prolonged intra uterine life they were not detectable by these light microscopic procedures

ELECTRON MICROSCOPIC OBSERVATIONS

The fine structure of epididymal sperm in *Myotis lucifugus* was partially characterized in several earlier papers by Fawcett and collaborators (Fawcett 58 62 Telkka Fawcett and Christensen 61) and recently in more comprehensive fashion by Fawcett and Ito (65) Our observations duplicate in most respects the observations of Fawcett's group Hence we shall restrict our description of fine structure of bat sperm to those observations which extend clarify differ from or confirm in certain instances where this is deemed useful the findings of the Harvard group We assert at the outset that at the ultrastructural as well as at the microscopic level we have observed no significant organizational differences between surviving intra uterine sperm in hibernating females and those

from the epididymus other than the absence of cytoplasmic droplets and a slight reorganization of the neck.

The cytoplasmic droplet

The cytoplasmic droplet has been little studied in reference to its fine structure. Bloom and Nicander (61) examined the droplets of bull, ram, rat and rabbit. They record differences in droplet morphology not only as between species but also in relation to the location of sperm within the epididymal tubule and the progressive phases of sperm maturation. Fawcett and Ito (65) provide a brief description of the cytoplasmic droplet in epididymal sperm of *Myotis* and while our observations accord with theirs a somewhat fuller characterization than they have provided seems warranted. Examples of terminalized (on the middle piece) droplets in epididymal sperm are depicted in figures 9 to 11 inclusive. The droplet is bounded externally by a single dense membrane (plasmalemma) continuous with that enclosing the middle piece above and the principal piece below. Where the membrane reflects from the caudal margin of the droplet onto the principal piece it passes over and is firmly adherent to the outer surface of the dense "annulus". The abundant cytoplasm of the droplet directly encloses and infiltrates the mitochondrial sheath and axial filaments which pass through it. The matrix is finely granular, relatively homogeneous and free of ribosomes and lipids.

The principal cytoplasmic inclusions are numerous double layered membranous sacculi, most of which present circular or semi-circular profiles in section view. The matrix invested by the membranous wall of these semi vesicles resembles and communicates widely with the surrounding general cytoplasmic matrix. The three dimensional form of many of the semi vesicles appears analogous to that of a hollow rubber ball in which one hemisphere is completely invaginated into the other, with or without elongation and "pursing" of the opening. The continuous circular profiles are presumably sections which miss the opening of the invaginated globes. Some of the flattened sacculi are less cupped than the majority and a few are adjudged to be semi tubular or ribbon like in three

dimensional aspect. Scattered among these larger double walled elements are variable numbers of smaller circular vesicles and tubular structures delimited by a single smooth surfaced membrane. A few similar bodies are scattered randomly between the mitochondria of the middle piece. All of these structures may or may not be components of a single membranous system. Since the membranes are non granulated and we lacked spermatid transformation stages for comparison we are uncertain as to their nature but they most probably are derived from Golgi lamellae, ER vesicles of the spermatid (a conclusion reached also by Fawcett and Ito (65)) or possibly lysosomes. In the more globate cytoplasmic droplets there is a distinct tendency for the membranous inclusions to be disposed peripherally adjacent to the outer limiting membrane leaving a zone of free cytoplasm immediately surrounding and within the mitochondrial sheath. These displaced bodies are visible as a dark peripheral band of granules in good phase contrast preparations of living sperm.

The absence of free or membrane associated RNP granules in the cytoplasmic droplet is consistent with its lack of basophilia. We are inclined however to ascribe the PAS and acid phosphatase reactivity of the droplet to the larger membranous inclusions just described for these alone are not shared by the confluent PAS and phosphatase negative cytoplasm of the middle piece. Furthermore their peripheral location coincides with the previously described distribution of the PAS and acid phosphatase reactions within the droplet.

The annulus

The annulus which we are unable to identify in our microscopic preparations is conspicuous enough in epididymal sperm when viewed under the electron microscope and has been well described by Fawcett and Ito (65). Whether it persists in mature intra uterine sperm we are unable to state with certainty for unfortunately clear sections at the precise level and plane necessary to determine this point were not available. The densities identified in the indicated cross section of the tail in figures 2 and 16 we believe to be portions of the annulus but there is suf

sufficient lack of definition here that we can not be certain. The annulus is well shown however in the longitudinal section of an epididymal spermatozoon in figure 10 where it has been bisected at two points on opposite sides of the tail. In section it appears acuminate and triangular and reveals a dense homogeneous texture which contrasts sharply with the closely apposed but less dense terminal members of the mitochondrial sheath. According to Fawcett (personal communication) the annulus has originally two distinct components a larger less dense part and a smaller denser part. In the bat only the smaller component persists in epididymal sperm.

The head

Earlier observations on bat spermatozoa emphasized the fine structure of the flagellum (Fawcett 58, 62; Telkka, Fawcett and Christensen 61) but Fawcett and

Ito (65) have now provided a detailed description of the head as well as epididymal sperm. The organization of the head in uterine sperm does not differ in any essential feature from that of epididymal sperm as described by Fawcett and Ito a point which becomes readily apparent if our figures of intra uterine sperm are compared with those of Fawcett and Ito. We shall therefore mention only features not emphasized by these authors or which extend their observations relative to particular organizational details.

The compressed nucleus has a remarkable symmetry the radius of curvature of its upper and lower surfaces being approximately equal throughout its length (fig 1). This contrasts with the situation in the rabbit sperm head (cf Bedford 64) which that of the bat otherwise resembles in many respects. An unusual feature of bat sperm noted by us and also by Fawcett and Ito is the extension of the

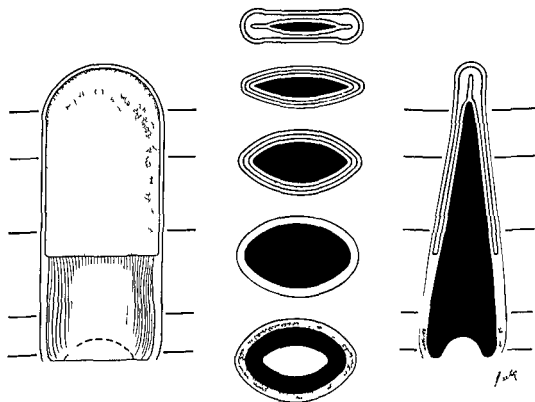


Fig 1 Semischematic reconstruction of the sperm head in *Myotis* based on microscopic and electron microscopic observations. The head is depicted at left in three dimensions as viewed in flat aspect far right is shown in longitudinal section a profile view cut at right angles to the plane of flattening. Successive transsections at levels represented by the horizontal lines are depicted at center. Nucleus black acrosomal cap grey post nuclear sheath stippled cytoplasm white. The outer line represents the plasmalemma.

uppermost pair of mitochondria of the mitochondrial sheath of the middle piece deep into the basal depression (implantation fossa) of the nucleus. The nuclear and mitochondrial outer membranes are in places virtually in contact within this fossa (figs 12 14 17 19). This close juxtaposition of uppermost mitochondria and nucleus has not been indicated in reference to the sperm of other mammals. The apparent constriction of the neck region observed by light and phase contrast microscopy is not evident in electron micrographs. In the former it is presumably an optical illusion created by a lack of density and chromophobia of the neck cytoplasm and its inclusions.

We can find little to add to Fawcett and Ito's account of the organization and relations of the acrosomal cap for they appear to be essentially the same in intra uterine sperm. The form and relations of the cap in uterine sperm are shown schematically in figure 1 and in various section views in the electron micrographs (figs 15-18 incl). For details of its structure consult Fawcett and Ito (65). We have noted in contrast to Fawcett and Ito that the inner face of the acrosomal cap is separated from the outer nuclear membrane by a narrow but relatively uniform zone of low density which in our preparations usually contains a finely granular or amorphous material. Anteriorly projecting for a distance into the terminal thickening of the acrosomal cap in the midline is a slit like extension of the subacrosomal zone of lower density just mentioned and it sometimes contains but more often does not a continuation of the amorphous material previously mentioned as filling in between the apposed acrosomal and nuclear membranes at lower levels (fig 17). This area has been termed the "subacrosomal space" by Fawcett and Ito (65) because it appeared to be empty in epididymal sperm. The entity in question resembles and corresponds to the "apical cone" or "apical body" described by Hadek (63) and Bedford (64) in rabbit sperm. On the other hand as noted by Fawcett and Ito (65) as well as ourselves the discrete triangular density which constitutes the apical body proper of rabbit sperm is absent in bat sperm. The

designation "cone" is inappropriate in any event for what appears to be conical or slitlike in section view has in reality the three-dimensional aspect of a semicircular lamina or ridge disposed parallel to the normal (flat) plane of the head. This "lamina" is tallest nearer the center of its arc but tapers in the lateral directions and disappears near the edge of the anterior curved segment of the nucleus. "Apical lamina" would be a more useful designation for this structure than "cone" for it is conical only in section profile.

Austin and Bishop (58) contend in reference to other mammalian sperm that this laminate entity or region is in fact comprised of modified nuclear membrane. Our micrographs of bat sperm provide no support for this notion for the apical nuclear membrane immediately beneath the area in question is discrete and unmodified. Nor are we persuaded that the term "subacrosomal space" proposed by Fawcett and Ito (65) and Fawcett (in press) is altogether appropriate for we have sometimes detected amorphous material within it as already mentioned. We believe the latter material when present to be cytoplasmic matrix for it appears continuous with the amorphous material separating the acrosomal and nuclear membranes posteriorly and which is in turn continuous with the thin investing layer of cytoplasm surrounding the basal third of the nucleus below the termination of the acrosomal cap. The discrete dense "apical body" of rabbit sperm (Hadek 63 Bedford 64) is presumably homologous with the "perforatorium" of murine and cricetine rodents. It should again be emphasized that these discrete structures have not been observed in bat sperm by us or by Fawcett and Ito (65).

The organization of the marginal region of the sperm head below the posterior end of the acrosomal cap that is the area of the "post nuclear cap" of earlier cytologists has been described in some detail by Fawcett and Ito (65) in epididymal sperm. The organization of this region in intra uterine sperm is generally similar and is depicted in figures 14 15 17 and 18 but differences between earlier observations and ours must be noted. Fawcett and Ito

the axial complex. These tend to be disposed in tandem extending radially to the circle defined by the columns of the connecting piece. Some of these granulae are homogeneously dense but others appear to have paler centers. It is our belief that these granulae are in fact transections of elements of the axial filament complex near their point of origin from the columns of the connecting piece. This view is strengthened by the details indicated by arrows in figures 19 and 20. Here are seen sharply defined fine parallel lines separated by a less dense intermediate layer the whole having a width corresponding to that of an individual axial filament. These structures are identified with the granulae previously noted and represent longitudinal or tangential sections of the axial filaments. Their peripheral location close association with the columns of the connecting piece and their lack of continuity with the proximal contriole above underscore our belief that the axial filaments originate from the columns of the connecting piece.

Fawcett and Ito (65) have already drawn attention to the aberrant form of the uppermost pair of mitochondria which lie in the neck and extend deep into the implantation fossa of the nucleus (figs 12 14 17). We can confirm all of their statements relative to the form and relations of these mitochondria including the presence of peculiar pleats or folds which extend between the segmented columns of the connecting piece into the central area occupied at lower levels by the axial filament complex (figs 15 16 19 20). There would seem little doubt that this constant and unique configuration of the neck mitochondria has some special functional significance perhaps in relation to the initiation of flagellar movements as Fawcett and Ito suggest. A further peculiarity of this pair of mitochondria also recognized by Fawcett and Ito but not given by them the emphasis it may well deserve concerns their spatial orientation relative to the lower mitochondria of the middle piece. As these authors have emphasized the mitochondria of the middle piece in the sperm of *Myotis lucifugus* have a more regular arrangement than observed in most mammalian sperm. They

are tightly packed and arranged serially in pairs the members of each pair lying at approximately the same level on opposite sides of the middle piece. As seen in trans section each mitochondrion has a plump crescentic shape and the truncated ends of each member of a pair meet in intimate contact along a plane which roughly corresponds to the dorsoventral axis of the flattened head (i.e. the xy axis of Telkka et al 61 Fawcett 62 and the xx axis of Fawcett and Ito 65). By contrast while the pair of neck mitochondria are less regularly crescentic and their ends seldom or ever actually meet they are oriented at right angles to those in the middle piece. Were their ends to meet it would be in a plane which coincides with the horizontal plane of the head (i.e. the yy axis of Fawcett 62 and Fawcett and Ito 65). These relationships may be visualized in figures 12 14 and 17. As to the significance of this axial rotation of the modified neck mitochondria we have at present no suggestion to offer.

The middle piece

We have little to add here to the observations of Fawcett and Ito (65) except to clarify the level and sequence of termination of the nine outer dense fibers. Their size rapidly diminishes in the lower half of the middle piece and as observed in the sperm of man and monkey but unlike the sperm of rat mouse and guinea pig they usually extend only a relatively short distance into the principal piece. The order of their disappearance with the exception of numbers 3 and 8 is in direct relation to their initial thickness. Fibers 3 and 8 which are intermediate in size disappear first (see below). They are followed by fibers 2 4 and 7. The four thickest fibers 1 5 6 and 9 disappear last with nine usually dropping out a little before the others (cf figs 2 15 16 19).

The principal piece

Our original observations on the fine structure of the fibrous sheath will not be presented for they add nothing to the detailed account of Fawcett and Ito (65). We shall comment on only one aspect of this region in which our observations differ somewhat from those of previous

workers and this involves a possible relationship between outer dense fibrils 3 and 3 and the longitudinal columns (raphes) formed on opposite sides of the principal piece by junction of the arcuate ribs of the fibrous sheath. Previous authors have made no definite reference to possible connections between outer dense fibers 3 and 8 and the elements of the fibrous sheath despite the fact that these fibers lie on opposite sides of the axial filament complex approximately on the XY axis and hence immediately beneath the longitudinal columns of the sheath on each side of the tail. Connections between dense outer fibers which are possibly contractile and the fibrous sheath which may have supportive or elastic properties (Fawcett '62) could if they exist have an important bearing on the dynamics of tail movement. Figure 9 section no. 1 is a tangential section through the junction between middle piece and principal piece in an epididymal spermatozoon. To the left it clearly portrays the ribs of the fibrous sheath joining the slender longitudinal column. To the right at the junction with the middle piece the column seems to continue on beyond the fibrous sheath into the middle piece where clearly it can no longer be column substance. It must be one of the coarse filaments 3 or 8. The picture by itself suggests that connections may exist between the elements of the sheath and fibrils 3 and 8 but the possibility exists that the coarse fiber passes beneath the raphe in line with it only creating an illusion of continuity between the two. However relations as viewed in cross-sections of the principal piece are more suggestive and it may be significant that fibers 3 and 8 while not the smallest are the first to disappear posteriorly. Within the mid section of the middle piece fibers 3 and 8 are smaller in cross sectional diameter than the largest fibers 1, 5, 6 and 9 but noticeably larger than 2, 4 and 7 (fig. 15). Their outline here is ovate and their long axes are directed radially the larger end facing outward. Normally too they are displaced outward somewhat and this becomes accentuated in the lower middle piece and upper principal piece. Within the latter they often appear to contact or be fused with the inner edge of the thin

longitudinal columns of the fibrous sheath. This is especially apparent in distorted sections where the various elements may be somewhat displaced here the two dense fibers usually cling to the fibrous columns rather than remaining proximate to axial filaments 3 and 8. In some cases they even appeared to be included wholly within the inner edge of the fibrous sheath. These appearances all suggest that there are areas of fusion between outer dense fibers 3 and 8 and the inner ends of the respective longitudinal columns of the fibrous sheath. Distally the broad inner ends characteristic of the longitudinal columns at higher levels are replaced by inwardly directed narrow projections of column substance whose ends may touch or nearly touch subfibrils 3 and 8 respectively (figs. 2, 16, 19).

We tentatively suggest that in *Myotis* spermatozoa at least outer dense fibers 3 and 8 gradually blend into the longitudinal columns of the fibrous sheath rather than ending freely without such attachment and that this may explain their apparent earlier disappearance posteriorly in the principal piece despite their intermediate size. The direction of flexion of the tail in swimming movements is primarily perpendicular to the plane which bisects outer dense fibers 3 and 8 (cf Fawcett '62). If the latter are contractile they could conceivably exert tension on the fibrous columns in the direction of their longitudinal axis thereby stiffening or polarizing the resistance of the sheath in the dorso ventral (xy) axis to the contraction waves that pass along the other elements of the axial filament complex. This might provide in the words of Fawcett ('62) "the necessary couple for the transverse bending movements of the tail."

DISCUSSION

For the most part our observations of sperm ultrastructure in *Myotis lucifugus* have paralleled those of Fawcett and Ito ('65). We have confirmed many of their findings and concur in most of their interpretations. Accordingly we have restricted the presentation of our own observations to those necessary to help clarify difficult points or which comple

ment and extend the findings of these authors. The Fawcett and Ito study was devoted wholly to epididymal sperm. The emphasis in our study of ultrastructure has been upon stored intra uterine sperm since we were especially interested in discovering adaptations which might help explain the remarkable longevity of bat sperm in the female reproductive tract. However as far as cytology and ultrastructure are concerned we have found no special modifications which might be related to sperm survival. Uterine sperm in hibernating *Myotis lucifugus* resemble in all essentials unejaculated sperm from the epididymis. The cytoplasmic droplet characteristic of epididymal sperm is lost at ejaculation but this is usual among mammals. Whether the loss by uterine sperm of the redundant nuclear membrane material (membranous scrolls of Fawcett and Ito '65) so characteristic of epididymal sperm has any special significance for sperm survival we cannot definitely say but we doubt it. It is conceivable that the disappearance of the redundant nuclear membrane is in some manner related to the process of sperm capacitation within the uterus but on the other hand the reversibility of the capacitation phenomenon under appropriate experimental conditions (Chang '57 Bedford and Chang '62) makes this too seem unlikely. We are forced to conclude that the mechanism of sperm survival in the female tract most probably resides either in special physiological characteristics of bat sperm which have very subtle or no morphological expression or alternatively in physiological adaptations of the uterus itself. Our observations concerning the latter possibility will be presented in a later communication.

In the process of spermatogenesis significant amounts of cytoplasm are sequestered into the lumen of the seminiferous tubules. These residual bodies (Regaud '01) have recently been studied with both the light microscope (Firlit and Davis '65) and with the electron microscope (Deitert personal communication in press). The residual bodies possess PAS positive granules. Deitert has also described a large number of lysosomes of varying structure within the cytoplasmic remnants. The cytoplasmic droplet present in the

epididymal sperm of this study but not in the intra uterine sperm is similar in many respects to the residual body. Our observations indicate that the vesicular bodies in the droplet are PAS positive and in many instances probably also contain acid phosphatase. Both of these reactions are characteristic of lysosomes (Novikoff '60). It appears then that the cytoplasmic droplet is the last remnant of unsequestered cytoplasm and is related to the residual body. With maturation of the epididymal sperm this element like the residual body is also lost.

We wish finally to call attention to an odd discrepancy between our microscopic and ultrastructural observations of the middle piece which may be of great functional importance and which has not been commented upon by previous workers. It is obvious in bat sperm that far more mitochondria are identifiable in electron micrographs of the middle piece than are revealed by conventional staining procedures of light microscopy indicating that some mitochondria are stained by the conventional methods whereas others are not. Moreover in microscopic preparations stained mitochondria alternate in a more or less regular pattern along the longitudinal axis of the middle piece and the stained ones tend to be staggered on its opposite sides i.e. stained mitochondria on one side of the middle piece generally lie opposite unstained ones on the other side and so on (fig. 4). It is this alternation of stained and unstained mitochondria on each side and their phase differences on opposite sides of the middle piece which create the illusion of a continuous mitochondrial spiral for at the low resolving power of the light microscope discontinuities between individual mitochondria are easily overlooked. Moreover the frequency with which the mitochondrial component of the middle piece has been described as a continuous spiral or helix suggests that comparable alternations of staining may characterize other mammalian sperm and lessens the likelihood that it has a merely random or fortuitous basis.

While this line of reasoning may explain how a misconception of middle piece organization might have arisen the phenomena itself could conceivably have

important physiological significance in relation to initiation and coordination of sperm tail movements. Why do some mitochondria stain whereas others do not and why does their stainability alternate more or less regularly on one side and in staggered on opposite sides of the middle piece? The bases of mitochondrial staining by conventional methods are little understood but they are presumably related to the chemical constitution of the organelles. Reversible or cyclic physiological activities within the mitochondria might conceivably alter their chemical makeup in such a way as to affect their stainability. It would be interesting to know whether certain mitochondria are permanently stainable and others non stainable or whether they are able to turn "on and off" in time relative to their staining affinity. This is not determinable in microscopic preparations of killed sperm but a rarely observed condition in the neck region of sperm in epididymal smears may provide a clue. In the preponderant majority of such sperm when stained by conventional methods for mitochondria the neck segment appears achromatic and transparent the uppermost gyre of the stained mitochondrial sheath lying some distance below the head. We have observed in such preparations an occasional spermatozoon in which the uppermost stained gyre extends through the neck and abuts against the nucleus (fig 4). In these occasional sperm the aberrant pair of mitochondria in the neck region evidently stain whereas in the vast majority of spermatozoa they do not. It is conceivable that these differences in the staining affinity of the peculiar mitochondria of the neck in different spermatozoa reflect a time lapse difference in their activity. If this can occur in the neck mitochondria there is no reason to suppose that it cannot among the mitochondria at lower levels in the middle piece. Interpreted in this light the apparent helical arrangement of stained and unstained mitochondria takes on additional significance for it is the appearance we would expect if the organelles fired in cyclic or pulsed fashion and in sequence along the middle piece. Experiments to test this possibility are currently in progress.

If this speculation has any validity then important questions (presumably answerable only in the domain of molecular biology) are raised concerning (1) the initiation and control of cyclic mitochondrial activities in the middle piece and (2) the dynamic relation between the pulsed sequential mitochondrial activity and the functional coordination of the individual contractile elements of the axial filament complex responsible for the spatially oriented movements of the tail. Successful demonstration that the mitochondria of the sperm middle piece are capable of coordinated cyclic functional sequences might also have more general significance in relation to the nature of mitochondrial activities in other types of cells as well as to the factors which determine their stainability by conventional cytological procedures.

LITERATURE CITED

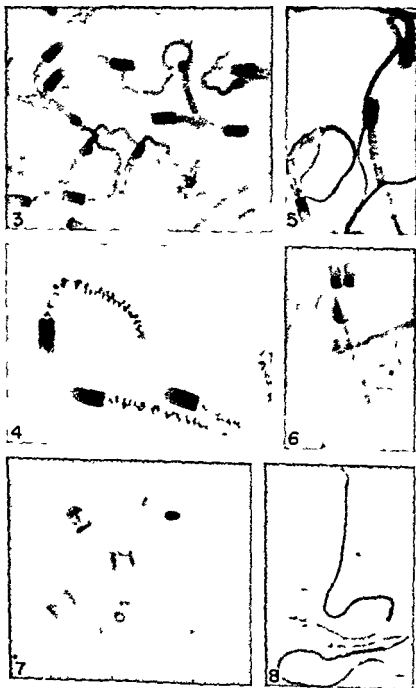
- Austin C R and M W H Bishop 1958 Role of the rodent acrosome and perforatorium in fertilization. *Proc Roy Soc Lond B* 149: 241-248.
- Bedford J M 1964 Fine structure of the sperm head in ejaculate and uterine spermatozoa of the rabbit. *J Reprod Fertil* 7: 221-228.
- Bedford J M and M C Chang 1962 Removal of decapacitation factor from seminal plasma by high speed centrifugation. *Am J Physiol* 202: 179-181.
- Bishop M W H and A Walton 1960 Spermatogenesis and the structure of mammalian spermatozoa. In *Marshall's Physiol Reprod* A S Parkes ed Vol 1 part 2 1-129. Longmans London.
- Bloom G and L Nicander 1961 On the ultrastructure and development of the protoplasmic droplet of spermatozoa. *Zischr f Zellforsch* 55: 833-844.
- Cavazos L F and R M Melampy 1954 A comparative study of periodic acid reactive carbohydrates in vertebrate testes. *Am J Anat* 95: 467-495.
- Chang M C 1957 A detrimental effect of seminal plasma on the fertilizing capacity of sperm. *Nature Lond* 179: 258-259.
- Clermont Y and C P Leblond 1955 Spermiogenesis of man monkey ram and other mammals as shown by the 'Periodic acid Schiff' techniques. *Am J Anat* 96: 229-254.
- Fawcett D W 1958 The structure of the mammalian spermatozoon. In *Int Rev Cytol* G Bourne and J Danielli ed vol VII 195-234. Academic Press New York.
- 1962 Sperm tail structure in relation to the mechanism of movement. *Spermatozoan Motility A.A.S.* 147-169. Wash D C.

- The anatomy of the mammalian spermatozoon with particular reference to the guinea pig Ztsch f Zellforsch (in press)
- Fawcett D W and S Ito 1965 The fine structure of bat spermatozoa *Am J Anat* 116 567-610
- Firlit C F, and J R Davis 1965 Morphogenesis of the residual body of the mouse testis *Quart J Microscop Sci* 106 93-98
- Hadek R 1963 Study on the fine structure of rabbit sperm head *J Ultrastr Res*, 9 110-122
- Hirth H F 1960 The spermatozoa of some North American bats and rodents *J Morph* 106 77-83
- Holmes W 1943 Silver staining nerve axons in paraffin section *Anat Rec* 86 157-187
- Karnovsky M J 1961 Simple methods for staining with lead at high pH in electron microscopy *J Bioph Bloch Cytol* 11 729-732
- Leblond C P and Y Clermont 1952 Spermiogenesis of rat mouse hamster and Guinea pig as revealed by the periodic acid fuchsin sulfurous acid techniques *Am J Anat* 90 167-216
- Matthews L H 1937 The female sexual cycle in the British horseshoe bats *Rhinolophus ferrum-equinum insulanus* Barrett Hamilton and *R hipposideros minutus* Montagu *Trans Zool Soc Lond* 23 224-266
- Novikoff A 1960 Lysosomes and related particles p 423-488 In J Brachet and A E Mirsky ed *The cell* Vol 2 Academic Press New York
- Regaud C 1901 Etude sur la structure des tubes seminifères et sur la spermatogenèse chez les mammifères *Arch d'Anat. Microscop* 4 101-155
- Telkka A D W Fawcett and A K Christensen 1961 Further observations on the structure of the mammalian sperm tail *Anat Rec* 141 231-246
- Wimsatt W A 1944 Further studies on the survival of spermatozoa in the female reproductive tract of the bat *Anat Rec* 88 193-204
- 1960 Some problems of reproduction in relation to hibernation in bats *Bull Mus Comp Zool* 124 249-267

PLATE 1

EXPLANATION OF FIGURES

- 3 Epididymal sperm suspension PAS hematoxylin and light green Only the cytoplasmic droplets are PAS positive all shown are located at the distal end of the middle piece $\times 1500$
- 4 Epididymal sperm suspension Altmann aniline acid fuchsin methyl green Cytoplasmic droplets are absent in these sperm Note the prominence of the middle piece within it the axial filament complex appears as a single strand and the apparent helical winding of mitochondria is clearly visible The unstained translucent acrosomal cap renders the anterior end of the nucleus indistinct $\times 2400$
- 5 Epididymal sperm suspension hematoxylin eosin and aniline blue Aniline blue stains selectively the fibrous sheath of the principal piece so the junction of the latter with the middle piece is sharply defined Cytoplasmic droplets not present $\times 1500$
- 6 Epididymal sperm suspension PAS and hematoxylin Abnormal spermatozoon with two heads and partial division of the middle piece The cytoplasmic droplet which is PAS positive is not terminalized on the middle piece as in most normal sperm in this preparation $\times 1500$
- 7 Epididymal sperm suspension Bodian protargol method Only the post nuclear sheath is stained by the Bodian procedure The stained area may not extend all the way forward to the posterior margin of the acrosomal cap $\times 4000$
- 8 Epididymal sperm suspension Holmes silver stain The procedure is highly specific for the fibrous sheath of the principal piece and the inner axial filaments Note the peculiar spatulate density at the terminal end of the principal piece characteristic of all sperm stained by the Holmes procedure Its structural basis and significance is unknown The post nuclear sheath region is faintly indicated but the remainder of the head is unstained $\times 1500$



- The anatomy of the mammalian spermatozoon with particular reference to the guinea pig Ztsch f Zellforsch (in press)
- Fawcett D W and S Ito 1965 The fine structure of bat spermatozoa *Am J Anat* 116 567-610
- Firlit C F and J R Davis 1965 Morphogenesis of the residual body of the mouse testis *Quart J Microscop Sci*, 106 93-98
- Hadek R 1963 Study on the fine structure of rabbit sperm head *J Ultrastr Res* 9 110-122
- Hirth H F 1960 The spermatozoa of some North American bats and rodents *J Morph* 106 77-83
- Holmes W 1943 Silver staining nerve axons in paraffin section *Anat Rec* 86 157-187
- Karnovsky M J 1961 Simple methods for staining with lead at high pH in electron microscopy *J Bioph Bioch Cytol* 11 729-732
- Leblond C P and Y Clermont 1952 Spermiogenesis of rat mouse hamster and Guinea pig as revealed by the periodic acid fuchsin sulfurous acid techniques *Am J Anat* 90 167-216
- Matthews L H 1937 The female sexual cycle in the British horseshoe bats *Rhinolophus ferrum-equinum insularis* Barrett Hamilton and R *hipposideros minutus* Montagu *Trans Zool Soc Lond* 23 224-266
- Novikoff A 1960 Lysosomes and related particles p 423-488 In J Brachet and A E Mirsky ed *The cell* Vol 2 Academic Press New York
- Regaud C 1901 Etude sur la structure des tubes seminifères et sur la spermatogenèse chez les mammifères *Arch d Anat Microscop* 4 101-155
- Telkka A D W Fawcett and A K Christensen 1961 Further observations on the structure of the mammalian sperm tail *Anat Rec* 141 231-246
- Wimsatt W A 1944 Further studies on the survival of spermatozoa in the female reproductive tract of the bat *Anat Rec* 88 193-204
- 1960 Some problems of reproduction in relation to hibernation in bats *Bull Mus Comp Zool* 124 249-267

PLATE 1

EXPLANATION OF FIGURES

- 3 Epididymal sperm suspension PAS hematoxylin and light green Only the cytoplasmic droplets are PAS positive all shown are located at the distal end of the middle piece $\times 1500$
- 4 Epididymal sperm suspension Altmann aniline acid fuchsin methyl green Cytoplasmic droplets are absent in these sperm Note the prominence of the middle piece within it the axial filament complex appears as a single strand and the apparent helical winding of mitochondria is clearly visible The unstained translucent acrosomal cap renders the anterior end of the nucleus indistinct $\times 2400$
- 5 Epididymal sperm suspension hematoxylin eosin and aniline blue Aniline blue stains selectively the fibrous sheath of the principal piece so the junction of the latter with the middle piece is sharply defined Cytoplasmic droplets not present $\times 1500$
- 6 Epididymal sperm suspension PAS and hematoxylin Abnormal spermatozoon with two heads and partial division of the middle piece The cytoplasmic droplet which is PAS positive is not terminalized on the middle piece as in most normal sperm in this preparation $\times 1500$
- 7 Epididymal sperm suspension Bodian protargol method Only the post nuclear sheath is stained by the Bodian procedure The stained area may not extend all the way forward to the posterior margin of the acrosomal cap $\times 4000$
- 8 Epididymal sperm suspension Holmes silver stain The procedure is highly specific for the fibrous sheath of the principal piece and the inner axial filaments Note the peculiar spatulate density at the terminal end of the principal piece characteristic of all sperm stained by the Holmes procedure Its structural basis and significance is unknown The post nuclear sheath region is faintly indicated but the remainder of the head is unstained $\times 1500$

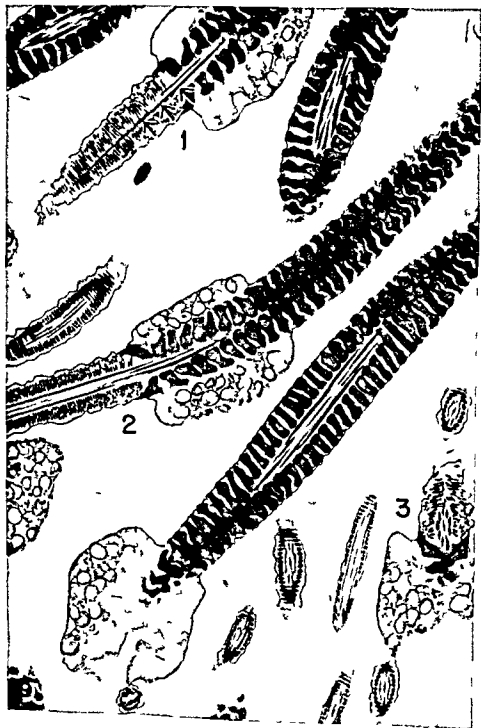


PLATE 2

EXPLANATION OF FIGURE

- 9 Epididymal spermatozoa showing structure and relations of middle piece principal piece and cytoplasmic droplets Three junctions between middle and principal pieces are depicted (1 2 3) note in each the intimate relation between lower mitochondrial pair and annulus and the firm adherence of the cell membrane to the outer face of the annulus In the upper section (1) arrows indicate the apparent confluence described in the text between one of the fibrous longitudinal columns of the principal piece and outer coarse fibril 3 or 8 of the middle piece

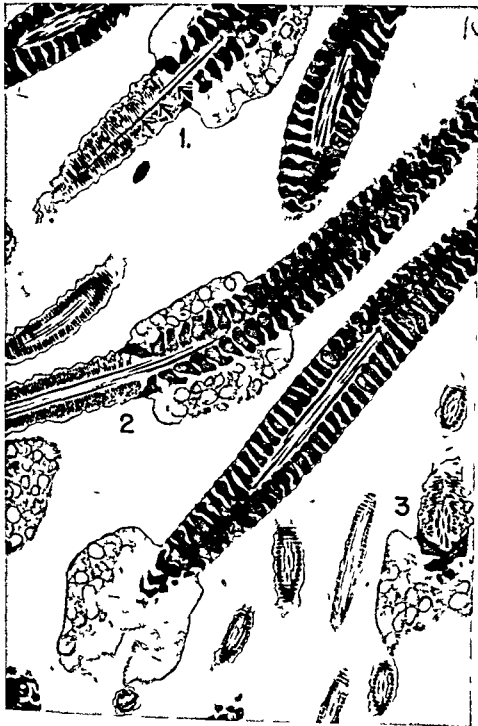


PLATE 3

EXPLANATION OF FIGURE

- 10 Enlargement of section 2 from preceding figure showing detail of cytoplasmic droplet and annulus (arrows). The peripheral distribution and organization of the membranous semi vesicles in the droplet cytoplasm is visible here as well as in the preceding and following figures. The section plane parallels the flat horizontal plane of the head i.e. is perpendicular to the X-Y axis of the tail.

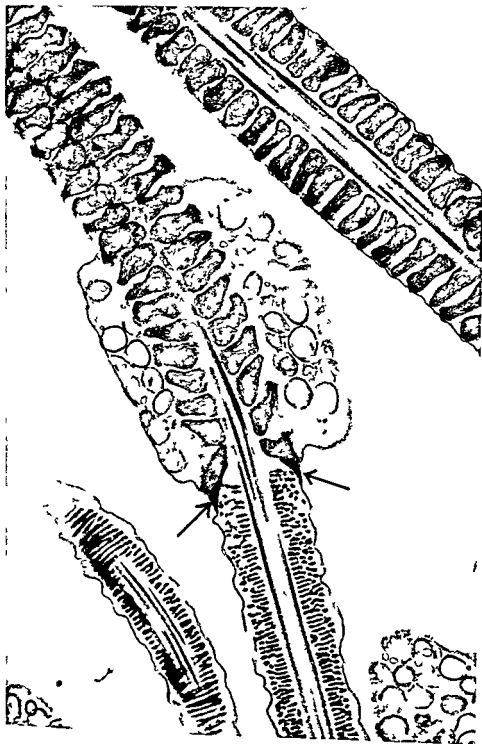


PLATE 4

EXPLANATION OF FIGURES

- 11 Cytoplasmic droplet enlarged showing membranous semi vesicles and tubules smaller vesicles and the tendency for these structures to occupy a peripheral location in the droplet. Note absence of RNP particles and lipid droplets. The membranous bodies are believed responsible for the PAS and acid phosphatase reactivity of the droplet (see text)
- 12 Tangential section through base of head neck and upper middle piece of an epididymal spermatozoon. The section is off center in relation to the axial complex of the middle piece and is perpendicular to the X-Y axis. Note that the uppermost mitochondrion appears unpaired in this plane of section crossing the midline perpendicular to the X-Y axis and skewed 90° in relation to the orientation of the lower pairs in the middle piece. Note also its intimate association with the nucleus within the implantation fossa. The section is not central enough to include the upper part of the connecting piece but two of its segmented columns are shown just below their junction. *M* mitochondrion *Ms* membranous scroll (nuclear membrane)

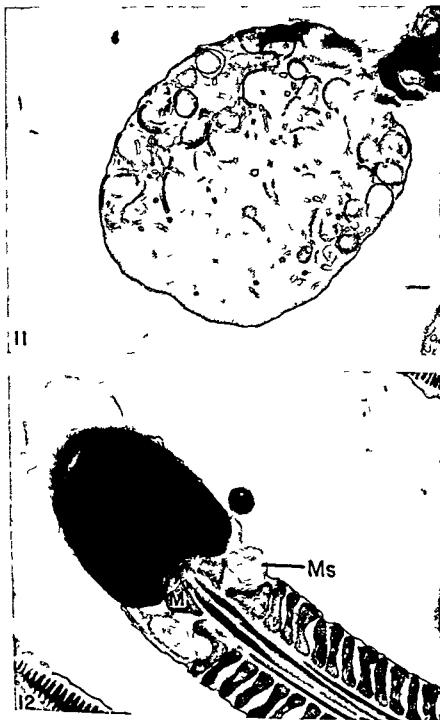


PLATE 5

EXPLANATION OF FIGURES

- 13 Epididymal spermatozoa stained by a modification of the Gomori lead sulfide method for acid phosphatase utilizing Na B glycerophosphate as substrate incubation time 30 minutes. Note the reactive bead at the junction between middle piece and principal piece representing the cytoplasmic droplet. The apparent staining of the fibrous sheath is less constant and is presumed to be an adsorption artifact. The same is probably true in respect to the bands on the head but the staining of the unidentified components at the top and base of the neck is consistent and is presumed to reflect enzymic activity. No staining occurred in control sections treated with NaFl.
- 14 Intra uterine spermatozoon whose head is embedded in an epithelial cell. The plane of section corresponds to the X-Y axis of the axial complex of the tail i.e. perpendicular to the plane of flattening of the head but it is tangential and off center. The plane is at right angles to that of figure 12 with which it should be compared. The dense structure (*) in the nuclear depression is apparently part of the connecting piece. The skewed orientation of the uppermost mitochondria pair (only one member shown) is indicated. The arrows show location of post nuclear sheath material. M mitochondria.

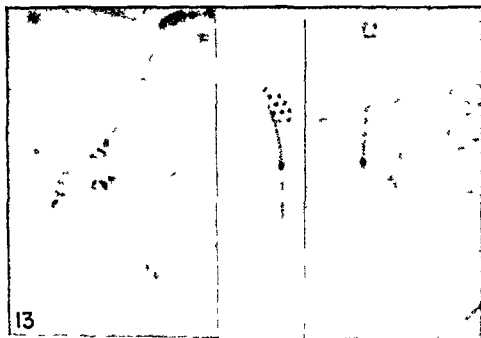


PLATE 5

EXPLANATION OF FIGURES

- 13 Epididymal spermatozoa stained by a modification of the Gomori lead sulfide method for acid phosphatase utilizing Na B glycerophosphate as substrate incubation time 30 minutes Note the reactive bead at the junction between middle piece and principal piece representing the cytoplasmic droplet The apparent staining of the fibrous sheath is less constant and is presumed to be an adsorption artifact The same is probably true in respect to the bands on the head but the staining of the unidentified components at the top and base of the neck is consistent and is presumed to reflect enzymic activity No staining occurred in control sections treated with NaCl
- 14 Intra uterine spermatozoon whose head is embedded in an epithelial cell The plane of section corresponds to the X-Y axis of the axial complex of the tail i.e. perpendicular to the plane of flattening of the head but it is tangential and off center The plane is at right angles to that of figure 12 with which it should be compared The dense structure (*) in the nuclear depression is apparently part of the connecting piece The skewed orientation of the uppermost mitochondria pair (only one member shown) is indicated The arrows show location of post nuclear sheath material M mitochondria

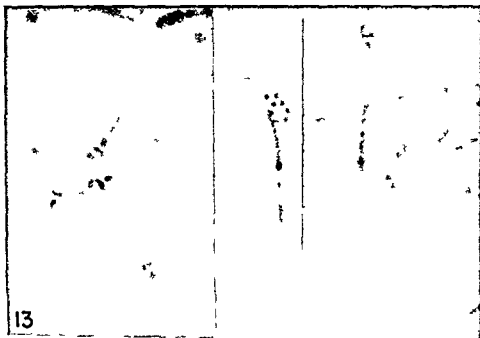


PLATE 5

EXPLANATION OF FIGURES

- 13 Epididymal spermatozoa stained by a modification of the Gomori lead sulfide method for acid phosphatase utilizing Na B glycerophosphate as substrate incubation time 30 minutes. Note the reactive bead at the junction between middle piece and principal piece representing the cytoplasmic droplet. The apparent staining of the fibrous sheath is less constant and is presumed to be an adsorption artifact. The same is probably true in respect to the bands on the head but the staining of the unidentified components at the top and base of the neck is consistent and is presumed to reflect enzymic activity. No staining occurred in control sections treated with NaFl.
- 14 Intra uterine spermatozoon whose head is embedded in an epithelial cell. The plane of section corresponds to the λ - λ axis of the axial complex of the tail i.e. perpendicular to the plane of flattening of the head but it is tangential and off center. The plane is at right angles to that of figure 12 with which it should be compared. The dense structure (*) in the nuclear depression is apparently part of the connecting piece. The skewed orientation of the uppermost mitochondria pair (only one member shown) is indicated. The arrows show location of post nuclear sheath material. M mitochondria.

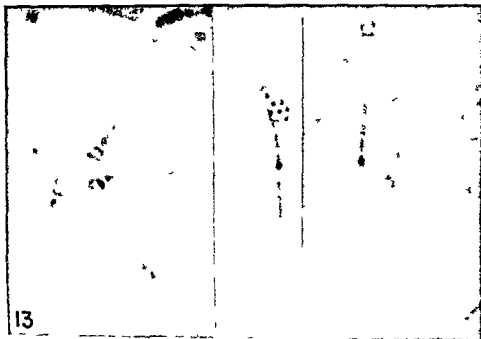


PLATE 5

EXPLANATION OF FIGURES

- 13 Epididymal spermatozoa stained by a modification of the Gomori lead sulfide method for acid phosphatase utilizing Na B glycerophosphate as substrate incubation time 30 minutes. Note the reactive bead at the junction between middle piece and principal piece representing the cytoplasmic droplet. The apparent staining of the fibrous sheath is less constant and is presumed to be an adsorption artifact. The same is probably true in respect to the bands on the head but the staining of the unidentified components at the top and base of the neck is consistent and is presumed to reflect enzymic activity. No staining occurred in control sections treated with NaF.
- 14 Intra uterine spermatozoon whose head is embedded in an epithelial cell. The plane of section corresponds to the X-Y axis of the axial complex of the tail i.e. perpendicular to the plane of flattening of the head but it is tangential and off center. The plane is at right angles to that of figure 12 with which it should be compared. The dense structure (*) in the nuclear depression is apparently part of the connecting piece. The skewed orientation of the uppermost mitochondria pair (only one member shown) is indicated. The arrows show location of post nuclear sheath material. M mitochondria.



PLATE 6

EXPLANATION OF FIGURE

- 15 Sections at various levels of spermatozoa lying within lumen of uterus (1) transection of head through flattened nuclear apex the acrosomal cap is complete and the lateral ends of its terminal bead (cf fig 1) are shown (2) transection of head at posterior margin of acrosomal cap which is deficient between arrows (3) transection of head posterior to acrosomal cap (4) transverse section through neck showing lower part of connecting piece (segmented columns) subfibrils near their point of origin and mitochondrial pleats (5) sections through lower neck or upper middle piece showing uniform size of the nine outer dense fibers at this level (6) typical transverse sections of middle piece showing larger size of outer dense fibers 1 9 5 and 6 and intermediate size of 3 and 8 the X-Y axis (of Fawcett '62) is indicated on one of the sections (7) section through upper part of principal piece showing association of outer dense fibers 3 and 8 with inner ends of fibrous longitudinal column (8) section of end piece

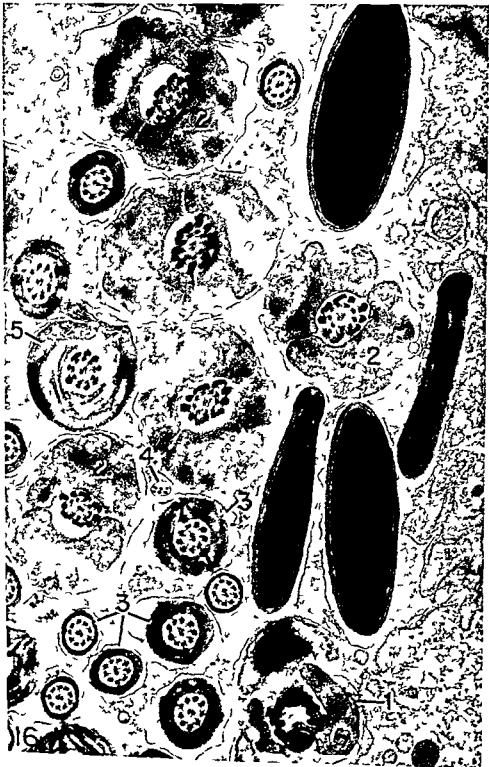


PLATE 7

EXPLANATION OF FIGURE

- 16 Sections of intra uterine (luminal) sperm cut at various levels and planes mostly transverse For detailed description see text (1) transections through neck (2) transections of middle piece (3) sections of principal piece at various levels showing variations in thickness of fibrous sheath and alignment of longitudinal columns on X-Y axis of tail (4) section near tip of end piece showing reduction of subfibrils to a ratio of 7+1 (5) transection at junction between middle piece and principal piece elements of the fibrous sheath are visible adjacent to the outer dense fibers and outside them portions of the lowermost pair of mitochondria of the middle piece the densities lying left and right are interpreted as portions of the annulus (End ring ring centriole)

William A Wimsatt, Philip H Krutzsch and Leonard Napolitano

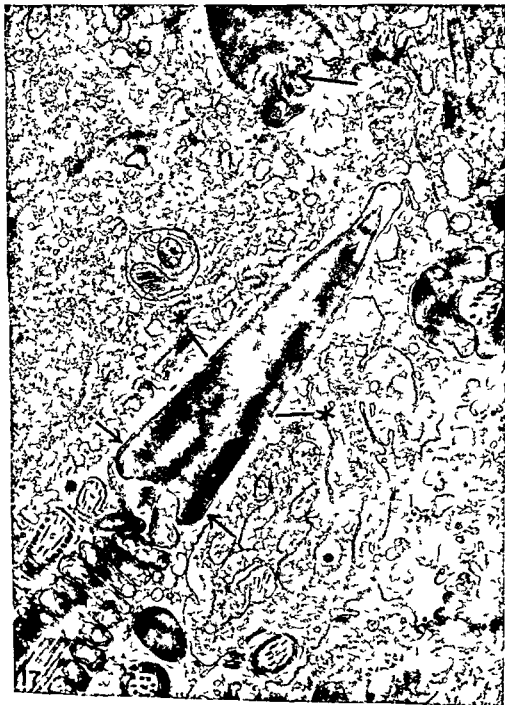


PLATE 8

EXPLANATION OF FIGURE

- 17 Intra uterine spermatozoa embedded in epithelial cell. In the large central section the head is cut slightly tangentially and in the plane of the X-Y axis of the tail i.e. at right angles to the plane of flattening of the head. Note especially relations in the neck the acrosomal cap which is shown in its full extent (* = its caudal margin) and the apical lamina. The arrow indicates in the upper spermatozoan a portion of a proximal centriole. The lower arrows indicate the basal thickenings of the post nuclear sheath presumed responsible for the argyrophilia of this region.



PLATE 9

EXPLANATION OF FIGURE

- 18 Tangential longi section of intra uterine spermatozoa lying within the lumen of a gland the section planes are approximately perpendicular to the plane of flattening of the head i.e. they parallel the X-Y axis of the tail. Arrows indicate the basal post nuclear sheath thickenings. The full extent of the acrosomal cap is visible in the larger head section.



PLATE 10

EXPLANATION OF FIGURES

- 19-20 Transections of sperm within the uterine lumen showing organization of tail segments at various levels (1) neck region (2) upper middle piece (3) upper principal piece (4) more distal levels of principal piece. In the neck sections (1) are seen the segmented columns of the connecting piece (B) and the mitochondrial laminae which project between them (see text). Note in the middle piece the larger size of outer coarse fibrils 1 5 6 and 9 the intermediate size of 3 and 8 and the smaller size of 2 4 and 7. The axial planes and other organizational details previously described by others are here confirmed. The two spermatozoa represented by sections through the distal portion of the middle piece (4) were facing in opposite directions the observer is looking toward the head in the upper one and toward the tail tip in the lower one. The arrows indicate tangential or longitudinal sections of the inner 9+2 array of subfibrils of the axial filament complex near their point of origin in the connecting piece. M mitochondria N nucleus

The Effect of Relaxin on the Endometrium of Monkeys

HISTOLOGICAL AND HISTOCHEMICAL STUDIES¹

G DALLENBACH HELLWEG A B DAWSON AND F L HISAW
*Biological Laboratories Harvard University Cambridge Massachusetts and
Department of Pathology Dartmouth Medical School
Hanover New Hampshire*

ABSTRACT Castrated or juvenile monkeys were given estrogen progesterone and relaxin in various doses and combinations. Relaxin induced (1) a dilatation of the superficial endometrial blood vessels and proliferation of their endothelial cells; this effect may be regarded as due to relaxin alone (2) an intensified differentiation of the endometrial stroma cells into predecidual cells and granulocytes dependent on estrogen priming and the simultaneous injection of progesterone (3) a periarteriole-like accumulation of granulocytes in the basal endometrium dependent on the above pretreatment (4) a degranulation of the granulocytes and hypersegmentation of their nuclei following prolonged administration of relaxin with estrogen and progesterone. Morphologically and histochemically the granulocytes of the monkey are almost identical with those of the human uterus and with the granular cells in the decidua and mesometrial gland of the pregnant rat. Immunohistologically relaxin has been demonstrated in the granulocytes of man and rat. The changes in the arterioles brought about by exogenous relaxin occur under physiological conditions only with the increased formation of endogenous relaxin during early pregnancy. They have been described in the immediate vicinity of ovum implantation in man, monkey and rat. Their function possibly lies in the preparation of blood spaces for nutrition of the young embryo.

Hisaw and Hisaw (64) studied the effects of relaxin in the female monkey stressing its influence on the thickness of the endometrium and myometrium and on the cervix and symphysis pubis. They concluded that relaxin tended to intensify the synergistic action between estrogen and progesterone on endometrial growth. Since granulocytic cells occur in the endometrium of the monkey (Cleveland 41 Bartelmez et al 51 Hellweg 59) and resemble the endometrial granulocytes of the human female and since relaxin has been demonstrated immunohistologically in the endometrial granulocytes of the human uterus (Dallenbach and Dallenbach Hellweg 64) a histological and histochemical study of the endometria of these monkeys treated with relaxin seemed to be of great interest. It appeared important therefore to determine if exogenously administered relaxin in certain dosages and in combination with estrogen and progesterone would have an effect on the number and distribution of the granulocytes and on the degree of granulation. Close attention was also given to the presence of other morphologically recog-

nizable effects which might eventually be ascribed to relaxin in addition to the increased endometrial growth recognized by Hisaw and Hisaw.

MATERIAL AND METHODS

The endometria of 64 monkeys (*Macaca mulatta*) were examined histologically and histochemically using essentially the same uteri which were studied by Hisaw and Hisaw (64). Since the treatments of the castrated animals were presented in detail in their paper they are not included here. Ten juvenile and non-castrated animals (nos 286-291 294-297) have been added to the treatment group. Controls consisted of 12 uteri of non-castrated untreated monkeys (ten obtained during the proliferative phase and two from the third month of pregnancy) these specimens were also used in a previous publication (Hellweg 59).

Paraffin sections of these uteri were stained with the following histological techniques: hematoxylin-eosin, phloxine

This work has been supported by U.S.P.H.S. grants HD 00422 and GM 10210.
Present address: Path.isches Institut, Städt. Krankenhaus, 48 Bielefeld, Germany.

but without the previous estrogen administration shows predecidual change and many granulocytes. The number of granulocytes which develop only in the presence of progesterone is closely proportional to the amount of progesterone administered. On the other hand under the influence of progesterone alone there is only little growth and consequently neither predecidual cells nor granulocytes develop (no 226). With progesterone given over prolonged periods (56 days no 231 234) a degranulation of the numerically unaltered granulocytes is evident. If relaxin is added to estrogen and progesterone the differentiation of the stromal cells into the pre-decidual type and into granulocytes is still further enhanced. The pre-decidual cells appear somewhat larger and the granulocytes seem to increase moderately in number (from +++ to +++) the shape of the granulocytes and the granulation of their cytoplasm remain unchanged (fig 2). Following the administration of only estradiol and relaxin (nos 288 290 292) only a few granulocytes are demonstrable and after estrinol alone followed by estrinol and relaxin (no 233) still fewer granulocytes are evident than when progesterone is administered simultaneously. When only progesterone and relaxin are given in the total (no 253) or in the final treatment (nos 249 and 287) the granulocytes become numerous.

When progesterone with or without relaxin is administered over a prolonged period of time (56 days nos 231 234 56 days no 256 with 41 days relaxin) an intense proliferation and differentiation of the periarterial cells into granulocytes becomes especially striking in the basal layers of the endometrium. Here these granulocytes invest the spiral arteries to produce thick mantles (fig 3). Such periarterial aggregates of granulocytes are demonstrable under the same hormonal conditions which lead to the differentiation of predecidual cells and granulocytes. The thickness of the mantle of cells about the arteries and arterioles (fig 4) is proportional to the total number of granulocytes in the uterus.

The granulocytes in the monkey endometria described here resemble morphologically the granulocytes of the human

endometrium hence further description of them is unnecessary. The histological and histochemical methods used are comparable to the studies carried out on the granulocytes of human uteri. The intra-cytoplasmic granules of the granulocytes stain weakly pink with H + E, thus they are difficult to recognize. With the phloxine tartrazin stain they contrast sharply from the remaining cytoplasmic structures because of their bright red phloxinophilia. In addition they are red with the Azan stain, Masson's trichrome stain and pentachrome stain. With Mallory's fibrin stain they are violet. The granules give a positive tetrazonium reaction which becomes negative after benzooylation. The reaction for tryptophan is strongly positive, those for histidine, lysine, tyrosine and SH groups are also positive. The isoelectric point as measured with methylene blue on formalin fixed sections is at pH 4.4. The PAS reaction after diastase digestion is weakly positive for some of the granules. The same is true for the aldehyde fuchsin stain after oxidation whereas it is negative without oxidation. In some of the granules the alcian blue reaction is positive. With the alcian blue PAS combination the granules appear blue. They fail to give an absolute (alcohol fast) metachromasia but a red color reaction is retained after dehydration with acetone. They react negatively to Sudan Black B. These histochemical results suggest that the granules consist of an acidophilic protein to which possibly an acid mucopolysaccharide is more or less loosely bound.

(d) In some animals in the superficial layers of the endometrial stroma lacunar dilatations of thin walled blood vessels (altered arterioles and capillaries) are evident which reveal a variably intense proliferation of their endothelial cells (fig 5 and 8). Some of the endothelial cells swollen and globular bulge into the lumen (fig 6) others are enlarged to the size and shape of the decidual cells, have round chromatin poor nuclei and are often multinucleate (fig 7). They have a homogeneous cytoplasm in which — with the above mentioned histochemical methods — only glycogen and neutral mucopolysaccharides are demonstrable with the

tartrazin after Lendrum Masson's trichrome stain⁴ Mallory's trichrome stain⁴ Heidenhain's Azan stain⁴ Movat's penta chrome stain⁴ Gomori's and Papanicolaou's reticulum stain⁴ and Mallory's fibrin stain (phosphotungstic acid hematoxylin⁵)

The histochemical reactions employed were Sudan Black B⁶ PAS with and without diastase⁷ aldehyde fuchsin with and without oxidation⁸ toluidine blue (at pH 4.5 and 7.0)⁹ alcian blue (at pH 2.5)¹⁰ alcian blue PAS (according to Manual of Histologic and Special Staining Techniques AFIP Washington D C 57) coupled tetrazolium reaction with and without benzoylation¹¹ Adams DMAB (p dimethyl amino benzaldehyde) nitrite method for tryptophan¹² Geyers modification of the Morel Sisky reaction for tyrosine hydroxy naphthaldehyde method for protein bound NH₂ groups after Weiss et al.¹³ reaction for histidine after Bachmann and Seitz reaction for SH groups after Barnett and Seligman¹⁴ and determination of the isoelectric point with methylene blue at controlled pH after Fischinger¹⁵

RESULTS

In table 1 the results of the study of the glands the stromal cells and the blood vessels of the 64 endometria are presented

(a) When viewed under low magnification the variations in thickness of the endometria are very striking. Even more striking are the *changing proportional relationships between the volumes of the glands and of the stroma*. In the normal proliferative phase (control cases) and after treatment with only estrogen or progesterone or with these combined in ineffectual doses or with estrogen and relaxin this relationship is 1:1 that is the straight glands extending through the functionalis from the basalis to the surface occupy about the same amount of space as does the intervening stroma. During pregnancy as well as after the combined administration of estrogen and progesterone in physiological doses the gland:stroma relationship is altered in favor of the stroma which is greatly thickened and has assumed a predecidual appearance especially in the more superficial levels of the endometrium (the so called

compacta) (fig 1). In contrast the dilated portions of the glands now form the spongiosa and lie adjacent to the basalis. The longer progesterone is administered the more the glands regress in the intensely developed almost decidual like stroma (no 231-234). On the other hand the addition of relaxin appears to have no effect on this relationship. If small doses of progesterone are given relative to a long pretreatment with estrogen the relationship may be altered in favor of the glands which at times may be found tightly coiled and extending to the surface (no 273).

(b) The *glandular secretion* is essentially dependent on a sufficient dose of progesterone which of course must have been preceded by an adequate treatment with estrogen. With an additional administration of relaxin the progesterone effect on the glands is not changed but hypersecretion and vacuolization occurs similar to the Arias-Stella Phenomenon in women. In the absence of progesterone relaxin alone cannot cause the glands to secrete (nos 288-290-293).

(c) Since the differentiation of the stroma cells into *predecidual cells* on one hand and into *granulocytes* on the other run practically parallel to one another the concomitant changes will be considered together. It should be noted that the granulocytes in the monkey uterus may be very numerous in the superficial compacta zone but occur in the basal portion of the endometrium as well and there in greater numbers than in the human uterus. The differentiation of both types of cells predecidual cells and granulocytes like the glandular secretion appears only after distinct combinations of hormones. Sufficient doses of progesterone and adequate pretreatment with estrogen or if no estrogen has been given progesterone and relaxin (no 253). If the daily doses of progesterone are too small (no 257) or preceded by a prolonged (80 days) estrogen treatment (from a previous experiment) (no 248) neither predecidual cells nor granulocytes develop normally. Monkey 274 treated the same as no 248

⁴ See Pearce
⁵ See Humason
⁶ See Romeis

but without the previous estrogen administration shows predecidual change and many granulocytes. The number of granulocytes which develop only in the presence of progesterone is closely proportional to the amount of progesterone administered. On the other hand under the influence of progesterone alone there is only little growth and consequently neither predecidual cells nor granulocytes develop (no 226). With progesterone given over prolonged periods (56 days no 231 234) a degranulation of the numerically unaltered granulocytes is evident. If relaxin is added to estrogen and progesterone the differentiation of the stromal cells into the pre-decidual type and into granulocytes is still further enhanced. The predecidual cells appear somewhat larger and the granulocytes seem to increase moderately in number (from +++ to ++++) the shape of the granulocytes and the granulation of their cytoplasm remain unchanged (fig 2). Following the administration of only estradiol and relaxin (nos 288 290 292) only a few granulocytes are demonstrable and after estradiol alone followed by estradiol and relaxin (no 233) still fewer granulocytes are evident than when progesterone is administered simultaneously. When only progesterone and relaxin are given in the total (no 253) or in the final treatment (nos 249 and 287) the granulocytes become numerous.

When progesterone with or without relaxin is administered over a prolonged period of time (56 days nos 231 234 56 days no 256 with 41 days relaxin) an intense proliferation and differentiation of the periarterial cells into granulocytes becomes especially striking in the basal layers of the endometrium. Here these granulocytes invest the spiral arteries to produce thick mantles (fig 3). Such periarterial aggregates of granulocytes are demonstrable under the same hormonal conditions which lead to the differentiation of predecidual cells and granulocytes. The thickness of the mantle of cells about the arteries and arterioles (fig 4) is proportional to the total number of granulocytes in the uterus.

The granulocytes in the monkey endometria described here resemble morphologically the granulocytes of the human

endometrium hence further description of them is unnecessary. The histological and histochemical methods used are comparable to the studies carried out on the granulocytes of human uteri. The intra cytoplasmic granules of the granulocytes stain weakly pink with H + E thus they are difficult to recognize. With the phloxine tartrazin stain they contrast sharply from the remaining cytoplasmic structures because of their bright red phloxinophilia. In addition they are red with the Azan stain Masson's trichrome stain and pentachrome stain. With Mallory's fibrin stain they are violet. The granules give a positive tetrazolium reaction which becomes negative after benzooylation. The reaction for tryptophan is strongly positive those for histidine lysine tyrosine and SH groups are also positive. The isoelectric point as measured with methylene blue on formalin fixed sections is at pH 4.4. The PAS reaction after diastase digestion is weakly positive for some of the granules. The same is true for the aldehyde fuchsin stain after oxidation whereas it is negative without oxidation. In some of the granules the alcian blue reaction is positive. With the alcian blue PAS combination the granules appear blue. They fail to give an absolute (alcohol fast) metachromasia but a red color reaction is retained after dehydration with acetone. They react negatively to Sudan Black B. These histochemical results suggest that the granules consist of an acidophilic protein to which possibly an acid mucopolysaccharide is more or less loosely bound.

(d) In some animals in the superficial layers of the endometrial stroma lacunar dilatations of thin walled blood vessels (altered arterioles and capillaries) are evident which reveal a variably intense proliferation of their endothelial cells (fig 5 and 8). Some of the endothelial cells swollen and globular bulge into the lumen (fig 6) others are enlarged to the size and shape of the decidual cells have round chromatin poor nuclei and are often multinucleate (fig 7). They have a homogeneous cytoplasm in which — with the above mentioned histochemical methods — only glycogen and neutral mucopolysaccharides are demonstrable with the

TABLE 1

The left half of this table is a condensation of treatments given to each monkey. In all animals receiving estradiol this was given first as pretreatment. Where the duration of estradiol therapy exceeds that of the other hormones the period of estradiol pretreatment may be calculated by subtracting the days of estradiol or progesterone therapy from the days estradiol was given. Where the duration of estradiol therapy does not exceed that of the other hormones estradiol was injected only as pretreatment and not included in the final treatment (nos 286-287, 291-249, 289, 285, 284, 271). Only one monkey was given estradiol as pretreatment (no 233). Monkey 248 had received estradiol in a previous experiment thus the long estradiol therapy. In monkeys 289 and 291 relaxin therapy was discontinued two days in 296 and 297 four days before the progesterone treatment ended. The right half of the table summarizes the histologic changes observed in the endometria. They are indicated by the signs¹.

Animal no	Hormone treatment (daily dose — days given)					Results				
	Estradiol	Estradiol	Progesterone	Relaxin	GPU	Gland/stroma ratio	Gland secretion	Predecidual change	Granulocytes	Endothelial proliferation
	10 µg	mg	mg							
11 normal controls	—	—	—	—	—	1 1	—	—	(+)	—
2 abortions	—	—	—	—	—	1 4	++	++	++	++
270	20d	—	—	—	—	1 1	—	—	—	—
225	—	0.5-35d	—	—	—	1 1	—	—	—	—
227	—	1-30d	—	—	—	1 1	—	—	—	—
228	—	1-34d	—	—	—	1 1	—	—	—	—
226	—	—	2-31d	—	—	1 1	—	—	—	—
263	45d	—	0.5-30d	—	—	1 1	—	—	+	—
245	51d	—	0.5-43d	—	—	1 1	—	—	—	—
267	51d	—	1-35d	—	—	1 1	—	—	—	—
237	40d	—	2-20d	—	—	1 1	++	—	++	—
251	39d	—	2-19d	—	—	1 1	++	+	++	—
259	49d	—	2-31d	—	—	2 1	++	++	++	—
269	59d	—	1-42d	—	—	1 1	—	—	+	—
238	53d	—	2-43d	—	—	1 2	++	++	++	—
231 234	71d	—	2-56d	—	—	1 8	++	++	++	—
293	—	—	—	6000-20d	—	1 1	—	—	—	—
288 290	44d	—	—	6000-20d	—	1 1	+	—	+	++
292	41d	—	—	6000-20d	—	1 1	+	—	+	+
295	15d	—	—	6000-20d	—	1 2	+	—	+	+
233	—	0.5-31d	—	6000-20d	—	1 2	+	—	+	+

Animal	Sex	Age	Period	Days	Observations	Endometrium	Capillaries	Subepithelial	Superficial	Remarks
237	♂	5 d	05-30d	11	—	—	—	—	—	+
273	♂	50d	1-35d	21	—	++	++	++	++	(+)
287	♂	20d	2-35d	12	—	++	++	++	++	++
288	♂	20d	2-13d	11	—	++	++	++	++	+
291	♂	20d	25-20d	11	—	++	++	++	++	+
292	♂	14d	2-10d	11	—	++	++	++	++	+
293	♂	50d	25-20d	12	—	++	++	++	++	++
294	♂	25d	2-35d	12	—	++	++	++	++	++
295	♂	20d	2-37d	12	—	++	++	++	++	++
296	♂	20d	2-13d	12	—	++	++	++	++	++
297	♂	13d	5-20d	12	—	++	++	++	++	++
298	♂	13d	2-10d	11	—	++	++	++	++	++
299	♂	73d	5-20d	13	—	++	++	++	++	++
300	♂	55d	2-58d	11	—	++	++	++	++	++
301	♂	57d	1-80d	11	—	++	++	++	++	++
302	♂	65d	1-40d	11	—	++	++	++	++	++
303	♂	65d	1-50d	11	—	++	++	++	++	++
304	♂	31d	1-50d	11	—	++	++	++	++	++
305	♂	67d	025-21d	12	—	++	++	++	++	++
306	♂	26d	1-41d	12	—	++	++	++	++	++
307	♂	54d	05-00d	12	—	++	++	++	++	++
308	♂	61d	1-20d	12	—	++	++	++	++	++
309	♂	55d	1-35d	13	—	++	++	++	++	++
310	♂	20d	2-40d	13	—	++	++	++	++	++
311	♂	20d	025-31d	12	—	++	++	++	++	++
312	♂	20d	05-32d	14	—	++	++	++	++	++
313	♂	15d	05-36d	21	—	++	++	++	++	++
314	♂	68d	1-42d	12	—	++	++	++	++	++
315	♂	51d	1-36d	11	—	++	++	++	++	++
316	♂	51d	4-36d	11	—	++	++	++	++	++

1 F the g n locyte — none; (+) 17 occasional cells in the sup rchial end metrium + few scattered cells mainly in the superficial endometrium; + + num rou g nubocytes local; 2 p ntr in the c + + comp u s g nubocytes in 11 layers of endometrium + + + + + very large num ber f g nubocytes entered 2 th of the decidua in 5 d other changed — non i + light; + + mode sig + + + + + extensive Und r endo metrial proliferati n (+) indic tes enlargement of the endothelial cells in a few non dilated subepithelial capillaries

PAS and alcian blue PAS reaction Often the cells are stratified in several layers In two monkeys (nos 288 and 290) some of these blood vessels are almost occluded by plump hillock like clusters of the hyperplastic endothelial cells (fig 9 and 10) They are delineated from the surrounding endometrial stromal cells only by the intact but inconspicuous basement membrane Most of these stromal cells next to the basement membrane are well differentiated granulocytes (fig 7) They replace the missing media and adventitia of these vessels Many of these dilated arterioles and capillaries pursue a tortuous course through the endometrial stroma others run parallel to the surface directly beneath the mucosal epithelium (fig 8) On cursory examination it is easy to mistake these vessels as glands With the alcian blue PAS reaction however they are readily differentiated The epithelial cells of the glands contain a secretion staining intensely blue (acid mucopolysaccharides) whereas the proliferating endothelial cells are filled with a finely granular red substance (neutral mucopolysaccharides and glycogen)

These changes of the arterioles as seen in this study are found only in those animals which received relaxin In addition in this series such changes were ob-

served always and only when comparatively little estradiol (0.25 mg no 285) or no estradiol (nos 249, 253, 256, 257, 264, 278, 286-292) was administered The arteriolar response after 0.25 mg estradiol with relaxin (6000 GPU) appears to be decreased, and 0.5-1.0 mg estradiol causes complete inhibition of this response in some endometria whereas in others a few non dilated subepithelial capillaries may have enlarged endothelial cells (see table 1) On the other hand the usual daily dose of estradiol (10 µg) or more does not seem to depress the action of relaxin on the blood vessels Furthermore there are no indications of an inhibitory influence on this action of relaxin when progesterone was given alone (no 253) or in combination with estradiol (nos 249, 256, 257, 264, 286, 287, 289) Hence these vascular changes appear after relaxin is administered in the absence of estrogen (no 233) or progesterone (nos 288, 290, 292) Actually the endothelial proliferation appears most pronounced after relaxin is given with only estradiol (nos 288 and 290) whereas the vascular dilatation is best seen after only progesterone and relaxin in the total (no 253) or final treatment (nos 289, 278) Prolonged doses of relaxin effect no further increase in these changes (compare no 256 with 264) The

TABLE 2

Although this represents a simplification of the results of the hormone treatments this table is supposed to provide a survey of the actions of these hormones when given in doses thought to be physiological and not over prolonged periods of time Hence e.g. the formation of endogenous relaxin following prolonged treatment with estrogen and progesterone with resulting endothelial proliferation is not considered in this table

Treatment	Decidual change	Granulocytes	Gland secretion	Endothelial proliferation
E	-	-	-	-
P	-	-	-	-
R	-	-	-	-
E+P	+	+	+	-
E+R	-	-	-	+
				(proliferation enhanced)
P+R	(+)	+	+	+
				(dilatation enhanced)
E+P+R	+	+	+	+

E estrogen P progesterone R relaxin

withdrawal of relaxin 2-4 days prior to discontinuing the progesterone (nos 291-296) brings about a decrease in the vascular dilatation and endothelial proliferation as compared to nos 286 and 287. This decrease fails to occur in monkeys 289 and 297 in which relaxin was also withdrawn 2-4 days early but in which the daily dose of progesterone was twice that given to no 291. Although the estrogen (and relaxin) doses were the same in animals 288-290 (juvenile monkeys) and 292 (an adult castrate) the latter had a reduced endothelial proliferation probably because of its castrated state and larger size.

(c) In those cases in which the endometrium is especially rich in granulocytes one may observe with silver impregnation techniques a focal dissolution of the reticulum fibers which normally envelop individual stromal cells. This is especially evident in monkey 256 which has received relaxin over a long period of time (41 days).

DISCUSSION

In order to evaluate the action of relaxin on the endometrium we must try to separate its activity from the combined effect of estrogen-progesterone treatment. This is indeed possible from the cases studied (see table 2).

The actions of relaxin on the monkey uterus may be summarized as follows: (1) The hormone functions as an intensifier of growth and differentiation of the endometrial stroma especially of the granulocytes but does not initiate these effects. With a suitable pretreatment with estrogen and a simultaneous administration of estrogen and progesterone or progesterone alone (nos 249-287) relaxin enhances their effect. In the absence of progesterone relaxin remains ineffective on the endometrial stromal cells. As suggested by one experiment (no 253) relaxin may be effective on the stromal cells in the absence of estrogen (pretreatment and final treatment) but this possibility requires further testing. (2) After prolonged administration and in the presence of adequate amounts of estrogen and progesterone relaxin calls forth an especially rich accumulation of granulo-

cytes about the spiral arteries of the basal endometrium as does a prolonged administration of progesterone without the addition of relaxin. (3) Relaxin as well as progesterone when given continuously over long periods of time may eventually lead to degranulation of the granulocytes and to hypersegmentation of their nuclei. (4) Relaxin induces an enlargement of the arterioles and capillaries and a proliferation of their endothelial cells in the superficial portions of the endometrium and alone seems responsible for this effect. The smallest dose and the shortest time interval needed for the appearance of these changes cannot be determined from these studies although the dose of relaxin given to monkey 278 appears to be quite small (low potency preparation of relaxin). Present results indicate that estrin may be more effective than estradiol in inhibiting the action of relaxin on the endothelium of endometrial blood vessels but this has not been proven on the basis of relative estrogenicity of the two compounds.

Of all these effects only the endothelial proliferation in the arterioles and capillaries may be interpreted as due solely to relaxin. The occurrence and physiology of these vascular changes in this series of monkeys have been described and interpreted by Hisaw and Hisaw (66). Whereas the granulocytes always occur only with a simultaneous change of the remaining stromal cells into predecidual or decidual cells the endothelial proliferation appears entirely independent of the degree of differentiation of the endometrial stroma and may be seen for example in a non-secretory endometrium (nos 288-290 and 292). The enhanced differentiation of the endometrial stroma after relaxin treatment in the presence of estrogen and progesterone is interesting for the following reasons. The synergism between estrogen and progesterone which occurs in the presence of endogenous relaxin may be the result of the relaxin action itself hence can be increased by the injection of exogenous relaxin. Hisaw and Hisaw (64) showed that in monkeys receiving estrogen and progesterone a formation of endogenous relaxin (0.2 to 0.3 GPU/ml blood serum)

takes place (no 259) its site of formation is to be looked for in the endometrial granulocytes. The periarteriolar mantle like accumulations of granulocytic cells like the granulocytes in the remaining decidua are therefore, to be regarded as evidence of an increased formation of relaxin, brought about by progesterone not however as being induced by relaxin. The degranulation of the granulocytes probably results from a prolonged excessive action of exogenous or endogenous relaxin that is formed following progesterone therapy over long periods. The mechanism of this degranulation remains unclear. The decrease in endothelial proliferation after relaxin withdrawal (nos 291-296) did not occur when the daily dose of progesterone was 5 mg (nos 289-297). It is presumed that this dosage of progesterone enhanced the formation of endogenous relaxin in the granulocytes. This endogenous relaxin most likely replaced the exogenous relaxin withdrawn.

An increase of the granulocytes in the endometrium of the monkey after treatment with estrogen and progesterone was also observed by Cleveland (41). This has also been seen in endometrial tissue from castrated women during experimental studies of hormone substitution therapy (Helleweg et al 60). Morphologically the endometrial granulocytes of the human uterus (Hamperl 54 Helleweg 54) and those of the monkey are virtually identical. Furthermore both resemble the frequently described granular cells of the mesometrial decidua and the metrial gland of the pregnant rat. Histochemically only slight differences exist between the granulocytes of these three species. These differences apparently are limited to a prosthetic group bound more or less firmly to the acidophilic protein. In monkeys this prosthetic group apparently consists of acid mucopolysaccharides corresponding consequently to that of the similar appearing granules of the rat (Wislocki et al 57). In human granulocytes such a prosthetic group is demonstrable only very rarely for the granules of the granulocytes are present almost always as a pure protein (Helleweg 56). Relaxin has been demonstrated immunohistologically in the endometrial granulocytes

of the human uterus and in the granular cells of the pregnant rat (Dallenbach and Dallenbach Helleweg 64 Dallenbach Helleweg et al 65). At the present time we are engaged in a study using similar techniques to determine if relaxin is also present in the endometrial granulocytes of the monkey. Differences between the granular cells in women monkeys and rats may be related to their localization and can be interpreted as an adaptation required by the varying types of placentation. In the rat these granular cells are present chiefly in the myometrium and appear only during pregnancy and pseudopregnancy. In the human uterus they are limited to the endometrium in nonpregnant and to the basal plate of the mature placenta in pregnant women. In the monkey these cells are so-to-speak intermediary being found in the superficial parts of the myometrium as well as in the endometrium in the nonpregnant animal and in the basal plate of the placenta and adjacent myometrial portion during pregnancy. A periarterial accumulation of specific decidual cells has been noticed in the pregnant monkey by Wislocki and Streeter (38) and by Ramsey (49) in the human decidua by Ercolani (1873) Waldeyer (1890) Paladino (1900) Litwak (31) and Brettner (64) and it is well known as constituting a major part of the metrial gland of the pregnant (Weill 19 and many others) and pseudopregnant rat (Selye and McKeown 35 Velardo et al 53 Ellis 57). It has furthermore been observed in the pregnant mouse (Goldmann 12 and many others) rabbit (Minot 1889 and others) golden hamster (Orsini, 54) and in insectivores *Macroscelides proboscideus* (Starck 49) *Naslio brachyrhynchus* (Gérard 23) *Elephantulus myurus* (van der Horst and Gillman 46) and *Tenrec ecaudatus* (Götz 37).

The endothelial proliferation similar to that brought about by exogenous relaxin has also been observed under normal physiologic conditions namely during early pregnancy which hormonally provides a favorable state for the secretion of endogenous relaxin apparently exceeding that of the menstrual cycle. Such proliferative changes of the vascular endo-

thelium were described by Wislocki and Streeter (38) and by Ramsey (49) in the decidua of the pregnant monkey. Wislocki and Streeter called this "cytotrophoblastic" because the walls of these enlarged vessels have undergone such a change with an apparent disappearance of the medial and adventitial coats the vessels easily may be mistaken for venous.

They are however continuous with the spiral arterioles as clearly shown by Ramsey (49). We therefore may assume that the structures of these vascular walls have been changed into or replaced by the granulocytes directly adjacent to the proliferated endothelial cells and separated from them only by the basement membrane. The numerous vessels beneath the endometrial surface showing endothelial proliferation are most likely proliferated and greatly dilated capillaries. Similar changes of the vascular endothelium have been known in the human uterus and have been described often in the basal decidua (Grosser 27 see literature there; Ortman 55; Wilkin 60). In the mesometrial decidua of the pregnant rat such changes of the arterioles were found in the immediate vicinity of the implantation of the ovum (Goldman 12; Szendi 33; Bridgman 48; Bulmer and Dickson 60; Dallenbach-Hellweg et al. 65) and beginning on the thirteenth day these modified arterioles were seen together with the first major appearance of the granular cells in the metrial gland (Gérard 25; Selje and McKeown 35; Baker 48). Endothelial proliferation has further more been seen in the pregnant rabbit (Minot 1889; Maximow 1898 and others), golden hamster (Orsini 54), guinea pig (Pytler and Strasser 25; Grosser 27), mouse (Goldman 12 and many others), ewe (Bjorkman 65), and in several insectivores: *Macroscelides proboscideus* (Starck 49), *Nasillo brachyrhynchus* (Gérard 23), *Tenrec ecaudatus* (Grosser 28; Goetz 37), *Sorex vulgaris* (Hubrecht 1894), *Sorex fumeus* and *Blarina brevicauda* (Wimsatt and Wislocki 47). That these cells are not of trophoblastic origin in spite of their morphologic similarities with syncytial trophoblastic cells is clearly evident in this series of non-pregnant monkeys. The proliferating endo-

thelial cells of the rat (Szendi 33) and of the monkey (see the above description) as well as those of the human uterus (Ortmann 55) contain polysaccharides or glycogen. Two histologic features suggest that these changes of the arterioles are closely related to the action of relaxin. They occur physiologically only with the marked accumulation of the granulocytes and only in their immediate vicinity. It is indeed interesting that Rossman (40) saw an identical endothelial proliferation in decidualomas of monkeys and Hisaw (44) in the endometrium of the monkey after menstruation was postponed by prolonging the functional activity of the corpus luteum with chorionic gonadotropin.

The function of these dilatations and endothelial proliferations of the arterioles and capillaries remains to be elucidated. It seems tempting to assume that in the preparation for implantation they enhance the blood supply and hence nutrition for the embryo. This action would be in accord with the concept that relaxin facilitates implantation and would permit the conclusion that relaxin is a true hormone of pregnancy.

ACKNOWLEDGMENT

The relaxin used in these experiments was supplied by the Warner-Lambert Research Institute, the research affiliate of Warner-Chilcott Laboratories, Morris Plains, New Jersey.

LITERATURE CITED

- Bachmann R. and H. M. Seitz 1961. Zur histochemischen Darstellung des Histidin mit Diazoniumsalzen. *Histochemie* 2: 307-312.
 Baker B. L. 1948. Histochemical variations in the metrial gland of the rat during pregnancy and lactation. *Proc. Soc. Exp. Biol. Med.* 68: 432-436.
 Bartelmez G. W., G. W. Corner and C. G. Hartman 1951. Cyclic changes in the endometrium of the rhesus monkey (*Macaca mulatta*). *Contrib. to Embryol.* 34: 99-144, no. 227. *Carnegie Inst. Wash. Publ.* 592.
 Bjorkman N. 1965. Fine structure of the ovine placenta. *J. of Anat.* 99: 283-297.
 Brettner A. 1964. Zum Verhalten der sekundären Wand der Uteroplacentalgefäße bei der decidualen Reaktion. *Acta Anat.* 57: 367-376.
 Bridgman J. 1948. A morphological study of the development of the placenta of the rat I. An outline of the development of the pla-

- centa of the white rat *J Morphol* 83 61-85 II An histological and cytological study of the development of the chorioallantoic placenta of the white rat *J Morphol* 83 195-223
- Bulmer D and A D Dickson 1960 Observations on carbohydrate materials in the rat placenta *J Anat* 94 46-58
- Cleveland R 1941 Cytologic and histologic observations on the epithelial connective and vascular tissues of the endometrium of macaques under various experimental conditions *Endocrinology* 28 388-405
- Dallenbach F D and G Dallenbach Hellweg 1964 Immunohistologische Untersuchungen zur Lokalisation des Relaxins in menschlicher Placenta und Decidua *Virchows Arch path Anat* 337 301-316
- Dallenbach Hellweg G J V Battista and F D Dallenbach 1965 Immunohistological and histochemical localization of relaxin in the metrial gland of the pregnant rat *Am J Anat* 117 433-450
- Ellis R A 1957 Histochemistry of the cellular components of the metrial gland of the rat during prolonged pseudopregnancy *Anat Rec* 129 39-51
- Ercolani G B 1873 *Della struttura anatomica della caduca uterina nei casi di gravidanza extrauterina nella donna* Mem Acad Sci Ist Bologna Ser 34 397-414
- Gérard P 1923 Etude sur les modifications de l'utérus pendant la gestation chez *Nasella brachyrhynchus* (Smith) *Arch de Biol* 33 197-227
- 1925 Sur la glande myométriale de la souris et du rat *C R Soc de Biol* 93 457-459
- Geyer G 1962 Eine Modifikation der Morel-Sisley Reaktion auf Tyrosin *Acta histochem* 13 355-356
- Goetz R H 1937 Studien zur Plazentation der Centetiden I Eine Neuuntersuchung der Centetes Plazenta *Zeitschr f Anat u Entwicklgesch* 106 315-342
- Goldmann E E 1912 Die aussere und innere Sekretion des gesunden und kranken Organismus im Lichte der vitalen Färbung *Beitr klin Chirurgie* 78 1-108
- Grosser O 1927 *Frühentwicklung Eihautbildung und Placentation des Menschen und der Säugetiere* München J F Bergmann pp 74-403
- 1928 Die Placenta von Centetes und ihre Lehren betreffs der Stoffaufnahme in den Placenten *Zeitschr f Anat u Entwicklgesch* 88 509-521
- Hamperl H 1954 Über endometriale Granulocyten (endometriale Kornchenzellen) *Klin Wochr* 32 665-668
- Hellweg G 1954 Über endometriale Kornchenzellen (endometriale Granulocyten) *Arch Gynak* 185 150-166
- 1956 Untersuchungen zur Charakterisierung der Granula in endometrialen Kornchenzellen *Virchows Arch* 329 111-120
- 1959 Über körnchenhaltige Zellen im menschlichen und tierischen Endometrium (endometriale Kornchenzellen metachromasie rende Zellen) *Zeitschr f Zellforsch* 49 555-568
- Hellweg G J Ferin and K G Ober 1960 Über die Bildung von endometrialen Kornchenzellen bei Kastrationen unter Hormoneinfluss *Acta Endocrinologica* 23 261-276
- Hisaw F L 1944 The placental gonadotrophin and luteal function in monkeys (*Macaca mulatta*) *Yale J Biol Med* 17 119-137
- Hisaw F L Jr, and F L Hisaw 1964 Effect of relaxin on the uterus of monkeys (*Macaca mulatta*) with observations on the cervix and symphysis pubis *Amer J Obstet Gynec* 89 141-155
- Hisaw F L and F L Hisaw Jr 1966 Effect of relaxin on the endothelium of endometrial blood vessels in monkeys (*Macaca mulatta*) In Press
- Horst van der C J and J Gillman 1946 The reactions of the uterine blood vessels before during and after pregnancy in elephant *S Afr J Med Sci* 11 Biol Suppl 103-111
- Hubrecht A A W 1894 Studies in mammalian embryology III The placentation of the shrew (*Sorex vulgaris* L.) *Quart J Micr Sci* 35 481-537
- Humason G L 1962 *Animal tissue techniques* San Francisco and London W H Freeman & Co
- Lendrum A C 1947 The Phloxine-tartraz method as general histological stain and for the demonstration of inclusion bodies *J Path Bact* 59 399-404
- Litwak M J 1931 Histologische Untersuchungen schwangerer und puerperaler Gebärmutter II Mitteilung *Arch f Gynak* 143 673-687
- Maximow A 1898 Zur Kenntnis des feineren Baues der Kaninchenplazenta *Arch f mik Anat* 51 68-136
- Minot C S 1889 Uterus and Embryo I Rabbit II Man *J Morphol* 2 341-462
- Orsinio M W 1954 The trophoblastic giant cells and endovascular cells associated with pregnancy in the hamster *Cricetus auratus* *Am J Anat* 94 273-331
- Ottmann R 1953 Histochemische Untersuchungen an menschlicher Placenta mit besonderer Berücksichtigung der Kernkugeln (Kernschlüsse) und der Plasmalipoideneinschlüsse *Zeitschr f Anat u Entwicklgesch* 119 28-54
- Paladino G 1900 De la genèse et du temp dans lequel apparaissent les cellules géantes dans le placenta humain *Arch Ital Biol* 33 290-295
- Pearse A G E 1961 *Histochemistry theoretical and applied* Little Brown & Co Boston
- Pytler R and H Strasser 1925 Die Vorgänge im Meerschweinchenuterus von der Inkulation des Eies bis zur Bildung des Plazentardiscus *Zeitschr f Anat u Entwicklgesch* 76 386-420
- Ramsey E M 1949 The vascular pattern of the endometrium of the pregnant rhesus monkey (*Macaca mulatta*) *Carnegie Inst Wash Publ* 583 *Contrib to Embryol* 33 113-148 no 219

- Romeis B 1962 Mikroskopische Technik. Olden-
burg Verlag Munchen
- Rossmann I 1940 The deciduomata reaction in
the rhesus monkey (*Macaca mulatta*) Am
J Anat 66 277-365
- Selye H and T McKeown 1935 Studies on
the physiology of the maternal placenta in the
rat Proc Roy Soc Lond 119 1-31
- Starck D 1949 Ein Beitrag zur Kenntnis der
Placentation bei den Macroscelididen Zeitschr
f Anat u Entwicklungsgesch 114 319-339
- Szendzi B 1933 Die Wege des Glykogens durch
die hämochoriale Placenta Zeitschr f Anat
und Entwicklungsgesch 101 791-798
- Velardo J T A B Dawson A G Olsen and
F L Hisaw 1953 Sequence of histological
changes in the uterus and vagina of the rat
during prolongation of pseudopregnancy as
associated with the presence of deciduomata
Am J Anat 93 273-305
- Waldeyer W 1890 Bemerkungen über den
Bau der Menschen und Affen Placenta Arch
mikr Anat. 30 1-51
- Weill P 1919 Glande myométriale endocrine
dans l'utérus de la rate gestante C R. Soc
Biol 82 1433-1435
- Wilkin P 1960 La vascularisation de l'endo-
mètre humain au cours de la phase progesta-
tive du cycle menstruel et au cours de la
nidation ovulaire Les fonctions de nidation
utérine et leurs troubles Masson et Cie Paris
pp 331-345
- Wimsatt W A and G B Wislocki 1947 The
placentation of the American shrews *blarina
brevicauda* and *sorex fumens* Am J Anat
60 361-435
- Wislocki G B and G L Streeter 1938 On
the placentation of the macaque (*Macaca
mulatta*) from the time of implantation until
the formation of the definitive placenta
Contr to Embryol 27 1-66 no 160 Carnegie
Inst Wash Publ 496
- Wislocki G B L P Weiss M H Burgos and
R A Ellis 1957 The cytology histochemistry
and electron microscopy of the granular cells
of the metrial gland of the gravid rat J of
Anat 91 130-140

PLATE 1

EXPLANATION OF FIGURES

- 1 Predecidual appearance of the endometrial stroma with scarcity of glands following administration of estrogen progesterone and relaxin Monkey 239 H and E stain Magnification 56 \times
- 2 Endometrial granulocytes with paranuclear accumulation of granules and peripheral vacuolization of cytoplasm surrounding a capillary in the compact layer of the endometrium after substitution with estrogen progesterone and relaxin Monkey 285 H and E stain Magnification 560 \times
- 3 Spiral arterioles in the basal layer of the endometrium surrounded by sheaths of granulocytes following prolonged relaxin administration for 41 days Monkey 256 H and E stain Magnification 138 \times
- 4 Periarterolar accumulation of granulocytes in the endometrium of the same monkey as in figure 1 H and E stain Magnification 560 \times

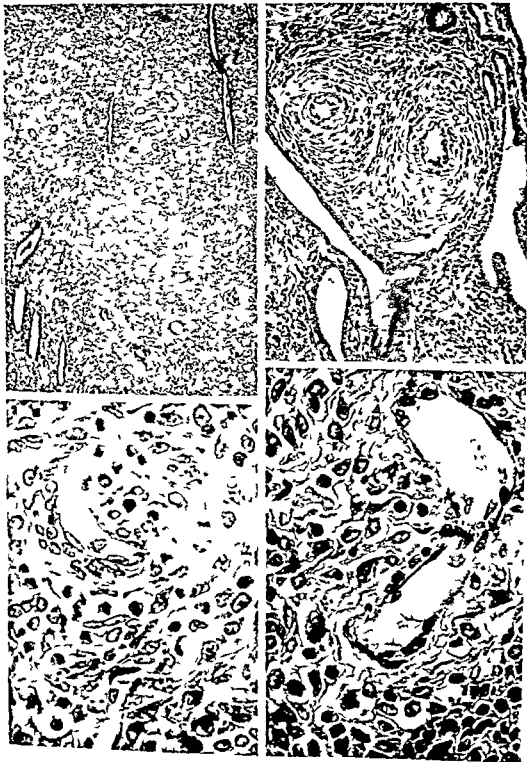


PLATE 1

EXPLANATION OF FIGURES

- 1 Precedual appearance of the endometrial stroma with scarcity of glands following administration of estrogen progesterone and relaxin Monkey 239 H and E stain Magnification 56 X
- 2 Endometrial granulocytes with paranuclear accumulation of granules and peripheral vacuolization of cytoplasm surrounding a capillary in the compact layer of the endometrium after substitution with estrogen progesterone and relaxin Monkey 285 H and E stain Magnification 560 X
- 3 Spiral arterioles in the basal layer of the endometrium surrounded by sheaths of granulocytes following prolonged relaxin administration for 41 days Monkey 256 H and E stain Magnification 138 X
- 4 Periarteriolar accumulation of granulocytes in the endometrium of the same monkey as in figure 1 H and E stain Magnification 560 X



PLATE 2

EXPLANATION OF FIGURES

- 5 Lacunar dilatation and endothelial proliferation of a capillary space underneath the surface epithelium of the endometrium of a monkey treated only with progesterone and relaxin no 253 H and E stain Magnification 90 X
- 6 Same monkey as in figure 5 The swollen endothelial cells bulge into the capillary lumen (upper half of the figure) The surrounding stroma and a neighboring gland (lower half) show incomplete progestational change in the absence of estrogen H and E stain Magnification 345 X
- 7 Endothelial proliferation with formation of large multinucleated giant cells and partial occlusion of the lumen of an arteriole in the compact layer of the endometrium following administration of estradiol progesterone and relaxin without estriol Next to the basement membrane of the arteriole groups of well differentiated granulocytes can be seen Monkey 249 H and E stain Magnification 560 X



PLATE 3

EXPLANATION OF FIGURES

- 8 Same monkey as in figure 7 Lacunar dilatation and tortuosity of arterioles and capillaries with endothelial proliferation underneath the surface epithelium In the lower middle of the figure a group of undilated spiral arteries At the upper right and lower left straight narrow portions of secreting glands H and E stain Magnification 70 \times
- 9 Endometrium from Monkey 288 treated only with estradiol and relaxin Proliferating glands and spindle shaped stromal cells in the absence of progestational change In the middle a capillary space occluded by extensive endothelial proliferation Phloxine Tartrazin stain Magnification 175 \times
- 10 Same monkey as in figure 9 A higher magnification (560 \times) of a capillary with partial occlusion of its lumen by large proliferated endothelial cells Phloxine Tartrazin stain

The Topographic Anatomy of the Muscles, Nerves, and Arteries of the Bovine Female Perineum

ROBERT E. HABEL

Department of Anatomy New York State Veterinary College
Cornell University Ithaca New York

ABSTRACT The perineal muscles and fasciae are described and illustrated and the diaphragma urogenitalis components of m sphincter urethrae and m ischio-cavernosus are described for the first time in the cow

The nerves of the pudendal plexus are discussed comparatively with the object of suggesting appropriate names based on their homology to the condition in other animals and man. The rami musculares to m. levator ani and m. coccygeus may originate from nn. sacrales 3 et 4 or n. pudendus or n. rectalis caudalis. The combination of rami musculares with n. rectalis caudalis was formerly called by veterinary anatomists n. hemorrhoidalis medius a term which should be abandoned because it is not listed in *Nomina anatomica* and because it has also been applied to n. splanchnicus pelvicius in the horse. N. pudendus is large and its rami cutanei supply regio femoris caudalis as well as regio perinealis. It also gives rise to n. perinealis profundus which supplies the genital muscles. The pudendal nerve ends by dividing into ramus mammarius and n. dorsalis clitoridis. There may be one or two nn. rectales caudales. They supply m. sphincter ani externus and adjacent parts of m. levator ani and the genital muscles.

The distribution of arteria urogenitalis (vaginalis) and a. pudenda interna are described and illustrated.

In spite of the clinical importance of the perineum of the cow no comprehensive study of it has been published. A brief description was included in a dissection guide (Habel 49-64). Various authors have described the muscles (Geiger 54, Bassett 61) and the blood vessels (Vollmerhaus 64) but the nerves have been described only in the male (Larson and Mitchell 58).

The purpose of this study was to prepare topographic descriptions and illustrations of the muscles, fasciae, nerves, and arteries. The veins were treated briefly as they were encountered in the dissection. Problems of comparative nomenclature of these structures required extensive reference to the literature of systematic anatomy in the effort to determine valid homologies among the domestic quadrupeds and man. Two essential criteria of veterinary anatomical nomenclature are homonymy of homologous structures in quadrupeds and the closest possible agreement with human nomenclature, the latter being modified to eliminate reference to the anatomical position. Thus the scope of the study was enlarged to include systematic

and comparative considerations and these are taken up in the discussions of individual structures. The genital organs and the anal canal were not examined because they have been adequately described in numerous works (Martin and Schauder 38, Schummer and Nickel 60).

MATERIALS AND METHODS

In addition to the specimens examined in the dissection room where six or seven cows are dissected each year by veterinary students using a laboratory guide that directs a study of the perineum (Habel 49) 22 preparations from 16 cows and six female calves were dissected especially for this investigation. Sixteen animals were fixed by arterial injection of 8% formalin and 2% phenol in water usually with the subject in the standing position (Lambert 16). After fixation the arteries were injected with colored starch glue or latex. Six preparations of the pelvic viscera were dissected in the fresh state with the aid of a stereoscopic microscope. Photographs and drawings were made during the dissections.

argued that the udder is not homologous to the scrotum but a similar objection applies to the ventral (anterior) limit of the human perineal region which includes the labia and excludes the scrotum. The perineal region was divided by a line connecting the ventromedial processes of the tubera ischiadica into an anal region and a urogenital region.

The perineal body lies in the median plane on the intertuberal line. In the cow it was formed by the junction of four striated muscles superficially and by a deeper mass of connective tissue and smooth muscle. The four striated muscles were sphincter ani externus, constrictor vulvae, transversus perinei superficialis

and the ventral band of the levator ani (fig 1). The smooth muscle of the perineal body was not identified histologically in this study. It has been well described by Geiger (54) as strands of the ventral longitudinal muscle of the rectum that turn ventrally decussate and pass into the smooth muscle of the labia and vestibule. This tract of smooth muscle known as the *Afterschamband* in German veterinary literature has received no Latin name in the NA but is apparently homologous to *m rectourethralis* in the male. Hayek (65) in his histological study of the smooth muscle of the human perineum suggested the term *m rectoperinealis* for the female. He showed a predominance of smooth muscle

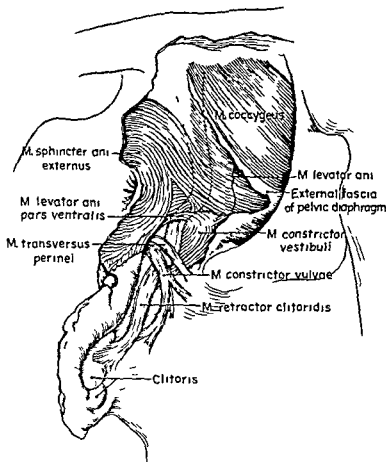


Fig 1 Perineal muscles of a cow exposed by removal of the deep fascia and retraction of the right labium. Caudolateral aspect.

MUSCLES AND FASCIAE

Regio perinealis

The terms in table 1 were extracted and rearranged from a list adopted by the World Association of Veterinary Anatomists for publication in *Nomina anatomica veterinaria*. The terms not applicable to this paper have been omitted and the order has been changed because the original typography identical with that of *Nomina anatomica* (NA Mitchell 61) gives the impression that the pelvic and urogenital diaphragms include all the structures in the anal and urogenital regions. According to Gray (59) and Gardner et al (63) the pelvic diaphragm is composed only of the levator ani and coccygeus muscles and the fasciae investing them; the urogenital diaphragm in man is composed of the transversus perinei profundus which does not occur in quadrupeds; the sphincter urethrae and the fasciae on the inner (superior) and outer (inferior) surfaces of these muscles.

Before the bovine perineum can be defined it is necessary to distinguish three concepts often confused: the perineum, the perineal region, and the perineal body. The perineum is the part of the body wall that covers the pelvic outlet and surrounds the anal and urogenital canals. As a part of the body wall it has an appreciable thickness and its deep boundaries — those of the pelvic outlet — are not the same as its superficial boundaries — those of the perineal region (Gray 59). An anatomical region is a surface area without depth but the perineal region was considered a part of the trunk by Gardner et al (63) and the same idea was implied by the change from Perineum to Regio perinealis under Partes corporis in the NA (Mitchell 61). The meaning of the term perineum is often restricted in obstetrics to the fibromuscular mass between the anus and vulva but this is more properly called the perineal body or Centrum tendineum perinei (NA).

The deep boundaries of the perineum in the cow were the first coccygeal vertebra, the sacrotuberous ligament, the dorsal and ventromedial processes of the tuber ischiadicum and the ischial arch (There is no pubic arch in domestic mammals). The superficial boundaries of the perineum or

TABLE 1

Nomenclature of muscles and fasciae

	Perineum
Regio perinealis	
Regio analis	
Regio urogenitalis	
Diaphragma pelvis	
M levator ani	
M coccygeus	
Fascia diaphragmatis pelvis interna	
Fascia diaphragmatis pelvis externa	
M sphincter ani externus	
Fossa ischiorectalis	
Corpus adiposum fossae ischiorectalis	
Canalis pudendalis	
Fascia pelvis	
F pelvis parietalis	
Fascia obturatoria	
F pelvis visceralis	
Septum rectovaginale	
Centrum tendineum perinei	
Diaphragma urogenitale	
M sphincter urethrae	
M urethralis	
M ischiourethralis	
M bulboglandularis	
Fascia diaphragmatis urogenitalis interna	
Fascia diaphragmatis urogenitalis externa	
M transversus perinei superficialis	
M ischioavernosus	
M bulbospongiosus	
M constrictor vestibuli	
M constrictor vulvae	
M retractor clitoridis	
Fascia superficialis perinei	
Fascia profunda perinei	

the boundaries of the perineal region had to be extended much farther ventrally than the ventral commissure of the labia to accommodate the perineal nerves and vessels in the area corresponding to that between the anus and the scrotum in the bull. Therefore the perineal region in the cow was bounded by the base of the tail, the sacrotuberous ligament (easily palpated), the dorsal and ventromedial processes of the tuber ischiadicum and a line from the tuber ischiadicum to the caudal attachment of the udder (fig 7). It could be

transverse processes of the first three coccygeal vertebrae. Its lateral surface was related to the internal pudendal artery, the branches of the pudendal nerve, the lesser sciatic foramen, and the fat in the ischio-rectal fossa.

Fasciae of the pelvic diaphragm (figs 41-5). The internal fascia of the pelvic diaphragm covered the medial surface of the coccygeus and levator muscles, forming a part of the parietal pelvic fascia, with which it was continuous cranially and dorsally. Caudally it passed from the levator to the rectum, where it was continuous with the visceral pelvic fascia. At the caudal border of the coccygeus muscle it fused with the external fascia. Ventrally it joined the external fascia at the ventral border of the levator and gave off the recto-vaginal septum.

The external fascia of the pelvic diaphragm covered the lateral surface of the coccygeus and levator muscles. It was attached cranially to the deep face of the sacrosciatic ligament and dorsally to the fascia on the sacrococcygeus. At the caudal border of the coccygeus it fused with the internal fascia of the pelvic diaphragm and joined the coccygeal fascia dorsal to the anus. It was attached to the tendinous inscription of the levator and was continuous with the deep fascia on the external anal sphincter and constrictor vestibuli. Ventrally it was continuous with the internal fascia at the ventral border of the levator, gave origin to the caudal part of the urethral muscle, and joined the urogenital diaphragm.

The pelvic diaphragm in quadrupeds is difficult to visualize as such because the right and left halves are so oblique that they lie almost in sagittal planes.

M. sphincter ani externus. The external anal sphincter completely encircled the anus (figs 3-4). Its most superficial fibers were radial and were attached to the skin. Most of the fibers crossed ventral to the anus and continued into the opposite labium as the constrictor vulvae. A few lateral fibers did not cross but passed into the labium on the same side.

The cranial part of the external anal sphincter was variably fused with the terminal portion of the levator. The dorsal band of the levator, which met its mate

over the anus, sometimes appeared to be long to the anal sphincter. An inconstant band of fibers took origin from the third coccygeal vertebra behind the coccygeus muscle and passed ventrally through the levator or across its deep surface to become continuous with the constrictor vestibuli. This band, when present, may be interpreted either as a coccygeal insertion of the levator or as a paired cranial part of the anal sphincter like that of the horse.

According to Bassett (65) the cranial part of the anal sphincter and the constrictor vestibuli in the sheep form a continuous muscle, the deep perineal sphincter. The functional concept may be useful, but the new term is unnecessary and undesirable because the anal and vestibular components are homologous to muscles that have received separate names in other domestic animals.

Fossa ischio-rectalis. The ischio-rectal fossa (Godina 39) lay lateral to the anus where it formed a visible depression in old multipara (figs 4-7). It was a triangular pyramid with three faces: a caudal base and a cranial apex. In animals in normal condition it was filled with fat. The medial wall was formed by the external fascia of the pelvic diaphragm and by the deep fascia on the constrictor vestibuli. The latero-dorsal wall was the sacrosciatic ligament and skin. The latero-ventral wall was the tuber ischiadicum and the obturator fascia. The apex was at the origin of the coccygeus muscle from the deep face of the sacrosciatic ligament. The base was covered by superficial fascia and skin. The internal pudendal artery and vein and the pudendal nerve ran obliquely caudoventrad in the ventral groove near the apex of the fossa between the obturator fascia and the fascia on the coccygeus. Laterally the distal cutaneous branch of the pudendal nerve passed along the medial surface of the tuber ischiadicum. Medially the deep perineal nerve ran along the genital tract to the urogenital muscles (fig 5).

Regio urogenitalis

M. transversus perinei profundus has not been demonstrated in quadrupeds with the possible exception of a muscle in the male goat called the ischio-urethralis by Heinemann (37). A similar muscle oc-

rather than tendinous tissue in the perineal center which has extensive connections in man and animals with the fasciae of the pelvic and urogenital diaphragms also shown by Hayek to have a large proportion of smooth muscle fibers

Regio analis

M levator ani (fig 3) The narrow tendon of origin was attached to the medial side of the sciatic spine near the lesser sciatic foramen. It was fused laterally with the tendon of the coccygeus which was adherent to the medial surface of the sacrosacral ligament (lig sacrospinotubercle). The levator was inserted by means of three main bands the fibers of which interpenetrated or were continuous with the fibers of the external anal sphincter. The middle band about 3 cm wide was inserted into the lateral part of the sphincter. The dorsal band about 1.5 cm wide blended with the sphincter dorsal to the anus where it was continuous with the contralateral muscle. The ventral portion blended with the ventral decussation of the external sphincter. A fourth inconstant insertion was attached to the coccygeal fascia (See cranial part of external anal sphincter).

The levator bore a transverse tendinous inscription (Geiger '54) where the fibers began to diverge to the insertion. At the ventral end of the inscription the constrictor vestibuli originated from the ventral border of the levator and from the fascia on its surface. The dorsal end of the inscription was attached to the coccygeal fascia. The external fascia of the pelvic diaphragm was loosely attached to the lateral surface of the levator except at the tendinous inscription with which it was fused.

The medial surface of the levator was related to the rectum and in the plane of the tendinous inscription to the retractor clitoridis. The caudal rectal nerve lay on the medial surface of the caudodorsal part of the muscle. The lateral surface was related to the coccygeus and to the ischio rectal fossa.

Bassett ('65) has raised again the question of the nomenclature of the levator ani in quadrupeds proposing that the coccygeus and levator be considered a single muscle the ischiococcygeus. This concept

and terminology should be rejected for the following reasons: (1) The muscles are quite distinct in other animals the coccygeus is lateral to the levator. Its fibers take a different direction and it is separated from the levator by a septum. Geiger's ('56) description and illustrations show the two muscles to be separate in the sheep. (2) The embryologic evidence presented by Bissett indicates that the coccygeus develops earlier than the levator. (3) Bassett's main argument against the use of the term levator ani in ungulates is that two parts of the human levator the iliococcygeus and pubococcygeus are not present with the same origins and insertions as in man. The human iliococcygeus is not directly attached to the ilium but originates in part from the spine of the ischium as in ungulates the insertion of the coccygeal fascia is much larger than in ungulates. The difference is a quantitative one readily explained by the increased supportive function in the erect posture. The human pubococcygeus originates from the pubis and is inserted in part on and around the external anal sphincter. The difference in ungulates is that the muscle is smaller and the pubic origin is lost or transferred to the spine of the ischium. According to Geiger ('56) the pubic origin is represented in the sheep by the arc tendineus which extends from the origin of the levator across the obturator internum to the pelvic symphysis. The arc tendineus was also described by Bassett ('65). The anal insertion is primary in ungulates and this idea would be lost if the term ischiococcygeus were adopted. (4) It is unfortunate that levator ani a gravitationally oriented term has been sanctioned by inclusion in the Basel, Jena and Paris nomenclatures of human anatomy (Kopsch '57) but since the function of the muscle as a part of the pelvic diaphragm is the same with regard to the long axis of the trunk in man and quadrupeds the name should be retained on functional as well as morphologic grounds.

M coccygeus (figs 3, 5) The common tendon of origin with the levator arose from the medial side of the sciatic spine and from the inside of the sacrosacral ligament. The muscle extended dorsocaudally crossing the lateral face of the levator obliquely and was inserted on the

separates *m. bulbospongiosus* (*m. constrictor vestibuli*) from *m. urethralis*.

M. urethralis in the cow covered the caudal half of the urethra, the suburethral diverticulum and the lateral walls of the genital tract at the junction of the vagina vestibule (fig 3). It was 6 mm thick ventrally but thin at the lateral attachments. The entire cranio-caudal extent was about 9 cm. Only the cranial 2 cm of the muscle was a true sphincter surrounding the urethra; the rest of the muscle consisted of fibers that passed around the ventral surface of the urethra and suburethral diverticulum from one side of the genital tract to the other. The vaginal segment of the muscle was 4 cm wide and the vestibular segment 3 cm wide, extending back to the urogenital diaphragm. The caudal part took origin from the fascia on the ventral border of the levator. The muscle fibers became shorter cranially, arising from the visceral pelvic fascia that extended ventrally from the rectovaginal septum onto the lateral wall of the vagina. Thus the muscle formed a broad sling under the urogenital tract. Its contraction would compress the urethra and suburethral diverticulum and constrict the mouth of the vagina. It was covered by a tightly adherent tunic of visceral pelvic fascia 1-2 mm thick.

M. ischiourethralis was 6-10 cm long, 3 cm wide, flat and rectangular (figs 2, 3). It took origin from the ischial arch and extended medioventrally to end in a flat thick aponeurosis which joined right and left muscles ventral to the vestibule. The aponeurosis was related ventrally to the crura clitoridis and dorsally to the tendon of the constrictor vestibuli. The cranial edge was continuous with the tunic on the caudal border of the ventral surface of the urethral muscle. The deep surface of the ischiourethralis was related to the ischial arch, the ischiocavernosus muscle and the internal fascia of the urogenital diaphragm. The superficial surface was covered by the external fascia of the urogenital diaphragm.

M. bulboglandularis (Heinemann 37) is proposed as a general term for the striated muscle covering the bulbourethral gland or its female homologue, the major vestibular gland. This muscle has been

described in the male of various species as a derivative of the urethralis ischiourethralis or bulbospongiosus and has been given different names in each instance (Brauell 1868). It is also subject to individual variation. The characteristic feature of the muscle is not its origin but its relation to the gland.

The bulboglandularis was present in the cow in varying degrees of development. It was usually a band from the urethral muscle about 5 mm wide that curved around the caudal dorsal and cranial borders of the major vestibular gland (fig 3). In some specimens it originated from fibers of the constrictor vestibuli that penetrated the external fascia of the urogenital diaphragm.

Fasciae diaphragmatis urogenitalis. In the cow the urogenital diaphragm was a strong semicylindrical sheet extending from the ischial arch inward and cranially to the ventral and lateral walls of the vestibule. It was partially separable into two layers of fascia which enclosed the ischiourethralis, the rudimentary ischiocavernosus and the major vestibular gland with the bulboglandularis (figs 2-5). Although *m. urethralis* must be included in *m. sphincter urethrae* and therefore in diaphragma urogenitalis in table 1 for comparative reasons, it is actually located cranial to the urogenital diaphragm in quadrupeds because of the elongation of the pelvic urethra. The ischiocavernosus is associated with the urogenital diaphragm only in the rudimentary female form. The diaphragm would appear to anchor the genital tract to the pelvic outlet against the forward pull of the gravid uterus and when everted during parturition against the expulsive efforts.

Geiger (56) in his description of the perineum of the sheep and goat said that the urogenital diaphragm was formed by *m. constrictor vestibuli* and *m. transversus perinei superficialis*. Such a diaphragm would not be homologous to the human urogenital diaphragm and should not be so named. These muscles are superficial to the diaphragm.

The external fascia of the urogenital diaphragm faced dorsally and caudomedially. It was attached to the ischial arch along the caudal border of the ischiourethralis.

curs as a variation in the ram and bull but as these muscles were described without reference to the urogenital diaphragm, they have not been shown to be homologous to the human transverse perineal muscle, which extends from the ischium to the perineal center between the fasciae of the urogenital diaphragm

M sphincter urethrae The human female sphincter urethrae is a flat transverse, striated muscle in the ventral part of the urogenital diaphragm. It originates from the inferior ramus of the pubis and most of its fiber bundles are inserted into the lateral wall of the vagina but a few pass ventral to the urethra and a few pass between the urethra and the vagina (Gardner et al 63). The bundles surrounding

the urethra are better developed in the male

No comparative study of the components of this muscle has been found. Because of the greater length of the pelvic urethra and the meager development of the urogenital diaphragm in quadrupeds the sphincter is more important than the transverse component. In veterinary anatomy the parts have been described as three separate muscles: *m urethralis*, *m ischiourethralis* and *m bulboglandularis*. Much confusion has arisen from a failure to distinguish between the smooth muscle in the urethral wall and the striated *m urethralis*; the smooth muscle is not named in NA. Another source of confusion is the failure to recognize the urogenital diaphragm which

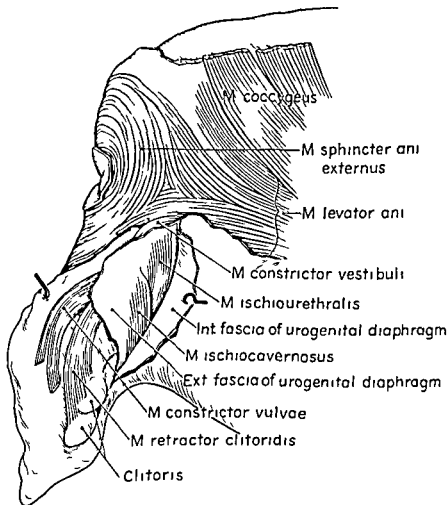


Fig 2 Perineal muscles of a cow in lateral view after removal from the pelvis. The urogenital diaphragm is split the labium is drawn back and the deep bands of the constrictor vulvae have been severed from their insertions on the fascia below the ischial arch

course of its fibers to the insertion on the crus clitoridis. The aponeurosis of insertion could be separated by dissection from the overlying aponeurosis of the ischiourethralis.

M. constrictor vestibuli (figs 1 3 4 6). The origin was from the ventral border of the levator ani at the tendinous inscription and from the fascia covering the levator. Variable fibers from other parts of the levator also joined the constrictor. The muscle became thin ventrally and ended in a flat tendon which passed under the floor of the cranial end of the vestibule to meet the tendon of the opposite muscle. This was over the caudal end of the pelvic symphysis. Contraction of the paired muscles raises a U shaped ridge inside the vestibule according to Geiger (54). When fixed *in situ* the upper part of the muscle was triangular in cross section. The medial surface was related to the vestibule and the *M. retractor clitoridis* the caudolateral surface to the fat in the ischiorectal fossa and the cranial surface to the urogenital diaphragm which contained the major vestibular gland. If the muscle exerts any pressure on the gland it does so by pressing against the urogenital diaphragm.

Bassett (65) basing the argument on dissections of the ewe denied that the constrictor vestibuli is homologous to the bulbospongiosus. Comparison to human anatomy is not helpful here because the extremely short human vestibule leaves no room for the development of a separate constrictor vestibuli. However in domestic animals a striated muscle surrounding the urogenital sinus just caudal (external) to the urogenital diaphragm is certainly homologous to the cranial part of the male bulbospongiosus.

M. constrictor vulvae (figs 1-7) was continuous with the external anal sphincter at the decussation. The superficial fibers spread out subcutaneously in the labia. They were thin and dispersed in the fascia and many of them were attached to the skin. The deep part of the muscle consisted of three or four bands which had a common origin from the anal sphincter and diverged ventrally on the fascia covering the semimembranosus muscle below the ischial arch.

M. retractor clitoridis (figs 1-3 6). This smooth muscle originated from the second and third or third and fourth coccygeal vertebrae and passed around the lateral surface of the rectum covered by the terminal part of the levator. Variable strands of smooth muscle joined the retractor from origins on the longitudinal muscle of the rectum the external anal sphincter and the levator ani. According to Bassett (61) the part between the rectum and the vertebrae may fail to develop in the sheep. It was present in all of the bovine specimens in this study. At the ventral border of the levator the retractor crossed obliquely the medial surface of the constrictor vestibuli and ran ventrally between the constrictors of the vestibule and vulva. Unlike the equine retractor (Habel 53) the bovine had no loop connecting right and left retractors through the perineal body. The termination was variable it divided into several strands one or more of which were inserted on the corpus clitoridis. Other branches were attached to the wall of the vestibule or to the fascia on the semimembranosus. The muscle in the ewe contained some scattered striated fibers (Bassett 61).

Fasciae perinei

Fascia superficialis perinei (fig 7). The superficial fascia was mingled with the subcutaneous fibers of the external anal sphincter and the constrictor vulvae. It was continuous with the fat that filled the ischiorectal fossa. The condensation of superficial fascia in the tail fold was attached to the deep fascia on the caudal border of the coccygeus and on the lateral border of the external sphincter. Elsewhere the superficial fascia was readily separable from the deep fascia that covered the perineal muscles.

Fascia profunda perinei (fig 5). The deep perineal fascia covered the circular fibers of the external anal sphincter the deep part of the constrictor vulvae and the constrictor vestibuli and extended to the scrotum or udder as a narrow zone continuous with the caudal femoral fascia on either side. It included the external fascia of the pelvic diaphragm and the fascia of the urogenital diaphragm.

and was continuous here with the caudal femoral fascia. It passed across the superficial surface of the ischiourethralis and around the cranial border of the constrictor vestibuli to its attachment on the wall of the vestibule. It covered the caudal surface of the major vestibular gland.

The internal fascia of the urogenital diaphragm faced ventrally and cranio-laterally. It arose from the ischial arch and the obturator fascia passed across the deep surface of the ischiourethralis and the cranial surface of the major vestibular gland and attached to the vestibule at the caudal border of the urethral muscle. It was continuous here with the visceral pelvic fascia on the surface of the muscle.

Dorsally both layers of the urogenital diaphragm were attached to the perineal center and to the fasciae of the pelvic diaphragm at the ventral border of the levator.

Ventral to the vestibule the fasciae of the urogenital diaphragm were fused with the tendons of the ischiourethralis and

ischiocavernosus, and formed a strong connection between the fascia on the ventral surface of the urethral muscle and the deep perineal fascia ventral to the vulva. An oval foramen with strong tendinous borders perforated the fascia at the caudal end of the pelvic symphysis. Through it passed the perineal vein, the nerve of the clitoris, the mammary branch of the pudendal nerve and the internal pudendal artery after leaving the pelvic cavity through the space between the crura clitoridis and the ischial arch.

M. transversus perinei superficialis was a rudimentary band about 5 mm wide which extended from the decussation of the external anal sphincter for a variable distance toward the tuber ischladicum in the superficial fascia (figs 1-4).

M. ischiocavernosus (figs 2-3) was 6 cm long, 2 cm wide and very thin. It lay on the medial part of the ischial arch covered by the ischiourethralis muscle. It was distinguished from the latter by the oblique

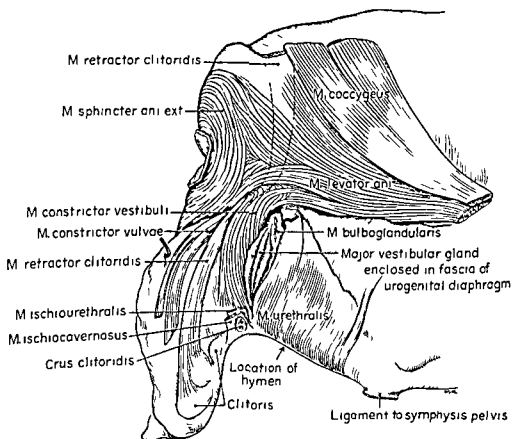


Fig. 3 Same specimen as figure 2 after removal of most of the urogenital diaphragm and removal of the visceral pelvic fascia from the urethral muscle.

Nn splanchnici pelvini (fig 5)

The largest pelvic splanchnic nerve was formerly called the middle hemorrhoidal nerve in the horse (Ellenberger and Baum 43) but the NA term should be adopted. In the cow it originated from sacral nerves 2 to 4 by means of the same branches that joined to form the pudendal nerve. The pelvic splanchnic nerve then left the medial surface of the proximal end of the pudendal and ran ventrally on the rectum to join the autonomic plexuses on the pelvic viscera. Smaller pelvic splanchnic nerves were given off from the pudendal near the vestibule from the deep perineal nerve from the muscular branches and from the caudal rectal nerves.

Rami musculares (fig 5)

In man (Gray 59) and dog (Miller et al 64) the branches to the levator ani and coccygeus extend directly from the sacral plexus to the muscles. In the horse (Habel 53) and pig (Reimers 13) the muscular branches are combined with the caudal rectal nerve.

In the cow the branches to the levator ani and coccygeus muscles were usually combined in a single nerve which originated from the fourth sacral nerve with a smaller contribution from S3 via the pudendal. Before passing to the medial surface of the coccygeus the muscular branch gave a ramus communicans to the distal cutaneous branch of the pudendal. Four variations from the usual pattern have been demonstrated: (1) Both muscular branches were incorporated in the pudendal leaving it just before the pudendal passed lateral to the coccygeus. When the muscular branches ran with the pudendal wholly or in part an unusually large branch of S4 joined the pudendal at its origin. (2) Both muscular branches were incorporated in the caudal rectal nerve. This combination was formerly called the middle hemorrhoidal nerve in the ox (Reimers 13). The reasons for eliminating the latter term are given in the discussion of *N rectalis caudalis*. When the muscular branches were separate from the pudendal they always gave off a communicating branch to the distal cutaneous branch of the pudendal. (3) One muscular

branch came from the pudendal and one from the caudal rectal. (4) One muscular branch was separate and the other was combined with the pudendal or caudal rectal.

N pudendus (figs 5-7)

The origin was from sacral nerves 2 to 4 with the largest contribution from S3. The pudendal nerve ran ventrocaudally on the medial surface of the sacrosclatic ligament dorsal to the internal iliac artery. From the medial side near its origin it gave off a large pelvic splanchnic nerve. It often contributed to the muscular branches to the coccygeus and levator ani. Near the lesser sciatic foramen it gave off the proximal and distal cutaneous branches. As it crossed the foramen it received the medial branch of the caudal cutaneous femoral and gave off the deep perineal nerve. Thus four parallel nerves were seen crossing the lesser sciatic foramen craniocaudally on the lateral surface of the coccygeus and levator muscles (fig 5). From dorsal to ventral they were: the proximal cutaneous branch, distal cutaneous branch, deep perineal and the continuation of the pudendal. The latter turned caudomedially between the vagina and the pelvic floor accompanied by the internal pudendal artery and vein. It gave small branches to the vestibule and ended as the dorsal nerve of the clitoris after giving off the mammary branch.

Ramus cutaneus proximalis (figs 5-7) emerged through the dorsal part of the lesser sciatic foramen or through the sacrotubular ligament near the dorsal process of the tuber ischiadicum. It turned ventrad and supplied the skin over the semitendinosus muscle, an area innervated by the caudal cutaneous femoral nerve in other species. Rarely the communication from the muscular branch joined the proximal instead of the distal cutaneous branch.

Ramus cutaneus distalis (figs 4-5-7) After receiving the communication from the muscular branch the distal cutaneous branch coursed caudally through the ischio-rectal fossa on the medial surface of the tuber ischiadicum about midway between the dorsal and ventromedial processes of the tuber (figs 4-7). It turned ventrally over the caudal surface of the tuber. The

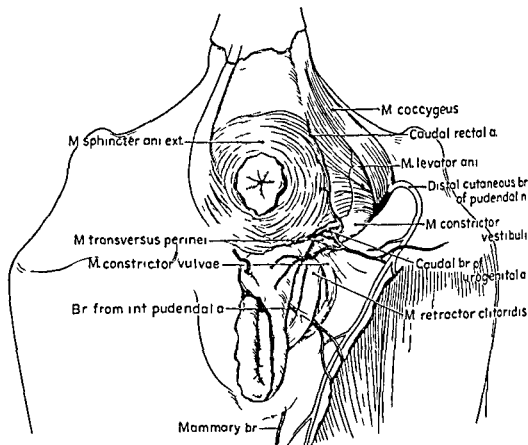


Fig 4 Perineal arteries of a cow in which the cutaneous branches to the region lateral and ventral to the vulva and to the mammary gland were supplied by the internal pudendal. These branches are supplied less frequently by the urogenital (vaginal) artery (fig 6)

NERVES

N cutaneus femoris caudalis (table 2 fig 5)

Because most of the caudal thigh region was supplied by the cutaneous branches of the pudendal nerve the caudal cutaneous femoral nerve was very small (Habel 56). It arose from the dorsal border of the sciatic nerve on the lateral surface of the sacrosciatic ligament at a variable distance from the greater sciatic foramen to a point half way between the sciatic foramina. The nerve ran caudally dorsal to the sciatic nerve on the lateral surface of the sacrosciatic ligament or on the origin of the deep gluteal muscle. At the lesser sciatic foramen it divided into two branches. The medial branch passed into the foramen between the caudal gluteal and internal pudendal arteries and joined either the pudendal nerve or its deep perineal branch or both. According to Schreiber (56) the lateral branch may be absent

it may join the proximal cutaneous branch of the pudendal or it may penetrate the caudal border of the biceps to supply the skin in an area parallel and lateral to the proximal cutaneous branch of the pudendal nerve.

TABLE 2
Nomenclature of nerves

Plexus sacralis	
<i>N cutaneus femoris caudalis</i>	
<i>Nn splanchnici pelvini</i>	
<i>Rami musculares</i>	
<i>N pudendus</i>	
	<i>Ramus cutaneus proximalis</i>
	<i>Ramus cutaneus distalis</i>
	<i>N perinealis superficialis</i>
	<i>Nn labiales</i>
	<i>N perinealis profundus</i>
	<i>Ramus mammarius</i>
	<i>N dorsalis clitoridis</i>
<i>Nn rectales caudales</i>	

ran caudally on the lateral surface of the coccygeus and levator ani muscles. The medial branch of the caudal cutaneous femoral nerve joined the pudendal or the deep perineal nerve or both near the origin of the latter. The deep perineal gave branches to the urethral muscle, the vagina and the major vestibular gland. It then perforated the urogenital diaphragm dorsal to the gland and passed medial to the origin of the constrictor vestibuli which it innervated. The nerve turned dorsally on the deep surface of the terminal bands of the levator and innervated them and the lateral margin of the external anal sphincter. A twig entered the adjacent caudal surface of the retractor clitoridis and communicated through the muscle with the caudal rectal nerve. Thus the deep perineal nerve innervated the urethral muscle and constrictor vestibuli and part of the external anal sphincter and levator ani.

The term deep perineal nerve was introduced into veterinary anatomy by Larson and Kitchell (58) who found that it innervated the homologous muscles in the male plus the ischiocavernosus. In man it is called the deep branch of the perineal nerve (Gray 59) but is not listed in the NA. It was called the perineal branch of the pudendal in the mare (Habel 53). In the dog it arises as a series of small branches from the pudendal (Miller et al 64).

Ramus mammarius (figs 5-7) This branch turned ventrally on the deep perineal fascia accompanied by the mammary branch of the perineal artery and the perineal vein and ran to the skin of the caudal surface of the udder. In some specimens a fine communicating branch joined the overlying superficial perineal nerve. In adult cows the perineal vein was often tortuous and its loops partially concealed the nerve and artery.

The mammary branch of the pudendal nerve (Habel 49) was called the perineal nerve by St Clair (42) and the superficial perineal nerve by Larson and Kitchell (58) who traced it in the male to the cranial aspect and median septum of the scrotum and to the prepuce. *Ramus mammarius* in the female and *ramus preputialis et scrotalis* in the male are preferable terms for the following reasons: (1) These nerves

do not supply the perineal region which does not include the udder, cranial surface of the scrotum or prepuce. (2) These nerves are not superficial in the perineal region; they do not supply the skin there. (3) In the ox the superficial nerves of the perineal region including the caudal scrotal nerve as described by Larson and Kitchell (58) are supplied by the distal cutaneous branch of the pudendal—not one of the terminal branches.

N. dorsalis clitoridis (fig 5) supplied the clitoris and sometimes gave a branch to the vestibule. Right and left nerves of the clitoris and mammary branches lay on the pelvic symphysis and emerged by passing between the crura clitoridis and the symphysis then through the foramen in the deep perineal fascia.

Nn. rectales caudales (figs 5-6)

One or two caudal rectal nerves originated from the fourth or fourth and fifth sacral nerves. They ran caudally between the rectum and the coccygeus supplying small pelvic splanchnic nerves to the rectum and sometimes giving off one or both muscular branches to the coccygeus and levator ani. The main caudal rectal nerve is easily exposed by dissection in the caudal angle between the coccygeus and levator (fig 6). On the deep surface of the levator cranial to the retractor clitoridis the nerve divided into several branches (fig 6). A dorsal branch went through the retractor clitoridis to the external anal sphincter and the dorsal band of the levator. A middle branch passed through or medial to the retractor clitoridis and deep into the perineal center where it entered the cranial surface of the decussation of the external anal sphincter. Some fibers reached the mucosa of the roof of the vestibule and others ran deep in the labium.

The largest or ventral branch passed through the retractor clitoridis and innervated it. Coursing medial to the origin of the constrictor vestibuli it gave twigs to that muscle and the adjacent part of the levator and communicated with the deep perineal nerve. It crossed obliquely the lateral surface of the retractor clitoridis in the labium and emerged through the deep part of the constrictor vulvae to end in the superficial fascia of the labium. The term

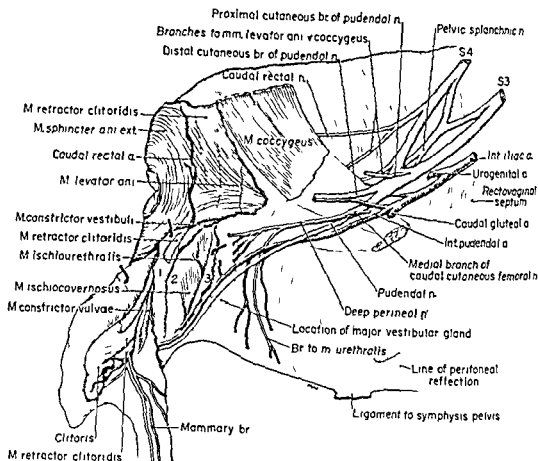


Fig 5 Lateral view of the pelvic viscera of a cow the superficial fascia of the labium is retracted by a hook 1 external layer of deep perineal fascia 2 external fascia of urogenital diaphragm 3 internal fascia of urogenital diaphragm The arterial pattern illustrated is the more usual one in which the internal pudendal artery supplies the region lateral and ventral to the vulva Another pattern is shown in figure 6

first branch was given off on the tuber ischiadicum and ran medially into the ischiorectal fossa. Another small medial branch was given off below the tuber at the level of the dorsal commissure of the labia. At the same level the trunk divided into three main branches. The medial branch gave two or three branches to the labium and ended by ramification on the midline over the perineal vein. It sometimes communicated with the mammary branch of the pudendal nerve. The middle branch supplied the skin over the semimembranosus and extended to the skin between the udder and thigh. The lateral branch ran along the septum between the semimembranosus and semitendinosus.

The branches to the perineal region and labia are the superficial perineal and labial nerves which are derived from the puden-

dal and emerge from the ischiorectal fossa as in man and dog. In the horse however the caudal rectal nerve after receiving a communicating branch from the pudendal supplies the superficial perineal nerves through the ischiorectal fossa (Habel 53). In the cow the caudal rectal nerve also reaches the labium but independently by passing medial to the levator ani (fig 5). This termination was called the perineal nerve by Reimers (13) it is best left unnamed (Larson and Kitchell 58).

In the bull the superficial perineal nerves (medial branches of the right and left distal cutaneous branches) joined to form the caudal scrotal nerve (Larson and Kitchell 58).

N. perinealis profundus (figs 5 6) This nerve arose from the dorsal border of the pudendal at the lesser sciatic foramen and

continued caudally giving small variable branches to the obturator muscle and divided at the cranial border of the lesser sciatic foramen into its terminal branches the caudal gluteal and internal pudendal arteries (see table 3)

A urogenitalis

This term (Miller 47) has been in use for many years in veterinary anatomy to designate the large artery that supplies the intrapelvic part of the urogenital system. It is partially homologous to the human vaginal artery but supplies a much larger area in ruminants and swine. Barone (57), Preuss (59) and Vollmerhaus (64) have adopted the term vaginal artery for use in domestic animals but they do not agree on the names of its branches.

TABLE 3
Nomenclature of arteries

<i>A iliaca interna</i>	
<i>A umbilicalis</i>	
<i>A uterina</i>	
<i>A iliofumbalis</i>	
<i>A glutea cranialis</i>	
<i>A urogenitalis (A vaginalis)</i>	
<i>Ramus cranialis</i>	
<i>R urethralis</i>	
<i>A vesicalis caudalis</i>	
<i>A ureterica</i>	
<i>R. uterinus</i>	
<i>Ramus caudalis</i>	
<i>Rami vaginales</i>	
<i>Rami rectales medii</i>	
<i>R glandularis</i>	
<i>R. vestibularis</i>	
<i>A rectalis caudalis</i>	
<i>A perinealis</i>	
<i>Rr labiales</i>	
<i>Rr perineales dorsales</i>	
(<i>Rr perineales ventrales</i>)	
(<i>R mammarius</i>)	
<i>A. glutea caudalis</i>	
<i>A pudenda interna</i>	
<i>R. vaginalis</i>	
<i>R. vestibularis</i>	
<i>R glandularis</i>	
<i>A profunda clitoridis</i>	
<i>A. dorsalis clitoridis</i>	
<i>Rr perineales ventrales</i>	
<i>R mammarius</i>	

After a short course to the lateral surface of the vagina the urogenital artery divided into cranial and caudal branches.

Ramus cranialis was the larger. It supplied branches to the urethra, bladder and ureter and was continued as the uterine branch. The latter was the largest branch of the urogenital artery in the parous cow and was formerly called the caudal uterine artery. Vollmerhaus (64) designated the cranial branch of the urogenital as the continuation of the vaginal artery and the caudal branch as the perineal artery. This is not helpful to understanding because the caudal branch is the one that supplies most of the vagina.

Ramus caudalis (figs 4-6) ran back along the dorsolateral surface of the vagina giving small branches to the vagina and rectum. It passed medial to the dorsal end of the major vestibular gland and gave off a branch to the gland. A small branch ran dorsally on the deep surface of the retractor clitoridis and the caudal branch crossed the medial surface of the muscle. After giving a branch to the vestibule the caudal branch emerged between the retractor clitoridis and the ventral branch of the levator and ended by dividing into the caudal rectal and perineal arteries. Because the caudal branch of the urogenital in ruminants and swine replaces a part of the internal pudendal artery of man, dog and horse it is not homologous to the human vaginal artery.

A rectalis caudalis (figs 4-7) ran dorsally on the lateral border of the external anal sphincter and ended in the tail fold. The nomenclature used by Vollmerhaus (64) for the middle and caudal rectal arteries is that of the Jena NA 1936 (Kopsch 57) in which they were listed as a rectalis caudalis and a analis.

A perinealis gave off a lateral branch to the region of the tuber ischiadicum and turned ventrally in the labium between the retractor clitoridis and constrictor vulvae. In two-thirds of the cows dissected the perineal artery derived from the urogenital terminated in the labium (figs 4-5). In one third it supplied the cutaneous branches to the perineal region lateral and ventral to the vulva and the branch to the mammary gland (fig 6).

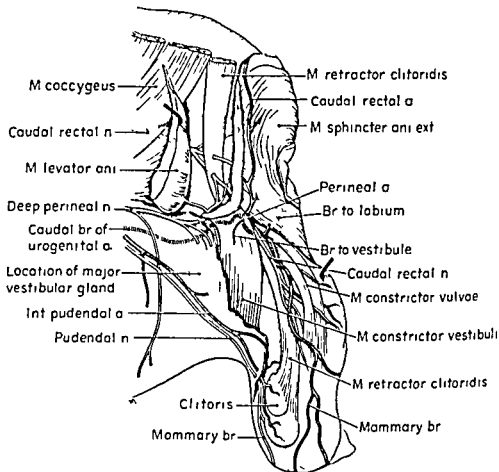


Fig 6 Lateral view of the pelvic viscera of a cow dissected to show the relation of the caudal rectal and deep perineal nerves. The arterial pattern shown here in which the cutaneous branches to the region lateral and ventral to the vulva and the branch to the mammary gland are supplied by the urogenital (vaginal) artery occurs less frequently than that shown in figure 5.

nal fibers of all three branches of the caudal rectal nerve may reach the skin but this was not demonstrated by dissection. Larson and Kitchell (58) showed that the nerve in the male was sensory and that it was also motor to the coccygeus levator ani external anal sphincter and retractor penis.

For many years the combination of a caudal rectal nerve with the muscular branches to the coccygeus and levator ani was called in the ox the middle hemorrhoidal nerve. The caudal hemorrhoidal (rectal) nerve was said to be often absent (Reimers 13, Habel 49, Larson and Kitchell 58). This was contrary to the nomenclature of the same nervous elements in man, dog and horse. It is better from a comparative and didactic standpoint to drop the term middle hemor-

rhoidal and to follow the NA in recognizing only nn rectales caudales in the plural. At least one caudal rectal nerve is always present. Lassoie (58) described it as one *nerf anal* which terminated in two parallel branches running caudally on the rectum.

ARTERIES

A iliaca interna (fig 5)

The first branch of the internal iliac artery was the common trunk of the uterine and umbilical arteries. After giving off the iliolumbar and cranial gluteal arteries the internal iliac coursed along the medial side of the ventral border of the sacrosacral ligament. The urogenital artery usually originated near the ischiatic spine although it sometimes arose more proximally or as far distally as the internal pudendal artery. The internal iliac

gave off a large branch that supplied the cutaneous branches to the perineal region lateral and ventral to the vulva and the small cutaneous branch to the mammary gland. In one third of the cows this area was supplied by the urogenital artery. Different arterial patterns may occur on right and left sides of the same cow.

ACKNOWLEDGMENTS

I wish to express my appreciation of the assistance of Dr Erwin Pearson who made many of the dissections and Miss Marion Newson who drew the illustrations.

LITERATURE CITED

- Barone R 1957 La vascularisation utérine chez quelques mammifères. Assoc Anat C R 44 124-131
- Bassett E G 1961 Observations on the retractor clitoridis and retractor penis muscles of mammals with special reference to the ewe. J Anat 95 61-77
- 1965 The anatomy of the pelvic and perineal region in the ewe. Aust J Zool 13 201-241
- Brauell 1868 Beitrag zur Myologie der männlichen Genitalien. Österr Vierteljahrsschr Wiss Vet 29 1-27
- Ellenberger W and H Baum 1943 Handbuch der vergleichenden Anatomie der Haustiere 18th ed. Springer Berlin
- Gardner E D J Gray and R O'Rahilly 1963 Anatomy A Regional Study of Human Structure. Saunders Philadelphia
- Geiger C 1954 Die anatomischen Grundlagen des Hymenalarings beim Rinde. Tierärztl Umsch 9 398-402
- 1956 Die anatomische Struktur des Beckenausganges der kleinen Wiederkäuer. Anat Anz 103 321-339
- Godina G 1939 Le fosse ischio-rettale dei bovini. Nuovo Ercolani 44 353-363
- Gray H 1959 Anatomy of the Human Body 27th ed. Ed by C M. Goss. Lea and Febiger Philadelphia
- Habel R E 1949 Guide to the Dissection of the Cow. Cornell Cooperative Soc. Ithaca N Y
- 1953 The perineum of the mare. Cornell Vet 43 249-278
- 1956 A source of error in the bovine pudendal nerve block. J Am Vet Med Assoc 128 16-17
- 1964 Guide to the Dissection of Domestic Ruminants. Publ by author. Ithaca N Y
- Hayek H 1965 La musculature lisse du plancher pelvien. C R Assoc Anat 126 829-835
- Heinemann K 1937 Einige Muskeln des männlichen Geschlechtsapparates der Haus saugetierte (M. bulbocavernosus, M. ischio-cavernosus, M. retractor penis). Diss. Hanover
- Kopsch F 1957 Nomina Anatomica 5th ed. Ed by K. H. Knese. Thieme Stuttgart
- Lambert F A 1916 Preservation and in situ fixation of veterinary anatomical subjects by intravascular injection. J Am Vet Med Assoc 49 381-391
- Larson L L and R L Kitchell 1958 Neural mechanisms in sexual behavior. II. Gross neuroanatomical and correlative neurophysiological studies of the external genitalia of the bull and the ram. Am J Vet Res 19 853-865
- Lassio L 1958 La portion postérieure du système nerveux chez la bête bovine. Ann Med Vét 102 529-549
- Martin F and M Schauder 1938 Lehrbuch der Anatomie der Haustiere. III. Band. Anatomie der Hauswiederkäuer. Schickhardt and Ebner. Stuttgart 302-348
- Miller M E 1947 Guide to the Dissection of the Dog. Publ by author. Ithaca N Y
- Miller M E, G C Christensen and H E Evans 1964 Anatomy of the Dog. Saunders Philadelphia
- Mitchell G A G Editor 1961 Nomina Anatomica 2nd ed. Excerpta Med. Amsterdam
- Preuss F 1959 Die A. vaginalis der Haus saugetierte. Berl Munch tierärztl Wschr 72 403-406
- Reimers H 1913 Der Plexus lumbalis und sacralis des Rindes und Schweines. Diss. Univ Leipzig
- Schreiber J 1956 Die anatomischen Grundlagen der Leitungsanästhesie beim Rind. IV. Die Leitungsanästhesie der Nerven der Hinterextremität. Wiener tierärztl Mschr 43 673-705
- Schummer A and R Nickel 1960 Lehrbuch der Anatomie der Haustiere. Band II. Eingeweide. Paul Parey Berlin 383-392
- St Clair L E 1942 The nerve supply to the bovine mammary gland. Am J Vet Res 3 10-16
- Vollmerhaus B 1964 Gefäßarchitektonische Untersuchungen am Geschlechtsapparat des weiblichen Hausrindes. Zbl Vet Med A 11 538-646

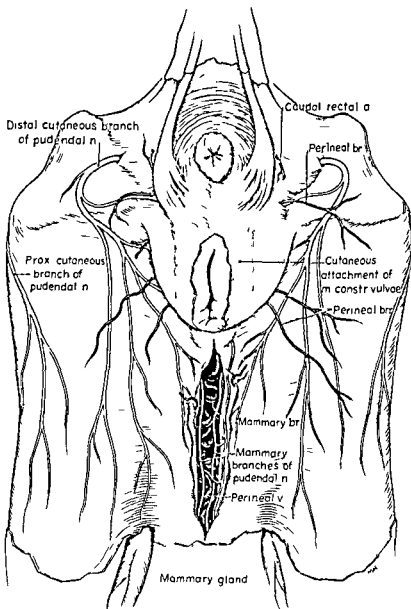


Fig 7 Perineal region of a cow after removal of the skin. The superficial fascia ventral to the vulva is incised and retracted. The arteries lateroventral to the anus are supplied by the urogenital (vaginal) artery. The arteries lateral and ventral to the vulva are usually supplied by the internal pudendal but may be from the urogenital.

A pudenda interna

After giving a muscular branch to the coccygeus and levator ani the artery ran caudally on the lateral surface of these muscles (fig 5). A branch accompanied the distal cutaneous branch of the pudendal nerve to the ischioanal fossa. Branches were given off to the vagina, vestibule and major vestibular gland as the trunk inclined ventrally on the internal surface of the urogenital diaphragm accompanied by the internal pudendal vein

and the pudendal nerve. Right and left vessels and nerves converged on the ventral surface of the vestibule and the veins joined to form one perineal vein. After emerging between the crura clitoridis and the pelvic symphysis and through the foramen in the deep perineal fascia the internal pudendal artery supplied the deep artery of the clitoris to the crus and ended as the dorsal artery of the clitoris. In two-thirds of the cows dissected the internal pudendal after perforating the deep fascia

Structure of the Surface of Mouse Hepatic Cells

TREVOR HEATH AND STEVEN L. WISSIG

Department of Veterinary Preclinical Sciences University of Melbourne
Parkville Victoria Australia and Department of Anatomy
University of California San Francisco Medical Center
San Francisco California

ABSTRACT Mouse hepatic cells appear in thin sections as polygons with six or more sides. The plasma membrane covering these sides may contact either bile canaliculi, the narrow intercellular space, the space of Disse or extensions of the space of Disse between adjacent cells. The plasma membrane covering microvilli in bile canaliculi and the space of Disse is thicker than that in contact with the narrow intercellular space. Bile canaliculi which contact about 6% of the perimeter of each cell are each separated by tight junctions from the narrow intercellular space. This space contacts more than one half the perimeter of each cell and is about 220 Å in width. It is continuous around the occasional studlike junctions which occur but is interrupted at frequent intervals by circumscribed tight junctions and occasionally by desmosomes. The narrow intercellular space is in free communication through the space of Disse with the plasma space. An interstitial fluid space separate from the plasma space does not occur in the liver lobule. Protein molecules from plasma enter hepatic cells in both coated and pinocytotic vesicles. These vesicles are derived from invaginations of the plasma membrane that borders the narrow intercellular space and the spaces between microvilli in the space of Disse. Pinocytotic vesicles may also incorporate fat droplets into hepatic cells.

Segments of the perimeter of parenchymal cells located in the interior of a hepatic lobule border one of three types of extracellular space: a lumen of a bile canaliculus, a perisinusoidal space of Disse or a narrow intercellular space separating adjacent hepatic cells. The plasma membrane and adjacent cytoplasm along each type of space have specific morphologic characteristics peculiar to that region and descriptions of some of these have already appeared in the literature (Fawcett '55, David '61, Biava '64).

Bile canaliculi in the mouse, rat, guinea pig and man are most often limited by segments of the plasma membrane of two and less often of three or more hepatic cells (David '61, Biava '64). The plasma membrane which limits the canaliculi at least in man is 100–110 Å thick but the thickness and density can vary depending on the procedures used to prepare the specimens for examination (Biava '64). The cytoplasm which borders each canaliculus contains a fine filamentous meshwork and strands from this meshwork extend into microvilli which project into the lumen (Wood '61). Minute tubules 70–90 Å in diameter have also been de-

scribed in canalicular microvilli in the rabbit liver (David '61).

There is some disagreement about the degree of continuity between the lumen of the canaliculi and the remainder of the extracellular space. In an early series of reports Rouiller ('54–'56) stated that bile canaliculi communicate freely with the space of Disse. As this statement has not been substantiated and as it cannot be reconciled with the known facts of liver physiology it seems likely that the author confused some extensions of the space of Disse for bile canaliculi. Later Ashworth and Sanders ('60) concluded that a cleft about 100 Å wide separated adjacent hepatic cells at the margins of canaliculi. They believed that this was just wide enough to allow water ions and small molecules to pass from the space of Disse into canaliculi but was too narrow to allow the passage of proteins. More recently Farquhar and Palade ('63) showed that the plasma membranes of adjacent hepatic cells in the rat and guinea pig fuse to form an apparently impermeable tight junction where they meet at the margins of a canaliculus. These tight junctions exist as a continuous band (zonula occlu-

ne Structure of the Surface of Mouse Hepatic Cells

TREVOR HEATH AND STEVEN L. WISSIG

Department of Veterinary Preclinical Sciences University of Melbourne
Parkville Victoria Australia and Department of Anatomy
University of California San Francisco Medical Center
San Francisco California

ABSTRACT Mouse hepatic cells appear in thin sections as polygons with six or more sides. The plasma membrane covering these sides may contact either bile canaliculi, the narrow intercellular space, the space of Disse, or extensions of the space of Disse between adjacent cells. The plasma membrane covering microvilli in bile canaliculi and the space of Disse is thicker than that in contact with the narrow intercellular space. Bile canaliculi, which contact about 6% of the perimeter of each cell, are each separated by tight junctions from the narrow intercellular space. This space contacts more than one half the perimeter of each cell and is about 220 Å in width. It is continuous around the occasional studlike junctions which occur but is interrupted at frequent intervals by circumscribed tight junctions and occasionally by desmosomes. The narrow intercellular space is in free communication through the space of Disse with the plasma space. An interstitial fluid space, separate from the plasma space, does not occur in the liver lobule. Protein molecules from plasma enter hepatic cells in both coated and pinocytotic vesicles. These vesicles are derived from invaginations of the plasma membrane that borders the narrow intercellular space and the spaces between microvilli in the space of Disse. Pinocytotic vesicles may also incorporate fat droplets into hepatic cells.

Segments of the perimeter of parenchymal cells located in the interior of a hepatic lobule border one of three types of extracellular space: a lumen of a bile canaliculus, a perisinusoidal space of Disse, or a narrow intercellular space separating adjacent hepatic cells. The plasma membrane and adjacent cytoplasm along each type of space have specific morphologic characteristics peculiar to that region, and descriptions of some of these have already appeared in the literature (Fawcett '55, David '61, Biava '64).

Bile canaliculi in the mouse, rat, guinea pig, and man are most often limited by segments of the plasma membrane of two and less often of three or more hepatic cells (David '61, Biava '64). The plasma membrane which limits the canaliculi at least in man is 100–110 Å thick but the thickness and density can vary depending on the procedures used to prepare the specimens for examination (Biava '64). The cytoplasm which borders each canaliculus contains a fine filamentous meshwork and strands from this meshwork extend into microvilli which project into the lumen (Wood '61). Minute tubules 70–90 Å in diameter have also been de-

scribed in canalicular microvilli in the rabbit liver (David '61).

There is some disagreement about the degree of continuity between the lumen of the canaliculi and the remainder of the extracellular space. In an early series of reports Rouiller ('54, '56) stated that bile canaliculi communicate freely with the space of Disse. As this statement has not been substantiated and as it cannot be reconciled with the known facts of liver physiology, it seems likely that the author confused some extensions of the space of Disse for bile canaliculi. Later Ashworth and Sanders ('60) concluded that a cleft about 100 Å wide separated adjacent hepatic cells at the margins of canaliculi. They believed that this was just wide enough to allow water ions and small molecules to pass from the space of Disse into canaliculi but was too narrow to allow the passage of proteins. More recently Farquhar and Palade ('63) showed that the plasma membranes of adjacent hepatic cells in the rat and guinea pig fuse to form an apparently impermeable tight junction where they meet at the margins of a canaliculus. These tight junctions exist as a continuous band (*zonula occlu-*

dens) along the length of the margins of all canaliculi and should effectively seal off the canalicular lumen from the adjacent intercellular space. Farquhar and Palade (63) described two other components of a junctional complex at the lateral margins of the canaliculi. These components, the intermediate junction (*zonula adhaerens*) and the desmosome (*macula adhaerens*) were believed to act as intercellular attachment devices. The junctional complex at the margins of human bile canaliculi consists of essentially the same components (Blava 64).

The segments of the hepatic cell surface which face the space of Disse and its extensions are covered by numerous microvilli (Rouiller 54). The cytoplasm immediately adjacent to the space of Disse contains many small vesicles and some of these vesicles appear to be connected to the space of Disse by tubular invaginations of the plasma membrane (Rouiller 54, Novikoff and Essner 60, Bruni and Porter 65). It has been suggested that these vesicles are pinocytotic in nature and that they are important in the uptake of materials by hepatic cells (Roth and Porter 62, Bruni and Porter 65). The observation of Hampton (58) that colloidal particles introduced into the space of Disse are incorporated into these vesicles seems to support this view.

Over much of their perimeter neighboring hepatic cells face each other across a narrow intercellular space. This space varies in width and is interrupted at intervals by various types of junctions between the adjacent cells (Fawcett 55, Ashworth and Sanders 60, Hampton 60, 64, David 61). Small dense droplets have been observed in the space (Cossel 62) and Hampton (64) described small vesicles in the adjacent cytoplasm.

The extracellular spaces in other tissues are believed to contain interstitial fluid which drains to the bloodstream in the lymphatics. Although the liver produces relatively large volumes of lymph little is known of its origin. Terminal lymphatics have not been described within the hepatic lobule and the relative contributions made by lobules and by periportal areas to the hepatic lymph have not been determined (Brauer 63). In this connection it would

be interesting to determine whether a true extravascular interstitial fluid space exists within the hepatic lobule and serves as a reservoir from which lymph drains in a manner analogous to its drainage from other tissues.

Although such topics as the differences in structure between different regions of the surface of hepatic cells, the nature of the junctions between neighboring hepatic cells and the existence of a true interstitial fluid space have been treated incidentally and sporadically by several papers in the literature, they have not been systematically investigated for their own sake. The present paper presents detailed quantitative and morphologic data concerning the entire surface of parenchymal cells of the mouse liver and also contains a description of the structure and location of various types of intercellular junctions along their perimeter. In addition ferritin was introduced into the circulating blood to serve as a tracer so that the accessibility of extravascular spaces within the lobule to constituents of plasma could be examined.

MATERIALS AND METHODS

Mice of either the Cal A or the C3H strain were allowed free access to food until the experiments were started in the mornings. The mice were anesthetized with pentobarbitone sodium. A midline incision was made through the abdominal wall and thin strips of liver were removed into a drop of chilled fixative. The strips were cut into small blocks which were immersed in fixative. In some experiments fixation was initiated by dripping chilled fixative onto the surface of the liver for ten minutes before a thin strip of fixed tissue was removed, cut into blocks and immersed in fixative.

Some mice received an intravenous or intraperitoneal injection of a 10% ferritin solution before the liver specimens were collected. Prior to injection the solution of ferritin was dialyzed against sodium versenate to remove traces of cadmium (Farquhar, Wissig and Palade 61). Specimens of liver were removed up to 80 minutes after 0.5 ml of ferritin solution was injected into the tail vein of unanesthetized mice or into the external jugular

in of anesthetized mice or 150 minutes after 10 ml was injected into the peritoneal cavity of unanesthetized mice.

The blocks of liver which were collected each experiment were all fixed for 2 hours in buffered solutions of either osmium tetroxide or glutaraldehyde. One 2% solution of osmium tetroxide were added to a pH of 7.5 with either acetate (Palade 52) phosphate (Millonig 62) or γ -collidine (Bennett and Luft 9). Redistilled glutaraldehyde was buffered to pH 7.5 with either cacodylate or phosphate (Sabatini, Bensch and Barnett 33).

The blocks were subsequently dehydrated in acetone and embedded in either araldite or Epon (Luft 61). Some of the blocks were immersed in a solution of 1% potassium permanganate in acetone for five minutes during dehydration (Parsons 31).

Thin sections were mounted on grids covered with formvar that had been stabilized with carbon and were stained with both uranyl acetate (Watson 58) and a lead salt (Millonig 61, Reynolds 63). The sections were examined with a Siemens Elmiskop 1.

Quantitative data

In the first series measurements were made of the total perimeter of hepatic parenchymal cells and of the percentage of the perimeter which bordered bile canaliculi, the space of Disse and its extensions and the narrow intercellular space. A flexible ruler was used to make these measurements on cells magnified 6400 \times that had been sectioned through the approximate center of their nuclei. It is possible that some of the cells contained more than one nucleus and in this case the plane of section may not have passed through the equator of the cell. In segments of the surface coated with microvilli the total length of the plasma membrane could not be accurately measured at this magnification. For this reason the linear extent of the surface bordering bile canaliculi was measured as the distance between the luminal extremities of the tight junctions at the canalicular margins (line A, fig 1a) and that bordering the space of Disse and its extensions was

measured across the bases of the microvilli (line A, fig 1b). Hepatic cells appeared polygonal in outline when viewed in equatorial section and the number of sides forming their perimeter as well as the number of bile canaliculi, desmosomes and stud like processes at their surface was recorded (figs 2-4). These measurements were all made on 22 cells from various regions of hepatic lobules from four mice.

In the second series the increase in length of the plasma membrane resulting from the presence of microvilli along segments of the cell surface was estimated on micrographs with a final magnification of 56 000-84 000 \times . Within bile canaliculi the total length of the plasma membrane covering microvilli, isolated profiles of microvilli and intermicrovillous spaces

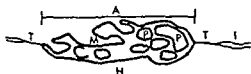


Fig 1a Diagram of bile canaliculus showing method used to estimate the increase in length of plasma membrane resulting from the presence of microvilli. The total length of the plasma membrane within the canaliculus (thick line) was compared with the length of the long axis of the canaliculus (line A). Abbreviations: H hepatic cell, M microvilli, T tight junction at margin of canaliculus, I intermediate junction, P isolated profile of microvilli.

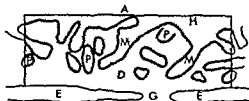


Fig 1b Diagram of hepatic cell surface facing the space of Disse showing method used to estimate the increase in length of the plasma membrane resulting from the presence of microvilli. The total length of hepatic plasma membrane within the stippled area (thick line) was compared with the linear extent of the cell surface upon which the microvilli are located (line A). Abbreviations: H hepatic cell, M microvilli, P isolated profiles of microvilli, E sinusoidal lining cell, G gap between sinusoidal lining cells.

(thick line fig 1a) was measured with a flexible ruler and compared with the linear extent of the surface bordering the canaliculi (line A fig 1a). Similar measurements were made within the space of Disse. A line was drawn across the bases of the microvilli and at either end a perpendicular line was drawn to intersect the plasma membrane of the endothelial cell lining the sinusoid. The total length of the hepatic plasma membrane within the roughly rectangular area defined by these three lines and the plasma membrane of the endothelial cell (stippled area fig 1b) was measured and compared with the linear extent of the surface (line A fig 1b).

In the third series the percentage of the narrow intercellular space occluded by tight junctions was estimated on a set of micrographs with a final magnification of $56\,000\text{--}84\,000\times$. The tight junctions at the margins of bile canaliculi were not included in these estimations.

No attempt was made to relate these linear measurements to the surface of the intact cell because of the complexity and lack of uniformity of the hepatic cell surface.

In the final series the thickness of different segments of the hepatic plasma membrane was measured by a method similar to that described by Millington (64). Electron micrographs taken at an initial magnification of $40\,000\times$ were enlarged photographically to $300\,000\times$ and the membrane was measured with a hand lens containing a scale calibrated to 0.1 mm . To minimize errors arising from the effects of fresnel fringes all micrographs used for these measurements were taken by one microscopist.

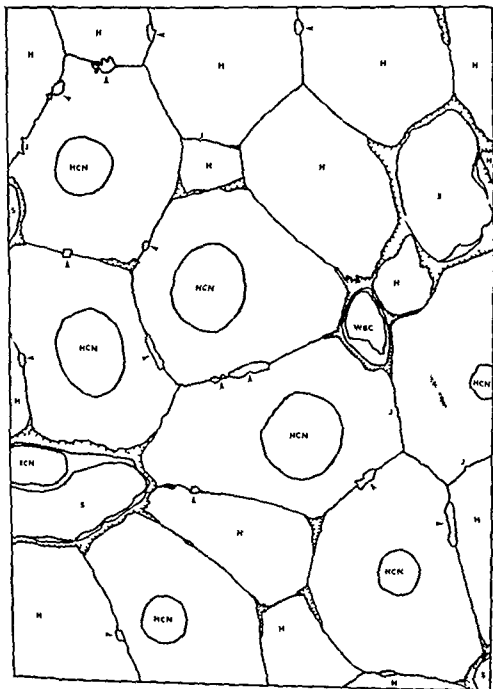
OBSERVATIONS

Mouse hepatic cells sectioned through the center of their nuclei appear polygonal in outline (fig 2). A typical hepatic cell has four sides facing its neighbors across a narrow intercellular space and two sides facing the space of Disse surrounding visible sinusoids (figs 2, 3). The narrow intercellular space is continuous with the space of Disse and its extensions between adjacent hepatic cells but is interrupted at intervals by bile canaliculi (figs 2-4).

The wall of a bile canaliculus is generally formed by two hepatic cells although as many as one quarter are limited by three cells. Each canaliculus formed by two cells is roughly elliptical in outline and its long axis which coincides with a line joining the luminal extremities of the tight junctions at its margins is often of the order of $1\text{ }\mu$ in length. The long axes of canaliculi comprise about 6% of the perimeter of hepatic cells (table 1) but because of the presence of microvilli the length of plasma membrane within the canaliculi represents a considerably higher percentage of the total plasma membrane of the cell. For example in one series of measurements the length of the plasma membrane within each canaliculus was 7.8 ± 0.4 times greater than the long axis of the elliptical cross section of the canaliculus. Although occasionally a canaliculus and part of the space of Disse are located in close proximity they are usually separated by a segment of narrow intercellular space several microns in length. This intercellular space is always separated from the lumen of the canaliculus by a tight junction (Farquhar and Palade 63). The constituents of junctional complexes at the margins of canaliculi will be considered in more detail in a subsequent section.

The space of Disse surrounds each sinusoid following its general contour but it also extends for considerable distances between hepatic cells adjacent to the sinusoid (figs 8, 15, 16). These extensions of

Fig 2 Tracing of the principle features in a montage of electron micrographs of part of a mouse hepatic lobule. The plane of section did not pass through the nuclei of most hepatic cells but did pass through the approximate center of the nuclei (HCN) of three cells near the middle of the picture. These cells each have six sides of which either one or two contact the space of Disse (stippled) surrounding visible sinusoids (S). Most of the remaining sides are in contact along part of their length with extensions of the space of Disse. These are shown as stippled areas between adjacent hepatic cells. The space of Disse is continuous with the narrow intercellular space which is interrupted at intervals by bile canaliculi (arrowed) tight junctions and desmosomes (not shown) but is generally continuous around studlike junctions (J). A white blood cell in the space of Disse (WBC) and a nucleus of a sinusoid lining cell (ECN) are also shown.



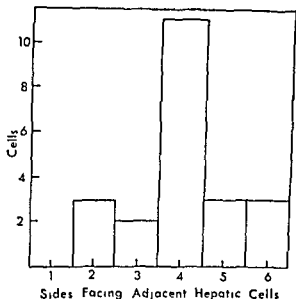
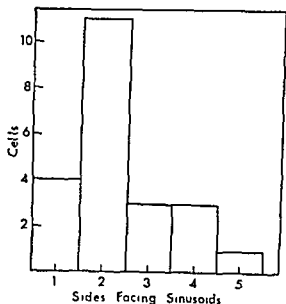


Fig 3 Number of sides of each hepatic cell which face sinusoids (top) and adjacent hepatic cells (bottom). Measurements were made on 22 cells sectioned through the center of the nucleus.

the space of Disse often appear in sections as isolated dilations of the intercellular space which may bear superficial resemblance to bile canaliculi (fig 9). The criteria used for distinguishing them will be discussed later. Although about one third of the sides of hepatic cells face the space of Disse surrounding visible sinusoids (fig 3) more than 80% of the remaining sides contact at least one extension of the space of Disse and about 10% are in contact with an extension of the space of Disse along their entire

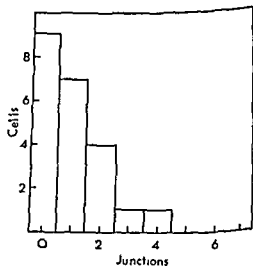
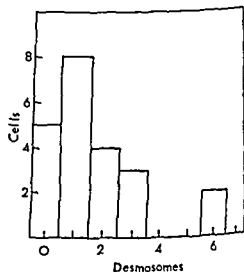
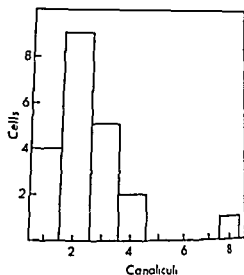


Fig 4 Number of bile canaliculi (top), desmosomes (middle) and studlike junctions (bottom) at the perimeter of each of 22 cells sectioned through the center of the nucleus.

TABLE 1

extracellular spaces in contact with the perimeter of hepatic cells

Average total perimeter ¹	76 \pm 3.4 μ
Percentage of perimeter facing	
Bile canaliculi ²	63 \pm 13%
Space of Disse ^{3,4}	17 \pm 21%
Extension of space of Disse ⁴	25 \pm 22%
Narrow intercellular space	54 \pm 45%

Mean perimeter of 22 cells (from four serial sections) surrounding the approximate center of the nuclei
¹ Long axis of canaliculi measured between horizontal streamlines of tight junctions at their margins (ie A, fig 1)
 Those portions of the surface facing space of Disse surrounding the sinusoid
² Line extent of cell surface measured as areas of microvilli (line "A" fig 1b)

length. In fact an average of more than 60% of the total linear extent of the perimeter of each hepatic cell is in contact with the space of Disse or its extensions (table 1). Because of the presence of microvilli in this region however a higher percentage of the total length of the plasma membrane is in contact with the space of Disse. In one series of measurements the length of plasma membrane covering microvilli and intermicrovillous spaces was 60 ± 0.8 times greater than the linear extent of the cell surface bordering this space.

Surfaces bordering bile canaliculi. The microvilli in bile canaliculi project in more or less random directions from the surface of the hepatic cells and those which are not oriented parallel to the plane of section appear as isolated profiles in the canalicular lumen (figs 9-11). The microvilli contain fine filaments which are more numerous near the limiting membrane and which appear continuous with a cytoplasmic feltwork of fine filaments which surrounds each canaliculus (figs 9-11). We did not observe the more complex structure of microvilli described by David (61) in canaliculi and by McNabb and Sanborn (64), Graney (64) and Rostgaard and Barnett (65) in the intestinal mucosa.

Vesicular invaginations were absent from the limiting membranes of canaliculi and no vesicles were present in the adjacent cytoplasm. These observations suggest that pinocytosis is not a prominent phenomenon at this surface but they provide no information about the mechanism by which bile constituents leave hepatic cells.

In sections that have been fixed in osmium tetroxide and stained with uranium and lead salts the plasma membrane limiting the canaliculi and the space of Disse is thicker than that along the narrow intercellular space (table 2). These membranes all appear slightly thicker in Epon embedded than in Araldite-embedded tissues. In all cases the inner and outer leaflets stain with similar intensity (fig 10) and all of the three leaflets are of approximately equal thickness (20-30 Å).

The outer dense leaflets of the plasma membranes of adjacent hepatic cells fuse to form the central leaflet of a tight junction at each lateral margin of a canaliculus (figs 9-11). These tight junctions which vary in length from 0.1-0.3 μ ($0.16 \pm 0.01 \mu$) are often continuous with intermediate junctions (Farquhar and Palade 63). These intermediate junctions are much less clearly defined than tight junctions and vary in length from 0.1-0.25 μ . They differ from tight junctions in that the apposed plasma membranes do not fuse but are separated by a space 130-220 Å in width. The cytoplasm adjacent to tight junctions and intermediate junctions is relatively dense especially in tissues fixed in osmium tetroxide and it contains a feltwork of fine filaments continuous with that which surrounds each canaliculus (figs 10-11). Intermediate junctions occur only near the bile canaliculi and are not present at any other points on the cell perimeter. At the distal end of an intermediate junction a desmosome or a second tight junction is occasionally present (figs 9-11) but in most cases the space between the plasma membranes is continuous with the narrow intercellular space.

Surfaces bordering the space of Disse. The microvilli which extend in various directions from this surface of the hepatic cell are curved and occasionally branched and in thin sections many appear as isolated profiles in the space of Disse (figs 6, 8, 12-14). These microvilli are of relatively uniform width (0.07-0.12 μ) but are often slightly constricted near their base (figs 12-14). They do not contain either vesicles or surface invaginations and do not appear to have any internal structure apart from a fine filamentous feltwork.

TABLE 2
Thickness of the plasma membrane of hepatic cells¹

Cell	Embedding medium	Location of membrane		
		Microvilli of bile canaliculi	Microvilli in space of Disse	Facing narrow intercellular space
1	Araldite	73	68	63
2	Araldite	75	70	66
3	Araldite	76	79	64
4	Araldite	79	72	66
5	Epon	88	82	75
6	Epon	88	80	66

¹ Means of ten measurements made along each of three segments of the plasma membrane are shown for six cells. These cells were from specimens fixed in osmium tetroxide and stained with both uranium and lead salts. In addition the specimens containing cells 1 and 2 were treated with potassium permanganate during dehydration.

(figs 13 14) This feltwork which extends into the microvilli from the adjacent cytoplasm can often be seen more clearly in specimens fixed in glutaraldehyde and post fixed in osmium tetroxide than in specimens fixed in buffered osmium tetroxide alone. The ends of almost all the microvilli in our preparations were free in the space of Disse and no microvilli were closely attached to sinusoidal lining cells in the manner described by Wasserman (58).

A finely fibrillar material extends throughout the space of Disse and is continuous with the plasma through gaps in the walls of the sinusoids. The fibrillar material in the space of Disse has a similar density and texture to that in the lumen of the sinusoids (figs 6 12) and is thought to represent the image of fixed plasma protein. Small fat droplets 0.1–0.15 μ in diameter may occur in the space of Disse and in the lumen of the sinusoids (figs 12 15 16) but their concentration is often higher in the space of Disse than within the sinusoids.

Two types of vesicular invaginations of the plasma membrane occur between the bases of the microvilli which project into the space of Disse. The first type, the coated invagination, is about 0.1 μ wide and may be sharply constricted at its opening into the space of Disse (figs 13 14). These invaginations contain material of the same density and structure as that in the space of Disse but do not appear to incorporate fat droplets. They are thought to represent stages in the formation of

coated vesicles which occur in the hepatic cell cytoplasm near the space of Disse (fig 13). Coated vesicles are also about 0.1 μ in diameter and are limited by a membrane of the same density and thickness as the plasma membrane. Each coated vesicle and coated invagination is bordered by a narrow band of increased cytoplasmic density which contains periodic dense striations oriented at right angles to the limiting membrane (figs 13 14). Coated vesicles do not appear to contain fat droplets but are filled with a fine filamentous material of slightly greater density than that in the space of Disse. Vesicles of this type have been described previously in a number of tissues including the rat liver and have been variously termed coated complex and alveolate vesicles (Farquhar, Wissig and Palade, 61; Gray, 61; Roth and Porter, 62, 64; Palay, 63; Rosenbluth and Wissig, 63; Bruni and Porter, 65).

The second type of invagination is also about 0.1 μ wide and may be constricted at its opening into the space of Disse (figs 12 15 16). Pinocytotic vesicles, limited by a membrane which appears identical to the plasma membrane, occur in the adjacent cytoplasm (fig 12) and are thought to be derived from these invaginations. Pinocytotic vesicles and invaginations differ from the coated structures in that the cytoplasmic leaflet of the limiting membrane lacks any form of specialization. They contain a finely filamentous material but fat droplets which completely fill some vesicles may also be

esent (fig 12) Pinocytotic vesicles are generally larger and more irregular than coated vesicles and vary in diameter from about 0.1–0.5 μ

A third type of vesicle the small dense vesicle is also present in the hepatic cell cytoplasm near the space of Disse and is more obvious in specimens fixed in glutaraldehyde (fig 15) These vesicles are all about 0.1 μ in diameter and are filled with a moderately dense homogenous material They do not resemble either of the types of surface invaginations described above but may contain fat droplets that could be derived from the space of Disse

In addition to these three types of vesicles large (up to 0.5 μ) and relatively irregular "vesicles" may occur in the hepatic cell cytoplasm very near the space of Disse in regions where the plasma membrane is tortuous (fig 8) These "vesicles" which are limited by a membrane identical to the plasma membrane contain material which appears the same as that in the space of Disse They are thought to represent cross sections of indentations of the space of Disse into the surface of the hepatic cell We did not observe the "granule-containing vacuoles with a dense matrix" which were described by Bruni and Porter (65) in the cytoplasm near the space of Disse in rat liver

Although extensions of the space of Disse may bear superficial resemblance to bile canaliculi they differ in a number of morphologic characteristics For instance a finely fibrillar material extends throughout the space of Disse but canaliculi are relatively empty except for sparse finely fibrillar or granular material (figs 9–11) The lumen of each canaliculus is always separated from the adjacent narrow intercellular space by tight junctions but tight junctions do not generally occur at the confluence of the space of Disse with the narrow intercellular space (figs 8–11 15) In sections from the livers of mice which have received exogenous ferritin ferritin molecules are present throughout the space of Disse but are absent from bile canaliculi (see later section) In addition vesicles and surface invaginations occur along the borders of the space of Disse (figs 12–16) but are absent from the borders of canaliculi

Surfaces bordering the narrow intercellular space A narrow intercellular space contacts a large proportion of the perimeter of hepatic cells (table 1) This space is relatively uniform in width (220 ± 14 Å) and the limiting membranes which are thinner than those covering other segments of the cell surface (table 2) are generally smooth or slightly curved (figs 5 7 8 17) They may be more convoluted in localized regions and may even separate to form small dilatations of the space These dilated segments often contain small droplets of fat (figs 17 18)

The plasma membranes of the apposed cells are modified at various points to form junctions across the narrow intercellular space The outer leaflets of the apposed membranes often fuse to form the central leaflet of a tight junction (figs 9 18 19) These central leaflets are always thinner than either of the outer leaflets from which they are derived and may be barely visible even at high magnification (figs 18 19) The tight junctions along the narrow intercellular space resemble those at the margins of bile canaliculi but the adjacent cytoplasm does not contain any evidence of filaments or of increased density (fig 19) The tight junctions are generally straight (fig 18) but irregular and tortuous forms may be present In some cases a series of tight junctions may occur in which the individual junctions are separated by short segments of narrow intercellular space The distance between the cytoplasmic margins of tight junctions remote from bile canaliculi is 100–150 Å and the junctions vary in length from 0.5–2.0 μ (1.0 ± 0.1 μ) They occupy about one fifth ($20 \pm 2.0\%$) of the length of cell sides which border the narrow intercellular space

Desmosomes which vary in length from 0.1–0.2 μ (0.13 ± 0.01 μ) may also occur along the narrow intercellular space (fig 11) The structure of hepatic desmosomes will not be considered as they have already been described in detail in the literature (Farquhar and Palade 63)

Studlike processes that project from the surface of one hepatic cell into a concavity in the surface of an adjacent cell (Fawcett 55) are the least common form of junction In this junction the apposed

plasma membranes are of the same thickness and staining intensity as the membranes that border the adjacent narrow intercellular space (figs 17, 19). This space is generally continuous around each studlike process (fig 19) but occasionally the apposed plasma membranes fuse to form a tight junction within the studlike junction.

Compound vesicular structures may occur in the hepatic cell cytoplasm near the narrow intercellular space and these are thought to represent transverse sections of studlike junctions (fig 5). The structures are 0.2–0.4 μ in diameter and contain a membrane bounded core which has the same density and texture as the surrounding cytoplasm. This core is separated from the external limiting membrane by a narrow (100–200 Å) ring of low density which presumably represents a segment of narrow intercellular space within the studlike junction. Both the external membrane and the membrane surrounding the core have the same thickness and structure as the plasma membrane bordering the narrow intercellular space.

The desmosomes, studlike junctions and tight junctions remote from bile canaliculi are distributed more or less at random along the narrow intercellular space. A few cell sides lack cell junctions except for those at the margins of the canaliculi and an occasional cell side lacks both cell junctions and bile canaliculi.

Coated and pinocytotic vesicles and invaginations occur in the region of the narrow intercellular space but are much less common than near the space of Disse. Neither small dense vesicles nor vesicular structures believed to be cross sections of pockets of the space of Disse have been observed in the hepatic cell cytoplasm near the narrow intercellular space.

Distribution of exogenous ferritin. A high concentration of ferritin molecules was present in the narrow intercellular space, the space of Disse and the hepatic sinusoids of all mice which had received injections of ferritin (figs 12, 13, 15, 16, 18, 19). We were not able to determine whether consistent variations existed in the concentration of ferritin molecules between these areas.

At the margins of bile canaliculi ferritin molecules were occasionally present between the apposed plasma membranes of intermediate junctions but did not appear either between the leaflets of tight junctions or in the lumens of canaliculi. Ferritin molecules were not found between the leaflets of tight junctions elsewhere on the plasma membrane although they do appear within short segments of narrow intercellular space separating adjacent tight junctions (fig 18). From these results we conclude that tight junctions are impermeable to ferritin and that the narrow intercellular space is continuous around circumscribed segments of tight junctions remote from bile canaliculi. Ferritin molecules were present between the apposed plasma membranes within studlike junctions (fig 19), verifying the continuity of the narrow intercellular space around these junctions.

Ferritin molecules were also present within coated and pinocytotic invaginations and vesicles in the region of the space of Disse and the narrow intercellular space (figs 12, 13). Some of the pinocytotic vesicles contained both fat droplets and ferritin molecules (fig 12). The concentration of ferritin molecules in the vesicular structures which are thought to represent cross sections of small pockets of the space of Disse was the same as the concentration in the adjacent areas of the space of Disse.

DISCUSSION

In conventional histologic sections of mammalian liver the lobule seems to consist of more or less straight cords of parenchymal cells in thickness that converge from the periphery of the lobule to terminate at the central vein. After analyzing such preparations Elias (49) concluded that the radial cords of parenchymal cells in fact represent sections through relatively flat plates of cells. These plates are separated from one another by sinusoids of relatively uniform diameter which converge towards the central vein into which they ultimately empty.

When thin sections of liver are examined with the electron microscope most sinusoids appear circular in outline. The appearance of the sinusoids in thin sec-

lans can best be reconciled with their appearance in the considerably thicker conventional histologic sections if we assume that they pursue a relatively serpentine course through fenestrations in the plates of liver cells. Their lateral digressions may not be sufficiently great to carry them out of the plane of a thick histologic section but could cause them to repeatedly leave and re-enter the plane of thin sections. If the sinusoids do pursue a serpentine course we should expect that the plane of thin sections would sometimes transect the space of Disse surrounding a sinusoid which was out of the plane of section (fig. 7). These tangential sections of the space may resemble transverse sections of radial extensions of the space of Disse. Thus some of the "extensions of the space of Disse" which we observed may have represented tangential sections through the roughly annular space surrounding the sinusoids. However most appeared to be sectioned normally and are thought to represent radial extensions of the space of Disse between hepatic cells adjacent to the sinusoids.

The extracellular spaces. Bile canaliculi extend throughout the liver lobule but are separated from the remainder of the extracellular spaces by tight junctions. Although Rouiller (56) and Ashworth and Sanders (60) described open connections between the canalicular lumen and the space of Disse a number of authors have provided evidence to the contrary (Fawcett 55, Hampton 58, Novikoff and Essner 60, Daems 61, Farquhar and Palade 63). Farquhar and Palade (63) demonstrated that tight junctions exist at the margins of canaliculi and concluded that these tight junctions are impermeable to protein molecules. In our studies tight junctions were always present at each canalicular margin and these appeared to prevent the entry of ferritin molecules into the canaliculi. Farquhar and Palade (63) also provided evidence which suggests that tight junctions may be impermeable to smaller molecules and possibly to water. If this is true all the biliary constituents from the blood must pass through hepatic cells in order to reach the canaliculi.

The narrow intercellular space was wider in our studies than in those of other authors (Fawcett 55, Ashworth and Sanders 60, Daems 61) but these variations may reflect different methods of specimen preparation (cf Hampton 60). Major changes in the width of the space may result from relatively minor changes in the volume of the adjacent cells during fixation and embedding. The width of the narrow intercellular space may also vary depending on the species (cf David 61) and on the physiological condition of the animal. For example the width of the space between epithelial cells in the intestine apparently varies in different nutritional conditions (Sjostrand 63).

Several types of modifications of the cell surfaces occur along the narrow intercellular spaces. In tissues embedded in methacrylate Fawcett (55) and Daems (61) described stud like processes which extend from one hepatic cell into a corresponding recess on the surface of an adjacent cell. However when Hampton (60) examined liver specimens embedded in Araldite he was unable to demonstrate these processes and concluded that they were alterations due to distortion during embedding or sectioning. We have found these processes in specimens embedded both in Araldite and in Epon and believe that they probably do occur in the living animal. However because they are relatively uncommon and because the narrow intercellular space is continuous around the processes we believe that they do not exert any significant function in cell cohesion.

Desmosomes are present along the narrow intercellular space but the apposed plasma membranes do not appear to be joined by any type of cement substance and the narrow intercellular space appears to continue without interruption between the two membranes. The apposed plasma membranes with their associated fibril containing areas of increased cytoplasmic density may act as focal points of structural rigidity. However as desmosomes are not common in the liver lobule and as each desmosome covers a very small proportion of the total cell surface their importance is probably slight.

It seems likely that the main intercellular attachment devices in the liver lobule are the tight junctions which occur at the margins of the canaliculi and at frequent intervals along the narrow intercellular space. These tight junctions appear to be essentially similar to the external compound membrane of Robertson (58) and the quintuple layered cell interconnections of Karrer (60). Those which occur along the narrow intercellular space remote from canaliculi are not constant in position with reference to any landmark of the hepatic cell and they are not present along all the cell sides which face the narrow intercellular space. For this reason we believe that these junctions do not form a belt of any length around the cells but that they are relatively circumscribed areas of fusion of the plasma membranes. The conclusion is supported by the results of experiments in which ferritin molecules introduced into the circulation were found along the length of the narrow intercellular space and between adjacent tight junctions. Although it is possible that ferritin molecules could have reached some parts of the narrow intercellular space by vesicular transport through hepatic cells, the amount of ferritin present in vesicles in these experiments did not appear sufficient to warrant serious consideration of this alternative explanation.

Transport of materials between hepatic cells and extracellular spaces. It has been suggested that some substances which are removed from the blood by cells lining the sinusoids are subsequently transferred to hepatic cells (Wasserman 58). However we were unable to find either microvilli closely attached to lining cells or any evidence to suggest that exogenous ferritin molecules could be transferred directly from the lining cells to microvilli of hepatic cells. These observations concur with those of Hampton (58) and seem to indicate that plasma constituents must enter the space of Disse before they can be absorbed by hepatic cells.

Coated and pinocytotic vesicles are both concerned with uptake of these plasma constituents by hepatic cells but show different degrees of selectivity in the nature of the materials they will ingest. Our observations on the uptake of exogenous fer-

ritin molecules by coated vesicles would seem to confirm that the role of coated vesicles in protein uptake in the liver resembles that in other tissues (Farquhar, Wissig and Palade 61; Rosenbluth and Wissig 63; Roth and Porter 64; Bruns and Porter, 65). However coated vesicles in liver cells do not appear to concentrate ferritin preferentially as they do in the cells of toad spinal ganglia (Rosenbluth and Wissig 63).

Pinocytotic vesicles also incorporate ferritin molecules but these vesicles are predominantly concerned with the uptake of fat droplets from the space of Disse and the narrow intercellular space. Fat droplets have been described previously in both the space of Disse and adjacent cytoplasmic vesicles but their mode of entry into the hepatic cells has remained obscure (cf Ashworth, Stenbridge and Sanders 60; French 63). Our observations appear to confirm the suggestion of Trotter (6a) that pinocytotic invaginations and vesicles play an important part in this process. However we were unable to confirm the observation of Schlesinger and Essner (65) that coated invaginations and vesicles may incorporate fat droplets into hepatic cells.

The fat droplets in our preparations were all between 0.1μ and 0.14μ in diameter and we were unable to determine whether they were chylomicrons synthesized in the gut wall from exogenous fat or lipoproteins derived from endogenous sources. The very low density lipoproteins vary in size up to 0.14μ and closely resemble small chylomicrons (cf Courtney and Garlick 62; French 63). In addition physiologic experiments have revealed that both chylomicrons and lipoproteins are removed from the blood in the liver (French and Morris 58; Bragdon and Gordon 58; Stein and Shapiro 60; Rodbell, Scow and Chernick 64). If the fat droplets present in our preparations were chylomicrons their uniform small size may indicate that only smaller chylomicrons can pass through the gaps in the sinusoidal walls. It is also possible that some of the droplets may have been lipoproteins which had been discharged from hepatic cells and were passing through the space of Disse to the bloodstream.

Although microvilli cover a large proportion of the surface of hepatic cells their role in the transfer of materials between the hepatic cell and the extracellular spaces is unknown. Vesicles and surface invaginations do not occur in microvilli; it appears to be confined to the intermicrovillous spaces. In this respect microvilli of hepatic cells resemble those of epithelial cells of the intestinal wall (cf. Lacey and Lacey 59; Lacey and Taylor 62). However fat droplets may be absorbed into intestinal microvilli (Rostgaard and Barnett 65) but do not appear in enter microvilli of hepatic cells.

Structure of the plasma membrane in the basis of studies of tissues fixed in potassium permanganate. Robertson (59, 61) postulated that cellular membranes consist of a central lipid leaflet bordered on both surfaces by layers of nonlipid material. Subsequent studies have revealed that considerable variations may occur within the framework of this simple unit membrane model. In tissues fixed in osmium tetroxide the structure of plasma membranes may vary between different cells and between different parts of the same cell (Wissig 62; Sjostrand 63; Farquhar and Palade 63; Millington 64). For instance the plasma membrane covering the microvilli of intestinal epithelial cells is substantially thicker than that covering the lateral and basal surfaces of the cell (Sjostrand 63; Millington 64) in the intestine. These differences may indicate that variations in the physiologic characteristics of the cell are reflected in slight changes in the structure of the membranes.

Variations in the methods used during preparation of specimens for examination may also cause alterations in the structure of membranes. In many epithelial cells which have been stained with either uranium or lead salts the outer leaflet of the plasma membrane is thinner and less dense than the inner leaflet. If the cells are treated with potassium permanganate during dehydration or if they are stained with both uranium and lead salts the outer leaflet can be visualized more readily (Farquhar and Palade 63). In our study no differences were apparent between the

inner and outer leaflets of the plasma membranes of hepatic cells stained with both uranium and lead salts.

ACKNOWLEDGMENTS

We thank Dr. W. O. Reinhardt and Miss Simona Ikeda for their help. These studies were made during the tenure of USPHS International Post-doctoral fellowship FF 612 and were also supported by USPHS grants HE-00749 and HE-04512.

LITERATURE CITED

- Ashworth C. T. and E. Sanders 1960 Anatomical pathway of bile formation. *Am J Path* 37: 343-355.
- Ashworth C. T., V. A. Stemberge and E. Sanders 1960 Lipid absorption transport and hepatic assimilation studied with electron microscopy. *Am J Physiol* 198: 1326-1328.
- Bennett H. S. and J. H. Luft 1959 α -collidine as a basis for buffering fixatives. *J Biophys Biochem Cytol* 6: 113-114.
- Blava C. G. 1964 Studies on cholestasis. A re-evaluation of the fine structure of normal human bile canaliculi. *Lab Invest* 13: 840-864.
- Bragdon J. H. and R. S. Gordon Jr. 1958 Tissue distribution of C after the intravenous injection of labelled chylomicrons and unesterified fatty acids in the rat. *J Clin Invest* 37: 574-578.
- Brauer R. W. 1963 Liver circulation and function. *Physiol Rev* 43: 115-213.
- Bruni C. and K. R. Porter 1965 The fine structure of the parenchymal cell of the normal rat liver. I. General observations. *Am J Path* 46: 691-750.
- Cossel L. 1962 Über den submikroskopischen Zusammenhang der interzellulären Räume und Sinusoide in der Leber. *Z. Zellforsch u mikroskop Anat* 58: 76-93.
- Courtice F. C. and D. G. Garlick 1962 The permeability of the capillary wall to the different plasma lipoproteins of the hypercholesterolaemic rabbit in relation to their size. *Quart J exp Physiol* 47: 221-227.
- Daems W. Th. 1961 The micro-anatomy of the smallest biliary pathways in mouse liver tissue. *Acta Anat* 46: 1-24.
- David H. 1961 Zur Morphologie der Leberzellmembran. *Z. Zellforsch u mikroskop Anat* 55: 220-234.
- Elias H. 1949 A re-examination of the structure of the mammalian liver. I. Parenchymal architecture. *Am J Anat* 84: 311-333.
- Farquhar M. G. and G. E. Palade 1963 Junctional complexes in various epithelia. *J Cell Biol* 17: 375-412.
- Farquhar M. G., S. L. Wissig and G. E. Palade 1961 Glomerular permeability. I. Ferritin transfer across the normal glomerular capillary wall. *J Exp Med* 113: 47-66.

- Fawcett D W 1955 Observations on the cytology and electron microscopy of hepatic cells *J Nat Cancer Inst* 15 (supp) 1475-1502
- French J E 1963 The behaviour of chylomicrons in the circulation. Observations with the electron microscope. In *Biochemical Problems of Lipids* A C Frazer ed Elsevier Publishing Company Amsterdam London New York pp 296-303
- French J E and B Morris 1958 The tissue distribution and oxidation of ^{14}C labelled chylomicron fat injected intravenously in rats *J Physiol* 140 262-271
- Graney D O 1964 Uptake and Fate of Tracer Protein in the Intestinal Epithelium of the Suckling Rat Thesis University of California San Francisco Medical Center
- Gray E G 1961 The granule cells mossy synapses and Purkinje spine synapses of the cerebellum. light and electron microscope observations *J Anat Lond* 95 345-356
- Hampton J C 1958 An electron microscope study of the hepatic uptake and excretion of submicroscopic particles injected into the blood stream and into the bile duct *Acta Anat* 32 262-291
- 1960 A re-evaluation of the submicroscopic structure of liver *Texas Rep Biol Med* 18 602-611
- 1964 Liver In *Electron Microscopic Anatomy* S M Kurtz ed Academic Press New York London pp 41-58
- Karrer H E 1960 The striated musculature of blood vessels. II Cell interconnections and cell surface *J Biophys Biochem Cytol* 8 135-150
- Lacy D and A B Taylor 1962 Fat absorption by epithelial cells of the small intestine of the rat *Am J Anat* 110 155-185
- Luft J H 1961 Improvements in epoxy resin embedding methods *J Biophys Biochem Cytol* 9 409-414
- McNabb J D and E Sanborn 1964 Filaments in the microvillous border of intestinal cells *J Cell Biol* 22 701-704
- Millington P F 1964 Comparison of the thicknesses of the lateral wall membrane and the microvillus membrane of intestinal epithelial cells from rat and mouse *J Cell Biol* 20 514-517
- Millonig G 1961 A modified procedure for lead staining of thin sections *J Biophys Biochem Cytol* 11 736-739
- 1962 Further observations on a phosphate buffer for osmium solutions in fixation. In *Fifth International Congress for Electron Microscopy Vol 2* S S Breese Jr ed Academic Press New York and London p 8-p 9
- Novikoff A B and E Essner 1960 The liver cell. Some new approaches to its study *Am J Med* 29 102-131
- Palade G E 1952 A study of fixation for electron microscopy *J Exp Med* 95 285-298
- Palay S L 1963 Alveolate vesicles in Purkinje cells of the rat's cerebellum *J Cell Biol* 19 89A-90A
- Palay S L and L J Karlin 1959 An electron microscopic study of the intestinal villus. II The pathway of fat absorption *J Biophys Biochem Cytol* 5 373-384
- Parsons D F 1961 A simple method for obtaining increased contrast in Araldite sections by using postfixation staining of tissues with potassium permanganate *J Biophys Biochem Cytol* 11 492-497
- Reynolds E S 1963 The use of lead citrate at high pH as an electron-opaque stain in electron microscopy *J Cell Biol* 17 208-215
- Robertson J D 1958 Structural alterations in nerve fibers produced by hypotonic and hypertonic solutions *J Biophys Biochem Cytol* 4 349-364
- 1959 The ultrastructure of cell membranes and their derivatives *Biochem Soc Symposium* 16 3-43
- 1961 The Unit Membrane. In *Electron Microscopy in Anatomy* J D Boyd F L Johnson and J D Lever eds Edward Arnold (Publishers) Ltd London pp 74-99
- Rodbell M R O Scow and S C Chernick 1964 Removal and metabolism of triglycerides by perfused liver *J Biol Chem* 239 385-391
- Rosenbluth J and S L Wissig 1964 The distribution of exogenous ferritin in toad spinal ganglia and the mechanism of its uptake by neurons *J Cell Biol* 23 307-325
- Rostgaard J and R J Barnett 1965 Fine structural observations of the absorption of lipid particles in the small intestine of the rat *Anat Rec* 152 325-350
- Roth T F and K R Porter 1962 Specialized sites on the cell surface for protein uptake. In *Fifth International Congress for Electron Microscopy Vol 2* S S Breese Jr ed Academic Press New York and London pp 114 to 115
- 1964 Yolk protein uptake in the oocyte of the mosquito *Aedes aegypti* *L J Cell Biol* 20 313-332
- Rouiller Ch 1954 Les canalicules biliaires. Etude au microscope électronique *Compt Rend Soc Biol* 148 2008-2011
- 1956 Les canalicules biliaires. Etude au microscope électronique *Acta Anat* 26 94-109
- Sabatini D D K Bensch and R J Barnett 1963 Cytochemistry and electron microscopy. The preservation of cellular ultrastructure and enzymatic activity by aldehyde fixation *J Cell Biol* 17 19-58
- Schlesinger M and E Essner 1965 Histochemical and electron microscopic studies of the liver in runt disease *Am J Path* 41 371-402
- Sjostrand F 1963 The ultrastructure of the plasma membrane of columnar epithelium cells of the mouse intestine *J Ultrastruct Res* 8 517-541
- Stein Y and B Shapiro 1960 Uptake and metabolism of triglycerides by the rat liver *J Lipid Res* 1 326-331
- Trotter N 1965 A fine structure study of the lipid-containing bodies which appear in hepatoma cells very soon after partial hepatectomy or sham-operation *Anat Rec* 151 427

- Masserman F 1958 The structure of the wall of the hepatic sinusoids in the electron microscope *Z Zellforsch u mikroskop Anat* 49 13-32
- Natanson M L 1958 Staining of tissue sections for electron microscopy with heavy metals *J Biophys Biochem Cytol* 4 475-478

- Wissig S L 1962 Structural differentiations in the plasmalemma and cytoplasmic vesicles of selected epithelial cells *Anat. Rec* 142 292
- Wood R. L. 1961 Some structural features of the bile canaliculus in calf liver *Anat. Rec* 140 207-215

Abbreviations

<i>c</i> bile canaliculus	<i>e</i> extension of the space of Disse
<i>d</i> space of Disse	<i>f</i> fine filaments
<i>dv</i> dense vesicle	<i>z</i> zonula occludens (tight junction)

The mice from which the specimens shown in figures 8 12 13 15 16 18 and 19 were obtained received an intraperitoneal or intravenous injection of ferritin solution prior to sacrifice

PLATE 1

EXPLANATION OF FIGURE

- 5 Hepatic cells of the mouse liver are shown at relatively low magnification. The borders of sinusoids appear at the upper and lower margins of the figure. The hepatic cells are roughly polygonal in outline. Two bile canaliculi (*c*) interrupt the narrow space between hepatic cells. A cross section of a studlike junction (arrow) is shown near the center of the figure. $\times 10,000$

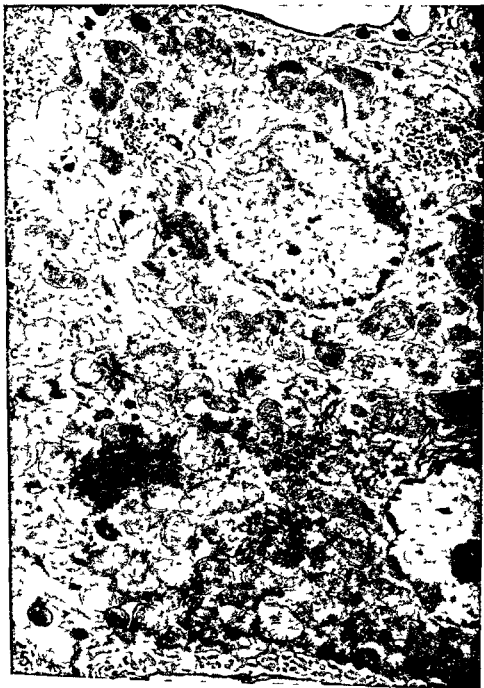


PLATE 2

EXPLANATION OF FIGURES

The figures illustrate the diversity of structure of intercellular spaces between hepatic cells. The intercellular space extends between spaces of Disse situated at the top and bottom of each figure.

- 6 The widely separated surfaces of the hepatic cells are coated with microvilli and the space between them is broadly continuous with the spaces of Disse at the top and bottom of the figure. The lining cells of both sinusoids are sectioned obliquely. This field probably contains a single sinusoid sectioned at a point where it makes a serpentine bend. In the center of the figure the sinusoid passes out of the plane of section which intercepts only its bordering space of Disse. $\times 27,000$
- 7 A narrow space separates the hepatic cells in this field. A bile canaliculus (c) with cross sections of microvilli filling its lumen interrupts the space midway along its length. A zonula occludens poorly visualized at this low magnification occurs at each lateral margin of the canaliculus. $\times 15,000$
- 8 A bile canaliculus (c) is situated close to a space of Disse (d) in the narrow space between hepatic cells. Its lumen filled with microvillous profiles is separated from the space of Disse above and the narrow intercellular space below by zonulae occludentes. A lumen (e) containing a few microvillous profiles dilates the narrow space near the sinusoid at the lower border of the figure. It is identified as an extension of the space of Disse because ferritin molecules can be detected in its lumen in the original micrograph and it lacks zonulae occludentes in its lateral margins (see text). A vesicular structure (arrow) believed to represent a cross section of an invagination of the space of Disse is present in the lower part of the figure. $\times 25,000$

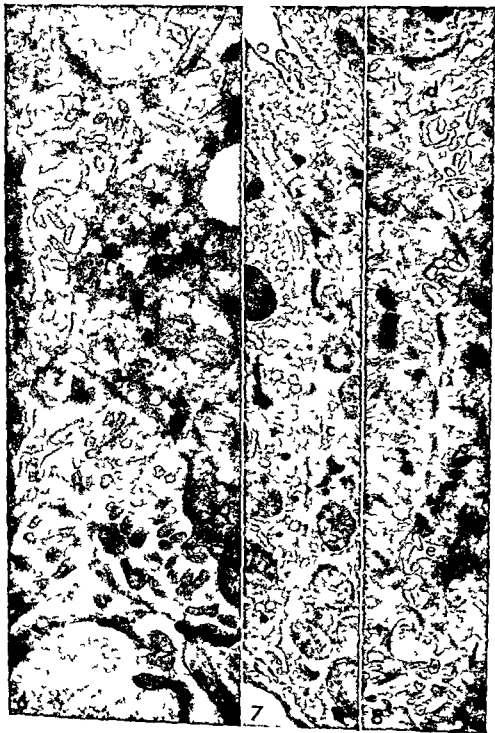


PLATE 3

EXPLANATION OF FIGURE

- 9 A bile canaliculus in a specimen fixed in buffered osmium tetroxide solution. The numerous microvillous profiles in its lumen are limited by distinct unit membranes and sparse filamentous or granular material is seen in their cores. Fine filaments (*f*) appear in the bordering cytoplasmic matrix. Zonulae occludentes (*z*) occur at the lateral margins of the canaliculus and are bordered by fine filaments. A short distance from one zonula occludens the narrow intercellular space is obliterated (arrow) where the plasma membranes of the hepatic cells are fused together. The lumen of the canaliculus appears empty and there is no sign of vesicles either forming or emptying along its border. $\times 88\,000$

SURFACE OF THE HEPATIC CELL
of He th and St ven L. W ssig



PLATE 4

EXPLANATION OF FIGURES

- 10 A zonula occludens (z) bordered by fine filaments is situated at a lateral margin of a bile canaliculus. Below it the plasma membranes are sectioned obliquely and their relationship to each other cannot be discerned. There are abundant fine filaments in the adjacent cytoplasm. The membranes again appear sectioned perpendicularly near the lower margin figure (arrow) and here they are fused together $\times 144\ 000$
- 11 At the lateral margin of a bile canaliculus the plasma membranes of adjacent hepatic cells fuse to form a zonula occludens (z) near its lumen. A desmosome (macula adherens) can be recognized in the lower portion of the figure. Between these two elements of a junctional complex the plasma membranes are sectioned obliquely for most of their length but they can be seen to be clearly separated at two points (arrows). It is not possible to decide with certainty whether an intermediate junction (zonula adherens) occurs in this region. A mesh of fine filaments stretching from the zonula occludens to the desmosome lines the cytoplasmic surface of the plasma membranes $\times 120\ 000$



PLATE 4

EXPLANATION OF FIGURES

- 10 A zonula occludens (z) bordered by fine filaments is situated at a lateral margin of a bile canaliculus. Below it the plasma membranes are sectioned obliquely and their relationship to each other cannot be discerned. There are abundant fine filaments in the adjacent cytoplasm. The membranes again appear sectioned perpendicularly near the lower margin figure (arrow) and here they are fused together. $\times 144\,000$
- 11 At the lateral margin of a bile canaliculus the plasma membranes of adjacent hepatic cells fuse to form a zonula occludens (z) near its lumen. A desmosome (macula adhaerens) can be recognized in the lower portion of the figure. Between these two elements of a junctional complex the plasma membranes are sectioned obliquely for most of their length but they can be seen to be clearly separated at two points (arrows). It is not possible to decide with certainty whether an intermediate junction (zonula adhaerens) occurs in this region. A mesh of fine filaments stretching from the zonula occludens to the desmosome lines the cytoplasmic surface of the plasma membranes. $\times 120\,000$



PLATE 5

EXPLANATION OF FIGURE

- 12 A dense concentration of ferritin molecules is seen in the sinusoidal lumen in the upper portion of the figure. Small droplets of moderate density (arrows) within it are identified as either chylomicrons or very low density lipoprotein particles. Several vesicles in the lining cell bordering the lumen contain numerous ferritin molecules. A few contain in addition a dense homogenous substance. Tortuous microvilli of the subjacent hepatic cell extend into the space of Disse which also contains a dense concentration of ferritin. The surface of the hepatic cell is deeply invaginated at one point (1) between the bases of adjacent microvilli. A pinocytotic vesicle containing ferritin molecules and faintly outlined lipid particles (2) appears free in the cytoplasm near the surface of the hepatic cell. $\times 91,000$



PLATE 6

EXPLANATION OF FIGURES

- 13 Arrows indicate coated vesicles containing ferritin in the sinusoidal lining cell (upper part of the figure) and hepatic cell (lower part of the figure) A vesicle containing only homogenous dense material (*dv*) appears near the surface of the hepatic cell $\times 67\ 000$
- 14 Two coated invaginations (arrows) appear along the surface of a hepatic cell A vesicle with dense homogenous content (*dt*) appears to the left of one of the invaginations $\times 128\ 000$

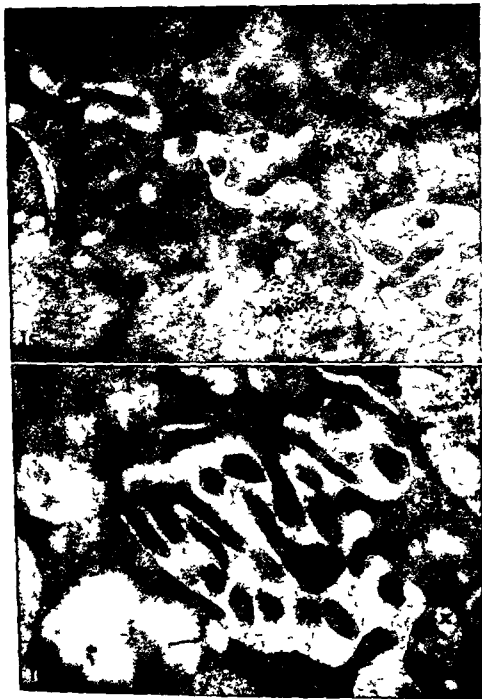


PLATE 7

EXPLANATION OF FIGURES

- 15-16 Both figures show portions of the space of Disse that extend some distance away from a sinusoid and dilate the space between hepatic cells. Numerous microvilli protrude into the extension of the space which contains many ferritin molecules and spherical particles presumably lipid which are not easily visualized because of their lack of density. The cytoplasm bordering the extensions contains numerous small dense vesicles (x) with a content that matches in diameter and density the spherical particles in the lumen. Some of the vesicles also contain ferritin. Two of them (arrows) are seen opening at the surface of hepatic cells. $\times 48\,000$ (fig 15) $\times 62\,000$ (fig 16)



PLATE 8

EXPLANATION OF FIGURES

- 17 Two studlike intercellular junctions appear in the upper part of the figure. The upper one is cut in cross section, the lower one in longitudinal section. Within both junctions the hepatic cells are separated by a distinct intercellular space. In the lower part of the figure a cluster of lipid droplets are seen in a localized dilation of the narrow intercellular space. $\times 102\,000$
- 18 At the top margin and in the center of the figure the plasma membranes of neighboring hepatic cells are fused together, obliterating the narrow intercellular space. Between the zones of fusion a distinct narrow space containing numerous ferritin molecules is present. $\times 122\,000$
- 19 Studlike junctions appear in the central and lower portions of the figure. Within each junction the adjacent hepatic cells are separated by a distinct space which contains ferritin. The plasma membranes of the hepatic cells are fused together in the lower part of the field. $\times 111\,000$

THE SURFACE OF THE HEPATIC CELL
 by H. H. H. and S. L. W. L.



On the Occurrence of a Fibrous Lamina on the Inner Aspect of the Nuclear Envelope in Certain Cells of Vertebrates¹

DON W. FAWCETT

Department of Anatomy Harvard Medical School Boston Massachusetts

ABSTRACT The fine structure of the fibrous lamina on the inner aspect of the nuclear envelope in cells of various invertebrates is reviewed and attention is drawn to the common occurrence of a similar but thinner layer in nuclei of cells in vertebrates. Certain superficial similarities are pointed out in the relations of fibrous lamina to the nuclear pores and of the basement lamina to the endothelial capillary pores. It is suggested that in future considerations of the physiological exchange of materials between nucleoplasm and cytoplasm the properties of the fibrous lamina must be taken into account.

A complex supporting layer of fine filaments closely applied to the inner aspect of the nuclear envelope has been described in *Amoeba proteus* (Pappas '56 Mercer '59) *Gregarina melanophila* (Beams et al. '57) and the neurones of the ventral nerve cord of *Hirudo medicinalis* (Gray and Guillery '63 Coggeshall and Fawcett '64). This structure has been called the fibrous lamina. No corresponding layer appears to have been described as yet for nuclei of vertebrate cells. Since the introduction of aldehyde fixatives for electron microscopy and the widespread practice of staining ultra thin sections with lead and uranyl ions the inner leaf of the nuclear envelope now often appears to be thicker than the outer. However at high magnification the membrane itself is found to have the usual dimensions. Its appearance of greater thickness being due to a continuous layer of closely compacted filamentous material applied to its inner surface. In view of the increased interest in the permeability properties of the nuclear envelope and the mechanisms of nucleocytoplasmic interaction (Baud '65 Lowenstein and Karno '63 '65) it would seem timely to draw attention to the occurrence of such a layer in a number of cell types in vertebrates and to suggest that it is the counterpart of the fibrous lamina already described for the nuclei of certain Protozoa, Gregarines and Annelids. Although the exact nature and functional significance of this layer cannot yet be specified it must be taken into ac-

count in future considerations of the physiological properties of the nuclear envelope.

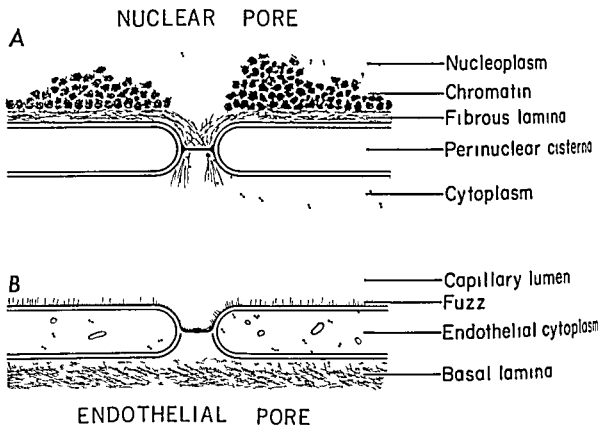
MATERIALS AND METHODS

The observations recorded here were incidental to investigations on the ventral nerve cord of the leech, the germinal epithelium and interstitial tissue of the cat testis, the guinea pig ductus epididymidis and the intestinal mucosa of the Congo eel. The fixation was accomplished in collidine buffered 1.3% osmium tetroxide in the case of the leech material. The vertebrate tissues were fixed in collidine buffered 5.5% glutaraldehyde followed by 1% osmium in the same buffer. Embedding was in Epon and the sections were stained with uranyl acetate and lead citrate. The micrographs were made on RCA EMU 3G electron microscope.

OBSERVATIONS

To facilitate comparison of the nuclear envelope of an invertebrate with that of vertebrates a micrograph of a ganglion cell nucleus from the leech is presented in figure 1. A prominent fibrous lamina (Gray and Guillery '63 Coggeshall and Fawcett '64) is found on the inner aspect of the nuclear envelope. In diametric sections it presents a scalloped profile with thin regions alternating with thicker re-

¹Supported in part by grants GM-6729 and GM 10182 from the Division of General Medical Sciences, National Institutes of Health, United States Public Health Service.



Text figure 1 Diagrams comparing the topographical relation of structures associated with a pore in the nuclear envelope (A) with the arrangement of components at a pore in a capillary endothelial cell (B). Both are traversed by a thin septum, the pore diaphragm, and by a layer of filamentous material — the fibrous lamina of the nuclear envelope in the one case and the endothelial basal lamina (basement membrane) in the other.

gions that project inward to form ridges or septa outlining a system of cylindrical compartments open at one end to the nucleoplasm and closed at the other by the nuclear envelope. In subtangential sections (fig 1 inset) the fibrous lamina presents a honeycomb appearance of dense septa delimiting circular areas of nucleoplasm of lower density. At high magnification the septa are observed to be composed of fine filaments 30 to 50 Å in diameter (see at arrows inset to fig 1). In the nuclear envelope at the bottom of each concavity in the fibrous lamina there is a typical nuclear pore. The filamentous material is very thin if not entirely lacking over the pore opening.

After glutaraldehyde and osmium fixation the chromatin in the nucleus of mammalian smooth muscle cells is disposed in masses around the periphery and is preserved in the form of granules that stain intensely with the combination of uranyl

and lead ions. The closely packed granular subunits of chromatin form a dark beaded row that runs parallel to but is not in contact with the smooth contour of the inner leaf of the nuclear envelope (fig 2). Instead the chromatin seems to be separated from the dense line representing the membrane proper by a layer 150 to 200 Å thick consisting of a very fine textured material of lower density than either the membrane or the chromatin. This layer therefore appears as a thin lighter zone of uniform thickness interposed between the dense chromatin and the innermost unit membrane of the bilaminar nuclear envelope (b in the inset to fig 2). Owing to its thinness and its compact organization the filamentous nature of this layer has not been convincingly demonstrated in the vertebrate material illustrated here. Nevertheless it seems permissible by analogy to assume that its ultimate structural components are basically similar to those of

corresponding layer in the nucleus of tannin invertebrates and to refer to it as *fibrous lamina*.

This layer lining the nuclear envelope of Schwann cells of peripheral nerve (fig 1) and endothelial cells (fig 8) is very similar in thickness and density to that of smooth muscle (figs 2 and 4). In the epidermal epithelium of the Congo eel the fibrous lamina is thicker and stains more heavily and therefore appears as a conspicuous dark layer (fig 3). Because it rarely matches the chromatin and the nuclear membrane in density its precise limits are more difficult to define.

In the nucleus of the interstitial cells of the cat testis the sparse heterochromatin occurs in small clumps scattered throughout the nucleoplasm and in a thin interrupted layer against the nuclear envelope (fig 7). Even at low magnification the inner element of the nuclear envelope appears unusually thick (see at arrows fig 7). At higher magnification this dark line is found to be made up of the inner leaf of the nuclear envelope and a heavily stained fibrous lamina of very uniform thickness (fig 9).

In the nucleus of leech neurones as described above there is invariably a circular discontinuity in the fibrous lamina over each pore in the nuclear envelope. It was anticipated that the same would be true in vertebrate nuclei and that where the central portion of a pore was included in the section the fibrous lamina would appear interrupted or greatly attenuated. This expectation is not borne out. The fibrous layer often appears to continue unchanged across the pore whether the section passes through the pore eccentrically or through the center. For example in figure 9 and the inset to figure 8 the sharpness of the image of the pore diaphragms and surrounding membranes would indicate that the sections pass through the center of the pores in a plane normal to the membranes. Yet in these figures the fibrous lamina clearly continues across the pore and has a sharply defined inner margin (see at arrows figs 8 and 9). In other cell types the inner edge of the fibrous lamina is poorly defined over the pore (figs 2 and 5). Nevertheless it contains material of appreciable density on both

sides of its diaphragm. This appearance suggests that in these instances the material of the fibrous lamina is present at the pores but more loosely organized there than it is elsewhere along the nuclear envelope.

The nucleus of the cat spermatocyte included here for comparison is representative of a number of cell types in which a continuous fibrous lamina cannot be detected. Its chromatin is dispersed and no dense clumps are present around the rim of the nucleus to provide the discontinuity in contrast that facilitates visualization of the fibrous lamina. Other small granular components of the nucleoplasm are scattered along the nuclear envelope however and it is quite evident that instead of being held away by an intervening layer these granules are often in direct contact with the inner membrane (fig 6). At the pores a moderately dense substance is found on either side of the pore diaphragm (see at arrow fig 6). This probably corresponds to the structure referred to by other authors as "the annulus." It is suggested that the substance of the annulus is the same as that comprising the fibrous lamina. If this is so it would seem that in some cells it forms a continuous layer lining the nuclear envelope while in others such as the spermatocyte it is lacking except at the pores.

DISCUSSION

In previous reports of a fibrous lamina in *Amoeba proteus* and in *Hirudo medicinalis* the suggestion was offered that this structure might have a supporting function providing a fibrous internal reinforcement for the nuclear envelope in cells with unusually large nuclei. This interpretation relating the fibrous lamina to nuclear size is difficult to defend however for among invertebrates there are many examples of cells with enormous nuclei in which this layer is not developed. Moreover in amoebae other than *Amoeba proteus* the fibrous lamina seems to be lacking even though the nuclei may be of comparable size. The published descriptions of the fibrous lamina in the leech were based upon examination of the very large peripheral glial and ganglion cells of the ventral nerve cord but it is also present in the endothelial

of nuclear pores is the same as that which in some cells forms a continuous lining for the nuclear envelope then further characterization of the pore substance will be facilitated by selection of cell types for study which have a well developed fibrous lamina

LITERATURE CITED

- Barnes R G and J M Davis 1959 The structure of nuclear pores in mammalian tissue J Ultrastruc Res 3 131-146
- Baud C A 1965 Nuclear membrane and permeability In Intracellular Membranous Structure, Japan Society for Cell Biology pp 323-330
- Beams H W T N Tahmisiian R Devine and E Anderson 1957 Ultrastructure of the nuclear membrane of a gregarine parasite in grasshoppers Exp Cell Res 13 200-204
- Coggeshall R E and D W Fawcett 1964 The fine structure of the central nervous system of the leech *Hirudo medicinalis* J Neurophysiol, 27 229-289
- Farquhar M G 1961 Fine structure and function in capillaries of the anterior pituitary gland Angiology 12 270-292
- Fawcett D W 1963 Comparative observations on the fine structure of blood capillaries In The Peripheral Blood Vessels J L Orbison and D E Smith Eds Williams and Wilkins Baltimore Maryland pp 17-44
- 1965 Surface specializations of absorbing cells J Histochem and Cytochem, 13 75-91
- Fawcett D W and F Witebsky 1964 Observations on the ultrastructure of nucleated erythrocytes and thrombocytes with particular reference to the structural basis of their discoidal shape Zeitschr f Zellforsch 62 785-806
- Feldherr C M 1962 The nuclear annulus as pathways for nucleocytoplasmic exchanges J Cell Biol 14 65-72
- Gray E G and R W Gullery 1963 On the nuclear structure in the ventral nerve cord of the leech *Hirudo medicinalis* Zeitschr f Zellforsch, 59 738-745
- Ito, S and W R Lowenstein 1965 Permeability of a nuclear membrane Changes during normal development and changes induced by growth hormone Science 150 909-910
- Kanno Y, and W R Lowenstein 1963 A study of the nucleus and cell membranes of oocytes with an intracellular electrode Exp Cell Res. 31 149-166
- Lowenstein W R and Y Kanno 1963 The electrical conductance and potential across the membrane of some cell nuclei J Cell Biol 16 421-425
- 1963 Some electrical properties of nuclear membrane examined with a microelectrode J Gen Physiol 46 1123-1140
- Luft J H 1965 The ultrastructural basis of capillary permeability In The Inflammation Process Chapter 3 Academic Press Inc New York pp 121-157
- Majno G and G E Palade 1961 Studies in inflammation I The effect of Histamine and Serotonin on vascular permeability an electron microscopic study J Biophys and Biochem Cytol 11 571-605
- Mercer E H 1959 An electron study of *Amoeba proteus* Proc Roy Soc B 150 216-232
- Merrill R W 1961 On the fine structure and composition of the nuclear envelope J Biophys and Biochem Cytol 11 559-570
- Pappas G D 1956 The fine structure of nuclear envelope of *Amoeba proteus* J Biophys and Biochem Cytol 2 Suppl 431-434
- Watson M 1959 Further observations on the nuclear envelope of the animal cell J Biophys and Biochem Cytol 6 147-156
- Wiener J D Spiro and W R Lowenstein 1965 Ultrastructure and permeability of membranes J Cell Biol 27 107-118
- Wischnitzer S 1960 The ultrastructure of the nucleus and nucleocytoplasmic relations Internat Rev Cytol 10 137-162

Footnote added in proof Since submission of this paper it has come to my attention that Dr Gianfranco Patrizi in an abstract in the Proceedings of the Eighth International Congress of Anatomists Wiesbaden 1965 described a similar dense layer on the inner aspect of the nuclear envelope to which he applied the term *zonula limitans nucleus*. This layer was reported to be of consistent occurrence in some cell types but absent in others. Among those in which it was found are Schwann cells endothelial cells fibroblasts kidney epithelium and amniotic and HeLa cells in tissue culture

PLATE 1

EXPLANATION OF FIGURE

- 1 An electron micrograph of a sector of the nucleus in a ganglion cell from the ventral nerve cord of the leech *Hirudo medicinalis*. The lower half of the figure is dominated by a large nucleolus consisting mainly of ribonucleoprotein granules. The nucleolus is held away from the nuclear envelope by a thick fibrous lamina whose alternate thick and thin regions give the margin of the nucleoplasm a scalloped appearance. Thickenings of the fibrous lamina project inward to form a hexagonal pattern of septa that delimit shallow cylindrical compartments of nucleoplasm. A nuclear pore is situated at the bottom of each compartment where the fibrous lamina is thinnest. In sub-tangential section the fibrous lamina presents the honeycomb configuration illustrated in the inset. The arrows indicate areas where the component filaments are resolved. (Micrograph by Dr Richard Coggeshall)

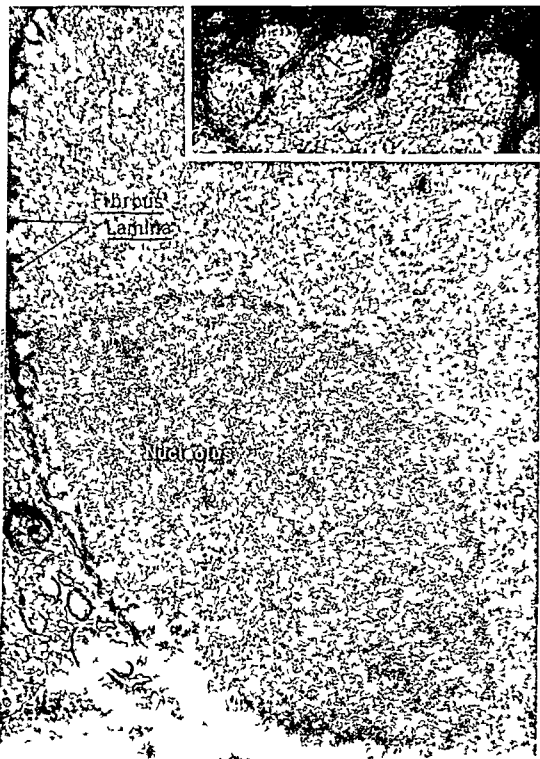


PLATE 2

EXPLANATION OF FIGURE

- 2 A portion of a smooth muscle cell from the guinea pig epididymis. The heavily stained nuclear chromatin is disposed around the periphery but does not appear to be in direct contact with the inner membrane of the bilaminar nuclear envelope. The thin layer of material of lower density intervening between the chromatin and the inner leaf of the nuclear membrane is believed to correspond to the fibrous lamina of the leech nucleus. At higher magnification in the inset the chromatin is indicated at *a*, the fibrous lamina at *b*, the inner membrane of the nuclear envelope at *c*, the perinuclear cisterna at *d*, and the outer membrane of the nuclear envelope at *e*.

c 11

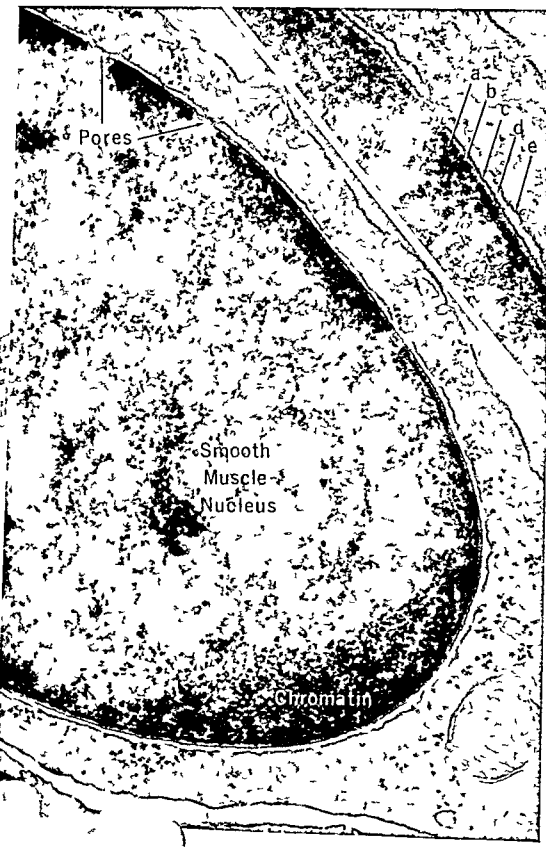


PLATE 3

EXPLANATION OF FIGURES

- 3 A small area of the nucleus and adjacent cytoplasm from an intestinal epithelial cell of *Amphiuma tridactylum*. In this case the fibrous lamina has stained more heavily and appears as a moderately dense fine textured layer about 300 A thick. The fibrous lamina appears to continue across the nuclear pore but is somewhat thinner and less dense in this region.
- 4-5 Additional examples from smooth muscle and Schwann cell nuclei showing the fibrous lamina as a thin layer of lower density interposed between the dense chromatin and the dark line representing the inner membrane of the nuclear envelope. At the arrows a fairly well demarcated inner margin of the fibrous lamina can be followed across the pore region. In the other pore without an arrow the material of the fibrous lamina appears less dense and has poorly defined limits.
- 6 A portion of the nucleus (above) and adjacent cytoplasm (below) from a cat spermatocyte. In contrast to the other examples on this plate a continuous fibrous lamina is absent. Granular components of the nucleoplasm are clearly in direct contact with the inner membrane of the nuclear envelope. There is however the usual moderately dense material associated with both sides of the diaphragm at the nuclear pore (at the arrow).

IF we ti

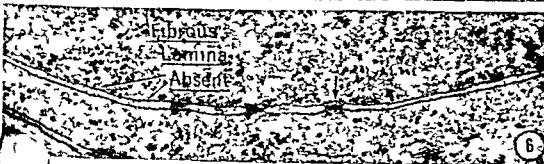
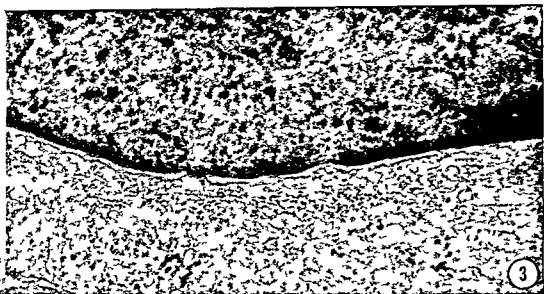


PLATE 4

EXPLANATION OF FIGURE

- 7 Nucleus of cat interstitial cell showing a thin peripheral accumulation of chromatin interrupted at the sites of nuclear pores. At this low magnification at the arrows the inner member of the bilaminar nuclear envelope appears to be several times the thickness of the membrane on the cytoplasmic surface. When an area such as that enclosed in the rectangle is examined at higher magnification (fig 9) it is found that this appearance of greater thickness is due to the presence of a fibrous lamina closely applied to the nuclear surface of a membrane of the usual thickness (80-90 Å).

S LAMINA OF THE NUCLEAR ENVELOPE
Fawcett

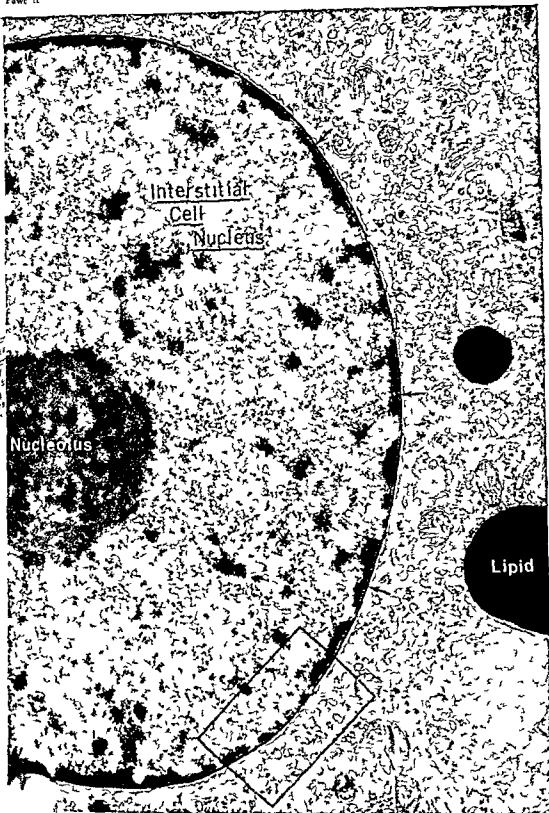


PLATE 5

EXPLANATION OF FIGURES

- 8 Two neighboring endothelial cells of a blood vessel in the interstitium of the cat testis. As in the smooth muscle and Schwann cells in figures 2, 4 and 5 the dense chromatin granules at the periphery of the nucleus are aligned in a row parallel to the nuclear envelope separated from it by a narrow zone of lower density representing the fibrous lamina. The region of a nuclear pore enclosed in the rectangle is shown at higher magnification in the inset. The arrows point to the sharp line of demarcation of the fibrous lamina over the pore and the area of low density in the adjacent nucleoplasm.
- 9 A portion of an interstitial cell nucleus similar to that enclosed in the rectangle on figure 7. The fibrous lamina is more heavily stained than in most of the other figures and has a texture suggesting that it is a feltwork of randomly oriented thin filaments. The arrows point to the sharp inner margin of the fibrous lamina which appears to continue across the pores.

LAMINA OF THE NUCLEAR ENVELOPE

awcett

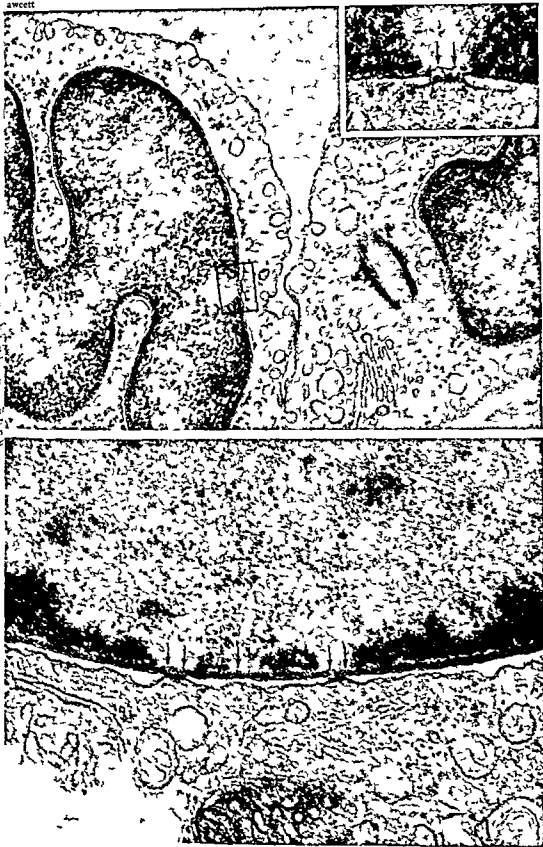


PLATE 5

EXPLANATION OF FIGURES

- 8 Two neighboring endothelial cells of a blood vessel in the interstitium of the cat testis. As in the smooth muscle and Schwann cells in figures 2, 4, and 5 the dense chromatin granules at the periphery of the nucleus are aligned in a row parallel to the nuclear envelope separated from it by a narrow zone of lower density representing the fibrous lamina. The region of a nuclear pore enclosed in the rectangle is shown at higher magnification in the inset. The arrows point to the sharp line of demarcation of the fibrous lamina over the pore and the area of low density in the adjacent nucleoplasm.
- 9 A portion of an interstitial cell nucleus similar to that enclosed in the rectangle on figure 7. The fibrous lamina is more heavily stained than in most of the other figures and has a texture suggesting that it is a feltwork of randomly oriented thin filaments. The arrows point to the sharp inner margin of the fibrous lamina which appears to continue across the pores.

Electron Microscopic Study of the Gingivo-dental Junction of Man¹

MAX A. LISTGARTEN

University of Toronto Faculty of Dentistry Toronto Canada

ABSTRACT Erupted teeth with attached gingival tissue were obtained from 15 patients ranging in age from 4 to 26 years. After preliminary glutaraldehyde fixation the area to be studied was excised with a high speed dental drill. The tissue was decalcified in Versene subdivided into smaller blocks and post fixed in 2% buffered osmic acid fixative. Epon embedded sections were stained with uranyl acetate and lead citrate prior to being examined in the electron microscope.

The results indicate that (1) an attachment is present between the epithelial cuff and enamel or cementum (2) the attachment apparatus of epithelium to tooth structure consists of hemidesmosomes and a cementing layer resembling the basement lamina of various epithelium-connective tissue junctions (3) the attachment may be to two types of cuticle of undetermined origin or directly to the tooth and (4) apical to the epithelial attachment the gingiva is connected to cementum by parallel bundles of collagen fibrils which extend from the gingiva into the cementum. The cementum itself consists of parallel collagen fibrils the periodicity of which is in register between adjacent fibrils. The fibrils are embedded in a rather sparse granular matrix.

In 1929 Orban and Mueller wrote a comprehensive and critical review on the microscopic structure of the gingival crevice area with particular emphasis on the structure of the epithelial attachment. Their conclusion at that time confirmed Gottlieb's previous findings (21) that an epithelial attachment can be found on enamel and that contrary to previous beliefs the attachment was not located at the cemento-enamel junction only (Black 15). This concept remained more or less unchallenged until 1952 when Waerhaug published a monograph in which he denied the existence of an organic epithelial attachment to enamel and provided some experimental proof that the bottom of the normal gingival crevice was situated at the cemento-enamel junction. He visualized the epithelium adjacent to the tooth as a tightly adapted cuff which could however be displaced from the tooth by the introduction into the potential space of thin metallic strips. Since that time numerous articles have been written to support Gottlieb's concept of an organic attachment (Becks '29 Kronfeld 30 Toller '39 Baume 52 Baume 53 Macapanpan 54 Ussing 55 Orban Bhatia Kollar and Wentz 56 Weinreb 60) as well as Waer

haug's proposal of an epithelial cuff (Greulich 61 Beagrie and Skougaard 62 Skougaard and Beagrie 62 Greulich 62 Trott and Gorenstein 63 Hunt and Paynter 63 Engler Ramfjord and Hiniker 65 McHugh and Zander 65).

Recently Stern (62-63) using electron microscopy described the epithelial attachment in the continuously erupting incisors of rats. This attachment appeared to exist both on enamel and cementum. However because morphologically and physiologically the dento-gingival relationship in rodent teeth is markedly different from that of primate teeth (Aldritt 61) it still remained to be shown that a true epithelial attachment was present in man.

In the present report which is part of a study to develop a satisfactory method for processing periodontal tissues for electron microscopic study evidence will be presented which confirms the existence of an attachment between gingival epithelium and the teeth of man. This attachment is morphologically similar to that which is found between epithelial lining membranes and their connective tissue support.

¹ This investigation was supported by grant DA 136 from the National Research Council of Canada Associate Committee on Dental Research.

cuticle A in the remainder of this paper occasionally appeared continuous with though structurally different from the enamel matrix (fig 6) Cuticle A frequently demonstrated appositional lines in its structure which was quite dense and angular (fig 7)

Although cuticle A was frequently quite prominent near the cemento-enamel junction (figs 4 7) it narrowed considerably coronally (fig 8) sometimes ending suddenly (fig 12) or continuing as a thin approximately 100 μ layer between the epithelial attachment and the enamel (fig 9) In one specimen cuticle A was allowed from the apical border of the enamel to a point coronal to the epithelial attachment In this instance the epithelial attachment was to cuticle A The most coronal cells of the attachment were separated from the cuticle This separation occurred between the cuticle and the basement lamina the latter remaining attached to the hemidesmosomes of the attachment apparatus (fig 10)

A second type of cuticle was observed either covering cuticle A (fig 11) or in direct apposition to enamel (fig 12 15) or cementum (fig 13) It was generally less granular than cuticle A usually presenting a mottled appearance (figs 14 15) It was usually found opposite the cells of the epithelial attachment and will be referred to as cuticle B Where the epithelial attachment extended onto cementum cuticle B continued along the external surface of the cementum to end near the apical portion of the epithelial attachment Although cuticle B was generally found as an intervening layer between the epithelial attachment and the tooth surface it was not always necessarily present in that position Thus an epithelial attachment could be found directly to cuticle A (figs 7 9 14) or directly to tooth enamel (fig 16) without any intervening structure resembling cuticle B It should also be noted that the cuticle binding bacterial plaque to tooth surface (fig 17) was morphologically indistinguishable from cuticle B

The junction between the tooth or the cuticles and the epithelial cells was actually mediated by a thinner less dense granular layer similar to the basement lamina of epithelium The basement la-

mina was always found between the epithelial cells and the adjacent tooth or cuticles (figs 8 to 15) It varied in width from 400 to 1200 \AA Together with the hemidesmosomes present along the portion of the plasma membrane facing the tooth it appeared to constitute the actual attachment apparatus of the epithelial cells to the teeth Occasionally invaginations of the cell membrane adjacent to the basement lamina were observed which were filled with a substance morphologically identical to that of the basement lamina (figs 11 12)

Circular profiles were occasionally found within the basement lamina of the attachment apparatus (figs 12 13 15) These probably correspond to microvilli from nearby epithelial cells They frequently demonstrated a series of concentric layers on their periphery which dimensionally corresponded to the layers observed in hemidesmosomes These layers have recently been described in detail by Stern (65) in the hemidesmosomes of gingival epithelium The reader should refer to this paper for further detail The appearance of the limiting membrane of these microvilli suggests the existence of belt like or cup-like hemidesmosomes completely surrounding the top of these cytoplasmic extensions

The connective tissue attachment

The epithelial membrane forming the epithelial attachment was connected to the gingival connective tissue by means of an attachment apparatus consisting of hemidesmosomes and a basement lamina similar to that found in other connective tissue-epithelial junctions (figs 7 18) Collagen fibrils from the connective tissue came in contact with but never crossed the basement lamina

Apical to the epithelial attachment the collagen fibrils of the gingival connective tissue became oriented into parallel bundles which were inserted into the cementum and became an important component of the organic matrix of cementum (figs 5 19 20) The other component of the organic matrix appeared as a dense often granular substance which surrounded the collagen fibrils within the cementum This interfibrillar granular material was most

METHOD AND MATERIALS

Teeth which visually and radiographically appeared free of periodontal disease were obtained at the time of extraction from 15 patients ranging in age from 4 to 26 years and immediately placed in ice cold buffered glutaraldehyde fixative. Concentrations of glutaraldehyde of 5% and 6.25% were used. Buffers which were adjusted to pH 7.4 included phosphate cacodylate, veronal acetate and collidine.

Some teeth were obtained with an intact lingual or facial covering of oral mucosa or bone and oral mucosa. Separation of the covering tissues from the adjacent tissues prior to extraction was achieved by the use of a sharp scalpel and when needed a mallet and chisel. Other teeth were obtained by extraction without regard for the preservation of an intact relationship between the teeth and surrounding soft tissues. Even though elevators which mechanically separate the tooth from the soft tissue were used in some of these extractions, some soft tissue invariably remained attached to the extracted tooth, especially in the cervical region.

After an interval of 1 to 3 hours of preliminary glutaraldehyde fixation the teeth were trimmed with a no. 56 fissure bur in a dental engine equipped with an air driven turbine under a water spray coolant so that only a very thin layer of mineralized dental tissue remained in contact with the surrounding soft tissue. The trimmed specimen was left to fix overnight in the glutaraldehyde fixative. It was then transferred to a 0.25 M solution of Verseyne¹ made up in the appropriate buffer or in the glutaraldehyde fixative itself. Demineralization generally required 3 to 7 days. After demineralization was completed the specimens were subdivided into smaller blocks approximately 1 mm thick. These were post fixed for 1 to 3 hours in 2% osmic acid fixative buffered to pH 7.4, dehydrated in graded aqueous solutions of ethanol and embedded in Epon (Luft 61). A total of 130 blocks were examined in this study. The preparation of the tissues for embedding is diagrammatically illustrated in figure 1. Sections were cut at 0.1 μ on a Porter Blum MT 2 ultramicrotome collected on either bare or carbon reinforced formvar coated grids and

stained with a saturated solution of uranyl acetate in 50% ethanol and with lead citrate (Reynolds 63). Sections were examined in a Phillips EM 200 microscope at 60 or 80 kv using the double condenser and a 20 μ objective aperture.

RESULTS

In all teeth examined whether extracted with care so as to not disturb the gingival attachment or whether extracted in routine fashion, evidence of a firm connection of soft tissue with tooth was always found. In routinely extracted teeth examination of the region between the remaining soft tissue and the tooth indicated that the actual junction between soft and hard tissue was frequently intact but tears were evident within the epithelium or connective tissue portion of the attachment (figs. 2, 3).

The examination of teeth erupted for as long as 20 years still revealed what appeared as a firm connection of soft tissue to enamel. No major differences in the appearance of the attachment could be attributed to the type of tooth, the age or sex of the patient.

In the remainder of this paper the term apical refers to the location of a structure closer to the root tip of the tooth. The term coronal signifies that the location is closer to the crown end of the tooth.

The epithelial attachment

Because the epithelial attachment of the tooth was frequently connected to cuticular structures covering the tooth rather than directly to enamel or cementum, it is first necessary to describe these cuticular structures.

In cases where the cementum did not overlap enamel, the cervical portion of the enamel was often covered with an electron dense layer which ended at the most apical border of the enamel flush with the cementum (fig. 4). Cementum was sometimes found over the enamel apical to the epithelial attachment. In such cases the dense layer continued uninterrupted between the enamel and the cementum to the most apical border of the enamel (fig. 5). This dense layer will be referred to as

¹ Ethylene diamine tetra acetic acid, Beresford Chemical Co., Framingham, Mass., U.S.A.

The material examined in this study included only fully erupted teeth with the gingival attachment consisting of reduced enamel epithelium having presumably been partially or completely replaced by an attachment consisting of cells derived from the oral epithelium and outer layers of the reduced enamel epithelium. The firmness of the attachment was evident despite the mechanical stress to which some of our material had been subjected during routine extractions; the attachment of epithelial cells to the tooth remained intact in some areas. When tears did occur they generally appeared within the epithelium itself. The finding of a firm attachment to the tooth and tears within the epithelium must however be interpreted with care in view of the preparative procedure. The latter included demineralization with a chelating agent despite the fact that tissues were first fixed in glutaraldehyde; it is possible that removal of calcium ions by chelation might result in loss of cellular adhesiveness with consequent tears within the epithelium without affecting the attachment of these cells to the tooth or its cuticles (Connan 61, Berwick and Connan 62). Thus the tears within the epithelium may not necessarily be due to mechanical stress but rather might reflect a sudden weakening of the desmosomes due to calcium depletion during the preparative procedure. Of particular interest is the finding that the attachment apparatus consisting of hemidesmosomes and the basement lamina which connects the epithelium to the tooth or its cuticles is remarkably similar to that seen at the junction of any epithelial lining with its underlying connective tissue. The basement lamina of most epithelial membranes including the gingiva consists of a dense homogeneous layer ~ 400 Å wide separated from the epithelial plasma membrane and its hemidesmosomes by a well defined less dense layer of ~ 400 Å (Listgarten 64, Melcher 65, Stern 65). The basement lamina of teeth does not reveal as clearly these double strata of different density. Also it is wider (~ 400-1200 Å) and of less constant width than the basement lamina of other epithelial membranes. However the average width (~ 800 Å) of the

basement lamina of the epithelial attachment closely approximates the combined width of the two layers of the basement lamina of other epithelial membranes.

Of additional interest is the fact that such an attachment apparatus can exist between epithelium and a tissue such as enamel which is not of mesenchymal origin. The finding adds further weight to the recent observations by Midgley and Pierce (63), Pierce, Midgley and Sri Ram (63), Pierce, Beals, Sri Ram and Midgley (64) and Mukerjee, Sri Ram and Pierce (65) that at least some basement membranes are of epithelial origin. The appearance in this study of structures resembling secretory vacuoles along the epithelial cell membrane facing the tooth suggests that cells of the epithelial attachment may be involved in some secretory activity. The fact that the contents of these vacuoles structurally resemble the substance of the cementing layer lends support to the possibility that the epithelial cells may be active in the synthesis of this layer.

The resemblance of the epithelial attachment to epithelial-connective tissue junctions does not end with the morphological appearance. It is well known that if an epidermal surface is locally denuded of epithelium the adjacent epithelial cells can quickly glide over the denuded connective tissue and cover the defect. Yet despite their relatively rapid motion along a connective tissue surface it is extremely difficult to separate the epithelial cells from the underlying connective tissue by means of a force applied perpendicularly to the epidermal surface.

A similar situation probably exists with respect to the epithelial attachment which is firmly resistant to forces which might tend to detach the epithelium from the tooth yet cells in contact with the tooth can quickly migrate from the basal portions of the epithelial attachment toward the gingival crevice (Greulich 61, Beagrie and Skougaard 62, Skougaard and Beagrie 62, Greulich 62, Hunt and Paynter 63). The theoretical aspects of some of the mechanisms which may play a part in the attachment of epithelial cells to tooth enamel have been recently reviewed by Schultz-Haude and co-workers (63) and the reader is advised to consult that pub-

clearly observed as localized deposits near to the cementum surface (fig 22) generally closely related to cytoplasmic extensions from adjacent connective tissue cells presumably cementoblasts

In the coronal portion of cementum near the cemento-enamel junction collagen fibrils were sometimes loosely arranged with a relatively large proportion of interfibrillar material (fig 4). More apically, the fibrils became denser and were arranged in remarkably parallel bundles both before and after entering the cementum (figs 20-21). The packing of these fibrils was so precise that the multiple bands which constitute the ~ 600 Å period of collagen fibrils could be followed over large areas of cementum as a series of lines roughly parallel to the cementum surface (fig 21). No evidence of spur-like cementum formations were evident at points on the cementum where collagen fibrils entered from the adjacent connective tissue.

The bundles of collagen fibrils extended in a more or less straight line from the cemental surface to the dentino-cemental junction. In general no marked curving of the fibrils was observed within the cementum. Within 1 to 3 μ from the dentino-cemental junction the cemental fibrils appeared to lose their closely packed parallel arrangement (fig 23). In this region the bands of adjacent fibrils were not as perfectly in register as the bands of fibrils closer to the surface. There was no apparent connection between the collagen fibrils of the cementum and dentine although the fibrils of one tissue were closely interdigitated with the fibrils of the other. The junction between dentine and cementum was easily identified because in this location the collagen fibrils of the dentine appeared to lack any kind of orientation in contrast to the more regularly arranged fibrils of cementum. No evidence of a basement lamina could be detected at the cemento-dentinal junction. Neither was there any evidence that cemental fibrils assumed a parallel relationship to the dentinocemental junction as is the case in rat incisors (Stern 64).

Where the epithelial attachment was located on cementum the collagen fibrils within the cementum ended abruptly at

the cementum surface. A couple of B was generally found on the surface between the attachment of the epithelium and the cementum (13).

DISCUSSION

Although much has been written with respect to the existence of an epithelial attachment versus an epithelial cuff, the two concepts regarding the relation of the epithelium to the tooth are necessarily mutually exclusive. Much of the recent work in this area points to the fact that the epithelium although tightly bound to the tooth is capable of rapid migration along its surface. Recent studies using autoradiographic techniques (Beagrie and Skougard 61, Skougard and Beagrie 62, Greulich 63, Hunt and Paynter 63, McHugh and Zander 65) have indicated not only that of the epithelial attachment are capable of rapid migration along the tooth but that the whole epithelial attachment probably turns over within a period of a little as five days in mice (Beagrie Skougard '62) and six days (Skougard and Beagrie 62). Ramfjord and Hiniker (65) in confirming the concept of a dynamic epithelial attachment observed that the turnover of cells in the attachment was slower than in the sulcus epithelium and that the turnover seemed to increase in inflamed areas. They interpreted these findings as an indication of decreased healing action by the epithelial attachment in inflamed areas.

The epithelial attachment in monkeys appears to undergo a period of maturation shortly after eruption during which the reduced enamel epithelium, its original component, is gradually replaced by the apical downgrowth of squamous epithelial cells derived from the oral epithelium and outer layers of the reduced enamel epithelium (McHugh 61, 63, Cohen 62, McHugh and Zander 65). McHugh (63) states that this replacement requires approximately 18 months in monkeys and is probably longer in man. Cohen's experiments indicated that the presence over the enamel of the reduced enamel epithelium is essential for the normal development of the mature attachment.

1) Kronfeld (28) and Gottlieb and Orban (38) are of the order of several hundred micron and are believed to be associated with increased occlusal stress. No dental spurs comparable in size with those seen in rat incisors were observed in this investigation.

The results of a study to determine the nature of the attachment found between erupted human teeth and their surrounding soft tissue has been recently completed. The findings to be published shortly indicate that morphologically the attachment of reduced enamel is similar to that of the epithelial attachment of erupted teeth (Listgarten 66).

ACKNOWLEDGMENTS

The author wishes to thank the members of the Department of Oral Surgery for their cooperation in obtaining the specimens for this study and Dr K J Paynter for his helpful suggestions.

LITERATURE CITED

- Adrian W S 1961 The epithelia in the dento gingival junction *Dent Pract* 11 213-223
- Awaza Y 1961 Electron microscopy of carious cementum — with special reference to early caries *J Nihon Univ School Dent* 3 89-106
- Burton J 1952 Observations concerning the histogenesis of the epithelial attachment *J Periodont* 23 71-84
- 1953 The structure of the epithelial attachment revealed by phase-contrast microscopy *J Periodont* 24 99-110
- Bagby G S and M R Skougard 1962 Observations on the life cycle of the gingival epithelial cells of mice as revealed by autoradiography *Acta Odont Scand* 20 15-31
- Berk H 1929 Normal and pathological pocket formation *J Am Dent Assoc* 16 2167-2188
- Berwick L and D R Coman 1962 Some chemical factors in cellular adhesion and stickiness *Cancer Res* 22 982-986
- Black G V 1915 Special dental pathology *Medico-dental Publishing Co Chicago*
- Bohen B 1962 A study of the periodontal epithelium *Brit Dent J* 112 55-64
- Coman D R 1961 Adhesiveness and stickiness. Two independent properties of the cell surface *Cancer Res* 21 1436-1438
- Engler W O S P Ramfjord and J J Hiniker 1965 Development of epithelial attachment and gingival sulcus in rhesus monkeys *J Periodont* 36 44-57
- Frank R M and J Nalbandian 1963 Comparative aspects of development of dental hard structures *J Dent Res* 42 422-437
- Gottlieb B 1921 Der Epithelansatz am Zahn *Dtsch Mtschr Zahnheilk* 39 142-147
- Gottlieb B and B Orban 1938 Biology and pathology of the tooth and its supporting mechanism *The Macmillan Co New York* p 70
- Greulich R C 1961 Epithelial DNA and RNA synthetic activities of the gingival margin *J Dent Res* 40 682-683 Abstract
- 1962 Cell proliferation and migration in the epithelial attachment collar of the mouse molar 40th General Meeting Int Assoc Dent Res Abstract no 304
- Heuser H 1962 Wird die Zementoberfläche des Menschlichen Zahnes durch die Funktion gestaltet? *Dtsch Zahnärztl Ztschr* 13 861-867
- Hunt A M and K J Paynter 1963 The role of cells of the stratum intermedium in the development of the guinea pig molar. A study of cell differentiation and migration using tritiated thymidine *Arch Oral Biol* 8 65-78
- Kronfeld R 1928 Zement und Scharpeysche Fasern *Ztschr Stomatol* 26 714-734
- 1930 The epithelial attachment and so-called Nasmyth's membrane *J Am Dent Assoc* 7 1889-1907
- Levine P T M J Glumcher and L C Bonar 1964 Collagenous layer covering the crown enamel of unerupted permanent human teeth *Science* 146 1676-1678
- Listgarten M A 1964 The ultrastructure of human gingival epithelium *Am J Anat* 114 49-70
- 1966 Phase-contrast and electron microscopic study of the junction between reduced enamel epithelium and enamel in unerupted human teeth *Arch Oral Biol* (in press)
- Luft J H 1961 Improvements in epoxy resin embedding methods *J Biophys Biochem Cytol* 9 409-414
- Macapanpan L C 1954 Union of the enamel and gingival epithelium *J Periodont* 25 243-245
- McHugh W D 1961 The development of the gingival epithelium in the monkey *Dent Pract* 11 314-324
- 1963 Some aspects of the development of gingival epithelium *Periodontics* 1 239-244
- McHugh W D and H A Zander 1965 Cell division in the periodontium of developing and erupted teeth *Dent Pract* 15 451-457
- Melcher A H 1965 The nature of the "basement membrane" in human gingiva *Arch Oral Biol* 10 783-792
- Midgley A R Jr and G B Pierce Jr 1963 Immunohistochemical analysis of basement membranes of the mouse *Am J Path* 43 929-943
- Murkerjee H J Sri Ram and G B Pierce Jr 1965 Basement membranes. V Chemical composition of neoplastic basement membrane mucoprotein *Am J Path* 46 49-57
- Orban B J 1926 Schmelz- und Zahnoberhäuten *Ztschr Stomatol* 24 136-167
- Orban B J and E Mueller 1929 The gingival crevice *J Am Dent Assoc* 18 1206-1242.

lication for further details and additional references

No evidence was found to support the concept of a fibrillar attachment as presented by Baume (53) with tonofibrils from the epithelial cells extending through the attachment area to become continuous with the enamel matrix

From the electron micrographs obtained in this study only two morphologically distinct types of cuticles could be identified. The first type referred to as cuticle A consisted of an electron dense granular layer which appeared to correspond by definition to a primary enamel cuticle (Gottlieb 21 Orban 26) mainly because of its location over the enamel only and between the enamel and cementum when the latter overlapped the enamel. This cuticle was occasionally followed past the epithelial attachment over the erupted portion of the enamel (fig 10)

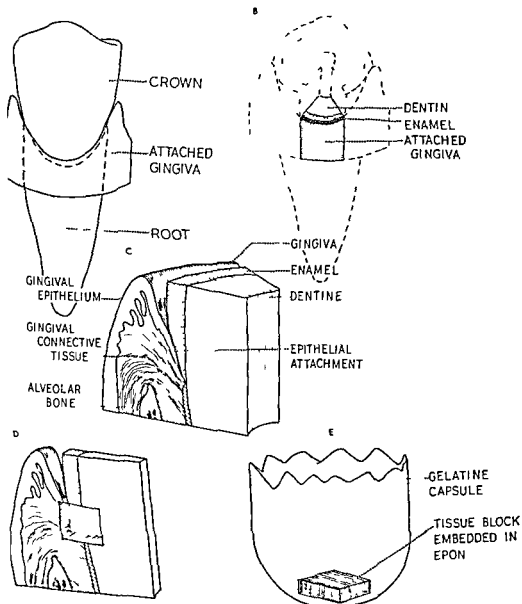
The other type of cuticle referred to as cuticle B was less granular than cuticle A and frequently presented a mottled appearance. It was generally found in contact with the epithelial attachment lying directly on enamel (fig 12) or cementum (fig 13) or over cuticle A (fig 11). However there was no evidence to suggest that cuticle B was secreted by epithelial cells. Furthermore the cuticle attaching bacterial plaque to the tooth surface (fig 17) appeared morphologically similar and is unlikely to be a secretion product of epithelial cells. It is quite possible that cuticle B is derived from organic probably protein components of tissue fluid or saliva.

Because demineralized material was employed in this study it was not possible to determine whether either or both types of cuticle were initially mineralized. It is of some interest however to note the morphological resemblance of cuticle A to the granular cementum matrix (fig 19). Perhaps it corresponds to a form of coronal cementum devoid of a collagenous fibrillar component. The existence of a cementum layer over tooth enamel of human teeth has been recently suggested by Levine, Glimcher and Bonar (64). However the coronal cementum described by these authors is morphologically different from cuticle A.

The connective tissue attachment of the gingiva to the tooth was mediated by collagen fibrils extending from the gingival connective tissue into the cementum where they formed the so-called Sharpey's fibrils. In close proximity to the denture these fibrils did not assume a parallel arrangement to the dentino-cemental junction. Such an arrangement of the collagen fibrils within the cementum had been reported by Selvig (63) and Stern (64). However these authors were working with mouse and rat incisors respectively. The difference in arrangements of fibrils within the cementum of continuously erupting teeth and human teeth could be explained simply on the basis of the relatively rapid rate of eruption of the rodent teeth. In contrast to cementum from continuously erupting rat incisors the cementum of human teeth contained a much higher concentration of collagen fibrils. This is in accord with similar observations by Wazwa (63), Frank and Nalbandian (63) and Stern (64). The concentration of interfibrillar matrix was correspondingly smaller in human cementum.

Some collagen fibrils which were embedded in cementum did not continue into the gingival connective tissue but rather stopped near the cementum surface. These were located under areas of new cementum matrix deposition (fig 22) or deep to the epithelial cuticle when the epithelial attachment was present on cementum (fig 13). Thilander (61) has recently described the dissolution of cemental fibrils near the cementum surface in rat molars affected with periodontal disease. Whether embedded fibrils become lysed at the cementum surface in disease only or whether such lysis may occur as part of a physiological process of tissue turnover is not clear.

Although cemental spurs have been described in rat incisors as well as in human teeth the order of magnitude of these structures is quite different from rat to man. The spurs described by Stern (64) in rat incisors are quite frequent along the cementum surface surrounding almost every individual fibril entering the cementum with a conical projection approximately 0.1-0.2 μ in size. The spurs described in human cementum by Heuser



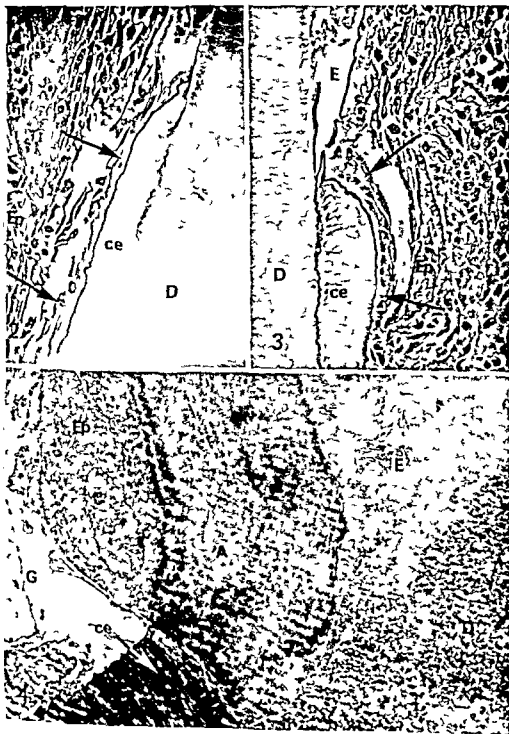
- Orban B J H Bhatia J A Kollar and F M Wentz 1956 The epithelial attachment J Periodont 27 167-180
- Pierce G B Jr T F Beals J Sri Ram and A R Midgley Jr 1964 Basement membranes IV Epithelial origin and immunologic cross reactions Am J Path 45 929-961
- Pierce G B Jr A R Midgley Jr and J Sri Ram 1963 The histogenesis of basement membranes J Exp Med 117 339-347
- Reynolds E S 1963 The use of lead citrate at high pH as an electron-opaque stain in electron microscopy J Biophys Biochem Cytol 17 208-212
- Schultz Haudt S D J Waerhaug S H From and A Attramadal 1963 On the nature of contact between the gingival epithelium and the tooth enamel surface Periodontics 1 103-108
- Selvig K A 1963 Electron microscopy of Hertwig's epithelial sheath and of early dentin and cementum formation in the mouse incisor Acta Odont Scand 21 175-186
- Skougaard M R and G S Beagrie 1962 The renewal of gingival epithelium in marmosets (*Callithrix jacchus*) as determined through autoradiography with thymidine- H^3 Acta Odont Scand 20 467-484
- Stern I B 1962 The fine structure of the ameloblast-enamel junction in rat incisors epithelial attachment and cuticular membrane in Electron Microscopy Fifth Congr Electron Microscopy New York 2 QQ6
- 1963 Electron microscopic observations of the dento-gingival attachment in rat incisors 41st General Meeting Int Res Abstract no 244
- 1964 An electron microscopic study of the cementum Sharpey's fibers and periodontal ligament in the rat incisor Am J Anat 137 377-410
- 1965 Electron microscopic study of oral epithelium I Basal cells and the basement membrane Periodontics 3 224-230
- Thilander, H 1961 Periodontal disease in a white rat Trans Roy Schools Dent Sci Holm and Umea 2 6
- Toller, J R 1939 The organic content of dentine the enamel and the epithelial attachment in dogs Brit Dent J 67 443-448
- Trott J E and S L Gorenstein 1963 Rates in the oral and gingival epithelium of rat Arch Oral Biol 8 425-434
- Ussing M 1955 The development of epithelial attachment Acta Odont Scand 12 123-154
- Waerhaug J 1952 The gingival pocket. Odont Tidskr 60 Supplement 1
- Weinreb M M 1960 The epithelial attachment J Periodont 31 186-196

PLATE 1

EXPLANATION OF FIGURES

Fig 1 Diagram illustrating the method used in obtaining and orienting specimens of the cemento-enamel junction area for study with the electron microscope

- A Tooth with attached gingiva Fixed as shown in glutaraldehyde for 1-3 hours
- B Tissue remaining after trimming away of excessive tissue Fixed as shown in glutaraldehyde for approximately 24 hours then demineralized in Versene
- C Side view of tissue block shown in B prior to subdivision into smaller blocks
- D Smaller blocks are excised under a dissecting microscope after demineralization in Versene The shape of the block facilitates its subsequent orientation in the gelatin capsule
- E Properly oriented block in an Epon filled gelatin capsule



Abbreviations

A type A cuticle
B type B cuticle
Ba bacteria
bm basement lamina adjacent
to connective tissue
ce cementum
Ceb cementoblast

cem interfibrillar cementum
matrix
CL basement lamina adjacent
to the tooth
D dentine
Dcej dentino cemental junction
E enamel space
Fm enamel matrix

Ep cells of epithelial attachment
G gingival connective tissue
Gc gingival crevice
Hd hemidesmosome
mv microvilli
v secretory vacuole
zo zonula occludens

PLATE 2

EXPLANATION OF FIGURES

- 2-3 Tear within epithelial attachment. Note that epithelial cells remain attached to the tooth structure (arrows). Lower first deciduous molar of five year old boy. Phase contrast $\times 400$
- 4 Cemento-enamel junction area. Upper second premolar of 15 year old boy $\times 4500$

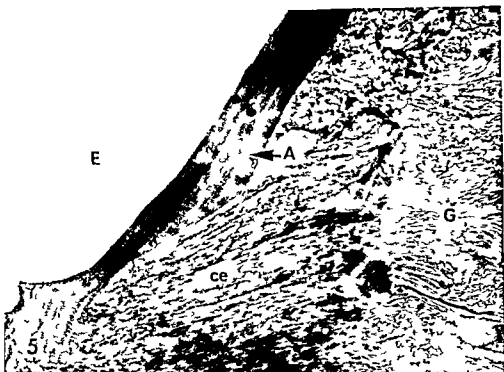


PLATE 3

EXPLANATION OF FIGURES

- 5 Cemento-enamel junction area just apical to epithelial attachment
Note type A cuticle between enamel space and cementum Lower
second deciduous molar of five year old boy $\times 10\,000$
- 6 Junction of type A cuticle and enamel matrix near cemento-enamel
junction Upper second premolar of 15 year old boy $\times 30\,000$



PLATE 4

EXPLANATION OF FIGURE

- 7 Epithelial attachment on type A cuticle just coronal to cemento-enamel junction area shown in figure 4. Note appositional layers within the cuticle. Upper second premolar of 15 year old boy
X7000

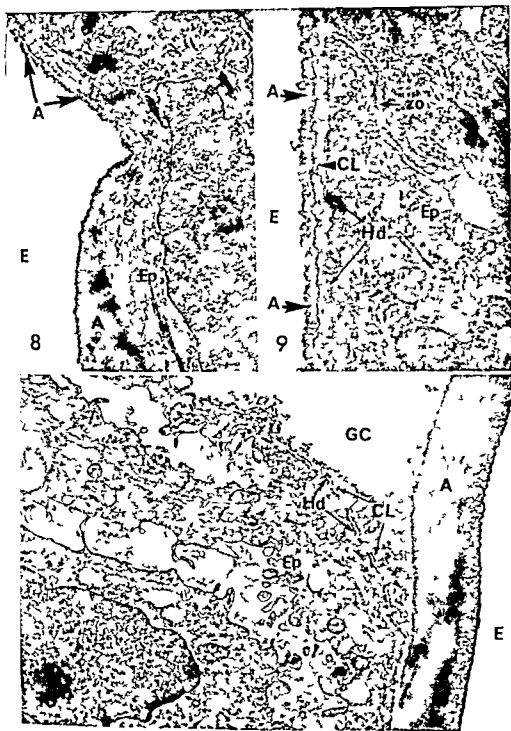


PLATE 5

EXPLANATION OF FIGURES

- 8 Type A cuticle narrowing to $\sim 100 \text{ m}\mu$ layer between enamel and epithelial attachment Upper second premolar of 15 year old boy $\times 14\,000$
- 9 Continuation of type A cuticle coronal to area shown in figure 8 between enamel space and basement lamina of epithelial attachment Upper second premolar of 15 year old boy $\times 36\,000$
- 10 Epithelial attachment to type A cuticle Note that where epithelium is separated from cuticle basement lamina is retained along cell surface opposite to the hemidesmosomes Lower first deciduous molar of five year old boy $\times 11\,000$



PLATE 6

EXPLANATION OF FIGURES

- 11 Epithelial attachment to type B cuticle which in turn lies over the type A cuticle covering the enamel. Structure resembling a discharging vacuole can be seen to contain a granular material similar to that of the basement lamina. Lower first deciduous molar of five year old boy $\times 37\,000$
- 12 Section just coronal to figure 11 showing the end of type A cuticle (arrow). The type B cuticle continues coronally in direct apposition to the enamel. Lower first deciduous molar of five year old boy $\times 39\,000$

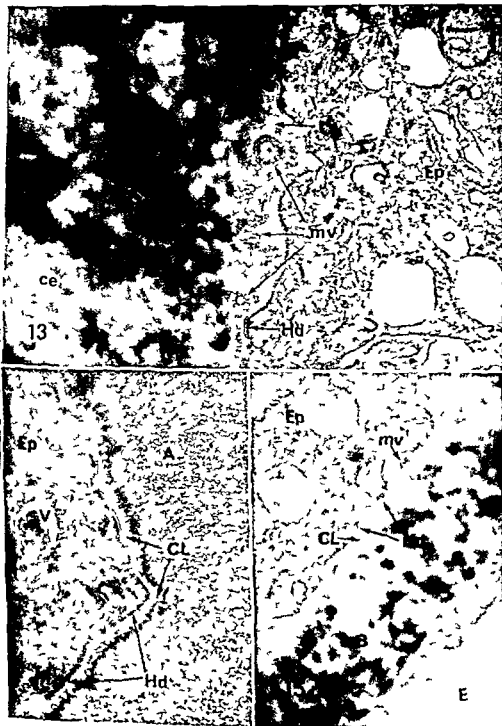


PLATE 7

EXPLANATION OF FIGURES

- 13 Epithelial attachment to cementum. Note the cemental fibrils ending at the cementum surface (small arrows) which is covered by a type B cuticle. The epithelial cell is attached by hemidesmosomes and a basement lamina to the cuticle. Cross sections of microvilli may be seen in the basement lamina. Peripheral appearance of microvilli is suggestive of cup like or belt like hemidesmosomes. Lower first deciduous molar of five year old boy $\times 50\,000$.
- 14 Magnified portion of figure 18 demonstrating the attachment of epithelium to a type A cuticle by hemidesmosomes and a basement lamina. Upper second premolar of 15 year old boy $\times 40\,000$.
- 15 Magnified portion of figure 12 showing the attachment of epithelium to a type B cuticle through hemidesmosomes and a basement lamina. Lower first deciduous molar of five year old boy $\times 45\,000$.

AN GINGIVO DENTAL JUNCTION
A. Li tgarten

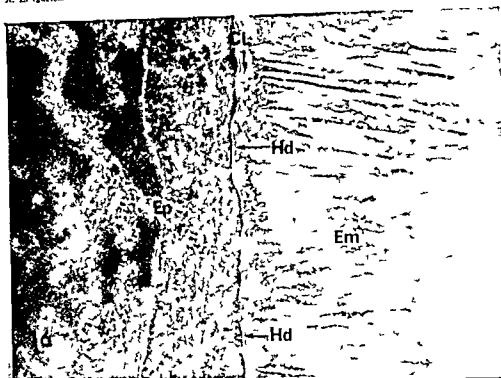


PLATE 8

EXPLANATION OF FIGURES

- 16 Epithelial attachment to enamel through hemidesmosomes and a basement lamina in the absence of a cuticle Upper lateral incisor of 26 year old man $\times 58\,000$
- 17 Bacterial plaque attached to enamel through a type B cuticle Lower first deciduous molar of five year old boy $\times 40\,000$



PLATE 9

EXPLANATION OF FIGURE

- 18 Epithelial attachment to type A cuticle. Note degenerative changes in the cells of the epithelial attachment (compare with connective tissue cells which are relatively well preserved). Degenerating epithelial cells may correspond to cells of the reduced enamel epithelium which have not yet been replaced by down growing cuff of oral epithelium. Upper second premolar of 15 year old boy $\times 14\,000$

AN GINGIVO-DENTAL JUNCTION
A Li tg rten

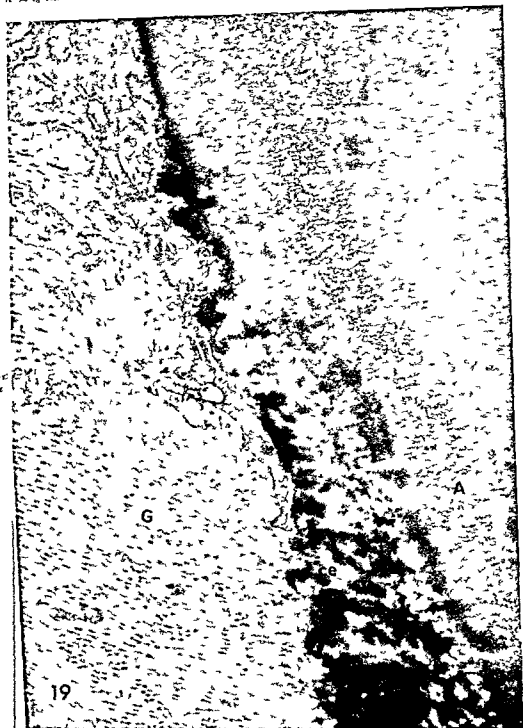


PLATE 10

EXPLANATION OF FIGURE

- 19 Section just apical to figure 18 showing a cementum layer with embedded collagen fibrils on the surface of a type A cuticle Upper second premolar of 15 year old boy $\times 19\ 000$

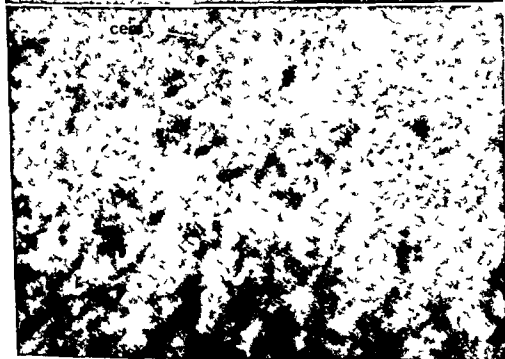
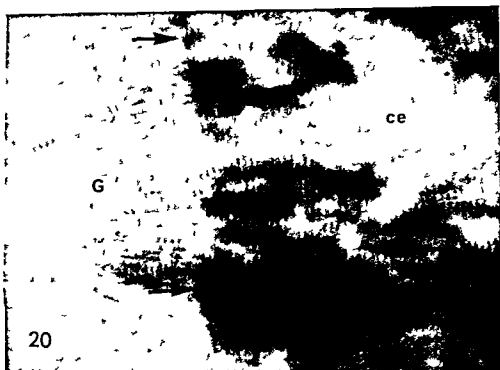


PLATE 11

EXPLANATION OF FIGURES

- 20 Insertion of gingival collagen fibrils into cementum immediately coronal to the alveolar bone margin. Note periodic striations of collagen fibrils in register within the cementum. Arrows indicate junction of cementum and gingival connective tissue. Lower second deciduous molar of five year old boy. $\times 35\,000$
- 21 Acellular cementum at level of alveolar bone margin. Parallel lines are due to arrangement of the cemental collagen fibrils with their periodic striations in register. Note relatively sparse cementum matrix. Upper second premolar of 20 year old woman. $\times 29\,000$

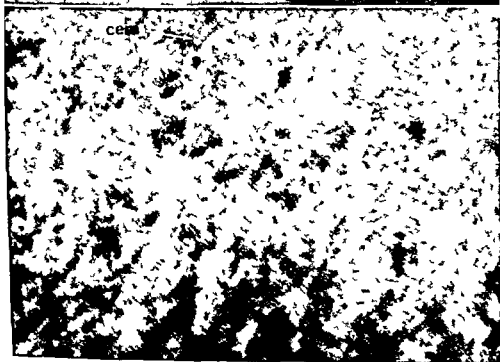
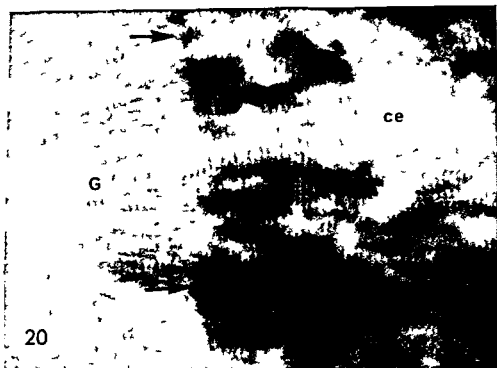
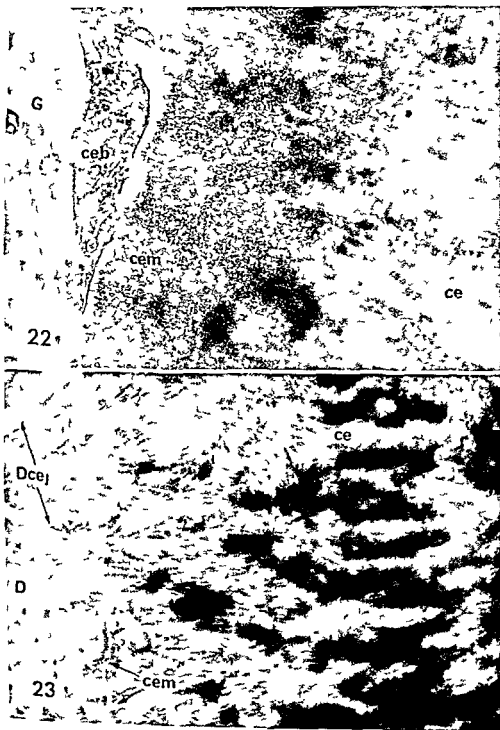


PLATE 12

EXPLANATION OF FIGURES

- 22 Granular cementum matrix on the gingival surface of cementum. The cementum matrix is closely related to a cytoplasmic process probably belonging to a cementoblast. Upper second premolar of 20 year old woman $\times 40\,000$
- 23 Dentino cemental junction. Note fraying of cemental fibrils near the junction with dentine. Compare parallel arrangement of fibrils in cementum to haphazard arrangement of collagen fibrils in dentine. Lower second deciduous molar of five year old boy $\times 14\,000$

Li tgarten



Development and Maintenance of Myelinated Tissue Cultures of Rat Trigeminal Ganglion¹

GERALD F WINKLER AND MERRILL K WOLF

The Department of Neurology and the Joseph P Kennedy Jr Memorial
Laboratories, Massachusetts General Hospital and the Laboratory of
Cellular Neuropathology, Harvard Medical School
Boston, Massachusetts

ABSTRACT Trigeminal ganglia of fetal or neonatal rats and mice have been cultured on collagen-coated coverslips in Maximow assemblies. The methods which proved optimal and the natural history of the resulting cultures are presented in detail. Cultures formed abundant myelin, remained healthy for at least three months, and resembled previously described cultures of other primary sensory ganglia in most but not all respects. New features included an exceptionally high requirement for glucose and apparently for other nutrients, migration of some neuron somas, and the occasional occurrence of stable but abnormally formed myelin segments. The advantages and limitations of such cultures for experimental study of isolated nervous tissues are discussed.

Tissue culture methods are now available which permit many fetal or neonatal nervous tissues to undergo part of their normal differentiation *in vitro* and to be maintained in this differentiated state for weeks or months. Such cultures are valuable experimental models for the study of many properties of the intact nervous system. This subject has been extensively reviewed by Murray (65) who has been a leader in the development of this experimental discipline.

This paper reports our experience with the behavior in Maximow double-coverslip cultures of a part of the nervous system which has not previously been cultivated *in vitro*, the trigeminal ganglion of late fetal or neonatal rat or mouse. Our technology was derived from that of Murray and her school but a number of minor new features appeared both in the specific methods which proved optimal in our hands and in the natural history of our cultures. A detailed description of our culture methods and results is therefore warranted as the indispensable baseline for the interpretation of experiments now in progress utilizing these cultures to analyze properties of peripheral nervous tissue (for example Asbury, Sidman and Wolf, 66 and Winkler, 65).

MATERIALS AND METHODS

Distilled water redistilled from glass was used for final rinsing of all glassware and to make up all culture media. Glassware other than coverslips was washed by Hanks metasilicate hydrochloric acid method (Paul, 59) and rinsed in three changes of distilled and one of glass-distilled water. Gold Seal brand coverslips were arranged in porcelain racks (Coors), boiled in metasilicate solution, rinsed in running hot tap water, immersed in pure nitric acid for half an hour, then rinsed in running distilled and two changes of glass-distilled water. All glassware was air dried and sterilized by dry heat.

Tyrodes balanced salt solution (BSS) was made up and autoclaved without bicarbonate and sodium bicarbonate solution separately sterilized by filtration (Millipore Swinny adaptor) was added to complete the formula.

Human placental blood (PS) was collected from normal term deliveries. After overnight clot retraction the serum was removed, kept at room temperature for a week, then tested for sterility and stored at 4°C. Serum was expected to be clear

¹ Supported by grants NB 04600 and NB 04792 from the National Institute of Neurological Diseases and Blindness.

and yellow specimens showing significant hemolysis (reddish or brownish hue) were rejected.

Embryo extract (EE) was made by grinding nine day chick embryos in a ten Broeck grinder with half their volume of BSS incubating the mash at 36° for one hour and centrifuging it at 2 000 RPM for 30 minutes. The supernatant was frozen in 0.5 ml aliquots which were thawed and recentrifuged on the day of use. The final supernatant was expected to be opalescent. After prolonged storage of EE the final supernatant became clear indicating deterioration. Therefore fresh EE was made about every two months.

The 22 mm round no. 1 coverslips destined to carry cultures were coated on one side with a drop of dialyzed rat tail collagen solution (Bornstein '58) exposed briefly to ammonia vapor and dried for 30 minutes to one hour and stored in BSS.

The first culture trials were made on trigeminal ganglia of mice several days old. It proved more advantageous to use younger animals and to use the rat rather than the mouse. The most reliable and abundant myelination in culture was obtained by using fetal rats of 18 to 19 days gestation. However cultures of newborn mouse ganglia when successful were similar in all essential features.

Noninbred Sprague Dawley rats were obtained from Charles River Laboratories or Gofmoor Farms.

Rat fetuses were delivered aseptically by Caesarian section. The calvarium was removed and the brain retracted caudally to expose the trigeminal ganglia on the floor of the middle cranial fossa. The overlying dura was removed, the nerves transected proximally and distally, the ganglia removed and stripped of connective tissue. Thorough stripping with disruption of the capsule seemed to favor prompt and abundant outgrowth. Good flattening of the explant and subsequent healthy development. There was no advantage however in dividing a ganglion into two or more pieces. Each suitably prepared ganglion was placed on a collagen coated coverslip bearing a drop (about 0.05 ml) of nutrient medium. The culture was then incorporated into a Maximow double coverslip assembly and incubated at $35.5^{\circ}\text{C} \pm 0.5$

in the lying drop position. The drop drained off and replaced twice weekly.

Originally, the nutrient medium consisted of equal parts of PS, EE or serum ultrafiltrate (commercially obtained) and BSS mixed with sufficient 5% glucose to give a final concentration of 0.3% in the complete medium. Before each feeding the cultures were washed by immersion in BSS. After several modifications of the medium were tested it was found best to increase the final glucose concentration to 1.1–1.2%, omit the ox serum ultrafiltrate and omit the washing. The richer medium reduced the incidence of spontaneous degeneration of cultures which was thought to result from exhaustion of some nutrient in the lying drop. The omission of washing reduced the incidence of bacterial contamination, simplified and speeded the feeding procedure and had no effect on the development of the cultures.

Maintenance of sterile technique has now been enormously simplified by carrying out all sterile operations in a hood through which flows a constant stream of filter sterilized air (White Rooms Inc.). This has eliminated the need for separate cubicles and gowns and masks.

Living cultures were examined by bright field microscopy. A long working distance immersion lens (Bausch and Lomb 40 \times fluorite) was indispensable for high magnification microscopy through the double coverslip. The development of cultures was unaffected by daily removal to room temperature for examination.

Cultures to be fixed and stained were handled as whole mounts. Some were fixed in 10% acrolein in M/10 phosphate buffer either for one hour at room temperature or overnight at 4°C and stained with sudan black B for myelin or with cresyl violet or toluidine blue for nuclei and Nissl substance. Others were fixed in 10% formalin in BSS for a week or longer in the refrigerator and impregnated with silver by an adaptation of Holmes' method for neurofibrils (Wolf '64).

For study of myelin development *in vivo* trigeminal ganglia of infant rats at various ages were fixed in 10% acrolein, embedded in polyester wax (Siddons, Mottla and Feder '61), sectioned at 8 μ and stained with Luxol Fast Blue.

RESULTS

The thin neurites began growing out of the explants almost immediately. Growing neurites as long as 50 μ have been observed as early as six hours after explantation (fig 1). At this stage of development the explants formed opaque masses approximately 1 mm in diameter. No neuron somas were observed out of the explant.

By one day after explantation the radially oriented outgrowth extended 0.5 to 0.75 mm beyond the edge of the explant. The outgrowing neurites were now taken up by a network of emigrating macrophages and fibroblasts. In addition, a few neuron somas started to move toward the most proximal part of the outgrowth (fig 2). As the cultures matured, these neurons increased their distance from the explant. Established cultures of explants contained a few healthy neuron somas as much as 300 to 400 μ beyond the original boundary of the explant (fig 7).

During early development occasional macrophages were observed ingesting erythrocytes and debris. Macrophages became far more numerous during the subsequent days as the explant thinned out and myelin formation commenced. As the architecture of the cultures stabilized, macrophages emigrated to the periphery or fell into the drop of medium as described by Bornstein and Murray (58). However, macrophages remained throughout the life of the cultures.

By the second week *in vitro* the explant became sufficiently thin that individual neuron somas could be distinguished within its original boundaries. Sometimes individual somas could be distinguished in all regions of the explant, but most somas occurred in clusters (fig 4) and the center of the explant usually remained too thick to resolve cellular detail (figs 7-9). Satellite cells were always closely applied to neuron somas (figs 5-8). Neuron nuclei were clear and usually centrally placed (figs 4-5-8) and contained a prominent nucleolus. The living cytoplasm appeared to contain evenly distributed small granules (figs 4-5). The Nissl bodies revealed by fixation and staining (fig 8) were also uniformly distributed throughout the peripheral cytoplasm but were too large to

correspond with the granules seen during life. Neuron somas were somewhat oval. The largest uninucleate neurons ranged from 30 to 35 μ in maximum diameter. Neuron somas much smaller than this were usually not clearly seen during life. Binucleate neurons were occasionally seen (fig 4) and were somewhat larger than uninucleate ones (largest diameter 50 to 60 μ).

The rat trigeminal ganglion *in situ* showed no myelin stainable by Luxol Fast Blue at birth. Some segments of myelin were seen by this method in sections of ganglia of two-day-old rats. Myelination was abundant at three and massive at four days of age. According to Dixon (63) the majority of myelin sheaths in ganglia of four-day-old rats have mature ultrastructure.

Cultures of trigeminal ganglia showed some myelin visible in the living state with the oil immersion objective as early as seven days *in vitro*. Since these ganglia were explanted about three days before birth, was expected this corresponds approximately to four days postnatal age. The earliest myelin (fig 3) appeared as single segments each with an associated Schwann cell nucleus. Over the ensuing days additional segments appeared on scattered nerve fibers. By 13 days *in vitro* over 90% of cultures contained some myelin segments and about 10% contained numerous axons possessing ten or more consecutive myelin segments. During the ensuing two weeks 60 to 75% of cultures came to form large closely interwoven networks of myelinated axons; some randomly oriented, some grouped in compact fascicles (figs 5-6-9-10). At the same time the diameter of individual axons and the thickness of their myelin sheaths both increased so that by four weeks *in vitro* myelin segments ranged from 0.5 μ to 5 μ in diameter. Nodes of Ranvier could regularly and incisures of Schmidt-Lantermann could sometimes be identified in the living cultures, but better photographs of these structures were obtained after fixation and staining (figs 11-14). Large myelinated axons were visible in living cultures at low magnification (10 \times objective) and often branched at nodes of Ranvier (Fig 11) distal to the branch point.

the fibers might or might not decrease in diameter

On one occasion an axon appeared traceable in a living culture from a neuron soma in the proximal outgrowth region to a myelin segment beginning 35 μ from that soma. Almost invariably however the unmyelinated initial segments of axons were invisible during life so that given neuron somas could not be traced in this way to their myelinated axons. Silver staining which revealed this initial segment was incompatible in our hands with the Luxol Fast Blue or sudan black B stains for myelin.

After four weeks *in vitro* no new myelin segments appeared to be formed but the myelin continued to increase somewhat in thickness became more irregular in contour and developed multiple small invaginations and protrusions which were more numerous near nodes of Ranvier (figs 5-13). This wrinkling gradually increased with time and became very conspicuous in the oldest cultures. Most cultures were terminated between 30 and 60 days *in vitro* but others set aside to test their longevity regularly attained three months and occasionally four months of age *in vitro*.

Silver staining revealed some additional structural features (fig 15). The total number of axons seen in any given culture after silver staining was much larger than the number of myelinated axons seen in the same culture during its life showing that the majority of axons were unmyelinated. In addition to the large neuron somas located primarily at the periphery of the explant where they had been recognized during life, numerous small neuron somas (10 μ or less in greatest diameter) were found in the center of the explant where they were only recognized after staining. Correlations between soma diameter and axon diameter could not be investigated because the extensive branching and interweaving of axons frustrated our attempts to trace them through the thick central regions of cultures.

The initial segments of axons were straight or had at most one or two turns or angulations. Sometimes the initial segments were broadly tapering and contained an extension of the delicate lightly

stained neurofibrillar network of the soma rather than being solid black like typical mature axons. Blunt, lobulated protrusions from the soma were sometimes seen but the tortuously folded "intracapsular networks" and "glomeruli of the terminal segments" described by Ramon y Cajal (3) and others were not recognized in silver-stained cultures. However the initial segments of axons could not be seen at all in many instances and it is possible that glomeruli and intracapsular networks existed in our cultures but were refractory to staining by Holmes' method or were obscured by the high optical density of successful Holmes preparations. The majority of the neurons were unipolar but many bipolar and some multipolar ones also were seen.

We observed in some cultures an abnormality of myelin formation (fig 14) consisting of grotesque, asymmetrical, ballooned myelin segments along the course of an axon which elsewhere might bear normally formed myelin. Often many axons in a particular fascicle were affected. The ballooned segments appeared to be abnormal in shape when first discovered and to survive intact for as long as the normally formed segments. This abnormality was most frequent in those cultures showing the most precocious and abundant myelin. Silver preparations of these cultures showed no abnormality of the axons.

Sporadic instances of spontaneous degeneration were observed. One type of degeneration primarily involved myelin which over a period of several days would break up into refractile granules and be phagocytosed. The neurons, Schwann cells and fibroblasts retained normal morphology. If such cultures were maintained for another 2 to 3 weeks in this unmyelinated state a few segments of myelin might appear, presumably regenerated in culture. Another type of degeneration consisted of overnight necrosis of all cellular elements in the culture with myelin retaining its structure for an additional 1 to 2 days before breaking up. Both of these types of degeneration were reduced in frequency though not eliminated by the modifications of the medium described under METHODS.

our days was the longest permissible interval between feedings. Cultures left for five days or longer began to show a kind of type of degeneration. Myelin segments developed smooth symmetrical oval dilatations broke up into ovoids and were degenerated neuron somas swelled and moved peripherally and the neurons died. Feeding before this process was complete would preserve those neurons intact but the myelinated axons which had developed oval dilatations would proceed to complete degeneration despite renewal of the nutrient medium.

Another very troublesome type of degeneration resulted from development of small holes or tears in the collagen film or partial detachment of the film from the underlying coverslip. Once the collagen film was broken the tension exerted on it by the maturing connective tissue cells in culture led to rapid increase in size of break culminating in physical disruption of the entire culture. These collagen tears could be initiated by any contact with an instrument or glass surface with the collagen but also occurred seemingly spontaneously. They were reduced in frequency by the use of highly viscous well polymerized collagen but it was necessary to avoid dialyzing the collagen to the point where it began to gel within the dialysis bag. Fragments of gelled collagen when incorporated into a collagen film on a coverslip served as foci for the initiation of subsequent collagen breaks. Careful dissection of connective tissue from the ganglia at the time of explantation and the use of younger animals also reduced the frequency of collagen breaks. Breaks were much more troublesome with mouse cultures perhaps because the small size of mouse ganglia increased the difficulty of moving connective tissues.

DISCUSSION

Cultures of rodent trigeminal ganglia resemble cultures of other sensory ganglia in most but not in all respects. A requirement for high glucose concentration in the medium and a preference for collagen gel as solid substrate are shared by trigeminal and spinal ganglia and central nervous tissue of rats mice cats and humans but

not by avian or amphibian nervous tissues (Bornstein and Murray 58 Murray 65 Peterson and Murray 55 Peterson Crain and Murray 65).

These characteristics seem therefore to be a function of phylogenetic rather than histologic class. The unusually high concentration of glucose and apparently of other nutrients required by our cultures of trigeminal ganglia may simply reflect the size of the cultures. It is our impression that the sheer bulk of neuron cytoplasm present on a single coverslip and therefore fed by a single drop of medium is much greater in healthy cultures of trigeminal ganglia (see figs 9 10) than in similar and equally healthy cultures of cerebellum pons spinal ganglion spinal cord or cerebral cortex (Wolf 64 and unpublished observations). It is unnecessary therefore to postulate any metabolic peculiarity of the trigeminal ganglion to explain the nutritional requirements shown by our cultures although the possibility remains that such peculiarities may some day be detected by other means.

The movement of neuron somas in our cultures away from the site of explantation could be interpreted as mere passive spread of the explant but it seems more likely that it represents active migration. Murray and Stout (47) observed active migration of postganglionic adult sympathetic neuron somas *in vitro*; those cells were embedded in clotted plasma and presumably had to overcome more passive resistance than cells growing on the surface of collagen gel. More recently Peterson Crain and Murray (65) observed that when fragments of fetal spinal cord were explanted on collagen film together with their attached dorsal root ganglia the ganglia migrated away from the cord fragments spinning out a tract of nerve fibers corresponding to the proximal dorsal root *in vivo*. Entire ganglia migrated over 0.5 mm during three months *in vitro*. Our cultures of trigeminal ganglia were set up without spinal cord or brainstem trigeminal neurons like those of sympathetic ganglia are apparently able to migrate without extrinsic influences.

The one major morphological feature of the trigeminal neuron *in situ* which appears to be lacking in cultured ganglia is

the fibers might or might not decrease in diameter

On one occasion an axon appeared traceable in a living culture from a neuron soma in the proximal outgrowth region to a myelin segment beginning 35 μ from that soma. Almost invariably however the unmyelinated initial segments of axons were invisible during life so that given neuron somas could not be traced in this way to their myelinated axons. Silver staining which revealed this initial segment was incompatible in our hands with the Luxol Fast Blue or sudan black B stains for myelin.

After four weeks *in vitro* no new myelin segments appeared to be formed but the myelin continued to increase somewhat in thickness became more irregular in contour, and developed multiple small invaginations and protrusions which were more numerous near nodes of Ranvier (figs 5-13). This wrinkling gradually increased with time and became very conspicuous in the oldest cultures. Most cultures were terminated between 30 and 60 days *in vitro* but others set aside to test their longevity regularly attained three months and occasionally four months of age *in vitro*.

Silver staining revealed some additional structural features (fig 15). The total number of axons seen in any given culture after silver staining was much larger than the number of myelinated axons seen in the same culture during its life showing that the majority of axons were unmyelinated. In addition to the large neuron somas located primarily at the periphery of the explant where they had been recognized during life, numerous small neuron somas (10 μ or less in greatest diameter) were found in the center of the explant where they were only recognized after staining. Correlations between soma diameter and axon diameter could not be investigated because the extensive branching and interweaving of axons frustrated our attempts to trace them through the thick central regions of cultures.

The initial segments of axons were straight or had at most one or two turns or angulations. Sometimes the initial segments were broadly tapering and contained an extension of the delicate lightly

stained neurofibrillar network of the soma rather than being solid black like typical mature axons. Blunt lobulated protrusions from the soma were sometimes seen but the tortuously folded intracapsular networks and glomeruli of the terminal segments described by Ramon y Cajal (1894) and others were not recognized in silver stained cultures. However the initial segments of axons could not be seen at all in many instances and it is possible that glomeruli and intracapsular networks existed in our cultures but were refractory to staining by Holmes method or were obscured by the high optical density of successful Holmes preparations. The majority of the neurons were unipolar but many bipolar and some multipolar ones also were seen.

We observed in some cultures an abnormality of myelin formation (fig 14) consisting of grotesque asymmetrically ballooned myelin segments along the course of an axon which elsewhere must bear normally formed myelin. Often many axons in a particular fascicle were affected. The ballooned segments appeared to be abnormal in shape when first observed and to survive intact for as long as the normally formed segments. This abnormality was most frequent in those cultures showing the most precocious and abundant myelin. Silver preparations of these cultures showed no abnormality of the axons.

Sporadic instances of spontaneous degeneration were observed. One type of degeneration primarily involved myelin which over a period of several days would break up into refractile granules and be phagocytosed. The neurons, Schwann cells, and fibroblasts retained normal morphology. If such cultures were maintained for another 2 to 3 weeks in this unmyelinated state a few segments of myelin might reappear presumably regenerated in culture. Another type of degeneration consisted of overnight necrosis of all cellular elements in the culture with myelin retaining its structure for an additional 1 to 2 days before breaking up. Both of these types of degeneration were reduced in frequency though not eliminated by modifications of the medium described under METHODS.

ur days was the longest permissible val between feedings Cultures left d for five days or longer began to show rd type of degeneration Myelin seg ts developed smooth symmetrical oval ations broke up into ovoids and were ocytosed neuron somas swelled nu moved peripherally and the neurons . Feeding before this process was plete would preserve those neuron as and myelinated axons which were intact but the myelinated axons h had developed oval dilatations would eed to complete degeneration despite wal of the nutrient medium

another very troublesome type of de eration resulted from development of ll holes or tears in the collagen film or ized detachment of the film from the lerying coverslip Once the collagen i was broken the tension exerted on it the maturing connective tissue cells in culture led to rapid increase in size of break culminating in physical disrupt i of the entire culture These collagen aks could be initiated by any contact an instrument or glass surface with the agen but also occurred seemingly ntaneously They were reduced in fre ency by the use of highly viscous well yzed collagen but it was necessary to id dialyzing the collagen to the point ere it began to gel within the dialysis g Fragments of gelled collagen when rporated into a collagen film on a verslip served as foci for the initiation subsequent collagen breaks Careful dis ction of connective tissue from the gan a at the time of explantation and the e of younger animals also reduced the equency of collagen breaks Breaks were uch more troublesome with mouse cul res perhaps because the small size of ouse ganglia increased the difficulty of moving connective tissues

DISCUSSION

Cultures of rodent trigeminal ganglia re mble cultures of other sensory ganglia in ost but not in all respects A require ent for high glucose concentration in the edium and a preference for collagen gel s solid substrate are shared by trigeminal nd spinal ganglia and central nervous ssue of rats mice cats and humans but

not by avian or amphibian nervous tissues (Bornstein and Murray 58 Murray 65 Peterson and Murray 55 Peterson Cram and Murray 65)

These characteristics seem therefore to be a function of phylogenetic rather than histologic class The unusually high concentration of glucose and apparently of other nutrients required by our cultures of trigeminal ganglia may simply reflect the size of the cultures It is our impres sion that the sheer bulk of neuron cytoplasm present on a single coverslip and therefore fed by a single drop of me dium is much greater in healthy cultures of trigeminal ganglia (see figs 9 10) than in similar and equally healthy cultures of cerebellum pons spinal ganglion spinal cord or cerebral cortex (Wolf 64 and unpublished observations) It is unneces sary therefore to postulate any metabolic peculiarity of the trigeminal ganglion to explain the nutritional requirements shown by our cultures although the pos sibility remains that such peculiarities may some day be detected by other means

The movement of neuron somas in our cultures away from the site of explanta tion could be interpreted as mere passive spread of the explant but it seems more likely that it represents active migration Murray and Stout (47) observed active migration of postganglionic adult sympa thetic neuron somas *in vitro* those cells were embedded in clotted plasma and pre sumably had to overcome more passive resistance than cells growing on the sur face of collagen gel More recently Peter son Cram and Murray (65) observed that when fragments of fetal spinal cord were explanted on collagen film together with their attached dorsal root ganglia the gan glia migrated away from the cord frag ments spinning out a tract of nerve fibers corresponding to the proximal dorsal root *in vitro* Entire ganglia migrated over 0.5 mm during three months *in vitro* Our cultures of trigeminal ganglia were set up without spinal cord or brainstem trigemi nal neurons like those of sympathetic gan glia are apparently able to migrate with out extrinsic influences

The one major morphological feature of the trigeminal neuron *in situ* which ap pears to be lacking in cultured ganglia is

the coiling of the initial segment of the axon into an elaborate intracapsular network or glomerulus. Other characteristics of the trigeminal ganglion such as the sizes and shapes of neuron somas, their relationships to satellite cells, the relationship of myelin segments to Schwann cells, the form and distribution of nodes of Ranvier and incisures of Schmidt-Lantermann are closely similar *in situ* and *in vitro*. The maximum diameter of myelin segments in rat trigeminal cultures is the same as found in the rat trigeminal ganglion *in situ* (Dixon '63) and the wrinkles and irregularities appearing in cultured myelin sheaths with advancing age *in vitro* correspond to those observed by Webster and Spiro ('60) in sciatic nerve of normal adult rats. The cultured neurons are of course abnormal in the sense of being isolated from their peripheral end organs from their postsynaptic target cells in the CNS and from much of their normal mesodermal environment. However, the isolation itself confers on these neurons the advantages of accessibility to direct microscopic observation and chemical or mechanical manipulation. Isolation also simplifies the interpretation of experimental findings: observed reactions must be intrinsic to those cells present in the culture rather than being possibly influenced by the participation of distant organs as may be the case *in situ*.

The usefulness of such cultures as test objects to study disease mechanisms has been well established (Bornstein '63, Winkler '65) and requires no extensive discussion here. A note of caution is introduced by the presence of some abnormally formed myelin segments and the occasional occurrence of spontaneous degeneration in even our best cultures. Rigorous controls are essential to establish that a deleterious effect obtained in an experiment concerned with disease mechanisms has actually been produced by that aspect of the experimental challenge which is relevant to the mechanisms of the disease under study.

Coverslip cultures of nervous tissues show some instructive limitations in other types of experiments. For example, as part of a recent study of porphyrin production by nervous tissues *in vitro* (As-

bury, Sidman and Wolf '66) measurements were desired of porphyrin production and of the activity of certain enzymes involved in porphyrin synthesis. One of the difficulties was that sometimes two, 10 μ l aliquots of the drop of medium could be recovered for analysis, although complete recovery was impossible because of adherence of medium to the small and large coverslips. The total enzyme activity of individual cultures appeared to be increased about 100% by appropriate chemical stimulation. However, no significance could be attached to this increase because the amount of actively metabolizing tissue per culture was variable and uncertain. By wet or dry weight and the protein content of different cultures varied as much as 100% and even these measurements were rendered meaningless by the inevitable inclusion of collagen film and dead or injured cells in uncertain proportions along with living nervous tissue. DNA measurements would also include dead and injured cells and would fail to reflect differences in cytoplasmic volume between the large neurons and the much smaller satellite and Schwann cells. Until means are found to solve or circumvent this measurement problem, cultures of nervous tissue will be refractory to quantitative enzymologic studies.

In the same study of porphyrin metabolism, fluorescence microscopy of cultures was undertaken in an attempt to determine the precise cell or structure in which the porphyrin was localized. Porphyrin fluorescence could be seen at high magnification but details of cell structure were almost completely obscured by background fluorescence from other cells lying above and below the plane of focus. Heat-treated neuron somas tended to occur in clusters three and four deep (see fig. 4). Even neuron somas and myelin segments that appear by conventional microscopy to be well isolated in the outgrowth zone proved to be completely enveloped by layers of Schwann and connective tissue cells whose diffuse fluorescence obscured detail. Thus, even if development might also be expected to increase the difficulty of other experimental manipulations such as the insertion of microelectrodes into neurons under direct microscopic visualization. Indeed, both Cris-

and Hild and Tasaki (62) have relied upon the great difficulty of achieving microelectrode penetrations of cultured neurons whether grown in a clot or on collagen gel. These trouble some multiple layers of cells cannot be used as merely a nuisance which might be eliminated by some improvement in the methodology. They are part and parcel of the conditions for optimum differentiation and survival of neurons *in vitro*.

Neurons seem to require intimate attachment and tridimensional support of their companion cells for healthy survival. Methods developed thus far for the cultivation of cultured neurons all have ended in some compromise with respect to differentiation and stability (for example see 56). The best isolated neurons in primary than cultures are in this respect not as reliable models of the behavior of the neuron *in situ* as their less accessible fellows in thicker cultures. The more precise information becomes available about specific macromolecules required by various cell types for survival and differentiation — such as the sympathetic nerve growth factor (Levi Montalcini 64) which must represent the first discovered example of a large class of specific trophic factors — it may become possible to maintain totally isolated differentiated neurons *in vitro*. At present healthy maintenance of neurons *in vitro* requires healthy maintenance of their surrounding matrix of associated cells. The problems thus presented are in the same class as the problems which the nervous system *in situ* has always posed for the experimenter because of its extraordinary heterogeneity. Limitations of present culture techniques serve to demonstrate the importance of this heterogeneity at the level of the intimate organization of nervous tissue.

LITERATURE CITED

Burns A K R L Sidman and M K Wolf 1966 Drug induced porphyrin accumulation in the nervous system. *Neurology* 16 320
 Bornstein M B 1958 Reconstituted rat tail collagen used as substrate for tissue cultures on coverslips in Maximow slides and roller tubes. *Laboratory Investigation* 4 134-137

—— 1963 A tissue culture approach to demyelination disorders. National Cancer Institute Monograph No 11 197-214
 Bornstein M B and M R Murray 1958 Serial observations on patterns of growth myelin formation maintenance and degeneration in cultures of newborn rat and kitten cerebellum. *Journal of Biophysical and Biochemical Cytology* 4 499-504
 Craun S M 1956 Resting and action potentials of cultured chick embryo spinal ganglion cells. *J Comp Neur* 104 285-330
 Dixon A D 1963 The ultrastructure of nerve fibers in the trigeminal ganglion of the rat. *Journal of Ultrastructure Research* 8 107-121
 Hild W and I Tasaki 1962 Morphological and physiological properties of neurons and glial cells in tissue culture. *Journal of Neurophysiology* 25 277-304
 Levi Montalcini R 1964 Growth control of nerve cells by a protein factor and its antiserum. *Science* 143 105-110
 Murray M R 1964 Nervous tissues *in vitro*. Chapter 9 Volume 2 In *Cells and Tissues in Culture Methods Biology and Physiology* ed E N Willmer Academic Press London and New York
 Murray M R and A P Stout 1947 Adult human sympathetic ganglion cells cultivated *in vitro*. *Am J Anat* 80 225-273
 Nakai J 1956 Dissociated dorsal root ganglia in tissue culture. *Am J Anat* 99 81-130
 Paul J 1959 Cell and Tissue Culture E and S Livingstone Ltd Edinburgh and London
 Peterson E R S M Craun and M R Murray 1965 Differentiation and prolonged maintenance of bioelectrically active spinal cord cultures (rat chick and human). *Zeitschrift für Zellforschung* 66 130-154
 Peterson E R and M R Murray 1955 Myelin sheath formation in cultures of avian spinal ganglia. *Am J Anat* 96 319-355
 Ramon y Cajal S 1952 *Histologie du système nerveux de l'homme et des vertébrés*. Consejo Superior de Investigaciones Científicas Instituto Ramon y Cajal Madrid
 Sidman R L P R Mottola and N Feder 1961 Improved polyester wax embedding for histology. *Stain Technology* 36 279-284
 Webster H DeF and D Spiro 1960 Phase and electron microscopic studies of experimental demyelination I Variations in myelin sheath contour in normal guinea pig sciatic nerve. *Journal of Neuropathology and Experimental Neurology* 19 42-69
 Winkler C F 1965 *In vitro* demyelination of peripheral nerve induced with sensitized cells. *Annals of the New York Academy of Sciences* 122 287-296
 Wolf M K 1964 Differentiation of neuronal types and synapses in myelinating cultures of mouse cerebellum. *Journal of Cell Biology* 22 259-279

the coiling of the initial segment of the axon into an elaborate intracapsular network or glomerulus. Other characteristics of the trigeminal ganglion such as the sizes and shapes of neuron somas, their relationships to satellite cells, the relationship of myelin segments to Schwann cells, the form and distribution of nodes of Ranvier and incisures of Schmitt-Lantermann are closely similar *in situ* and *in vitro*. The maximum diameter of myelin segments in rat trigeminal cultures is the same as found in the rat trigeminal ganglion *in situ* (Dixon 63) and the wrinkles and irregularities appearing in cultured myelin sheaths with advancing age *in vitro* correspond to those observed by Webster and Spiro (60) in sciatic nerve of normal adult rats. The cultured neurons are of course abnormal in the sense of being isolated from their peripheral end organs from their postsynaptic target cells in the CNS and from much of their normal mesodermal environment. However the isolation itself confers on these neurons the advantages of accessibility to direct microscopic observation and chemical or mechanical manipulation. Isolation also simplifies the interpretation of experimental findings: observed reactions must be intrinsic to those cells present in the culture rather than being possibly influenced by the participation of distant organs as may be the case *in situ*.

The usefulness of such cultures as test objects to study disease mechanisms has been well established (Bornstein 63, Winkler 65) and requires no extensive discussion here. A note of caution is introduced by the presence of some abnormally formed myelin segments and the occasional occurrence of spontaneous degeneration in even our best cultures. Rigorous controls are essential to establish that a deleterious effect obtained in an experiment concerned with disease mechanisms has actually been produced by that aspect of the experimental challenge which is relevant to the mechanisms of the disease under study.

Coverslip cultures of nervous tissues show some instructive limitations in other types of experiments. For example, as part of a recent study of porphyrin production by nervous tissues *in vitro* (As-

bury, Sidman and Wolf 66) measurements were desired of the amount and of the activity of certain enzymes involved in porphyrin synthesis. One sometimes two 10 μ l aliquots of the drop of medium could be recovered for analysis although complete recovery impossible because of adherence of medium to the small and large cultures. The total enzyme activity of individual cultures appeared to be increased 100% by appropriate chemical stimulation. However no significance could be attached to this increase because amount of actively metabolizing tissue in culture was variable and uncertain, wet or dry weight and the protein of different cultures varied as much as 100% and even these measurements rendered meaningless by the inevitable inclusion of collagen film and dead or dying cells in uncertain proportions along with living nervous tissue. DNA measurements would also include dead and dying cells and would fail to reflect differences in cytoplasmic volume between the large neurons and the much smaller satellite cells and Schwann cells. Until means are found to solve or circumvent this measurement problem, cultures of nervous tissue will be refractory to quantitative enzymological studies.

In the same study of porphyrin metabolism, fluorescence microscopy of cultures was undertaken in an attempt to determine the precise cell or structure in which the porphyrin was localized. Porphyrin fluorescence could be seen at high magnification but details of cell structure were almost completely obscured by background fluorescence from other cells lying above and below the plane of focus. Heat-labile neuron somas tended to occur in clusters three and four deep (see fig. 4). Even the somas and myelin segments that appeared by conventional microscopy to be well isolated in the outgrowth zone proved to be completely enveloped by layers of Schwann and connective tissue cells whose diffuse fluorescence obscured detail. This envelopment might also be expected to complicate the difficulty of other experimental manipulations such as the insertion of microelectrodes into neurons under direct microscopic visualization. Indeed both Cra-

and Hild and Tasaki (62) have relied upon the great difficulty of achieving microelectrode penetrations into cultured neurons whether grown in a clot or on collagen gel. These trouble some multiple layers of cells cannot be dealt as merely a nuisance which might be eliminated by some improvement in the methodology. They are part and parcel of the conditions for optimum differentiation and survival of neurons in culture. Neurons seem to require intimate attachment and tridimensional support from companion cells for healthy survival. Methods developed thus far for the cultivation of cultured neurons all have ended some compromise with respect to differentiation and stability (for example, see 56). The best isolated neurons in particularly thin cultures are in this respect not as reliable models of the behavior of the neuron *in situ* as their less accessible fellows in thicker cultures. Even more precise information becomes available about specific macromolecules required by various cell types for survival and differentiation—such as the sympathetic nerve growth factor (Levi Montalcini, 64) which must represent the first covered example of a large class of specific trophic factors—it may become possible to maintain totally isolated differentiated neurons *in vitro*. At present healthy maintenance of neurons *in vitro* requires a healthy maintenance of their surrounding matrix of associated cells. The problems thus presented are in the same class as the problems which the nervous system *in situ* has always posed for the experimenter because of its extraordinary heterogeneity. Limitations of present culture techniques serve to demonstrate the importance of this heterogeneity at the level of the intimate organization of nervous tissue.

LITERATURE CITED

- Levi Montalcini, R. 1964 Growth control of nerve cells by a protein factor and its antiserum. *Science* 143 105-110.
- Murray, M. R. 1965 Nervous tissues *in vitro*. Chapter 9 Volume 2. In *Cells and Tissues in Culture*. Methods Biology and Physiology, ed. E. N. Willmer. Academic Press, London and New York.
- Murray, M. R. and A. P. Stout. 1947 Adult human sympathetic ganglion cells cultivated *in vitro*. *Am. J. Anat.* 80 225-273.
- Nakai, J. 1956 Dissociated dorsal root ganglia in tissue culture. *Am. J. Anat.* 99 81-130.
- Paul, J. 1959 Cell and Tissue Culture. E. and S. Livingstone Ltd. Edinburgh and London.
- Peterson, E. R., S. M. Craun and M. R. Murray. 1965 Differentiation and prolonged maintenance of bioelectrically active spinal cord cultures (rat chick and human). *Zeitschrift für Zellforschung* 66 130-154.
- Peterson, E. R. and M. R. Murray. 1955 Myelin sheath formation in cultures of avian spinal ganglia. *Am. J. Anat.* 96 319-355.
- Ramon y Cajal, S. 1952 Histologie du système nerveux de l'homme et des vertébrés. Consejo Superior de Investigaciones Científicas. Instituto Ramon y Cajal, Madrid.
- Sidman, R. L., P. R. Mottla and N. Feder. 1961 Improved polyester wax embedding for histology. *Stain Technology* 36 279-284.
- Webster, H. DeF. and D. Spiro. 1960 Phase and electron microscopic studies of experimental demyelination. I. Variations in myelin sheath contour in normal guinea pig sciatic nerve. *Journal of Neuropathology and Experimental Neurology* 19 42-69.
- Winkler, C. F. 1965 *In vitro* demyelination of peripheral nerve induced with sensitized cells. *Annals of the New York Academy of Sciences* 122 287-296.
- Wolf, M. K. 1964 Differentiation of neuronal types and synapses in myelinating cultures of mouse cerebellum. *Journal of Cell Biology* 22 259-279.
- Bornstein, M. B. and M. R. Murray. 1958 Serial observations on patterns of growth, myelin formation, maintenance and degeneration in cultures of newborn rat and kitten cerebellum. *Journal of Biophysical and Biochemical Cytology* 4 499-504.
- Craun, S. M. 1956 Resting and action potentials of cultured chick embryo spinal ganglion cells. *J. Comp. Neur.* 104 285-330.
- Dixon, A. D. 1963 The ultrastructure of nerve fibers in the trigeminal ganglion of the rat. *Journal of Ultrastructure Research* 8 107-121.
- Hild, W. and I. Tasaki. 1962 Morphological and physiological properties of neurons and glial cells in tissue culture. *Journal of Neurophysiology* 25 277-304.

PLATE 1

EXPLANATION OF FIGURES

Living cultures of rat trigeminal ganglion showing features of early development

- 1 Six hours *in vitro* A few delicate neurites are already growing out of the explant $\times 485$
- 2 Two days *in vitro* Some neuron somas have started to move away from the edge of the explant $\times 725$
- 3 Seven days *in vitro* A myelin sheath has appeared around an axon. Both the myelin and the underlying axon appear smaller in diameter than the mature ones shown at the same magnification in Plate 2 $\times 725$



PLATE 1

EXPLANATION OF FIGURES

Living cultures of rat trigeminal ganglion showing features of early development

- 1 Six hours *in vitro* A few delicate neurites are already growing out of the explant $\times 485$
- 2 Two days *in vitro* Some neuron somas have started to move away from the edge of the explant $\times 725$
- 3 Seven days *in vitro* A myelin sheath has appeared around an axon. Both the myelin and the underlying axon appear smaller in diameter than the mature ones shown at the same magnification in Plate 2 $\times 725$

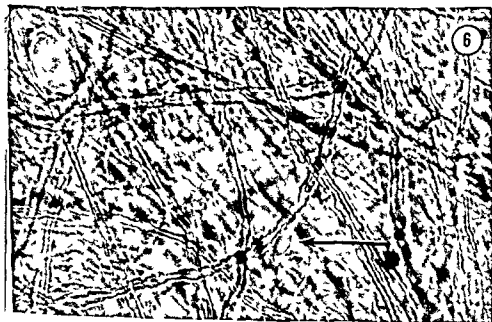


PLATE 2

EXPLANATION OF FIGURES

Living neuron somas and myelin sheaths in mature cultures

- 4 Twenty five days *in vitro*. A cluster of neuron somas. Note the centrally placed nuclei and uniform small cytoplasmic granules. One binucleate neuron is present (arrow). Satellite cell nuclei are seen between neuron somas. Myelinated axons course through the lower part of the field. $\times 725$
- 5 Isolated neuron soma in the proximal outgrowth zone. The apparent bumps on its surface are the nuclei of satellite cells surrounding it. Segments of myelin course in and out of the plane of focus. $\times 725$
- 6 Field of myelinated axons. The Schwann cell associated with one of the myelin segments is in focus (arrow). This myelin segment and some others in the picture show conspicuous wrinkling. $\times 725$



PLATE 2

EXPLANATION OF FIGURES

Living neuron somas and myelin sheaths in mature cultures

- 4 Twenty five days *in vitro* A cluster of neuron somas Note the centrally placed nuclei and uniform small cytoplasmic granules One binucleate neuron is present (arrow) Satellite cell nuclei are seen between neuron somas Myelinated axons course through the lower part of the field $\times 725$
- 5 Isolated neuron soma in the proximal outgrowth zone The apparent bumps on its surface are the nuclei of satellite cells surrounding it Segments of myelin course in and out of the plane of focus $\times 725$
- 6 Field of myelinated axons The Schwann cell associated with one of the myelin segments is in focus (arrow) This myelin segment and some others in the picture show conspicuous wrinkling $\times 725$



PLATE 3

EXPLANATION OF FIGURES

Trigeminal ganglion 29 days *in vitro* Stained with toluidine blue

- 7 Survey view The edge of the explant above proximal outgrowth below Several neuron somas (arrows) occupy positions 200 to 400 μ away from the explant $\times 200$
- 8 High magnification view of the neuron in the center of figure 7 showing centrally placed nucleus uniformly distributed clumps of Nissl substance and on the upper right margin a closely apposed satellite cell nucleus $\times 1350$

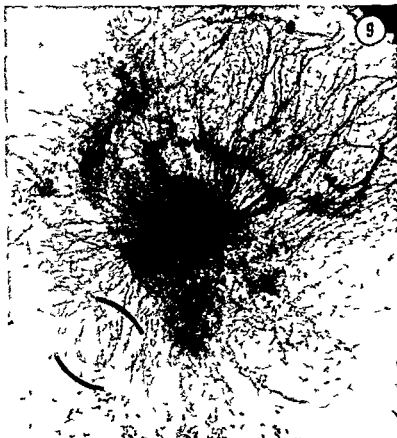


PLATE 4

EXPLANATION OF FIGURES

Trigeminal ganglion 30 days *in vitro* Stained with sudan black B

- 9 Survey view of entire culture The explant is surrounded by a dense halo of outgrowing myelinated axons some coursing at random some especially in the upper right quadrant travelling in compact parallel fascicles Macrophages intensely stained because of their phagocytosed fat droplets are scattered in the outgrowth About $\times 23$
- 10 Higher magnification of the area bracketed in figure 9 A lightly myelinated area was chosen to permit individual myelinated axons to be distinguished These two figures show how much healthy nervous tissue may be present on a single coverslip in the best cultures of trigeminal ganglion About $\times 92$

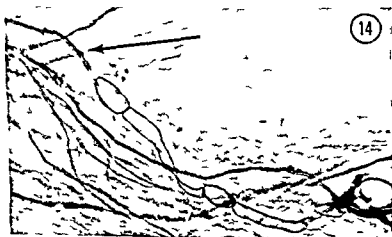


PLATE 5

EXPLANATION OF FIGURES

Features of myelin sheath structure at high magnification. Cultures stained with sudan black B

- 11 Bifurcation of a myelinated axon at a node of Ranvier. The segment proximal to the bifurcation shows two incisures of Schmitt-Lantermann (arrows). Three additional myelinated axons are in the field. Forty-two days *in vitro* $\times 725$
- 12 Another incisure of Schmitt-Lantermann. Thirty days *in vitro* $\times 1000$
- 13 Extensive wrinkling of myelin adjacent to a node of Ranvier. Thirty days *in vitro* $\times 1000$
- 14 Abnormal grotesquely ballooned myelin segments. Note that the adjacent myelin segment on the same axon (arrow) and other segments in this field are normally formed. Thirty days *in vitro* $\times 400$



PLATE 6

EXPLANATION OF FIGURE

Structural features revealed by silver impregnation

- 15 Trigeminal ganglion 45 days *in vitro* Holmes silver method. Note the extremely numerous axons more numerous than myelin sheaths in any corresponding field examined during life or after sudan black staining. The large neuron in the center has a protoplasmic extension of its soma (P). Its axon appears as a solid black line following the left margin of the cell soma and then turning away to the left of the field. Another large neuron near the bottom of the field has an axon which contains a loose neurofibrillar network and makes a hairpin turn close to the soma (A). No greater tortuosity of the initial segment was observed in silver impregnated cultures. Numerous small neurons under $20\ \mu$ in diameter are also present in this field (N). Small neurons such as these were not usually identified during the life of the culture. Approximately $\times 1000$.



PLATE 6

EXPLANATION OF FIGURE

Structural features revealed by silver impregnation

- 15 Trigeminal ganglion 45 days *in vitro* Holmes silver method Note the extremely numerous axons more numerous than myelin sheaths in any corresponding field examined during life or after sudan black staining The large neuron in the center has a protoplasmic extension of its soma (P) Its axon appears as a solid black line following the left margin of the cell soma and then turning away to the left of the field Another large neuron near the bottom of the field has an axon which contains a loose neurofibrillar network and makes a hairpin turn close to the soma (A) No greater tortuosity of the initial segment was observed in silver impregnated cultures Numerous small neurons under $20\ \mu$ in diameter are also present in this field (N) Small neurons such as these were not usually identified during the life of the culture Approximately $\times 1000$



acts of Triton WR 1339 on the Rat Yolk Sac Placenta¹

PHYLLIS W. SCHULTZ², JAMES F. REGER³ AND RICHARD L. SCHULTZ⁴
Department of Anatomy University of Colorado Medical Center
Denver, Colorado

ABSTRACT The cytochemistry and ultrastructure of the lysosomal area of the rat's yolk sac placenta was studied at various stages of development. The lysosomal area located at the apical end of the yolk sac epithelial cell between the microvillous border and the nucleus consisted of dense bodies that persisted from day 10 of pregnancy through gestation and multivesicular bodies that are present only through day 12. Acid phosphatase activity was restricted to the dense material and to the membranes of this area. Two types of pinocytotic vesicles were present in all stages of development. One was a tubular structure containing dense material and the other a saccular clear structure containing a "fuzz lining" and membrane remnants. Possible relationships between the pinocytotic vesicles and the dense and multivesicular bodies were considered.

The injection of Triton WR 1339 on day 11 of pregnancy resulted in a vacuolation of the dense and multivesicular bodies. This vacuolation began 15 minutes after injection and maximum effect was reached within 12-24 hours. A reorganization of the lysosome area occurred on days 15-16 in those animals in which pregnancy continued to term. This reorganization consisted of an increase in the dense material within the vacuoles and a reduction in vacuole size. The vacuoles remained distended in those animals in which death and resorption of the fetus occurred. The first cellular changes associated with death occurred between 48-60 hours post injection. The microvilli became shorter, thicker and reduced in number; the pinocytotic vesicles disappeared from the cell surface; the endoplasmic reticulum became dilated and vesiculated; and vesicles were formed from the cristae of the mitochondria.

With the injection regimen used in this study 25% of the litters were resorbed while the remainder of the pregnant rats delivered viable fetuses at term.

Termination of pregnancy and resorption of the rat fetus and placenta can be induced in many ways, but the mechanism of this phenomenon has not been studied. It may be that the lysosomes of the fetus and placenta play a role in the digestion of the conceptus since lysosomes have been implicated in other types of tissue degeneration (de Duve 63; Weissmann 65). Previous histochemical study of the distribution of lysosomes in ethionine-induced resorption of conceptuses gave evidence in support of this idea in that the size and distribution of these organelles appeared to change with resorption (Schultz and Schultz 62).

The structure in the rat conceptus with the most pronounced acid phosphatase activity, the reference enzyme for lysosomes, was the yolk sac placenta. Acid phosphatase activity was found to be localized in the supranuclear region of the visceral yolk sac epithelial cell (Wislocki, Deane and Dempsey 46; Padykula 48; Schultz and Schultz 62). This region has also been shown to contain a heavy concen-

tration of diastase-resistant carbohydrate (Wislocki and Padykula 61) which has been related to lysosomes (Koenig 62). Other studies have shown that the apical region of the yolk sac cell is a region in which foreign materials, especially vital dyes, are concentrated (Everett 35; Wislocki, Deane and Dempsey 46; Wilson, Beaudoin and Free 59; Al Abbass and Schultz 66). For this reason it has been suggested that the yolk sac cell acts as a placental barrier to prevent foreign materials from reaching the fetus (Wislocki, Deane and Dempsey 46; Al Abbass and Schultz 66).

Fine structural studies of the supranuclear region of the visceral yolk sac epithelial cell have shown the region to contain

Supported by U.S. Public Health Service grant HD-00496 and by National Science Foundation grant CB-29223.

¹ Faculty Fellow, University of Colorado, Denver, Center. The author gratefully acknowledges the assistance of the Council for Research and Creative Work.

² Present address: Department of Anatomy, University of Tennessee, Memphis.

³ Supported by Research Career Development Award K3 HD 7680.

post fixed for 45 minutes in cold buffer 1% osmium tetroxide pH 7.4. The sections were dehydrated in methanol and embedded with a propylene oxide Epon mixture and embedded in Epon 812.

Control morphology. A number of sections were fixed in buffered glutaraldehyde (3-6.25%) pH 7.4, post fixed in cold 1% osmium tetroxide pH 7.4 and embedded as described above. As a control for the specificity of localization of the reaction product a number of samples were fixed in varying concentrations of glutaraldehyde (1-6.25%) pH 7.35 and used for acid phosphatase activity after the method of Miller (62) but because of the capriciousness of this method in yolk sac cells it was not used routinely.

Sections 600-900 Å were cut with diamond knives on the LKB or Blum MT2 ultramicrotome, stained with 7.5% uranyl acetate and 0.2% lead citrate and examined with the Phillips electron microscope at 60 KV. Photographs were taken on Kodak Contrast film.

RESULTS

Control observations

The normal fine structure of the lysosomal area of the yolk sac epithelial cell was studied at various stages of development and was considered in relation to the distribution of acid phosphatase activity in this region. Particular attention was given to the cellular elements: pinocytotic vesicles, dense bodies and multivesicular bodies.

Pinocytotic vesicles. There were two types of pinocytotic vesicles present in all stages of development studied. One type was tubular containing very dense material. These vesicles retained their tubular appearance after they were separated from the cell surface, sometimes forming U-shaped structures and ultimately appeared to fuse with dense bodies located at the apical portion of the yolk sac cell (figs 2, 3, 12). Their contents were of the same opacity as the material present in the adjacent dense bodies. These structures have been referred to as canaliculi (Vislocki and Padykula, 61).

Pinocytotic vesicles of the second type are larger than the tubular type and were

expanded distally so that they appeared to be saccular. Each vesicle contained an outer ring of slightly dense material adjacent to the membrane ("fuzz lined" Carpenter and Ferm, 66) and membrane remnants were frequently found in the lumen (figs 2, 3, 8, 12). The type of membrane remnant in the clear pinocytotic vesicle was also found free in the lumen of the yolk sac (figs 1, 8, 10, 16). These vesicles were found at various depths within the supranuclear region of the cell.

Neither of these vesicles reacted for acid phosphatase except in cases where the reaction product was also present on the microvilli and upon the nuclear membrane. This reaction has been said to be an artifact (Novikoff, 63).

Dense bodies. In all of the stages studied the yolk sac epithelial cells contained large dense bodies varying in size (2-6 µ in diameter) and opacity (figs 1, 2, 3, 6, 7). Those bodies nearest the cell surface were much more opaque than those more proximally located. A gradual reduction in the size of the dense bodies occurred in later stages of pregnancy. By day 20 the dense bodies ranged in size from 1-3 µ and occupied the greater portion of the apical part of the cell. The membranes of mitochondria and the endoplasmic reticulum fused with the smooth membrane of the dense bodies. Frequently membrane remnants were found in the space between the dense material and the limiting membrane of the dense bodies (figs 2, 3, 6). Projections of cytoplasm containing free ribosomes often extended into the area.

Reaction for acid phosphatase was observed in the dense bodies located the greatest distance from the cell surface and in the cytoplasm between these bodies (figs 1, 2). Reaction product was often lacking or sparsely distributed in the distally located dense bodies.

"Multivesicular" bodies. In the younger stages, days 10 and 11, the epithelial cells of the yolk sac had relatively clear vacuoles containing disorganized membrane remnants, myelin figures and scattered particles of dense material. On day 12 these vacuoles 3-9 µ in diameter were filled with large numbers of small spherical vesicles interspersed within the dense material (figs 3, 4, 5). Frequently the

dense and fuzz lined vesicles the membranes of which are continuous with the plasma membrane and several types of vacuoles containing dense material and vacuolated clear areas (Wislocki and Dempsey '55 Wislocki and Padykula '61). Materials injected into the uterine cavity were absorbed by the vesicles of the yolk sac cell and became concentrated in the vacuoles in the supranuclear region of the cell (Luse '57 Carpenter and Ferm '66). The vacuoles then correspond to the digestive vacuoles of the lysosome concept (de Duve '63). If acid phosphatase activity were to be demonstrated within the vacuoles this would substantiate the idea that they are lysosomal in character.

To test the hypothesis that lysosomes may be directly involved in necrosis of the conceptus (Schultz and Schultz '62), Triton WR 1339 a non ionic detergent known to lyse the lysosomes of other tissues *in vivo* (Wattiaux, Wibo and Baudhuin '63) was injected into pregnant rats. A histochemical study had demonstrated that 20-60% of the rat litters were resorbed after Triton injection and that the most marked morphological change in the conceptus was a pronounced vacuolation of the apical region of the epithelial cells of the visceral yolk sac. These vacuoles were ringed by acid phosphatase activity and by non glycogen PAS reacting material suggesting lysosomal origin (Schultz and Schultz '66).

This report presents cytochemical and fine structural observations of the lysosomal area of developing normal yolk sac cells the vacuolation of this area following Triton injection and the ensuing changes associated with survival or death of the conceptus.

MATERIALS AND METHODS

Injection regimen Sprague Dawley rats were injected intravenously (vena cava inferior) on day 11 of pregnancy with 200 mg Triton WR 1339 in 1 ml rat Ringer's solution 300 mg Triton in 1.5 ml Ringer's or 400 mg Triton in 2 ml Ringer's solution. Control animals were injected with an equivalent amount of rat Ringer's solution. Conceptuses were obtained by laparotomy on days 11, 12, 13, 14, 15, 16 and 20 of pregnancy. A total of sixty yolk sacs

from 29 control rats and 87 yolk sacs from 50 experimental animals was used in this study.

Another series of experiments involved intravenous injections of 200 mg Triton WR 1339 on day 12 of pregnancy and removal of conceptuses by laparotomy at 30, 60, 120, 240 and 360 minutes after injection. A minimum of six yolk sac samples were taken at each time interval.

At the time of injection the membranes of the yolk sac had been completely detached, the chorion allantoic placenta had been excised, and the parietal yolk sac and Reichert's membrane were intact.

Laparotomy Consecutive samples were taken from individual animals at the following time intervals: 1. at a specific time conceptuses were removed by laparotomy; 2. the pregnancy allowed to continue; 3. at each of the next time intervals the procedure was repeated. In this manner a critical time after Triton treatment could be determined with fair accuracy. Approximately 75% of the Triton treated animals handled this way delivered live fetuses at term. Laparotomy did not reduce resorption in the control arm.

Sample preparation The folded portion of the visceral yolk sac placenta (day 15 of pregnancy) was dissected from the conceptus in cold 0.25 M sucrose and cut into small pieces approximately 5 × 5 mm × 15-50 μ. The samples were fixed for 12 hours in either cold Bouin's (Holt and Hicks '61) or Pease's fixative stored overnight in cold buffer sucrose solution pH 7.3 rinsed with 7.5% sucrose and reacted for acid phosphatase activity with Daems' modification of Gomori substrate pH 5 (Daems '60) for 20 minutes at 37°C. Thinner membranes from older conceptuses (day 16) were fixed whole, chopped in 0.5 day slices with the McIlwain mechanical tissue chopper (McIlwain and Buddle '57 Smith and Farquhar '63) and reacted for acid phosphatase activity. Duplicate samples were inhibited by incubation in Gomori substrate containing 0.01 M NaF. After reaction the tissues were washed in 0.05 M acetate buffer containing 4% formaldehyde and 7.5% sucrose pH 4.

careed from the apical border of the the endoplasmic reticulum became fed with an increased accumulation of material within the cisternae and all vesicles were formed from the crs of the mitochondria (figs 16 17 18)

The vacuolated bodies remained ger than those of yolk sac cells which lived the Triton effect. The acid phosphate reaction was localized upon the ques of dense material and on the membrane of the vacuoles (figs 16 17). At 60-72 hours after injection the early fences of approaching cell death were lanced and were accompanied by pyk of the nucleus and a total disorganization of the membranes in the apical ion of the cell. The apical region of the became filled with many small vesi some of which had ribosomes associated with them and were probably ded from the endoplasmic reticulum (figs 18 19). The vacuolated dense and ultivesicular" bodies became very large and occupied the major portion of the apical region of the cell.

When a cell could no longer be recognized morphologically as a yolk sac epithelial cell the acid phosphatase activity was ill present and there was no change in the distribution of the reaction product en in cases of most advanced disorganization. In the final stages of degeneration the cells ruptured and the cell contents ere expelled into the extracellular area.

DISCUSSION

The histology histochemistry fine structure and absorptive function of the yolk sac epithelial cell have been described in detail (Wislocki Deane and Dempsey 46 Amoroso 58 Wislocki and Padykula 61 Al Abbass and Schultz 66). These studies demonstrated that the apical region of the visceral yolk sac cell was absorptive in function had localized acid phosphatase activity and contained proteinaceous droplets and non glyco-gen PAS reacting substances. These structural and biochemical characteristics of the lysosome have been established during the last few years. This study has verified the lysosomal and absorptive nature of the supranuclear area of the yolk sac cell and we have attempted to relate this area with the survival or

death of the cell under adverse conditions. A complete review of current concepts of the lysosome function has been presented by Weissmann (65).

The presence of acid phosphatase in the transitory "multivesicular" bodies and the proximal dense bodies indicated that they were lysosomes (Novikoff 63). The successive transformation of the autophagic vacuoles of days 10 and 11 to multivesicular bodies on days 12 and 13 and the transformation of multivesicular bodies to dense bodies in later stages of pregnancy corresponded to similar transformations in the lysosomal areas of other tissues (Gordon Miller and Bensch 65). Electrophoretic studies on the yolk sac have shown changes in acid phosphatase distribution between days 10 and 11 and between days 13 and 14 of pregnancy (Johnson and Spinuzzi 66). These days coincide with the time of occurrence of morphological changes in the lysosomes of the yolk sac epithelial cell. It may be that the acid phosphatase in the lysosomes changes molecularly in conjunction with changes in fine structure.

We have assumed that the vacuolation of all of the bodies in the supranuclear region of the cell was due to the absorption and accumulation of the Triton WR 1339 since the detergent administration was the only imposed variable in the experimental conditions. This area has been shown to accumulate colloidal gold (Luse 57) and thorotrast (Carpenter and Ferm 66). It therefore seemed reasonable to assume that it was also capable of incorporating Triton. Vacuolation of the lysosomes of the liver following Triton WR 1339 administration has been demonstrated (Wattiaux Wibo and Baudhuin 63) and the Triton filled vacuoles of the liver were morphologically similar to those of the yolk sac cell.

The marked increase in resorption following the administration of Triton was evidence that the detergent was detrimental to the conceptus. Although it was clear from this study that Triton had a marked effect upon the morphology of the yolk sac placenta of resorbing animals we do not know whether the death of the yolk sac was a cause of or a result of the interruption of pregnancy. Ultrastructural stud

membranes of mitochondria and endoplasmic reticulum fused with the surrounding membrane of the vacuoles (fig 4). The lack of organization of the membrane remnants within the vacuoles at days 10 and 11 was characteristic of autophagic vacuoles of other tissues while the uniformity in size and appearance of the inclusions of the vacuole on day 12 was similar to that of the multivesicular bodies of other tissues (Novikoff, 63; Novikoff, Essner and Quintana, 64; Gordon, Miller and Bensch, 65). We have referred to both structures as multivesicular bodies. The multivesicular bodies disappeared completely by the fourteenth day and therefore were interpreted to be transitory structures in the differentiation of the lysosomal area of the yolk sac epithellium.

The acid phosphatase activity was associated with the dense material within the vesicles and with the outer limiting membrane of the multivesicular body. Acid phosphatase activity also appeared in the cytoplasm between these inclusions and the dense bodies.

Disposition of other organelles. Great numbers of mitochondria were found clustered about the lysosomal area (figs 2, 3, 4). The endoplasmic reticulum became more regularly disposed in the later stages of development and frequently contained dense material similar in opacity to that of the dense bodies (fig 15). The Golgi apparatus was localized in the perinuclear region and did not appear to be related to the lysosomal area. None of these structures reacted for acid phosphatase.

Observations following injection of triton

In 75% of the pregnant rats injected with Triton WR 1339 the conceptuses survived any detrimental Triton effects and live fetuses were delivered at term. In 25% of the pregnancies the conceptuses died and were resorbed.

Survival. The time before response of the yolk sac cell to Triton injection varied from animal to animal. Some yolk sacs showed increased vacuolation within the dense and multivesicular bodies 15 minutes after injection while others did not show this until two hours after injection. The maximum "swelling" and vacuolation

effect was obtained 4-6 hours after injection (fig 9).

Within 12 hours after injection the membrane remnants of the multibodies (9-17 μ) had disappeared entirely. The opaque material of both multivesicular bodies and the dense bodies appeared to be pushed to the periphery of the vacuoles where it formed dense plaques (figs 10, 11, 12). Fusion of the membranes of mitochondria and the endoplasmic reticulum with the membrane of the vacuoles was common (fig 12).

Acid phosphatase reaction was confined to the dense plaques, the membrane of the vacuoles and the cytoplasm between vacuoles (fig 10, 11).

The large clear vacuoles, through days 13 and 14 of pregnancy, membrane remnants and myelin began to reappear in the lumen of the vacuoles. Random dead cells and debris from lysed cells were found on these although the fetus was alive at the time the samples were taken. By the fifteenth and sixteenth days, the vacuoles came smaller and again began to contain large amounts of dense material (figs 13, 14). By the twentieth day the yolk sac appeared similar to those of the control with the exception of small clear dilated areas within the dense bodies, the presence of a larger amount of residual membrane (fig 15).

Occasionally after Triton treatment intercellular spaces between epithelial cells became dilated and disorganized and cell figures and membrane remnants were found in these spaces (fig 16). At this time was there a measurable change in the size distribution or appearance of the dense or clear pinocytotic vesicles and membrane remnants within the clear pinocytotic vesicles did not disappear upon Triton injection as did those of the multivesicular body.

Death. All Triton treated yolk sac cells whether destined to survive or to die were morphologically similar through the 48 hour interval after injection. The cellular changes in the yolk sac associated with death of the fetus occurred between 48-60 hours post injection. The villi became shorter, thicker and reduced in number, the pinocytotic vesicles &

lets of other cells (Novikoff 63) If the other hand these dense vesicles involved in the process of pinocytosis (fig 1B) they are acting as phagosomes (Straus 64) and would eventually with lysosomes to form digestive roles

The saccular fuzz lined vesicles are probably pinocytotic in that other studies have shown that these vesicles incorporate marker substances gold and thorotrast (see 57 Carpenter and Ferm 66) They also be concerned with the process of pinocytosis for the removal of membrane remnants from the cell (text fig 1A) Juve (63) suggested that a mechanism of exocytosis might exist but the phenomenon has rarely been observed in a complex system

ACKNOWLEDGMENTS

The authors gratefully acknowledge the technical assistance of Barbara D Fleischer Gabrielle C Rouiller Juanita Reyes and Catharine Zahler

LITERATURE CITED

Abbas A H and R. L. Schultz 1966 Phagocytic activity of the rat placenta J Anat (Lond) 100 349-359

Abbas E C 1958 Placentation In Marshall's Physiology of Reproduction chapt 15 (A S Parkes editor) Longmans Green and Company New York 2 127-311

Carpenter S J and V H Ferm 1966 Electron microscopic observations on the uptake and storage of Thorotrast by rodent yolk sac epithelial cells Anat Rec 154 327-328

Chen W T 1962 Mouse liver lysosomes and storage: a morphological and histochemical study Ph.D thesis University of Leiden

Duve C 1963 The lysosome concept In Ciba Foundation Symposium on Lysosomes (A V S de Reuck and M P Cameron eds) Little Brown and Company Boston pp 1-31

Faziani M V 1963 Lysosome changes in liver injury In Ciba Foundation Symposium on Lysosomes (A V S de Reuck and M P Cameron editors) Little Brown and Company Boston pp 335-352

Ferm J W 1935 Morphological and physiological studies of the placenta in the albino rat J Exp Zool 70 243-286

Ford G B L R Miller and K G Bensch 1965 Studies on the intracellular digestive process in mammalian tissue culture cells J Cell Biol 25(2) 41-55

Gil, S J and R M Hicks 1961 The localization of acid phosphatase in rat liver cells as revealed by combined cytochemical stain

ing and electron microscopy J Biophysic Blochem Cytol 11 47-66

Johnson E M and R Spinuzzi 1966 Molecular differentiation of the rat's yolk-sac "placenta" as effected by a teratogenic agent J Embryol Exp Morph (In press)

Koenig H 1962 Histochemical distribution of brain gangliosides lysosomes as glycolipoprotein granules Nature (Lond) 195 782-784

Luse S A 1957 The morphological manifestations of uptake of materials by the yolk sac of the pregnant rabbit In Gestation (C A Villee editor) Josiah Macy Jr Foundation Madison New Jersey pp 115-141

Mellwain H and H L Buddle 1953 Techniques in tissue metabolism 1 A mechanical chopper Biochem J 53 412-420

Miller F 1962 Acid phosphatase localization in renal protein absorption droplets In Fifth International Congress for Electron Microscopy Academic Press 2 Q2

Novikoff A B 1963 Lysosomes in the physiology and pathology of cells contributions of staining methods In Ciba Foundation Symposium on Lysosomes (A V S de Reuck and M P Cameron editors) Little Brown and Company Boston pp 36-73

Novikoff A B E Essner and N Quintana 1964 Golgi apparatus and lysosomes Fed Proc 23 1010-1022

Padykula H A 1958 A histochemical and quantitative study of enzymes of the rat's placenta J Anat (Lond) 92 118-129

Pease D C 1962 Buffered formaldehyde as a killing agent and primary fixative for electron microscopy Anat. Rec 142 342

Schultz R L and P W Schultz 1962 Enzyme distribution in the rat fetus and placenta following the administration of ethionine J Cell Biol. 15 211-225

— 1966 Morphological and histochemical changes in the rat conceptus following the administration of a nonionic detergent Proc Soc Exp Biol and Med 122 874-877

Smith R E and M G Farquhar 1963 Preparation of thick sections for cytochemistry and electron microscopy by a nonfreezing technique Nature 200 691

Sorokin S P and H A Padykula 1964 Differentiation of the rat's yolk sac in organ culture Am J Anat. 114 457-477

Straus W 1964 Occurrence of phagosomes and phago-lysosomes in different segments of the nephron in relation to the reabsorption transport digestion and extrusion of intravenously injected horseradish peroxidase J Cell Biol. 21 295-308

Wattiaux R, M Wilbo and P Baudhuin 1963 Influence of the injection of Triton WR 1339 on the properties of rat liver lysosomes In Ciba Foundation Symposium on Lysosomes (A V S de Reuck and M P Cameron eds) Little Brown and Company Boston pp 176-196

Weber R. 1963 Behavior and properties of acid hydrolases in regressing tails of tadpoles.

ies of the resorbing chorio-allantoic placenta have not yet been done but histological preparations indicated that none of the layers of the chorio-allantoic placenta or the decidua basalis responded to Triton treatment as markedly as the yolk sac placenta (Schultz and Schultz, 66).

In resorbing conceptuses the continued distension and vacuolation of the dense and multivesicular bodies was characteristic of the lysosomal area of the yolk sac cells. It may be that continued enlargement of these structures was incompatible with the life of the cell. In all cases the membrane of the vacuoles appeared to be intact and there was no obvious change in distribution of the acid phosphatase. Although acid phosphatase appeared stable during resorption the other acid hydrolases of the lysosomes may have behaved differently.

Although the morphology of the vacuoles and the localization of acid phosphatase activity did not change appreciably, drastic changes in structure and presumably function of other organelles occurred during the course of death and resorption of the yolk sac cell. These changes loss of the mitochondrial cristae, vesiculation of the endoplasmic reticulum, decrease in the number and size of the microvilli, loss of the pinocytotic vesicles and nuclear pyknosis were definite indications of impending cell death. Other studies of cell death have shown that mitochondrial swelling and decay and damage to the endoplasmic reticulum occurred prior to obvious lysosomal degeneration (Weber 63, Dianzani 63).

The survival of the conceptus after Triton treatment was characterized by reorganization of the lysosomal area of the yolk sac cell. We cannot say whether the decrease in size of the vacuoles and reaccumulation of the dense material was associated with release of Triton from the cell or was an indication of repackaging of the detergent into smaller vacuoles. Survival of the yolk sac cells may not have depended upon reorganization of the lysosomal area since the latter may have occurred as a consequence of the recovery of other cellular systems primarily affected by Triton.

The absorptive function of epithelial cell has been well. Recently, it has been shown the yolk sac is also secretory in (Sorokin and Padykula, 64). Both these functions must be related in some way to the structures of the distal part of the cell, i.e., the microvilli, pinocytotic vesicles, dense bodies and vacuoles. Figure 1 presents the types of structures that may occur in this area. If the pinocytotic vesicles represent droplets budding off the dense material (fig. 1A) the loss of acid phosphatase activity from the droplet as it moves toward the apical end of the cell corresponds to the loss of the enzyme activity in

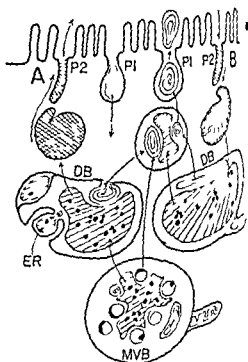
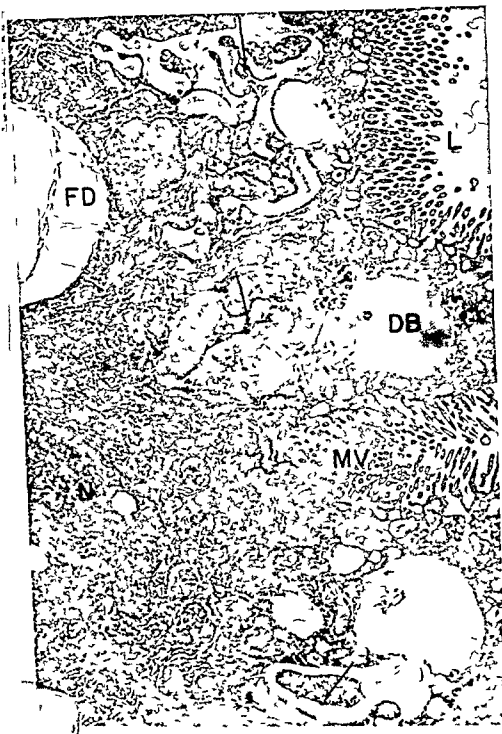


Fig. 1. Diagram indicating possible interrelationships of the pinocytotic vesicles with the dense and multivesicular bodies. The clear pinocytotic vesicles (P1) are presumed to serve the process of exocytosis eliminating membrane remnants from the yolk sac epithelial cell. The clear vesicles may also result from the process of endocytosis. Scheme A indicates elimination of a secretory product from the yolk sac cell. In this scheme the secretory product is formed in the endoplasmic reticulum (ER) and accumulates in the dense bodies (DB). The dense material moves toward the apical region of the cell and is eliminated from the cell via the dense tubular pinocytotic vesicles (P2). Scheme B indicates an alternate way of dense material within the yolk sac cell (i.e., endocytosis).



- during spontaneous and induced metamorphosis *in vitro* In Ciba Foundation Symposium on Lysosomes (A V S de Reuck and M P Cameron editors) Little Brown and Company Boston pp 282-300
- Weissmann G 1965 Lysosomes N Eng J Med 273 1084-1090 1143-1149
- Wilson J R A R Beaudoin and H J Free 1959 Studies on the mechanism of teratogenic action of trypan blue Anat Rec 133 115-128
- Wislocki G B H W Deane and E W Dempsey 1946 The histochemistry of the rodent placenta Am J Anat 78 381-321
- Wislocki G B and E W Dempsey 1955 Electron microscopy of the placenta of the mouse Anat Rec 123 33-63
- Wislocki G B and H A Padykula 1961 Histochemistry and electron microscopy of the placenta In Sex and Internal Secretions chapt 15 (W C Young editor) Williams and Wilkins Company Baltimore pp 853-877

Abbreviations

CP clear pinocytotic vesicle	LA lysosomal area
DB dense body	M mitochondria
DP dense pinocytotic vesicles	MB multivesicular body
ER endoplasmic reticulum	MV microvilli
FD fat droplet	N nucleus
IS intercellular space	TV vacuole following Triton treatment
L yolk sac lumen	V vesiculated region of cell

PLATE 1

EXPLANATION OF FIGURE

- 1 Twelve day control yolk sac epithelial cells Fixative Pease's Acid phosphatase reaction (arrows) 7400 \times

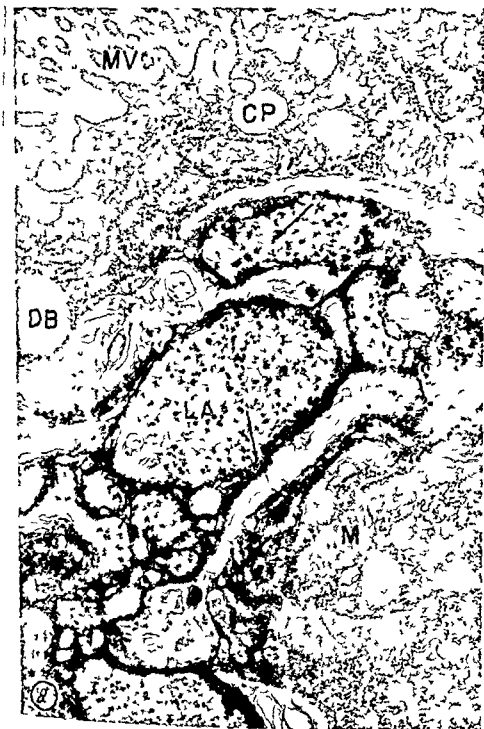


PLATE 2

EXPLANATION OF FIGURE

- 2 Twelve day control supranuclear region of yolk sac cell Fixative
Pease's Acid phosphatase reaction (arrows) 27 000 X

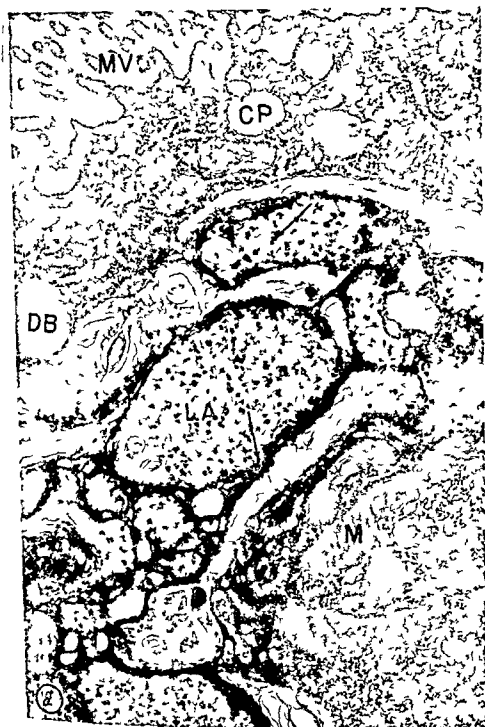


PLATE 3

EXPLANATION OF FIGURE

- 3 Twelve day control supranuclear region of cell Fixative Peases
Acid phosphatase reaction inhibited by NaF 15 000 X



PLATE 4

EXPLANATION OF FIGURES

- 4 Twelve day control example of fusion of mitochondria with multi vesicular body Fixative glutaraldehyde 45 000 X
- 5 Twelve day control Fixative Pease s Acid phosphatase reaction (arrows) 18 000 X

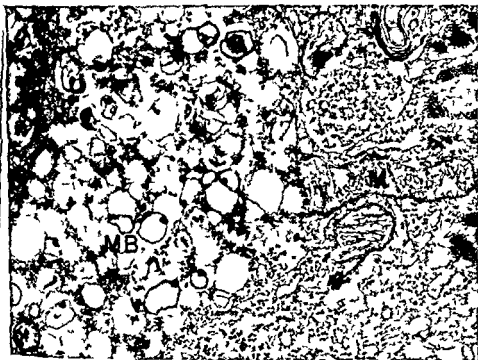


PLATE 4

EXPLANATION OF FIGURES

- 4 Twelve day control example of fusion of mitochondria with "multi vesicular body" Fixative glutaraldehyde 45 000 X
- 5 Twelve-day control Fixative Pease's Acid phosphatase reaction (arrows) 18 000 X

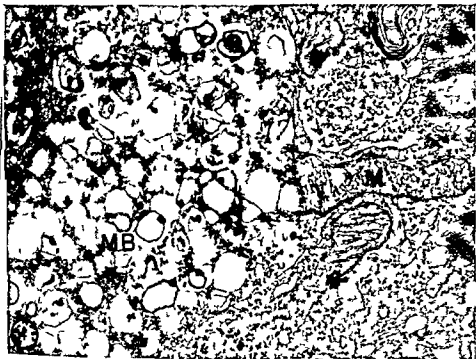


PLATE 5

EXPLANATION OF FIGURES

- 6 Fifteen day control supranuclear region of yolk sac cell Peases
fixative Acid phosphatase reaction (arrow) 32 000 X
- 7 Twenty-day control supranuclear region of yolk sac cell Holt's
fixative Acid phosphatase reaction (arrow) 15 000 X

1: W. Schultz, Jam. F. Rege, and R. hard L. S. hultz



PLATE 6

EXPLANATION OF FIGURES

- 8 Twenty-day control apical area of yolk sac cell Holt's fixative
27 000 X
- 9 Four hour Triton treated (200 mg) yolk sac cell day 12 of pregnancy Pease's fixative Acid phosphatase reaction (arrows)
15 000 X

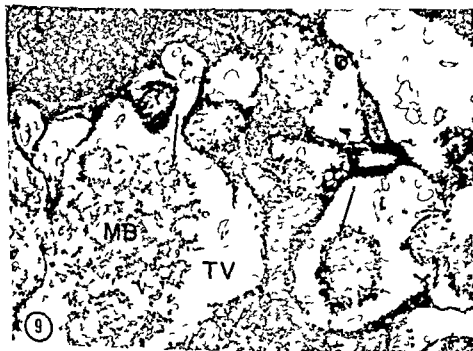


PLATE 7

EXPLANATION OF FIGURE

- 10 Thirteen day Triton treated (300 mg) yolk sac cells 48 hours after injection Pease's fixative Acid phosphatase reaction (arrows)
6500 \times



PLATE 7

EXPLANATION OF FIGURE

- 10 Thirteen day Triton treated (300 mg) yolk sac cells 48 hours after
injection Pease's fixative Acid phosphatase reaction (arrows)
6500 \times



PLATE 8

EXPLANATION OF FIGURE

- 11 Thirteen day Triton treated (300 mg) yolk sac cells 48 hours after
injection Pease's fixative Acid phosphatase reaction (arrows)
20 000 \times



PLATE 9

EXPLANATION OF FIGURE

- 12 Thirteen day Triton treated (200 mg) yolk sac cells 48 hours after injection Example of blebbing of endoplasmic reticulum into vacuoles (arrows) Pease's fixative Acid phosphatase reaction reaction inhibited with NaF 14 000 \times



PLATE 9

EXPLANATION OF FIGURE

- 12 Thirteen day Triton treated (200 mg) yolk sac cells 48 hours after injection. Example of blebbing of endoplasmic reticulum into vacuoles (arrows). Pease's fixative. Acid phosphatase reaction reaction inhibited with NaF. 14 000 \times

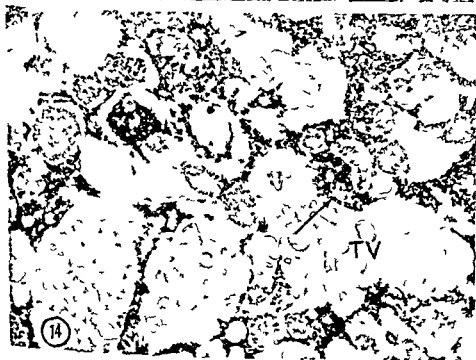


PLATE 10

EXPLANATION OF FIGURES

- 13 Fifteen day Triton treated (200 mg) yolk sac epithelial cell 96 hours after injection Viable fetuses at term Pease's fixative Acid phosphatase reaction (arrow) 13 000 \times
- 14 Sixteen-day Triton treated (300 mg) yolk sac cell 120 hours after injection Viable fetuses at term Pease's fixative Acid phosphatase reaction (arrow) 10 000 \times



PLATE 11

EXPLANATION OF FIGURE

- 15 Twenty day Triton treated (300 mg) yolk sac cell nine days after
Triton injection Viable fetuses Holt's fixative Acid phosphatase
reaction (arrow) 12 000 \times

YOLK SAC CYTOCHEMISTRY
as W Schultz, James F R Jr and Richard L Schultz

PLATE 12

EXPLANATION OF FIGURE

- 16 Fourteen day Triton treated (300 mg) yolk sac cell 72 hours after injection. Five dying yolk sac cells from animal that resorbed litter before term. Pease's fixative. Acid phosphatase reaction (arrow). 7000 X



PLATE 13

EXPLANATION OF FIGURE

- 17 Fourteen day Triton treated (200 mg) yolk sac cell 72 hours after injection Litter resorbed Pease's fixative Acid phosphatase reaction (arrow) 15 000 \times

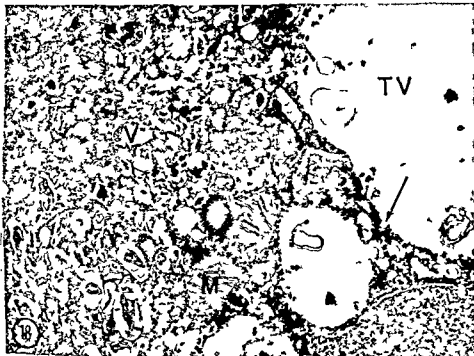


PLATE 14

EXPLANATION OF FIGURES

- 18 Fourteen day Triton treated (200 mg) yolk sac cell apical region
Litter resorbed Pease's fixative Acid phosphatase reaction (arrow)
27 000 X
- 19 Fourteen-day Triton treated (200 mg) yolk sac cell apical region
Litter resorbed Pease's fixative Acid phosphatase reaction (arrow)
17 500 X

Histochemical Study of the Esterases in the Rat Heart¹

EL-SAYED H H HEGAB AND VICTOR J FERRANS

Departments of Anatomy and Medicine Tulane University School of
Medicine New Orleans Louisiana

ABSTRACT The histochemistry of esterases was studied in the rat heart using various methods of tissue preparation and a large number of substrates inhibitors and activators

Non-specific esterase and cholinesterase was demonstrated in the fibers of the atrioventricular conduction system in atrial and ventricular muscle fibers in cardiac neurons and in some of the nerve fibers of the heart The highest concentration of both types of enzymes was found in the conduction system and in the neural elements Pericytes and macrophages showed only non specific esterase activity

Two broad types of non specific esterase activity cytoplasmic and lysosomal were distinguished in the pericytes macrophages and cardiac muscle fibers by the use of selective inhibitors and activators The cytoplasmic activity is due to the presence of B and C esterases and was better demonstrated with esters of a naphthol than with naphthol AS derivatives or indigogenic esters The esterase activity of lysosomes appears to be due to a group of fluoride- and organophosphate resistant enzymes some of which are probably cathepsins

Although the histochemical localization of cholinesterase and thioacetate acid esterase in cardiac muscle recently has been studied by electron microscopy (Barnett and Palade 59 Karnovsky and Hug 63 Karnovsky 64) the general topography of these various esterases of the rat heart has been the subject of relatively few investigations Nachlas and Seligman (49) Mori (52) and Chessick (53) described unidentified cells in the rat heart that reacted with a naphthyl acetate in paraffin sections of acetone fixed tissues The remainder of the myocardium showed no activity Ravin Zacks and Seligman (53) reported the hydrolysis of β -naphthyl acetate in unfixed frozen sections of rat heart with the formation of a diffuse granular precipitate in the muscle fibers Carbonell (56) found a naphthyl acetate esterase activity in interstitial cells believed to be macrophages scattered throughout the myocardium the atrioventricular conduction system (AVCS) reacted strongly with choline esters but not with a naphthyl acetate More recently Joo and Csillik (62) applied the thioacetate acid and the indoxyl acetate methods to sections pretreated with hyaluronidase and found esterase activity in the cytoplasm and intercalated discs of the rat heart

Significant advances in the histochemical methodology of esterases (Pearse 61a Burstone 62 Barka and Anderson 63) have been made since the publication of some of the preceding histochemical reports and the present investigation appeared justified by the fact that these improvements have not been applied systematically to the study of the heart

MATERIAL AND METHODS

Fixation

Male albino rats weighing from 250 to 300 gm were used In some experiments the hearts were removed rapidly after decapitation and frozen in dry ice isopentane fresh frozen sections were then cut in a cryostat and post fixed for periods of time varying from 30 minutes to 16 hours in one of the following fixatives 4% neutralized formaldehyde containing 1% calcium chloride (formol-calcium) with and without the addition of 0.44 M sucrose 4% formaldehyde in 0.1 M phosphate buffer 7.4 4% glutaraldehyde in 0.1 M phosphate buffer pH 7.4 and 4% glutaraldehyde in 0.1 M cacodylate buffer pH 7.2 In other experiments the heart was per-

Supported by research grant HE-06100-04 and by Training Grant ES-01793 from the United States Public Health Service

RESULTS

terase activity was demonstrated in following structures of the heart

The cytoplasm of the specialized cells of the atrioventricular node the bundle of His and its two main branches (figs 1-4 23 25-28 31 32)

The cytoplasm and lysosomes of the l and ventricular muscle cells (figs 17-20 23 24 31 32)

The neural elements including the ganglia and their postganglionic fibers the nervous plexuses surrounding the atrioventricular node and bundle of His and some of the nerve fibers in the atria ventricles and atrioventricular ring (figs 2 3 6 24 28-30)

The cytoplasm and lysosomes of various types of interstitial and pericapillary present throughout the myocardium epicardium in the mural and valvular myocardium and in the adventitia of the blood vessels at the base of the heart (figs 1-4 7-17 19-22)

The intensity of the reaction at the various enzymatic loci the extent of diffusion the quality of the morphological presentation of tissues varied according to the method of fixation For the study of non-specific esterases pre-fixation for two hours with 4% glutaraldehyde in 0.1 M cacodylate buffer pH 7.2 gave the best results particularly when preceded by *in situ* perfusion of the heart with the fixative Higher enzymatic activity and greater evenness of fixation were demonstrated after this procedure than after fixation by immersion overnight in formal-calcium which otherwise gave excellent results Less satisfactory morphology much more diffusion and considerably less enzymatic activity were found with all post-fixation procedures Of the latter fixation in the cold for 30 minutes with formal-calcium gave the most acceptable results Prolongation of the time of post-fixation resulted in gradual reduction of the esterase activity of the muscle fibers which showed only a slight reaction after 12 hours of post-fixation

Variable amounts of non-specific esterases are known to be extracted from fresh frozen sections during the process of post-fixation and during exposure to the solutions of buffers and inhibitors (Nachlas

et al 56 Hannibal and Nachlas 59) For this reason the studies on the effects of enzymatic inhibitors and activators were made on free floating sections from pre-fixed tissues in which such losses are minimal

Cholinesterases were best studied in fresh frozen sections briefly fixed in cold buffered formaldehyde since the enzymatic activity was strongly inhibited by prolonged formaldehyde fixation and by the glutaraldehyde mixtures

As shown in table 1 the patterns of histochemical staining observed in each of the esterase active sites depended primarily on the chemical structures of the substrates employed for the reaction and our results will be described accordingly

Esters of a naphthol The strongest staining was produced by a naphthyl acetate Progressively less intense staining was observed with the propionate and butyrate esters and only a faint reaction was given by a naphthyl valerate No staining was noted with a naphthyl caprylate laurate or myristate Of the two types of coupling agents best results were obtained with hexazotized p-rosanilin which produced much better defined localization than Diazo Blue B

A moderately intense reaction was obtained in the cytoplasm of the specialized muscle cells of the atrioventricular node and the bundle of His and its two main branches (figs 1-4) The esterase activity of the peripheral ramifications of the AVCS was similar to that of ventricular myocardial cells Atrial muscle fibers reacted less intensely than the AVCS but more strongly than ventricular muscle Two distinct types of enzymatic activity towards esters of a naphthol were distinguished in the muscle fibers by the use of selective inhibitors (table 2) One was responsible for the diffuse cytoplasmic staining (fig 5) the other was localized in sarcoplasmic bodies that were identified as lysosomes on the basis of electron microscopy and staining for acid phosphatase No staining was observed in the intercalated discs The diffuse cytoplasmic esterase activity which is sensitive to prolonged aldehyde fixation was completely inhibited by 10^{-4} M DFP (diisopropylfluorophosphate) 10^{-5} M E... (diethyl p-

fused *in situ* for 15 minutes with one of the fixatives listed above and then subjected to further fixation with the same solution for two hours in the glutaraldehyde mixtures and overnight in the formaldehyde solutions. Specific areas of the heart were then dissected washed in several changes of buffer or 0.44 M sucrose frozen rapidly and sectioned in a cryostat.

For the study of the atrioventricular conduction system it became necessary to use post fixed frozen sections cut serially since considerable difficulty was often encountered in handling free floating pre fixed sections of the area of the atria and the atrioventricular ring.

Histochemical staining

Seven groups of esterase substrates were used

1 *The following a naphthyl esters of straight chain aliphatic acids were employed* Acetate propionate butyrate valerate caprylate laurate and myristate. Two types of agents were utilized to couple the liberated a naphthol stabilized diazonium salts and hexazotized prosanilin. In both cases the incubation was performed at a pH ranging from 6.5 to 8.2. Since best results were obtained at pH 7.0 this was used throughout the study. For the hexazotized prosanilin the method of Barka and Anderson (63) was followed and sections were incubated at room temperature for 15 minutes. Of the diazonium salts used (Diaz Blue B, Diaz Blue RR, Diaz Blue BB, Diaz Red RC and Fast Violet B) best results were obtained with Diaz Blue B which was used in all subsequent experiments. Sections were incubated at room temperature for ten minutes in a medium prepared according to the method of Pearse (61b).

2 *Naphthol AS esters* Naphthol AS D acetate, naphthol AS D chloroacetate, naphthol AS LC acetate and naphthol AS BG acetate were used. Sections were incubated for 30 minutes at room temperature according to the method of Burstone (62). The double staining technique of Shnitka and Seligman (61) was followed for the differential demonstration of cytoplasmic and lysosomal esterase activity in the same tissue section.

3 *Indigogenic substrates* The technique of Holt and Withers (58) was followed using indoxyl acetate, 5-bromoindoxyl acetate and 5-bromo-4-chloroindoxyl acetate as substrates. In some experiments the ferricyanide-ferrocyanide redox system was used in reduced concentrations (0.0005 M instead of 0.005 M). Sections were incubated for 30 minutes at 37°C. Incubation times were prolonged to 1 hour in media containing high concentrations of the redox system.

4 *Choline esters of long-chain acids* The modified Gomori technique of Barka and Anderson (63) was used. Sections were incubated for two hours at 37°C in media containing either lauroyl or myristoyl choline as substrate.

5 *Thiocholine esters* The procedure of Koelle and Friedenwald (49) was followed using acetyl and butyrylthiocholine. Sections were incubated for two hours at 37°C.

6 *Thioacetic acid* The method of Wachstein, Meisel and Falcon (61) was used. Sections were incubated at room temperature for 15–30 minutes.

7 *Tucons* The method of Gomori (45) was followed using Tween 80. Sections were incubated with and without the addition of 10^{-4} M sodium taurocholate at 37°C for periods of time ranging from 30 minutes to 16 hours.

Control procedures included the incubation of heat inactivated sections and the use of media that contained all reagents except the substrate.

The effect of the enzymatic activators and inhibitors listed in table 2 was studied. In these experiments the sections were pre-incubated for one hour at room temperature in a buffered solution containing the inhibitor after which they were transferred to a complete incubating medium and processed in the same manner as sections that had been (a) untreated, (b) treated with the buffered solution without the inhibitor. Whenever possible (i.e. when it did not react with any of the components of the medium) the inhibitor was also added to the final incubating medium.

RESULTS

ase activity was demonstrated in following structures of the heart

The cytoplasm of the specialized cells of the atrioventricular node the bundle of His and its two main branches (figs 1-4 23 25-28 31 32) The cytoplasm and lysosomes of the atrioventricular muscle cells (figs 17-20 23 24 31 32)

The neural elements including the autonomic ganglia and their postganglionic fibers the nervous plexuses surrounding the atrioventricular node and bundle of His and some of the nerves in the atria ventricles and atrioventricular ring (figs 2 3 6 24 28-30)

The cytoplasm and lysosomes of various types of interstitial and pericapillary present throughout the myocardium epicardium in the mural and valvular myocardium and in the adventitia of the blood vessels at the base of the heart (figs 1-4 7-17 19-22)

The intensity of the reaction at the various enzymatic loci the extent of diffusion and the quality of the morphological presentation of tissues varied according to the method of fixation For the study of non-specific esterases pre-fixation for two hours with 4% glutaraldehyde in 0.1 M cacodylate buffer pH 7.2 gave the best results particularly when preceded by *in situ* perfusion of the heart with the fixative Higher enzymatic activity and greater evenness of fixation were demonstrated after this procedure than after fixation by immersion overnight in formal-calcium which otherwise gave excellent results Less satisfactory morphology much more diffusion and considerably less enzymatic activity were found in all post-fixation procedures Of the three methods of fixation in the cold for 30 minutes formal-calcium gave the most acceptable results Prolongation of the time of fixation resulted in gradual reduction of the esterase activity of the muscle fibers which showed only a slight reaction after 12 hours of post-fixation

Variable amounts of non-specific esterases are known to be extracted from frozen sections during the process of post-fixation and during exposure to the solutions of buffers and inhibitors (Nachlas

et al 56 Hannibal and Nachlas 59) For this reason the studies on the effects of enzymatic inhibitors and activators were made on free floating sections from pre-fixed tissues in which such losses are minimal

Cholinesterases were best studied in fresh frozen sections briefly fixed in cold buffered formaldehyde since the enzymatic activity was strongly inhibited by prolonged formaldehyde fixation and by the glutaraldehyde mixtures

As shown in table 1 the patterns of histochemical staining observed in each of the esterase active sites depended primarily on the chemical structures of the substrates employed for the reaction and our results will be described accordingly

Esters of a naphthol The strongest staining was produced by α -naphthyl acetate Progressively less intense staining was observed with the propionate and butyrate esters and only a faint reaction was given by α -naphthyl valerate No staining was noted with α -naphthyl caprylate laurate or myristate Of the two types of coupling agents best results were obtained with hexazotized p-rosaniline which produced much better defined localization than Diazo Blue B

A moderately intense reaction was obtained in the cytoplasm of the specialized muscle cells of the atrioventricular node and the bundle of His and its two main branches (figs 1-4) The esterase activity of the peripheral ramifications of the AVCS was similar to that of ventricular myocardial cells Atrial muscle fibers reacted less intensely than the AVCS but more strongly than ventricular muscle Two distinct types of enzymatic activity towards esters of α -naphthol were distinguished in the muscle fibers by the use of selective inhibitors (table 2) One was responsible for the diffuse cytoplasmic staining (fig 5) the other was localized in sarcoplasmic bodies that were identified as lysosomes on the basis of electron microscopy and staining for acid phosphatase No staining was observed in the intercalated discs The diffuse cytoplasmic esterase activity which is sensitive to prolonged aldehyde fixation was completely inhibited by 10 M DFP (diisopropylfluorophosphate) 10⁻⁵ M E₆₀₀ (diethyl p-

TABLE 1

Distribution of esterase activity in rat heart as shown by different types of histochemical substrates. Tissues were pre-fixed for two hours in cacodylate buffered glutaraldehyde for the experiments in which naphthol and indigenic substrates and thiolaetic acid were used. Post-fixation for 30 minutes in cold formal-calcium was used for the study of cholinesterase substrates. The intensity of staining is expressed in a scale from 0 to 4+ in reference to the structure showing the highest activity with each substrate

Incubating medium	Cardiac muscle cells			Interstitial cells		Neural elements	Mast cells
	Atrial	AVCS	Ventric	Cytoplasm	Lysosomes		
a Naphthol acetate hexazotized pro-saunin	+	+	+	+	+	+	+
Naphthol AS-D acetate Fast Garnet GBC salt	+	+	+	+	+	+	+
Indigenic substrates with 0.005 M redox system	+	+	+	+	+	+	+
Thiolaetic acid	+	+	+	+	+	+	+
Lauroyl choline	+	+	+	+	+	+	+
Myristoyl choline	+	+	+	+	+	+	+
Acetylthiocholine iodide	+	+	+	+	+	+	+
Butyrylthiocholine iodide	+	+	+	+	+	+	+
Tween 80	0	0	0	0	0	0	0

nitrophenylphosphate) 10^{-4} M mercuric acetate and by 0.005 M concentration of the ferricyanide ferrocyanide redox system of Holt. It was slightly inhibited by 10^{-4} M copper sulfate 10^{-4} M silver nitrate and was unaffected by 10^{-4} M Iso-OMPA (isopropylpyrophosphoramidate) 10^{-4} M phenylpropionic acid 10^{-4} M sodium tartrate 10^{-4} M lead nitrate 10^{-4} M sodium iodoacetate and by 0.1 M N-ethylmaleimide. The diffuse cytoplasmic esterase activity was activated by 10^{-4} M cysteine. No activation could be demonstrated with 10^{-4} M PCMB (p-chloromercuribenzoate) except after treatment with 10^{-4} M E_{400} which irreversibly inhibited all the diffuse cytoplasmic esterase activity.

The small number of lysosomes present in the cardiac muscle cells particularly in the perinuclear area contained a fluoride and organophosphate resistant type of esterase activity similar to that of the lysosomes of the interstitial cells. In view of the fact that the localization of this type of esterase activity was restricted to lysosomes the term lysosomal esterase will be used throughout this paper in reference to the fluoride and E_{400} resistant esterase activity present in lysosomes. Similarly the fluoride and E_{400} sensitive esterase activity responsible for the diffuse cytoplasmic staining will be referred to as cytoplasmic esterase.

Various types of interstitial cells present throughout the heart (figs 7-17) gave an intense esterase reaction. Many of these cells were pericytes (figs 9-13) which had numerous elongated cytoplasmic processes and were closely related to the walls of the capillaries and the endocardium and subepicardium (figs 13-15). Others mostly macrophages and fibroblasts were unrelated to small blood vessels and were especially prominent in the upper portion of the interventricular septum in the atrioventricular ring in the adventitia of the great vessels and in the stroma of the cardiac valves (figs 14-16). The cytoplasmic processes of these cells were best demonstrated in sections from prefixed tissue blocks. Mast cells gave only a faint reaction with the a naphthol substrates.

TABLE 2

Effect of inhibitors and activators on the hydrolysis of naphtholic substrates by rat myocardium pre fixed in cacodylate buffered glutaraldehyde

Inhibitors or activator	Cytoplasm of muscle fibers	Interstitial cells	
		Cytoplasm	Lysosome
Serine 10 ⁻³ M	I+	0	0
DFP 10 ⁻⁴ M	I++++	I++++	I++
NaF 10 ⁻³ M	I++++	I++++	I++
NaF 10 ⁻⁴ M	I++++	I++++	0
iso-OMPA 10 ⁻³ M	0	0	0
Sodium fluoride 10 ⁻³ M	I++++	I++++	0
Mercuric acetate 10 ⁻³ M	I++++	I++++	I+++
Copper sulfate 10 ⁻³ M	I+	I++	I+
Silver nitrate 10 ⁻³ M	I+	I++	I+
Lead nitrate 10 ⁻³ M	0	0	0
Phenylpropionic acid 10 ⁻³ M	0	0	0
Cysteine 10 ⁻³ M	A+++	A+++	A+
Taurocholate 10 ⁻³ M	0	0	0
Sodium iodoacetate 10 ⁻³ M	0	0	0
N-ethylmaleimide 0.1 M	0	0	0
PCMB 10 ⁻³ M	0	0	0
Inhibition by E ₄₀₀ 10 ⁻³ M followed by PCMB 10 ⁻³ M	0	0	0
Inhibition by E ₄₀₀ 10 ⁻³ M followed by PMCB 10 ⁻³ M	A++	A+	A±

At 100% fixation by A and inhibition by I. ++ 50% +++ 75%
 +++ 100% fixation by A and inhibition by I. ++ 50% +++ 75%

As in the muscle fibers two types of esterase, cytoplasmic and lysosomal, were demonstrated in the interstitial cells (table 1). The cytoplasmic enzyme (figs 9, 10) is less sensitive to aldehyde fixation than that of the muscle fibers and was completely inhibited by organophosphates. 10⁻³ M sodium fluoride (fig 11), 10⁻³ M mercuric acetate, and by 0.005 M concentration of the ferricyanide-ferrocyanide redox system of Holt. It was partially inhibited by silver nitrate and by 10⁻³ M copper sulfate but was not affected by 10⁻³ M iso-OMPA, 10⁻³ M serine, 10⁻³ M phenylpropionic acid, 10⁻³ M lead nitrate, 10⁻³ M iodoacetate, 10⁻³ M sodium taurocholate, or by 0.1 M N-ethylmaleimide. The enzyme was activated by cysteine, however, the cytoplasmic esterase of the interstitial cells in contrast to that of the muscle fibers was only slightly activated by 10⁻³ M PCMB after inhibition by 10⁻³ M E₄₀₀. Many of the interstitial cells also contained lysosomal esterase activity which was best demonstrated in sections in which the other types of esterase had been inactivated either by fixation or by the use of selective inhibitors (fig 11). These experiments showed that there was considerable

variation in the number of lysosomes present in the various types of interstitial cells. The lysosomal esterase was prominent in macrophages; the cytoplasmic enzyme accounted for the major part of the esterase activity of the pericytes which had few lysosomes.

Naphthol AS esters. In general the staining pattern obtained with these substrates was qualitatively similar to that given by the esters of α -naphthol (table 1). The best localization was obtained with naphthol AS D acetate which produced intense staining of the interstitial cells and neural elements but only a very weak reaction in the cytoplasm of the muscle cells. The cytoplasmic processes of the interstitial cells were not as well delineated by the naphthol AS substrates (fig 12) as by the α -naphthyl esters. This was at least partly due to the granular character of the dye deposits produced by the naphthol AS compounds. Mast cells reacted much more intensely with naphthol AS esters than with the α -naphthyl substrates. Their reactivity toward naphthol AS D acetate was similar to that of the interstitial cells; however, naphthol AS D chloroacetate, a substrate that gave only a faint reaction in all other myocardial components, was hydro-

lyzed by the mast cells at a much faster rate than by the interstitial cells. Studies on the influence of enzymatic inhibitors upon the hydrolysis of naphthol AS substrates gave results similar to those obtained with the esters of a naphthol.

The double staining technique of Shnitka and Seligman (61) based on the reversible inhibition of the cytoplasmic esterase by fluoride was used to show histochemically the presence of both types of esterase i.e., lysosomal and cytoplasmic in the interstitial cells. An attempt was made to demonstrate the cytoplasmic esterase by using various naphtholic substrates after staining for the lysosomal esterase by the indigogenic method of Holt followed by prolonged washing to remove the ferricyanide ferrocyanide redox system. However it was found that as shown by Shnitka and Seligman (61) the inhibition of the cytoplasmic esterase by the redox system is to a large extent irreversible.

Indigogenic esters Best results were obtained with 5-bromo-4-chloroindoxyl acetate. Only an extremely faint reaction was observed in the muscle fibers even after long periods of incubation when Holt's complete indigogenic medium was used. For this reason several changes were made in the composition of the incubating medium; the results obtained are summarized in table 3. With Holt's complete medium esterase activity was demonstrated in the AVCS in neurons and nerves of the cardiac ganglia and in the lysosomes of the cardiac muscle fibers and interstitial cells.

The cytoplasmic esterase of the interstitial and muscle cells was inhibited by the pH and by the 0.005 M concentration of the ferricyanide ferrocyanide redox system (fig. 17). Histochemical localization similar to that produced by the naphthol esters was observed (figs. 18-20) when the final concentration of the redox buffer was reduced to 0.0005 M and the pH of the incubating solution was changed from 8.5 to 7.0. Omission of the 1 M sodium chloride or its replacement by sucrose also resulted in a modest increase in the activity of the cytoplasmic esterase. Even under apparently optimal conditions for the reaction the staining of the interstitial cells was less well defined than seen with the naphtholic substrates and the number of cells stained by the indirect methods appeared smaller. At pH 7.0 and using the 0.0005 M concentration of the redox system the effect of the various inhibitors tested (figs. 19-21) was similar to that found with the naphtholic substrates.

Choline esters The results obtained with these esters (figs. 25-32) differed from those of the other substrates employed in this study (table 1). With lauroyl and myristoyl choline a positive reaction was observed in some of the nerve fibers and in the cytoplasm of the neurons and specialized muscle fibers of the bundle of His (figs. 25-28). Staining of the cardiac muscle fibers however faint and diffuse was obtained with lauroyl choline but not with myristoyl choline. The interstitial

TABLE 3
Effect of various modifications made in Holt's indigogenic medium on the intensity of the esterase reaction of rat myocardium pre-fixed in cacodylate buffered glutaraldehyde
The relative intensity of staining is expressed in a scale from 0 to 4+

Composition of the medium	Cardiac muscle fibers	Interstitial cells		Neural elements
		Cytoplasm	Lysosomes	
Complete Holt's medium	±	±	++++	+
Concentration of ferricyanide ferrocyanide redox system reduced from 0.005 M to 0.0005 M	++	+++	++++	+++
Complete Holt's medium pH reduced from 8.5 to 7.0	+	+	++++	++
Complete Holt's medium NaCl omitted	+	+	++++	+++

and mast cells did not react with any of the esters of choline or thiocholine. Butyrylthiocholine was hydrolyzed more slowly than was the acetyl ester both of these compounds were hydrolyzed at a faster rate than the long chain choline esters. In both instances the fibers in the bundle of His gave a more intense reaction than the atrial fibers the latter reacted more strongly than the ventricular fibers (figs 31 32).

The hydrolysis of all choline esters (table 1) was completely inhibited in all sites by 10^{-4} M eserine and by 10^{-3} M moderate inhibition was produced by 10^{-2} M iso-OMPA (figs 29 30) and blocked inhibition by 10^{-1} M sodium fluoro-Taurocholate had no effect on the reaction.

Thiolacetic acid Using fresh frozen unfixed sections thiolacetic acid revealed moderate diffuse staining of the cytoplasm of the muscle fibers and neural elements the cytoplasm of the interstitial cells failed to stain. Staining in the specialized muscle fibers of the bundle of His was more intense than in the atrial muscle fibers the latter gave a stronger reaction than the ventricular muscle fibers. This reaction was little affected by 10^{-3} M eserine but was totally inhibited by 10^{-1} M

staining of tissues pre fixed with glutaraldehyde revealed primarily the lysosomes of the interstitial cells (fig 22) which could not be clearly distinguished in the unfixed sections. Staining of the cytoplasm of the muscle cells was faint and

no reaction could be detected in the cytoplasm of the interstitial cells.

DISCUSSION

Esterases are a group of enzymes that hydrolyze the carboxylic acid esters of mono- and polyhydric alcohols and phenols (Gomori 52 Gomori and Chessick 53). They possess a low degree of substrate specificity and occur in a wide variety of molecular forms (isozymes) with broadly overlapping enzyme-substrate characteristics (Markert and Hunter 59 Hunter and Burstone 60). Esterases may be classified according to the following scheme based on that of Pearse (61a).

1 Non specific esterases Their activity is not affected by eserine. According to their sensitivity to other inhibitors and activators they can be classified into

a A-esterases (arom-esterases organophosphate resistant type I esterases) which are completely inhibited by 10^{-4} M eserine partially inhibited by 10^{-3} M PCMB and activated by cysteine. Their activity is also inhibited by heavy metal ions such as Hg^{+} Ni^{+} Ph^{++} and by N-ethylmaleimide.

b B esterases (alcali-esterases organophosphate sensitive esterases) which are completely inhibited by 10^{-3} M eserine they are not affected by heavy metal ions and are activated by cysteine. Sodium fluoride in a concentration of 10^{-2} M is a potent inhibitor of the activity of this type of esterases (Shnitka and Seligman 61).

c C-esterases (organophosphate resistant type II esterases cathepsin like ester

TABLE 4

The effect of enzymatic inhibitors on the hydrolysis of choline esters by sections of rat heart post fixed for 30 minutes in cold formal-calcium

Inhibitor	Substrate	Myocardial fibers	Bundle of His	Neural elements
DFP 10^{-4} M	All choline esters	I + + + +	I + + + +	I + + + +
Eserine 10^{-4} M	All choline esters	I + + + +	I + + + +	I + + + +
Eserine 10^{-3} M	All choline esters	I + + + +	I + + + +	I + + + +
Iso-OMPA 10^{-2} M	Acetylthiocholine	I + + +	I +	I +
	Butyrylthiocholine	I + + +	I + +	I + +
	Long-chain choline esters	I +	I +	I +

I = inhibition expressed on a scale from 0 to 4+

ases), which are inhibited by 10^{-3} M β phenylpropionic acid and activated by PCMB. They resemble A esterases in their resistance to organophosphates and in their sensitivity to heavy metal ions and N-ethyl maleimide.

2 Cholinesterases Their activity is completely inhibited by 10^{-3} M eserine, 10^{-4} M DFP, and by 10^{-3} M E₆₀₀. They are subdivided into

a true cholinesterases (specific cholinesterases, acetylcholinesterases) which are not affected by 10^{-3} M iso-OMPA and

b pseudocholinesterases which are selectively inhibited by 10^{-3} M iso-OMPA.

3 Lipases, which are activated by sodium taurocholate and preferentially hydrolyze esters of aliphatic fatty acids with a straight carbon chain that contains more than 12 carbon atoms.

The capacity of these enzymes to act upon a number of different substrates renders their characterization very difficult. Furthermore, the use of histochemical substrates permits only a limited characterization of the esterases of the heart since as shown by electrophoretic experiments (Hunter and Burstone '60, Barron et al. '63), histochemical reactions demonstrate the total activity of a family of isozymes that are capable of hydrolyzing a wide variety of substrates. Thus thiolacetic acid (Cr  vier and Belanger '55, Wachstein, Meisel and Falcon '61) and the naphtholic and indigogenic substrates (Hobbiger '57, Pearse '61a) are attacked by cholinesterases and by various types of non specific esterases. However, the hydrolysis of choline esters by rat tissues is considered to be exclusively due to true and pseudocholinesterases (Aldridge '54, Allen et al. '58, Hobbiger '57).

For these reasons the use of selective inhibitors is necessary for the classification of esterases (Aldridge '54, Bayliss and Todrick '56, Pearse '61a, Burstone '62) and several distinctive features emerge from a comparison of the effects of inhibitors and activators on the esterase activity present in the various components of the rat heart.

The atrioventricular conduction system Non specific esterase and cholinesterase activity were demonstrated histochemically in the specialized muscle fibers of the

atrioventricular node and bundle of His and its two main branches but not in the peripheral ramifications. Both types of enzymes were also present in the cardiac ganglia and in the nervous plexuses surrounding the AVCS.

Non specific esterase activity has been detected previously in the AVCS of the rat but is known to occur in that of other mammalian species (Carbonell '56). The negative reaction towards naphtholic substrates observed by Carbonell ('56) in the AVCS of the rat was probably due to the inhibition of the enzymatic activity by prolonged fixation and by the use of incubating media adjusted at a high pH. Carbonell ('56) reported the presence of cholinesterase in the fibers of the AVCS of the rat and other workers have made similar observations in other species (Gouras '48, Gerebtzoff, '53). This enzyme has been studied in the nervous plexuses of the AVCS of other mammals (Iltis, Kakueva, '58, Robb '65) but not in that of the rat.

The enzymatic activity of the muscle fibers of the AVCS against naphtholic and indigogenic substrates appeared to be caused by the presence of both non specific esterase and cholinesterase. This was shown by the partial inhibition of the hydrolysis of these substrates by eserine which inhibits both true and pseudocholinesterases but has no influence upon non specific esterases (Pearse '61a). Iso-OMPA which is known to inhibit almost completely the pseudocholinesterases but not the true cholinesterases of rat tissues (Bayliss and Todrick '56) had little effect on the hydrolysis of naphtholic and choline esters by the AVCS and surrounding nerve fibers. However, eserine inhibited completely the hydrolysis of choline esters by these structures which indicated that the major part of their cholinesterase activity is of the true cholinesterase type.

Cardiac ganglia The neurons of the cardiac ganglia and their post ganglionic nerve fibers were intensely stained for cholinesterase and non specific esterase. Most of their cholinesterase activity was of the true type which conforms to the histochemical pattern of other parasympathetic ganglia.

cardiac ganglia (Koelle 62) and agrees with the findings of Gerebtzoff (53) on cardiac ganglia of other species. The atrial and ventricular muscle fibers esterase activity was found in the lysosomes and in the cytoplasm of the cardiac muscle fibers. The lysosomal esterase was demonstrated only in sections from fixed blocks presumably because of the disruption of the lysosomes during freezing and thawing of unfixed tissues. The lysosomes of the cardiac muscle fibers are very small in size and number and esterase activity appeared similar to that of the lysosomes of other tissues (Lt 63).

The cytoplasmic esterase which is sensitive to the effects of fixatives was best shown in sections of glutaraldehyde-cacodylate fixed tissues. As recognized by Zacks and Seligman (53) the failure of some investigators to detect this enzyme was caused by its inactivation during prolonged fixation. Subsequent investigations (Shnitka and Seligman 61) have fully documented the fact that the cytoplasmic esterase of liver and kidney is inhibited by prolonged formaldehyde fixation. The negative results obtained by Pearson and Defendi (57) using Holt's indigogenic method on rat myocardium fixed for a short period of time may be explained by their use of a relatively high concentration of the ferricyanide ferrocyanide redox system which is known to produce complete and partially irreversible inhibition of the cytoplasmic esterase of liver and kidney (Shnitka and Seligman 61) and as shown in this study of cardiac muscle. The hydrolysis of choline esters by the cytoplasm of the muscle fibers was completely inhibited by eserine. However, eserine produced only minimal inhibition of the hydrolysis of naphtholic and indigogenic esters by the muscle fibers. These results and the marked inhibition by isonitrophenyl acetate (INPA) of the reaction of the muscle fibers against choline esters suggest that both nonspecific esterase and pseudocholinesterase are present in the cytoplasm of the cardiac muscle cells.

The intensity of staining obtained with naphtholic and choline esters was greater in the atria than in the ventricles. These results agree with the biochemical studies of Ord and Thompson (50) which showed that in the rat the cholinesterase activity of atrial tissue is three times higher than that of ventricular muscle. Our observations on the relationship of the relative rates of hydrolysis of various naphtholic esters by the muscle fibers and interstitial cells to the length of the carbon chain of the esterified acids are also in agreement with biochemical measurements (Hug and Moulton 48) of the rates of the *in vitro* hydrolysis of a series of p-nitrophenyl esters by rat myocardial and testicular esterases.

The presence of lipase activity has been observed histochemically in the myocardium of several mammals but not in the rat (George and Iype 60). However, the negative reaction obtained with Tween 80 in the presence and absence of taurocholate tends to exclude the possibility that the histochemically detectable esterase activity of the muscle fibers of the rat heart is caused by lipase.

The use of selective inhibitors revealed that the major part of the nonspecific esterase activity of the cardiac muscle fibers conforms to the criteria of a B esterase, i.e., an organophosphate sensitive esterase similar to that present in the cytoplasm of other cell types (Wachstein and Meisel and Falcon 61; Shnitka and Seligman 61). After treatment with 10^{-4} M E600, no esterase activity could be detected in the cytoplasm of the muscle fibers, however, when sections exposed to this inhibitor were further treated with 10^{-4} M PCMB, a small but definite activation of the reaction was noted. PCMB is used to classify the types of organophosphate resistant esterases since it activates C esterase and inhibits A esterase (Pearse 61a). Therefore, the preceding data were interpreted as indicating that in addition to the B type of esterase the muscle fibers also contain a small amount of C esterase, the activation of which could not be histochemically detected unless other types of esterase were simultaneously inhibited.

The presence of B and C esterases in rat ventricular muscle fibers has been recognized by Karnovsky and Hug (63) in their electron microscopic study of thioacetic acid esterase. As pointed out by these

authors it is unusual to find an organo phosphate resistant aldehyde sensitive esterase and the significance of this observation is unclear

Our studies using other inhibitors are less conclusive since the specificity of some of these agents is less well established (Karnovsky and Hug 63 Barron et al 63) particularly at the histochemical level Furthermore in some cases the degree of inhibition can be assessed only from quantitative studies which are often obtained under conditions that differ substantially from those employed in histochemical techniques The preceding factors which account for a large part of the difficulties encountered in the classification of esterases assume critical importance when the enzymatic activity is low and when more than one type of enzyme is present at the site where the final product of the histochemical reaction is localized

Interstitial cells A large number of interstitial cells rich in non specific esterase were observed throughout the rat heart Many of these cells were identified as pericytes which in other tissues have been found to contain large amounts of non specific esterase (Gomori 53) As in the muscle fibers two types of esterase activity cytoplasmic and lysosomal were demonstrated in the interstitial cells

The cytoplasmic esterase of the interstitial cells was better demonstrated by the α naphtholic than by the naphthol AS or indigogenic esters This enzyme reacted only very weakly with thiolacetic acid and did not react with any of the choline esters or with naphthol ASD chloroacetate It differed from the muscle fiber enzyme in several respects it reacted more intensely with naphthol AS esters it was less sensitive to the inhibitory effect of aldehyde fixation and following treatment with 10^{-3} M E_{600} it was activated by PCMB to a much lesser degree than the cytoplasmic esterase of the muscle fibers However the two enzymes reacted in a similar manner to various inhibitors (table 2) These results indicate that as in the muscle fibers the major part of the non specific esterase activity of the cytoplasm is caused by a

B esterase and that only a very small amount of C esterase is present in the cytoplasm of the interstitial cells

The fluoride and E_{600} resistant esterase activity of the lysosomes present in the cardiac muscle fibers and the interstitial cells could be shown with all the substrates except the choline esters and was best demonstrated in sections in which the cytoplasmic esterase had been suppressed by fluoride ions The biochemical characteristics of this type of esterase activity i.e. lack of inhibition by fluoride iodoacetate N ethylmaleimide and by relatively high concentrations of organophosphates are similar to those found by Holt (63) in the lysosomes of other tissues According to the evidences presented by Hess and Pearse (58) Wachstein and Hess and Falcon (61) Sabatini Bensch and Barnett (63) and Holt (63) these characteristics suggest that the hydrolysis of esterase substrates by lysosomes rather than resulting from the action of esterases may be due to cathepsins which are known to be present in lysosomes and are capable of attacking a large variety of substrates Further studies will be necessary to investigate this possibility

LITERATURE CITED

- Aldridge W N 1954 Some esterases of the rat *Biochemical J* 57 692-702
 Allen J M O Eranko and R L Hunter 1961 A histochemical study of the esterases of the adrenal medulla of the rat *Am J Anat* 151 93-116
 Barka T and P J Anderson 1963 *Histochemistry Theory Practice and Bibliography* Chapter 11 pp 257-277 Hoeber New York
 Barnett R J and G E Palade 1959 Enzymatic activity in the M band *J Biophys Biochem Cytol* 6 163-169
 Barron K D J Bernsolin and A R Hess 1961 Separation and properties of human brain esterases *J Histochem Cytochem* 11 139-144
 Bayliss B J and A Todrick 1956 The use of a selective acetylcholine inhibitor in the demonstration of pseudocholinesterase activity in brain *Biochem J* 62 62-67
 Burstone M S 1962 *Enzyme histochemistry and its application to the study of neoplasia* Chapter 6 pp 293-330 Academic Press New York
 Carbonell L M 1956 Esterases of conducting system of the heart *J Histochem Cytochem* 4 87-95
 Chessick R D 1953 Histochemical study of the distribution of esterases *J Histochem Cytochem* 1 471-485

- r M and L F Bélanger 1955 Simple method for histochemical detection of esterase activity *Science* 122 556
- J C and P T Iype 1960 A histochemical study of the atrioventricular bundle (bundle of His) and the myocardium of the sheep *J Anim Morph Physiol* 7 78-85
- troff M A 1953 Recherches histochemiques sur les acetylcholine et cholinesterases *Anat.* 19 366-379
- ri G 1945 The microtechnical demonstration of sites of lipase activity *Proc Soc Exp Biol Med* 58 362-364
- 1948 Histochemical demonstration of sites of cholinesterase activity *Proc Soc Exp Biol Med* 68 354-358
- 1952 The histochemistry of esterases *Ann Rev Cytol* 1 323-335
- 1953 Esterases and phosphatases of brain: a histochemical study *J Neurobiol Exp Neurol* 12 387-396
- ori G and R D Chessick 1953 Histochemical studies of the inhibition of esterases *Cell and Comp Physiol* 41 51-63
- nal M J and M M Nachlas 1959 Further studies on the lyso- and desmo components of several hydrolytic enzymes and their histochemical significance *J Biophysical Biochem Cytol* 5 279-288
- R. and A G E Pearse 1958 The histochemistry of indoxyl esterase of rat kidney with special reference to its cathepsin-like activity *Brit J Exp Path* 39 292-299
- biger E E 1957 The hydrolysis of indoxyl esters by rat esterases *Biochem J* 67 600-607
- l S J 1963 Some observations on the occurrence and nature of esterases in lysosomes *Lysosomes* Ciba Foundation Symposium 15 S de Reuck and M P Cameron ed Little Brown and Company Boston Massachusetts pp 114-125
- l S J and R F J Withers 1958 Studies in enzyme histochemistry V An appraisal of the endogenous reaction for esterase localization *Proc Roy Soc (B)* 148 520-532
- gins C and S H Moulton 1948 Esterases of testis and other tissues *J Exp Med* 88 169-179
- er R L and M S Burstone 1960 The symposium as a tool for the characterization of enzyme substrate specificity *J Histochem Cytochem* 9 58-62
- skakueva E I 1958 A histochemical study of cholinesterase activity of the nerve fibers and conducting system of the heart *Bull Exp Biol Med* 46 1270-1273
- F and B Cullik 1962 Cholinesterase activity of intercalated discs in mammalian heart muscle *Nature* 193 1192-1193
- arnovsky M J 1964 The localization of cholinesterase activity in rat cardiac muscle by electron microscopy *J Cell Biol* 23 217-232
- Karnovsky M J and K Hug 1963 The nature of the M band enzyme in rat ventricular muscle *J Cell Biol* 19 255-260
- Koelle G B 1962 A new general concept of the neurohumoral functions of acetylcholine and acetylcholinesterase *J Pharm Pharmacol* 14 65-90
- Koelle G B and J S Friedenwald 1949 A histochemical method for localizing cholinesterase activity *Proc Soc Exp Biol Med* 70 617-622
- Markert C L and R L Hunter 1959 The distribution of esterases in the mouse tissues *J Histochem Cytochem* 7 42-49
- Nachlas M M W Prinn and A M Seligman 1956 Quantitative estimation of lyso- and desmoenzymes in tissue sections with and without fixation *J Biophys Biochem Cytol* 2 487-502
- Nachlas M M and A M Seligman 1949 The comparative distribution of esterases in the tissues of five mammals by a histochemical technique *Anat Rec* 105 677-695
- Ord M G and R H S Thompson 1950 Distribution of cholinesterase types in mammalian tissues *Biochem J* 46 346-352
- Pearse A G E 1961a *Histochemistry Theoretical and Applied* 2nd ed Chapter 16 pp 456-490 Little Brown and Co Boston Mass
- 1961b *Loc Cit* Appendix 16 p 886
- Pearson B and V Defendi 1957 A comparison between the histochemical demonstration of non specific esterase activity with 5-bromo-indoxyl acetate, a naphthyl acetate and naphthol AS acetate *J Histochem Cytochem* 5 72-83
- Ravin H A S I Zacks and A M Seligman 1953 The histochemical localization of acetylcholinesterase in nervous tissue *J Pharmacol* 107 37-53
- Robb J S 1965 *Comparative Basic Cardiology* Chapter 15 pp 449-452 Grune and Stratton New York and London
- Sabatini D D K Bensch and R J Barnett 1963 *Cytochemistry and electron microscopy* The preservation of cellular ultrastructure and enzymatic activity by aldehyde fixation *J Cell Biol* 17 19-58
- Shrout T A and A M Seligman 1961 Role of esterase inhibition on the localization of esterase and the simultaneous cytochemical demonstration of inhibitor sensitive and resistant enzymes species *J Histochem Cytochem* 9 504-527
- Wachstein M E Meisel and C Falcon 1961 *Histochemistry of thioacetic acid esterase* A comparison with non-specific esterase with special regard to the effect of fixatives and inhibitors on intracellular localization *J Histochem Cytochem* 9 325-339

PLATE 1

EXPLANATION OF FIGURES

- 1 Cross section through the bundle of His 200 \times Post fixation for 30 minutes in cold formol-calcium a naphthyl acetate Diazo Blue B Staining is most intense in the specialized fibers of the bundle and in the surrounding interstitial cells and nerve fibers
- 2 Left branch of the bundle of His 200 \times Post fixation for 30 minutes in cold formol calcium a naphthyl acetate Diazo Blue B There is strong staining of the specialized muscle fibers and adjacent interstitial cells and nerve fibers
- 3 Atrioventricular node 200 \times Post fixation for 30 minutes in cold formol calcium a naphthyl acetate Diazo Blue B Section through a portion of the atrioventricular node showing the staining pattern of the AV nodal fibers and their loose irregular arrangement
- 4 Bundle of His 600 \times Post fixation for 30 minutes in cold formol calcium a naphthyl acetate Diazo Blue B A moderately intense reaction is obtained in the fibers of the bundle of His



PLATE 2

EXPLANATION OF FIGURES

- 5 Right ventricular wall 1 000 \times Post fixation for 30 minutes in cold Formol-calcium a naphthyl acetate Diazo Blue B Cross section showing moderately intense esterase activity in the cytoplasm of the ventricular muscle fibers
- 6 Right atrial wall 400 \times Post fixation for 30 minutes in cold formol calcium a naphthyl acetate Diazo Blue B A strong esterase reaction is seen in the cardiac neurons their post ganglionic nerve fibers and in the cytoplasmic rim of adipose tissue cells
- 7 Base of the septal leaflet of the mitral valve 200 \times Post fixation for 30 minutes in cold formol calcium a naphthyl acetate Diazo Blue B There is a large number of intensely stained interstitial cells in the connective tissue at the base of the valve
- 8 Upper part of the muscular portion of the interventricular septum 200 \times Pre fixation for 24 hours in formol calcium a naphthyl butyrate hexazotized prosanilin The staining and general distribution of the interstitial cells are observed The cytoplasm of the muscle cells shows no esterase activity

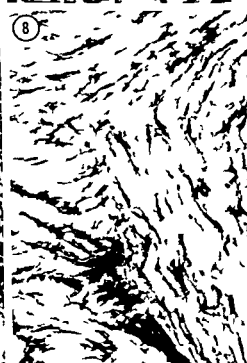
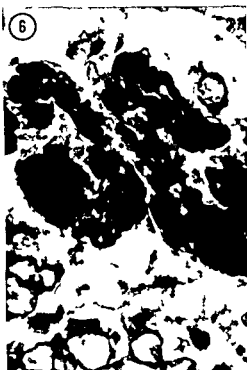


PLATE 3

EXPLANATION OF FIGURES

- 9 Left ventricular myocardium 1 000 \times Pre fixation for 24 hours in formol-calcium a naphthyl butyrate Diazo Blue B There is very intense staining of the interstitial cells their cytoplasmic processes are less clearly evident than in figure 10 Very faint staining is observed in the muscle fibers
- 10 Left ventricular myocardium 1 000 \times Pre fixation for two hours in cacodylate buffered glutaraldehyde a naphthyl acetate hexazotized prosanilin Note the intensely stained pericyte and its cytoplasmic processes Distinct staining is also observed in the muscle cells
- 11 Left ventricular myocardium 1 000 \times Pre fixation for two hours in cacodylate buffered glutaraldehyde a naphthyl acetate hexazotized prosanilin Section preincubated with 0.01 M sodium fluoride The cytoplasmic staining of the muscle fibers and interstitial cells is completely inhibited The lysosomes of the interstitial cells remain intensely stained
- 12 Left ventricular myocardium 1 000 \times Post fixation for 30 minutes in cold formol-calcium Naphthol ASD acetate Fast Garnet GBC salt 1 000 \times The interstitial cells are strongly stained A discrete reaction is evident in the muscle fibers however the dye deposits are granular in character Compare with figure 10

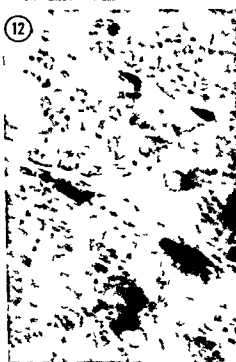
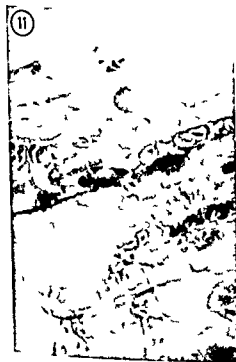


PLATE 4

EXPLANATION OF FIGURES

- 13 Epicardium and part of the wall of the left ventricle 600 \times Pre fixation for 24 hours in formol-calcium a naphthyl butyrate hexazotized prosanilin The subepicardial interstitial cells are intensely stained
- 14 Septal leaflet of the tricuspid valve 200 \times Pre fixation for 24 hours in formol-calcium a naphthyl butyrate hexazotized prosanilin A large number of esterase positive cells is present in the valve leaflet
- 15 Interventricular septum 200 \times Pre fixation for 24 hours in formol calcium a naphthyl acetate hexazotized prosanilin Numerous esterase positive cells are seen in the subendocardial connective tissue of the interventricular septum
- 16 Part of the media and adventitia of the aortic wall 600 \times Pre fixation for two hours in cacodylate buffered glutaraldehyde a naphthyl acetate hexazotized prosanilin There is a large number of intensely stained connective tissue cells in the adventitia of the aorta



PLATE 5

EXPLANATION OF FIGURES

- 17 Left ventricular myocardium 400 \times Pre fixation for two hours in cacodylate buffered glutaraldehyde. Holt's indigogenic medium employing 5 bromo-4-chloroindoxyl acetate. There is faint staining of the muscle fibers. The interstitial cells show mainly lysosomal staining.
- 18 Left ventricular myocardium 200 \times Pre fixation for two hours in cacodylate buffered glutaraldehyde. Holt's indigogenic medium employing 5 bromo-4-chloroindoxyl acetate but with the concentration of the ferricyanide/ferrocyanide redox system reduced from 0.005 to 0.0005 M. There is a marked increase in the intensity of the staining of the muscle fibers and of the interstitial cells.
- 19 Left ventricular myocardium 1000 \times Pre fixation for two hours in cacodylate buffered glutaraldehyde. Holt's indigogenic medium employing 5 bromo-4-chloroindoxyl acetate and 0.0005 M ferricyanide/ferrocyanide redox system. Section pretreated with 0.01 M sodium fluoride. Staining is now confined to the lysosomes of the interstitial cells.
- 20 Left ventricular myocardium 200 \times Pre fixation for 24 hours in formal calcium. Holt's indigogenic medium employing 5 bromo-4-chloroindoxyl acetate and 0.0005 M ferricyanide/ferrocyanide redox system (as in figs 18-19). Prolonged fixation has caused a considerable decrease in the intensity of the esterase reaction of the muscle fibers.
- 21 Left ventricular myocardium 200 \times Pre fixation for 24 hours in formal calcium. Holt's indigogenic medium using 5 bromo-4-chloroindoxyl acetate and 0.0005 M ferricyanide/ferrocyanide redox system. Section pretreated with 10^{-3} M E_{600} . Comparison with figure 20 demonstrated the inhibition of the cytoplasmic staining of the muscle fibers and interstitial cells.
- 22 Left ventricular myocardium 1000 \times Pre fixation for two hours in cacodylate buffered glutaraldehyde. Thiobarbituric acid medium. Staining is mainly localized in the lysosomes of the subendocardial interstitial cells.



PLATE 6

EXPLANATION OF FIGURES

- 23 Section through the bundle of His and adjacent atrial and ventricular myocardium 100 \times Post fixation for 30 minutes in cold formal calcium Holt's indigogenic medium using 5-bromo-4-chloroindoxyl acetate and 0.0005 M ferricyanide-ferrocyanide redox system. The most intense staining is observed in the elements of the conduction system; staining of atrial muscle is greater than that of ventricular myocardium.
- 24 Right atrial wall 100 \times Post fixation for 30 minutes in cold formal calcium Holt's indigogenic medium using 5-bromo-4-chloroindoxyl acetate and 0.0005 M ferricyanide-ferrocyanide redox system. The nerve cells and postganglionic nerve fibers of a cardiac ganglion are intensely stained. A moderate reaction is observed in the surrounding atrial muscle cells.



PLATE 7

EXPLANATION OF FIGURES

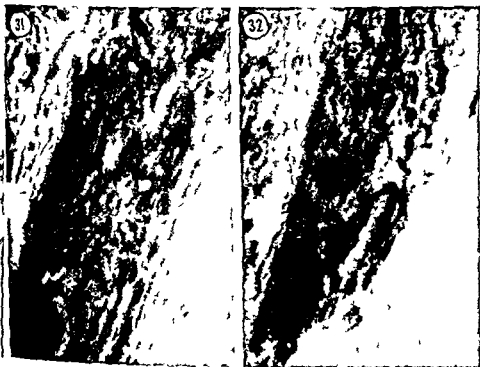
- 25 Bundle of His and surrounding areas 50 \times Post fixation for 30 minutes in cold formol-calcium Myristoyl choline The bundle is intensely stained No staining is observed in the interventricular septum and only a very faint reaction is seen in the atrial muscle cells
- 26 Section serial to that shown in figure 25 50 \times Post fixation for 30 minutes in cold formol-calcium Myristoyl choline after treatment with 10^{-4} M eserine Cholinesterase activity is completely inhibited by eserine
- 27 Same section as in figure 25 200 \times Post fixation for 30 minutes in cold formol-calcium Myristoyl choline There is intense cholinesterase activity in the right branch of the bundle
- 28 Bundle of His 400 \times Post fixation for 30 minutes in cold formol-calcium Lauroyl choline The nerve fibers surrounding the bundle of His are intensely stained The specialized muscle cells show weak but distinct staining
- 29 Cardiac Ganglion 600 \times Post fixation for 30 minutes in cold formol-calcium Acetylthiocholine iodide The nerve cells show intense cholinesterase activity
- 30 Cardiac Ganglion 600 \times Post fixation for 30 minutes in cold formol-calcium Acetylthiocholine iodide Section pretreated with 10^{-3} M iso OMPA Comparison with figure 29 shows the reduction in cholinesterase activity produced by iso OMPA



PLATE 8

EXPLANATION OF FIGURES

- 31 Bundle of His and adjacent atrial and ventricular myocardium
200 \times Post fixation for 30 minutes in cold formol-calcium Butyryl
thiocholine iodide The most intense reaction is observed in the
bundle of His (center) the atrial myocardium (upper left) shows
more intense staining than the ventricular myocardium (lower right)
- 32 Section similar to that shown in figure 31 200 \times Post fixation for
30 minutes in cold formol-calcium Acetylthiocholine iodide The
staining pattern is the same as that obtained with butyrylthiocholine
iodide



Instant Cell Populations in Normal, Testosterone- Deprived and Testosterone Stimulated Levator Ani Muscles¹

JOHN H. VENABLE

Department of Anatomy Harvard Medical School Boston Massachusetts

ABSTRACT Castration of adult male mice produces a true atrophy of their levator ani muscles until the muscle reaches a stable weight within 45 days. Subsequent treatment with testosterone produces a true hypertrophy from the stable neutered state. The weight changes in the muscle are accounted for solely by changes in the size of the muscle fibers. No mitotic activity accompanies atrophy or hypertrophy. The number of cell nuclei and the amount of DNA in the muscle is unaltered.

In the adult male mouse the mass of levator ani dwindles following castration then waxes after a parenteral injection of testosterone. Concomitantly there are marked changes in the diameters of muscle fibers (Wainman and Shipoun 41). Whether the change in muscle mass involves only the pre-existing muscle fibers or includes new tissue components has not been clearly established. It is generally accepted that mammalian skeletal muscles enlarge during the later stages of growth and following persistent increase by a hypertrophy of the individual muscle fibers; the number of fibers remains constant (MacCallum 1898; Morpurgo 197). One wonders whether testosterone sensitive muscles accomplish their weight changes similarly. Kochakian (64) has demonstrated that enlargement of the testosterone-stimulated masseter muscle of the guinea pig involves no increase in DNA, implying no increase in the number of nuclei. Corollary information on the contributions of the different tissue components to the total muscle mass is lacking.

Herein is evidence that the changing mass in the levator ani is essentially a vacuolation of sarcoplasmic mass in the muscle fibers. This is demonstrated by four characteristics of the atrophied and hypertrophied levator ani: (1) the relation of the size of its muscle fibers to its total weight; (2) the mitotic activity of its cells; (3) the relative numbers of its different cell types; and (4) its total quantity of DNA.

These characteristics are discussed in comparing the levator ani and other skeletal muscles during growth, maintenance, atrophy and hypertrophy. The morphological changes in the levator ani are described in an accompanying report (Venable 66).

MATERIALS AND METHODS

Male white mice were obtained from the Charles River mouse farms, North Wilmington, Massachusetts. They formed three experimental groups: intact, neutered, and testosterone-treated neuter groups. The mice of the intact group were left uncastrated and received no testosterone. The mice of the neuter group were castrated as adults at 40 days of age and left untreated for 45 days to allow maximum atrophy of the levator ani (Venable 66). The mice of the testosterone-treated neuter group were treated identically to the neuters but subsequently received 0.5 mg of Depo-testosterone (Upjohn) intramuscularly. All mice in any one experiment had the same date of birth, experienced identical environmental influences, and were sacrificed on the same day.

For the comparison of muscle fiber size to total muscle weight, mice from all three

¹ Research supported by National Science Foundation Fellowship grant GM-406 and by grant GM-10182.

Received by the Division of Medical Science, The Graduate School of Arts and Sciences, Harvard University, in partial fulfillment of the requirements for the Degree of Doctor of Philosophy in Anatomy.

Present address: Department of Veterinary Anatomy, College of Veterinary Medicine, Oklahoma State University, Stillwater, Oklahoma.

groups — four intact six neuter, six testes terone treated neuter mice — were anesthetized with sodium pentobarbital killed by cervical dislocation, and their levator ani muscles dissected with blunt scissors under isotonic saline. After blotting off the excess saline these muscles were weighed quickly and then fixed with glutaraldehyde (Gordon et al, 64). As with most aldehyde fixatives glutaraldehyde caused the muscle to swell. Even when the swelling was dissipated in a normal saline bath the weight changes of the individual muscles were quite variable. It proved important to use the weights of the unfixed muscles in correlations with muscle fiber size.

To measure muscle fiber diameters fixed muscle samples were washed in normal saline and the individual fibers dissociated by low speed action of a microblender. Samples of dispersed fragments of muscle fibers were stored in isotonic saline allowing osmotic equilibration before measurement on a standard light microscope equipped with a 25 \times water immersion objective and a calibrated eyepiece micrometer. The muscle fibers from the levator ani were of uniform diameter throughout the muscle therefore errors due to inappropriate sampling were avoided. The diameters of 50 successively encountered fragments of muscle fibers were measured where they were most nearly cylindrical avoiding flattened regions. Each diameter was halved to give a radius. Each radius was squared and the arithmetic mean of the 50 squared radii (\bar{r}^2) served as the statistic to be compared with the weight of the muscle.

The relationship between muscle fiber size and muscle weight can be formulated in the following manner. The weight of the muscle (W) equals the weight of the muscle fibers (F) plus the weight of the interstitial tissues (C).

$$W = F + C \quad (a)$$

The weight of the fibers (F) can be expressed as a function of the product of their mean number (N) their mean density (D) their mean length (L) and their mean cross sectional area ($\pi\bar{r}^2$). Substituting this approximation for F in equation (a) produces the equation

$$W = NDL\pi\bar{r}^2 + C \quad (b)$$

If N D L and C are constants equation (b) is a linear one with the useful characteristic of relating muscle weight (W) to the mean squared fiber radius (\bar{r}^2). Expressed in standard form this equation is of the type

$$W = m\bar{r}^2 + b \quad (c)$$

The degree of constancy of m and b can be estimated by a correlation coefficient (Snedecor 56) calculated from the data of muscle weight and mean squared fiber radii. A high correlation coefficient indicating these terms to be relatively constant. A high coefficient would then imply that changing fiber radius accounts for most if not all of the changing muscle mass.

This equation was useful in this study because morphological observations (Venable 66) indicated that fiber length fiber density and connective tissue mass remained relatively constant. The equation can be adapted to other situations to compare any two of its parameters or groups thereof provided that the remaining parameters can be estimated.

Mitotic activity was sought both by microscopic examination of sections for mitotic figures and by administering tritiated thymidine to label nuclei synthesizing DNA. The thymidine H^3 (6.05 c.m.i.) was injected intraperitoneally at a dose of 10 μ c per gram body weight. Autoradiographs of epon sections one and one-half microns thick were made by coating them with the Ilford L-4 nuclear emulsion (Hay and Revel 63). Development of the latent image with 1 part Dektol (Kodak) and 3 parts water followed a three week exposure of the emulsion.

The relative number of nuclei of the different cell types was determined from epon sections three-quarter micron thick. The accompanying report on the morphology of the levator ani (Venable 66) presents the technique of preparing the muscle for epon embedding and the criteria for identifying the cell types.

For the determination of the total DNA in the muscle mice were decapitated, the levator ani muscle dissected, weighed, minced and homogenized in a 1 ml homogenization tube. The homogenate was washed subsequently in a 15 ml centrifuge tube with 1 ml of saline where the acid

le fraction and phospholipid fraction were extracted by the method of Ceder (45). The remaining proteins, including the nucleoproteins, contained between 20 and 30 μ g of DNA. Colorimetric analysis of these quantities by the modified method of Schmid et al. (63) followed Beer's Law closely. This method is used for hydrolysis of the nucleic acids at 100°C for 80 minutes in 2 ml of 5% chloroacetic acid adjusted to pH 2.45.

NaOH. The hydrolysis was stopped by rinsing the reaction tubes. One milliliter of 0.06% indole solution and 1 ml of 1N HCl were added and the tubes were placed in an 85°C water bath for an additional 80 minutes where colored products from indole-pentose reactions formed. These reactions were stopped also by rinsing the reaction tubes. Spurious colored products absorbing light in the range of indole-deoxyribose 490 m μ were removed by four extractions with chloroform. The remaining optical density of the solution at 490 m μ was measured with a Bausch and Lomb electronic 20 spectrophotometer. Control measurements included a reagent blank and duplicate samples of 30 μ g of highly polymerized DNA from calf thymus (Sigma Chemical Co., St. Louis).

RESULTS

Relation between muscle fiber size and total muscle weight

The degree of linear correlation between weight of the muscle and the mean squared radius of its fibers is high (correlation coefficient equals 0.90). Figure 1 presents a graph of the data. An analysis of variance attributes 55% of the total variation to the regression line. The residual variation of 45% includes variation in dissecting the muscles as well as variation in the assumed constants N (number of muscle fibers), L (length of fibers), D (density of fibers), and C (amount of connective tissue). At the point on the regression line where the average squared radius of the muscle fibers equals zero, a residual muscle weight of 3.7 mg remains which is a reasonable estimate of the weight of the connective tissues.

The high degree of linear correlation between fiber size and muscle weight indicates that the product of N , L , and D ap-

proaches constancy. There is the possibility that the product remains constant though each parameter varies but this is unlikely. The majority of the fibers are known to run the full length of the muscle so L (mean length of fiber) is not altered appreciably. Neither is it likely that D (density) makes any radical change because the morphology of the muscle fibers in the three groups are similar. Therefore N must be a fairly stable number.

Lack of mitotic activity

No mitoses are evident in approximately 20,000 sectioned nuclei. One half of these nuclei are from animals that received colchicine intraperitoneally six hours prior to sacrifice. Neither castration nor testosterone treatment produces mitotic division in any of the cell types in the muscle.

Tritiated thymidine administered from the thirtieth through the forty-second hour following testosterone treatment of three neuter mice labeled only one fibroblast among 1,000 cells. In two neuter mice untreated with testosterone but receiving the tritiated thymidine, the thymidine labeled one fibroblast and two endothelial cells, the latter located in adjacent adipose tissue. Though the time chosen for the administration of the thymidine may have been inappropriate for demonstrating an early burst of mitotic activity in view of the other observations, these negative results provide additional support for the concept of a static number of cells participating in the alterations in mass in the muscle.

Differential nuclear counts in primary muscle bundles

Of 1,217 sectioned nuclei from two intact mice, 57% belong to muscle cells, 21% to endothelial cells, 14% to fibroblasts, 6% to pericytes, and 2% to satellite cells. Table 1 presents these percentages and the 95% confidence intervals corresponding to an assumption that the samples are from a binomially distributed set of like samples. Infrequently encountered cells such as mast cells, macrophages, and Schwann cells have been ignored.

Differential counts from two mice from the neuter group display a decreased fre-

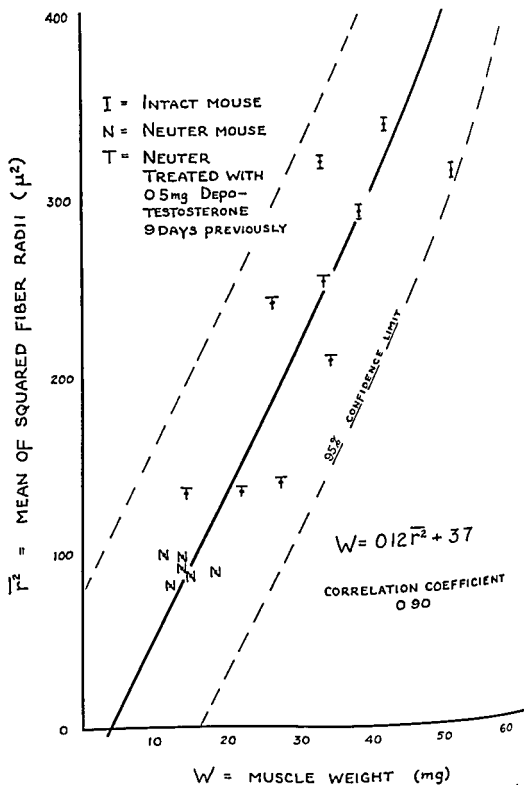


Fig 1 A comparison of muscle weights and means of squared muscle fiber radii in levator ani muscles from intact neuter and testosterone treated neuter mice. The linear regression is plotted along with a 95% confidence limit calculated from the data. The equation for the regression line is presented this being a unique characterization of the levator ani muscle of the adult mice studied. It includes the factors of muscle fiber number density of fibers length of fibers and amount of stroma (see text). The calculated correlation coefficient is 0.90.

TABLE 1

Frequency of encounter of the nuclear types in sections from two intact mice¹

Nuclear type	Number	95% Confidence interval ²	
		n	%
Leucocyte	690	57	54-60
Endothelial	257	21	19-24
Myoblast	165	14	12-16
Myocyte	78	6	5-8
Satellite cell	27	2	1-3

¹ Correction is made for the three-quarter micron thickness of the sections and the dimensions of the field at right angles to the plane of the section (Abercrombie 46). The percentages are rounded off to the nearest whole number.

² The confidence intervals are selected from the author's (56) table 1.3.1

Frequency of encounter of endothelial nuclei (16%) and a corresponding increase in the frequency of encounter of muscle nuclei (62%). The differential counts from *testosterone treated neuter* mice are remarkably similar to those of the *intact* group. The null hypotheses that there are no differences in the differential counts of the *neuter* and the *testosterone treated neuter* as compared of the *intact* in the *intact* mice has been tested by the chi-square method. The data and chi-square calculations appear in table

The *neuter* is significantly different from the *intact* mouse in the frequency of encounter of muscle nuclei ($P < 0.005$ one

degree of freedom and of endothelial nuclei ($P < 0.005$ one degree of freedom). This might be interpreted as a change in cellular populations but this seems doubtful considering the insignificant difference between the counts from *testosterone treated neuter* and *intact* mice. It is much more likely that in the *neuter* state the subtle geometric changes in nuclear orientation and perhaps nuclear size is sufficient to change the probability of the inclusion of these nuclei in sections three quarter micron thick (Abercrombie 46).

Constant DNA content of the levator ani

Considering the lack of mitotic activity and the similar proportions of the several cell types in the *intact* and *treated neuter* mice it was predicted that the total DNA content of the muscle would be independent of both castration and testosterone treatment.

To test this prediction the *levator ani* muscles from five *intact* five *neuter* and five *testosterone treated* mice were analyzed for their total content of DNA. The *treated neuter* mice had received their parenteral testosterone nine days previously. Table 3 presents the data.

The weights of the muscles fall into three distinct groups: the heavy muscles of the *intact* mice (45.3 mg) the light

TABLE 2
Frequency of encounter of the nuclear types in the three experimental groups and calculation of chi squares¹

Group	Nuclei						Total
	Muscle	Endothelium	Fibroblast	Myocyte	Satellite cell		
Intact							
Number	690	257	165	78	27		1217
Per cent	56.7	21.1	13.6	6.4	2.2		
Neuter ²							
Number	1093	290	211	128	46		1768
Per cent	61.8	16.4	12.0	7.2	2.6		
Treated neuter ³							
Number	450	160	117	55	21		809
Per cent	56.4	19.7	14.5	6.8	2.6		

¹ $\chi^2 = (f - F)^2 / F$ where f equals the hypothetical number of nuclei calculated from the percentage found in the *intact* mice and F equals the observed values.

² $\chi^2 = \frac{(1093 - 1002)^2}{1002} + \frac{(290 - 373)^2}{373} + \frac{(211 - 241)^2}{241} + \frac{(128 - 113)^2}{113} + \frac{(46 - 39)^2}{39}$

$\chi^2 = 8.264 + 18.469 + 3.734 + 1.991 + 1.258 = 33.714$ null hypothesis rejected $P < 0.005$

³ $\chi^2 = 0.020 + 0.588 + 0.445 + 0.173 + 0.800 = 1.726$ null hypothesis accepted $P < 0.005$

TABLE 3

Total DNA in the levator ani muscles of intact neuter and testosterone treated¹ neuter mice

Animal	Group	Body weight	Muscle weight	Total DNA	Means and standard deviations		
					Body weight	Muscle weight	Total DNA
		gm	mg	μ g	gm	mg	N
1	Intact	46.0	51.5	24.9			
2		44.0	46.6	25.0			
3		44.5	42.4	21.0			
4		44.0	38.7	20.5			
5		45.5	47.5	28.2	44.8 \pm 0.9	45.3 \pm 4.9	35.1
6	Neuter	43.5	16.4	23.6			
7		35.0	12.9	20.3			
8		36.0	16.0	27.5			
9		41.0	14.6	15.5			
10		35.0	16.7	28.3	38.1 \pm 3.9	15.3 \pm 1.6	23.0
11	Neuter treated with testosterone	46.0	31.4	28.6			
12		39.0	31.2	25.9			
13		43.0	24.8	21.5			
14		50.0	36.7	24.5			
15		39.0	28.2	24.3	43.4 \pm 4.7	30.5 \pm 4.4	18

¹ 0.5 mg Depotestosterone (Upjohn) nine days previous to sacrifice

muscles of the *neuters* (15.3 mg) and the intermediate muscles of the *neuters treated with testosterone* (30.5 mg). The total DNA content of the muscles varies between 20 and 29 μ g except for one unusually low reading of 15.5 μ g. But there is no significant difference between the means representing the three groups. This does not mean that the number of cells in this muscle is stable throughout adulthood. Indeed, when data from adult mice of widely varying ages are compared differences are noted. But it is clearly evident that the cell number is independent of the effects of castration and testosterone treatment.

DISCUSSION

The concept of a stable number of skeletal muscle fibers forming early in mammalian life is well supported. MacCallum (1898) has reported that the fixed number is established before birth in the human *sartorius*. This is questioned by Montgomery (62) who finds new fibers forming postnatally. In the mouse Goldspink (62) also notes formation of new muscle fibers postnatally. Taken as a whole the evidence presented indicates a stabilization of fiber number relatively early in the growth period. This constant number of fibers persists into adulthood and is refractory to change even during

the muscular hypertrophy of exercise (Morpurgo 1898). The data from the *levator ani* confirms this constancy. A manipulation of testosterone levels can not alter the established number of muscle fibers.

Though the number of fibers in an adult remain unchanged there is growing evidence that the number of muscle nuclei continually increase. Montgomery (61) reports a nuclear increase in the human *sartorius* from birth through the seventh decade of life. He hypothesizes a continual fusing of an expanding population of myoblasts into existing muscle fibers. The studies of skeletal muscle made by Morpurgo (1898), Morpurgo and Benda (1898) and Schiefferdecker (69) provide many instances of an increasing number of muscle nuclei as muscles age. They postulate mitosis of muscle nuclei as the cause. Enesco and Puddy (64) confirm these observations present a histometric study of skeletal muscles in the rat that demonstrates constancy in the number of muscle fibers and yet a 10 to 50 fold increase in the number of muscle nuclei from the sixteenth to the eleventh fourth day of age. MacConaichie, Enesco and Leblond (64) working with the same material demonstrate that these nuclei incorporate thymidine and divide mitotically at rates in accordance with their increase.

numbers. The nature of these mitotically active cells is not fully established. MacConnachie notes that in many they resemble the "satellite cells" of the fibers first described by Mauro (1) and now recognized to be a distinct cell type in many striated muscles (2, 3, 4, 5, 6, 7, 8, 9, 10, 11, 12, 13, 14, 15, 16, 17, 18, 19, 20, 21, 22, 23, 24, 25, 26, 27, 28, 29, 30, 31, 32, 33, 34, 35, 36, 37, 38, 39, 40, 41, 42, 43, 44, 45, 46, 47, 48, 49, 50, 51, 52, 53, 54, 55, 56, 57, 58, 59, 60, 61, 62, 63, 64, 65, 66). These observations tempt speculation that the slowly increasing number of nuclei in muscle fibers represents the latent proclivity to myogenesis that can be demonstrated by injecting mature skeletal muscles (Allbrook and Walker 63, Zhunkin and Andreeva 64, Price et al 64) and that this propensity may burst forth when the *levator ani* is stimulated hormonally to produce exceptionally large number of muscle fibers. This speculation proves untenable through the number of muscle nuclei in *levator ani* is increasing slowly as in other mature skeletal muscles (limited published data on DNA content) the rate of increase is altered negligibly by castration and subsequent testosterone treatment. Mice in the three experimental groups analyzed show equal quantities of DNA in their muscles because they were sacrificed at identical ages.

Kochakian (64) in his study of the nucleic acid content of the *masseter* and *temporalis* muscles of growing guinea pigs notes that testosterone "retards the attainment of the adult level of DNA" but does not prevent it. The implication is that the *masseter* and *temporalis* either assume a constant quantity of DNA or the accumulation slows to an immeasurable rate below the adult level" is unaltered by administering testosterone.

The concept of Stockdale and Holtzer (61) that synthesis of DNA and synthesis of specific muscle proteins are antagonistic processes" is supported by the response of the mature *levator ani* to testosterone. In this instance the muscle fibers are differentiated to synthesize maintain and perhaps destroy sarcoplasmic proteins. During atrophy these muscle cells do not dedifferentiate (Venable 66) and therefore their nuclei are mitotically dormant as if locked to processes associated with functional muscle cells. During enlargement the increase in muscle

mass is wholly the response of these same fully differentiated muscle cells so here also mitotic activity is repressed.

It may seem remarkable that the endothelial cells of the capillary beds and the fibroblasts of the connective tissues are unresponsive to the considerable change in girth of the muscle fibers. This becomes less surprising if one realizes that the capillaries and the connective tissues are more sensitive to changes in the lengths of muscle fibers than to changes in their girths. This is so because capillaries and connective tissue elements are oriented primarily in parallel with the longitudinal axis of muscle fibers. In the atrophying and hypertrophying *levator ani* the length of the muscle changes very little. As the girths of the muscle fibers decrease capillaries, fibroblasts and collagenous fibers are brought more closely together. As the girths increase these elements move apart.

The distances metabolites must diffuse from capillaries to deeply situated metabolic sites in the sarcoplasm does not seem to limit total muscle mass provided the muscle fibers remain smaller than 70 μ in diameter the largest measured in this study.

The conclusions drawn are these. Testosterone alters neither the total number of nuclei nor the total number of muscle cells in the *levator ani* of mature mice though there is evidence from studies in guinea pigs that the rate of the accumulation of nuclei during the growth period may be affected. This androgen's stimulatory effect is associated specifically with the synthesis and maintenance of the sarcoplasmic mass of the muscle fibers (see Venable 66).

Castration of a mature male mouse produces true atrophy of the muscle fibers of the *levator ani*. Subsequent administration to the stable neuter produces true muscular hypertrophy.

ACKNOWLEDGMENTS

The author is grateful to Drs. Jean Paul Revel, Elizabeth Hay and James Adelstein for the use of their laboratories and their helpful suggestions during the course of this study.

LITERATURE CITED

- Allbrook D 1962 An electron microscopic study of regenerating skeletal muscle *J Anat* 96 137-152
- Abercrombie M 1946 Estimation of nuclear population from microtome sections *Anat Rec* 94 239-247
- Enesco M and Della Puddy 1964 Increase in the number of nuclei and weight in skeletal muscles of rats of various ages *Am J Anat* 114 235-244
- Flood P R 1964 Myosatellite cells in myxine and axolotl *Proc 3rd European Regional Conf on Electron Micros* p 575
- Gordon G B L R Miller and K G Bensch 1963 Fixation of tissue culture cells for ultrastructural cytochemistry *Exp Cell Res* 31 440-443
- Hay Elizabeth and J P Revel 1963 Autoradiographic studies of the origin of the basement lamella in amblystoma *Dev Biol* 7 152-168
- Kochakian C D J Hill and D G Harrison 1964 Regulation of nucleic acids of muscles and accessory sex organs of guinea pigs by androgens *Endocrinology* 74 635-642
- MacCallum J B 1898 On the histogenesis of the striated muscle fiber and the growth of the human sartorius muscle *Bull Johns Hopk Hosp* 9 208-215
- MacConnachie H F M Enesco and C P Leblond 1964 The mode of increase in the number of skeletal muscle nuclei in the postnatal rat *Am J Anat* 114 245-253
- Mauro A 1961 Satellite cell of skeletal muscle fibers *J Biophysic Biochem Cytol* 9 493-494
- Midsukami M 1964 Electron microscopic studies of satellite cells in the cardiac muscle of the brachyura *Okajimas Fol Anat Jap* 40 173-185
- Montgomery R D 1962 Growth of human striated muscle *Nature* 195 194-195
- Morpurgo B 1897 Ueber Activitäts Hypertrophie der willkürlichen Muskeln *Virchows Arch Path Anat* 150 522-554
- 1898 Über die postembryonale Entwicklung der quergestreiften Muskeln von weissen Ratten *Anat Anz* 15 200-206
- Morpurgo B and F Bindi 1898 Ueber die numerischen Schwankungen der Kerne der quergestreiften Muskelfasern der Menschen und Thiere *Arch Path Anat* 151 181-188
- Muir A R A H M Kanyo and D Allbrook 1965 The structure of the satellite cell in skeletal muscle *J Anat* 99 435-444
- Price H M E L Howes Jr and J M Ellenberg 1964 Ultrastructural alterations in skeletal muscle fibers injured by cold *Lab Invest* 13 1279-1302
- Schaefferdecker P 1909 *Muskeln und Muskelkern* Leipzig
- Schmid P Charlotte Schmid and D Broca 1963 The determination of the total deoxyribose of deoxyribonucleic acid *J Biol Chem* 238 1068-1072
- Schneider W C 1945 Phosphorus compounds in animal tissues I Extraction and estimation of deoxypentose nucleic acid and of pentose nucleic acid *J Biol Chem* 161 293-331
- Stockdale F E and H Holtzer 1961 DNA synthesis and myogenesis *Exp Cell Res* 21 508-520
- Snedecor G W 1956 *Statistical Methods* The Iowa State College Press Ames Iowa Chapter 7
- Venable J H 1964 The cytology of hypertrophy in a skeletal muscle *Anat Rec* 148 347 (abstract)
- 1966 Morphology of the cells of normal testosterone deprived and testosterone stimulated levator ani muscles *Am J Anat* 119 271-302
- Wainman P and G C Shipounoff 1941 The effects of castration and testosterone propionate on the striated perineal musculature of the rat *Endocrinology* 29 975-978
- Walker B E 1963 The origin of myoblasts and the problem of dedifferentiation *Exp Cell Res* 30 80-92
- Zhinkin L N and L F Andreeva 1963 Nuclear synthesis and nuclear reproduction during embryonic development and regeneration of skeletal tissue *J Embryol Exp Morph* 11 357-367

Morphology of the Cells of Normal, Testosterone deprived and Testosterone stimulated levator Ani Muscles¹

JOHN H. VENABLE²

Department of Anatomy Harvard Medical School Boston Massachusetts

ABSTRACT The atrophy of the *levator ani* following castration of an adult mouse or rat results from the dissolution of the myofilaments from myofibrils and eventual loss of two-thirds of the sarcoplasm. Within 45 days the atrophy ceases. The morphology of the now smaller muscle fibers is indistinguishable from those from intact males. Treatment of the stable neuter with testosterone produces rapid enlargement of the muscle fibers but negligible changes in the morphological patterns of the sarcoplasm. Observations indicate that new myofilaments form in register along the myofibrils the enlarging myofibrils being divided to maintain a diameter between 0.5 and 1.5 μ . The cytology of each of the five cell types common to the primary bundles is described. Satellite cells of the muscle fibers are a consistent component, but do not contribute to the processes of atrophy or hypertrophy.

In 1935 Papanicolaou and Falk reported administering testosterone to female and castrated male guinea pigs to stimulate enlargement of their masticatory muscles to a size characteristic of the intact male. Three years later Wainman and Shipounoff (41) reduced the weight of the perineal muscles in male rats by castration. This wasting could be prevented by administering testosterone. Testosterone treatment of intact males resulted in abnormal enlargement of their perineal muscles. The individual muscle fibers seemed to change their size harmoniously with the change in size of the muscle as a whole. Surprisingly there was no alteration in the internal structure of the muscle fibers resolvable by light microscopy. No mitotic activity was noted but the number of nuclei per unit area of section seemed to be greater in samples from the wasted muscles. This was ascribed either to a crowding to either of the original nuclei or possibly to an infiltration of connective tissue cells.

In 1949 Eisenberg et al. treated the neutered male rat with testosterone and measured the remarkable increase in weight of a single muscle of the perineal complex the *levator ani*. They suggested this measurement as a biological indicator of myotropic activity of androgens. Subsequently Kochakian (59) reported a

similarly induced weight increase in the *levator ani* of the mouse. Other organs of the mouse such as the lacrimal and salivary glands urinary bladder and kidney also enlarged discernibly under the influence of parenterally administered testosterone.

Because fine structural changes in muscles responsive to testosterone remained unknown and these changes seemed essential to understanding maintenance and growth of muscle tissue a re-examination of the morphology of the atrophying and enlarging *levator ani* was undertaken utilizing both light and electron microscopy of thin sections of the muscle embedded in epoxy resin. This report presents the microscopical observations made during the study. A preceding report (Venable 66) demonstrates the stability of the cell populations involved in these phenomenon and shows the changing weight of the muscle to be due solely to a change in sarcoplasmic mass.

¹ Research supported by National Science Foundation Science Faculty Fellowship 2G-406 training grant GM-406 and by grant GM-10182.

² Based on a thesis submitted to the Division of Medical Sciences The Graduate School of Arts and Sciences Harvard University in partial fulfillment of the requirements for the Degree of Doctor of Philosophy in Anatomy.

³ Present address: Department of Veterinary Anatomy College of Veterinary Medicine Oklahoma State University Stillwater Oklahoma.

LITERATURE CITED

- Allbrook D 1962 An electron microscopic study of regenerating skeletal muscle *J Anat* 96 137-152
- Abercrombie M 1946 Estimation of nuclear population from microtome sections *Anat Rec* 94 239-247
- Enesco M and Della Puddy 1964 Increase in the number of nuclei and weight in skeletal muscles of rats of various ages *Am J Anat* 114 235-244
- Flood P R 1964 Myosatellite cells in myxine and axolotl *Proc 3rd European Regional Conf on Electron Microsc* p 575
- Gordon G B L R Miller and A G Bensch 1963 Fixation of tissue culture cells for ultrastructural cytochemistry *Exp Cell Res* 31 440-443
- Hay Elizabeth and J P Revel 1963 Autoradiographic studies of the origin of the basement lamella in amblystoma *Dev Biol* 7 152-168
- Kochakian C D J Hill and D G Harrison 1964 Regulation of nucleic acids of muscles and accessory sex organs of guinea pigs by androgens *Endocrinology* 74 635-642
- MacCallum J B 1898 On the histogenesis of the striated muscle fiber and the growth of the human sartorius muscle *Bull Johns Hopk Hosp* 9 208-215
- MacConnachie H F M Enesco and C P Leblond 1964 The mode of increase in the number of skeletal muscle nuclei in the postnatal rat *Am J Anat* 114 245-253
- Mauro A 1961 Satellite cell of skeletal muscle fibers *J Biophysic Biochem Cytol* 9 493-494
- Midsukami M 1964 Electron microscopic studies of satellite cells in the cardiac muscle of the brachyura *Okajimas Fol Anat Jap* 40 173-185
- Montgomery R D 1962 Growth of human striated muscle *Nature* 195 194-195
- Morpurgo B 1897 Ueber Activitts Hypertrophie der willkrlichen Muskeln *Virchows Arch Path Anat* 150 522-554
- 1898 Ueber die postembryonale Entwicklung der quergestreiften Muskeln von weissen Ratten *Anat Anz* 15 200-206
- Morpurgo B and F Bindi 1898 Ueber die numerischen Schwankungen der Kerne den quergestreiften Muskelfasern der Menschen *Virchows Arch Path Anat* 151 181-183
- Muir A R A H M Kanji and D Allbrook 1965 The structure of the satellite cell skeletal muscle *J Anat* 99 435-441
- Price H M E L Howes Jr and J M Ellenberg 1964 Ultrastructural alterations in skeletal muscle fibers injured by cold *Lab Invest* 13 1279-1302
- Schlefferdecker P 1909 *Muskeln und Muskelkern* Leipzig
- Schmid P Charlotte Schmid and D Brod 1963 The determination of the total deoxyribose of deoxyribonucleic acid *J Biol Chem* 238 1068-1072
- Schneider W C 1945 Phosphorus compounds in animal tissues I Extraction and estimation of deoxyribose nucleic acid and of ribose nucleic acid *J Biol Chem* 161 933-937
- Stockdale F E and H Holtzer 1961 DNA synthesis and myogenesis *Exp Cell Res* 1 508-520
- Snedecor G W 1956 *Statistical Methods* The Iowa State College Press Ames Iowa 7
- Venable J H 1964 The cytology of trophy in a skeletal muscle *Anat Rec* 347 (abstract)
- 1966 Morphology of the cells of normal testosterone-deprived and stimulated levator ani muscles *Am J* 119 271-302
- Wainman P and G C Shipounoff 1941 effects of castration and testosterone propionate on the striated perineal musculature of *Endocrinology* 29 975-978
- Walker B E 1963 The origin of myoblasts and the problem of dedifferentiation *Cell Res* 30 80-92
- Zhinkin L N and L F Andreeva 1963 DNA synthesis and nuclear reproduction during embryonic development and regeneration of cle tissue *J Embryol Exp Morph* 11 367

muscle is embedded in dense deep anal and coccygeal fascia and is connected posteriorly with the external anal sphincter. Figure 5 demonstrates these relationships.

Histologically the levator ani is a typical striated skeletal muscle (figs 6-12). Its parallel cross striated muscle fibers range in diameter from 10-70 μ in both adult mice and rats. The frequency distribution of fiber diameters is skewed slightly positively with a mean and standard error of the mean of $36.1 \pm 0.5 \mu$ (fig 11). Single fibers have a fairly uniform diameter throughout their length.

Serially and sagittally cut celloidin sections of one half the levator ani from one male mouse demonstrate that most muscle fibers extend the full length of the specimen with the exception of the fibers positioned at the outer margins of the muscle. These latter ones end short of the perineal insertion and may not reach the mid-line. Whether or not fibers cross the midline dorsal to the rectum was not investigated directly but the lack of a visible raphe coupled with a lack of fibers ending in the near mid sagittal sections suggests that they are continuous.

The muscle is primarily closely packed muscle fibers. The meager collagenous connective tissue recognizable by light microscopy is confined to a perimysium forming the adventitial sheaths of the distributed blood vessels and nerves. Elastic fibers are confined to the walls of arteries. The capillaries are plentiful and regularly spaced. Most run parallel to the long axis of the muscle but are interconnected at occasional intervals by oblique anastomoses. In cross sections of the muscle each muscle fiber abuts at least two and usually three capillaries.

Other than the muscle fibers the four common cell types found in every primary muscle bundle are in order of their frequency of occurrence the endothelial cell of the capillary the fibroblast the pericyte (undifferentiated perivascular cell) and a cell appearing as a satellite to the muscle fibers. The latter seemingly identical to the cell described by Mauro (61) will be referred to as "the satellite cell." Histocytes and mast cells are sometimes encountered but are present more typically

in the perimyseal connective tissues. Myelinated nerves and Schwann cells are seen occasionally particularly since the chosen region for sampling often includes motor end plates. The quantitative distribution of 1170 nuclei of cells in the primary bundles of muscles of three intact mice is presented in figure 1. In the accompanying report (Venable '66) data is presented showing a constancy of the nuclear types in all of the three experimental groups of mice. The percentages of encounter seen in the three intact mice are: muscle nuclei (57%), endothelial nuclei (20%), fibroblast nuclei (14%), pericyte nuclei (7%), and satellite cell nuclei (2%). These data are not modified to account for differences in average nuclear size and section thickness (Abercrombie '46).

The morphology of the muscle fiber

In electron micrographs the bulk of the muscle fiber is a continuum of myofilaments divided into anastomosing bundles by many thin longitudinally oriented planes of the remaining sarcoplasm (fig 12). These bundles the myofibrils present polygonal and often asymmetrical cross-sections. Their widths range from 0.5-1.5 μ in both the mouse and rat. These myofibrils exhibit the banding and sarcomere structure recognized as typical of vertebrate skeletal muscle (Huxley '57).

Sarcoplasm between the myofibrils is usually scant. It exhibits mitochondria, a reticulum of membranous tubes — the sarcoplasmic reticulum — and many small granules of varying size (figs 12-13).

Most mitochondria are scattered throughout the sarcoplasm appearing singularly or in rows along myofibrillar interspaces. The majority of sarcomeres make no direct contact with mitochondria. A few mitochondria aggregate either beneath the sarcolemma or at the poles of the muscle nuclei. These small subsarcolemmal aggregates generally represent sites close to capillaries. Mitochondria are more numerous in the muscles from mice than in the muscles from rats, an expected observation in view of Gauthier and Padykula's correlation (63) between increased concentration of mitochondria and decreased body mass.

MATERIALS AND METHODS

To avoid the superposition of the effects of normal muscle growth on the effects of testosterone the levator ani muscles of only adult male mice and rats were studied. All the mice (55) were young adults. The rats were either young adults (12) or old neuters (10).

Both the young adult mice and the young adult rats were divided into three groups: the *intact neuter*, and *testosterone treated neuter* groups. *Intact* animals were uncastrated and received no testosterone. *Neuter* animals were castrated as adults at 40 days of age and maintained under standard animal room conditions long enough to allow near maximal atrophy of the levator ani. *Testosterone treated neuter* animals were likewise castrated as adults and maintained for a minimum of 40 days, but this group then received an intermuscular injection of Depo testosterone (Upjohn). At the time of sacrifice all young adult mice were between 80 and 100 days old; all young adult rats between 95 and 150 days of age.

Two young adult neuter rats were sacrificed to study the fine structure of atrophying muscle fibers: one at 22 days and one at 45 days following castration.

The ten old neuter rats had been castrated prior to puberty and were approximately 300 days old. Five were treated with Depo testosterone; the others served as untreated controls.

Preparation of the levator ani for morphological study included exposing it by blunt dissection through the excised perineum and fixing it *in situ* by flooding the dissected space with a 0.5–4.0% solution of glutaraldehyde buffered to pH 7.4 by 0.05–0.2 M sodium cacodylate. Mosquito forceps attached to the rim of the anus and suspended by tape from a position above and behind the dorsally recumbent animal produced a slight tension on the muscle during fixation. After 30 minutes exposure *in situ* to the fixative the muscle was dissected free and placed in fresh cold fixative. Samples were taken from the fixed muscle at a site located originally just lateral to the rectum (fig 5). These were left in the fixative for an additional three hours.

The samples were washed subsequently¹ in several changes of a cacodylate-sucrose buffer solution (Gordon, Mille, and Bensch 63) in which they were left overnight and then treated 1 to 2 hours the following morning with a 1% solution of osmium tetroxide in fresh washing solution. Rapid dehydration through increasing concentrations of cold ethanol and embedding in Epon 812 as described by Leff (61) completed the preparation of the samples for sectioning.

In a few instances muscles were fixed *in situ* with 1% osmium tetroxide buffered with 0.1 M phosphate or *s-collidine* instead of the glutaraldehyde osmium fixation.

For light microscopy sections were cut which averaged one square micron in area and one half to three quarters of a micron in thickness. These were stained with 1% toluidine blue in 1% borax and the entire section imaged on a 4 × 5 photographic film using a 25 × plan apochromatic (Zeiss) microscope objective. Enlarged prints of these developed films served as work sheets. Types of nuclei identified on the original section by means of a 100 × Neofluor Phase Objective (Zeiss) were recorded on the large photographic print and provided the data on frequency of occurrence of nuclear types.

Silver to gold thin sections for electron microscopy were stained with lead cacodylate (Karnovsky 61) or lead citrate (Venable, Coggeshall 65) — with and without previous treatment with uranyl acetate — and photographed in a RCA EMU 3E or 3 electron microscope.

Measurements of muscle fiber diameter were made from glutaraldehyde fixed samples taken from regions near the sectioned areas and from similar areas from the opposite half of the muscle. The technique is described in the preceding article.

OBSERVATIONS

The levator ani in the male mouse or rat is a loop of muscle forming a collar dorsally and laterally around the last few millimeters of the rectum. Ventral to the rectum the two ends of the loop attach to two paired caudal extensions of the fibrous capsule of the urethral bulb. The muscular loop and the fibrous capsule completely encircle the rectum. Dorsal to the rectum

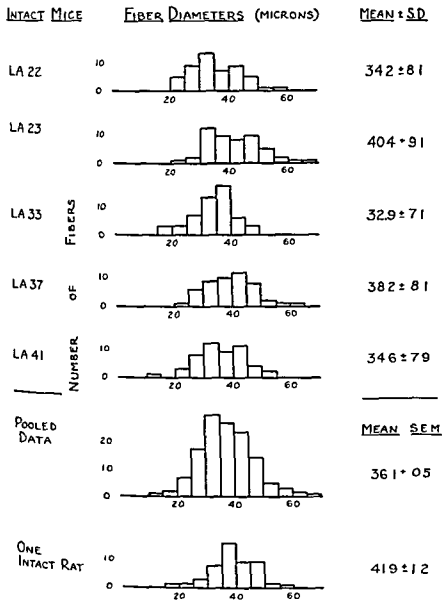


Fig 2 Histograms of muscle fiber diameters of the levator ani of five intact adult mice and one intact adult rat. The much larger size of the levator ani muscle in the rat is due to a larger number of muscle fibers rather than larger fibers.

bands. A very small number of triads run longitudinally across A bands. In old *new* rats it is common to find occasional pentads (Revel 62). These are not found in the muscles of younger animals.

Granules are numerous in the sarco-plasma. They average 25 μ in diameter

with a range of 10–40 μ . They have an affinity for lead stains. Uranyl acetate staining alone adds little contrast to these granules — or to any other structures in these glutaraldehyde-osmium fixed muscle fibers. A very few multilocular granules can be found. One might assume all the

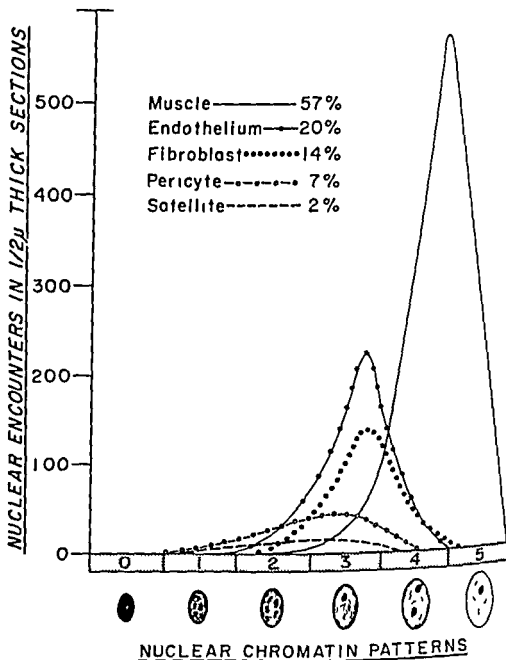


Fig 1 Relative numbers of nuclei of the five cell types common to primary muscle bundles of the *levator ani* of three adult male mice. Variations in the chromatin patterns common to the nuclear types is indicated by position on the abscissa. Examples of the chromatin patterns are found in figure 8 through 11 where they are labeled by the number system appearing here.

The sarcoplasmic reticulum of the *levator ani* is morphologically similar in basic respects to that described by Porter and Palade (57) for the rat and now regarded as typical for white fibers of mammalian skeletal muscle. A longitudinal system of tubules closely invests each myofibril and is fused to them at the Z-lines. The trans-

verse system of tubes or T system (15) (son Cedergren 59) is apparent in association at the A-I junctions with transverse cistern formed by one of the more longitudinally oriented sarcoplasmic tubules. The transversely organized triads appear at 75% of the border of the longitudinally sectioned A and

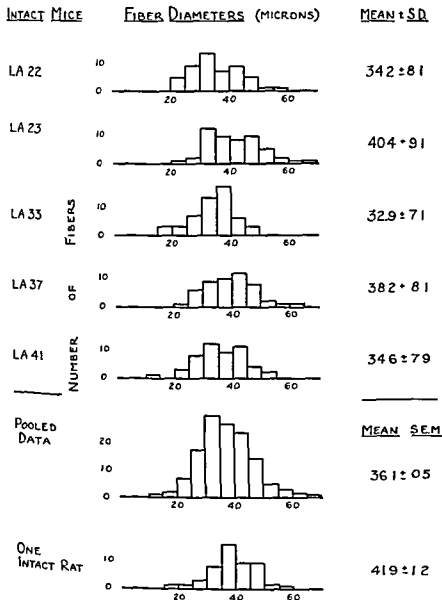


Fig 2 Histograms of muscle fiber diameters of the levator ani of five intact adult mice and one intact adult rat. The much larger size of the levator ani muscle in the rat is due to a larger number of muscle fibers rather than larger fibers.

bands. A very small number of triads run longitudinally across A bands. In old neuter rats it is common to find occasional pentads (Revel 62). These are not found in the muscles of younger animals.

Granules are numerous in the sarcolemma. They average 25 μ in diameter

with a range of 10–40 μ . They have an affinity for lead stains. Uranyl acetate staining alone adds little contrast to these granules — or to any other structures in these glutaraldehyde-osmium fixed muscle fibers. A very few multilocular granules can be found. One might assume all the

granules to be glycogen on the basis of these characteristics (Revel 64) but due to uncertainties as to the effect of the glutaraldehyde fixation on these staining characteristics the possibility that some or many may be ribosomes can not be excluded.

Muscle nuclei are typically located at the periphery of the muscle fibers though a few are buried among the myofibrils. They are shaped most often like elongated platters. Their average length is $16\ \mu$ their average width measured tangentially and transversely to the fiber is $7\ \mu$ their average depth is $2.5\ \mu$. The glutaraldehyde osmium fixed muscle nuclei show a thin rim of densely stained chromatin at the periphery of the karyotheca but only a few chromatin strands scattered in the karyoplasm. The thin rim of chromatin is more electron opaque than that seen in muscle nuclei fixed by osmium alone though the patterns of chromatin clumping seem identical. One to three per cent of the muscle nuclei have thicker, coarser patterns of chromatin than the rest. Such patterns are similar to those characteristic of satellite cell and pericyte nuclei.

Muscle nuclei invariably are within $30\ \mu$ of the myofibrils in this mature muscle a space unresolved by light microscopy. This is a useful criterion for differentiating muscle nuclei from nuclei of indenting satellite cells, fibroblasts and endothelial cells.

The satellite cell

Satellite cells must be considered normal components of the *levator ani*. These cells lie inside the muscle fibers glyco-calyx (of Bennett 63) often referred to as the basement membrane yet are distinctly outside the sarcolemma (plasmal emma). They nestle into the muscle fiber so as to leave the fibers outer contour relatively undistorted (fig 7). The plasmal emmae of the satellite cell and the muscle fiber lie within $30\ \mu$ of each other with no intervening glycocalyx.

The cytoplasm of the satellite cell in the mature *levator ani* is usually sparse and shows little specialization. It contains a small but distinct Golgi complex, a few scattered smooth vesicles and tubules, a

pair of centrioles, a few scattered mitochondria, and cytoplasmic granules suggestive of both glycogen and ribosomes (fig 14). The cytoplasm contains a granular endoplasmic reticulum.

A striking differential characteristic of the satellite nucleus more readily discerned after glutaraldehyde-osmium fixation than osmium fixation alone is its coarse pattern of chromatin clumping. The chromatin is in thicker strands and clumps in the karyoplasm and is in thicker aggregates at the karyotheca than that characteristic of the usual muscle cell nucleus.

With thinly sectioned glutaraldehyde-osmium fixed specimens it is possible to differentiate between satellite cells and muscle nuclei by light microscopy (figs 7-10). Stained sections one half to three quarters of a micron in thickness are scanned at a magnification of 400. Nuclei lying within the outer contours of the muscle fibers which exhibit coarser chromatin patterns than those of usual muscle nuclei are critically examined for a narrow light line less than $0.4\ \mu$ in thickness between the karyotheca and the dark stained A bands of the adjacent myofibrils. Such a light line can not be resolved between muscle nuclei and adjacent A bands. Encroaching fibroblasts and endothelial cells have a wider space between their nuclei and the nearest myofibrils of the muscle cell. It is usually possible to see the cytoplasm of the satellite cell contrasted against the sarcoplasm since the former's staining and optical properties differ somewhat from the latter. Using these criteria approximately 4% of what otherwise could be mistaken easily for muscle nuclei are more accurately identified as nuclei of satellite cells.

The satellite cell nuclei average $13\ \mu$ in length, $4.5\ \mu$ in width and $2.8\ \mu$ in depth. They are thus smaller and more fusiform than muscle nuclei. By being smaller they have a lower probability of appearing in sections (Abercrombie 46) making the figure of 4% satellite nuclei given above an underestimate. Adjusting for the decreased probability of their appearance in sections the true percentage of satellite cell nuclei to muscle nuclei in the *levator*

of adult mice likely falls between 48 and 58%

The pericyte

Pericytes (Rouget 1873) are very similar morphologically to satellite cells (fig 16) but they do differ however in three characteristics: their position in relation to the muscle cells, their slightly coarser chromatin pattern and their completely circumferential glycocalyx.

The pericyte's differentiation by light microscopy depends upon its adjacency to capillaries: its paucity of cytoplasm and coarseness of chromatin pattern. On electron micrographs the pericyte has the additional identifying characteristic of a glycocalyx. This glycocalyx

is unattached to the one surrounding the adjacent capillary. Cytoplasmic structure of the pericyte is identical to that of the satellite cell.

The pericytes of the capillaries and the satellite cells of muscle fibers are indeed similar in morphology that it is feasible to consider them to be two forms of the same cell. This feasibility is strengthened by instances of pericytes indenting muscle fibers where the two usually separate glycocalyxes are fused to form a single line. In figure 14 the glycocalyx dips between the satellite cell and muscle fiber existing first as a double line then as a single fused membrane and finally disappearing leaving the plasma lemmas in close apposition. Figure 15 shows a longitudinal view of a nested satellite cell or perhaps a pericyte. Here the glycocalyxes are double in some areas and single fused membranes in others. Early in this study it was speculated that pericytes become satellite cells

during the testosterone stimulated hypertrophy of the muscle. However the quantitative data indicate no significant shift between these two cell populations.

The fibroblast

By light microscopy fibroblasts sometimes prove difficult to differentiate from pericytes. This is particularly true on cross sections of the muscle where the usual longitudinal streaming of the cytoplasm from both ends of the fibroblast nucleus does not appear in the section. In these instances one must rely for its differentiation on the lighter staining surrounding cytoplasm and a usually less dense chromatin pattern. In electron micrographs by contrast fibroblasts are identified easily for they are devoid of a glycocalyx (fig 16) and present a notable amount of a granular endoplasmic reticulum.

The endothelial cell

Endothelial cells form capillaries typical of those in other muscles (Fawcett 63). Their nuclei are easily identified by light microscopy in sections one half to three quarters of a micron thick for the boundaries of capillaries can always be distinguished with certainty (figs 6-11). This is seldom the case when the muscle is studied in thicker paraffin sections.

The levator ani of the neuter

Atrophy of the levator ani following castration of the male mouse and rat involves a loss of myofilaments from muscle fibers but no frank degeneration of muscle tissue. Table 1 compares the muscle weights of intact mice, neuter mice, and

TABLE 1
Atrophy of the levator ani of the mouse 45 days and six months after castration¹

Intact control		45 D y neuter		Six month neuters	
Muscle weight	Body weight	Muscle weight	Body weight	Muscle weight	Body weight
mg	gm	mg	gm	mg	gm
51.5	(46.0)	16.4	(43.5)	14.2	(66.5)
46.6	(44.0)	12.9	(35.0)	16.0	(54.0)
42.4	(44.5)	16.0	(36.0)	15.7	(41.0)
38.7	(44.0)	14.6	(41.0)	12.5	(44.0)
47.5	(45.5)	16.7	(35.0)	13.0	(56.0)
Mean muscle weight \pm SD		15.3 \pm 1.6		14.3 \pm 1.6	
45.3 \pm 4.9					

¹The intact animals and 45-d y neuter were 89 d y old. The six month neuters were 227 days old. Both groups of neuters were castrated when they were 43 d y old.

trated for 45 days and neuter mice castrated for six months. By the forty fifth day after castration the muscles from neuter males have reached a new stable weight one third that found in intact males. Little, if any further atrophy occurs.

A comparison between electron micrographs of levator ani muscles of neuter males castrated for 45 days and micrographs from muscles of intact males shows no remarkable difference in morphology other than a decrease in the average diameter of the muscle fibers. In the castrated mouse the average diameter drops from 36.1μ to 20.8μ (fig. 3).

A few samples were collected and examined during the earlier stages of atrophy in one rat, a young adult castrated for 22 days. These samples exhibit alterations from the intact and neuter morphology that seem to characterize the process of atrophy. These alterations are a fraying of myofilaments from myofibrils, a disorganization of the sarcoplasmic reticulum and a wrinkling of the sarcolemma and nuclear envelope. Thick myofilaments disperse first from their interconnections at the M line (fig. 17) then appear free in the sarcoplasm. Additional sarcoplasmic space appears between fraying myofibrils. The sarcoplasmic reticulum in these areas is often either absent or has lost its intimate association with the myofibrils. These alterations are not found uniformly throughout the muscle; some fibers appear to be normal. The myofibrils in the muscle fibers of neuters tend to be of smaller average diameter than those in muscle fibers of intact animals.

The levator ani of the testosterone treated neuter

Fifteen days following treatment of two old neuter rats with 1 mg of Depo-testosterone ($2\mu\text{g}$ per gram body weight) their levator ani muscles had increased in weight 2.3 times those of two untreated controls (table 2).

The same dose in young adult mice is much less effective. A dose of $12\mu\text{g}$ per gram body weight however produces within nine days an enlargement twice that of untreated controls (Venable '66). Response to the treatment seems to be

TABLE 2
Muscle weights and muscle fiber diameters in old neuter rats treated with Depo-testosterone¹

Animal	Group	Muscle weight	Fiber diameter (Mean \pm SEM)
		mg	μ
LA 17	untreated	71.0	19.3 ± 1.1
LA 19	untreated	74.6	21.0 ± 1.5
LA 18	treated	174.0	27.6 ± 1.3
LA 20	treated	156.4	30.9 ± 1.8

¹ Two micrograms per gram body weight 15 days previous to sacrifice.

varied as might be expected from variable rates of absorption of the repository drug used. However the hypertrophy is in every case remarkable.

Figure 4 compares the muscle fiber diameters of the treated and untreated neuter mice. The histogram of fiber diameters from the treated muscles is lower and wider than that of the untreated ones—the mean and maximum fiber diameter of the treated muscles has shifted to the right, some 40% above that of the untreated ones. This new position is intermediate between that of neuter and intact animals.

Electron micrographs of treated muscles show no striking structural alterations associated with this rapid enlargement. There is a seeming increase in the average myofibril diameter but it is too small to explain the greatly expanded girth of the muscle fibers. There is no great number of very small myofibrils to indicate new myofibrils forming by aggregation of new myofilaments. Neither is there randomly scattered single myofilaments. A site for the formation of myofilaments can not be detected.

The presence of many incomplete intermyofibrillar septa of sarcoplasm (fig. 12) suggests that existing myofibrils are being split. In some instances septa seem to be invading single I bands. Micrographs can give no direct evidence of a dynamic process such as myofibrillar splitting, but as will be explained in the Discussion this and other related evidence points to a conclusion that the myofibrillar mass is continuously subdivided as it expands.

Components of the sarcoplasm, i.e., mitochondria, sarcoplasmic reticulum and sarcoplasmic granules do not alter their structure discernibly during muscle en-

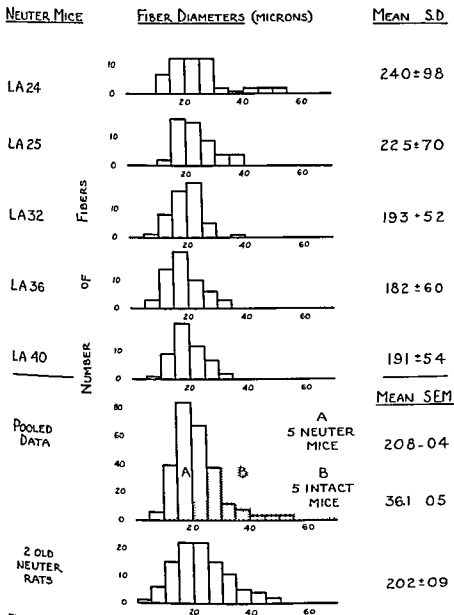


Fig 3 Histograms of muscle fiber diameters of the *levator ani* of five neuter mice and two neuter rats castrated 45 days previously. The data of the neuter mice (A) are compared to the data on intact mice (B) presented in figure 2.

largement. If these components are not replicated during this doubling of muscle volume one should expect volume dilution of organelles in each muscle fiber. In fact, there appears to be little change in the relative distributions of the organelles.

This would imply that the formation of new organelles keeps pace with the expanding sarcoplasmic mass. Whether or not such an increase occurs can not be proved or disproved easily by examining electron micrographs because of the prob-

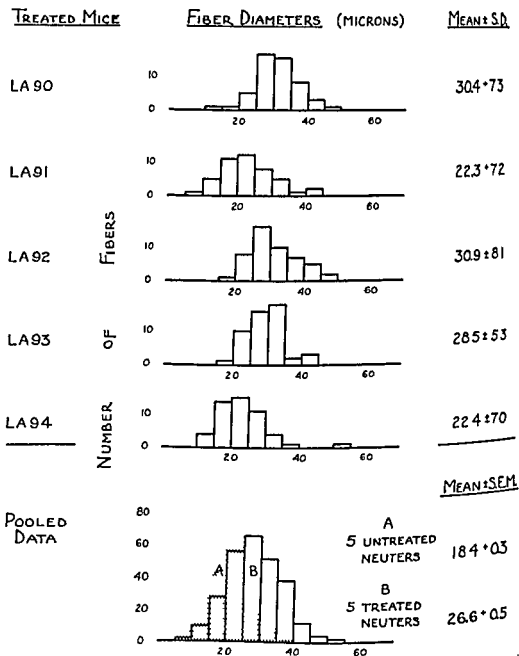


Fig 4 Histograms of muscle fiber diameters of the levator ani of five neuter mice treated eight days previously with 0.5 mg of Depo testosterone

lems of small sample size and non homogeneous distribution of the elements studied Leonard (50) has shown succinic dehydrogenase concentration to remain unchanged during enlargement of perineal musculature a fact conforming to a concept of replication of mitochondria during the process

DISCUSSION

Kochakian has demonstrated (64) that the enlargement of the masseter muscle

of the guinea pig which occurs after administration of testosterone involves no increase in the quantity of DNA in the muscle. This is true also both in the atrophy of the levator ani of the mouse following castration and in its reenlargement following testosterone treatment (Venable 66). The constancy of DNA is consistent with the lack of mitotic activity during these phenomena (Wainman and Shipounoff 41). The decrease and increase in size and weight of the muscle can be accounted

solely by a change in the average diameter of existing muscle fibers (Venable) therefore these phenomena represent a true atrophy and in reference to a stable neuter condition a true hypertrophy of the muscle cells. This atrophy and hypertrophy is produced by a decrease and increase respectively of the usual contractile proteins and supporting cytoplasm.

With castration of the adult male mouse rat the rapid removal of testosterone of testicular origin apparently upsets drastically the metabolic balance that maintains the muscle cells at their characteristic size. The resulting metabolic imbalance does not kill cells but the loss of muscle mass becomes so rapid initially that the usual pattern of packed myofibrils is disrupted. The apparent increase in the amount of sarcoplasm around the myofibrils results probably as much from a thinning of myofibrils as from formation of new sarcoplasm. Many myofibrils particularly those at the periphery are completely lost others are only decreased in size. The manner of dissolution of the contractile proteins and the sarcoplasm is unclear.

Gori and Pelligrino (64) have presented a preliminary report on the morphological aspects of the atrophy of the *levator ani* in rats following castration. They note lysosomes at the periphery of the fibers near the nuclei. In the present study lysosomal like bodies are not observed at 22 days post-castration but their presence earlier in the atrophy can not be denied. It seems improbable however that lysosomal enzymes would be responsible for the degradation of myofilaments since it would mean that lysosomes release specific enzymes into the sarcoplasm for proteolytic digestion of the myofilaments and associated sarcoplasmic proteins. One could except that if the usual complement of acid hydrolases and proteases from a lysosome would be released into the sarcoplasm there would be more drastic alterations in muscle structure than what is observed. Indeed it is difficult to postulate any result less than disruption of the cell. Gori (64) has demonstrated that the loss of muscle proteins from muscles atrophy following denervation has a non-enzymatic

character despite the fact that lysosomal enzymes as measured by such means as hemoglobin degradation are in greater concentration.

Gori and Pelligrino also report that large blocks of "undifferentiated sarcoplasm" appear sometimes as folds extending from the periphery of the fibers that "will subsequently be phagocytized by macrophages." Though such folds occur this method of removing sarcoplasmic material would likely be of little significance in the total reduction of size of the fibers since encounters of histiocytes or other phagocytes particularly in primary muscle bundles are rare. The elimination of sarcoplasm occurs in what appears to be morphologically viable cells with neither massive destruction of all its elements nor accumulation of deposits of debris. The method of autolytic breakdown of the sarcoplasmic elements remains for future investigation.

It is significant that atrophy of the *levator ani* is self limiting. Gori and Pelligrino (64) report a rapid 60% loss in weight of the muscle in male rats within one month after castration but that after this period the rate slows. The muscle weights of castrate mice as reported herein drop at a similar rate nearing zero by 45 days. By this time the muscles are one third their initial weights. By 45 days the muscle fibers show none of the alterations in the cytoplasm described as atrophic and are apparently in a stable condition. There is no reason to doubt that the muscle is functionally active at this new decreased size since its fine structure can not be differentiated from that of other white skeletal muscles. A metabolic balance within the muscle fiber apparently has again been achieved that is commensurate with the hormonal balance of the neuter state. Therefore testicular testosterone is not essential to the existence of this muscle as a functional unit. It is necessary only to maintain the muscle at the masculine size.

It is surprising that the testosterone stimulated muscle can double its mass in nine days while maintaining a normal structural pattern in its muscle fibers. No distinct areas of differentiating myoplasm appear. Simply more and somewhat larger myofibrils fill the expanded fiber. It is im-

possible to characterize morphologically a myofibril either as a new or an old one. This muscular hypertrophy is reminiscent of Morpurgo's early description of hypertrophy in the canine *sartorius* following forced exercise (1897). He showed the hypertrophy to result from an increased diameter of existing fibers by accumulation of a greater number of myofibrils of similar size to those found in the unhypertrophied muscle. It would seem that muscle hypertrophy, whether resulting from exercise or from stimulation by testosterone, is accomplished by similar processes though initiated by differing triggering mechanisms.

Loring Spencer and Vilee (61) provide evidence that testosterone may be linked with the metabolism of the *levator ani* via control of the activity of DPN cytochrome C reductase. A high testosterone level by increasing this enzyme's activity would promote a greater abundance of ATP. The availability of ATP could be the important rate limiting step in the synthesis of sarcoplasmic and myofibrillar proteins. Assuming this to be true, the concentration of ATP is probably influenced by multiple factors of which testosterone and exercise are only two. Different factors apparently are expressed in varying degrees in different muscle groups. Why testosterone expresses its effect most dramatically on the perineal musculature of the rodent and the muscles of mastication in the guinea pig remains a puzzle.

From the evidence at hand the possibility emerges that there is a common general process by which skeletal muscle fibers synthesize and organize their unique cytoplasmic components, the differences in growth rate and final mass of different skeletal muscles depending on basic controls of energy producing metabolism.

The data of Dreyfus et al (60) and Kruh et al (60) show a slow but distinct turnover of myofibrillar proteins in skeletal muscles of the rat and mouse. These workers further interpret their data as indicating a myofibril life span of 30 days in the rat and 20 days in the mouse. Since myofibrils may be synthesized and destroyed continuously in adult animals by hypertrophy and atrophy can be thought of

as an imbalance where the rate of either myofilament production or myofilament destruction predominates over the other.

The fine structural patterns presented by myofilaments and myofibrils in a muscle fiber must, therefore be transient, either being formed being temporary, stable or being broken down. That each of these conditions in the adult has morphologically distinct characteristics is open to question particularly if the rate of change is as slow as Dreyfus data would indicate. Electron micrographs can demonstrate the rapid destruction of myofibrils as seen in the earlier stages of atrophy of the *levator ani*. It is doubtful that they can be used alone to demonstrate slow destruction. Myofilaments and myofibrils that are forming can not be identified with certainty on micrographs whether the synthesis is rapid or slow though it is of interest attempting to describe areas of slight disarrangement of myofilaments in these terms. It will be necessary to combine other evidence of synthesis with a particular morphological pattern before interpretation becomes possible.

The present study provides one hypothesis for the structural manner in which the *levator ani* hypertrophies. This hypothesis includes the assumption that myofibrillar patterns are not static and that new myofilaments are formed in their normal positions upon the sarcomere. If ribosomal synthesis of proteins is represented, where there is presently no reason to doubt the many of the granules in the sarcoplasm between myofibrils must be ribosomes. As myofilaments accumulate on existing myofibrils these myofibrils enlarge. But no without limit because the sarcoplasmic reticulum divides the larger ones keeping the range of myofibril diameters within 0.5–1.5 μ . Thus the number of myofibrils continues to increase yet very small myofibrils — presumably new ones — self appear.

The presence of the satellite cell of the muscle fiber as a consistent component of the *levator ani* representing over 5% of the nuclei enclosed within the glycocalyx of the muscle cell strengthens the acceptance of this cell type as one common to many skeletal muscles. Since Maurer (61) first description of this cell in fr

rat skeletal muscle it has been reported to be present in cardiac muscle of species of crabs (*Chionoecetes opilio* *Charybdis japonica*) by Midsukami in the trunk musculature of the hsh (*Myxine glutinosa*) and axolotl (*Ambystoma tigrinum*) by Flood (64). In the web muscles of the wings of bats (*Eidolon helvum*) and several scales of white mice by Muir et al (65) frequency of occurrence has been noted in two instances other than the reported herein. In the hagfish they present two nuclei per 50 nuclei of muscle fibers (Flood 64b). In the bat 10% nuclei associated with web muscle are satellite cells (Muir et al 65) and his co-workers have noted also that muscles of new born mice may have to 20% satellite nuclei associated with muscle fibers. The satellite cells consist of presence in the levator ani in the same percentage from animal to animal eliminates any notion that it is only a wandering mononuclear cell caught in an unusual position on a micrograph. It is present throughout the usual life of white mice and rats (1 year). It is quite probable that the cells reported by MacConnachie et al (64) to exhibit mitotic activity in growing rat muscle are satellite cells as he has indicated and perhaps represent cells with myoblastic activity associated with muscle development and maturation. This study of the levator ani provides no insight into the function of the satellite cell. It apparently plays no roll in the atrophy and hypertrophy of the levator ani in adult mice.

ACKNOWLEDGMENTS

The author is grateful to Drs Don Fawcett, Susumu Ito, Jean Paul Revel and Elizabeth Hay for their encouragement and aid during the course of this study.

LITERATURE CITED

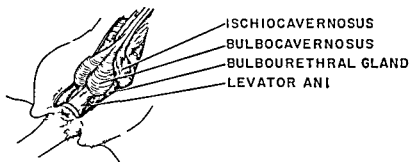
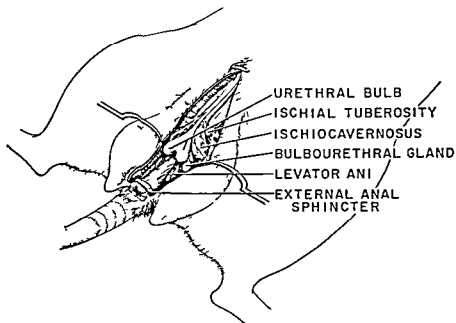
- Abercrombie M 1946 Estimation of nuclear population from microtome sections Anat. Rec. 94 239-247
- Andersson-Cedergren Ebba 1959 Ultrastructure of motor end plate and sarcoplasmic components of mouse skeletal muscle fibers as revealed by three-dimensional reconstruction from serial sections J Ultrastructure Res supplement 1
- Bennett H S 1963 Morphological aspects of extracellular polysaccharides J Histochem and Cytochem. 11 14-23
- Dreyfus J C J Kruh and G Schapira 1960 Metabolism of myosin and life time of myofibrils Biochem J 75 574-578
- Eisenberg E G S Gordon and H W Elliott 1949 Testosterone and tissue respiration of the castrate male rat with a possible test for myotropic activity Endocrinology 45 113-119
- Fawcett D W 1963 Comparative observations on the fine-structure of blood capillaries. In The Peripheral Blood Vessels The Williams and Wilkins Co Baltimore
- Flood P R 1964a Myosatellite cells in myxine and axolotl. Proc 3rd European Regional Conf on Electron Microsc p 575
- 1964b Personal communication
- Gauthier Geraldine and Helen Padykula 1963 Comparative cytological studies of the heterogeneity of skeletal muscle fibers Anat Rec 145 232 (abstract)
- Gordon G B L R Miller and K G Bensch 1963 Fixation of tissue culture cells for ultrastructural cytochemistry Exp Cell Res 31 440-443
- Gori M Zina and Claudio Pellegrino 1964 Ultrastructural observations on the atrophy by castration of the levator ani muscle of the rat and on the following regeneration caused by testosterone Proc 3rd European Regional Conf on Electron Microsc p 83
- Huxley H F 1957 The double array of filaments in cross-striated muscle J Biophysic Biochem Cytol 3 631-648
- Karnovsky M J 1961 Simple methods for "staining with lead" at high pH in electron microscopy J Biophysic Biochem Cytol 11 729-732
- Kochakian C D 1959 Mechanisms of androgen actions Lab Invest 8 538-556
- Kochakian C D J Hill and D G Harrison 1964 Regulation of nucleic acids of muscles and accessory sex organs of guinea pigs by androgens Endocrinology 74 635-642
- Kohn R R 1964 Mechanisms of protein loss in denervation muscle atrophy Amer J Path 45 435-447
- Kruh J J C Dreyfus G Schapira and G Gay 1960 Abnormalities of muscle protein metabolism in mice with muscular dystrophy J Clin Invest 60 1180-1184
- Leonard S L 1950 Succinic dehydrogenase levels in striated muscle in relation to male hormone Endocrinology 47 260-264
- Loring J M J M Spencer and C A Vallee 1961 Some effects of androgens on intermediary metabolism in muscle Endocrinology 68 501-506
- Luft J H 1961 Improvements in epoxy resin embedding methods J Biophysic Biochem Cytol 9 405-414
- MacConnachie H F M Enesco and C P Leblond 1964 The mode of increase in the number of skeletal muscle nuclei in the postnatal rat Am J Anat. 114 245-253

- Mauro A 1961 Satellite cell of skeletal muscle fibers J Biophysic Biochem Cytol 9 493-494
- Midsukami M 1964 Electron studies of satellite cells in the cardiac muscle of brachyura Okayimas Fol Anat Jap 40 173-185
- Morpurgo B 1897 Ueber Activitatz Hypertrophie der willkurlichen Muskeln Virchow's Arch Path Anat 150 522-554
- Muir A R A H M Kanji and D Allbrook 1965 The structure of the satellite cell in skeletal muscle J Anat 99 435-444
- Papanicolaou G N and E A Falk 1938 General muscular hypertrophy induced by androgenic hormone Science 87 238-239
- Porter K R and G E Palade 1957 Studies on the endoplasmic reticulum III Its form and distribution in striated muscle cells J Biophysic Biochem Cytol 3 269-300
- Revel J P 1962 The sarcoplasmic reticulum of the bat cricothyroid muscle J Cell Biol 12 571-588
- 1964 Electron microscopy of glaucoma J Histochem Cytochem 12 104-114
- Rouget C 1873 Mémoire sur le développement la structure et les propriétés physiques des capillaires sanguins et lymphatiques Arch Physiol Norm et Pathol 5 603-663
- Venable J H 1966 Constant cell populations in normal testosterone-deprived and testosterone stimulated levator ani muscles Am J Anat 119 263-270
- Venable J H and R Coggeshall 1965 Amplified lead citrate stain for use in electron microscopy J Cell Biol 25 40-408
- Wainman P and G C Shipounoff 1941 The effects of castration and testosterone propionate on the striated perineal musculature of the rat Endocrinology 29 9/5-9/8

PLATE I

EXPLANATION OF FIGURE

- 5 The gross relationships of the levator ani of the intact mouse are illustrated here with the perineum dissected. The upper drawing provides a view of the urethral bulb with the bulbocavernosus removed. The lower drawing depicts the degree of dissection performed in preparation for the *in situ* fixation of the levator ani. The dotted rectangle on the levator ani represents the sample used for morphological study.



- Mauro A 1961 Satellite cell of skeletal muscle fibers J Biophysic Biochem Cytol, 9 493-494
- Midsukami M 1964 Electron studies of satellite cells in the cardiac muscle of brachyura Okajimas Fol Anat Jap 40 173-185
- Morpurgo B 1897 Ueber Activitatz Hypertrophie der willkürlichen Muskeln Virchows Arch Path Anat 150 522-554
- Muir A R A H M Kanji and D Allbrook 1965 The structure of the satellite cell in skeletal muscle J Anat 99 435-444
- Papanicolaou G N and E A Falk 1938 General muscular hypertrophy induced by androgenic hormone Science 87 238-239
- Porter K R and G L Palade 1957 Studies on the endoplasmic reticulum III Its form and distribution in striated muscle cells J Biophysic Biochem Cytol 3 269-300
- Revel J P 1962 The sarcoplasmic reticulum of the bat cricothyroid muscle J Cell Biol 12 571-588
- 1964 Electron microscopy of chrysa J Histochem Cytochem 12 104-114
- Rouget C 1873 Mémoire sur le développement la structure et les propriétés physiologiques des capillaires sanguins et lymphatiques Arch Physiol Norm et Pathol 5 603-661
- Venable J H 1966 Constant cell population in normal testosterone-deprived and testosterone stimulated levator ani muscles Am J Anat 119 263-270
- Venable J H and R Coggeshall 1965 Amplified lead citrate stain for use in electron microscopy J Cell Biol 25 401-408
- Wainman P and G C Shipounoff 1941 The effects of castration and testosterone propionate on the striated perineal musculature of the rat Endocrinology 29 975-988

PLATE 1

EXPLANATION OF FIGURE

- 5 The gross relationships of the levator ani of the intact mouse are illustrated here with the perineum dissected. The upper drawing provides a view of the urethral bulb with the bulbocavernosus removed. The lower drawing depicts the degree of dissection performed in preparation for the *in situ* fixation of the levator ani. The dotted rectangle on the levator ani represents the sample used for morphological study.

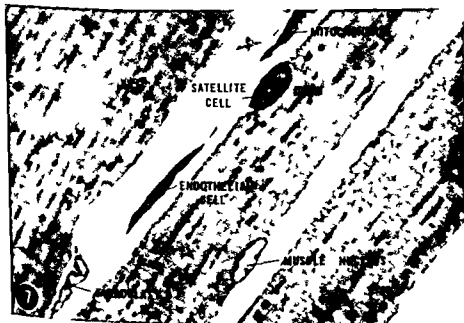
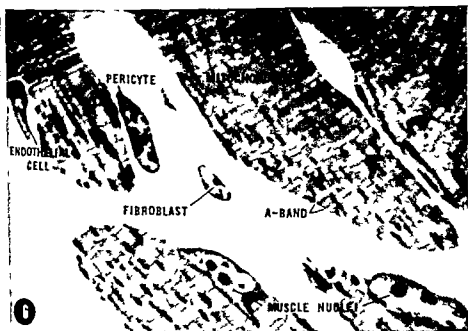


PLATE 2

EXPLANATION OF FIGURES

Epon sections three quarters of a micron thick of the *levator ani* from an *intact* mouse. Stained with toluidine blue in borax $\times 1700$

- 6 The structure of the muscle is depicted at the limits of resolution provided by light microscopy. Myofibrils pack the sarcoplasmic mass. Mitochondria (dense sarcoplasmic masses) are scattered throughout the fiber. Four nuclear types are noted. Pericyte nuclei have darker chromatin patterns than muscle nuclei.
- 7 A satellite cell appears in this section with the typical dark chromatin pattern. Note the thin white line between the nuclear membrane of the satellite and the adjacent myofibrils. This is a distinguishing characteristic of satellite nuclei in sections less than $1\ \mu$ in thickness. Note that endothelial cells the fibroblasts (figs 6-11) are separated from the sarcoplasmic mass by a wider space. No space is visible between muscle nuclei and the adjacent myofibrils.

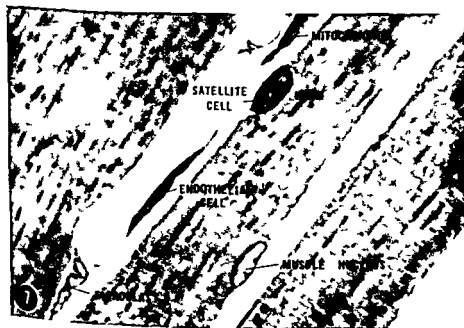
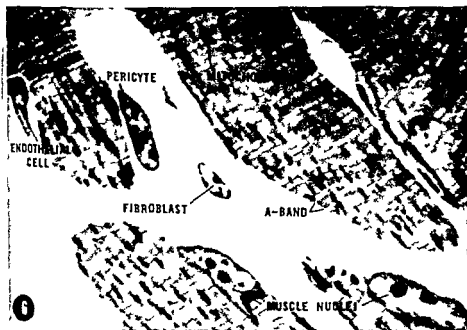


PLATE 3

EXPLANATION OF FIGURES

Examples of cellular types and chromatin patterns in the *levator ani*. Figures 8 9 and 10 are from *neuter* mice while figure 11 is from an *intact* mouse. There are no obvious differences in sarcoplasmic structure of the muscle fibers between the two groups. Nuclei are labeled by letter and number the letter being the initial of the cell type and the number indicating the chromatin pattern as ranked from 1 to 5 according to figure 1. $\times 1500$

- 8 The pericyte nucleus (P_1) has the typical chromatin pattern ranked 2 as does the endothelial nucleus (E_2). The muscle nuclei are typical (M_4). One fibroblast (F_3) is in view. Erythrocytes fill the capillary.
- 9 The pericyte, fibroblast and endothelial cell nuclei all have chromatin patterns ranked 3.
- 10 An intermediate form of pericyte satellite cell has a chromatin pattern ranked 2 ($P-S_2$). A motor end plate containing two terminal nerve endings appears at the lower right. A Schwann cell satellite to a myelinated axon appears at the upper right.
- 11 Various chromatin patterns of muscle nuclei. Muscle nuclei with chromatin patterns darker and denser than the upper one (M_2) are rare. Muscle nuclei with lighter chromatin patterns than those shown ranked 5 are common, having a very thin layer of chromatin at the karyotheca and exhibiting a karyoplasm relatively free of chromatin strands (less than five thin strands).

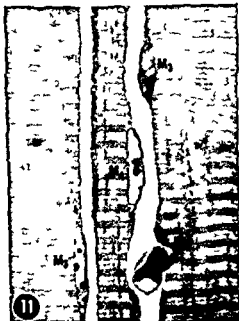


PLATE 4

EXPLANATION OF FIGURE

- 12 The *levator ani* of a *testosterone treated neuter* mouse. The morphology is in basic respects no different from that found in intact and *stable neuter* mice. A possible splitting of myofibrils in this hypertrophying muscle fiber is indicated by the incomplete division of many myofibrils by granular and tubular elements of the sarcoplasm. No misoriented myofilaments are seen. Sites of myofilament synthesis can not be located. Glutaraldehyde-osmium fixation. Lead citrate staining. $\times 16\ 000$

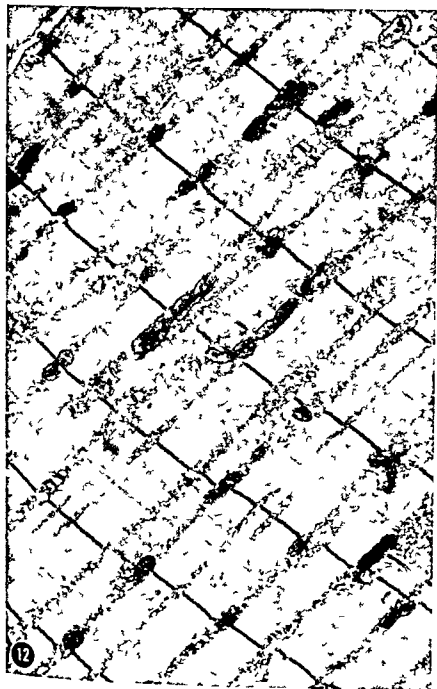


PLATE 5

EXPLANATION OF FIGURE

- 13 The *levator ani* from an intact mouse showing details of the organelles. Mitochondria are scattered singly in the interfibrillar space. The infoldings of the inner membrane form both cristae and tubules. Small dark intermitochondrial granules are common. The sarcoplasmic tubules of the longitudinal system are extensive and attached to the myofibrils at the Z lines (arrows). Triadic association of the longitudinally oriented tubules with the transverse tubules of the T system appears at all A-I junctions in this micrograph but may be missing at 25% of the usual sites. Sarcoplasmic granules must represent both glycogen and ribosomes but a distinct differentiation of two types is not possible in this preparation. Glutaraldehyde-osmium fixation. Lead citrate staining. $\times 40,000$



PLATE 6

EXPLANATION OF FIGURE

- 14 A cross section of a satellite cell nested into a muscle fiber in the *levator ani* of a *neuter* mouse. The nucleus shows much coarsely granulated chromatin and an ill-defined nucleolus. A small Golgi complex lies to the left of the nucleus. A few small mitochondria appear in the sparse granulated cytoplasm. The plasmalemmae of the satellite cell and the muscle fiber are in close proximity. There is no intervening glycocalyx except at the lateral margins. Here (see inset) there is a separate glycocalyx for each cell. More deeply along the interface of the two cells the two glycocalyces fuse thin and finally disappear. Glutaraldehyde-osmium fixation. Uranyl acetate-lead citrate staining. $\times 10\,000$



PLATE 7

EXPLANATION OF FIGURE

- 15 A longitudinal view of a satellite cell in an intact mouse. Only portions of the lips of the tangentially sectioned muscle fiber are seen encircling the satellite cytoplasm. An intervening glycocalyx is double in some areas and fused in others. The common close association of satellite cell, muscle nucleus, and capillary is illustrated. Glutaraldehyde-osmium fixation. Lead citrate staining. $\times 10,000$.



PLATE 8

EXPLANATION OF FIGURE

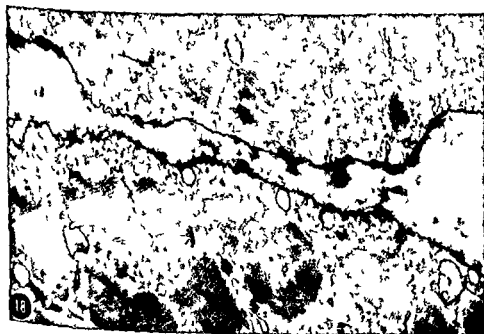
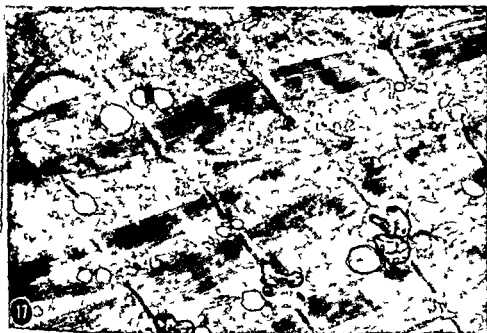
- 16 Cells of the endomysium of the *levator ani* of a *neuter* mouse. The pericyte displays two centrioles and an associated small Golgi complex. The cytoplasm is sparse and granular like the satellite. The nucleus characteristically shows thick clumps of coarsely granular chromatin at the karyotheca and in the karyoplasm. The pericyte is encircled by a glycocalyx which is in close apposition but is not fused with the glycocalyx of the capillary. The fibroblast lacks the glycocalyx. Its nuclear chromatin pattern is lighter than the pattern in pericytes and its cytoplasm contains fewer free ribosomes. The capillary is the type common to skeletal muscles. Glutaraldehyde-osmium fixation. Uranyl acetate lead citrate staining. $\times 16\ 000$

PLATE 9

EXPLANATION OF FIGURES

Levator ani from a rat castrated 22 days showing sarcoplasmic changes associated with atrophy Osmium fixation Lead cacodylate staining
× 20 000

- 17 A longitudinal section of the atrophying muscle fiber The myofibrils are separated by abnormal amounts of sarcoplasm Sarcoplasmic tubules are in disarray and apparently missing between some myofibrils Tubular attachments at the Z line are missing at many sites Myofilaments are frayed from the myofibrils Attachments at the Z-line appear more tenacious than attachments at the M line Dark granules appear (arrow) in the regions of overlap of thick and thin filaments
- 18 A cross section of the atrophying muscle fiber Dissassociation of myofilaments from myofibrils is evident Sarcolemma remains intact but wrinkled Sarcoplasmic tubules are sparse Arrow indicates dark granules corresponding to those indicated in figure 17



dies on Guinea Pig Oocytes

HISTOCHEMICAL OBSERVATIONS ON SOME PHOSPHATASES AND LIPID IN DEVELOPING AND IN ATRETIC OOCYTES AND FOLLICLES¹

ELEANOR C ADAMS ARTHUR T HERTIG AND SUSANNE FOSTER
*Department of Pathology Harvard Medical School
Boston Massachusetts*

ABSTRACT Normal guinea pig oocytes develop in an environment of AMPase within the granulosa cells of the wall the cumulus and the latter's projections that traverse the zona pellucida to terminate at the surface of the oocyte. Oocytes in developing non vesicular and small vesicular follicles have an ATPase activity at their surface which appears to indicate specialized absorptive mechanisms confined to these early stages of development. Acid phosphatase present in granules scattered throughout the cytoplasm of all developing oocytes may be evidence of a mechanism in this species whereby the oocyte hydrolyzes unidentified nutritional reserves.

Histologically normal appearing oocytes in atretic vesicular follicles may show deviations from the normal histochemical pattern i.e. clumping and subsequent loss of acid phosphatase activity or a band of AMPase activity at the periphery of the oocyte representing apparent enlargement of the terminals of projections of the cumulus. These deviations may reflect disturbances of granulosa cell-oocyte transfer as a consequence of beginning atretic processes in the follicle wall. By the eighth day of the estrous cycle the granulosa layer of many medium sized follicles has been invaded by a few long strands of nucleoside polyphosphatase positive thecal connective tissue often carrying a small blood vessel. This early stage of atresia is apparently followed by shedding of the granulosa layer and hypertrophy of the thecal layer which begins the transformation of atretic follicles into interstitial masses.

This histochemical study and a correlated electron microscopic study (Adams and Hertig 64) were initiated as preparation for a similar study now underway on human oocytes (Adams and Hertig 65). We hoped that by applying a variety of reparatory techniques in histochemistry and electron microscopy to developing or atretic follicles and their contained oocytes in an available laboratory animal we would be able to evaluate more efficiently similar but much less easily obtained material from human patients in the younger reproductive age. The guinea pig was chosen because its relatively long estrous cycle (16-17 days) allows a controlled study of the sequence of events in the maturation of follicles and oocytes. The histologic evidence for the maturation of a vesicular follicle within one estrous cycle in the guinea pig was reported in 1936 by Myers Dempsey and Young. Their observations on developing vesicular follicles were used as the basis for this study.

The application to guinea pig oocytes and follicles of histochemical techniques for a variety of phosphatases produced some results which vary considerably from those previously published for other mammalian species. The results of our studies are reported here in order to add to the growing evidence of species differences and similarities in the cellular physiology of maturing oocytes and their follicle walls.

In addition our histochemical studies of atretic oocytes indicate that certain precautions should be taken in the interpretation of the ultrastructure of any mammalian oocytes in vesicular follicles. Even though the oocyte may show no histologic evidence of atresia and the follicle wall only minimal evidence of atresia our histochemical studies show that subtle changes frequently have occurred in the oocyte. Such changes apparently involve

This research was supported entirely by grant HD-00137 Division of Human Development and Child Health formerly C 2451 of the National Institute of Health.

tional undoubtedly also reflect alterations in the ultrastructure. Therefore it seems hazardous to evaluate electron microscopic evidence of developmental vs. degenerative processes in mammalian oocytes in vesicular follicles unless the follicular stage is known and unless the follicle can be fixed intact so that both the oocyte and the follicle wall can be carefully examined for the earliest evidence of atresia.

MATERIAL AND METHODS

Immature female guinea pigs purchased locally, were held until they began to establish a regular estrous cycle of 16-17 days. This was confirmed by the periodic opening of the vagina for 2-3 days every 15-17 days. Thereafter they were checked at least once each evening and morning for evidence of copulatory response indicating active estrus (heat). This was indicated when a female (1) attempted to mount other females (2) exhibited lordosis when stroked or placed with a male or (3) allowed a male to actively mount her (Young 61). Thirty animals 3-9 months of age were sacrificed by a blow on the head on various scheduled days after at least one and usually multiple recorded heats. Ovaries were obtained on the first, second, fourth, eighth, twelfth and sixteenth days of the cycle and during heat (counting the estimated day of ovulation as day 1). Since ovulation occurs 8-10 hours after the onset of heat, those animals to be sacrificed for the recovery of matured follicles were sometimes observed constantly during the evening of expected estrus in order to time the onset of heat and thus to determine the time of subsequent sacrifice.

One ovary from each animal was fixed in Bouin's fluid for histologic survey of follicular and oocyte development. These ovaries were sectioned at 7 μ and every third section was serially mounted and stained with hematoxylin and eosin. The other ovary was fixed overnight in either chilled formol calcium (Baker 51) or formol phosphate with 7.5% sucrose (Holt 61). After washing for one to one and one half hours in running water it was placed in a freshly prepared solution of gum sucrose for three hours and was then rapidly frozen in a beaker of isopentane pre-

cooled to -70°C in a bath containing dry ice and acetone. These ovaries were serially sectioned in a cryostat at 10-12 μ —each section was mounted separately on a precooled gelatinized slide and dried briefly on a warm plate at 35°C. The slides were quickly examined with a phase microscope to record those serial sections containing oocytes and then were stored overnight at 4°C. By this means serial slides of a individual oocyte could be used for several different techniques the following day.

Incubation media for the nucleoside phosphatase activities were freshly prepared according to the method of Wachstein and Meisel (57) using 0.5 mg of substrate per ml of medium at pH 7.2. Adenosine triphosphate (ATP), adenosine diphosphate (ADP), adenosine 5-phosphate (AMP), and sodium glycerophosphate (NaGP) were the substrates used at this pH. Sodium glycerophosphate served as a control for the specificity of the nucleoside phosphatases. An additional slide was run as a water blank control in the complete medium without substrate. Sections were incubated 25 minutes at 37°C then thoroughly rinsed in distilled water and placed in dilute ammonium sulphate for 1-2 minutes. After a thorough wash in water they were mounted in glycerine jelly.

Slides for acid phosphatase activity were incubated for one hour according to the Gomori method at pH 5.0 as reported by Becker et al (60) using sodium glycerophosphate as substrate. Sodium glycerophosphate was also the substrate for alkaline phosphatase activity performed according to the Gomori method at pH 9.4 (Pearse 60).

Additional sections were stained by Sudan Black for lipid and occasionally others were post fixed on slides in Roseman's fluid and stained by the periodic acid Schiff method for glycogen.

OBSERVATIONS

Normally developing follicles

Histologic description

Primordial and non vesicular (primordial) follicles. At all stages of the estrous cycle, primordial and small primary follicles are found at the periphery of the ovary (fig. 2). Primordial oocytes measuring 20-25 μ in

eter surrounded by a single layer of and primitive follicular cells contain central nucleus with clumped chromatin. Ioannou (64) reported that this attracted stage of development follows large diplotene stage and becomes pre- dominant in resting oocytes of guinea pigs less than 60 days. These small follicles in a narrow band of dense cortex just beneath the subepithelial tunica albuginea.

Initial evidence of development to the primary follicle stage is an increase in the number of follicle cells as they become cuboidal. The oocyte begins to enlarge in diameter and its nucleus becomes vesicular. The single layer of cuboidal cells with prominent nucleoli are not observed after mitosis. Once the cuboidal cells of the follicle wall begin to become double layered however mitoses are frequently seen (fig. 3). During the development of the intraluminal non-vesicular follicle the oocyte grows markedly in diameter the granulosa wall becomes multilayered the zona pellucida is formed and the theca externa differentiates. In addition the follicle is carried deeper into the ovary where it lies within the cortex usually adjacent to an interstitial mass.

Vesicular (secondary) follicles. The histologic survey of our serial sections of ovaries examined on the first second fourth sixth twelfth and sixteenth days following an observed estrus indicates a maturation of the vesicular follicles during the period of one estrous cycle. These observations are in agreement with those reported by Myers Young and Dempsey (36). The growth and atresia of guinea pig follicles is schematically illustrated in figure 1 which is reprinted from Everett (61). As Myers et al. reported only a few of the many small vesicular follicles found in each ovary at about the fourth day of the estrous cycle are destined to produce the 1-3 mature follicles of the sixteenth day. (Although similar small follicles are present on later days of the cycle all apparently undergo atresia without maturing (fig. 1).) Developing follicles characteristic of the fourth day of the cycle have an eccentric crescent shaped antrum surrounded by a multilayered granulosa wall and a central granulosa mass forming a cumulus around the oocyte and a broad theca

interna layer (figs. 4, 5). They measure 0.2-0.3 mm in diameter to the periphery of the granulosa layer the external boundary of theca being hard to define in any follicle. Mitoses are prevalent in the cumulus and throughout both granulosa and theca interna layers. The oocyte is spherical measuring 65-70 μ in diameter (fig. 5). It has a vesicular nucleus which is central in the smaller follicles and often more eccentric in the larger ones of 0.3 mm. In Bouin's fixed material the substance of the zona pellucida is not preserved and is seen merely as a space traversed by projections from the inner layer of the cumulus.

By the eighth day normally developing follicles measure 0.6-0.7 mm in diameter have a thick wall of granulosa cells loosely attached to each other and a weblike cumulus attached at several points to the granulosa wall (fig. 6). Many mitoses can be seen in both the granulosa and thecal layers. The oocyte has an eccentric nucleus with a large vacuolated nucleolus (fig. 7). Its cytoplasm appears mottled due to lipid droplets having been dissolved out in the histologic preparation.

By the twelfth day of the cycle in each ovary there are usually 1 to 3 follicles

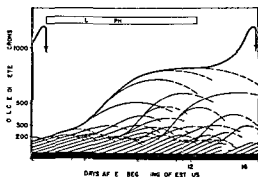


Fig. 1 A schematic representation of the follicular cycle in the guinea pig. The heavy solid curve represents the diameters of the largest follicles recalculated from the data of Myers Young and Dempsey (36). The arrow point indicates ovulation. The other solid curves and broken lines represent impressionistically the growth and atresia respectively of other groups of follicles that are not ordinarily destined for ovulation.

This diagram of the development and atresia of secondary follicles in guinea pig oocytes is reproduced from Everett (61).

measuring 0.8–0.9 mm whose peripheral granulosa layer is often luteinized or eosinophilic. Lacunae of fluid begin to collect forming a spongy zone at the base of the cumulus — actually a septum traversing the follicle (fig. 9). In contrast to the follicular cells the nuclei of the cumulus cells are widely separated by indistinct cytoplasm. The innermost row of these cells is forming a corona radiata. Their nuclei lie distal to the oocyte in an elongated cytoplasm which is adherent to the zona pellucida (fig. 8). Their delicate cytoplasmic processes project through the zona to the oocyte membrane.

During the sixteenth day the maturing follicles measure 1.0 mm or more and the granulosa cells become strikingly eosinophilic as luteinization continues. The lacunae of fluid in the base of the cumulus are larger (fig. 11). Just before the beginning of heat the eccentric nucleus of the oocyte develops a network of pale fibrils and a dense basophilic chromatin mass (fig. 10).

During heat the oocyte forms the first meiotic spindle (fig. 12), extrudes a polar body and begins to form the second meiotic spindle. The cells of the cumulus disperse and a coagulum is formed which loosely attaches the oocyte and surrounding corona radiata to the follicle wall (fig. 13). The follicle expands to over 1 mm in diameter. Only a very few ovaries examined during heat contained any normal appearing secondary follicles of any size other than the 1 to 3 matured follicles destined to ovulate.

HISTOCHEMICAL OBSERVATIONS

In contrast to oocytes in later stages of development the cytoplasm of most resting primordial oocytes has been somewhat difficult to preserve in frozen sections without distortion. Thus we have been unable to assess accurately the results of histochemical procedures in the primordial oocyte itself. Nevertheless no resting primordial oocyte appeared to contain any cytoplasmic enzymatic activity by any of the methods employed.

The superficial cortical cells as well as those of the tunica albuginea in the guinea pig ovary contain an *adenosine monophosphatase* activity indistinguishable from

that seen in the thin single layered primordial follicle cells (fig. 14). In developing early primary follicles AMPase activity is present at the periphery of the cuboidal follicle cells but is most prominent in the area between the innermost layer of these cells and the oocyte (fig. 15). From electron microscopic studies on guinea pig oocytes in these stages this area has been observed to contain a concentration of broad interdigitating projections arising from follicle cells (Adams and Hertig 1964). In later stages of multilaminar non vesicular follicles AMPase activity is seen in these projections that now traverse the developing zona pellucida to terminate at the cellular membrane of the oocyte. As intercellular spaces between granulosa cells become more prominent AMPase becomes localized at the periphery of each cell.

In small secondary follicles developing on the fourth day of the estrous cycle *adenosine monophosphatase* remains prominent at the margins of all granulosa cells (fig. 16). In these follicles just beginning to form an antrum the enzyme is now active immediately peripheral to the oocyte where it again delineates the meshwork of granulosa projections surrounding the zona. The delicate projections that traverse the zona, and the blunt terminals of these same projections at the oocyte membrane (fig. 17). By the eighth day stage there is no longer a dense band of activity peripheral to the zona (fig. 18) and in addition AMPase in the entire granulosa layer becomes somewhat less prominent (fig. 19). The projections of the follicle cells that traverse the zona become more delicate and widely spaced but retain their AMPase activity until the onset of heat at which time it is lost (figs. 18, 20, 21). Occasionally cytoplasmic granules of AMPase activity are present in the oocyte on the twelfth and later days of follicular development.

In double or multilayered non vesicular follicles a fuzzy rim of *adenosine triphosphatase* activity becomes prominent at the periphery of the oocyte (figs. 22, 23). While *adenosine diphosphate* is a substrate for ever activity in this area is only rarely seen (fig. 24). The rim of ATPase activity is still present around oocytes in 0.5–1.0 mm follicles of the four day stage (fig. 24).

(26) but we have never seen it in nor-
mally developing oocytes in larger follicles
after development. Oocytes in follicles
of similar size (0.2-0.3 mm) present at
later stages of the estrous cycle also show
ATPase activity (fig. 59).

A less specific nucleoside polyphospha-
tase activity produced with both ATP and
ADP develops in cytoplasmic granules in
oocytes of the larger primary follicles
(fig. 22). These remain small and dif-
ferentially distributed in the four-day follicles
(fig. 26) but subsequently become less
numerous. By the twelfth day those seen
with ATP as a substrate appear coarse and
somewhat more peripherally located (figs.
28) whereas with ADP as a substrate
the granules are smaller, more numerous
and more evenly distributed in the cyto-
plasm (fig. 29). Nucleoside polyphospha-
tase activity with both ATP and ADP as
substrates is also present in the vascular
and supporting cells of the theca in-
terna of all follicles (fig. 25) in interstitial
masses and in the supporting connective
tissue of the ovary. It is less prominent in
the tunica albuginea and is absent in the
serosal epithelium.

Sodium glycerophosphate as a substrate
at a similar neutral pH produces no activ-
ity in oocytes of any stage but in the theca
interna layer produces a slight reaction
localized similarly to an alkaline phosphatase
(fig. 60). In sections reacted as a
water blank the granulosa and theca cells
frequently contain a single black granule
which is interpreted as inorganic phos-
phate reaction produced in some unidentified
lipid. The oocytes are always free
from these granules.

In the small primary follicle stage the
oocyte begins to develop a few cytoplasmic
granules of acid phosphatase (fig. 30).
Such granules are distributed throughout
the cytoplasm of oocytes in developing
vesicular follicles of all sizes (figs. 32-33).
Cells of the cumulus also have a fine
dispersion of cytoplasmic activity. Activity
in macrophages invading the theca interna
is often seen in larger vesicular follicles.
During estrus there is a faint reaction in
the granulosa cells of matured follicles
and strongly reactive macrophages begin
to invade this layer as well (fig. 34).

Water blank controls frequently show a
granule of precipitate in the granulosa and
thecal layers as well as in the serosal
surface similar to that seen at neutral
pH (fig. 31).

As the primary follicle enlarges and
moves deeper in the ovarian cortex it be-
comes associated with the alkaline phos-
phatase positive cells of the interstitial
masses (fig. 36). Reactive theca interna
cells begin to appear around the primary
follicle (figs. 36 and 37). In the maturing
vesicular follicles alkaline phosphatase
activity in this layer continues to be pres-
ent (fig. 55) but does not become so prom-
inent as that seen in the hypertrophied
theca of atretic follicles (fig. 61).

Sudanophilia is diffuse in oocytes of pri-
mary follicles and probably represents
mitochondrial staining (fig. 38). Fat vacu-
oles develop in the small vesicular follicles
characteristic of the fourth day stage (fig.
39). These vacuoles increase rapidly in
number and fill the cytoplasm as the nu-
cleus becomes eccentrically located (figs.
40-42). Fine sudanophilic droplets are
present in the peripheral layers of the
granulosa wall of the mature 16-day fol-
licle and increase in prominence during
heat (fig. 41). Previous to this only a
single small granule of sudanophilia was
visible in some cells of the cumulus (fig.
42) and granulosa wall. These were in-
terpreted to be the same granules seen in
the water blank slides of neutral and acid
phosphatases (fig. 31). The cells of the
thecal layer are finely sudanophilic in the
secondary follicles.

Glycogen confined to the cells of the
cumulus only is prominent in mature fol-
licles of the sixteenth day. During heat it
is seen throughout the coagulum contain-
ing the oocyte.

Atretic follicles and oocytes

Normal and abnormal appearing pri-
mordial and primary follicles have been
observed throughout the estrous cycle. In
the primordial oocyte it is difficult to dis-
tinguish atretic processes from nuclear or
cytoplasmic distortion that may be caused
by preparatory technique. Occasionally
primordial sized oocytes with contracted
nuclei are seen in follicles whose cells are
cuboidal and are prematurely undergoing

mitosis. In primary follicles extreme eccentricity of the nucleus and irregularly arranged granulosa layers are evidence of atresia (fig. 43).

Early in the estrous cycle as new small vesicular follicles develop the follicles from the previous cycle are in various stages of atresia leading to the formation of new interstitial masses (figs. 46-50). This transition proceeds gradually by the sloughing of the granulosa layer into the cavity and the hypertrophy of the theca interna followed by the organization of the antrum. The thecal hypertrophy results in an interstitial mass in whose central cavity a degenerating oocyte can often be seen (figs. 49-50). These oocytes usually have undergone cleavage (fig. 49) or fragmentation but occasionally they may show bizarre nuclear changes such as large astral rays associated with clumps of basophilic (fig. 82) or multiple micronuclei (fig. 83). These degenerating oocytes contain large deposits of lipid (fig. 69). Although their acid phosphatase activity has previously been lost (fig. 75) a cytoplasmic substance occasionally is found that gives a black precipitate with the acid phosphatase reaction and also with its water blank control (figs. 76-77). Such a reaction is characteristic of the deposition of insoluble salts. Acid phosphatase (fig. 75) and sudanophilin (fig. 69) are seen in the macrophages of the organizing antrum. As the thecal layer hypertrophies to form an interstitial mass its alkaline phosphatase (figs. 61-62) and lipid content becomes more pronounced (figs. 75-39) and acid phosphatase (fig. 32) appears faintly in a perinuclear distribution.

The atretic processes which overwhelm the great majority of vesicular follicles may become apparent at any stage of their development. At all stages of the cycle the oocytes in small vesicular follicles may show a precocious eccentricity of the nucleus (fig. 44). The granulosa layer or the cumulus is often abnormally thin in spite of the presence of mitotic figures in these layers (fig. 44). In these small follicles there also may be sloughing of granulosa cells into the cavity (fig. 45). The cells of the granulosa layer retain their AMPase activity until they are shed (fig. 68). In the oocyte acid phosphatase is

occasionally seen in paranuclear clumps rather than in dispersed granules (fig. 49). Oocytes in non-developing small follicles often retain their peripheral rim of ATPase (fig. 59).

Prominent on the eighth day of the cycle in medium sized follicles that seem to be otherwise developing normally is an invasion of the granulosa wall and the cumulus by one or two long strands of connective tissue cells from the theca interna (figs. 51-52). These strands which usually carry a small blood vessel (fig. 54) traverse the cumulus but do not invade the oocyte or zona. Histologic study of serial sections through many follicles in the eighth day of the cycle reveals that only a few medium sized follicles appear to escape this form of atresia. The nucleoside polyphosphatase activity (with ATP as ADP) of the invading cells allows one to identify quickly this atretic process in scanning an ovary of this stage for normally maturing follicles (fig. 53). The invading cells are not the alkaline phosphatase positive theca interna cells (fig. 55).

After the twelfth day of the cycle the two or three follicles destined to ovulate from each ovary are usually recognizable histologically by the increased eosinophilia of the granulosa layer. This distinguishes them from other non-maturing follicles of similar or smaller size which may not yet show evidence of atresia. Most of the non-maturing follicles however do show beginning or widespread sloughing of the granulosa cells into the antrum or hypertrophy of the theca or both (fig. 46). The sloughed granulosa cells are rounded and AMPase negative (fig. 63) but those still within the wall retain an active cytoplasmic reaction. In spite of this indication of involution, mitoses still occur in the wall or the cumulus (fig. 46). In the granulosa layer of some sloughing atretic follicles occasional strands of nucleoside polyphosphatase positive thecal elements are present. This finding is the residual evidence of the earlier invasive (8th day) stage. In other involuting follicles of the twelfth to sixteenth days of the cycle showing more advanced shedding of the granulosa layer a broad stalk of thecal tissue projects into the cavity near the base of the cumulus (fig. 56). This again is interpreted as a

due to the thin vascular strands seen in the invasive stage observed initially on the eighth day of the cycle (figs 51-52-53). Alkaline phosphatase activity becomes more pronounced in the hypertrophied cells of most moderate to large atretic follicles (fig 61). Lipid is only very gradually accumulated in this layer (fig 66). Few follicles of this size fail to show such marked hypertrophy and thus apparently do not contribute to the interstitial tissue. Additional evidence of atresia is a faint, generalized nucleoside polyphosphatase activity in the cytoplasm of the basal granular layers of follicles (figs 57-59). Toward the end of the cycle many medium to large non-maturing follicles contain a prominent row of sudanophilic and acid phosphatase positive cells limited to the destruction of granulosa and thecal layers. These are interpreted as the macrophages which only in the matured preovulatory follicle go on to invade the granulosa (fig 34). In atretic follicles the granulosa remains free from both lipid (fig 66) and acid phosphatase activity (fig 74).

Although many oocytes in medium to large follicles with some evidence of atresia may look normal histologically (fig 46) they frequently show deviations from the normal histochemical pattern. AMPase activity may appear at the oocyte surface as a dense ring interpreted as enlargement or even fusion of the terminals of the projections of the follicle cells (figs 5-67). This contrasts sharply with the normal (figs 17-18-20). Acid phosphatase granules may be clumped into masses during early atresia (figs 71-72) but with increasing granulosa shedding become strikingly reduced in number and size (fig 74) and subsequently disappear again. This differs significantly from the normal (figs 33-35). Fat droplets in the oocyte increase in size or coalesce (figs 64-66) in contrast to the normal distribution (fig 42).

With the onset of heat most oocytes in non-ovulating follicles of varied sizes and stages of atresia begin to form spindles and to extrude a polar body (figs 78-80). Some undergo cleavage to morula-like forms (fig 81). Occasionally this abnormal nuclear maturation is seen in oocytes

in small follicles that do not yet show cytologic evidence of atresia (fig 78).

At all stages of the cycle there are a variable number of normal appearing follicles which are not developing synchronously with those follicles whose growth was initiated soon after estrus. They vary greatly in size and may be derived from small follicles arising throughout the cycle (fig 1). It is difficult to determine how many of them will eventually contribute to the pool of interstitial masses seen in the ovary throughout the cycle.

DISCUSSION

Normally developing oocytes and follicles

1 Nucleoside monophosphatase (AMPase)

Although the function of this enzyme in the economy of the guinea pig oocyte is unknown it is always present at the immediate periphery of the resting and maturing oocyte. Its presence in the follicular projections that terminate at the oocyte membrane suggests that there may be specialized routes for various substances reaching or leaving the developing guinea pig oocyte. These projections may transport material synthesized in the cells of the cumulus and delivered directly to the surface of the oocytes. During estrus the loss of the activity of this enzyme in the projections traversing the zona pellucida correlates with the time of dispersal of the outer layers of cumulus cells. It is an indication that these cells rather abruptly are no longer required for the further maturation of the oocyte. The reactivity of the entire granulosa layer may indicate some role in the production or regulation of the follicular fluid. Anderson and Beams (60) the first to study the ultrastructure of the guinea pig oocyte postulated that the follicle cells of the cumulus synthesize a nutrient which is liberated into the zona pellucida and reaches the oocyte by diffusion or pinocytosis.

Other mammalian species have not to our knowledge been reported to contain AMPase in the granulosa wall of developing follicles. McKay et al (61) reported the presence of this enzyme only in the stroma surrounding follicles in the human ovary. In the mouse Novikoff et al (61) reported its presence only in the germinal

mitosis. In primary follicles extreme eccentricity of the nucleus and irregularly arranged granulosal layers are evidence of atresia (fig 43).

Early in the estrous cycle as new small vesicular follicles develop the follicles from the previous cycle are in various stages of atresia leading to the formation of new interstitial masses (figs 46-50). This transition proceeds gradually by the sloughing of the granulosal layer into the cavity and the hypertrophy of the theca interna followed by the organization of the antrum. The thecal hypertrophy results in an interstitial mass in whose central cavity a degenerating oocyte can often be seen (figs 49-50). These oocytes usually have undergone cleavage (fig 49) or fragmentation but occasionally they may show bizarre nuclear changes such as large astral rays associated with clumps of basophilia (fig 82) or multiple micronuclei (fig 83). These degenerating oocytes contain large deposits of lipid (fig 69). Although their acid phosphatase activity has previously been lost (fig 75) a cytoplasmic substance occasionally is found that gives a black precipitate with the acid phosphatase reaction and also with its water blank control (figs 76-77). Such a reaction is characteristic of the deposition of insoluble salts. Acid phosphatase (fig 75) and sudanophilia (fig 69) are seen in the macrophages of the organizing antrum. As the thecal layer hypertrophies to form an interstitial mass, its alkaline phosphatase (figs 61-62) and lipid content becomes more pronounced (figs 75-39) and acid phosphatase (fig 32) appears faintly in a perinuclear distribution.

The atretic processes which overwhelm the great majority of vesicular follicles may become apparent at any stage of their development. At all stages of the cycle the oocytes in small vesicular follicles may show a precocious eccentricity of the nucleus (fig 44). The granulosal layer or the cumulus is often abnormally thin in spite of the presence of mitotic figures in these layers (fig 44). In these small follicles there also may be sloughing of granulosal cells into the cavity (fig 45). The cells of the granulosal layer retain their AMPase activity until they are shed (fig 68). In the oocyte acid phosphatase is

occasionally seen in paranuclear clumps rather than in dispersed granules (fig 40). Oocytes in non developing small follicles often retain their peripheral rim of ATPase (fig 59).

Prominent on the eighth day of the cycle in medium sized follicles that seem to be otherwise developing normally is an invasion of the granulosal wall and the cumulus by one or two long strands of connective tissue cells from the theca interna (figs 51-52). These strands which usually carry a small blood vessel (fig 54) traverse the cumulus but do not invade the oocyte or zona. Histologic study of serial sections through many follicles in the eighth day of the cycle reveals that only a few medium sized follicles appear to escape this form of atresia. The nucleoside polyphosphatase activity (with ATP or ADP) of the invading cells allows one to identify quickly this atretic process. In scanning an ovary of this stage for normally maturing follicles (fig 53) the invading cells are not the alkaline phosphatase positive theca interna cells (fig 50).

After the twelfth day of the cycle the two or three follicles destined to ovulate from each ovary are usually recognizable histologically by the increased eosinophilia of the granulosal layer. This distinguishes them from other non maturing follicles of similar or smaller size which may not yet show evidence of atresia. Most of the non maturing follicles however do show beginning or widespread sloughing of the granulosal cells into the antrum or hypertrophy of the theca or both (fig 46). The slow shed granulosal cells are rounded and AMPase negative (fig 63) but those still within the wall retain an active cytoplasmic rim. In spite of this indication of involution, mitoses still occur in the wall or the cumulus (fig 46). In the granulosal layer of some sloughing atretic follicles occasional strands of nucleoside polyphosphatase positive thecal elements are present. This finding is the residual evidence of the earlier invasive (8th day) stage. In other involuting follicles of the twelfth to sixteenth days of the cycle showing more advanced shedding of the granulosal layer a broad stalk of thecal tissue projects into the cavity near the base of the cumulus (fig 56). This again is interpreted as a

vel to the thin vascular strands seen in the invasive stage observed initially on the eighth day of the cycle (figs 51 52 53). Alkaline phosphatase activity becomes more pronounced in the hypertrophied ca of most moderate to large atretic follicles (fig 61). Lipid is only very gradually accumulated in this layer (fig 66). Few follicles of this size fail to show such local hypertrophy and thus apparently do not contribute to the interstitial tissue. Additional evidence of atresia is a faint generalized nucleoside polyphosphatase activity in the cytoplasm of the basal granular layers of follicles (figs 57-59). Toward the end of the cycle many medium to large non maturing follicles contain a prominent row of sudanophilic and acid phosphatase positive cells limited to the junction of granulosa and thecal layers. These are interpreted as the macrophages which only in the matured preovulatory follicle go on to invade the granulosa (fig 34). In atretic follicles the granulosa remains free from both lipid (fig 66) and acid phosphatase activity (fig 74). Although many oocytes in medium to large follicles with some evidence of atresia may look normal histologically (fig 46) they frequently show deviations from the normal histochemical pattern. AMPase activity may appear at the oocyte surface as a dense ring interpreted as an invagination or even fusion of the terminals of the projections of the follicle cells (figs 5 67). This contrasts sharply with the normal (figs 17 18 20). Acid phosphatase granules may be clumped into masses during early atresia (figs 71 72) but with increasing granulosa shedding become strikingly reduced in number and size (fig 44) and subsequently disappear again. This differs significantly from the normal (figs 43 35). Extracellular material in the oocyte increases in size or coalesce (figs 64 66) in contrast to the normal distribution (fig 42). With the onset of heat most oocytes in non-ovulating follicles of varied sizes and stages of atresia begin to form spindles and to extrude a polar body (figs 78-80). Some undergo cleavage to morula like forms (fig 81). Occasionally this abnormal nuclear maturation is seen in oocytes

in small follicles that do not yet show cytologic evidence of atresia (fig 78).

At all stages of the cycle there are a variable number of normal appearing follicles which are not developing synchronously with those follicles whose growth was initiated soon after estrus. They vary greatly in size and may be derived from small follicles arising throughout the cycle (fig 1). It is difficult to determine how many of them will eventually contribute to the pool of interstitial masses seen in the ovary throughout the cycle.

DISCUSSION

Normally developing oocytes and follicles

1 Nucleoside monophosphatase (AMPase)

Although the function of this enzyme in the economy of the guinea pig oocyte is unknown it is always present at the immediate periphery of the resting and maturing oocyte. Its presence in the follicular projections that terminate at the oocyte membrane suggests that there may be specialized routes for various substances reaching or leaving the developing guinea pig oocyte. These projections may transport material synthesized in the cells of the cumulus and delivered directly to the surface of the oocytes. During estrus the loss of the activity of this enzyme in the projections traversing the zona pellucida correlates with the time of dispersal of the outer layers of cumulus cells. It is an indication that these cells rather abruptly are no longer required for the further maturation of the oocyte. The reactivity of the entire granulosa layer may indicate some role in the production or regulation of the follicular fluid. Anderson and Beams (60) the first to study the ultrastructure of the guinea pig oocyte postulated that the follicle cells of the cumulus synthesize a nutrient which is liberated into the zona pellucida and reaches the oocyte by diffusion or pinocytosis.

Other mammalian species have not to our knowledge been reported to contain AMPase in the granulosa wall of developing follicles. McKay et al (61) reported the presence of this enzyme only in the stroma surrounding follicles in the human ovary. In the mouse Novikoff et al (61) reported its presence only in the germinal

epithelium Arvy (60) reported its presence in the rabbit ovary at the periphery of the oocyte between the zona pellucida and the surface of the oocyte. Although she did not report the visualization of the projections of the cumulus cells in the zona it is possible that the rabbit may be similar to the guinea pig in the localization near the oolemma. Her report however described a granulosa rich only in alkaline phosphatase.

2 Nucleoside polyphosphatases

The strong reaction for this class of enzymes using either ATP or ADP as a substrate seen in many structures of the guinea pig ovary is similar in distribution to that reported by Novikoff et al (61) in the mouse ovary and by Arvy (60) in the rabbit. In addition guinea pig oocytes within large primary follicles or small secondary follicles contain numerous fine cytoplasmic granules of activity. In oocytes of larger follicles only a few coarse granules were seen. The precise localization of these intracytoplasmic granules is unknown and awaits histochemical electron microscopic study.

A somewhat more specific reaction namely for nucleoside triphosphatase was seen in a narrow fuzzy halo at the periphery of the oocyte during the primary and very early secondary follicle stages. It is during these early stages that microvilli begin to protrude from the oocyte membrane into the zona pellucida and a complex system of peripheral organelles is being differentiated within the oocyte cytoplasm (Adams and Hertig 64). Therefore we believe this nucleoside triphosphatase may well be localized on or near these microvilli. Thus in contrast to the AMPase of the follicular projections this enzyme may be involved in the absorptive capacity of the oolemma for substances perhaps filtering across the zona pellucida from the follicular fluid. Moreover the presence of this enzyme at the periphery of the oocyte in its early stages of development and its absence as the follicle enlarges beyond 0.3 mm diameter appear to reflect changes in the absorptive mechanism during development of the oocyte. Our unpublished electron microscopic data show that microvilli are present in maturing

oocytes as late as the twelfth day stage. This is however long after the disappearance of ATPase and may represent altered function of the microvilli. In mouse ovaries Novikoff et al (61) observed that with ATP as a substrate there was intense staining of the zona pellucida whereas with ADP as a substrate the zona of an occasional oocyte was negative. These authors also postulated a correlation between this activity and the presence of microvilli on the surface of the oocyte and interpreted the activity as indicating the presence of either a polyphosphatase or the presence of both ATPase and ADPase. In the guinea pig oocyte reactivity with ADP as a substrate was only rarely observed and even the reactivity with ATP appeared to be dependent on a very brief fixation time. This particular localized sensitivity to technical procedures may indicate the presence of an enzyme or enzymes in the oolemma different from nucleoside polyphosphatases elsewhere in the ovary. The latter enzymes withstood longer fixation times in our hands.

3 Acid phosphatase

This enzyme is present as discrete cytoplasmic granules in all developing guinea pig oocytes. We have been unable to correlate the size or number of reactive granules with the stage of development. The variation in size of the granules has seemed to depend on subtle differences in technical preparation since all normal oocytes in any one ovary regardless of their stage of development contain similar sized granules. Therefore we have attributed this variation to the degree to which the organelles containing the enzyme became swollen during the fixation and freezing processes.

Although the presence of this enzyme in a variety of cells has been correlated with the presence of lysosomes — membrane bound structures containing a variety of hydrolytic enzymes — our previous electron microscopic study of the early developing guinea pig oocytes did not reveal an organelle morphologically recognizable to us as a lysosome. We did however find large vesicles containing a slightly dense substance which might from the point of view of cytoplasmic distribution be p

the sites for the ultrastructural localization of this enzyme. These were expanded into vesicles of rough endoplasmic reticulum and were postulated to be areas for possible storage or synthesis of material within the oocyte (Adams and Hertig 64). Histochemical observations on an electron microscopic level will obviously be required to localize the intracytoplasmic site of activity. The function of acid phosphatase within the developing oocyte is unknown but its presence could indicate this hydrolytic enzyme is required for the utilization of some nutritional reserve. Although in the guinea pig lipid appears to be the principal material stored in the cytoplasm, the acid phosphatase granules can be seen by light and phase microscopy to be distinct structures separate from the lipid droplets. This enzymatic activity appears in developing oocytes before the stage when fat droplets can be identified histologically.

Acid phosphatase is also present in macrophages in the thecal layer of the follicle. Just before ovulation considerable numbers of these phagocytic cells invade the granulosa layer of the matured follicle. Their presence here may be related to the loosening of this layer in preparation for the penetration of thecal vessels and its conversion into a corpus luteum.

Arvy (60) reported that the oocyte and granulosa layer in rabbit ovaries were rich in acid phosphatase. McKay et al (61) studying the human and using acetone fixation and paraffin sections reported the presence of acid phosphatase in oocytes, granulosa and theca in preantral follicles and in the granulosa and thecal layers of large Graafian follicles. Our own recent unpublished studies of similar human material in formalin fixed frozen sections show acid phosphatase activity in the follicular wall but not in the oocyte. It is now recognized that an acetone paraffin technique allows diffusion of acid phosphatase activity. Lobel et al (61) reported the absence of acid phosphatase in healthy follicles and in all oocytes of rat ovaries.

4 Alkaline phosphatase

This enzyme was never found in the oocytes nor in the granulosa layer of de-

veloping follicles. Its presence in the thecal cells of non vesicular and vesicular follicles and in the interstitial masses may be involved in some unknown way in the production of estrogen.

Studies of other mammalian species have indicated a variety of combinations of alkaline phosphatase localizations as reported in a review by Jacoby (62). Both the hamster (Knigge and Leatham 56) and the rabbit (Arvy 60) have a granulosa layer rich in alkaline phosphatase with lesser amounts or absence of activity in the theca. Most other species however including humans (McKay et al 61) have been reported to contain alkaline phosphatase in the thecal layer (Jacoby 62). We know of no other species that has been reported to have a combination similar to that reported here for guinea pigs i.e. a strong nucleoside monophosphatase activity in the granulosa combined with a strong alkaline phosphatase activity in the thecal layer.

5 Sudanophilus

Fat droplets appear in the guinea pig oocyte in developing follicles at about the fourth day of the cycle. De Geeter (54) who studied some histochemical aspects of oocytes and fertilized ova in guinea pigs, rats and rabbits suggested that lipid appears to be the main nutritional storage reserve in guinea pig oocytes. In this connection it is of interest that lipid droplets appear soon after the stage when our previous electron microscopic observations on primordial and primary follicles led us to conclude that the oocyte had become equipped for the absorption, utilization and intracellular transport of material delivered to its surface membrane (Adams and Hertig 64). The presence of fat droplets in oocytes of the sow, horse, cat and dog were noted by Jacoby (62) who reviewed reports of their possible source from the yolk nucleus and/or from cells of the cumulus.

A faint sudanophilia is present in cells in the thecal layer of developing follicles. It also appears in the peripheral layers of the granulosa in matured follicles where it may be related to the "luteinization" of this layer and its subsequent transformation to a corpus luteum. The true relation

ship of sudanophilia in the follicle wall to steroid production and/or secretion is uncertain since we did not attempt to demonstrate steroid 3B or dehydrogenase activity on these formalin fixed frozen sections. The relationship of sudanophilia to other indirect histologic tests for hormone production is discussed fully by Jacoby (62) who reviewed a variety of reports on several species.

6 Glycogen

Glycogen deposits appear in the cells of the cumulus just before heat as well as in the coagulum during heat. This may be evidence of the cessation of the transport to the oocyte of glycogen precursors from the cells of the cumulus and the consequent deposition of glycogen in these cells. The appearance of glycogen in these areas occurs at the same time that the follicular projections lose their adenosine monophosphatase reactivity. In the guinea pig the cells of the outer layers of the cumulus are dispersed during heat and those of the corona radiata are detached from the ovum soon after ovulation (Hunt and Chang 64).

Atretic oocytes and follicles

There are three morphologic aspects of atresia: those involving the oocyte, the follicle, and the combination of these two in relation to the cycle. In primordial primary (non vesicular) and very small secondary (vesicular) follicles, the earliest sign of abnormality is frequently detected by the eccentric location of the egg nucleus. This would seem to indicate that at these stages abnormal differentiative processes are initiated within the oocyte itself and are independent of the stage of the cycle. Hisaw (47) observed that the arrangement of the granulosa of a primordial follicle is apparently under the control of the ovum. Whether or not abnormal oocytes are indeed the cause of the poorly developed or disorganized granulosa layers seen in many of our non maturing primary and small secondary follicles has not been clarified by any of the present observations.

The phase of the estrous cycle seems to be related to the atretic processes that overwhelm the great majority of vesicular follicles whose apparently normal development is initiated soon after estrus. This

cyclic atresia appears to be initiated in the follicle wall with secondary effects on the oocyte. Initially this form of atresia can be seen in ovaries examined on the eighth day of the cycle when an invasion of the granulosa layer and the cumulus by delicate strands of vascularized connective tissue is taking place. It is easily observed in nucleoside polyphosphatase preparations of moderately large follicles but less easily seen in sections stained by H and E. The invasive process appears to be evanescent since examination of ovaries on later days of the cycle shows no continuation of the process. Instead of the latter beginning or advanced shedding of granulosa cells is seen in follicles with residual strands of invasive thecal elements in the granulosa layer. This phenomenon of thecal invasion appears to be the earliest indication of a selective atretic process which is possibly under endocrine control. This interpretation is based on two observations: (1) that these invasive stages are seen in many follicles that had apparently begun their development normally and (2) that the number of 0.6-0.7 mm follicles that had escaped this invasion by the eighth day of the cycle approximately equals the number of follicles which by the twelfth day show obvious evidence of atresia, i.e. eosinophilia of the granulosa wall. Thus the critical period when the follicles destined to undergo atresia are separated from those destined for maturation has been reached by the eighth day—well before the twelfth day when Dempster (37) reported that some guinea pig follicles are competent, i.e. capable of being ovulated. A causal relationship between the vascularized connective tissue invasion and the subsequent shedding of the granulosa and the hypertrophy of the thecal layer in atretic follicles has not been clearly defined by this study. In fact we do not know whether this invasion is cause of or a response to a subtle beginning of atresia. In a discussion of causal factors of atresia, Ingram (62) observed that many experimental procedures which affect the rate of atresia also involve some alteration of the supply of gonadotropin. In commenting on the possible control of the pituitary of the variation of atretic processes he observed that the "vascular

individual follicles may also participate in the process provided by a relatively poor blood supply (and hence a low level of gonadotropin) probably being the first to become atretic.

By our criteria the presence of even one sloughed granulosa cells in any serially sectioned follicle indicated atresia irrespective of the presence of mitotic figures. As previously observed by Schmidt (12) the stimulus to growth in the follicle wall revealed by mitotic figures continues despite rather widespread sloughing of mitotic figures in the cumulus. Indeed mitotic figures in the cumulus can often be found in follicles with advanced antral shedding. The abnormal appearance of nucleoside polyphosphatase in the cytoplasm of the basal granulosa cells often appeared to be an early evidence of atresia and to be correlated with shedding of the more distal layers into the antrum. This breakdown of the granulosa layer was accompanied by neither the appearance of acid phosphatase as was reported by Lobel et al. (61) in the rat nor the dramatic increase in lipids reported in a variety of mammals by Guraya and Greenwald (64).

In many follicles with sloughing granulosa cells the oocyte often appears normal histologically as observed previously by Rowlands (56). In some of our follicles with only minimal atresia however the contained oocyte though appearing normal histologically showed histochemical evidence of abnormality. The nature of these aberrations appears to indicate the sensitivity of the oocyte to the integrity of its follicular environment. In AMPase preparations the visualization of the apparent fusion of the terminals of the granulosa projections at the periphery of the oocyte appeared to be histochemical evidence of interruption of granulosa cell-oocyte transfer. The clumping of acid phosphatase activity in the cytoplasm of oocytes in follicles with early atresia may also reflect the lack of orderly transport to the oocyte of some nutrient supplied to it from the environment. The apparently rapid disappearance of this activity in the oocyte as the follicle continues to degenerate indicates that this hydrolytic enzyme is not involved in the dissolution of this cell. The enlarged lipid droplets in de-

generating oocytes may be an indication that this nutritional reserve can no longer be utilized.

Just before ovulation most oocytes of non-ovulating follicles contain maturation spindles with or without polar body formation. This phenomenon and the subsequent development of micronuclei morula like formation and bizarre nuclear transformations can be followed in degenerating oocytes as the follicle becomes transformed into an interstitial mass. Harman and Kargis (38) postulated that the stimulus for this abnormal maturation division in the guinea pig is related in some way to the presence of sloughed or necrotic granulosa cells. On the other hand our observation of the presence of spindles in oocytes in occasional small follicles not yet showing cytologic evidence of atresia supports suggestions made in discussions by Hammond (61), Chang (61) and Pincus (61). These authors postulate that such spindles may form at about the time of ovulation due to release from an unidentified factor that inhibits maturation and cleavage.

ACKNOWLEDGMENT

The authors gratefully acknowledge the participation in this project by Mr Arlo Collins who faithfully recorded his observations on the estrous cycles of these guinea pigs. In addition thanks are due to Mrs Audrey Hadfield for photographic assistance and to Mrs Millicent Snow for secretarial help.

LITERATURE CITED

- Adams E. C. and A. T. Hertig 1964 Studies on guinea pig oocytes. I. Electron microscopic observations on the development of cytoplasmic organelles in oocytes of primordial and primary follicles. *J. Cell Biol.* 21: 397-427.
- 1965 Annulate lamellae in human oocytes in primordial and primary follicles. *J. Cell Biol.* 27: 119A.
- Anderson E. and H. W. Beams 1960 Cytological observations on the fine structure of the guinea pig ovary with special reference to the oögonium, primary oocyte and associated follicle cells. *J. Ultrastruct. Res.* 3: 432-446.
- Arvy L. 1960 Contribution à l'histoenzymologie de l'ovaire. *Z. Zellforsch.* 51: 406-420.
- Baker J. R. 1951 *Cytological Technique*. John Wiley and Sons Inc. New York.
- Becker N. H., S. Goldfisher, W. Shin and A. B. Novikoff 1960 The localization of enzyme

ship of sudanophilia in the follicle wall to steroid production and/or secretion is uncertain since we did not attempt to demonstrate steroid 3 β ol dehydrogenase activity on these formalin fixed frozen sections. The relationship of sudanophilia to other indirect histologic tests for hormone production is discussed fully by Jacoby (62) who reviewed a variety of reports on several species.

6 Glycogen

Glycogen deposits appear in the cells of the cumulus just before heat as well as in the coagulum during heat. This may be evidence of the cessation of the transport to the oocyte of glycogen precursors from the cells of the cumulus and the consequent deposition of glycogen in these cells. The appearance of glycogen in these areas occurs at the same time that the follicular projections lose their adenosine monophosphatase reactivity. In the guinea pig the cells of the outer layers of the cumulus are dispersed during heat and those of the corona radiata are detached from the ovum soon after ovulation (Hunt and Chang '64).

Atretic oocytes and follicles

There are three morphologic aspects of atresia: those involving the oocyte, the follicle, and the combination of these two in relation to the cycle. In primordial primary (non vesicular) and very small secondary (vesicular) follicles the earliest sign of abnormality is frequently detected by the eccentric location of the egg nucleus. This would seem to indicate that at these stages abnormal differentiative processes are initiated within the oocyte itself and are independent of the stage of the cycle. Hisaw (47) observed that the arrangement of the granulosa of a primordial follicle is apparently under the control of the ovum. Whether or not abnormal oocytes are indeed the cause of the poorly developed or disorganized granulosa layers seen in many of our non maturing primary and small secondary follicles has not been clarified by any of the present observations.

The phase of the estrous cycle seems to be related to the atretic processes that over-whelm the great majority of vesicular follicles whose apparently normal development is initiated soon after estrus. This

cyclic atresia appears to be initiated in the follicle wall with secondary effects on the oocyte. Initially this form of atresia can be seen in ovaries examined on the eighth day of the cycle when an invasion of the granulosa layer and the cumulus by delicate strands of vascularized connective tissue is taking place. It is easily observed in nucleoside polyphosphatase preparations of moderately large follicles but less easily seen in sections stained by H and E. The invasive process appears to be evident since examination of ovaries on later days of the cycle shows no continuation of the process. Instead of the latter beginning or advanced shedding of granulosa cells is seen in follicles with residual strands of invasive thecal elements in the granulosa layer. This phenomenon of thecal invasion appears to be the earliest indication of a selective atretic process which is possibly under endocrine control. This interpretation is based on two observations: (1) that these invasive stages are seen in many follicles that had apparently begun their development normally and (2) that the number of 0.6-0.7 mm follicles that had escaped this invasion at the eighth day of the cycle approximates the number of follicles which by the twelfth day show obvious evidence of maturity, i.e. eosinophilia of the granulosa wall. Thus the critical period when the follicles destined to undergo atresia are separated from those destined for maturation has been reached by the eighth day, well before the twelfth day when Dempsey (37) reported that some guinea pig follicles are competent, i.e. capable of being ovulated. A causal relationship between the vascularized connective tissue invasion and the subsequent shedding of the granulosa and the hypertrophy of the thecal layer in atretic follicles has not been clearly defined by this study. In fact we do not know whether this invasion is a cause of or a response to a subtle beginning of atresia. In a discussion of causal factors of atresia Ingram (62) observed that many experimental procedures which affect the rate of atresia also involve some alteration of the supply of gonadotropin. In commenting on the possible control by the pituitary of the variation of atretic processes he observed that the "vascular-

- activities in the rat brain J Biophysic and Biochem Cytol 8 649-663
- Chang M C 1961 Discussion p 54 following Pincus G and A P Merrill The Role of Steroids in the Control of Mammalian Ovulation In Control of Ovulation Ed by C A Villee Pergamon Press New York
- Dempsey E W 1937 Follicular growth rate and ovulation after various experimental procedures in the guinea pig Am J Physiol 120 126-132
- Everett J W 1961 The mammalian female reproductive cycle and its controlling mechanisms In Sex and Internal Secretions Ed by W C Young Williams and Wilkins Company Baltimore Vol I Chap VIII 497-555
- de Geeter L 1954 Études sur la structure de l'oeuf vierge et les premiers stades du développement chez le cobaye et le lapin Arch Biol (Paris) 65 363-436
- Guraya S S and G S Greenwald 1964 A comparative histochemical study of interstitial tissue and follicular atresia in the mammalian ovary Anat Rec 149 411-434
- Hammond J Jr 1961 Discussion p 35 following Noyes R W T H Cleve and A M Yamate Follicular Development Ovarian Maturation and Ovulation in Ovarian Tissue Transplanted to the Eye In Control of Ovulation Ed by C A Villee Pergamon Press New York
- Harmon M T and H D Kirgis 1938 The development and atresia of the Graafian follicle and the division of intra ovarian ova in the guinea pig Am J Anat 63 79-99
- Hisaw F L 1947 Development of the Graafian follicle and ovulation Physiol Rev 27 95-119
- Holt S J and R M Hicks 1961 The localization of acid phosphatase in rat liver cells as revealed by combined cytochemical staining and electron microscopy J Cell Biol 11 47-66
- Hunt D M and M C Chang 1964 Fertilization and cleavage of guinea pig ova Anat Rec 148 378
- Ingram D L 1962 Atresia In The Ovary Ed by S Zuckerman A M Mandl and P Eckstein Academic Press New York vol I Chap IV 247-273
- Ioannou J M 1964 Oogenesis in the guinea pig J Embryol exp Morph 12 673-691
- Jacoby F 1962 Ovarian Histochemistry In The Ovary Ed by S Zuckerman A M Mandl and P Eckstein Academic Press New York vol I Chap III 189-245
- Knigge K M and J H Leatham 1956 Growth and atresia of follicles in the ovary of the hamster Anat Rec 124 679-698
- Lobel B L R M Rosenbaum and H W Dore 1961 Enzymic correlates of physiological regression of follicles and corpora lutea in ovaries of normal rats Endocrinology 68 247
- McKay D G J H M Pinkerton A T Hertz and S Danziger 1961 The adult human ovary a histochemical study Obst and Gynec 18 13-39
- Myers H I W C Young and E W Dempsey 1936 Graafian follicle development throughout the reproductive cycle in the guinea pig with especial reference to changes during oestrus (sexual receptivity) Anat Rec 65 381-401
- Novikoff A B J Drucker W Shin and S Goldfisher 1961 Further studies of the adenosine triphosphatase activity of cell membranes in formal-calcium fixed tissues J Histochem and Cytochem 9 434-451
- Pearse A G E 1960 Histochemistry Theoretical and Applied Little Brown and Company Boston
- Pincus G 1961 Discussion p 54 following Pincus G and A Merrill The Role of Steroids in the Control of Mammalian Ovulation In Control of Ovulation Ed by C A Villee Pergamon Press New York
- Rowlands I W 1956 Discussion p 66 following Williams P C The History and Fate of Redundant Follicles CIBA Foundation Colloquia on Ageing vol II Ageing in Transient Tissues Ed by G E W Wolstenholme and E C P Millar Little Brown and Company Boston
- Schmidt I G 1942 Mitotic proliferation in the ovary of the normal mature guinea pig treated with colchicine Am J Anat 71 245-273
- Wachstein M and E Meisel 1957 Histochemistry of hepatic phosphatases at a physiological pH Am J Clin Path 27 13-23
- Young W C 1961 The Hormones and Male Behavior In Sex and Internal Secretions Third edition Ed by W C Young Williams and Wilkins Company Baltimore Vol I Chap XIX 1173-1239

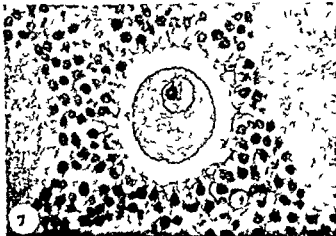
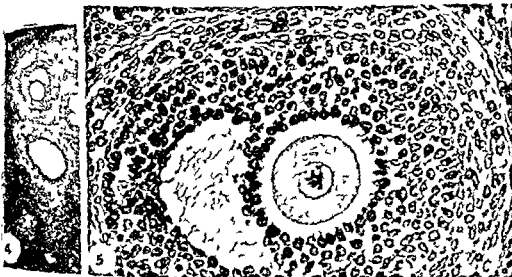
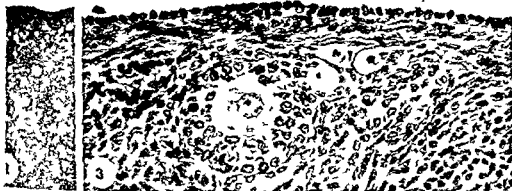


PLATE 1

EXPLANATION OF FIGURES

Normal development of oocytes and follicles

- 2 Low power survey of primordial and primary follicles at periphery of ovary GP 55 — in heat $\times 56$
- 3 High power of primordial oocytes with contracted nuclei a small primary follicle and a large primary follicle with granulosa cell mitoses GP 34 Second day $\times 350$
- 4 Low power of a fourth day follicle GP 38 $\times 56$
- 5 High power of figure 4 to show developing theca layer and many mitotic figures in granulosa wall and cumulus Nucleus of oocyte is centrally located Projections from cells of the cumulus can be seen traversing the zona G1 38 $\times 350$
- 6 Low power of an eighth day follicle to show the wide granulosa layer made up of cells loosely adherent to each other and the weblike cumulus attached at several points to granulosa wall GP 36 $\times 56$
- 7 High power of oocyte in figure 6 to show eccentric nucleus with vacuolated nucleolus GP 36 $\times 350$

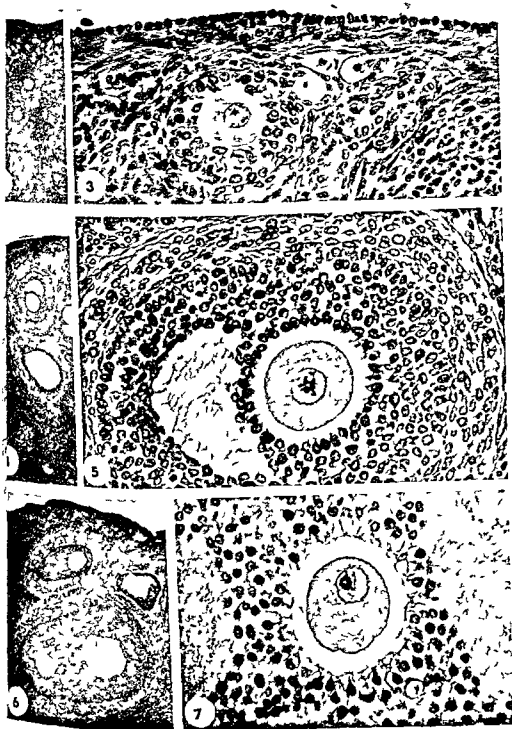


PLATE 2

EXPLANATION OF FIGURES

Normal development of oocytes and follicles

- 8 High power of figure 9 to show oocyte of twelfth day of cycle A corona radiata is developing Extracted lipid droplets can be seen in the cytoplasm of the oocyte GP 35 \times 350
- 9 Low power of twelfth day follicle to show compact granulosa and enlarging cavity GP 35 \times 56
- 10 High power of figure 11 to show just before the onset of heat nuclear changes in the oocyte with the appearance of a network of fibrils and a dense basophilic mass GP 46 \times 350
- 11 Low power of a sixteenth day follicle before the beginning of heat The granulosa wall is compact the cavity is enlarged and the theca is not hypertrophied Note lakes of fluid at base of cumulus GP 46 \times 56
- 12 High power of oocyte in figure 13 from animal in heat The first maturation spindle has formed and an anaphase is seen in a tangential cut The adjacent section contained the rest of the spindle and the chromosomes of the opposite pole The cells of the corona radiata are elongated their nuclei appear pycnotic GP 62 \times 350
- 13 Low power of follicle from an animal in heat Note dispersal of cells of the cumulus to form a loose coagulum GP 62 \times 56

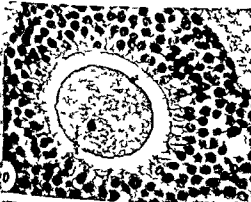
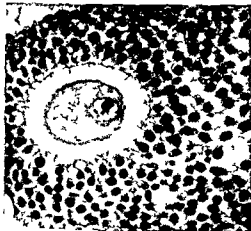


PLATE 3

EXPLANATION OF FIGURES

Adenosine monophosphatase in normally developing oocytes and follicles

- 14 The flat follicular cells around these two primordial oocytes and the surrounding cortical cells show AMPase activity. Note lack of activity in the oocyte. GP 41 fourth day $\times 1400$
- 15 A portion of a multilayered primary follicle (right) and the contained oocyte (left). AMPase activity is seen around each granulosa cell and in a dense band formed by their projections at the periphery of the developing zona pellucida. GP 41 fourth day $\times 1400$
- 16 Low power view of a small follicle of the fourth day of the estrous cycle. The dense tunica albuginea and superficial cortical layer (top) and the granulosa cells are strongly positive for AMPase activity. Note atretic follicle with degenerating oocyte at lower left. GP 41 $\times 140$
- 17 A high power of portion of the oocyte, zona pellucida and cumulus seen in figure 16. Note AMPase activity in periphery of granulosa cells (right) in dense band of their projections at periphery of zona (center) and in their projections that traverse zona to terminate at oocyte surface. GP 41 $\times 1400$
- 18 A portion of an oocyte (lower left) from a follicle from the eighth day of the estrous cycle. The granulosa cells and their projections that cross the zona are reactive for AMPase. The dense band of projections at the periphery of the zona is no longer present. GP 74 $\times 1400$
- 19 A low power of a follicle developing on the twelfth day of the cycle. AMPase activity is still present in the granulosa cells but has diminished since the fourth day. GP 60 $\times 90$
- 20 A high power of part of an oocyte (left) from a follicle just prior to the onset of heat (seventeenth day). The granulosa projections are still positive for AMPase. GP 47 $\times 1400$
- 21 A high power of part of an oocyte (left) from a follicle during heat. The granulosa projections though reactive for AMPase in the corona radiata are no longer seen in the zona pellucida. GP 77 $\times 1400$

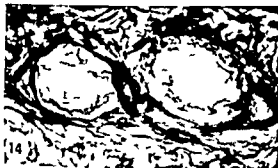


PLATE 3

EXPLANATION OF FIGURES

Adenosine monophosphatase in normally developing oocytes and follicles

- 14 The flat follicular cells around these two primordial oocytes and the surrounding cortical cells show AMPase activity. Note lack of activity in the oocyte. GP 41 fourth day $\times 1400$
- 15 A portion of a multilayered primary follicle (right) and the contained oocyte (left). AMPase activity is seen around each granulosa cell and in a dense band formed by their projections at the periphery of the developing zona pellucida. GP 41 fourth day $\times 1400$
- 16 Low power view of a small follicle of the fourth day of the estrous cycle. The dense tunica albuginea and superficial cortical layer (top) and the granulosa cells are strongly positive for AMPase activity. Note atretic follicle with degenerating oocyte at lower left. GP 41 $\times 140$
- 17 A high power of portion of the oocyte, zona pellucida and cumulus seen in figure 16. Note AMPase activity in periphery of granulosa cells (right) in dense band of their projections at periphery of zona (center) and in their projections that traverse zona to terminate at oocyte surface. GP 41 $\times 1400$
- 18 A portion of an oocyte (lower left) from a follicle from the eighth day of the estrous cycle. The granulosa cells and their projections that cross the zona are reactive for AMPase. The dense band of projections at the periphery of the zona is no longer present. GP 74 $\times 1400$
- 19 A low power of a follicle developing on the twelfth day of the cycle. AMPase activity is still present in the granulosa cells but has diminished since the fourth day. GP 60 $\times 90$
- 20 A high power of part of an oocyte (left) from a follicle just prior to the onset of heat (seventeenth day). The granulosa projections are still positive for AMPase. GP 47 $\times 1400$
- 21 A high power of part of an oocyte (left) from a follicle during heat. The granulosa projections though reactive for AMPase in the corona radiata are no longer seen in the zona pellucida. GP 77 $\times 1100$

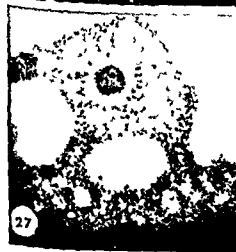


PLATE 4

EXPLANATION OF FIGURES

Nucleoside polyphosphatase in normally developing oocytes and follicles

- 22 With ATP as a substrate oocytes in primary follicles have a band of activity at their periphery and usually contain reactive granules in their cytoplasm. The ovarian stroma is strongly reactive, the tunica albuginea weakly positive and the serosal epithelium of the ovary is negative. GP 28. Fourth day. $\times 140$
- 23 With ATP as a substrate this oocyte has a reactive rim. Compare with figure 1. GP 46. Sixteenth day. $\times 140$
- 24 Serial section to figure 23. With ADP as a substrate there is usually no reactivity around the oocyte and stromal activity is slightly less. GP 46. $\times 140$
- 25 Reactivity with either ATP or ADP as substrates is seen in the ovarian stroma and the supporting cells of the theca interna. Slight activity with ATP is seen at the periphery of the oocyte in this follicle from the fourth day of the cycle. Precipitate was frequently seen over the cavity of small follicles and was interpreted to be artifactitious. GP 41. $\times 140$
- 26 A high power of an oocyte (left) from a small follicle of the fourth day. Reactivity with ATP as a substrate is seen at the periphery of the oocyte, possibly associated with ovular microvilli, and in granules in the cytoplasm of the oocyte. The zona pellucida (right center) and the granulosa cells (right) are negative. GP 3. $\times 1400$
- 27 An oocyte and cumulus in a follicle from the twelfth day of the cycle. With ATP as a substrate the oocyte has lost its peripheral rim of activity. See figures 3 and 29 for serial sections through this oocyte. GP 60. $\times 140$
- 28 A higher power of oocyte in figure 27. With ATP as a substrate a few coarse granules of activity are seen in the cytoplasm. GP 60. $\times 560$
- 29 A serial section to that in figure 28. With ADP as a substrate somewhat smaller granules are seen in the oocyte. The single granules seen in the cells of the cumulus are not enzymatically produced since the water blank controls contain similar granules. GP 60. $\times 560$

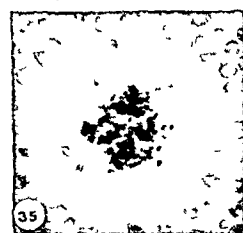
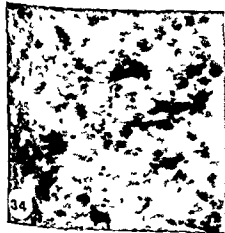
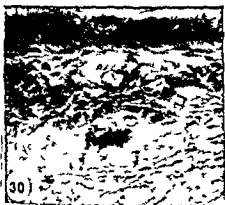


PLATE 5

EXPLANATION OF FIGURES

Acid phosphatase in developing oocytes

- 30 Acid phosphatase activity is seen in granules in the oocyte of this primary follicle GP 28 Fourth day $\times 350$
- 31 Acid phosphatase water blank control in a serial section to that in figure 30 The granules seen in the serosal epithelium (top) are not enzymatically produced and may represent an inorganic phosphate reaction associated with a lipid compound GP 28 $\times 350$
- 32 A small follicle of the fourth day to show acid phosphatase activity in the contained oocyte and negative granulosa An interstitial mass at left of oocyte shows faint activity GP 84 $\times 140$
- 33 A higher power of the oocyte seen in figure 32 Discrete granules of activity are seen throughout the oocyte cytoplasm A faint dusting of activity is seen in the cumulus GP 84 $\times 560$
- 34 A high power of a matured follicle wall to show the acid phosphatase positive macrophages that during heat invade the granulosa (right) from the theca (left) This same follicle is seen in figure 41 (Sudan black) and at the left in figure 61 (alkaline phosphatase) GP 77 $\times 350$
- 35 An oocyte from a follicle of the twelfth day showing that the acid phosphatase positive granules are clearly unassociated with the lipid droplets GP 60 $\times 560$

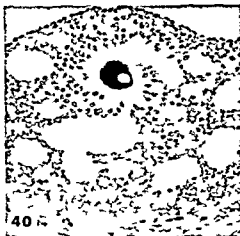


PLATE 6

EXPLANATION OF FIGURES

Alkaline phosphatase and lipid in developing follicles

- 36 The primordial follicles seen in the superficial cortex (top) are negative. The developing theca interna of the primary follicle (bottom) and the cells of the interstitial mass are reactive for alkaline phosphatase. GP 77 — in heat $\times 280$
- 37 The oocyte and granulosa layer are negative for alkaline phosphatase. The theca interna is strongly positive. GP 77 — in heat $\times 280$
- 38 The sudanophilia in this oocyte in a primary follicle is diffuse and probably represents mitochondrial staining. GP 74. Eighth day $\times 280$
- 39 Sudanophilic droplets appear in oocytes in developing follicles of the fourth day. The interstitial mass surrounding this follicle shows dense sudanophilia. GP 84 $\times 140$
- 40 This mature pre-estrous follicle of the seventeenth day shows sudanophilia in the oocyte and in the macrophages of the theca interna. Its granulosa wall at higher magnification showed fine sudanophilia. GP 47 $\times 140$
- 41 During heat the granulosa cells rapidly become sudanophilic. This follicle is also seen in figure 34 (acid phosphatase) and at the left in figure 61 (alkaline phosphatase). GP 77 $\times 350$
- 42 A high power of the oocyte seen in figure 40 showing sudanophilic droplets throughout cytoplasm. GP 47 $\times 560$

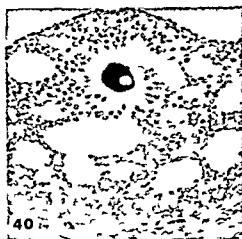
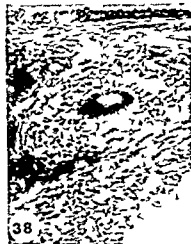


PLATE 7

EXPLANATION OF FIGURES

Atretic follicles and the development of interstitial masses

- 43 The granulosa layer in this primary follicle is disorganized The oocyte has an eccentrically located nucleus GP 47 Seventeenth day $\times 140$
- 44 A small follicle whose cumulus is thin Several mitoses are seen in the granulosa layer Note extreme eccentricity of the nucleus in this oocyte GP 40 Twelfth day $\times 140$
- 45 The granulosa layer in this small follicle is sloughing into the cavity GP 62 — in heat $\times 140$
- 46 This is an early atretic follicle owing to the granulosal slough and thecal hypertrophy Note mitoses in granulosa in spite of atresia The oocyte appears histologically normal GP 35 Twelfth day $\times 140$
- 47 The granulosal layer has degenerated there is a maturation spindle in the oocyte the theca interna layer is wide and contains many mitoses GP 62 — in heat $\times 140$
- 48 This follicle with advanced atresia shows complete shedding of the granulosa layer beginning organization at the periphery of the cavity and a wide thecal layer The oocyte is degenerating GP 65 Twelfth day $\times 140$
- 49 This follicle has a more advanced stage of organization of the former cavity an oocyte that has undergone fragmentation or cleavage and a thecal layer now forming an interstitial mass GP 64 — in heat $\times 140$
- 50 An interstitial mass showing remnants of an oocyte within its central cavity GP 38 Fourth day $\times 140$

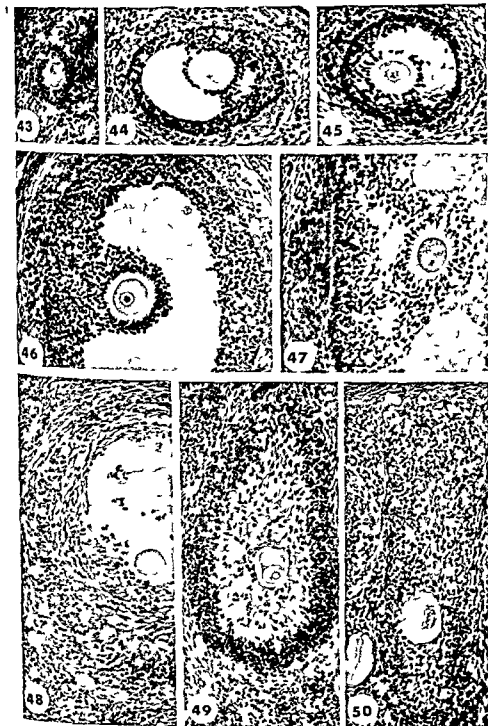


PLATE 8

EXPLANATION OF FIGURES

Atretic follicles with invasion of granulosa by vascularized connective tissue from the theca

- 51 Delicate strands from the theca invade the granulosa and cumulus in this eighth day follicle GP 36 $\times 140$
- 52 Nucleoside polyphosphatase activity is present in the invading cells GP 74 Eighth day $\times 140$
- 53 Two similar follicles of the eighth day one of which shows evidence of early atresia in the nucleoside polyphosphatase positive invasive thecal elements (right) Follicle on left is normal Compare with a nearby section of same two follicles (alkaline phosphatase) in figure 55 GP 74 $\times 56$
- 54 A thecal invasion with small blood vessels near the base of a cumulus There are a few sloughed granulosa cells Note apparently normal oocyte GP 40 Twelfth day $\times 140$
- 55 Alkaline phosphatase reaction on same two follicles as in figure 53 Note the absence of this enzyme in the cumulus on the right This indicates that the invasive strands are not the alkaline phosphatase positive thecal cells GP 74 $\times 56$
- 56 A follicle with advanced atresia showing a stalk of cells continuous with the theca at base of former cumulus GP 65 Twelfth day $\times 140$

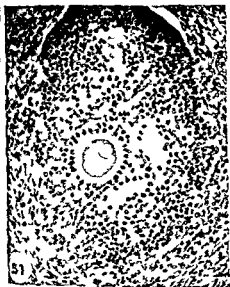


PLATE 9

EXPLANATION OF FIGURES

Atretic follicles — all alkaline and neutral phosphatases

- 57 This follicle of the thirteenth day shows minimal atresia. The basal layers of the granulosa are nucleoside polyphosphatase positive. See figure 58 for higher power of follicle wall and figures 61 and 72 for histochemical evidence of abnormality in its contained oocyte.
- 58 High power of wall of follicle shown in figure 57. The granulosa layer is beginning to slough into the cavity distally and its basal layers are nucleoside polyphosphatase positive. C P 51 $\times 560$.
- 59 With ATP as a substrate the oocytes in the non-developing small follicles found throughout the cycle frequently maintain a peripheral rim of activity. The large follicle at lower left shows advanced sloughing and a basal granulosa layer with nucleoside polyphosphatase activity. G P 14 Twelfth day $\times 140$.
- 60 Sodium glycerophosphate at pH 7.2 was used as a control for the specificity of the nucleoside polyphosphatase reactions. It gave a moderate reaction in the thecal layer only in locations similar to that seen with alkaline phosphatase. The granules in the granulosa are not enzymatically produced since they are present also in the water blank control. C P 51 Thirteenth day $\times 140$.
- 61 The follicle at left is matured and about to ovulate. Its theca interna is prominent and shows only moderate alkaline phosphatase activity as compared with the two non-ovulating follicles (at the right) with hypertrophied theca. G P 77 — in heat $\times 88$.
- 62 This shows a variety of stages of interstitial masses. Alkaline phosphatase remains prominent in the thecal layer as it becomes transformed into an interstitial mass. G P 71 Eighth day $\times 88$.



PLATE 10

EXPLANATION OF FIGURES

Atretic oocytes — Adenosine monophosphatase and lipid

- 63 This follicle shows beginning atresia in the sloughing granulosa layer. The sloughed granulosa cells lose their AMPase activity. See figure 65 for details of oocyte. GP 44 Twelfth day $\times 140$
- 64 This oocyte has abnormally large lipid droplets in its cytoplasm. This section is serial to those seen in figures 72 and 73. The follicle wall showed minimal atresia (see figures 57 and 58). GP 54 Thirteenth day $\times 560$
- 65 A higher power of the oocyte seen in the atretic follicle in figure 63. The AMPase reactive terminals of the granulosa projections are enlarged at the oocyte surface. GP 44 Twelfth day $\times 560$
- 66 The oocyte in this atretic follicle shows clumped or coalesced lipid droplets. The shedding granulosa remains negative for sudanophilia. GP 44 Twelfth day $\times 140$
- 67 This oocyte from a follicle that showed only moderate sloughing of the granulosa layer nevertheless contains a dense band of AMPase activity at the periphery of the oocyte. This is interpreted to result from enlargement or possibly fusion of the terminals of the granulosa projections. GP 84 Fourth day $\times 140$
- 68 The surviving granulosa cells still retain their AMPase activity in this follicle with advanced atresia and a fragmented or segmenting oocyte. GP 84 Fourth day $\times 140$
- 69 This atretic follicle is developing into an interstitial mass. Its oocyte has large clumps of sudanophilia. The macrophages in the organizing cavity contain lipid. The theca cells only gradually develop sudanophilia. GP 28 Fourth day $\times 140$

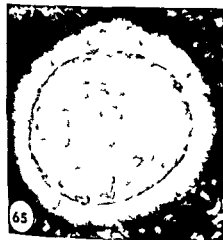


PLATE 11

EXPLANATION OF FIGURES

Acid phosphatase in atretic oocytes and follicles

- 70 A small follicle with disorganized granulosa cells contains an oocyte with clumped acid phosphatase activity GP 41 Fourth day $\times 140$
- 71 A larger follicle with minimal sloughing of the granulosa layer contains an oocyte with clumped acid phosphatase activity GP 74 Eighth day $\times 100$
- 72 This oocyte with clumped acid phosphatase activity was found in the follicle with minimal atresia shown in figures 57 and 58 Serial sections of the oocyte are seen in figure 64 (sudanophilia) and figure 73 (acid phosphatase control) GP 54 Thirteenth day $\times 560$
- 73 Acid phosphatase water blank control through a serial section of the oocyte in figure 72 No precipitate is seen GP 54 Thirteenth day $\times 560$
- 74 With moderate to advanced atresia the oocyte shows reduced or no acid phosphatase activity The shedding granulosa layer remains negative Macrophages in the thecal layer (right) contain reactive granules GP 44 Twelfth day $\times 560$
- 75 With advanced atresia the oocyte is negative for acid phosphatase activity The macrophages in the organizing cavity are positive and the thecal layer becomes faintly positive as it is transformed to an interstitial mass GP 28 Fourth day $\times 140$
- 76 Occasionally degenerating oocytes contain a substance that blackens in both this acid phosphatase preparation and in its water blank control (fig 77) This precipitate is characteristic of the presence of inorganic phosphates GP 28 Fourth day $\times 140$
- 77 Acid phosphatase water blank control on a section serial to that in figure 76 to show that the black precipitate in the degenerating oocyte is not enzymatically produced GP 28 Fourth day $\times 140$

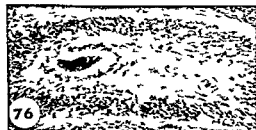
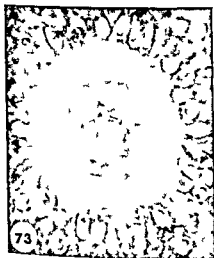
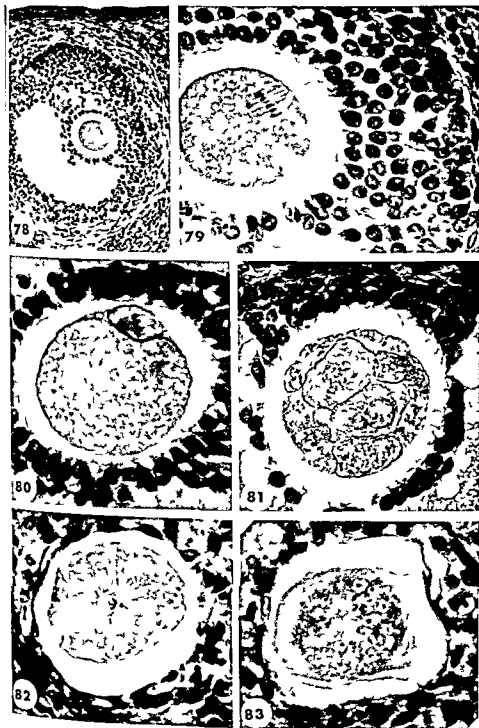


PLATE 12

EXPLANATION OF FIGURES

Atretic oocytes with abnormal nuclear changes

- 78 This follicle shows little histologic evidence of atresia yet the nucleus of its oocyte is in the first maturation spindle. This nuclear change is seen in most oocytes about the time of estrus. GP 31. Second day $\times 140$.
- 79 A higher power of figure 78 to show maturation spindle. There are definite mitotic figures in the granulosa layer (lower right). GP 34. Second day $\times 560$.
- 80 This oocyte shows a spindle in the polar body and another section contained the second maturation spindle. It was contained in an atretic follicle with moderate sloughing of the granulosa layer. Note mitosis in cumulus. GP 60. Twelfth day $\times 560$.
- 81 This oocyte appears to have undergone several cleavages to form a morula like structure. The atretic follicle which contained it had a very thin granulosa layer. Note poorly formed cumulus. No granulosa slough was apparent. GP 31. Second day $\times 560$.
- 82 This oocyte is degenerating in an atretic follicle that is becoming organized to form an interstitial mass. A polar body is seen at left. The large astral ray with associated basophilic clumps appears to be derived from the oocyte nucleus. GP 47. Seventeenth day $\times 560$.
- 83 This degenerating oocyte in an organizing follicle contains several micronuclei without any evidence of cytoplasmic cleavage. GP 40. Twelfth day $\times 560$.



Differentiation of Mouse Thymus Cultured in Diffusion Chambers

EMMA SHELTON

Laboratory of Biochemistry National Cancer Institute National Institutes of Health Public Health Service U S Department of Health Education and Welfare Bethesda Maryland

ABSTRACT Considerable evidence has been brought forward in recent years to show that thymus growing in intraperitoneally implanted diffusion chambers will partially restore immunological competence to mice thymectomized at birth (Osoba and Miller 63) Levey Trainen and Law 63 Law Trainen Levey and Barth 64 Law Dunn Trainen and Levey 64 Osoba 65) Since it was suggested that the thymus cells secrete a factor that mediates the restoration it was of interest to examine the thymic cells that grew or survived in the diffusion chamber. Whole thymuses from newborn mice were grown in thymectomized or intact syngeneic or allogeneic hosts of various ages. Whole mount preparations were made of the thymus tissue after it had grown for from 9-86 days. Thymic lymphocytes, granulocytes, macrophages and fibroblasts migrated rapidly from the explant, the latter forming a sheet that covered the entire chamber. Viable lymphocytes were present in chambers removed from the host after 86 days. The striking feature of the cultures was the differentiation of the epithelium into sheets, clusters and cords of cells reminiscent of glandular epithelium. Whorls of cells resembling Hassall's bodies were occasionally seen. These epithelial cells were distinguished by the presence of large lipid filled vacuoles and neutral mucopolysaccharide in the cytoplasm. It is suggested that the epithelial cells were engaged in secretory activity.

Considerable evidence has been brought forward in recent years to show that embryonic or neonatal thymus growing in intraperitoneally implanted diffusion chambers will partially restore immunological competence to mice thymectomized at birth (Osoba and Miller 63, 64; Levey, Trainen and Law 63; Law, Trainen, Levey and Barth 64; Law, Dunn, Trainen and Levey 64; Osoba 65). These and other experiments (Metcalf 56, 60) have suggested that the thymus cells secrete a "humoral substance" that mediates the restoration and for this reason it has been of interest to examine the type of cells that grow or survive in the diffusion chamber. Previous descriptions of thymic tissue grown in diffusion chambers which have relied upon the examination of sections of paraffin-embedded material have shown that epithelial reticular cells and possibly lymphocytes (Levey, Trainen and Law 63; Osoba 65) may survive for periods as long as 18 weeks; however, these preparations provide limited information as to the survival and growth pattern of the thymic tissue as a whole. The descrip-

tions that follow are based upon "whole mounts" of the thymic tissue recovered from intraperitoneally implanted diffusion chambers. These show that the epithelial cells grow as sheets or clusters or as a network of cords and that thymic lymphocytes while steadily decreasing in numbers may continue to survive for as long as 12 weeks.

MATERIAL AND METHODS

Thymuses and in one experiment spleens were removed as nearly intact as possible from newborn donors that were anesthetized with ether or by low temperature. They were blotted free of blood on filter paper soaked in chilled phosphate buffered saline, pH 7.2, and dissected free of extraneous tissue. The tissues were kept on ice in a Petri dish containing a saline moistened filter paper until they were put into the chambers. The center filter of each chamber was moistened with saline before the tissues were enclosed by sealing the top filter. Immediately after sealing each chamber was inserted into the peritoneal cavity of the host mouse and the

abdominal muscle and skin were closed separately with silk sutures. Sterile technique was used throughout.

Double diffusion chambers of a design previously described (Shelton and Rice, '58) were used. They consisted of two lucite rings (20 mm o.d., 10 mm i.d., for adult hosts; 12 mm o.d., 6 mm i.d. for three week hosts) between which a Millipore filter¹ (type HA pore size $0.45 \mu \pm 0.02 \mu$) was cemented. On the outside of the rings were cemented Schleicher and Schuell B1 or T Flex B12 filters² (average pore diam. 0.15μ). The chambers were fabricated except for the top filter and sterilized by dry heat at 80°C for 48 hours.

A total of 53 chambers containing thymus and eight chambers containing spleen are included in this study. The following combinations of donor \rightarrow host were used: BalbC \rightarrow BalbC, BalbC \rightarrow A, C₃H \rightarrow (C₃H \times C₃H)_{F₁}, C₃H \rightarrow (C₃H \times C₃H)_{F₁}, and DBA/2 \rightarrow DBA/2. In the thymus series 12 of the host mice were three weeks of age and had been thymectomized at birth; 33 were three months of age and were intact. The spleens were put into three week old thymectomized hosts.

When the chambers were removed from the animals, the top filter was removed and the accumulated fluid was aspirated from around the tissue with a pipette and rubber bulb. Small droplets of this fluid were placed on slides for examination with the phase microscope. The bottom filter of the chamber was removed, the fluid discarded and the center filter on which the thymus was growing was fixed in one of the following fixatives:

- (1) 3% potassium dichromate (pH 6) to which 10% formalin had just been added, (Orth's fluid)
- (2) 95% ethyl alcohol to which 10% of formalin had just been added (alcohol formalin)
- (3) 10% formalin, 2% calcium acetate, 0.5% cetylpyridinium chloride in water (CPC formalin)

With the exception of one group of eight thymus chambers the tissues were fixed, processed and mounted on slides as whole mounts (Shelton and Rice '58). Tissue from the group of eight thymus chambers was sectioned "frontally" after paraffin embedding. Material fixed in Orth's fluid was

stained with Glemsa's stain. Lillie's alcohochrome connective tissue stain and iron hematoxylin. Tissues fixed in alcohol formalin were stained in azure-eosin hematoxylin, tissues fixed in CPC formalin were stained with oil red O for lipid (Lillie '54) and with alcian blue PAS (after diastase digestion) for mucopolysaccharide (Spicer, '60).

RESULTS

Neither the genetics of the donor \rightarrow host combination nor the age nor the presence or absence of the thymus in the host affected the growth pattern or the survival of the thymus in the diffusion chambers. The explanation of the gland to the diffusion chamber resulted in concomitant death and proliferation of cells and, as is common with all cultures of organs and tissues, there was considerable variability in the growth pattern and cell survival from chamber to chamber. Complete necrosis of the tissue was never observed but necrosis was always present in the central portion of the explant. Dying thymic lymphocytes were quite clearly recognized but it was difficult to ascertain to what extent the epithelial stroma of the glands was involved in the necrotic process. Lymphocytes present in profusion in some chambers were sparse in others. Similar variability was observed in the proliferation of sheets and cords of epithelium but in only five of the 45 whole mount preparations examined were epithelial cells missing entirely. In these five preparations only fibroblasts proliferated and it is worth remarking that very little evidence of necrotic cells could be detected, a fact which attested to the remarkable activity of the macrophages in the chambers. Table 1 shows the number of whole mounts of thymus tissue examined at various time intervals.

The tissue of the freshly explanted thymus was too compact to be examined as a whole mount but after nine days of growth in the diffusion chamber it had loosened up and spread out so that its structure could be discerned. During these nine days fibroblasts had migrated out from the gland to form two thin sheets while

¹ Millipore Filter Corp. Bedford, Massachusetts.
² Carl Schleicher and Schuell Co., Keene, New Hampshire.

TABLE 1

Chambers	9-15 day	26-40 days	55-86 days
Stal with epithelial proliferation	17	19	4
Stal without epithelial proliferation	—	4	1

extended on the roof and the floor to the edges of the chambers. There were many free macrophages and thymic lymphocytes present in the fluid of the chamber and wandering between and on the surface of the sheets of fibroblasts. The epithelial portion of the gland remained localized where it had been initially placed and reorganization and growth of the epithelial cells had begun. In favorable preparations the outline of each of the two thymic lobes could be seen as a pattern of clusters or interconnected cords of epithelial cells completely surrounded by fibroblasts (fig 1). These clusters and cords of cells were only one or two cells thick although they could be many cells wide (fig 2). During the first two weeks of growth thymic lymphocytes were invariably present floating free in the fluid of the chamber or scattered in clusters throughout the solid tissue on the filter. Clusters of granulocytes and occasional foci of myelopoiesis were seen in several of the chambers and mast cells were ubiquitous.

Later as the tissue of the thymus spread out more extensive and elaborate proliferation of the clusters and cords of cells became evident. In some chambers sheets of epithelium were more prominent than cords or clusters while in others both sheets and cords were present. After four weeks epithelial cells were still actively proliferating (figs 3 4 5) and many thymocytes were present in the chamber fluid (figs 7 8 9) and intercellular spaces of the tissue. Whorls of cells strongly resembling Hassall's bodies were now present at intervals along the epithelial cords (fig 6). By 55 days thick cords of cells could still be seen (figs 10 11 12) but many now had become more irregular in outline and their thin walls enclosed an empty or necrotic lumen. Clusters of thymocytes were still present (fig 12). In

chambers opened between 70 and 86 days sheets and cords of cells still persisted and clusters of viable lymphocytes were observed (figs 13 14 15).

In addition to a characteristic pattern of growth a feature distinguishing the epithelial cells was the presence of large vacuoles in the cytoplasm (figs 2 11).

When explants that had grown in the chambers for from 9 to 28 days were stained with oil red O the vacuoles were found to contain lipid (figs 18 19). When other explants were digested with diastase to remove glycogen and then were stained with Alcian Blue PAS the cytoplasm of the epithelial cells were PAS positive indicating the presence of neutral mucopolysaccharide (fig 20) (Spicer 60). The vacuoles in the cytoplasm did not stain with PAS but accumulations of PAS positive material were found in what appeared to be a lumen in some of the cords of cells (fig 21). Accumulation of lipid and PAS positive material in macrophages varied greatly and appeared to be related to the state of the phagocytic activity of the individual cells. Surprisingly lipid droplets were also found in some of the thymic lymphocytes and presumably the vacuoles seen in the lymphocytes after 86 days in culture (figs 14 15) were also due to the presence of lipid. The fibroblasts frequently contained very fine dust like lipid droplets and were very faintly PAS positive.

The serial sections of the eight paraffin embedded tissues recovered from chambers after four weeks of growth would have been exceedingly difficult to interpret had it not been for the prior experience with the whole mounted tissues. The epithelial sheets and tubules were so thin that they were not easy to follow through the 5 μ sections and it would have been almost impossible to recognize that the clusters of epithelial cells scattered through the fibroblastic matrix were sections through a network of cords. However it was easy to see in the sections that the center of the explant was necrotic and it appeared that the proliferation of the epithelium came mainly from cells in the cortex of the gland. It thus appeared probable that the central necrosis of the explant involved all cell types.

New born spleen The eight chambers containing new born spleen were opened after four weeks. The growth consisted of flat sheets of reticular cells (fig 16) with clusters of macrophages and polymorphonuclear leucocytes. In three of the chambers, extensive myelopoiesis was observed (fig 17). If lymphocytes were present they could not be distinguished.

DISCUSSION

In the past experiments with the *in vitro* cultivation of the thymus were largely concerned with the problem of the origin of the thymic lymphocytes, but some investigators (Emmart 36, Popoff 26 Murray 37) did describe the characteristics of the epithelial outgrowth of their cultures. Popoff (26) a student of Maximow believed that the thymic lymphocytes originated from the mesenchyme and migrated into the epithelial rudiment of the gland and he thus considered the question of the origin of the thymic lymphocyte to be a closed issue. He concentrated his efforts therefore, upon the examination of the characteristics of the epithelium of 100 explants from new born, half grown and adult rabbits. It is worth noting from the point of view of technique that these cultures were prepared from fragments of minced tissue since the explanation of whole organs into a static culture environment usually met with no success because of insufficient gas and nutrient exchange in thick explants and in spite of this he always observed necrosis in his cultures. He found as we have that the epithelium remained relatively stationary while lymphocytes, histiocytes and polymorphonuclear leucocytes migrated rapidly from the explants and that the fibroblasts formed a sheet that eventually enveloped the epithelium. In his cultures the epithelium contracted to form islands and he noted that clear vacuoles became prominent in and between the cells of the epithelial foci that they could attain quite a large size and were probably to be looked upon as a manifestation of a kind of secretory activity. In his conclusions Popoff states unequivocally that the epithelial cells were engaged in secretory activity. Twenty-one years later in the same laboratory, Murray (47) succeeded in obtaining pure cultures

of rabbit thymus epithelium which he said grew in tongues sheets and cords. The illustrations of his cultured cells are remarkably similar to figures 4 and 5 of the present paper. He concluded that the stroma of the gland was entirely epithelial and that there was no difference between the medulla and the cortex of the gland so far as the capacity for epithelial proliferation was concerned.

The evidence that the cells of thymus glands grown in diffusion chambers secrete a diffusible substance that influences the immunological reactivity of the hosts has raised the question of the cellular origin of the substances and provided the impetus for examining the morphology of such cultures. It was perhaps naive to expect successful cultivation of the explants of whole thymic lobes. Necrosis of the cells in the center of the explant promptly occurred but at the same time there was growth and reorganization of the epithelial cells and a remarkably rapid proliferation and migration of the fibroblasts and wandering cells of the gland. This concomitant death migration and growth produced a sheet of cells thick enough to permit the penetration of gas and nutrients so that successful cultures were established.

The striking feature of the diffusion chamber cultures was the epithelial differentiation a feature for which the morphological appearance of the gland in the adult animal provides little evidence although the embryonic anlage of the thymus is clearly epithelial. These cells proliferate and rearranged themselves into structures very reminiscent of glandular epithelium [Murray (47) could not distinguish between the epithelial outgrowth from cultures of either gall bladder intestine or thymus so similar was their morphology]. The question to be answered is are these thymic epithelial cells engaged in secretory activity and are they secreting a material that influences the immunological competence of the host? In agreement with the conclusions of others (Osoba and Miller 64 Metcalf 60 Popoff 26) circumstantial evidence implicates the epithelial cell as being involved in such activity if indeed it exists. The histochemical evidence shows that while lipid ac-

AS positive material was present in macrophages lymphocytes and fibroblasts. These materials were more consistently present in the epithelial cells and served clearly to distinguish them from all other cells in the chambers. In addition it has been shown (Osoba 65) that diffusion chamber cultures of new born spleen are ineffective in restoring the immunological competence of the host and it was shown in the present experiments that spleen cultures are devoid of epithelial cells. Finally the lymphocytes are probably not involved in the restoration of immunological competence since although some were still present after 86 days in the chamber their number steadily decreased from the time of explantation and they could be considered to be a dying population.

In experiments where the immunological capacity of the host has been restored considerable animal to animal variation has been observed (Osoba and Miller 63, 64 Osoba 65 Law Traenen Levey and Barth 64). Such variation may have been due to variation in the survival of the thymic epithelium. Further experiments designed to correlate the survival of specific cell types in the chamber with the immunological reactivation of the hosts should provide more insight into the function of the thymus in diffusion chamber cultures.

ACKNOWLEDGMENTS

The author is grateful to Mr Charles Mock whose skillful technical assistance made these experiments possible to Dr S S Spicer for many helpful discussions and to Mrs Jacqueline Henson for preparing the mucopolysaccharide stains.

LITERATURE CITED

- Emmart E 1936 A study of the histogenesis of the thymus *in vitro* Anat Rec 66 59-73
- Law L W T B Dunn N Traenen and R H Levey 1964 Studies of thymic function. In The Thymus The Wistar Symposium Monograph no 2 Wistar Institute Press Philadelphia, pp 105-120
- Law L W N Traenen R H Levey and W F Barth 1964 Humoral thymic factor in mice further evidence Science 143 1049-1051
- Levey R H N Traenen and L W Law 1963 Evidence for function of thymic tissue in diffusion chambers implanted in neonatally thymectomized mice Preliminary report J Nat Cancer Inst 31 199-218
- Lallie R 1954 Histopathologic Technic and Practical Histochemistry The Blakiston Company Inc New York
- Metcalf D 1960 The effect of thymectomy on the lymphoid tissues of the mouse British J Haemat 6 324-333
- 1956 The thymic origin of the plasma lymphocytosis stimulating factor British Jour of Cancer 10 442-457
- Murray R G 1947 Pure cultures of rabbit thymus epithelium Am J Anat 81 369-412
- Osoba David 1965 The effects of thymus and other lymphoid organs enclosed in Millipore diffusion chambers on neonatally thymectomized mice JEM 122 633-650
- Osoba D and J F A P Miller 1963 Evidence for a humoral thymus factor responsible for the maturation of immunological faculty Nature 199 653-654
- 1964 The lymphoid tissues and immune responses of neonatally thymectomized mice bearing thymus tissue in Millipore diffusion chambers JEM 119 177-194
- Popoff N 1926 The histogenesis of thymus as shown by tissue culture Arch f Exp Zellforsch 4 395-416
- Shelton E and M E Rice 1958 Studies on mouse lymphomas II Behavior of three lymphomas in diffusion chambers in relation to their invasive capacity in the host Jour Nat. Cancer Inst 21 137-161
- Spicer S S 1960 A correlative study of the histochemical properties of rodent acid mucopolysaccharides Jour Histochemistry and Cytochemistry 8 18-36

PLATE 1

EXPLANATION OF FIGURES

- 1 Low power view of BALB/c thymus explant after nine days of culture in an intact adult BALB/c host. The fenestrated pattern formed by the growth of the thymus epithelium clearly delineates the two lobes of the thymus. Arrow points to a contracted sheet of fibroblasts that had pulled off the top filter of the chamber when it was removed. Allochrome stain 23 \times
- 2 Enlargement of a portion of the thymus shown in figure 1. Broad cords of epithelial cells are surrounded by a matrix of fibroblasts. Living and dead thymocytes are dispersed singly or in clusters in the fibroblastic matrix. The preparation is too dense to permit good resolution of cellular detail but the epithelial cells can be seen to be filled with large vacuoles (compare with fig 11). These vacuoles correspond to the large lipid deposits seen in appropriately stained material. 500 \times

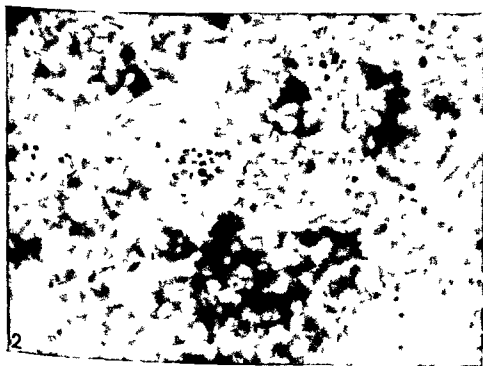


PLATE 2

EXPLANATION OF FIGURES

- 3 Twenty-eight day-old explant of C₃H Black thymus placed into three week old thymectomized (Bl \times C₃H)_{F1} host. Epithelial cords and tubules have proliferated extensively into the sheet of fibroblasts. Azure eosin 100 \times
- 4 Detail of epithelial cord of cells seen in figure 3. Note lymphocytes still present in connective tissue next to epithelial cord 500 \times
- 5 Detail of epithelium seen in figure 3. Mitoses can be seen in this proliferating cord of cells 500 \times
- 6 Hassall's bodies are formed by some of the epithelial cells. Same culture as figure 3



PLATE 2

EXPLANATION OF FIGURES

- 3 Twenty-eight day-old explant of C_{37} Black thymus placed into three-week-old thymectomized $(B1 \times C_{37}H)_{F1}$ host. Epithelial cords and tubules have proliferated extensively into the sheet of fibroblasts. Azure-eosin 100 \times
- 4 Detail of epithelial cord of cells seen in figure 3. Note lymphocytes still present in connective tissue next to epithelial cord. 500 \times
- 5 Detail of epithelium seen in figure 3. Mitoses can be seen in this proliferating cord of cells. 500 \times
- 6 Hassall's bodies are formed by some of the epithelial cells. Same culture as figure 3.



PLATE 3

EXPLANATION OF FIGURES

Representative phase optical photographs of the cell population in the fluid of a culture of new born BALB/c thymus grown for 26 days in an intact adult strain A host

- 7 Thymic lymphocytes two of which display typical hand mirror form of locomotion 2 000 \times
- 8 Two thymic lymphocytes and a macrophage in metaphase 2 000 \times
- 9 Group of thymic lymphocytes and macrophages The large vacuol in the macrophage at the left probably corresponds to the PAS positive material seen in stained preparations 1 000 \times



PLATE 4

EXPLANATION OF FIGURES

- 10 Fifty five days after explantation of BALB/c thymus into intact adult BALB/c host the pattern of epithelial cord like structures can clearly be distinguished from the surrounding connective tissue Giemsa stain 80 \times
- 11 A cord of epithelial cells thrusts into the sheet of fibroblasts covering the floor of the chamber Many of the cells contain large vacuoles which probably represent lipid inclusions Detail of figure 10 500 \times
- 12 In this epithelial cord there is very little evidence of lipid inclusions although some of the cells appear to be degenerating Thymic lymphocytes which are still viable at this time can be seen scattered or in clusters in the fibroblastic matrix of the culture Detail of figure 10 500 \times

Emm Sh Item

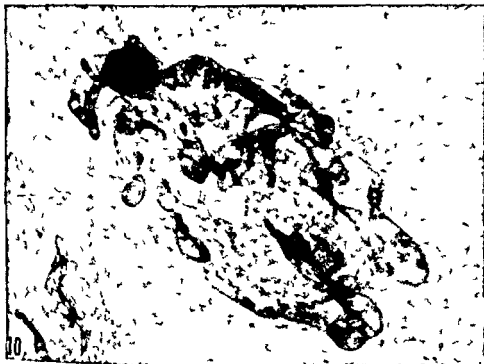


PLATE 5

EXPLANATION OF FIGURES

- 13 Eighty six days after explantation of BALB/c thymus into an intact adult BALB/c host pale staining tubules can still be seen Only the outer cells of the tubules are still viable at this time Lymphocytes can be seen as pepper like dots Giemsa stain 80 \times
- 14-15 Detail of clusters of thymic lymphocytes present in 86-day-old thymus culture shown in figure 13 Many of the lymphocytes contain vacuoles which are presumed to denote the presence of lipid 1 000 \times
- 16 Spleen from new born C₃ black donor grown in diffusion chamber placed into three week old thymectomized (C₃H \times C₃H/Bl)_{F1} host The reticular cells form a criss-cross pattern in some areas of the culture Twenty nine days Azure cosin 500 \times
- 17 Extensive myelopoiesis was present in several of the spleen cultures Twenty nine days 500 \times

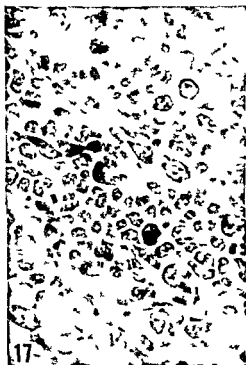
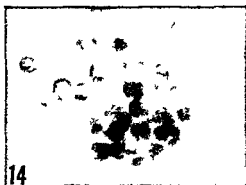


PLATE 6

EXPLANATION OF FIGURES

- 18 DBA/2 thymus stained for lipid after 11 days of growth in an intact DBA/2 host. The epithelial cells forming long strands in the center of the explant can be distinguished by the accumulation of lipid droplets in the cytoplasm. The discrete dense red deposits seen in this preparation are lipid containing vacuoles in the cytoplasm of macrophages. Oil red O with hematoxylin counterstain. 65 \times .
- 19 High power view of the strand of epithelial cells showing detail of lipid deposits in the cytoplasm. The discrete densely stained bodies scattered through the preparation represent the deeply stained lipid deposits in the cytoplasm of macrophages. Same preparation as shown in figure 18. 500 \times .
- 20 DBA/2 thymus after 25 days of growth in intact DBA/2 host. The red stained material in the cytoplasm of the epithelial cells growing in closely packed cord like arrangements denotes the presence of neutral mucopolysaccharide. The hypertrophied cytoplasm of two macrophages also contains PAS positive material. Alcian Blue Periodic acid Schiff reaction after diastase digestion. 400 \times .
- 21 Higher power view of same preparation shown in figure 20 showing the accumulation of PAS positive material in what appears to be a lumen in a cord of epithelial cells. 500 \times .

suprarenal Gland Lymphatic Drainage¹

ROBERT J MERKLIN

Jefferson Medical College Philadelphia Pa

ABSTRACT The gross and microscopic anatomy of the suprarenal gland lymphatic system was studied in post mortem specimens and specimens in which the venous system was injected with blue latex solution

Extensive subserous lymphatic networks overlie the suprarenal gland Deep to these networks are the lymphatic vessels proper of the suprarenal gland These vessels lie within the suprarenal gland capsule and communicate with the subserous lymphatic network Their primary routes of drainage however are directed medialward passing to the thoracic duct or cisterna chyli either directly or by way of regional lymph nodes A few capsular lymphatic vessels extend toward the diaphragm or the kidney The regional lymph nodes are small few in number and situated at the lower medial aspect of the gland

Microscopic examination of serially sectioned suprarenal glands revealed a complete absence of lymphatic vessels in the cortical and medullary parenchymal tissue Lymphatic vessels were found only in the capsule and in the adventitia of the central vein and its major tributaries

A close association between capsular lymphatic vessels and veins was noted and in a number of specimens capsular lymphatic vessels were traced to the inferior vena cava where they assumed a close relationship with vasa vasorum

Although studies of the lymphatic system go back several centuries the methods applied to their study have undergone little change down to the present time Parke and Michels (63) reviewed these methods and remarked that the only new procedure since the seventeenth century has been lymphangiography Even this procedure they pointed out has limitations in common with earlier methods namely getting the radiopaque material into the lymphatic vessels This requirement is a serious obstacle in lymph vessel studies since they are difficult to inject in either anagrade or retrograde fashion Parke and Michels described a technique for studying subserous lymphatic vessels that overcame this problem They applied solutions of hydrogen peroxide to post mortem specimens and found a fairly selective inflation of lymphatic vessels under this treatment In their hands a 3% solution of hydrogen peroxide was found most effective since it produced a gaseous swelling of lymphatics lasting several hours This period of time is adequate for gross study photographic recording and preparation of specimens for additional histological study I have applied the technique to a study of the suprarenal gland lymphatic system and a search for lymphatic

covenous connections between the suprarenal gland and the inferior vena cava or its tributaries

MATERIAL AND METHODS

Sixty eight adult post mortem specimens were studied by the technique of Parke and Michels Each specimen consisted of the suprarenal gland (24 left 44 right) and surrounding tissue including a portion of the diaphragm portions of the renal artery and vein and either the aorta or inferior vena cava Most specimens included both major vessels thus insuring the presence of the thoracic duct Three per cent hydrogen peroxide was applied before and during the dissection of the serous membrane and fascia covering the suprarenal gland Repeated applications of hydrogen peroxide were made as the dissections progressed

In addition selected histological material from previous studies of the suprarenal blood vessels was reexamined with the focus of attention on the lymphatic vessels This material consisted of ten adult and ten neonatal suprarenal glands in which the venous system had been in

¹ Supported by research grant HE 08441-03 of the National Institutes of Health of the United States Public Health Service

jected with blue latex before fixation, staining and sectioning. In these histological sections the lymphatic channels were identified by structure and absence of injection material in their lumina. Serial sections of each gland were followed in a search for tributaries from the cortex or medulla with particular care given to the area where the suprarenal vein makes its exit from the gland. Sections of the inferior vena cava containing adventitial lymphatic vessels were also examined microscopically to determine their relationship to the vein.

RESULTS

Lymphatic vessels occur in great profusion under the serous lining of the abdominal cavity. The gaseous swelling of lymphatic vessels produced by hydrogen peroxide solution makes them easily visible in the connective tissue and fascia and distinguishes them from accompanying veins (figs 1-2-3). They may be followed for considerable distances through the tissues as the dissection progresses and they respond to repeated application of the hydrogen peroxide solution.

In the area of the suprarenal gland the subserous lymphatic channels form an extensive plexus running at several levels and in several directions within the fascia and loose connective tissue covering the suprarenal gland. Deeper still are the lymphatic channels proper of the suprarenal gland. These vessels are within the suprarenal gland capsule and usually number four to five on the ventral surface and two to three on the dorsal surface. In figures seven and eight all the capsular lymphatic vessels seen in the dissection of 68 gross specimens are recorded in superimposed fashion. The purpose of this is to show the variation in position of these vessels and the prevalence of vessels in the vicinity of the suprarenal vein. Figure nine is a composite drawing intended to show a typical lymphatic drainage pattern for both glands. Study of gross specimens and serial sections of the histological material mentioned under material and methods established the fact that these suprarenal capsular channels begin blindly at scattered points on the gland surface usually in close association with one of the cap-

sular veins that form a small but important part of the suprarenal gland venous drainage system. Histological study revealed the additional fact there are no tributaries from the cortical or medullary parenchyma to these capsular lymphatic channels. This observation was carefully verified by comparison of the capsular veins and lymphatic vessels. Since the former contained blue latex they were easily distinguished from the lymphatic vessels containing pink staining plasma. While numerous venous channels were seen coming from within the gland and joining capsular veins there was not a single instance of similar lymphatic tributaries to the capsular lymphatic vessels. The possibility that parenchymal lymphatic channels exist but follow a drainage route along the central vein was considered and carefully investigated. Lymphatic channels were found in the connective tissue surrounding the central vein and its larger tributaries but they began blindly and had no tributaries from the parenchymal tissue. In the neonatal gland the central vein and its larger tributaries are surrounded by a wide band of connective tissue and muscular tissue is absent. In the adult gland prominent longitudinal muscle bundles are present in the connective tissue and the lymphatic channels are usually found external to the muscle tissue (fig 5).

The majority of capsular lymphatic channels run medialward to the thoracic duct often without the intervention of lymph node. Some channels run downward toward the kidney or superiorly toward the diaphragm. More channels are found on the ventral than on the dorsal surface and on either surface they are generally parallel to that of the suprarenal gland blood vessels. Regional lymph nodes that is nodes specifically associated with the suprarenal gland are few in number and rather small. They are usually situated medial to the lower portion of the gland.

In over a dozen instances capsular lymphatic channels from the right suprarenal gland were traced directly to the surface of the inferior vena cava and appeared to terminate in this vessel (fig 6). Microscopic study was required to clarify the

relationship. The lymphatic channels were found to take a position alongside the vasorum of the inferior vena cava. The intimal walls of these two structures were seen to come in contact (fig 6) and the lymphatic channel abruptly ended just before the vasa vasorum emptied into the vena cava. In summary there was no apparent lymphaticovenous connections in any of the specimens examined in this study.

DISCUSSION

Although there have been earlier studies of visceral lymphatics the first comprehensive report on adrenal gland lymphatics was made by Kumita (1959a,b). He repeated studies by Stilling (1938) on both the adrenal lymphatic vessels and carried out additional studies on canine and new-born human adrenal glands. Kumita's results substantially the same as Stilling's were that the adrenal gland of lower forms and of man were well supplied with lymphatic vessels.

According to Kumita these vessels are disposed throughout the capsule, cortex and medulla and drain into a lymphatic meshwork surrounding the central vein. This meshwork in turn empties into two lymphatic trunks accompanying the suprarenal vein and terminating in regional lymph nodes. Not only did Kumita describe intercellular lymphatic channels but he reported and included figures of what he believed to be intracellular lymph channels.

Aside from a number of abbreviated reports 50 years elapsed before another comprehensive study was made on this subject. In 1959 the Russian Sapin published a study of the lymphatic system in 120 adult human specimens. He reported essentially the same distribution of lymphatic vessels in the cortex and medulla as Kumita reported except for the drainage pattern of the cortex. Sapin reported a centrifugal drainage of the cortex into capsular lymphatic vessels rather than a drainage inward into the medullary vessels.

My results differ substantially from those of Kumita and Sapin. In the present investigation suprarenal gland lymphatic vessels were found only in the capsule of

the gland and in the adventitia of the central vein and its largest tributaries. It would seem that Kumita and Sapin mistook the medullary venous sinuses and the small veins passing out through the cortex into the capsule for lymphatic vessels. Both men used a technique of random injection of dye into the tissue. This method results in hit or miss filling of the lymphatic vessels and frequently fills adjacent veins as well. From figures in both reports it appears that capsular veins were also filled and the fluid backed up into the small cortical veins and the medullary sinuses. In several of Sapin's figures he also appears to be labeling cortical sinusoids (sinusoidal capillaries fenestrated capillaries) as lymphatic vessels.

The suprarenal glands examined microscopically in the present study were injected with blue latex via the suprarenal vein. This single discrete injection filled the central vein, its tributaries, medullary sinuses and the veins running out through the cortex and into the capsule. The capsular lymphatic vessels were distinguished by the presence of valves and the presence of pink staining plasma instead of blue latex in their lumina (fig 4). The lymphatic vessels were followed through complete serial sections of each gland in a search for tributaries from within the gland but none were found anywhere in the cortical or medullary parenchymal tissue.

The arrangement of suprarenal gland lymphatics as reported in the present study is similar to that of the liver or kidney. Lymphatics of the former were described by Mall (1906) who found them in close company with the blood vessels in the interlobular tissue and never in association with the parenchymal tissue within the liver lobule. Of further note is Mall's observation that particulate matter injected into the hepatic artery or portal vein quickly appears in the liver lymphatics.

Clark and Clark (1937) commented on Mall's classical study and stressed the point that a large proportion of lymph entering the thoracic duct (the liver being a major source of thoracic duct lymph) represents direct "leakage" from interlobular portal venules of fluid that has never

been in contact with cells of the liver lobule. The Clarks using their rabbit ear chamber technique made a thorough study of the relation of lymph vessels to blood vessels. They found veins and lymphatics lying side by side with no intervening tissue for long distances and verified Malls observation that substances passed from vein to lymphatic. In their experiments intravenously injected methylene blue quickly appeared in adjacent lymphatics and leucocytes and red blood cells passed from vein to lymphatic under conditions of chemical thermal and mechanical stimulus. The Clarks noted too that in spite of this close association and easy passage of material from vein to lymphatic, open communication between the two types of vessels was never established.

In contrast to these reports of transfer of material from vein to lymphatic but without open communication are reports of flow from lymphatic to vein and by way of very definite anastomoses. Silvester (12) in a study of 25 new world species of monkey found constant communications between the intestinal and lumbar lymphatic channels on the one hand and the inferior vena cava or left renal vein on the other. Interestingly enough he was unable to find any similar communications in 16 species of old world monkeys. Job (18) found lymphaticovenous communications at the level of the iliac renal and subclavian veins in 48% of the rats he studied. Job also noted an increase in the number of connections per animal under certain physiological conditions. Blalock et al (37) demonstrated the development of lymphaticovenous anastomoses in dogs following ligation of the thoracic duct and found the greatest number of communications between the abdominal lymphatics and the inferior vena cava at the level of the renal veins. Threefoot et al (63) obtained similar results after ligation of the cisterna chyli and found the development of anastomoses to be more rapid in animals pretreated with hexamethonium. Threefoot et al (63) developed a method of radioisotope detection of lymphaticovenous connections and recorded their presence within five days of the occlusion of the thoracic duct in rats. The intimate relation between lymphatic

vessels and vasa vasorum of the inferior vena cava noted in the present study (6, 6) could well be the site for the development of anastomoses under the conditions mentioned above.

From the foregoing reports it is evident that much remains to be learned about the lymphatics as a system and about their relation to the venous system. In man it appears that lymphaticovenous connections are normally present only in the cervical region (thoracic duct and right lymphatic duct). However this arrangement can not be considered typical of all mammals since reports mentioned above clearly indicate the presence of lymphaticovenous communications in other areas of the body in a number of mammalian species. Phylogenetic and ontologic studies of the lymphatic system similar to the early studies by Huntington and McClure (10), Huntington (10) and Sablin (28) are badly needed to clarify this situation.

The dynamics of the lymphatic system warrant additional investigation not only in the area of the development of new connections in response to various stimuli but also in regard to the dynamics involved in the transfer of material in the opposite direction from vein to lymphatic. Finally the role of lymphatic vessels in structures such as the suprarenal gland where they are limited to the capsule and connective tissue elements requires additional study.

LITERATURE CITED

- Blalock A C S Robinson R S Cunningham M T Cray 1937 Experimental study on lymphatic blockage Arch 34 1049-1051
Clark E R and E L Clark 1937 Observations on living mammalian lymphatic capillaries—their relation to the blood vessels Am J Anat 60 253-298
Huntington C S 1908 The genetic interpretation of the development of the mammalian lymphatic system Anat Rec 11 19-45
Huntington C S and C F W McClure 1909 The anatomy and development of the jugular lymph sacs in the domestic cat Anat Rec 11 1-18
Job T T 1918 Lymphaticovenous communications in the common rat and their significance Am J Anat 24 467-491
Kumita K 1909 Über die lymphgefäß- und nieren- und nebennierenkapsel Arch f Anat Physiol 1909-38
——— 1909 Über die parenchymatösen lymphgefäße der nebenniere Arch f Anat Physiol 321-326

- all F P 1906 A study of the structural unit of the liver *Am J Anat* V 227-308
- Wright W W and N A Michels 1963 A method for demonstrating subserous lymphatics with hydrogen peroxide *Anat Rec* 146 165-171
- Johnson F R 1908 Further evidence on the origin of the lymphatic endothelium from the endothelium of the blood vascular system *Anat Rec* II 46-54
- Johnson M R 1959 Intraorganic lymphatic system of human adrenals *Arkiv Anat Histol Embryol* 36 52-59
- Thwester C F 1912 On the presence of permanent communication between the lymphatic and the venous systems at the level of the renal veins in adult South American monkeys *Am J Anat* 12 447-472
- Stilling H 1898 The anatomy of the adrenal gland *Arch mikroskop Anat* 52 176-195
- Threefoot S A W T Kent and B F Hatchett 1963 Lymphatico venous and lymphatico lymphatic communications demonstrated by plastic corrosion models of rats and post mortem lymphangiography in man *J Lab Clin Med* 61 9-22
- Threefoot S A M F Kossover and D W Aiken 1965 Radioisotopic detection of lymphatico-venous communication in living animals *J Lab Clin Med* 65 688-697

PLATE 1

EXPLANATION OF FIGURES

- 1 Subserous lymphatic vessels in the fascia overlying the suprarenal gland Mag 2 \times
- 2 Lymphatic vessels (arrows) from the suprarenal gland at right to a regional lymph node held by two hemostats
- 3 Several lymphatic vessels (arrows) passing from the right suprarenal gland to the dorsal surface of the inferior vena cava

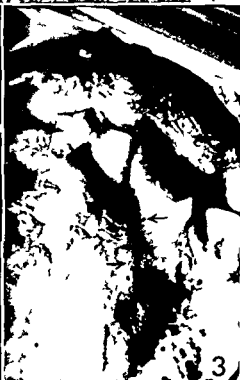


PLATE 1

EXPLANATION OF FIGURES

- 1 Subcutaneous lymphatic vessels in the fascia overlying the suprarenal gland. Mac 25.
- 2 Lymphatic vessels (arrows) from the suprarenal gland & run to a regional lymph node held by two hemostats.
- 3 Several lymphatic vessels (arrows) passing from the right suprarenal gland to the dorsal surface of the inferior vena cava.



PLATE 2

EXPLANATION OF FIGURES

- 4 Suprarenal capsular vessels. The thick walled arteries and veins filled with dark injection material are easily recognized. The remaining vessels are lymphatics. Note the close relationship between vein and lymphatic. Mag 180 \times
- 5 The central vein containing injection material and surrounded by longitudinal muscle. Two lymphatic vessels are seen external to the muscle. A valve can be seen in the right lymphatic. Mag 180 \times

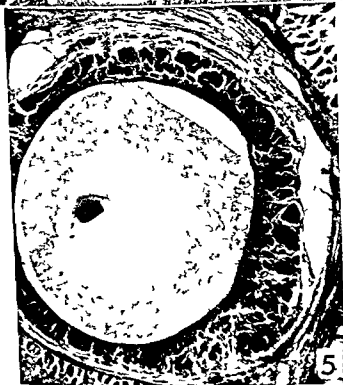


PLATE 3

EXPLANATION OF FIGURE

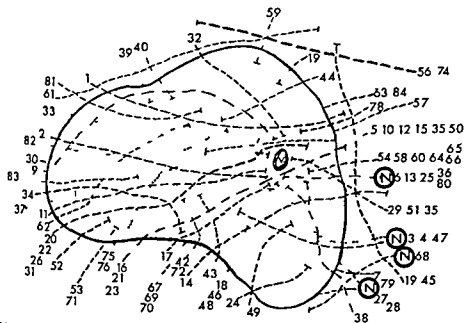
- 6 A section through the wall of the inferior vena cava. A vas vasorum (V) is seen in two sections with a lymph vessel (L) sandwiched in between. The vas vasorum opens into the vena cava at the upper right.



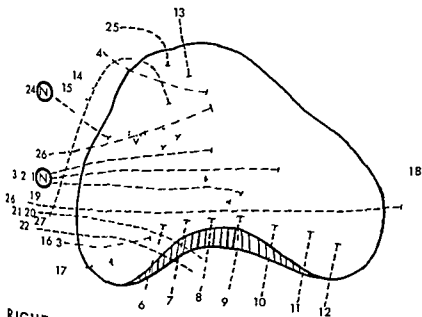
PLATE 4

EXPLANATION OF FIGURE

- 7 All the lymphatic vessels seen in the study of 68 post mortem specimens are charted and numbered consecutively on a single drawing of the ventral and dorsal surface of the right suprarenal gland. This presentation indicates the areas where lymphatic vessels are most commonly found. V suprarenal vein N lymph node



RIGHT VENTRAL

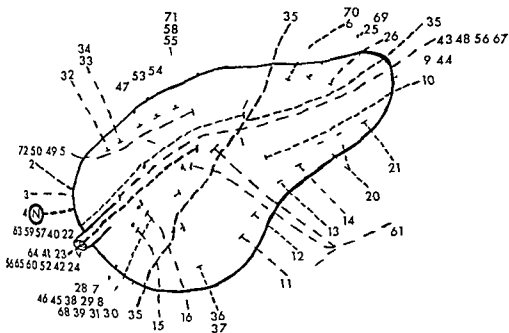


RIGHT DORSAL

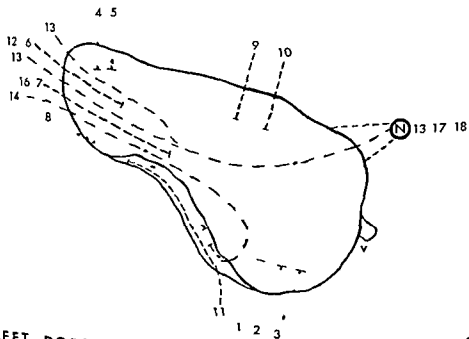
PLATE 5

EXPLANATION OF FIGURE

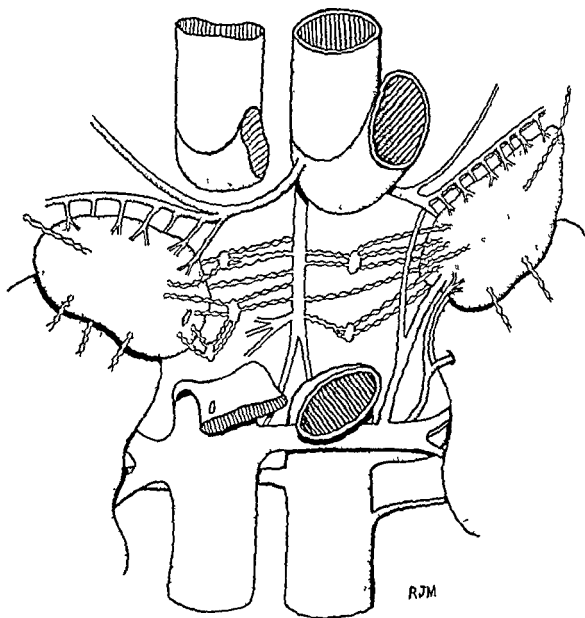
- 8 Same as for figure 7 but for the left suprarenal gland



LEFT VENTRAL



LEFT DORSAL



EXPLANATION OF FIGURE

- 9 An idealized drawing of the suprarenal gland lymphatic drainage based on observations of post mortem specimens

The Synthesis and Storage of Protein by Isolated Lymphoid Cells, Examined by Autoradiography with the Electron Microscope¹

SAM L. CLARK JR.²

Department of Anatomy Washington University School of Medicine
St. Louis Missouri

ABSTRACT Autoradiography with the electron microscope was employed to locate sites of synthesis and storage of newly formed protein in cells isolated from lymph nodes of immunized rabbits and incubated with tritium labelled leucine. The chief object of the investigation was to locate the site of sequestration of newly formed antibody during the half hour that intervenes between its synthesis and release from the plasma cell. By making counts of grains over nuclei Golgi complex and ergastoplasm and relating these to the relative volume of each region evidence was obtained that during the latent period of secretion antibody moves into the Golgi region from its site of synthesis in the ergastoplasm. In analyzing the data some of the difficulties involved in quantitative autoradiography were considered and the statistical inappropriateness of using mean grain counts and their standard errors to estimate the concentration of isotope was discussed. As an alternative with a sounder theoretical basis the ratio estimate was adopted and Fisher's theorem was used to obtain conservative estimates of confidence limits. The results of statistical analysis supported the biological conclusion that newly formed antibody migrates to the Golgi region but the role of the Golgi complex in secretion of antibody remains to be explained.

The hypothesis that plasma cells originate by differentiation from large lymphocytes received circumstantial support from the observation that among those cells active in synthesis of protein a series transitional in structure from large lymphocytes to mature plasma cells could be assembled.

These experiments were undertaken to examine the mechanism of secretion of antibody by plasma cells. While studying the secretion of antibody *in vitro* by cells isolated from lymph nodes of immunized rabbits Helmreich Kern and Eisen (61) observed a latent period of approximately 30 minutes intervening between the addition of radioactive amino acid to the culture medium and the first detectable release of labelled antibody from the cells. This delay was not due to a slow rate of synthesis; complete labelled antibody was recovered from cellular homogenates prepared during the latent period. Further more binding of antibody to ribosomes — as newly formed albumin is bound in the liver (Peters 57) — did not account for the latent period; most of the intracellular antibody recovered from homogenates was found free in the cell sap. To test whether the delay was due to slow adaptation to the cultural environment C¹⁴ labelled amino acid was added to cells already actively secreting tritium labelled antibody. The usual latent period preceded release

of C¹⁴ labelled antibody even though secretion of tritium labelled antibody had continued unabated. The process of secretion not only was orderly as demonstrated by these double labelling experiments it also proceeded to completion almost no intracellular labelled antibody remained 90 minutes after labelled cells had been washed and reincubated in a medium free of radioactive amino acid. However when synthesis of protein was interrupted by the addition of puromycin the release of preformed antibody stopped short of completion (Helmreich Kern and Eisen 62). On the basis of these experiments the authors concluded that the secretion of antibody by plasma cells is a continuous orderly active process in which antibody moves from its site of synthesis to some other intracellular compartment for temporary storage prior to its release from the cell. They also concluded that cellular dissolu

¹ Supported in part by grants GM 7176 and GM 3784 from the National Institutes of Health, United States Public Health Service.
² Recipient of a Research Development Award from the United States Public Health Service.

tion is not required to release antibody lysis would be expected to release intracellular proteins indiscriminately but little labelled protein other than gamma globulin accumulated in the incubation medium and the extracellular activity of the enzyme, aldolase did not increase during incubation

In the secretion of protein by pancreatic acinar cells and by chondroblasts similar latencies have been observed and the Golgi complex has been implicated as a site for temporary sequestration of the secretory product (Warshawsky Leblond and Droz, 63 Caro and Palade, 64 Jamieson and Palade 66 Revel and Hay, 63)

In the present experiments lymphoid cells were incubated with tritium labelled leucine and autoradiography was employed in a search for the site where labelled antibody is sequestered during the latent period of secretion. Leucine labels all newly formed protein and thus could not be used to identify antibody directly but the intracellular distribution of immunoglobulin has been determined by immunohistochemical staining (Rifkind Osserman Hsu and Morgan 62 de Petris and Karlsbad 65) and lymphoid cells can be depleted of labelled antibody by re-incubation in unlabelled medium (Helmreich Kern and Eisen 62). Therefore re-incubation in unlabelled leucine was used to distinguish between immunoglobulin and structural proteins in plasma cells. The results can be interpreted to implicate the Golgi complex in sequestration of antibody but it has seemed necessary to re-evaluate the statistical basis for quantitative autoradiography at the level of the electron microscope in order to support such a conclusion.

MATERIAL AND METHODS

Immunization

Male white rabbits weighing approximately 2 kg were injected in the hind footpads with an emulsion of antigen in Freund's complete adjuvant (Difco Laboratories). In experiments I and II (table 1), the antigen was 5 mg of dinitrophenyl coupled bovine gamma globulin (DNP BGG) (Helmreich, Kern and Eisen 61)

In experiments III V, 60 mg of human serum albumin (HSA) (Merck Sharp and Dohme) was injected with adjuvant both into the footpads and subcutaneous over the scapulae

Cell suspensions

Two to seven weeks after infection the rabbits were anesthetized with sodium pentobarbital (Nembutal Abbott) the popliteal lymph nodes excised and a suspension of cells was prepared by teasing the nodes gently with stainless steel rakes and stirring slowly for 15 to 2 hours at 0°C in oxygenated tris buffered balanced salt solution (Helmreich Kern and Eisen 61). After large fragments of tissue had been removed by straining through gauze the suspended cells were washed three times by centrifuging at 100 × for ten minutes at 0°C and resuspended in fresh medium. For incubation the cells were resuspended finally in a medium fortified with phosphates and bicarbonate but free of leucine. In experiment V bit serum that had been heated to 56° for an hour was added to the medium at a final concentration of 0.2% to more favorable conditions for cellular metabolism.

At this point in the procedure of the cell suspension were tested for viability by staining with a dilute solution of eosin by a procedure that is said to provide conservative estimates of viability (Black and Berenbaum 64). The suspensions contained approximately 0.5 × 10⁶ cells/ml but accurate counts were not attempted because of clumping of the cells.

Incubation (table 1)

Three ml aliquots of the cell suspension were incubated in siliconized 20 ml beakers in a metabolic shaker at 37°C in an atmosphere of 95% oxygen and 5% carbon dioxide. The cells were agitated by gentle agitation for at least ten minutes before the addition of tritium labelled leucine. Each beaker received 100 to 200 microcuries of D.L. leucine 4-5 H³ in specific activity from 3.5 to 5.5 curies/millimole (New England Nuclear). The resulting concentration of the

TABLE I
Experimental protocol

Experiment	Imm i t i n		Imm i l i n g I n t r v l	No. f b b i s	Group	In b t i n		In t e r v l t i m n t	R i n b t i n p e r i o d	A u t o r d i s t r i b u t i o n	
	Antigen	Antigen				Inc b t i n p e r i o d	minutes			Expo s u r e	No. of c e l l s
d y											
I II	DNP BGG DNP BGG	50 22	6 3	{	1	10				17	23
					2	20				15	13
					3	30				15 and 43	10
					4	60				43	23
					5	90				15	26
					6	120				43	20
					7	60	P			21	10
					8	60	P			35 and 42	19
					9	60	C				
					10	60	C				
					11	60	PC				
					12	60	PC				
III	HSA	14	3	{	1	0.5				77	7
					2	1				77	11
					3	2				77	16
					4	4				77	5
					5	30				51	32
IV	HSA	14	2	{	1	0.5				84	21
					2	0.5	C		0.5	84	21
					3	0.5	C		1.5	84	14
					4	0.5	C		3.5	84	26
					5	0.5	C		29.5	84	16
V	HSA	23	3	{	3	10				9	14
					4	10	C		180	19	15
					1	90				17	20
					2	90	C		180	9	22

Abbreviations: DNP BGG dinitrophenyl-coupled bovine gamma globulin; HSA human serum albumin; P, puromycin; C, unlabeled leucine.

cine approximately 0.01 millimolar, was similar to that of the other amino acids present and presumably did not limit the rate of protein synthesis.

Reincubation in unlabeled leucine was carried out by adding L-leucine to the incubation medium in a final concentration of ten millimolar for experiments I, II and V and 0.03 millimolar in experiment IV. In experiment V, the cells were washed once in leucine free medium before reincubation and NaCl was added to groups one and three in a final concentration of ten millimolar in order to simulate the osmotic effect of the leucine added to groups two and four.

In experiments I and II puromycin was added in a final concentration of 3×10^{-4} molar (Helmreich, Kern and Eisen '62) (Puromycin 2 HCl Lot 1326B 156.1 obtained through the generosity of Dr J. M. Rueggsegger of Lederle Laboratories and Dr J. L. Strominger of the Department of Pharmacology University of Wisconsin School of Medicine).

Fixation and imbedding

Incubation was terminated by fixing the cells for 15 minutes at 0°C in 1% osmium tetroxide dissolved in incubation medium. Fixed cells were dehydrated in ethanol and imbedded in epon 812 (Luft '61) using two different methods for incorporating the suspended cells into blocks suitable for dehydration and imbedding.

1 In experiments I and II the incubation mixture was sedimented at $100 \times g$ for five minutes at 0°C, the medium decanted and the cells resuspended in the fixing solution. After fixing ten minutes the cells were centrifuged again, the fixative decanted and the cells resuspended in 1 ml of molten 3% agar agar. The solidified agar was cut into small blocks for dehydration and imbedding.

2 In experiments III-V more rapid interruption of synthesis and better cytological preservation were achieved by diluting the incubating mixture to two volumes with cold 2% osmium tetroxide in incubation medium. After fixing ten minutes the cells were sedimented into a hard pellet ($10,000 \times g$ for 5 minutes at 0°C) which could be dehydrated *in toto* and cut

into small blocks for imbedding (Malame '63).

Autoradiography

For light microscopy sections 2 μ thick were cut with glass knives on a Portablum microtome (Servall) mounted on glass slides coated with chromated gelatin and dipped into diluted melted emulsion (Kodak NTB 3 Ilford L-4 or G-5) (Caro and van Tubergen '62). Dried slides were sealed in plastic boxes containing silica gel with a small piece of dry ice added to retard fading of the latent image. After exposure at room temperature for 1 to 3 weeks autoradiographs were developed in Kodak D 72 and stained through the emulsion with ice-cold Giemsa stain (Benge '60) or with hot 1% azar B bromide.

For electron microscopy thin sections with pale gold interference color were mounted on collodion-coated copper grids and covered with a film of diluted Kodak NTB 3 or Ilford L-4 emulsion according to the method of Revel and Hay ('63) or of Caro and van Tubergen ('62). After exposures of 2 to 12 weeks under conditions similar to those described above the autoradiographs were developed in Kodak Microdol X placed in 0.02 molar NaOH for 30 minutes to digest away the gelatin of the emulsion (Revel and Hay '63) and stained with lead hydroxide or uranyl acetate. Electron micrographs were obtained with an RCA EMU 3C electron microscope.

Grain counts

Crude estimates of radioactivity in a types of cells were made by counting grains in low power electron micrographs and recording the number/cell in nucleus, nucleolus and cytoplasm. Only cells containing at least two grains were counted and because of irregularities in labelling unlabelled cells were not recorded.

Grain counts in plasma cells were made by photographing every plasma cell when it was first encountered then choosing for counting only those that contained at least two grains showed no signs of degeneration and possessed a recognizable Golgi complex. Electron micrographs were made at a constant magnification of 5,400 \times .

X and enlarged to a final magnification of 21 600 X. To avoid prejudice during the counting procedure sections of cells from several experimental groups were mixed and the identities of individual cells were not known. Nevertheless obvious differences in total numbers of grains made some prejudice unavoidable. Cells were subdivided into four regions:

- 1 Nucleus (N) if present in the section
- 2 Golgi complex (G) demarcated from the surrounding cytoplasm by drawing a line on each micrograph to enclose smooth surfaced vesicles sacs and vacuoles but exclude all recognizable ribosomes and rough surfaced endoplasmic reticulum (fig 12)

- 3 The cytoplasm immediately surrounding the Golgi region (juxtagolgi or J) defined as an area extending the width of one grain or approximately 0.35μ beyond the limits of G

- 4 The outer cytoplasm (O)

The cytoplasm exclusive of G (O and J taken together) was designated ER for its chief constituent ergastoplasm.

The volumes of N G and ER were estimated by cutting electron micrographs into appropriate pieces weighing each region to measure its area and multiplying by an estimated section thickness of 0.08μ . Fourteen whole electron micrographs measuring 206 by 256 mm weighed from 9.364 to 9.583 gm with a mean of 9.421 gm and standard deviation of 0.0034 gm. Therefore at a final magnification of 21 600 X each gm of paper represented approximately $1 \mu^3$ of protoplasm.

Statistical analysis was undertaken with the advice of Mrs Barbara Bartels Hixon of the Department of Preventive Medicine and Mr George Whitlow of the Computer Research Laboratory Washington University School of Medicine. Computations were made at the Washington University Computer Facilities supported in part by grant G-22296 from the National Science Foundation.

RESULTS

Viability of cells

Sixty to 80% of the cells failed to stain with eosin Y at the beginning of each experiment and a similar proportion re-

mained apparently viable at the end of incubation. Cells might have died and degenerated into unrecognizable debris during the course of incubation but Helreich et al (61) obtained evidence that few cells degenerated in their experiments. In any case only cells that showed no signs of degeneration were chosen for grain counts. Therefore the results presumably represent the activities of viable cells.

Morphology of cells

Lymphocytes plasma cells monocytes macrophages granular leucocytes and erythrocytes could be recognized in electron micrographs by their resemblance to cells described previously by others (Bessis 61) (fig 7). Neither reticular cells nor connective tissue fibers appeared in the suspensions which were selected populations including only those cells that survived the process of isolation. The term "large lymphocyte" will be used to designate all those large round basophilic cells with vesicular nuclei and prominent nucleoli but lacking ergastoplasm — variously called lymphoblasts plasmablasts hemocytoblasts or primitive reticular cells — because there seemed to be no adequate criteria for distinguishing between them in electron micrographs.

Lymphocytes predominated in all preparations with small lymphocytes comprising 50 to 60% medium sized lymphocytes 20 to 25% and large lymphocytes 5 to 10% of the cells present. Five to 15% were plasma cells and other types were scarce. Two weeks after an injection of HSA (experiments III and IV) approximately 15% of the cells were large lymphocytes and 5% were plasma cells. 3 to 7 weeks after an injection of DNP BGG (experiments I and II) these proportions were reversed.

By arbitrary choice of electron micrographs a transitional series of cells from large lymphocyte to plasma cell could be assembled just as de Petris and Karlsbad (65) and Harris et al (65) have demonstrated. Some of the large lymphocytes were in mitosis. The most immature plasma cells could be distinguished from large lymphocytes only by the presence of ergastoplasm in the cytoplasm. Mature plasma

cine, approximately 0.01 millimolar was similar to that of the other amino acids present and presumably did not limit the rate of protein synthesis.

Reincubation in unlabeled leucine was carried out by adding L leucine to the incubation medium in a final concentration of ten millimolar for experiments I, II and V and 0.03 millimolar in experiment IV. In experiment V the cells were washed once in leucine free medium before reincubation and NaCl was added to groups one and three in a final concentration of ten millimolar in order to simulate the osmotic effect of the leucine added to groups two and four.

In experiments I and II puromycin was added in a final concentration of 3×10^{-4} molar (Helmreich, Kern and Eisen '62) (Puromycin 2 HCl Lot 1326B 156 1, obtained through the generosity of Dr. J. M. Rueggsegger of Lederle Laboratories and Dr. J. L. Strominger of the Department of Pharmacology, University of Wisconsin School of Medicine).

Fixation and imbedding

Incubation was terminated by fixing the cells for 15 minutes at 0°C in 1% osmium tetroxide dissolved in incubation medium. Fixed cells were dehydrated in ethanol and imbedded in epon 812 (Luft '61) using two different methods for incorporating the suspended cells into blocks suitable for dehydration and imbedding.

1. In experiments I and II, the incubation mixture was sedimented at $100 \times g$ for five minutes at 0°C, the medium decanted and the cells resuspended in the fixing solution. After fixing ten minutes the cells were centrifuged again, the fixative decanted and the cells resuspended in 1 ml of molten 3% agar agar. The solidified agar was cut into small blocks for dehydration and imbedding.

2. In experiments III-V, more rapid interruption of synthesis and better cytological preservation were achieved by diluting the incubating mixture to two volumes with cold 2% osmium tetroxide in incubation medium. After fixing ten minutes the cells were sedimented into a hard pellet ($10,000 \times g$ for 5 minutes at 0°C) which could be dehydrated *in toto* and cut

into small blocks for imbedding (Malama '63).

Autoradiography

For light microscopy, sections 2 μ thick were cut with glass knives on a Portablum microtome (Servall) mounted on glass slides coated with chromated gelatin, and dipped into diluted melted emulsion (Kodak NTB 3 Ilford L-4 or G-1) (Caro and van Tubergen '62). Dry slides were sealed in plastic boxes containing silica gel, with a small piece of dry ice added to retard fading of the later image. After exposure at room temperature for 1 to 3 weeks, autoradiographs were developed in Kodak D 72 and stained through the emulsion with ice-cold Giemsa stain (Benge '60) or with hot 1% azur B bromide.

For electron microscopy, thin sections with pale gold interference color were mounted on collodion coated copper grids and covered with a film of diluted Kodak NTB 3 or Ilford L-4 emulsion according to the method of Revel and Hay ('63) or of Caro and van Tubergen ('62). After exposures of 2 to 12 weeks under conditions similar to those described above, the autoradiographs were developed in Kodak Microdol X placed in 0.02 molar NaOH for 30 minutes to digest away the gelatin of the emulsion (Revel and Hay '63) and stained with lead hydroxide or uranyl acetate. Electron micrographs were obtained with an RCA EMU 3C electron microscope.

Grain counts

Crude estimates of radioactivity in all types of cells were made by counting grains in low power electron micrographs and recording the number/cell in nucleus, nucleolus and cytoplasm. Only cells containing at least two grains were counted and because of irregularities in labelling, unlabelled cells were not recorded.

Grain counts in plasma cells were made by photographing every plasma cell when it was first encountered, then choosing for counting only those that contained at least two grains. Grains showed no signs of degeneration and possessed a recognizable Golgi complex. Electron micrographs were made at a constant magnification of 5,400

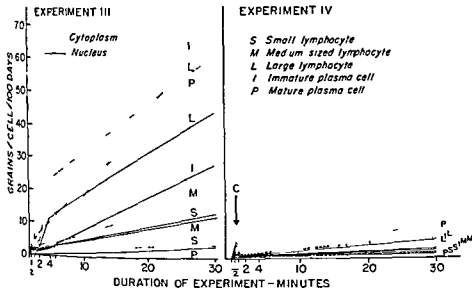


Fig 1 Average grain counts taken from low power electron micrographs of experiments III and IV expressed as grains per cell per 100 days autoradiographic exposure. In experiment IV unlabelled leucine (C) was added to the incubation medium 30 seconds after the addition of tritium labelled leucine. Apparently tritium labelled leucine was incorporated by all types of cells progressively for at least 30 minutes but the addition of excess unlabelled leucine interrupted this incorporation. Large lymphocytes and plasma cells incorporated the largest quantities and — to judge by inspection of electron micrographs — the greatest concentrations of leucine but nuclei of mature plasma cells were relatively inactive.

cytological preservation was inadequate for electron microscopy but the results of this experiment when assessed by light microscopy were comparable to those of experiment I. Groups 7, 9, 11 and 12 of experiment I were omitted because the label seen by light microscopy in these groups accorded with predictions based on grain counts made in groups 8 and 10 and no new or critical information seemed forthcoming from the omitted groups.

Some experimental groups were small, the few plasma cells counted were all that could be found. Scarcity of suitable cells can be attributed in part to the small proportion of plasma cells present in the cell suspensions, to defects in preparation of autoradiographs and to the scarcity of silver grains in preparations incubated less than ten minutes even after prolonged autoradiographic exposure.

Uncontrolled sources of variation in grain count — among the several experiments within individual experiments and even within individual autoradiographs — make direct comparisons of results risky.

Two different emulsions and several variants in the technique of their application were employed. Among and within experiments the autoradiographic exposures required to produce usable grain counts varied widely creating possibilities for variation in fading of the latent image. Within individual autoradiographs there were obvious variations in thickness of section and emulsion that were associated with variations in overall density of labeling. Accordingly direct comparisons of grain counts between experimental groups were made with circumspection and reliance was placed as much as possible on comparisons of the several regions within each cell. The statistical precautions taken to achieve these aims will be dealt with in the Discussion.

The results (figs 2-6) can be interpreted to indicate that ergastoplasm began to incorporate leucine without delay but that within 10 to 30 minutes it reached a steady state in which the concentration of radioactivity varied little thereafter just as Mitchell has reported on the basis of

cells had condensed nuclei and no nucleoli. Some plasma cells showed signs of degeneration, including condensed ergastoplasm, a reduced Golgi complex and a nucleus separated into two homogeneous phases differing in density (fig 8). Similar signs of degeneration can be found in plasma cells in intact lymph nodes (unpublished observations) and in thymic lymphocytes dying after an injection of hydrocortisone (Cowan and Sorenson 64). Therefore this probably represents the usual fate of effete plasma cells rather than an artifact of isolation.

In most plasma cells ergastoplasmic sacs were relatively collapsed and only a few cells contained inclusions that could be interpreted as stored antibody. These were of three types:

- 1 Dilated ergastoplasmic sacs with contents of low density
- 2 Condensed ergastoplasmic contents (Russell bodies)
- 3 Dense bodies enclosed in smooth membranes lying near the Golgi complex (fig 12)

There were no obvious indications as to how antibody is released from plasma cells. Signs of cytoplasmic shedding (the clasmatosis of Thierly 59) were not recognized but any such dynamic interpretation of static electron micrographs is difficult. Some plasma cells did possess microvilli (figs 10-13) similar to those cited by Sorenson (64) to support his contention that antibody is released from peripheral ergastoplasmic sacs by what might be called reverse pinocytosis but we saw no other evidence to support his hypothesis. There seemed to be no direct path of communication between the Golgi complex and the surface of the cell.

Although a hypothetical transitional series from large lymphocyte to plasma cell could be assembled some macrophages also possessed features in common with immature plasma cells. Most macrophages had condensed nuclei and cytoplasm containing few ribosomes but a few possessed vesicular nuclei with prominent nucleoli and concentrations of ergastoplasm in the peripheral cytoplasm (fig 9). Therefore the possibility that plasma cells differentiate from immature phagocytic cells should not be overlooked.

Indeed, the heterogeneous inclusions seen in some plasma cells may represent phagocytic debris (fig 12).

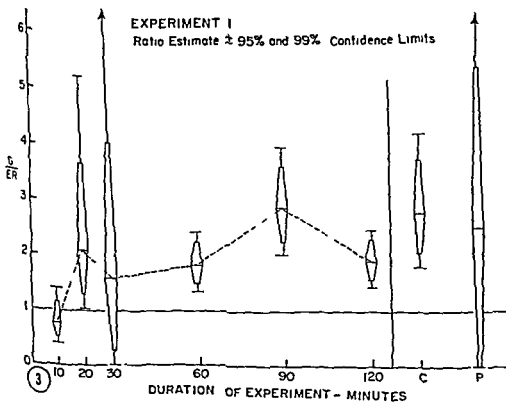
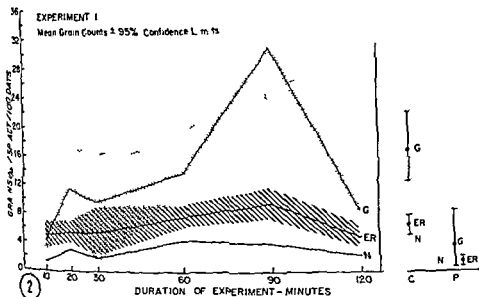
Autoradiography

As judged by both light and electron microscopy, all types of cells—including erythrocytes—incorporated radioactive leucine within 30 seconds after its addition to the incubation medium and continued to do so for at least 30 minutes (figs 1-7). Although differences in the degree of labelling among the various types of cells are exaggerated in figure 1 by differences in size of the cells it was apparent by both light and electron microscopy that large lymphocytes and immature plasma cells contained the greatest concentrations of radioactivity. Medium sized lymphocytes and mature plasma cells were intermediate and most small lymphocytes contained little or no label at autoradiographic exposures adequate for demonstrating radioactivity in other cells. Macrophages with condensed nuclei contained little label, but those immature macrophages described above were labelled as heavily as medium sized lymphocytes (fig 9). Other types of cells incorporated leucine sparsely. Among cells that labelled heavily nuclear radioactivity was prominent in all but mature plasma cells. During the first ten minutes nuclear label was concentrated along the nuclear membrane and at the line of junction between light and dense chromatin; by 30 minutes nucleoli were radioactive.

Autoradiographic background as judged by the dearth of grains over regions of section containing only imbedding plastic was negligible. A few grains lay over intercellular spaces (figs 7-9, 10, 11, 13) but these may indicate either extracellular labelled protein or an occasional beta particle from intracellular tritium that penetrated more than half a micron before encountering a silver bromide crystal. Cellular debris incorporated some leucine (fig 7).

Quantitative autoradiography

As indicated in table 1 material for grain counts in plasma cells was obtained from all but experiment II and selected groups of experiment I. In experiment II



Figures 2 and 3

light microscopy (64b) The Golgi region incorporated little or no leucine during the first four minutes but had begun to accumulate radioactivity by ten minutes and within 20 minutes had surpassed the rest of the cytoplasm This sequence of events in ergastoplasm and Golgi region corresponds in timing to the course of synthesis intracellular accumulation and subsequent release of antibody described by Helmreich Kern and Eisen (61) In experiment V, the Golgi region was already labelled more heavily than the ergastoplasm after only ten minutes exposure to radioactive leucine but the addition of serum to the incubation medium made this experiment different from the others perhaps it accelerated the accumulation of newly formed protein in the Golgi region

Reincubation in unlabelled leucine produced varied results In experiment I after exposure to radioactive leucine for one hour it made little difference (figs 2 3) In experiment IV after only 30 seconds exposure to radioactive leucine the addition of unlabelled leucine—in a concentration only three times greater than that of the radioactive leucine—seemed to retard the incorporation of radioactive leucine by 30 minutes the label in the ergastoplasm was not as great as in experiment III and the Golgi region had not yet exceeded the ergastoplasm in radioactivity (figs 4 5) In experiment V in which serum was added to the incubation medium to improve conditions for the cells and in which the cells were washed to free them of radioactive leucine before the addition of a high concentration of unlabelled leucine both Golgi region and ergastoplasm were reduced by reincubation to the same low level of radioactivity (fig 6) As might be expected from the fact that antibody has not been identified in nuclei (Rifkind et al 62 de Petris and Karlsbad 65) nuclear label was not reduced by reincubation in unlabelled leucine

Puromycin reduced the label in both Golgi region and ergastoplasm, but counts in the Golgi region varied greatly from cell to cell and correlated poorly with counts in the ergastoplasm (figs 2 3)

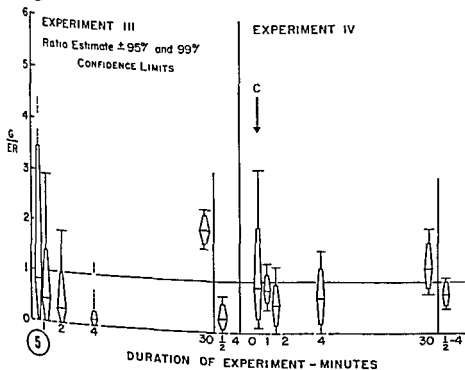
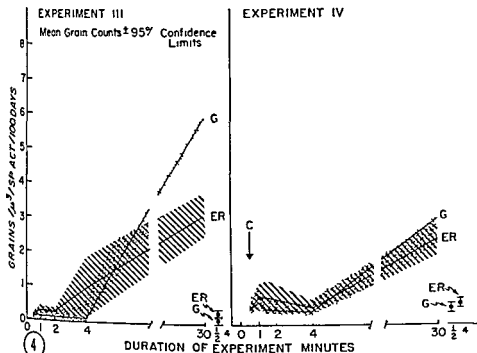
DISCUSSION

Cellular differentiation and the origin of plasma cells

Our observations furnish indirect support for the contention that plasma cell originate from large lymphocytes (de Petris and Karlsbad 65) All the cells in the putative transitional series actively manu

Fig 2 Grain counts over plasma cells in experiment I The numbers of grains over nuclei (N) the Golgi region (G) and the remainder of the cytoplasm (ER) were related to the volume of each region estimated by weighing the appropriate areas cut from electron micrographs and the results were expressed as a ratio estimate (mean grains per region)/(mean volume of region) normalized to a specific activity of one curie of tritium per millimol of leucine and an autoradiographic exposure of 100 days Confidence limits were computed from Fieller's theorem (Cochran 63) Labelled leucine was added to all groups at the beginning of the experiment after one hour's incubation unlabelled leucine (C) or puromycin (P) was added to groups 10 and 8 respectively and the cells were reincubated for an additional hour It appears that grain counts in the Golgi region had exceeded those in the remainder of the cytoplasm as early as 20 minutes after the addition of labelled leucine and—except for the variable results at 30 minutes—remained higher thereafter Reincubation in unlabelled leucine seemed to have little effect but puromycin lowered grain counts generally However such comparative interpretations are subject to question because variations in thickness of sections and emulsion made obvious differences in autoradiographic efficiency—even within individual autoradiographs—and variations in exposure introduced possibilities for variation in fading of the latent image Therefore a statistical means was sought to make comparisons between regions within individual cells where variations in autoradiographic efficiency were minimal (See fig 3)

Fig 3 Intracellular comparisons of grain counts in the Golgi region (G) to those in the remainder of the cytoplasm (ER) in plasma cells of experiment I made cell by cell to avoid uncontrolled variations in autoradiographic efficiency and expressed as ratio estimates (see page 16) Fieller's theorem takes account of the skewness inherent in the distribution of some ratios therefore confidence limits are not always symmetrically related to the ratio estimates Arrowheads in place of upper 99% confidence limits indicate that the limits extend beyond the top of the graph The ratio of G to ER was significantly greater than 1.0 after incubation for 20 60 90 and 120 minutes and after reincubation in unlabelled leucine (C—group 10) but not after reincubation in puromycin (P—group 8) thus the results reinforce the tentative conclusions drawn from figure 2



Figures 4 and 5

factured protein, as judged by autoradiography, and not all of this new protein was removed by reincubation in unlabelled leucine presumably some of it was structural protein—the building material for cellular reproduction and differentiation. Much protein was manufactured in the nuclei of immature cells of the series, but not in mature plasma cells—a parallel with Mitchell's observations on the synthesis of RNA (64a, 64b). Mitosis was observed in large lymphocytes. All of these observations are consistent with the hypothesis that mature plasma cells are the effete end products of cellular differentiation from proliferating clones of large lymphocytes and immature plasma cells (Nossal 62). On the other hand, differentiation of plasma cells from phagocytic cells has not yet been ruled out. If one takes a properly dynamic view of the question however then the categorization of cellular types on the basis of the morphology of dead cells—however detailed the analysis of that morphology may be—seems limited in its usefulness because of its failure to consider that any particular morphology may be only a passing phase in a rapidly and reversibly modulating population of cells.

Quantitative autoradiography

Autoradiography with the light microscope was inconclusive in demonstrating the intracellular migration of antibody partly due to limitations in autoradiographic resolution but even more because it was difficult to distinguish Golgi region from ergastoplasm. Nevertheless qualitative assessment by light microscopy supported the conclusions drawn from electron micrographs.

Grain counts obtained from electron micrographs could be interpreted to indicate that antibody was synthesized in the ergastoplasm and migrated to the Golgi complex before being released from the plasma cell but before such conclusions can be defended from the biological viewpoint the chemical specificity of the method and the rationale for effective quantitation need to be established.

1 *Chemical specificity* The object of the experiments was to identify newly formed protein. There is strong evidence that cells incorporate leucine almost ex-

clusively into new protein (Caro and Palade 64), and that after the usual preparation of tissue for autoradiography more than 90% of the remaining radioactivity represents protein (Warshawski, Leblond and Droz 63), but Caro and Palade (64) discovered that when tissue were fixed in osmium tetroxide as much as 4% of the free amino acid present at the time was bound to the tissue in such a way that it survived preparation for autoradiography and produced silver grains.

Thus except in groups reincubated in unlabelled leucine, some of the label seen in the present experiments might have represented free leucine rather than newly formed protein—this could account for the few silver grains seen over erythrocytes, as noted by Caro and Palade (64). If the intracellular distribution of amino acids was relatively uniform as suggested by the autoradiographic experiments of Benditt et al (65) then the spurious background thus produced might have obscured regional differences in the concentration of labelled protein but it would not have created false differences. On the other hand if recently acquired amino acid failed to mix freely with the

Fig 4 Grain counts over the Golgi region (G) and the remainder of the cytoplasm of plasma cells in experiments III and IV expressed as in figure 2. Groups 1 to 4 were combined to obtain values for incubations of one-half to four minutes inclusive. In experiment IV, unlabelled leucine (C) was added 30 seconds after the addition of tritium labelled leucine. During the first four minutes incubation label in the ergastoplasm appeared to exceed that in the Golgi region whereas the reverse was true by 30 minutes after addition of labelled leucine. Unlabelled leucine seemed to reduce the rate of incorporation of label and erase the differences between regions. However the objections raised in relation to figure 2 apply to these interpretations as well intracellular comparisons are needed.

Fig 5 Intracellular comparisons between grain counts in the Golgi region (G) and those in the remainder of the cytoplasm (ER) expressed as in figure 3. Groups for one-half to four minutes incubation were combined and unlabelled leucine (C) was added to experiment IV as in figure 4. Using Fieller's theorem confidence limits are derived from the roots of a quadratic equation if imaginary roots are obtained as occurred for the upper 99% limits after one-half and four minutes incubation in experiment III no limit can be estimated. The results of these intracellular comparisons reinforce the conclusions drawn from figure 4.

ports. Therefore it seems unlikely that bound leucine was a source of erroneous localization of protein accordingly the reduction of label in Golgi region and ergastoplasm produced by reincubation in unlabelled leucine in experiment V will be interpreted as excretion of labelled immunoglobulin.

2. Resolution Caro (62) estimated that the resolution for tritium in electron micrographs fell between 0.1 and 0.5 μ depending upon experimental conditions. The Golgi complex in our micrographs had a minimum width of 0.7 μ therefore labeling of the Golgi complex should be distinguishable from radioactivity in the surrounding cytoplasm but the spread of beta particles across the boundaries of such a small region could distort grain counts. However most Golgi complexes were wider than 0.7 μ and in any case errors of resolution would tend to obscure true differences in radioactivity between adjacent regions rather than creating false differences. For example the few grains seen over the Golgi region after incubation for less than ten minutes might have arisen from tritium in the "juxtagolgi" cytoplasm if so then the true difference between Golgi complex and ergastoplasm was greater than it seemed.

Another problem of resolution is not so easy to rationalize. Many grains occurred above the nuclear membrane and were included in the counts for nuclei or ergastoplasm depending upon their exact location. de Petris and Karlsbad (65) found concentrations of antibody within the cavity of the nuclear membrane a space continuous with the cavities of the ergastoplasm. If silver grains along the nuclear membrane represented such antibody then inclusion of some grains in the counts for nuclei would have produced a falsely low estimate of the radioactivity in ergastoplasm and exaggerated the extent to which the Golgi complex appeared to exceed the ergastoplasm in label after prolonged incubation. However recounting a group of autoradiographs to include all rich grains in the ergastoplasm increased the average count by less than 4% such an error is too small to compromise the observed differences (fig 2).

3. Quantitation The basis for quantitation of autoradiographs lies in the presumption that grain counts are proportional to the total quantity of radioisotope present in the specimen. This will be true only if the specimen is thin enough for a representative proportion of beta particles to reach the emulsion and if all other factors affecting the probability that grains will form are held constant. The adaptation of autoradiography to the electron microscope has been haunted by the fear that constancy of conditions would need to be sacrificed for improvement in resolution. This ghost has been laid by recent work. Techniques have been standardized (Caro and van Tubergen 62 Salpeter and Bachmann 64) to such an extent that reproducible quantitative results can be obtained. Caro and Shnos (65) obtained reliable estimates of efficiency for tritium but they pointed out its great sensitivity to variations in thickness of the emulsion. Bachmann and Salpeter (65) looked for non linearity of response by testing for fading of the latent image in the emulsion during prolonged autoradiographic exposure. They reported that fading did not occur in Ilford L-4 emulsion exposed at room temperature in dry air for 2 months but others have not been so fortunate and the factors that control fading are poorly understood. Thus reproducible autoradiographic efficiency is achievable but definitive methods for maintaining conditions constant and controlling fading of the latent image have not yet been developed. In the present experiments obvious variations in thickness of sections and emulsion made visible differences in efficiency and some exposures exceeded two months. Therefore constant efficiency cannot be taken for granted when comparing different experimental groups. Different autoradiographs within one experimental group or even different plasma cells with in individual autoradiographs. A statistical method is needed for dealing with the large variability in the data and for making intracellular comparisons.

Before statistical analysis can be attempted there must be some assurance that the data were collected from samples that because they were randomly chosen truly represented the phenomena under

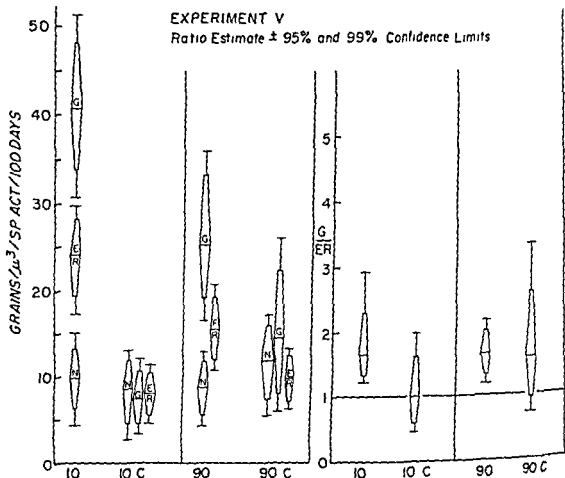


Fig 6 Grain counts over plasma cells in experiment V expressed both as grain counts for each region as in figure 2 and as the ratio of grain counts in the Golgi region to those in the ergastoplasm (ER) made cell by cell as in figure 3. After incubation in labelled leucine for 10 or 90 minutes the cells were washed, resuspended in unlabelled leucine and reincubated for three hours (10 C and 90 C). Grain counts in the Golgi region had already exceeded those in the ergastoplasm after only ten minutes incubation but this experiment differed from the others in that rabbit serum was added to the incubation medium to improve conditions for the cells perhaps this accelerated the accumulation of newly formed protein in the Golgi region. Reincubation in unlabelled leucine reduced the label in both Golgi region and ergastoplasm but made little difference in nucleolus (N). These observations are consistent with the reported identification of immunoglobulins in ergastoplasm and Golgi complex by immunohistochemical methods and they are interpreted to indicate that the label removed by reincubation in unlabelled leucine was newly formed immunoglobulin. If this interpretation is correct then antibody not only accumulates in the Golgi complex it also is removed from there in the course of secretion.

total intracellular pool as proposed by Kipnis, Reiss and Helmreich (61) then local concentrations of labelled leucine might have been a source of confusion. However, there is indirect evidence in the experimental results that such confusion was not a source of serious error. First intracellular label was low during the first four minutes of incubation, when labelled leucine should already have entered the cells in high concentration (Kipnis, Reiss and Helmreich 61). Second reincubation

in unlabelled leucine by making labelled leucine relatively unavailable should have reduced any spurious label due to bound amino acid but nuclear label was never reduced by this procedure and in experiment I label was not reduced in the Golgi region or ergastoplasm either. In contrast when cells were reincubated in puromycin which presumably interrupted the synthesis of protein but did not change the availability of labelled leucine label appeared to be reduced in all three re-

distribution (Snedecor 56) Hanawalt et al (61) demonstrated that this was true for whole cells of uniform size and specific activity and Caro and Shnos (65) used Poisson means to express grain counts over sections of uniformly labelled bacteria in electron micrographs. In large samples Poisson distributions approach normality. Hastenbaum and Hanna (65) studying mixed populations of whole cells assumed that their data were distributed normally and used analysis of variance to test the significance of differences between mean grain counts. However, Stewart et al (65) demonstrated that small errors in estimation of background skew the distribution of grain counts over whole cells and they adopted the "grain median" as a more reliable estimate of radioactivity than the mean grain count.

In electron micrographs background was negligible but the use of sections introduces other difficulties both for light and electron microscopy. Poisson statistics are based on specimens of uniform size but intracellular regions in sections are variable in size. This difficulty could be circumvented by subdividing each region into uniform areas by superimposition of a standard grid on the electron micrograph but the Golgi region was too small and irregular in shape to be subdivided with any accuracy.

Another approach can be based on the statement that in homogeneously labelled regions where the probability that grains will occur is proportional to the total radioactivity present grain counts should be proportional to the volume of the region. In other words if grain count is plotted against volume of the region for a homogeneously labelled sample of regions the graph should describe a straight line that passes through the origin and the slope of the line should be a measure of the concentration of radioactivity in the specimen. Schultz et al (65) found that such linear regressions adequately described the distribution of grain counts over nuclei in sections from mice injected with tritium labelled amino acid and they concluded that this indicated a uniform specific rate of protein synthesis per unit volume of nucleus. Our data also fit such

linear regressions but with considerable variation.

Thus the ratio of grain count to volume seems a reasonable estimate of the concentration of radioactivity but the average of such ratios which other authors have used for statistical comparisons is not the best estimate when groups are small and grain counts are low. This is because in an average of the ratios all specimens in the sample — regardless of volume — receive the same weight. Where counts are low and many counts of zero occur as in the Golgi region after short incubation periods this error in weighting can be particularly serious. A count of zero in a large volume is a more impressive indication of low radioactivity than a count of zero in a small volume but both would influence an unweighted average equally. What is needed is a weighted average; the ratio estimate is such a weighted average that provides theoretically unbiased values for the slopes of linear regressions which pass through the origin (Cochran 63). The ratio estimate is calculated as the ratio of total grain count for a sample to total volume of the sample or — what is the same thing — the ratio of mean grain count to mean volume.

The difficulty with using ratio estimates is that there is no exact method for calculating variance because ratios by nature are not normally distributed. In large samples the approach to normality may be close enough to allow use of an approximate "normal" solution but in small samples where the coefficient of variation of the denominator (volume) exceeds 0.1 as in most of our experimental groups estimated variances would be misleadingly small. In this event Fieller's theorem still provides an approximate estimate of confidence limits for the ratio estimate; it takes some account of the natural skewness in distribution of ratios and it is relatively safe for use with small samples.

Therefore ratio estimates and confidence limits for grain counts were computed and selected results are presented graphically in figures 2, 4 and 6. Although there seemed to be significant differences between Golgi region and ergastoplasm in many experimental groups differences were not clear after brief incubation peri-

study and were not biased by some artifact of selection. In order to achieve randomness of selection all recognizable plasma cells were photographed as soon as encountered and from these all were chosen for counting that contained at least two grains (but not so many that accurate counting was impossible) had a visible Golgi complex and showed no signs of degeneration. Thus subjective judgements were required for selecting cells for counting; other real or potential sources of non-random selection also operated. Single cells may have appeared in successive sections and been counted twice. The choice of cells with visible Golgi complex although necessary for intracellular comparisons, led to greater representation of the juxtagolgi cytoplasm than of the outer cytoplasm. Accidental coincidence of grains may have reduced the apparent grain count in heavily labelled cells (fig. 11) but to have eliminated all possibility of coincidence would have been to reduce the size of the samples too much. Errors of resolution in which grains over one region arose from tritium in an adjacent region would have operated more in heavily labelled than lightly labelled cells; however as pointed out above these errors would tend only to obscure true differences in concentration rather than creating false differences. In addition to these non-random sources of selection heterogeneity of the material may have been a source of bias. Plasma cells varied in maturity, and the relative numbers of mature and immature plasma cells varied from experiment to experiment. The Golgi complex was not homogeneous in structure if the distribution of label was similarly heterogeneous then thin sections of Golgi complex may not all have represented the same population of labelled protoplasm. Thus there were several real or potential sources of bias in the sampling procedure. None seems—from the theoretical point of view—large enough to compromise statistical analysis but it will be important to seek independent reassurance that the results are logically consistent. As evidence for this results obtained under similar conditions in different experiments should be comparable and results obtained under varying con-

ditions within individual experiments should vary in an appropriate fashion.

The method used for expressing grain counts imposes limits on the conclusions that can be drawn. When expressed as the proportional distribution of grains in several compartments, the data may provide evidence as to the timing of change in distribution but it allows no conclusions concerning the concentrations of isotope present (Caro and Palade, 1964). In measuring the area of each compartment in the section relative concentrations of isotope can be estimated and changes in small compartments can be detected with greater sensitivity, as pointed out by Ross and Benditt (1965).

Thus there is the basis in previous work for estimating the concentration of isotope by counting the grains per unit volume of protoplasm according to the following expression: Concentration of isotope (grains/area of region/thickness of section/exposure) \times efficiency \times error. Errors would include variations in efficiency due to inconsistencies in thickness of section and emulsion, non-linearity due to fading of the latent image and other unknown factors. Because autoradiographic efficiency was not measured in the present experiments, only relative concentration of isotope can be estimated.

4. Statistical analysis. There is as yet no firmly established rationale for analysis of grain counts over sections of heterogeneous cells or tissues. Many investigators have avoided statistical testing altogether; others have calculated mean grain counts and standard errors and have used the *t* test to evaluate the significance of differences without discussing the rationale for their use (Warshwsky, Leblond and Droz, 1963; Ross and Benditt, 1965). The use of these statistics presupposes a normal distribution of the data but neither *a priori* reasons for expecting a normal distribution nor tests to demonstrate normality have been presented. Our data were not normally distributed and judged by graphic methods.

Theoretically with specimens of uniform size and radioactivity the small but uniform probability that grains will occur over any individual specimen should result in grain counts that follow a Poisson

formed protein had accumulated in the Golgi region. In attempting physiological interpretation of these conclusions three questions will be discussed: 1. What part of the newly formed protein is antibody or immunoglobulin? 2. What is the source of the protein that accumulates in the Golgi region? 3. What role does the Golgi complex play in the secretion of antibody?

1. Identification of antibody. Judging from the results of reincubation in unlabelled leucine both ergastoplasm and Golgi region contained newly formed antibody but there was little or none in nuclei. Immunohistochemical staining has led to similar conclusions (Rifkind et al. 62; de Petris and Karlsbad 65). On the other hand some of the label in ergastoplasm and Golgi region was not removed by reincubation in unlabelled leucine. This label may represent structural protein or it may be due to antibody that was not released because of cellular injury as discussed above.

2. The source of label in the Golgi region. Ribosomes were not seen within the Golgi complex and the label there was low during the first 4 to 10 minutes of incubation. Others have concluded that the Golgi complex in the pancreas does not synthesize protein (Warshawsky et al. 63; Ca o and Palade 64) and a similar conclusion seems warranted for plasma cells. Therefore the label that accumulated in the Golgi region and was removed by reincubation in unlabelled leucine presumably represents antibody that had migrated to the Golgi region after synthesis in the ergastoplasm. Jamieson and Palade recently have obtained evidence for such a migration in the pancreas (66). If the label not removed by reincubation was structural protein its source might have been either ergastoplasm or nucleus.

3. Pole of the Golgi complex in secretion. The foregoing evidence can be interpreted to indicate that antibody migrates from the ergastoplasm to the Golgi region during the latent period of secretion and that it reaches a high concentration there just at the time when the concentration of labelled antibody in the ergastoplasm reaches a plateau and antibody first appears extracellularly (Helmreich and Eisen 61). Therefore in

the plasma cell as elsewhere the Golgi region is by implication a way station on the route of secretion.

However the "role" of the Golgi complex in secretion of antibody is not yet obvious. In the pancreas the Golgi complex seems to be the site where secretory material is concentrated into zymogen granules but few plasma cells contain anything that might be called secretory granules—Russell bodies lie within the ergastoplasm not in the Golgi complex. Synthesis of carbohydrate has been attributed to the Golgi complex (Peterson and Leblond 64) perhaps the carbohydrate moiety of antibody (Cohen and Porter 64) is manufactured there. Whether continued synthesis of protein is necessary for the Golgi complex to play its role in secretion was not determined by our experiments because puromycin produced equivocal results. If the label remaining in the Golgi region after reincubation in unlabelled leucine was structural protein it may be an indication that the Golgi complex serves as a depot for membranes involved either in the formation of ergastoplasm or the release of antibody from the cell.

The mechanisms for release of antibody remain as obscure as the role of the Golgi complex. As mentioned in RESULTS the Golgi complex is remote from the surface of the cell and no morphological indications of transport of antibody from the Golgi region or its excretion from the cell were detected. Even when all this is understood it will still be necessary to explain what mechanisms coordinate synthesis, storage and excretion—why some plasma cells accumulate antibody in dilated ergastoplasmic sacs or in condensed Russell bodies whereas most plasma cells seem to excrete antibody as fast as it is manufactured.

In other words more work needs to be done to understand the secretion of antibody. This study has produced evidence of the importance of the Golgi complex in the process and has demonstrated some of the possibilities and difficulties of quantitative autoradiography with the electron microscope. Future work might profitably be concerned with synthesis of membranes and of carbohydrates by plasma cells.

ods and as pointed out earlier, direct comparisons had to be made with caution because of variations in the thickness of sections and emulsion.

Therefore more reliable estimates were sought in intracellular comparisons where thickness of section and emulsion were relatively constant. To achieve such comparisons as for example between Golgi region and ergastoplasm ratio estimates were constructed as follows

$$\frac{G_{\text{grains}}/G_{\text{volume}}}{E_{\text{grains}}/E_{\text{volume}}}$$

However in order to give proper weight to Golgi regions in which no grains were found and to make comparisons cell by cell the ratio estimates actually were computed by isolating Golgi grains in the numerator as follows

$$\frac{G_{\text{grains}}}{G_{\text{volume}}/E_{\text{grains}}/E_{\text{volume}}}$$

This seemed justifiable because volume could be considered as a given quantity rather than an independent variable and therefore both numerator and denominator each contained only one independent variable. These intracellular comparisons some of which are presented in figures 3, 5 and 6 supported the conclusions drawn from individual ratio estimates and, in addition indicated that the Golgi region was significantly lower in label than the ergastoplasm after incubation for one half to four minutes.

These statistically significant results when examined for logical consistency were for the most part reproducible among the several experiments and varied with differing experimental conditions. Therefore it will be presumed either that selection of samples was adequately random or that selective biases operated so uniformly in all experiments that the results are true only for some particular segment of the population of plasma cells. In either case biological interpretation seems justified.

Biological interpretation

Before interpreting the results in terms of normal cellular physiology the possibility needs to be considered that the mechanisms of secretion were altered

either by the damaging effects of radiation from tritium or by unfavorable conditions of incubation. This possibility applies particularly to those experimental groups which underwent prolonged incubation and reincubation. It might explain for instance the fact that in experiment I grain counts were lower after two hours incubation (group 6) than after incubation for one hour (group 5) (fig. 2). That tritium may damage cells is adequately tested by Wimber's review (64) but most of the experiments he cites involved thymidine and damage was indicated by reduction in mitotic rate. There is little evidence from which to evaluate the damaging effects on secretory processes of short exposures to tritium labelled amino acids. Helmreich et al. (61) reported that synthesis and release of antibody continued unabated for at least five hours but the concentrations of tritium used in the present experiments were as much as 2.5 times greater than they used and must also have been considerably greater than those to which cells have been exposed in studies of secretion *in vivo* (Caro and Palade 64). However, the cells used for grain counts in our experiments showed no visible signs of damage at the end of incubation — as seen in electron micrographs — and they failed to stain with eosin Y. The reduction of grain counts in both Golgi region and ergastoplasm upon reincubation in unlabelled leucine in experiment V where the greatest care was taken to insure favorable conditions for incubation can be taken as evidence that mechanisms for release of antibody continued to operate perhaps the failure of grain counts to diminish with reincubation in experiment I group 10 is evidence that in this group mechanisms of release had been damaged. Therefore although morphological evidence and dye exclusion indicated that the cells were undamaged altered mechanisms of secretion must remain as possible explanations for the results.

On the basis of all the previous considerations it seems appropriate to conclude that incorporation of leucine into new protein began without delay in nuclei and ergastoplasm — but not in the Golgi region — and that within 20 minutes newly

protein had accumulated in the Golgi region. In attempting physiological interpretation of these conclusions three questions will be discussed: 1. What part of the newly formed protein is antibody or immunoglobulin? 2. What is the source of the protein that accumulates in the Golgi region? 3. What role does the Golgi complex play in the secretion of antibody?

1. *Identification of antibody* Judging from the results of reincubation in unlabelled leucine both ergastoplasm and Golgi region contained newly formed antibody but there was little or none in nuclei. Immunohistochemical staining has led to similar conclusions (Rifkind et al. 1965; de Petris and Karlsbad 1965). On the other hand some of the label in ergastoplasm and Golgi region was not removed by reincubation in unlabelled leucine. This label may represent structural protein or it may be due to antibody that was not released because of cellular injury as discussed above.

2. *The source of label in the Golgi region* Ribosomes were not seen within the Golgi complex and the label there was low during the first 4 to 10 minutes of incubation. Others have concluded that the Golgi complex in the pancreas does not synthesize protein (Warshawsky et al. 1961; Caro and Palade 1964) and a similar conclusion seems warranted for plasma cells. Therefore the label that accumulated in the Golgi region and was removed by reincubation in unlabelled leucine presumably represents antibody that had migrated to the Golgi region after synthesis in the ergastoplasm. Jamieson and Palade recently have obtained evidence for such a migration in the pancreas (1966). If the label is not removed by reincubation was structural protein its source might have been either ergastoplasm or nucleus.

3. *Pole of the Golgi complex in secretion* The foregoing evidence can be interpreted to indicate that antibody migrates from the ergastoplasm to the Golgi region during the latent period of secretion and that it reaches a high concentration just at the time when the concentration of labelled antibody in the ergastoplasm reaches a plateau and antibody first appears extracellularly (Helmreich and Eisen 1961). Therefore in

the plasma cell as elsewhere the Golgi region is by implication a way station on the route of secretion.

However the "role" of the Golgi complex in secretion of antibody is not yet obvious. In the pancreas the Golgi complex seems to be the site where secretory material is concentrated into zymogen granules but few plasma cells contain anything that might be called secretory granules—Russell bodies lie within the ergastoplasm not in the Golgi complex. Synthesis of carbohydrate has been attributed to the Golgi complex (Peterson and Leblond 1964) perhaps the carbohydrate moiety of antibody (Cohen and Porter 1964) is manufactured there. Whether continued synthesis of protein is necessary for the Golgi complex to play its role in secretion was not determined by our experiments because puromycin produced equivocal results. If the label remaining in the Golgi region after reincubation in unlabelled leucine was structural protein it may be an indication that the Golgi complex serves as a depot for membranes involved either in the formation of ergastoplasm or the release of antibody from the cell.

The mechanisms for release of antibody remain as obscure as the role of the Golgi complex. As mentioned in RESULTS the Golgi complex is remote from the surface of the cell and no morphological indications of transport of antibody from the Golgi region or its excretion from the cell were detected. Even when all this is understood it will still be necessary to explain what mechanisms coordinate synthesis, storage and excretion—why some plasma cells accumulate antibody in dilated ergastoplasmic sacs or in condensed Russell bodies whereas most plasma cells seem to excrete antibody as fast as it is manufactured.

In other words more work needs to be done to understand the secretion of antibody. This study has produced evidence of the importance of the Golgi complex in the process and has demonstrated some of the possibilities and difficulties of quantitative autoradiography with the electron microscope. Future work might profitably be concerned with synthesis of membranes and of carbohydrates by plasma cells.

ACKNOWLEDGEMENT

I wish to express grateful appreciation to Dr Ernst Helmschick, of the Department of Biological Chemistry, Washington University School of Medicine, who called my attention to the usefulness of this experimental system for studying secretion of antibody, carried out immunization, isolation of cells and incubations in experiments I and II and served as a valuable source of advice and help throughout the course of the work.

LITERATURE CITED

- Bachmann L and M M Salpeter 1965 Autoradiography with electron microscope A quantitative evaluation *Lab Invest* 14 1041-1053
- Benditt E P G M Martin and H Platter 1965 Application of freeze drying and formaldehyde vapor fixation to radioautographic localization of soluble amino acids In *The Use of Radioautography in Investigating Protein Synthesis* Edited by C P Leblond and K B Warren Academic Press New York and London pp 65-75
- Benge W P J 1960 Staining autoradiographs at low temperature *Stain Tech* 35 106-108
- Bessis M C 1961 Ultrastructure of lymphoid and plasma cells in relation to globulin and antibody formation *Lab Invest* 10 1040-1067
- Black L and M C Berenbaum 1964 Factors affecting the dye exclusion test for cell viability *Exp Cell Res* 35 9-13
- Caro L G 1962 High resolution autoradiography II The problem of resolution *J Cell Biol* 15 189-199
- Caro L G and G E Palade 1964 Protein synthesis storage and discharge in the pancreatic exocrine cell An autoradiographic study *J Cell Biol* 20 473-495
- Caro L G and M Schnos 1965 Tritium and phosphorus 32 in high resolution autoradiography *Science* 149 60-62
- Caro L G and R P van Tubergen 1962 High resolution autoradiography I Methods *J Cell Biol* 15 173-188
- Cochran W G 1963 *Sampling Techniques* John Wiley and Sons Inc New York London
- Cohen S and R R Porter 1964 Structure and biological activity of immunoglobulins *Adv Imm* 4 287-349
- Cowan W K and G D Sorenson 1964 Electron microscopic observations of acute thymic involution produced by hydrocortisone *Lab Invest* 13 353-370
- de Petris S and G Karlsbad 1965 Localization of antibodies by electron microscopy in developing antibody-producing cells *J Cell Biol* 26 759-778
- Hanawalt P C O Maalge D J Cummings and M Schaeffer 1961 The normal DNA replication cycle II *J Mol Biol* 3 156-165
- Harris T N K Hummel and S Harris 1965 Electron microscopic observations on antibody producing lymph node cells *J Exp Med* 123 161-172
- Helmschick E M Kern and H N Eisen 1961 The secretion of antibody by isolated lymph node cells *J Biol Chem* 236 464-473
- 1962 Observations on the mechanism of secretion of γ globulins by isolated lymph node cells *J Biol Chem* 237 1975-1981
- Jamieson J D and G E Palade 1966 Role of the Golgi complex in the intracellular transport of secretory proteins *Proc NAS* 55 424-431
- Kastenbaum M A and M G Hanna 1965 Statistical analysis of autoradiographic and histologic data *Arch Path* 79 462-465
- Kipnis D M E Reiss and E Helmschick 1961 Functional heterogeneity of the intracellular amino acid pool in mammalian cells *Biochim Biophys Acta* 51 519-521
- Luft J H 1961 Improvements in epoxy resin embedding methods *J Biophys and Biochem Cytol* 9 409-414
- Malamed S 1963 Use of a microcentrifuge for preparation of isolated mitochondria and cell suspensions for electron microscopy *J Cell Biol* 18 696-700
- Mitchell J 1964a Autoradiographic studies of nucleic acid and protein metabolism in lymphoid cells I Differences amongst members of the plasma cell sequence *Aust J Exp Biol Med Sci* 42 347-362
- 1964b Autoradiographic studies of nucleic acid and protein metabolism in lymphoid cells II The stability and actinomycin sensitivity of rapidly formed RNA and protein *Aust J Exp Biol Med Sci* 42 363-372
- Nossal G J V 1962 Cellular genetics of immune responses *Adv Imm* 2 163-204
- Peters T 1957 A serum albumin precursor in cytoplasmic particles *J Biol Chem* 229 659-677
- Peterson M and C P Leblond 1961 Synthesis of complex carbohydrates in the Golgi region as shown by radioautography after injection of labeled glucose *J Cell Biol* 21 143-148
- Revel J and E D Hay 1963 An autoradiographic and electron microscopic study of collagen synthesis in differentiating cartilage 2 *Zellforsch* 61 110-144
- Rifkind R A E F Osserman K C Hsu and C Morgan 1962 The intracellular distribution of gamma globulin in a mouse plasma cell tumor (X5563) as revealed by fluorescence and electron microscopy *J Exp Med* 116 423-432
- Ross R and E P Benditt 1965 Wound healing and collagen formation V Quantitative electron microscope radioautographic observations of proline 14 C utilization by fibroblasts *J Cell Biol* 27 83-106
- Salpeter M M and L Bachmann 1964 Autoradiography with the electron microscope A procedure for improving resolution sensitivity and contrast *J Cell Biol* 22 469-477
- Schultz B P Citoler K Hempel K Citoler and W Maurer 1965 Cytoplasmic protein synthesis in cells of various types and its relation

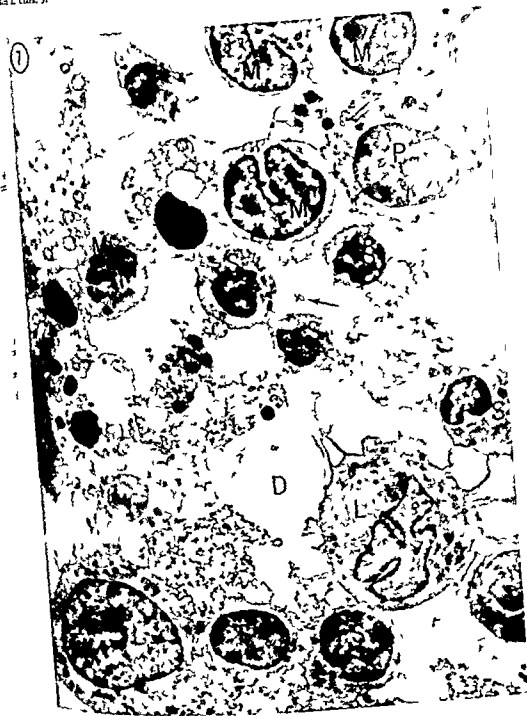
- to nuclear protein synthesis In *The Use of Radioautography in Investigating Protein Synthesis*. Edited by C P Leblond and K B Wimer Academic Press New York and London, pp 107-139
- Snedecor C W 1956 *Statistical Methods* The Iowa College Press Ames Iowa
- Szymon, C D 1964 Electron microscopic observations of bone marrow from patients with multiple myeloma *Lab Invest* 13 196-213
- Lwert, P A, H Quastler M R Skougaard D A Wimer M F Wolfsberg C A Ferrotta B Fabel and M Carlough 1965 Four factor model analysis of thymidine incorporation into mouse DNA and the mechanism of radiation effects *Radiation Res* 24 521-537
- Thiery J P 1959 Microcinematographic contributions to the study of plasma cells In *Cellular Aspects of Immunity* Edited by G E W Wolstenholme and M O'Connor Little Brown and Company Boston pp 59-81
- Warshawsky H C P Leblond and B Droz 1963 Synthesis and migration of proteins in the cells of the exocrine pancreas as revealed by specific activity determination from radioautographs *J Cell Biol* 16 1-23
- Wimer D E 1964 Effects of intracellular irradiation with tritium *Adv Radiation Biol* 1 85-115

Figures 7-13 are electron micrographs and autoradiographs of cells isolated from popliteal lymph nodes of immunized rabbits and incubated with tritium labelled leucine. Sections were stained with uranyl acetate after removing gelatin of the photographic emulsion with NaOH

PLATE 1

EXPLANATION OF FIGURE

- 7 These cells were incubated 90 minutes in labelled leucine (experiment V group 1) and the autoradiograph was exposed for 18 days every cell is labelled. Lymphocytes — identified as small (S) medium sized (M) and large (L) — predominate one plasma cell (P) is present and the remainder is debris — presumably derived from cells that degenerated during the course of isolation or incubation. The plasma cell with its large vesicular nucleus and prominent nucleolus was designated as immature there is label in both nucleus and cytoplasm. The large lymphocyte in the lower left is typical of those large basophilic cells with vesicular nuclei and prominent nucleoli that stand at the beginning of the hypothetical transitional series leading from lymphocytes to plasma cells. The large lymphocyte in the lower right with contorted nucleus and narrow pseudopods has the appearance of becoming a macrophage. The medium sized lymphocyte on the left appears to be in mitosis. The large lipid droplet (D) contains two silver grains similar labelling over erythrocytes where synthesis of protein is equally unexpected was taken as evidence that a small quantity of free leucine was bound to cells and debris by fixation in osmium tetroxide as reported by Caro and Palade (64). The few silver grains seen over intercellular spaces (arrow) probably do not represent background in view of the observation that areas of imbedding plastic outside the pellet of cells were free of grains perhaps the intercellular label represents newly formed antibody or other protein released from the cells $\times 1500$

PROTEIN SYNTHESIS IN LYMPHOID CELLS
S. L. Clark, Jr.

Figures 7-13 are electron micrographs and autoradiographs of cells isolated from popliteal lymph nodes of immunized rabbits and incubated with tritium labelled leucine. Sections were stained with uranyl acetate after removing gelatin of the photographic emulsion with NaOH.

PLATE 1

EXPLANATION OF FIGURE

- 7 These cells were incubated 90 minutes in labelled leucine (experiment V group 1) and the autoradiograph was exposed for 18 days. Every cell is labelled. Lymphocytes — identified as small (S), medium sized (M) and large (L) — predominate. One plasma cell (P) is present and the remainder is debris — presumably derived from cells that degenerated during the course of isolation or incubation. The plasma cell with its large vesicular nucleus and prominent nucleolus was designated as immature; there is label in both nucleus and cytoplasm. The large lymphocyte in the lower left is typical of those large basophilic cells with vesicular nuclei and prominent nucleoli that stand at the beginning of the hypothetical transitional series leading from lymphocytes to plasma cells. The large lymphocyte in the lower right with contorted nucleus and narrow pseudopods has the appearance of becoming a macrophage. The medium sized lymphocyte on the left appears to be in mitosis. The large lipid droplet (D) contains two silver grains. Similar labelling over erythrocytes where synthesis of protein is equally unexpected was taken as evidence that a small quantity of free leucine was bound to cells and debris by fixation in osmium tetroxide as reported by Caro and Palade (64). The few silver grains seen over intercellular spaces (arrow) probably do not represent background. In view of the observation that areas of imbedding plastic outside the pellet of cells were free of grains perhaps the intercellular label represents newly formed antibody or other protein released from the cells. \ 1500

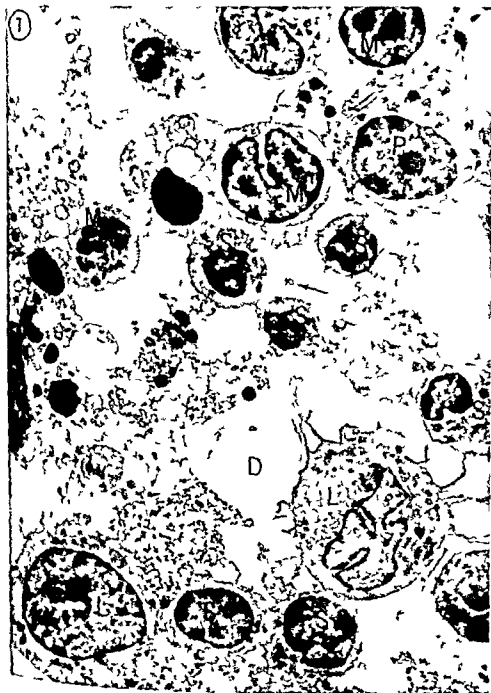


PLATE 2

EXPLANATION OF FIGURES

- 8 This plasma cell incubated ten minutes in labelled leucine (experiment V group 3) and exposed for nine days is typical of those described in the text as degenerating or senescent. The nucleus (N) has separated into two phases and the cytoplasm consists chiefly of condensed ergastoplasm. Although this cell seems relatively active in the synthesis of protein many such cells were not. The mottled appearance of the intercellular space probably indicates the original spacing of silver bromide crystals in the emulsion $\times 15\,000$
- 9 This large cell appears to have been actively ingesting membranous debris along with large quantities of incubation medium. It is typical of one type of macrophage seen in these preparations characterized by a large vesicular nucleus (N) prominent nucleoli cytoplasmic accumulations of ergastoplasm (arrows) and moderately heavy label in both nucleus and cytoplasm. Perhaps this type of cell is a progenitor of plasma cells (Experiment V group 3 incubated ten minutes exposed 47 days) $\times 12\,000$

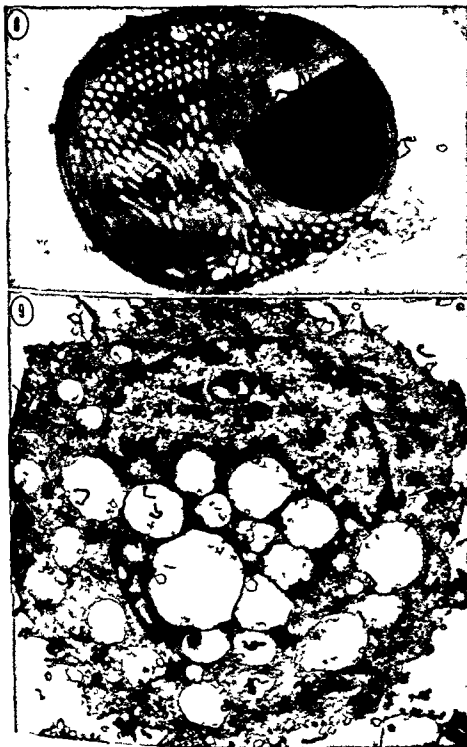


PLATE 3

EXPLANATION OF FIGURES

- 10 This plasma cell was incubated in labelled leucine for ten minutes and reincubated in unlabelled leucine for three hours (experiment V group 4, exposed 20 days) There are three grains over the nucleus (N) two over the Golgi region (G) and seven over the remainder of the cytoplasm (LR) The grain in the upper left lies more than one grain's width (approximately 0.3μ) beyond the edge of the cell and was considered extracellular The dense material at the arrow was identified as dirt rather than a silver grain In terms of the concentration of grains $N = 2.4$ $G = 3.6$ and $LR = 3.1$ grains/ μ^2 /sp act / 100 days $\times 15,000$
- 11 This plasma cell was incubated 90 minutes in radioactive leucine (experiment V group 1 exposed 17 days) The nucleus contains eight grains the Golgi region (G) six grains and the remainder of the cytoplasm 21 grains The large grain at the arrow may be two grains superimposed and thus represent a source of error in counting heavily labelled cells In terms of concentration $N = 7.3$ $G = 28.0$ and $LR = 10.2$ grains/ μ^2 /sp act / 100 days The cytoplasm contains a dense heterogeneous inclusion (I) (S small lymphocyte) $\times 15,000$

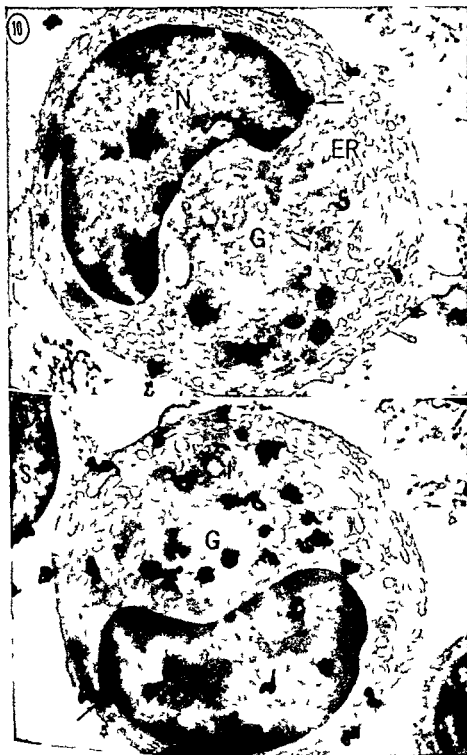


PLATE 3

EXPLANATION OF FIGURES

- 10 This plasma cell was incubated in labelled leucine for ten minutes and reincubated in unlabelled leucine for three hours (experiment V group 4 exposed 20 days) There are three grains over the nucleus (N) two over the Golgi region (G) and seven over the remainder of the cytoplasm (ER) The grain in the upper left lies more than one grain's width (approximately 0.3μ) beyond the edge of the cell and was considered extracellular The dense material at the arrow was identified as dirt rather than a silver grain In terms of the concentration of grains $N = 2.4$ $G = 3.6$ and $ER = 3.1$ grains/ μ^2 /sp act / 100 days $\times 15,000$
- 11 This plasma cell was incubated 90 minutes in radioactive leucine (experiment V group 1 exposed 17 days) The nucleus contains eight grains the Golgi region (G) six grains and the remainder of the cytoplasm 21 grains The large grain at the arrow may be two grains superimposed and thus represent a source of error in counting heavily labelled cells In terms of concentration $N = 7.3$ $G = 28.0$ and $ER = 10.2$ grains/ μ^2 /sp act / 100 days The cytoplasm contains a dense heterogeneous inclusion (I) (S small lymphocyte) $\times 15,000$



PLATE 4

EXPLANATION OF FIGURE

- 12 An enlargement of figure 11 marked to indicate how the Golgi region (G) was delimited from the ergastoplasm for grain counts. As can be seen subjective judgement was important in drawing this line. In this electron micrograph five grains lie entirely within the Golgi region and two others lie on the boundary. One was assigned to the Golgi region and the other to the ergastoplasm. Five grains were considered to lie within one grain's width of the Golgi region and were designated as juxtagolgi. The dense cytoplasmic inclusion (I) is enclosed by a smooth surfaced membrane and resembles inclusions in macrophages $\times 27\ 000$.

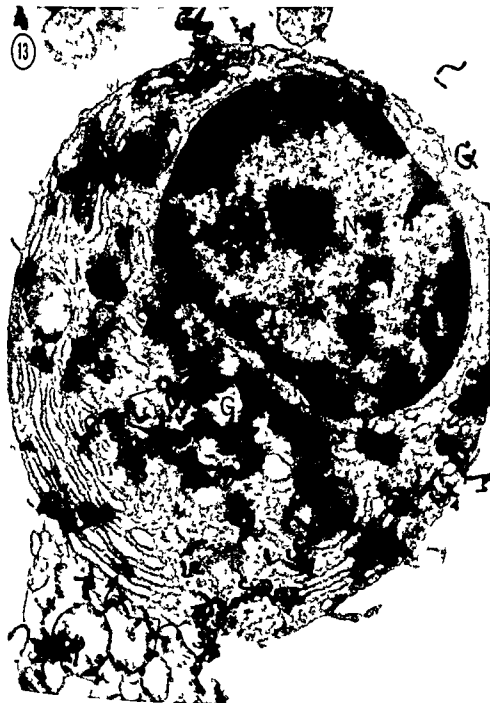
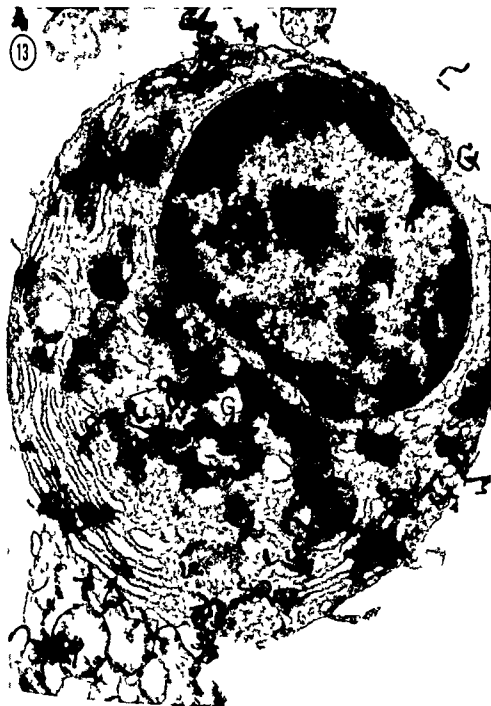


PLATE 5

EXPLANATION OF FIGURE

- 13 This plasma cell was incubated ten minutes in labelled leucine in an incubation medium containing rabbit serum (experiment V group 3 exposed 47 days) In this over exposed autoradiograph the concentration of newly formed protein in the Golgi region (G) and the relatively sparse labelling of the nucleus (N) can be appreciated by inspection (Arrow centriole) $\times 21\ 000$



Dual Innervation of the Mammalian Urinary Bladder¹

A HISTOCHEMICAL STUDY OF THE DISTRIBUTION OF CHOLINERGIC AND ADRENERGIC NERVES

AHMAD EL-BADAWI* AND ERIC A. SCHENK

Division of Urology and Department of Pathology The University of Rochester School of Medicine and Dentistry Rochester New York

ABSTRACT The pattern of autonomic innervation of the urinary bladder was studied in the cat dog rabbit and rat using specific histochemical techniques for acetylcholinesterase and norepinephrine. Cholinergic and adrenergic ganglion cells exist in all layers throughout the bladder wall. Large cholinergic and adrenergic nerve trunks coursing in the adventitial coat and deep lamina propria branch into the muscularis. The terminal cholinergic ramifications form a neuroterminal plexus which surrounds every smooth muscle cell in the bladder wall. The terminal adrenergic fibers are less abundant, do not form a plexus and show regional variations in number at different levels and depths of the muscularis. These variations suggest that two regions of the bladder, namely the base and body, may be distinguished on the basis of differences in muscular innervation.

In the lamina propria cholinergic and adrenergic nerves are grouped as deep and superficial subepithelial nerves. The latter form networks of variable complexity and supply fibers to the epithelium. Throughout the bladder wall the blood vessels have a dual cholinergic and adrenergic perivascular plexus from which fibers extend into the media.

Although the basic pattern of innervation is similar in the species studied, certain variations exist in the relative abundance and arrangement of epithelial and subepithelial nerves. The muscularis has a uniform cholinergic and a variable adrenergic innervation in different species.

The intrinsic innervation of the mammalian urinary bladder, including that of man, is still unsettled. Extensive studies on bladder function in different animals after selective stimulation of vesical nerves, partial or complete denervation and administration of various autonomic drugs have led to the following contradictory conceptions:

- (1) The bladder musculature in its entirety is supplied by purely motor fibers from both sympathetic and parasympathetic nerves (Budge 1864).
- (2) Both sympathetic and parasympathetic nerves supply the entire bladder musculature; the former are motor to the trigone and inhibitory to the rest of the bladder and the latter perform a reciprocal function (Zeiss 1892, 1893, 1894, 1901, Elliott 1901, Learmonth 31).
- (3) The detrusor muscle is supplied exclusively by parasympathetic and the trigone exclusively by sympathetic nerves (Rehlfisch 1897, Page 1902, Langworthy and Murphy 39).
- (4) The detrusor muscle is antagonistically supplied by both parasympathetic and sym-

pathetic nerves and the trigone only by the latter (Kuntz and Succomano 44).

Morphologic data on the distribution of intrinsic vesical nerves have been based entirely on material stained by supravital methylene blue or silver impregnation techniques which are neither fully reliable nor specific. Recently developed histochemical techniques for the selective demonstration of cholinergic (acetylcholinesterase-containing) and adrenergic (norepinephrine-containing) nerves have been used in the present work to define specifically the distribution of these two types of autonomic nerves in the bladder of the cat, dog, rabbit and rat.

MATERIAL AND METHODS

The urinary bladders studied were obtained under light nembutal anesthesia (in

This investigation was supported in part by USPHS Intramural Grant FR 5403 from the National Institute of General Medical Sciences by USPHS grant HE 06089 and by grant from the American Cancer Society. Lecturer in Urology, Faculty of Medicine, University of Alexandria, Alexandria, U.A.R. Presently on leave as a Research Fellow in Urology, Research Unit, University of Rochester School of Medicine and Dentistry, Rochester, New York 14620.

travenous or intraperitoneal) from 49 adult animals: eight male and three female cats, four male and ten female dogs, fifteen male and five female rats, and four male rabbits. In the rat the bladder was removed in toto; in the other animals it was sectioned transversely at 3 to 6 levels or bisected in the median sagittal plane. The specimens were quick frozen with dry ice acetone and stored in a sub zero refrigerator at -80°C . Two to $14\ \mu$ sections were cut at -30°C with a Lipshaw cryostat. Each specimen was so oriented that the entire transverse or sagittal diameter of the bladder was represented on the slide. As many as 30 consecutive or alternate serial sections of the full bladder thickness were obtained from single blocks.

Demonstration of norepinephrine (NE)
The following modification of Falck's (62) technique was employed. Mounted cryostat sections were rapidly transferred to a desiccator and dried over phosphorus pentoxide under vacuum for 25 to 45 minutes or dried at room temperature by a continuous current of cold air for a period of 5 to 15 minutes. The dried slides were transferred to a Coplin jar containing 5 to 10 gm of trioxymethylene (paraformaldehyde) powder; the jar was sealed and heated in an oven at $+80^{\circ}\text{C}$ for 60 to 80 minutes. At the end of this period the slides were dehydrated in absolute alcohol for 15 to 20 seconds, passed in succession through a 1:1 absolute alcohol:xylene mixture and two changes of xylene for 15 seconds each, and mounted in Permount. The dehydrating alcohol bath was replaced by 0.005% Eosin Y in absolute alcohol as a counterstain for some of the sections.

The sections were examined with a Zeiss fluorescent microscope utilizing a high pressure mercury (Osram HBO 200) burner, a BG 12 excitation filter and a 470 m μ barrier filter. Under these conditions the NE-containing nerves stand out prominently as finely beaded bright green fluorescent lines in marked contrast to the dull faint greenish yellow autofluorescent background.

Black and white photographs were taken on 3000 ASA 4×5 Polaroid film (exposure time 8–120 seconds). Color photographs were taken on Kodak high speed Ektachrome EHB 35 mm roll films

(exposure time 10–40 seconds); the processing of the films was modified to give a film sensitivity equivalent to 400 ASA.

Demonstration of acetylcholinesterase (AChE)
The following modification of the technique described by Karnovsky (64) was used. Mounted cryostat sections were dried at room temperature for 5 to 10 minutes and then fixed in 4% neutral formalin at -4°C for 15 to 20 minutes. The sections were rinsed in distilled water and incubated at 37°C for one and a half to three hours. The incubation medium was prepared by dissolving 12 mg of the substrate acetylthiocholine iodide in 16.3 ml acetate buffer (15.8 ml of 0.06 N sodium acetate + 0.5 ml of 0.1 N acetic acid) and then adding the following solutions in the order given: 12 ml of 0.1 N sodium citrate, 2.5 ml of 30 mM cupric sulfate, 0.5 ml of 4 mM tetraso-propylpyrophosphoramidate (iso OMPA), 2.0 ml of distilled water, and 2.5 ml of 5 mM potassium ferricyanide. The pH ranged between 5.5 and 5.6. Following incubation the sections were rinsed in distilled water, counterstained in Harris hematoxylin for 30 to 45 seconds, blued in 1% lithium carbonate washed in tap water (1 minute), dehydrated in 95% and absolute alcohol (15 seconds each), cleared in 1:1 absolute alcohol:xylene mixture and three changes of xylene (30 seconds each), and mounted in Permount. Sites of AChE activity are marked by a finely granular reddish brown precipitate of cupric ferrocyanide.

RESULTS

Innervation of the cat bladder

A. Subepithelial nerves

Two freely interconnected groups of nerves are discernible in the lamina propria, namely the deep and superficial subepithelial nerves.

Deep subepithelial nerves
In the deepest part of the lamina propria numerous sizable cholinergic (fig. 1) and adrenergic nerve trunks and thin nerve bundles run in various directions circumferentially, i.e., in a plane concentric with the epithelial lining. Some of the nerves join ganglia (fig. 2) or individual ganglion cells in the lamina propria. Both types of nerves are

is closely associated with deep subepithelial vessels as neurovascular bundles and give rise to three sets of branches

(a) *Vascular nerves* These accompany the deep subepithelial vessels chiefly the arterioles which like the related nerve trunks and bundles run in a circumferential plane. The vascular nerves ramify around each vessel and arborize in the adventitia to form prominent and intricate cholinergic and adrenergic plexuses (figs 3 4) which send fine fibers into the outer part of the tunica media. Occasionally the nerves also give off slender fiber groups or isolated nerve fibers which run independently in the lamina propria. The vascular nerves and perivascular plexuses closely follow the deep subepithelial vessels their deep muscular branches which run in an outward direction between the innermost muscle bundles and their superficial subepithelial branches which proceed in a radial direction inwards i.e. perpendicular to and towards the epithelium (figs 5 6). Just before reaching the junction of the two layers of the lamina propria each vessel branches dichotomously to smaller channels which continue divergently into the superficial layer of the lamina propria. In this layer the corresponding vascular nerves and perivascular networks become incorporated in the superficial subepithelial plexus.

(b) *Radial subepithelial nerves* These are thin nerve bundles both cholinergic and adrenergic which are seen running through the deep layer of the lamina propria parallel to but independent of nearby vessels (fig 8). While most bundles ramify as a part of the superficial subepithelial plexus a few do not divide till they actually reach the epithelium. Some isolated cholinergic and adrenergic fibers derived from the deep subepithelial nerves or their radial branches seem to end freely at various depths in the lamina propria (fig 7).

(c) *Muscular nerves* In many areas a deep subepithelial cholinergic or adrenergic nerve trunk or one or more of its branch bundles run into the inner muscularis (fig 1) where they ramify.

Rich cholinergic and adrenergic perivascular networks in the deep layer of the lamina propria are present throughout the

bladder. However the complexity of arrangement of the deep subepithelial nerves is more striking in the base than in the dome of the bladder commensurate with the more abundant vascular channels and nerve trunks or bundles that exist in the former region. Large nerve trunks and sizable ganglia in the lamina propria are found only in the dome and upper part of the body of the bladder.

Superficial subepithelial nerves These fibers are derived partly from the cholinergic and adrenergic radial subepithelial nerves and partly from the nerve bundles and networks associated with the radial subepithelial vessels. Traversing the deep layer of the lamina propria the nerves follow distinctly tortuous courses with many U or S turns a loops or corkscrew-like spirals. In the dome and upper part of the body of the bladder the superficial subepithelial nerves are represented by a few scattered cholinergic and adrenergic nerves situated for the most part along the arterioles and some of the venules in the superficial layer of the lamina propria (fig 9). They have few branches and scarcely intercommunicate. At more distal levels of the bladder the nerves progressively increase in number undergo more extensive ramification and inosculate more freely (fig 8). Consequently the nerves become more and more intricately arranged till at the bladder base they are interwoven into a highly complex network.

The superficial subepithelial plexus is typically seen in the region corresponding to the trigone (figs 5 10). Radially directed adrenergic nerve fibers running in the deep layer of the lamina propria ramify and inosculate in the inner third of that layer to form a wide meshed network. This pattern is seen in both transverse and sagittal sections of the bladder indicating a tridimensional arrangement of this plexus. On the epithelial side the plexus sends a few branch fibers which traverse the superficial layer of the lamina propria and intercommunicate sporadically on their way to the epithelium.

By "base" is meant the part of the bladder in which the anterior wall and lateral wall are the posterior wall, while the distal to the bladder is the ureters pierce the bladder wall on its posterior aspect. The rest of the bladder is referred to as the body and its uppermost part the "dome".

The main part of the cholinergic superficial subepithelial plexus is located within the narrow superficial layer of the lamina propria. In both transverse and sagittal sections of the bladder two continuous layers of cholinergic nerves are seen: one at the junction of the two layers of the lamina propria and the other immediately beneath the epithelium. The deeper network receives its component fibers from the nerves running in the deep layer of the lamina propria and the more superficial one sends fine twigs to the epithelium. The two networks are joined together by numerous freely ramifying nerve fibers which have a predominantly radial direction and form a narrow meshed plexus. On the whole the cholinergic superficial plexus is more intricate than its adrenergic counterpart.

B Epithelial nerves

The epithelial nerve fibers arise from the cholinergic and adrenergic superficial subepithelial plexuses as radial branches or continuations of their component fibers. Besides a few thin nerve bundles — chiefly cholinergic — continue uninterruptedly from the deep subepithelial nerves through the whole thickness of the lamina propria without branching or communicating with other nerves on the way to end by breaking up into fine fibers upon reaching the epithelium. Many epithelial fibers are associated with small epithelial blood vessels, often apparently of capillary size.

The innervation of the epithelium ranges from a meager supply by a few widely spaced fibers at the bladder dome to a rich arborization in the distal part of the bladder base.

In the first part of their course the adrenergic epithelial fibers lie almost perpendicular to the epithelium. They enter the basal epithelial layer as undivided fibers or after branching in a Y or T shaped manner (fig. 11). In the latter case the branch fibers run divergently for a short distance in contact with the epithelium and bending sharply they penetrate the epithelium almost perpendicularly. Inside the epithelium the fibers are identified only with difficulty being as a rule very thin and faintly fluorescent. They follow straight or more commonly wavy courses

and becoming more or less parallel to the surface they come to abrupt endings in the basal third of the epithelium.

The cholinergic epithelial fibers originate from the superficial network lying beneath the epithelium. Like the adrenergic epithelial fibers they enter the epithelium immediately or after branching in a Y or T shaped manner. Most intraepithelial cholinergic fibers have slightly clubbed terminations (fig. 12); some divide into two, three or more branches which end widely apart and some — especially in the bladder base — arborize as a rich network between the basal epithelial cells. No fiber extends through more than half the thickness of the epithelium.

C Muscular nerves

General pattern. The cholinergic muscular nerves ramifying inside the musculature arise as branches of intermuscular nerve bundles (fig. 13). Most of these are derived from larger juxtamural nerve trunks which course in the connective tissue on the external surface of the organ. Sizeable nerves are always found between outer muscle bundles and progressively become smaller as they repeatedly subdivide into the depth of the muscle. Some of the latter are derived from deep subepithelial bundles and some communicate with the deep subepithelial vascular nerves and perivascular network. Most bundles show numerous interposed or superimposed nuclei.

The cholinergic intermuscular nerve bundles follow a wavy course in the connective tissue separating large muscle bundles. Together with their parent trunks they accompany interstitial and adventitial blood vessels collectively forming neurovascular bundles. Vascular branches proceed towards the arteries along which they run for variable distances as individual fibers, thin bundles or interanastomosing fiber groups. Ramifying to fine fibers in the adventitia of the vessel they form intricate intermuscular and juxtamural perivascular plexuses which save for the larger size of the vessels differ in no way from their subepithelial analogues already described. Many muscular nerves are derived from the vascular nerves or perivascular plexus. The nerve fibers related

to some of the moderate sized venules are in the form of loose and poorly developed networks

The adrenergic muscular nerves are derived partly from nerve bundles and large nerve trunks composed of cholinergic and adrenergic nerve fibers (fig 14) and partly from purely adrenergic nerve bundles (fig 15) which are commonly associated with blood vessels. They give rise to vascular branches which form a rich perivascular plexus (fig 16) and to thin fiber groups which run in the connective tissue between and inside muscle bundles. Although the adrenergic perivascular plexus is uniformly rich throughout the musculature the adrenergic nerve bundles vary in number in different regions of the bladder. They are more abundant in the base than in the body of the bladder and in the latter region between the outer than between the inner muscle bundles. In the bladder base the adrenergic bundles are about equally abundant at all depths in the muscle layer but still are much less in number than the corresponding cholinergic nerves. As a rule the adrenergic intermuscular nerves are equally distributed in the anterior posterior and lateral walls of the bladder.

Many cholinergic nerves are connected with intermuscular and juxtamural ganglia of different sizes (fig 17). They are present throughout the bladder at all depths in the muscle layer but are larger and more abundant in the base especially between the outer muscle bundles and in the adventitial coat. The ganglia are composed of a variable number of cells of different shapes. The majority of the cells show a heavy staining of their cytoplasm and appear dark brown; all are related to and are usually encircled by fine cholinergic fibers. Some ganglia are connected with adrenergic bundles as well. These ganglia enclose scattered moderately or faintly stained cells and cells which show a diffuse faint or bright fluorescence or a diffuse stippling with fluorescent granules. In addition they constantly contain fine adrenergic fibers that run between or even surround individual ganglion cells (fig 18). Aside from the purely and predominantly cholinergic ganglia a few purely adrenergic ones composed of small clusters of brightly fluorescent cells may be

encountered in the depth of the muscle layer particularly in the bladder base.

In most bladders examined one or more paraureteric cholinergic ganglia were constantly encountered in the cleavage plane between the intravesical part of the ureter and the surrounding bladder musculature. They were frequently connected with moderately thick cholinergic nerve bundles that ran principally parallel to the ureter.

Terminal ramifications. Coursing for variable distances between the larger muscle bundles the cholinergic intermuscular nerves divide and give rise to smaller branch bundles which follow the connective tissue between smaller muscle bundles. These in turn give still thinner fiber groups that lie between groups of muscle fibers. Traced inside the latter the nerve bundles together with the muscular branches of vascular nerves lose their identity and their component fibers become incorporated in an extremely intricate nucleated plexiform network (fig 25). This "cholinergic neuroterminal plexus" is composed of fine sharply defined strands showing a high AChE activity which run along and inosculate between and around individual muscle fibers. Such is the complexity of this plexus that its extensive ramifications virtually entangle each and every muscle cell in the bladder wall (figs 1, 13, 17).

On the whole the terminal ramifications of adrenergic muscular nerves have a far less intricate pattern than the cholinergic terminals. The nerves apparently ramify dichotomously and their finer branches run divergently (fig 23) along and around smooth muscle cells. Here and there the fibers communicate between or across the surface of contiguous muscle cells. Nowhere in the bladder however is the picture of an extensively ramifying terminal plexus found. Many terminal adrenergic muscular nerves take origin from the vascular nerves or perivascular plexus lying in the lamina propria between muscle bundles or in the outer adventitial coat of the bladder.

The distribution of terminal adrenergic fibers shows distinct regional differences. In the bladder dome only few terminal fibers are found in relation to large groups of muscle fibers (fig 20). In the inner

The main part of the cholinergic superficial subepithelial plexus is located within the narrow superficial layer of the lamina propria. In both transverse and sagittal sections of the bladder two continuous layers of cholinergic nerves are seen one at the junction of the two layers of the lamina propria and the other immediately beneath the epithelium. The deeper network receives its component fibers from the nerves running in the deep layer of the lamina propria and the more superficial one sends fine twigs to the epithelium. The two networks are joined together by numerous freely ramifying nerve fibers which have a predominantly radial direction and form a narrow meshed plexus. On the whole the cholinergic superficial plexus is more intricate than its adrenergic counterpart.

B Epithelial nerves

The epithelial nerve fibers arise from the cholinergic and adrenergic superficial subepithelial plexuses as radial branches or continuations of their component fibers. Besides a few thin nerve bundles — chiefly cholinergic — continue uninterruptedly from the deep subepithelial nerves through the whole thickness of the lamina propria without branching or communicating with other nerves on the way to end by breaking up into fine fibers upon reaching the epithelium. Many epithelial fibers are associated with small epithelial blood vessels often apparently of capillary size.

The innervation of the epithelium ranges from a meager supply by a few widely spaced fibers at the bladder dome to a rich arborization in the distal part of the bladder base.

In the first part of their course the adrenergic epithelial fibers lie almost perpendicular to the epithelium. They enter the basal epithelial layer as undivided fibers or after branching in a Y or T shaped manner (fig 11). In the latter case the branch fibers run divergently for a short distance in contact with the epithelium and bending sharply they penetrate the epithelium almost perpendicularly. Inside the epithelium the fibers are identified only with difficulty being as a rule very thin and faintly fluorescent. They follow straight or more commonly wavy courses

and becoming more or less parallel to the surface they come to abrupt endings in the basal third of the epithelium.

The cholinergic epithelial fibers take origin from the superficial network underlying the epithelium. Like the adrenergic epithelial fibers they enter the epithelium immediately or after branching in a Y or T shaped manner. Most intraepithelial cholinergic fibers have slightly clubbed terminations (fig 12) some divide to two three or more branches which end wide apart and some — especially in the bladder base — arborize as a rich network between the basal epithelial cells. No fiber extends through more than half the thickness of the epithelium.

C Muscular nerves

General pattern The cholinergic muscular nerves ramifying inside the bladder musculature arise as branches of intermuscular nerve bundles (fig 13). Most of these are derived from larger juxtamural nerve trunks which course in the connective tissue on the external surface of the organ. Sizeable nerves are always found between outer muscle bundles and progressively become smaller as they repeatedly subdivide into the depth of the muscle. Some of the latter are derived from deep subepithelial bundles and some communicate with the deep subepithelial vascular nerves and perivascular network. Most bundles show numerous interposed or superimposed nuclei.

The cholinergic intermuscular nerve bundles follow a wavy course in the connective tissue separating large muscle bundles. Together with their parent trunks they accompany interstitial and adventitial blood vessels collectively forming neurovascular bundles. Vascular branches proceed towards the arteries along which they run for variable distances as individual fibers, thin bundles or interanastomosing fiber groups. Ramifying to fine fibers in the adventitia of the vessel they form intricate intermuscular and juxtamural perivascular plexuses which save for the larger size of the vessels differ in no way from their subepithelial analogues already described. Many muscular nerves are derived from the vascular nerves or perivascular plexus. The nerve fibers related

part of the muscle scarcely any fibers exist apart from the perivascular plexus (fig 19). At more distal levels in the body of the bladder the terminal fibers progressively become more abundant and are related to smaller and smaller groups of nerve fibers but still more fibers are present in the outer (fig 22) than in the inner (fig 21) muscle bundles. Therefore in the body of the bladder the relative abundance of adrenergic terminals follows two gradients: the nerves increase progressively in number as they are traced (1) at a given level from within outwards and (2) at the same depth in the muscle layer from the dome distally. In the bladder base the terminal adrenergic fibers are much more abundant than in the body of the bladder each fiber being related to one or a few muscle fibers. This picture is uniform throughout the depth of the muscularis in the base (figs 23-24). No differences in the innervation pattern exist between the anterior, posterior and lateral walls of the bladder.

Bladder innervation in other animals

A Subepithelial nerves

In the dog, rabbit and rat bladder the subepithelial nerves generally have a much less complicated arrangement than those in the cat bladder though as in the latter they are considerably more abundant in the base than in the body of the bladder. This applies to both cholinergic and adrenergic fibers. In the rabbit and rat more nerves are consistently seen in the posterior wall than in either the anterior or lateral walls.

In the rabbit deep and superficial nerves can be discerned only in the base. In this region the main arborization of the subepithelial nerves is represented by a single narrow meshed network that underlies the epithelium and lies in the circumferential plane. Otherwise the arrangement of the nerves resembles that seen in the cat bladder save for the difference in number and intricacy of arrangement (figs 26-27).

In the dog the subepithelial nerves are conspicuously less abundant than in either cat or rabbit. The superficial plexus in

the bladder base lies at the junction of the two layers of the lamina propria. The epithelial branches of the plexus run through the compact zone of the submucosa with few connections, so that the picture is that of a very wide meshed network.

In the rat definite subepithelial nerves, whether individual fibers or perivascular plexuses, cholinergic or adrenergic, are seen only in the base of the bladder, especially near the bladder outlet. Even in this region they are sparse, do not mesh late and include no definite nerve bundles or ganglia. Nowhere in the bladder are the fibers discernible as deep and superficial networks.

B Epithelial nerves

In the rabbit the innervation of the epithelium closely resembles that seen in the cat except that a far less number of nerves are seen in the former animal. In the dog intraepithelial fibers can be identified only in the bladder base. Even in this region they are widely separated and undergo very limited branching. No plexiform basal network like that seen in the cat or to a less extent in the rabbit is found; the fibers as a rule remaining individually discernible to their termination. In the rat neither cholinergic nor adrenergic epithelial fibers could be seen.

C Muscular nerves

A uniformly rich cholinergic innervation of all parts of the bladder musculature including the trigone or the corresponding area is found in all three animal species. The distribution of cholinergic ganglia and nerves and the appearance of the neuroterminal plexus are similar to the cat bladder. Paraureteric ganglia occur in all. In the rat a stout nerve trunk is constantly seen penetrating the whole thickness of the posterior bladder wall in a very oblique direction a short distance above the level of the bladder outlet.

The adrenergic muscular innervation in the dog is very similar to that in the cat but in the rabbit and rat it presents some special features.

Like in the cat the base of the rabbit bladder has the richest adrenergic mus-

cular innervation. In the musculature of the bladder body the relative abundance of the adrenergic nerves follows the same "gradients as in the cat bladder. In both the base and body of the rabbit bladder a third gradient" is noted: the muscular nerves increase progressively as they are traced from the anterior aspect of the bladder posteriorly. Throughout the bladder the intermuscular and juxtamural perivascular networks around both arterioles and venules are exceptionally prominent. No adrenergic ganglia were encountered in the rabbit bladder.

In the rat the proximal third of the bladder is totally devoid of adrenergic muscular nerves and shows only poorly developed networks around the few arterioles in the adventitial and interstitial connective tissue that exist at that level. In the middle third small groups of nerve fibers appear between the muscle bundles of the posterior and lateral walls of the bladder. Their terminal ramifications are related to groups of muscle fibers and are about equally abundant throughout the muscle layer. Meanwhile the perivascular plexuses become more prominent. In the anterior wall very few nerves with limited branching are seen. In the distal third of the bladder more intermuscular nerves, more extensive terminal ramification and more complex perivascular networks are found. The nerves are equally abundant at all depths in the muscle layer although they are still more prominent posteriorly and laterally. The general pattern in the distal third of the bladder thus resembles that in the bladder base of other animals. No adrenergic ganglia could be identified in the rat bladder. A few juxtamural nerve bundles on the anterior and lateral aspects of the bladder are apparently continuous with nerve bundles or fibers in the adjacent connective tissue capsules of the corresponding lobes of the prostate.

DISCUSSION

The autonomic nerve fibers in the bladder wall are classified functionally according to their staining characteristics as cholinergic or adrenergic. The adrenergic fibers whether they run individually as nerve bundles or in conjunction with cholinergic fibers in large nerve trunks

are unequivocally postganglionic sympathetic fibers. On the other hand the origin of cholinergic fibers cannot be ascertained; actually they may represent preganglionic or postganglionic sympathetic or parasympathetic efferent fibers or afferent sensory fibers. All preganglionic fibers whether sympathetic or parasympathetic in origin are cholinergic and are present only within large nerve trunks. Since both sympathetic and parasympathetic ganglia are present in the bladder wall many of the larger nerve trunks in the adventitial coat muscularis and lamina propria undoubtedly contain preganglionic fibers. Certain sympathetic postganglionic fibers, namely the vasodilator (Burn 38) and sudomotor (Dale and Feldberg 34) are known to be cholinergic. Whether or not sympathetic cholinergic vasodilator nerves exist in the urinary bladder remains unknown. It has also been proposed by Burn and Rand (59, 60) that the adrenergic postganglionic sympathetic fiber is in essence a cholinergic fiber at the termination of which the adrenergic transmitter norepinephrine (NE) is released. That this hypothesis is not universally applicable is apparent from a variety of experimental histochemical and pharmacological data in the recent literature (Koelle and Valk 54, Koelle 55, 62, 65, Euler 56, Giacobini 57, Goodall and Kirschner 58, Muscholl and Vogt 58, Carlsson et al. 64, Dahlstrom and Fuxe 64, Dahlstrom 65, Rice and Long 66). Our finding of adrenergic fibers intermingled with cholinergic fibers in large nerve trunks or occurring as nerve bundles which give rise to smaller fiber groups and individual fibers also offers no support to the Burn-Rand hypothesis. It may therefore be proposed that the majority of cholinergic nerve fibers in the bladder wall, excluding those running in large nerve trunks, are parasympathetic postganglionic fibers.

The presence of autonomic ganglia in the mammalian bladder has been well documented. Although it is generally conceded that the region near the entrance of the ureters has the richest supply of ganglia, there is no agreement as to their relative distribution in the different layers of the bladder wall. While Michailow

part of the muscle scarcely any fibers exist apart from the perivascular plexus (fig 19). At more distal levels in the body of the bladder the terminal fibers progressively become more abundant and are related to smaller and smaller groups of nerve fibers but still more fibers are present in the outer (fig 22) than in the inner (fig 21) muscle bundles. Therefore in the body of the bladder the relative abundance of adrenergic terminals follows two gradients: the nerves increase progressively in number as they are traced (1) at a given level from within outwards and (2) at the same depth in the muscle layer from the dome distally. In the bladder base the terminal adrenergic fibers are much more abundant than in the body of the bladder; each fiber being related to one or a few muscle fibers. This picture is uniform throughout the depth of the muscularis in the base (figs 23-24). No differences in the innervation pattern exist between the anterior, posterior and lateral walls of the bladder.

Bladder innervation in other animals

A Subepithelial nerves

In the dog, rabbit and rat bladder the subepithelial nerves generally have a much less complicated arrangement than those in the cat bladder, though as in the latter they are considerably more abundant in the base than in the body of the bladder. This applies to both cholinergic and adrenergic fibers. In the rabbit and rat more nerves are consistently seen in the posterior wall than in either the anterior or lateral walls.

In the rabbit deep and superficial nerves can be discerned only in the base. In this region the main arborization of the subepithelial nerves is represented by a single narrow meshed network that underlies the epithelium and lies in the circumferential plane. Otherwise the arrangement of the nerves resembles that seen in the cat bladder, save for the difference in number and intricacy of arrangement (figs 26-27).

In the dog the subepithelial nerves are conspicuously less abundant than in either cat or rabbit. The superficial plexus in

the bladder base lies at the junction of the two layers of the lamina propria. The epithelial branches of the plexus run through the compact zone of the submucosa with few connections so that the picture is that of a very wide meshed network.

In the rat definite subepithelial nerves, whether individual fibers or perivascular plexuses, cholinergic or adrenergic, are seen only in the base of the bladder especially near the bladder outlet. Even in this region they are sparse, do not mesh and include no definite nerve bundles or ganglia. Nowhere in the bladder are the fibers discernible as deep as superficial networks.

B Epithelial nerves

In the rabbit the innervation of the epithelium closely resembles that seen in the cat, except that a far less number of nerves are seen in the former animal. In the dog intraepithelial fibers can be identified only in the bladder base. Even in this region they are widely separated and undergo very limited branching. No plexiform basal network like that seen in the cat or to a less extent in the rabbit is found; the fibers as a rule remaining individually discernible to their termination. In the rat neither cholinergic nor adrenergic epithelial fibers could be seen.

C Muscular nerves

A uniformly rich cholinergic innervation of all parts of the bladder musculature, including the trigone or the corresponding area, is found in all three animal species. The distribution of cholinergic ganglia and nerves and the appearance of the neuroterminal plexus are similar to the cat bladder. Paraureteric ganglia occur in all. In the rat stout nerve trunk is constantly seen penetrating the whole thickness of the posterior bladder wall in a very oblique direction, a short distance above the level of the bladder outlet.

The adrenergic muscular innervation in the dog is very similar to that in the cat, but in the rabbit and rat it presents some special features.

Like in the cat, the base of the rabbit bladder has the richest adrenergic mus-

or regenerative functions of the bladder epithelium. The majority of the intraepithelial nerve terminations closely resemble sensory nerve endings and may therefore subserve an afferent sensory function.

While most of the subepithelial nerves are associated with blood vessels in the lamina propria some apparently run in dependently and end freely in simple branched or complex terminations similar to sensory nerve endings described in that layer. Some nerve fibers within the muscularis also join specific end bodies which are apparently concerned with proprioceptive muscular sensation. Like those in the epithelium these apparently sensory nerve fibers are much more abundant in the bladder base than in the dome. These findings indicate that the sensory function is particularly prominent in — though by no means restricted to — the bladder base. In relation to the epithelium this would be at variance with the view entertained by Schabadasch (34) that the afferent terminations in the mucosa are limited to the trigone.

Up to the present the mammalian trigone — in conformity with its ontogenic and anatomical distinction (Kalischer '00) — has been believed to possess an innervation pattern which is distinctly different from that of the rest of the bladder (detrusor muscle). Although opinion still differs as to the innervation of the detrusor muscle it is unanimously agreed that the trigone is supplied exclusively by sympathetic nerves. In this study it is shown that the trigone not only is richly supplied by both sympathetic and parasympathetic nerves but also has the same innervation pattern as the detrusor muscle on the anterior and lateral aspects of the bladder base. In contrast to the parasympathetic innervation which is uniformly rich throughout the bladder the sympathetic supply shows important regional variations. Though sympathetic nerves are equally abundant in all parts of the musculature of the bladder base their number varies significantly at various levels and at different depths of the musculature of the body of the bladder. It is thus evident that if a regional functional differentiation of the bladder musculature is at all present on the basis of differences

in innervation it is to be defined between the body and base of the bladder rather than between the detrusor muscle and trigone. We would propose therefore that the two regions of the bladder namely the base and body differing in the type richness and pattern of innervation have distinctive motor as well as sensory functions.

Whether or not all muscle cells in the bladder are supplied by nerve fibers has been a matter of contention. The ratio of nerve fibers to muscle fibers has been variously estimated at 2-4:1 (Csiky, '11) (Obregia 1875 Gscheidlen 1877 Lustig 1881 Agababow '12) 1:25-50 (Englemann 1869) or 1:100 (Langley Stohr '28). Though a ratio of 1:100 is the one currently accepted (Bors '57) Caesar et al ('57) obtained evidence in an electron microscopic study of the mouse bladder that "each and every muscle cell shows a close relationship to the axon at a well defined locus." The construction of the cholinergic neuroterminal plexus outlined in this report accords well with that of the peripheral autonomic innervation apparatus described in the literature (Stohr '32 Boeke '33 '38 '49 Hillarp '46 '59 Jabonero '48 '51 Myelung '53) and indicates that the terminal parasympathetic ramifications probably come in contact with every muscle cell in the bladder wall. In view of its striking uniformity and continuity throughout the bladder musculature it is unlikely that the neuroterminal plexus would evoke a different response in different parts of the bladder musculature following one stimulus as advocated by the proponents of the reciprocal innervation theory. Nor is it conceivable that the plexus would exert its influence on the muscularis on a strictly segmental or unilateral basis as emphasized in many previous reports (Giannuzzi 1863 Sherrington 1892 Griffiths 1894 Stewart 1899 Langworthy et al '34 Langworthy and Kolb '38 Jacobson '45 Carpenter and Root '51 Torbey and Leadbetter '63).

The sympathetic terminal fibers have an entirely different arrangement than the parasympathetic ramifications and are not associated with individual muscle cells. Not even in the bladder base which

(08b), and Muller ('19) described ganglia in the submucosa as well as in other layers of the bladder wall. Bobin (24) Hryntschak ('25) and Stohr (28) admitted their presence only in the adventitia and muscularis. Kuntz (65) in a recent review asserted that an extensive area in the dome of the bladder is devoid of ganglia. Our findings indicate that ganglia are present in all parts of the bladder and at all depths in its wall, including the lamina propria. In conformity with previous reports the bladder base, especially at the entrance of the ureters and near the bladder outlet, contains the richest supply of ganglia. Generally the deeper in the wall the ganglia lie, the smaller and fewer they are. It is noteworthy that large ganglia and nerve trunks in the lamina propria occur only in the dome and upper part of the body of the bladder. In the bladder base only thin nerve bundles and occasional isolated ganglion cells are present in the lamina propria.

It was repeatedly pointed out that the intramural ganglia of the bladder are predominantly parasympathetic and partly sympathetic (Langley and Anderson, 1894; Stewart, 1899; Kuntz and Moseley, '36; Moseley, '36) and not exclusively parasympathetic as maintained by some authors (Iljina and Lawrentjew, '32; Polakowa, '35). In a study of the distribution of ganglia in the cat bladder Kuntz and Moseley ('36) stated that while parasympathetic ganglia — with few exceptions — are embedded in the deep portion of the serosa sympathetic ganglia are present in both serosa and external part of the muscularis. In this study the ganglion cells in the bladder were found to contain AChE, NE or both. In the cat and dog NE-containing cells were encountered in all layers of the bladder wall, and in the body as well as the base of the bladder. Though no NE-containing ganglion cells were encountered in the rabbit or rat bladder in this study, their presence cannot be entirely excluded until they are specifically looked for in serial sections of the whole bladder.

The interpretation of the relationship of the different ganglion cell types to the parasympathetic and sympathetic systems

has to be largely speculative. Three types of ganglion cells are present in the bladder.

(a) *Cholinergic cells* These are the most frequently observed. They are ACh-rich cells associated only with cholinergic fibers which ramify as postganglionic presumably parasympathetic fibers. Therefore they are considered to be a part of the parasympathetic system.

(b) *Adrenergic cells* These are quite rare, contain only NE and show a diffuse bright fluorescence. They give rise to adrenergic postganglionic sympathetic fibers and thus belong to the sympathetic system.

(c) *Intermediate type cells* These are commonly found and are related to both cholinergic and adrenergic nerve fibers inside the ganglia. While some stain heavily for AChE, others stain moderately or faintly for the enzyme and show as well a diffuse faint or bright fluorescence or stippling with brightly fluorescent N granules. Whether this population of cells belongs entirely to either parasympathetic or sympathetic system or represent peripheral regulatory centers through which one system exerts a control over the other remains to be elucidated.

Intraepithelial fibers have been depicted and described by a host of authors (Kisselw 1868; Retzius 1892; Grünstein '00; Lendorf '01; Michailow '08a; Iljina and Lawrentjew '32; Schabadash '34; Kleynjens and Langworthy, '37; Langworthy and Murphy '39; Yokoyama '49; Yamaguchi '60; Seto '63). In this study it was found that the epithellium is supplied by both sympathetic and parasympathetic fibers which can be traced through approximately half of its thickness. As a rule the adrenergic fibers are fewer and less complicated in arrangement than the cholinergic fibers. However, both types of fibers show the same tendency to be more abundant in the base than in the dome of the bladder. Many of the epithelial fibers are clearly associated with vascular channels. Whether or not some fibers directly innervate the epithelial cells as well cannot be ascertained with the degree of microscopic resolution utilized in this study. Should a cellular innervation exist it may prove to be related to the secretory

- Dale, H. H. and W. Feldberg 1934 The chemical transmission of secretory impulses to the sweat glands of the cat. *J Physiol* 82 121-133.
- Elliott, T. R. 1907 The innervation of the bladder and urethra. *J Physiol* 35 367-445.
- Engelmann, T. W. 1869 Zur Physiologie des Ureters. *Pflüger's Arch ges Physiol* 2 243-253.
- Engel, U. S. von 1936 "Noradrenaline Chemistry physiology pharmacology and clinical aspects. Thomas Springfield Illinois
- Fagge, C. H. 1902 On the innervation of the urinary passages in the dog. *J Physiol* 28 304-315.
- Falk, B. 1962 Observations on the possibilities of the cellular localization of monoamines by a fluorescence method. *Acta physiol scand* 58 suppl 197 pp 26.
- Fellow, B. 1935 Nervous control of the blood vessels. *Physiol Rev* 35 629-663.
- 1950 Nervous control of the blood vessels. In "The Control of the Circulation of the Blood" by R. J. S. McDowall. Dawson London. Suppl. vol. pp 1-85.
- Giacobini, E. 1957 Quantitative determination of cholinesterase in individual sympathetic cells. *J Neurochem*, 1 234-244.
- Giamuzzi, J. 1863 Recherches physiologiques sur les nerfs moteurs de la vessie. *J de la Physiol* 6 22-29.
- Goodall, McC. and N. Kirschner 1958 Biosynthesis of epinephrine and norepinephrine by sympathetic nerves and ganglia. *Circulation* 1 366-371.
- Guthrie, J. 1894 Observations of the urinary bladder and urethra. II The nerves. *J Anat Physiol* 29 61-83.
- Grunstein, N. 1900 Zur Innervation der Harnblase. *Arch mikr Anat* 55 1-11.
- Gschlösser, R. 1877 Beiträge zur lehre von der Nervenendigung in den glatten Muskel fasern. *Arch. mikr Anat* 14 321.
- Hilary, N. A. 1946 Structure of the synapse and the peripheral innervation apparatus of the autonomic nervous system. *Acta Anat* 2, suppl. 4 pp 153.
- 1959 The construction and functional organization of the autonomic innervation apparatus. *Acta physiol. scand* 46 suppl 57 pp 38.
- Knack, T. 1925 Zur Anatomie und physiologie des Nervenapparates der Harnblase und des Ureters. II Über den ganglienzellapparat von Nierenbecken und Harnleiter des Menschen und einiger Säugetiere. *Ztschr urol. Gyn* 18 86-110.
- Law, W. J., and B. J. Lawrentjew 1932 Experimental-morphologische Studien über den inneren Bau des autonomen Nervensystems. II Über die Innervation der Harnblase. *Zschr mikr Anat Forsch.* 30 543-550.
- 1948a Etudes sur le système neurovégétatif périphérique I Structure des fibres nerveuses. *Acta Anat* 6 14-50.
- 1948b Etudes sur le système neurovégétatif périphérique II. Innervation efférente des vaisseaux sanguins et de la musculature lisse. *Acta Anat* 6 376-409.
- 1951 La synapse plexiforme à distance du système neurovégétatif périphérique. *Experientia* 7 471-475.
- Jacobson, C. E. Jr 1945 Neurogenic vesical dysfunction an experimental study. *J Urol* 53 670-695.
- Kalischer, O. 1900 Die Urogenitalmuskulatur des Damms. Berlin.
- Karnovsky, M. J. 1964 A "direct-coloring" thiocholine method for cholinesterases. *J Histochem Cytochem* 12 219-221.
- Kisselw, J. 1868 Ueber die Endigung der Sensiblen Nerven der Harnblase. *Zentralbl. med Wissensch* 6 337-338.
- Kleynjens, R. and O. R. Langworthy 1937 Sensory nerve endings on the smooth muscle of the urinary bladder. *J Comp Neur* 67 367-380.
- Koelle, G. B. 1955 The histochemical identification of acetylcholinesterase in cholinergic adrenergic and sensory neurons. *J Pharmacol Exp Therap* 114 167-184.
- Koelle, G. B. 1962 A new general concept of the neurohumoral functions of acetylcholine and acetylcholinesterase. *J Pharma Pharmacol* 14 65-90.
- Koelle, G. B. 1965 The roles of acetylcholine and acetylcholinesterase in junctional transmission. In "Pharmacology of cholinergic and adrenergic transmission" Eds G. B. Koelle, W. W. Douglas and A. Carlsson. Macmillan New York pp 29-40.
- Koelle, G. B. and T. Valk 1964 Physiological implications of the histochemical localization of monoamine oxidase. *J Physiol* 126 434-447.
- Kuntz, A. 1965 Physiology of urinary bladder and urethra normal and pathological. In "Handbuch der Urologie" Springer Verlag Berlin Vol 2 p 550.
- Kuntz, A. and R. L. Moseley 1936 Experimental analysis of pelvic autonomic ganglia in the cat. *J Comp Neur* 64 63-75.
- Kuntz, A. and G. Succomano 1944 The sympathetic innervation of the detrusor muscle. *J Urol* 51 535-542.
- Langley, J. N. and H. K. Anderson 1894 The constituents of the hypogastric nerves. *J Physiol* 17 177-191.
- 1896 On the innervation of the pelvic and adjoining viscera. VII Anatomical observations. *J Physiol* 20 372-406.
- Langley, J. N. Cited by C. M. Gruber 1933 The autonomic innervation of the genito-urinary system. *Physiol Rev* 13 497-609.
- Langworthy, O. R. and L. C. Kolb 1938 Histological changes in the vesical muscle following injury of the peripheral innervation. *Anat. Rec* 71 249-263.
- Langworthy, O. R. and E. L. Murphy 1939 Nerve endings in the urinary bladder. *J Comp Neur* 71 487-509.
- Langworthy, O. R. D. L. Reeves and E. S. Tauber 1934 Autonomic control of the urinary bladder. *Brain* 57 266-290.

has the richest sympathetic supply does a 1:1 nerve to muscle ratio occur. The ratio is least in the bladder dome where sympathetic terminals are related only to large groups of muscle fibers or even to muscle bundles. These findings are contradictory to the statement of Langworthy and Murphy (39) that while the sympathetic innervation of the bladder shows more of the characteristics of a true nerve net, the parasympathetic fibers do not form as complicated a plexus being similar in their mode of branching to the somatic motor fibers innervating striated muscle. The relationship of sympathetic terminals to the parasympathetic neuroterminal plexus remains to be defined.

Most of the blood vessels in the bladder wall including the arterioles many moderate sized venules and perhaps some capillaries are innervated by both adrenergic and cholinergic fibers. The adrenergic (postganglionic sympathetic) fibers as elsewhere may be assumed to have a vasoconstrictor function. It is a well known fact that active vasodilatation mediated by parasympathetic cholinergic fibers occurs in pelvic vascular beds (Folkow 55, 56; McDowall 56). Whether the cholinergic vascular fibers in the bladder represent such parasympathetic vasodilator fibers or sympathetic cholinergic vasodilator fibers akin to those demonstrated in skeletal muscle (Uvnäs 54; Folkow 55, 56) remains unanswered.

It is evident that this work not only provides for the first time a clear picture of the innervation pattern of the urinary bladder in the experimental animal but also shows that the construction of the peripheral autonomic innervation apparatus is far more complex than has hitherto been recognized. Although the basic pattern of innervation is essentially the same in the four animal species studied certain differences exist in the relative abundance and arrangement of the epithelial and subepithelial sympathetic and parasympathetic ramifications. Although the parasympathetic muscular innervation is uniformly similar the sympathetic innervation shows prominent species variations. These features may be teleologically related to the variable micturition habits acquired by different animals and more

specifically, to the degree of involvement of afferent and efferent stimuli from and to the different layers of the bladder wall in the various reflexes concerned with urine storage and expulsion.

LITERATURE CITED

- Agababow A 1912 Über die Nerven der Augenhaut von Graefes Arch Ophthalmol 83: 317
- Bobin W 1924 Zur Frage nach den Harnblasen nerven bei Kaninchen Kubanski Wissenschaftl med Westnik 4
- Boeke J 1933 Innervationsstudien. Der sympathische Grundplexus und seine Beziehungen zu den quergestreiften Muskelfasern und zu den Herzmuskelfasern. Ztschr mikr Anat Forsch 34: 330-378
- 1938 Sympathetic ground plexus and reticulate fibers. Anat Anz 86: 150-162
- 1949 The sympathetic end formation: its synaptology, the interstitial cells, the peripheral terminal network and its bearing on the neuron theory. Discussion and Critique. Acta Anat 8: 18-61
- Bors E 1957 Neurogenic bladder. Urol Surv 7: 177-250
- Budge J 1864 Ueber den Einfluss des Nervensystems auf die Bewegung der Blase. Ztschr Rat Med 21: 1-16, 174-191
- Burn J H 1938 Sympathetic vasodilator fibers. Physiol Rev 18: 137-153
- Burn J H and M J Rand 1959 Sympathetic postganglionic mechanism. Nature 184: 163-165
- 1960 Sympathetic postganglionic cholinergic fibers. Brit J Pharmacol 15: 56-66
- Caesar R G A Edwards and H Ruska 1957 Architecture and nerve supply of mammalian smooth muscle tissue. J Biophys Biochem Cytol 3: 867-877
- Carlsson A B Falck K Fuxe and N A Hillarp 1964 Cellular localization of monoamines in the spinal cord. Acta physiol scand 60: 112-119
- Carpenter F G and W S Root 1951 Effect of parasympathetic denervation on feline bladder function. Amer J Physiol 166: 686-691
- Csiky von Cited by P Stohr Jr 1926 Über die Innervation der Harnblase und Samenblase beim Menschen. Zugleich ein Beitrag über die Beziehung zwischen Nerv und glatten Muskulatur. Ztschr Anat Entwickl 78: 555-584 (p 571)
- Dahlström A 1965 Observations on the accumulation of noradrenaline in the proximal and distal parts of peripheral adrenergic nerves after compression. J Anat 99: 677-689
- Dahlström A and K Fuxe 1964 Evidence for the existence of monoamine containing neurons in the central nervous system. I. Demonstration of monoamines in the cell bodies of brain stem neurons. Acta physiol scand 62 suppl 232 pp 55

- Dak, H. H. and W. Feldberg 1934 The chemical transmission of secretory impulses to the sweat glands of the cat. *J Physiol* 82 121-133.
- Ellott, T. R. 1907 The innervation of the bladder and urethra. *J Physiol* 35 367-445.
- T. W. 1869 Zur Physiologie des Urters. *Pflüger's Arch. ges. Physiol.* 2 243-253.
- U. S. von 1956 "Noradrenaline Chemistry physiology pharmacology and clinical aspects. Thomas Springfield Illinois.
- Fager, C. H. 1909 On the innervation of the urinary passages in the dog. *J Physiol* 28 304-315.
- Falk, B. 1962 Observations on the possibilities of the cellular localization of monoamines by a fluorescence method. *Acta physiol. scand.* 56 suppl. 197 pp. 26.
- Fallow, B. 1935 Nervous control of the blood vessels. *Physiol. Rev.* 35 629-663.
- 1956 Nervous control of the blood vessels. In "The Control of the Circulation of the Blood," by R. J. S. McDowall. Dawson London. Suppl. vol. pp. 1-85.
- Giachini, E. 1957 Quantitative determination of cholinesterase in individual sympathetic cells. *J Neurochem.* 1 234-244.
- Gianuzzi, J. 1863 Recherches physiologiques sur les nerfs moteurs de la vessie. *J. de la Physiol.* 6 22-29.
- Guthrie, McC. and N. Kirschner 1958 Biosynthesis of epinephrine and norepinephrine by sympathetic nerves and ganglia. *Circulation* 1 36-371.
- Guthrie, J. 1894 Observations of the urinary bladder and urethra. II. The nerves. *J. Anat. Physiol.* 29 61-83.
- Grunstein, N. 1900 Zur Innervation der Harnblase. *Arch. mikr. Anat.* 55 1-11.
- Gschwend, R. 1877 Beiträge zur Lehre von der Nervenendigung in den glatten Muskelfasern. *Arch. mikr. Anat.* 14 321.
- Harp, N. A. 1946 Structure of the synapse and the peripheral innervation apparatus of the autonomic nervous system. *Acta Anat.* 2, suppl. 4 pp. 153.
- 1959 The construction and functional organization of the autonomic innervation apparatus. *Acta. physiol. scand.* 46 suppl. 57 pp. 3.
- Hirschbach, T. 1925 Zur Anatomie und physiologie des Nervensystems der Harnblase und des Ureters. II. Über den ganglienzellapparat von Nierenbecken und Harnleiter des Menschen und einiger Säugetiere. *Ztschr. urol. Ch.* 13 86-110.
- , W. J. and B. J. Lawrentjew 1932 Experimentell-morphologische Studien über den feineren Bau des autonomen Nervensystems. II. Über die Innervation der Harnblase. *Ztschr. mikr.-Anat. Forsch.* 30 543-550.
- Lakero, V. 1948a Etudes sur le système nerveux périphérique I. Structure des fibres nerveuses. *Acta Anat.* 6 14-50.
- 1948b Etudes sur le système nerveux périphérique II. Innervation éfferente des vaisseaux sanguins et de la musculature lisse. *Acta Anat.* 6 376-409.
- 1951 La synapse plexiforme à distance du système nerveux végétatif périphérique. *Experientia* 7 471-475.
- Jacobson, C. E. Jr 1945 Neurogenic vesical dysfunction an experimental study. *J. Urol.* 53 670-695.
- Kalischer, O. 1900 "Die Urogenitalmuskulatur des Damms." Berlin.
- Karnovsky, M. J. 1964 A direct-coloring thiocholine method for cholinesterases. *J. Histochem. Cytochem.* 12 219-221.
- Kisselw, J. 1863 Ueber die Endigung der Sensiblen Nerven der Harnblase. *Zentralbl. med. Wissensch.* 6 337-338.
- Kleynjens, R. and O. R. Langworthy 1937 Sensory nerve endings on the smooth muscle of the urinary bladder. *J. Comp. Neur.* 67 367-380.
- Koelle, G. B. 1955 The histochemical identification of acetylcholinesterase in cholinergic adrenergic and sensory neurons. *J. Pharmacol. Exp. Therap.* 114 167-184.
- Koelle, G. B. 1962 A new general concept of the neurohumoral functions of acetylcholine and acetylcholinesterase. *J. Pharma. Pharmacol.* 14 65-90.
- Koelle, G. B. 1965 The roles of acetylcholine and acetylcholinesterase in junctional transmission. In "Pharmacology of cholinergic and adrenergic transmission. Eds G. B. Koelle, W. W. Douglas and A. Carlsson. Macmillan New York. pp. 29-40.
- Koelle, G. B. and T. Valk 1954 Physiological implications of the histochemical localization of monoamine oxidase. *J. Physiol.* 126 434-447.
- Kuntz, A. 1965 Physiology of urinary bladder and urethra normal and pathological. In "Handbuch der Urologie. Springer Verlag Berlin. Vol. 2 p. 550.
- Kuntz, A. and R. L. Moseley 1936 Experimental analysis of pelvic autonomic ganglia in the cat. *J. Comp. Neur.* 64 63-75.
- Kuntz, A. and G. Succomano 1944 The sympathetic innervation of the detrusor muscle. *J. Urol.* 51 535-542.
- Langley, J. N. and H. K. Anderson 1894 The constituents of the hypogastric nerves. *J. Physiol.* 17 177-191.
- 1896 On the innervation of the pelvic and adjoining viscera. VII. Anatomical observations. *J. Physiol.* 20 372-406.
- Langley, J. N. Cited by C. M. Gruber 1933 The autonomic innervation of the genito-urinary system. *Physiol. Rev.* 13 497-609.
- Langworthy, O. R. and L. C. Kolb 1938 Histological changes in the vesical muscle following injury of the peripheral innervation. *Anat. Rec.* 71 249-263.
- Langworthy, O. R. and E. L. Murphy 1939 Nerve endings in the urinary bladder. *J. Comp. Neur.* 71 487-509.
- Langworthy, O. R., D. L. Reeves and E. S. Tauber 1934 Autonomic control of the urinary bladder. *Brain* 57 266-290.

has the richest sympathetic supply does a 1:1 nerve to muscle ratio occur. The ratio is least in the bladder dome where sympathetic terminals are related only to large groups of muscle fibers or even to muscle bundles. These findings are contradictory to the statement of Langworthy and Murphy (39) that while the sympathetic innervation of the bladder shows more of the characteristics of a true nerve net, the parasympathetic fibers do not form as complicated a plexus being similar in their mode of branching to the somatic motor fibers innervating striated muscle. The relationship of sympathetic terminals to the parasympathetic neuroterminal plexus remains to be defined.

Most of the blood vessels in the bladder wall including the arterioles many moderate sized venules and perhaps some capillaries are innervated by both adrenergic and cholinergic fibers. The adrenergic (postganglionic sympathetic) fibers, as elsewhere may be assumed to have a vasoconstrictor function. It is a well known fact that active vasodilatation mediated by parasympathetic cholinergic fibers occurs in pelvic vascular beds (Folkow 55, 56; McDowall 56). Whether the cholinergic vascular fibers in the bladder represent such parasympathetic vasodilator fibers or sympathetic cholinergic vasodilator fibers akin to those demonstrated in skeletal muscle (Uvnäs 54; Folkow 55, 56) remains unanswered.

It is evident that this work not only provides for the first time a clear picture of the innervation pattern of the urinary bladder in the experimental animal but also shows that the construction of the peripheral autonomic innervation apparatus is far more complex than has hitherto been recognized. Although the basic pattern of innervation is essentially the same in the four animal species studied certain differences exist in the relative abundance and arrangement of the epithelial and subepithelial sympathetic and parasympathetic ramifications. Although the parasympathetic muscular innervation is uniformly similar the sympathetic innervation shows prominent species variations. These features may be teleologically related to the variable micturition habits acquired by different animals and more

specifically, to the degree of involvement of afferent and efferent stimuli from and to the different layers of the bladder wall in the various reflexes concerned with urine storage and expulsion.

LITERATURE CITED

- Agababow A 1912 Über die Nerven der Augenhaut von Graefes Arch Ophthalmol 83 317
- Bobin W 1924 Zur Frage nach den Harnblasen nerven bei Kaninchen Kubanski Wissenschaftl med Westnik 4
- Boeke J 1933 Innervationsstudien Der sympathische Grundplexus und seine Beziehungen zu den quergestreiften Muskelfasern und zu den Herzmuskelfasern Ztschr mikr Anat Forsch 34 330-378
- 1938 Sympathetic ground plexus and reticulate fibers Anat Anz 86 150-162
- 1949 The sympathetic end formation its synaptology the interstitial cells the peripheral terminal network and its bearing on the neuron theory Discussion and Critique Acta Anat 8 18-61
- Bors E 1957 Neurogenic bladder Urol Surv 7 177-250
- Budge J 1864 Ueber den Einfluss des Nerven systems auf die Bewegung der Blase Ztschr Rat Med 21 1-16 174-191
- Burn J H 1938 Sympathetic vasodilator fibers Physiol Rev 18 137-153
- Burn J H and M J Rand 1959 Sympathetic postganglionic mechanism Nature 184 163-165
- 1960 Sympathetic postganglionic cholinergic fibers Brit J Pharmacol 15 56-66
- Caesar R G A Edwards and H Ruska 1957 Architecture and nerve supply of mammalian smooth muscle tissue J Biophys Biochem Cytol 3 867-877
- Carlsson A B Falck K Fuxe and N A Hillarp 1964 Cellular localization of monoamines in the spinal cord Acta physiol scand 60 112-119
- Carpenter F G and W S Root 1951 Effect of parasympathetic denervation on feline bladder function Amer J Physiol 166 686-691
- Csiky von Cited by P Stohr Jr 1926 Über die Innervation der Harnblase und Samenblase Beim Menschen Zugleich ein Beitrag über die Beziehung zwischen Nerv und glatter Muskulatur Ztschr Anat Entwickl 78 555 584 (p 571)
- Dahlstrom A 1965 Observations on the accumulation of noradrenaline in the proximal and distal parts of peripheral adrenergic nerve after compression J Anat 99 677-689
- Dahlstrom A and K Fuxe 1964 Evidence for the existence of monoamine containing neurons in the central nervous system I. Demonstration of monoamines in the cell bodies of brain stem neurons Acta physiol scand 62 suppl 232 pp 55

- Learmonth J R 1931 A contribution to the neurophysiology of the urinary bladder in man *Brain* 54 147-176
- Lendorf A 1901 Beiträge zur Histologie der Harnblasenschleimhaut *Anat Hefte* 17 55-171
- Lustig A 1881 Über die Nervenendigung in den glatten Muskelfasern Sitzungsber kais Akad Wissensch Wien 83 186
- McDowall R J S 1956 The Control of the Circulation of the Blood Dawson London pp 46-65
- Michailow S 1908a Über die sensiblen Nervenendigungen in der Harnblase der Säugetiere *Arch mikr Anat* 71 254-283
- 1908b Die feinere Struktur der sympathischen Ganglien der Harnblase bei den Säugetieren *Arch mikr Anat* 72 554
- Moseley R L 1936 Preganglionic connections of the intramural ganglia of the urinary bladder *Proc Soc exp Biol* 34 728-730
- Müller L R 1919 Die Blaseninnervation *Deut Arch klin Med*, 128 81-106
- Muscholl E, and M Vogt 1958 The action of reserpine on the peripheral sympathetic system *J Physiol* 141 132-155
- Myelung H A 1953 Structure and significance of the peripheral extension of the autonomic nervous system *J Comp Neur* 99 495-535
- Obregia A 1875 Über die Nervenendigungen in den glatten Muskelfasern beim Hunde *Verhandl. 10 Internat med kong Berlin* 1890
- Polykarpowa G A 1935 Experimentell morphologische Analyse der autonomen Innervation der Harnblase *Ztschr Anat Entwickl* 104 378-388
- Rehlfisch E 1897 Über den Mechanismus des Harnblasenverschlusses und der Harnentleerung *Virch Arch path Anat* 150 111-151
- Retzius G 1892 Cited by L Testut 1923 In *Traité d'Anatomie Humaine* Doin Paris T 4 p 491
- Rice A J and J P Long 1966 An unusual venoconstriction induced by acetylcholine *J Pharmacol Exp Therap* 151 423-429
- Schabadasch A 1934 Studien zur Architektur des vegetativen Nervensystems I Neue Intramurale Nervengeflechte der Harnblase und des Harnleiters *Ztschr Zellforsch* 21 657-732
- Seto H 1963 Sensibility of the urogenital organs In *Studies on the sensory innervation* Thomas Springfield Illinois pp 250-265
- Sherrington C S 1892 Notes on the arrangement of some motor fibers in the lumbosacral plexus *J Physiol* 13 621-772
- Stewart C C 1899 On the course of impulses to and from the cat's bladder *Amer J Physiol* 2 182-202
- Stöhr P Jr 1928 Die peripherischen Anteile des vegetativen Nervensystems In von Mollendorff's *Handbuch der mikroskopische Anatomie des Menschen* Springer Berlin H 4/1 pp 265-447
- 1932 Mikroskopische Studien zur Innervation des Magen-Darmkanals II Über die Nerven des menschlichen Magens und ihre Veränderungen beim Ulcus *Ztschr Zellforsch* 16 123-197
- Torbey K and W F Leadbetter 1963 Innervation of the bladder and lower ureter studies on pelvic section and stimulation in the dog *J Urol* 90 395-404
- Uvnäs B 1954 Sympathetic vasodilator outflow *Physiol Rev* 34 608-618
- Yamaguchi D 1960 Supplementary study on the sensory nerve supply of the human urinary bladder *Arch Histol Jap* 19 667-684
- Yokoyama H 1949 Nervous supply of the urinary bladder and the inferior part of the ureter in adult man with special reference to the sensory innervation *Tohoku Igaku Zasshi* 42 28-36
- Zeissl M von 1892 Recherches expérimentales de l'innervation de la vessie *Ann Malad org Genito urin* 10 828-832
- 1893 Ueber die Innervation der Blase *Pflügers Arch ges Physiol* 53 560-575
- 1894 Weitere Untersuchungen über die Innervation der Blase *Pflügers Arch ges Physiol* 55 569-578
- 1901 Neue Untersuchungen über die Innervation der Blase *Wien med. Wchnschr* 51 465-472

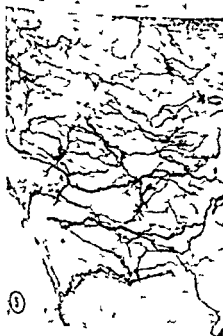


All figures represent cat bladder except figures 14 and 18 (dog bladder) and figures 26 and 27 (rabbit bladder)

PLATE 1

EXPLANATION OF FIGURES

- 1 Deep part of lamina propria (LP) in upper part of body. Large cholinergic deep subepithelial nerve trunks (NT) and smaller nerve bundles run circumferentially on the inner aspect of the muscularis (M). A nerve bundle (NB) courses into the inner muscularis. The smooth muscle cells are surrounded by the extensive ramifications of cholinergic nerve fibers. AChE $\times 40$
- 2 Deep part of lamina propria in upper part of body. Moderate sized cholinergic ganglion with adjoining nerve bundles. AChE $\times 100$
- 3 Deep part of lamina propria in base. A cholinergic nerve bundle (NB) next to a deep subepithelial arteriole (A) sends vascular branches which form a plexus around the arteriole. AChE $\times 100$
- 4 Deep part of lamina propria in lower part of body. Adrenergic perivascular plexus around arterioles (A). NE $\times 125$
- 5 Superficial part of lamina propria in base cut tangentially. The perivascular plexus around a radial subepithelial arteriole and its branches join the cholinergic superficial subepithelial plexus. AChE $\times 40$
- 6 Epithelium (E) and lamina propria in lower part of body. The adrenergic perivascular plexus around a radial subepithelial arteriole joins the adrenergic superficial subepithelial plexus. NE $\times 80$



All figures represent cat bladder except figures 14 and 18 (dog bladder) and figures 26 and 27 (rabbit bladder)

PLATE 1

EXPLANATION OF FIGURES

- 1 Deep part of lamina propria (LP) in upper part of body. Large cholinergic deep subepithelial nerve trunks (NT) and smaller nerve bundles run circumferentially on the inner aspect of the muscularis (M). A nerve bundle (NB) courses into the inner muscularis. The smooth muscle cells are surrounded by the extensive ramifications of cholinergic nerve fibers. AChE $\times 40$
- 2 Deep part of lamina propria in upper part of body. Moderate sized cholinergic ganglion with adjoining nerve bundles. AChE $\times 100$
- 3 Deep part of lamina propria in base. A cholinergic nerve bundle (NB) next to a deep subepithelial arteriole (A) sends vascular branches which form a plexus around the arteriole. AChE $\times 100$
- 4 Deep part of lamina propria in lower part of body. Adrenergic perivascular plexus around arterioles (A). NE $\times 125$
- 5 Superficial part of lamina propria in base cut tangentially. The perivascular plexus around a radial subepithelial arteriole and its branches join the cholinergic superficial subepithelial plexus. AChE $\times 40$
- 6 Epithelium (E) and lamina propria in lower part of body. The adrenergic perivascular plexus around a radial subepithelial arteriole joins the adrenergic superficial subepithelial plexus. NE $\times 80$



PLATE 2

EXPLANATION OF FIGURES

- 7 Deep part of lamina propria in lower part of body Free branches and complex terminations of cholinergic subepithelial fibers AChE $\times 100$
- 8 Epithelium and lamina propria in lower part of body Neurovascular bundle (NVB) in deep layer of lamina propria cholinergic superficial subepithelial plexus and epithelial fibers AChE $\times 40$
- 9 Epithelium and lamina propria in dome In contrast to the rich cholinergic superficial subepithelial plexus and abundant epithelial fibers seen in the lower part of the body (fig 8) and the base (fig 5) only a few scattered cholinergic subepithelial fibers and no epithelial fibers are seen in the dome AChE $\times 40$
- 10 Epithelium (E) and lamina propria in base cut tangentially The adrenergic superficial subepithelial plexus is more prominent than that in the body (fig 6) NE $\times 80$
- 11 Epithelium (E) and superficial layer of lamina propria in base The epithelial branches of the adrenergic superficial subepithelial plexus run parallel to and immediately beneath the epithelium NE $\times 200$
- 12 Epithelium and superficial layer of lamina propria in base The cholinergic superficial subepithelial plexus gives rise to many epithelial fibers which have free or branched clubbed terminations in its basal third AChE $\times 400$

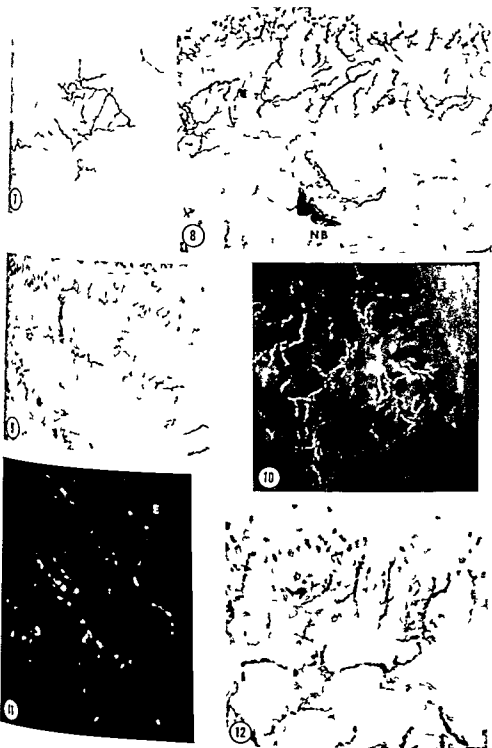


PLATE 3

EXPLANATION OF FIGURES

- 13 Outer part of muscularis in lower part of body. Large cholinergic intermuscular nerve trunks and neuroterminal plexus (*cf* figs 1 25) AChE $\times 40$
- 14 Trigonal muscle. Adrenergic nerve fibers in a large intermuscular nerve trunk. NE $\times 320$
- 15 Inner part of muscularis in lower part of body. Moderate sized branching nerve bundle composed entirely of adrenergic nerve fibers. NE $\times 125$
- 16 Outer part of muscularis in lower part of body. The adrenergic perivascular plexus around an intermuscular arteriole sends a branch fiber (BF) to adjacent muscle. Adrenergic nerve fibers (NF) are seen inside a muscle bundle (lower right hand corner). NE $\times 125$
- 17 Outer part of muscularis in base. AChE rich ganglion cells in a large juxtamural ganglion. A large cholinergic nerve trunk joins the ganglion. AChE $\times 10$
- 18 Outer part of muscularis in upper part of body. Moderate sized intermuscular ganglion. Adrenergic fibers surround the ganglion cells some of which contain NE granules. NE $\times 200$

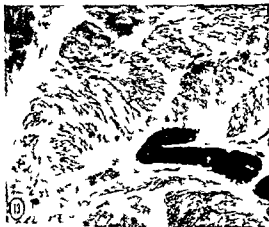


PLATE 4

EXPLANATION OF FIGURES

- 19 Inner part of muscularis in dome Adrenergic intermuscular perivascular plexus no muscular adrenergic terminal fibers NE $\times 125$
- 20 Outer part of muscularis in dome Adrenergic intermuscular perivascular plexus few terminal fibers inside muscle bundles NE $\times 80$
- 21 Inner part of muscularis in lower part of body Adrenergic intermuscular perivascular plexus more muscular nerve fibers than in the dome (figs 19 20) NE $\times 125$
- 22 Outer part of muscularis in lower part of body More adrenergic muscular terminal fibers than in the inner part of muscularis at the same level (fig 21) NE $\times 80$
- 23 Inner part of muscularis in base Adrenergic muscular innervation more than in the body (figs 21 22) Dichotomous branching and divergent course of terminal fibers NE $\times 125$
- 24 Outer part of muscularis in base Same innervation pattern as inner part of muscularis at the same level (fig 23) NE $\times 80$

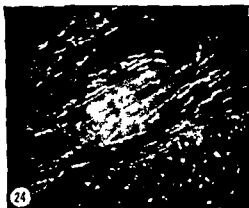
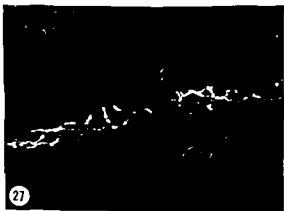
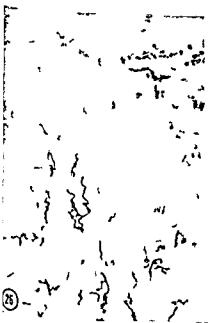


PLATE 5

EXPLANATION OF FIGURES

- 25 Muscularis in base. Smooth muscle cells cut transversely and longitudinally are surrounded by a rich network of cholinergic fibers which are related to AChE-containing interstitial cells (neuroteriminal plexus). A nerve bundle gives rise to several branch fibers which are continuous with the plexus. AChE $\times 160$
- 26 Epithelium and lamina propria in base. In contrast to the cat bladder (figs 5-8) the cholinergic subepithelial nerves are less numerous, less frequently communicating and are mainly related to subepithelial vessels. They send few fibers to the epithelium. AChE $\times 40$
- 27 Epithelium (top) and lamina propria in dome. In contrast to the cat bladder (fig 9) only deep subepithelial perivascular adrenergic fibers are seen. NE $\times 80$



Fine Structure of Adrenocortical Cells in Adult Male Rhesus Monkeys¹

ROBERT M. BRENNER

Department of Electron Microscopy

Oregon Regional Primate Research Center Beaverton Oregon

ABSTRACT Adrenals of ten mature male rhesus monkeys were studied by electron microscopy

Mitochondria had lamelliform cristae in the zona glomerulosa and tubular cristae in the zona fasciculata and zona reticularis. Agranular reticulum of tubular form was scarce in the zona glomerulosa but present in great abundance in the fasciculata and reticularis. The Golgi complex was prominent in the cells of the zona glomerulosa but poorly developed in the cells of the inner cortical zones.

Zona fasciculata cells contained large highly ordered "stacks" of granular endoplasmic reticulum which showed multiple connections with the random network of tubular agranular reticulum. In the reticularis granular endoplasmic reticulum was present in more disordered whorl-like arrays.

Lipid droplets in the inner cortical regions were enveloped by tubules of agranular endoplasmic reticulum. Occasional sections showed these tubules ending blindly at or near the surface of the lipid droplets. This association was strongly suggestive of a functional relationship.

Dense bodies varied in size and complexity of structure throughout the cortex. They were smallest and simplest in form in the zona glomerulosa; those in the zona reticularis were the largest and most complex.

The adrenal cortex of the rhesus monkey (*Macaca mulatta*) has not been examined previously by electron microscopy. Reports have been published on the electron microscopy of the following animals: the frog (Burgos '59), the garter snake (Sheridan '63), the brown pelican (Sheridan et al. '63), Belt et al. '66), the alligator and sea gull (Harrison '66), the domestic fowl (Fujita '61), the guinea pig (Sheridan and Belt '64), the opossum (Long and Jones '66), the rabbit (Cotte et al. '63), the hamster (Yates '65), Fawcett, '66), the mouse (Zelander '59), the rat (Lever '55), Sabatini and DeRobertis '61), Sabatini et al. '62), Yamori et al. '61), Giacomelli et al. '65), and man (Ross et al. '58, Carr '61). Considerable species differences have been reported in mitochondrial structure, the form of the agranular reticulum, the amount and distribution of the granular reticulum, the characteristics of the lipid droplets and the distribution of so-called dense bodies.

The purpose of this report is to describe the fine structure of the adrenal cortex of adult male rhesus monkeys and to compare the findings with those in other species.

MATERIALS AND METHODS

Ten mature male monkeys ranging in weight from 8 to 14 kg were sacrificed according to a standard procedure. Each autopsy was performed between 9:00 a.m. and 11:00 a.m. The animal was held immobile in a squeeze cage and Sernylan (Phencyclidine hydrochloride, Parke Davis) was injected intramuscularly at a dose rate of 2 mg/kg 5 to 15 minutes before the scheduled autopsy time. The abdomen was opened, the abdominal aorta was catheterized and 25-50 cc of blood were withdrawn for clinical test. The adrenals were removed, halved and placed directly into fixative. The composition of which was 0.75% glutaraldehyde (prepared from Union Carbide 25% stock solution), 8% formalin (Merck analytical reagent grade), 1% sodium cacodylate, 4.5% sucrose and 0.05% calcium chloride (the latter was added just before use).

The adrenals were fixed for 30 minutes and then sliced by hand into rectangular blocks representing complete radial sec-

¹ Publication 143 of the Oregon Regional Primate Research Center, supported in part by grant AM 09060(03) and FR 00163 from the National Institutes of Health.

tions of the cortex. These slices were fixed for a total period of 24 hours. Subsequently they were washed a minimum of 24 hours in two changes of a solution containing 4.5% sucrose and 1% sodium cacodylate. Blocks were post fixed for two hours in a mixture of 1% osmium tetroxide, 4.5% sucrose and 1% sodium cacodylate. The osmicated tissues were rapidly dehydrated through an alcohol series to a 1:1 mixture of 70% alcohol and 70% acetone, after which they were carried through an acetone series to a 1:1 mixture of acetone and Epon, and then embedded in Epon (Luft 61). Sections with bright gold interference colors were double stained with uranyl acetate and lead citrate and examined in a Philips EM 200 electron microscope.

The glutaraldehyde formaldehyde fixative listed above was devised after several trials in which the concentrations of each of the components were varied over a wide range. In all such trials the criteria for optimal fixation were the minimization of shrinkage effects, the preservation of intact mitochondrial structure, the maintenance of homogeneous lipid droplet structure, and the preservation of general tissue integrity. Preliminary experiments were also carried out on the effect of the length of fixation time on general tissue integrity. Tissues were fixed for 3, 6, 12, or 24 hours. Cell preservation was best after fixation for 24 hours.

OBSERVATIONS

Capsule and zona glomerulosa

The capsule of the adrenal gland is a multilayered feltwork of collagen fibers in which circular longitudinal and oblique layers of fibers alternate with one another in a fairly regular order. The collagen bundles are in intimate contact with the arterioles and nerves which traverse the capsule before entering the cortex (fig. 6).

Fibroblasts and macrophages are the only cellular components of the capsule. The numerous fibroblasts are arranged in layers throughout the depth of the capsule (fig. 1). The macrophages are fewer in number and are large cells containing several large electron dense granules, a prominent Golgi complex and a considerable

amount of agranular reticulum. The membrane of these macrophages is often extensively folded. These cells are usually found either at the capsule glomerular junction or in the subendothelial space within the zona glomerulosa (fig. 5).

The zona glomerulosa consists of short looped cords of cells which at the capsule end of the gland are separated from the collagen fibrils of the capsule only by the width of the narrow subendothelial space (figs. 1, 5, 6). At the glomerulosa fascicula junction the glomerulosa cords either merge with the outermost cells of the zona fasciculata or form loops which abut against the blood vessels of the fascicula, forming a sharp transitional boundary (figs. 1, 2).

The nuclei of the glomerulosa cells vary widely in shape. The majority are spherical (fig. 6) but many are deeply lobulated (fig. 10).

The mitochondria have lamelliform cristae which are plate like inward reflections of the inner mitochondrial membrane (fig. 8).

Small dense bodies are consistently found at the periphery of many glomerulosa cells. Most of these bodies are round, uniformly dense and bounded by a unit membrane, but some are irregular in shape and have granular contents (figs. 5, 6, 8). Their diameters range from 120 m μ to 420 m μ and they probably are lysosomes, although their content of acid hydrolase has not yet been measured.

The endoplasmic reticulum is predominantly of the granular type. Surprisingly, most glomerulosa cells show no agranular reticulum at all. In figures 5, 6, 7, and 8, large areas of cytoplasm are visible which are completely devoid of agranular endoplasmic reticulum. Figure 9 shows some regions which do contain tubules of agranular endoplasmic reticulum in association with the cell membrane. The much more prevalent granular endoplasmic reticulum is randomly arranged except for an occasional region where mitochondria and lipid droplets are closely bounded by curved cisternal profiles of the granular endoplasmic reticulum (fig. 7).

Numerous ribosomes, in addition to their presence on the membranes of the granular endoplasmic reticulum, are scat-

red throughout the cytoplasm in the form of polysomes (fig 7)

The Golgi region is quite prominent in the cells of the glomerulosa. Figure 9 illustrates the stacked cisternae and small vesicles characteristic of the Golgi complex in glomerulosa cells. No large Golgi vacuoles are present.

The cell membrane is highly convoluted and is bounded by a basal lamina composed of a matted fibrillar material (figs 5, 6). The glomerulosa cells adjoin the characteristic subendothelial space which in this zone contains numerous collagen fibrils (figs 5, 6).

The inner cortical zones

On the basis of their cytological characteristics the inner cortical zones in adult male rhesus monkeys can be divided into three subregions. The first zone is the outermost portion of the zona fasciculata the cells of which contain the largest number of lipid droplets (figs 2, 11). This zone the extent of which is quite variable merges imperceptibly with the inner region of the zona fasciculata whose cells possess smaller amounts of lipid (figs 3, 11). The latter zone then merges with the zona reticularis which in this species is not a very highly reticular zone (fig 4). The cells of the reticularis abut against the blood vessels, nerves and fibroblasts which surround the adrenal medulla (figs 4, 24). As in many other species reticularis cells may be found scattered among groups of medullary cells (fig 4). Only a few fibroblasts accompanied by very small amounts of collagen are present at the reticularis-medulla junction (fig 24).

In all of the cells of the inner cortical zones the mitochondria have tubular cristae. This is most clearly seen in figures 12 and 14 but details of mitochondrial structure are also visible in figures 13, 17, 18 and 24. There are no mitochondria which purely vesicular cristae in any region of the cortex. Further there is no evidence of any centripetal gradation of mitochondria throughout the inner cortical zones.

All of the cells of the inner cortical zones have an extensive network of agranular endoplasmic reticulum the tubules of which have a cross-sectional diameter of approximately 600 Å. Figure 12 is perhaps

the best demonstration of this network but figures 13, 14, 17, 18 and 19 also illustrate the tubular form and pervasive distribution of this organelle.

In certain regions of the cytoplasm of the inner cortical zone cells the tubules of the agranular reticulum become continuous with discrete layered masses or stacks of granular reticulum (figs 16, 17). In the cells of both the outer and inner regions of the zona fasciculata the stacks are large and highly ordered containing up to twenty layers of ribosome-studded cisternae with a regular spacing between the cisternal plates of approximately 140 mμ (fig 17). In the zona reticularis the stacks occur in more disordered whorl-like patterns (figs 20, 21, 22). It is important to note that there is considerable variation in the size of these stacks both from animal to animal and from cell to cell.

As in the zona glomerulosa those ribosomes not attached to the surface of the granular reticulum are scattered at random in the cytoplasm in the form of polysomes (fig 13).

The lipid droplets in the inner fasciculata and the zona reticularis are less numerous and smaller than those in the upper fasciculata. In occasional sections which graze the ends of small lipid droplets groups of tubules of the agranular endoplasmic reticulum appear to end blindly against the surface of the droplet (fig 18). In other sections which transect droplets at or near their centers numerous circular profiles of tubules appear in close apposition to the lipid droplet surface (fig 19). These images suggest that lipid droplets are surrounded by runs of tubules which envelop the droplet and end blindly at various points on its surface. A complete analysis of the junctional relationships between the lipid droplets and the tubules of the agranular endoplasmic reticulum must await serial sectioning.

Most inner cortical zone cells contain dense bodies which are larger and more granular than those in the zona glomerulosa (fig 20). The granules within the dense bodies vary in both size and density and one or more of the larger granules often forms a bulge at the periphery of the dense body. These large peripheral gran-

ules are composed of a light, homogeneous matrix surrounded by a narrow layer of extremely electron dense material (figs 20 21 22). In the zona reticularis cells, where the dense bodies are of greater size and complexity than those in any other region, there are frequent mergers between dense bodies (fig 20). A unit membrane can usually be seen around the fused bodies (fig 22). These mergers create a new class of structures which shall be referred to here as complex dense bodies (figs 22 23 24). Their contents, which are extremely variable include several sizes of granules with or without dense limiting membranes short runs of membranous material and a granular background matrix. Presumably these complex dense bodies are the lipofuscin or lipofuscin like pigment granules seen with the light microscope in the adrenal cortex of a variety of species (Deane 62), no histochemical tests on these structures in the monkey have as yet been performed.

There is a marked centripetal gradation in the size and complexity of the dense bodies throughout the inner cortical zones. The smallest ones are found in the outermost zona fasciculata (approximately 0.5μ in diameter) and the largest in the innermost cells of the zona reticularis (approximately 1.5μ to 2.0μ in diameter). Dense bodies which are intermediate in size and complexity are found in the intermediate regions of the cortex.

The subendothelial space

There is an ubiquitous subendothelial space in the adrenal cortex of the adult male rhesus monkey similar to that described in other species. The ramifications of this space are clearly seen in figure 3 a light micrograph of the inner zona fasciculata. Figures 11, 12 13 and 14 illustrate this space at much higher magnifications and also show the great number of microvilli which extend into it from the cortical cell surfaces. This extreme multiplication of surface area by the microvillous extension of the cell membrane is most marked in the inner regions of the zona fasciculata. Note however that even in the fasciculata the degree of development of the microvillous surface may be

variable. Figure 16 illustrates a portion of the inner fasciculata in which the cells show long regions of intimate contact interrupted only at intervals by small microvillous zones.

Throughout the subendothelial space is a loosely dispersed, fibrillar material which also forms the basal laminae adjoining the surfaces of the cortical and endothelial cells (fig 13).

Collagen fibrils are found in considerable quantity in the subendothelial space particularly in the zona glomerulosa (figs 5 6) there are lesser amounts in the inner cortical zones.

The endothelial cells are similar to those found in the adrenals of other species. Their cytoplasm is highly attenuated and marked by the presence of characteristic annular pores. These pores are capable of transporting relatively large masses of material. Figure 15 shows a fragment of cytoplasmic material caught in the process of traversing an annular pore. The source and motive power of the cytoplasmic fragment is not known however, pieces of cytoplasm may break away from the surface of a degenerating cell (of which there are always some in the cortex) wander within the subendothelial space and ultimately find their way into the blood stream via an annular pore. This phenomenon is either rare or extremely rapid because it was observed only twice in this study.

Macrophages frequently seen in the subendothelial space of the zona glomerulosa (fig 5), are not very common within the inner cortical zones.

DISCUSSION

Mitochondria

In the adrenal cortex of all species which have been described to date with the exception of the guinea pig and the opossum the mitochondria throughout the cortex have the tubular rather than the lamellar type of cristae. In the guinea pig mitochondria with lamelliform cristae are found throughout the cortex (Sheridan and Belt 64). In the opossum (Long and Jones 66) mitochondrial cristae are lamelliform in the glomerulosa and tubular in the fasciculata. The mitochondria in

the zona glomerulosa of the male rhesus monkey have lamelliform cristae while those in the inner cortical zones have cristae of the tubular type

Although there are as yet no published data on secretion of aldosterone by the adrenal cortex in the rhesus monkey we now have preliminary evidence that the adrenal of these animals secretes aldosterone *in vitro* (Hittinger '66). It is reasonable to assume that the zona glomerulosa is the source of aldosterone in the monkey as it is in the rat the cow and man (Stadenko and Giroud '62). Consequently we may infer that the presence of mitochondria with lamelliform cristae in the glomerulosa cells of the rhesus monkey is evidence that mitochondria with tubular cristae are not necessary components of steroid secreting cells. The same conclusion must, of course, be drawn from the presence of lamelliform mitochondrial cristae in the adrenal cortex of the guinea pig and the opossum.

Golgi complex

The cells of the zona glomerulosa have a well developed Golgi complex in contrast to the cells of the inner cortical zones. However there is no evidence to permit even a reasonable speculation concerning the possible role of the Golgi in the cells of the zona glomerulosa.

Agranular endoplasmic reticulum

There is considerable evidence (recently reviewed by Christensen '65) that the agranular reticulum in steroid secreting cells contains many of the enzymes essential to steroidogenesis. Yet the cells of the zona glomerulosa of the rhesus monkey have very small amounts of agranular reticulum. If aldosterone is really made in rhesus monkey glomerulosa cells as discussed above then the agranular reticulum may not be absolutely essential for steroidogenesis. This however must be a tentative conclusion until we have biochemical data on aldosteronogenesis in the rhesus monkey adrenal. A tentative conclusion would also apply to the adrenal of the opossum. Long and Jones ('66) report that the cells of the zona glomerulosa of the opossum adrenal like those of the rhesus monkey

have relatively small amounts of agranular reticulum.

In contrast to the zona glomerulosa however the cells of the inner cortical zones are rich in agranular reticulum. In the rhesus monkey this organelle always appears as a randomly disposed cytoplasmic network of inter-connecting tubules whereas in the adrenals of most other species which have been described the agranular reticulum has been observed in the form of isolated vesicles.

Fawcett ('66) and Christensen ('65) have pointed out the difficulties involved in preserving the delicate tubules of the agranular endoplasmic reticulum in the interstitial cells of the testis. Christensen ('65) has shown that the tubular form of the agranular reticulum in the interstitial cells of the guinea pig is only preserved when the testis is fixed by perfusion with glutaraldehyde fixation by immersion in glutaraldehyde always produces the vesicular form.

In the adrenal cortex of the mouse (Brenner unpublished data) I have observed that immersion in glutaraldehyde or glutaraldehyde formaldehyde mixtures containing 4.5% sucrose always preserves the tubular form whereas the same fixative mixture without sucrose invariably results in the formation of vesicles.

The tissues used in the present study were immersed in a glutaraldehyde formaldehyde fixative which contained 4.5% sucrose. Immersion fixation was evidently adequate to protect the tubular system from breaking down into vesicles. Perfusion fixation is therefore not essential for the preservation of the tubular form of the agranular endoplasmic reticulum in the adrenal cortex. It must be remembered that species differences and organ differences in response to fixatives greatly complicate the task of finding a fixation technique which preserves all steroid secreting cells perfectly. However the presence of the vesicular form of the agranular endoplasmic reticulum seems to be evidence of inappropriate fixation technique.

Granular endoplasmic reticulum

The large and highly ordered stacks of granular endoplasmic reticulum present in

the inner cortical zones are undoubtedly of functional significance. It seems reasonable to assume that high rates of protein synthesis occur within these stacks. Since there is no cytological evidence of protein being made for export in adrenal cells the proteins manufactured in the stacks may be enzymes needed in adrenal cortical cell metabolism. Since the stacks are in direct continuity with the tubules of the agranular endoplasmic reticulum where steroidogenesis is presumed to occur, the enzymes made may be involved in steroidogenesis. The size of the stacks varies from cell to cell and from animal to animal. Therefore variations in functional state may be reflected in variations in the amount of agranular reticulum converted by the cells into protein synthetic machinery. This possibility is currently being investigated.

In the guinea pig the adrenal contains a considerable amount of granular reticulum but Sheridan and Belt (64) did not describe stacks equivalent to those in the rhesus monkey adrenal. Christensen (65) has observed junctions between the agranular reticulum and small stacks of granular reticulum in the interstitial cells of the guinea pig testis. However the stacks were not prominent features of these cells and Christensen mentions that they occur in small patches (see his figs 3 4 12). Whether this structure is present in the adrenal cortices of other subhuman primates is currently under investigation. Published electron micrographs of the adrenal of man do not show similar structures (Ross, 58 Carr 61) although Long and Jones (66) have reported that the human adrenal cortex does have similar large stacks of granular endoplasmic reticulum.

Lipid droplets and the agranular endoplasmic reticulum

It has been amply demonstrated with the light microscope that lipid droplets diminish in volume and often disappear completely during periods of maximal secretory activity of the adrenocortical cells. When the secretory rates decrease the lipid droplets become larger. This waxing and waning of the lipid droplets is presumed to correspond to the storage and

release of steroid precursor molecule. (Deane 51). The mechanism where the adrenocortical cell shuttles these precursors back and forth from lipid droplets to steroidogenic sites remains obscure and it is not known whether or not there is an ultrastructural correlate for the function of precursor transport.

The areas of contact described above (figs 18 19) between the tubules of the agranular reticulum and the surfaces of the lipid droplets might be junctions across which steroid precursor transport could occur. If this were the case the frequency of appearance of these junctions might vary directly with secretory rate. This possibility is currently being investigated.

Two recent studies in other species provide evidence that the tubules of the agranular reticulum may become confluent with the surfaces of lipid droplets in organs other than the adrenal. Geer (65) found lipid accumulations in small cisternae of the agranular endoplasmic reticulum in the foam cells and smooth muscle cells of fatty streaks in the human aorta. Smuckler et al (65) found stellate aggregates of cisternae of both the granular and agranular endoplasmic reticulum surrounding and apparently leading into lipid droplets in the livers of guinea pigs intoxicated with carbon tetrachloride.

Although these are studies of pathological tissue they suggest that the tubules of the agranular reticulum have the potential to transport lipid.

Effects of handling stress

One must bear in mind that all of the observations in this study were made on the adrenals of animals which had undergone some stress because of handling. True resting conditions in the adrenal are very difficult to obtain short of sudden death of an unaware animal (Glick et al 54). Undoubtedly there were increases in ACTH blood levels in these animals before they were sacrificed.

Consequently the cytological observations reported here pertain not to resting cells but to normal cells mildly stimulated by endogenous ACTH. In future reports shall compare the ultrastructural effect of intense exogenous ACTH stimulation

of the effects of severe cortisone suppression with the observations reported here ultimately this should provide a complete picture of the full range of micromorphological variation which the adrenocortical cells of the monkey can express

ACKNOWLEDGMENT

I wish to express my thanks to Miss V. J. June Kamm for her excellent technical assistance during this study

LITERATURE CITED

- W. D. M. N. Sheridan, R. A. Knouff and F. A. Hartman 1966 Fine structural study of a possible mechanism of secretion by the adrenal cells of the brown pelican *Z f Zellforsch u Mikrosk Anat* 68 864-873
- M. H. 1959 Histochemistry and electron microscopy of the three cell types in the adrenal gland of the frog *Anat Rec* 133 103-174
- Cori 1961 The ultrastructure of the human adrenal cortex before and after stimulation with ACTH *J Path Bact* 81 101-105
- Christensen A. K. 1965 The fine structure of testicular interstitial cells in guinea pigs *J Cell Biol* 26 911-935
- Corre, G. N. Michel Bechet, D. Picard and A. M. Besson 1963 Etude comparative en microscopie électronique de la cortico-surrénale du cobaye et de la lapine et du hamster *Annales d'Endocrinologie* 24 1040-1043
- Deane H. W. 1951 Physiological regulation of the zona glomerulosa of the rat's adrenal cortex, as revealed by cytochemical observations. In: *Primary Adrenal Function* R. C. Christman, ed. AAAS Washington D C 31-38
- 1962 The anatomy chemistry and physiology of adrenocortical tissue. In: *Deane H. W. Ed., The Adrenocortical Hormones Their Origin Chemistry Physiology and Pharmacology* Handbuch der Experimentellen Pharmakologie Springer-Verlag Berlin Part 1 56-58
- Freeman D. W. 1966 An atlas of cell fine structure. The Cell Saunders Philadelphia and London. 195-199
- Fujita H. 1961 An electron microscopic study of the adrenal cortical tissue of the domestic fowl *Z f Zellforsch u Mikrosk Anat* 55 56-63
- Guy J. C. 1965 Fine structure of human adrenal interstitial thickening and fatty streaks *Lab Invest* 14 1 64-1783
- Guzonell F. J. Winer and D. Spiro 1965 Cytochemical alterations related to stimulation of the zona glomerulosa of the adrenal gland *J Cell Biol* 16 472-52
- Gluck D. R. H. Swigart R. C. Bahn and D. W. Hastings 1954 A technique for killing animals to obtain tissues on studies of stress effects *Endocrinology* 54 706-708
- Harrison G. A. 1966 Some observations on the presence of annulate lamellae in alligator and sea gull adrenal cortical cells *J Ultrastruct Res* 14 158-166
- Kittinger G. 1966 Personal communication
- Lever J. D. 1955 Electron microscopic observations on the adrenal cortex *Am J Anat* 97 409-430
- Long J. A. and A. L. Jones 1966 The fine structure of the zona glomerulosa and the zona fasciculata of the opossum *Anat Rec* 154 378-379
- Luft J. H. 1961 Improvements in epoxy resin embedding methods *J Biophys Biochem Cytol* 9 409-414
- Ross M. H. G. C. Pappas J. L. Lanman and J. Lind 1958 Electron microscope observations on the endoplasmic reticulum in the human fetal adrenal *J Biophys Biochem Cytol* 4 659-662
- Sabatini D. and E. D. P. DeRobertis 1961 Ultrastructural zonation of adrenocortex in the rat *J Biophys Biochem Cytol* 9 105-120
- Sabatini D. E. D. P. DeRobertis and H. B. Bleichmar 1962 Submicroscopic study of the pituitary action on the adrenal cortex of the rat *Endocrinology* 70 390-406
- Sheridan M. N. 1963 Fine structure of the interrenal cell of the garter snake (*Thamnophis sirtalis*) *Anat Rec* 145 285
- Sheridan M. N. and W. D. Belt 1964 Fine structure of the guinea pig adrenal cortex *Anat Rec* 149 73-98
- Sheridan M. N. W. D. Belt and F. A. Hartman 1963 The fine structure of the interrenal cells of the brown pelican *Acta Anatomica* 53 55-65
- Smuckler E. A. R. Ross and E. P. Benditt 1965 Effect of carbon tetrachloride on guinea pig liver *Exper and Mol. Path* 4 328-339
- Stachenko J. and C. J. P. Giroud 1960 Some aspects of steroidogenesis in the zona glomerulosa. In: *Currie A. R. T. Symington and J. K. Grant eds The Human Adrenal Cortex* Williams and Wilkins Company Baltimore 30-43
- Yamori T. S. Matsuura and S. Sakamoto 1961 An electron microscopic study of the normal and stimulated adrenal cortex in the rat *Z f Zellforsch u Mikrosk Anat* 55 179-199
- Yates R. D. 1965 Fine structural observations on untreated and ACTH treated adrenal cortical cells of the zona reticularis of Syrian hamsters *Z f Zellforsch u Mikrosk Anat* 66 384-395
- Zelander T. 1959 Ultrastructure of mouse adrenal cortex. An electron microscopical study in intact and hydrocortisone treated male adults *J Ultrastruct Res Suppl* 2

Abbreviations

aer	agranular endoplasmic reticulum	ger	granular endoplasmic reticulum
ap	annular pore	gr	granule
bv	blood vessel	gv	golgi vesicles
C	capsule	J	junctions
CDB	complex dense body	L	lipid droplet
cf	cell fragment	M	macrophage
cg	chromaffin granule	Med	medulla
cm	cell membrane	m	mitochondria
co	collagen	mv	microvilli
db	dense body	N	nucleus
ec	endothelial cytoplasm	n	nerve
F	fasciculata	P	polysome
f	fibroblast	rbc	red blood cell
G	glomerulosa	SES	subendothelial space
g	golgi	wbc	white blood cell
gc	golgi cisternae		

PLATE 1

EXPLANATION OF FIGURES

- 1 Portion of the capsule glomerulosa and outer fasciculata. The glomerulosa cords can be seen to merge with the fasciculata cords in lower right of micrograph. Looped glomerulosa cords are evident at lower left of picture $\times 250$
- 2 Glomerulosa fasciculata junction. Lower end of a looped glomerulosa cord is evident in upper half of micrograph. Note that outer most fasciculata cells are very rich in lipid $\times 1850$
- 3 Inner fasciculata. Cells here are much less rich in lipid than those in the outer fasciculata. Note extensive ramifications of the subendothelial space $\times 760$
- 4 Reticularis medulla junction. Note the minimal degree of reticularization. Some cortical cells are scattered about the medullary islands $\times 332$

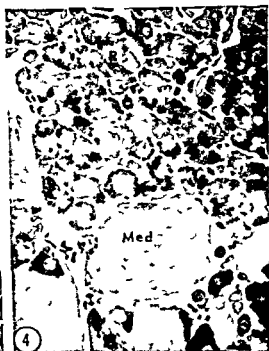


PLATE 2

EXPLANATION OF FIGURES

- 5 Capsule glomerulosa junction. A large macrophage is present at the capsule glomerulosa junction. The arrow points to the highly convoluted cell membrane of a glomerulosa cell. Dense bodies are present in the cytoplasm of a glomerulosa cell. $\times 8310$
- 6 Capsule glomerulosa junction. Collagen bundles, nerve fibers, and blood vessels typical of the capsule are shown here. Note small dense bodies in glomerulosa cells. $\times 4680$



PLATE 2

EXPLANATION OF FIGURES

- 5 Capsule glomerulosa junction A large macrophage is present at the capsule glomerulosa junction The arrow points to the highly convoluted cell membrane of a glomerulosa cell Dense bodies are present in the cytoplasm of a glomerulosa cell $\times 8310$
- 6 Capsule glomerulosa junction Collagen bundles nerve fibers and blood vessels typical of the capsule are shown here Note small dense bodies in glomerulosa cells $\times 4680$

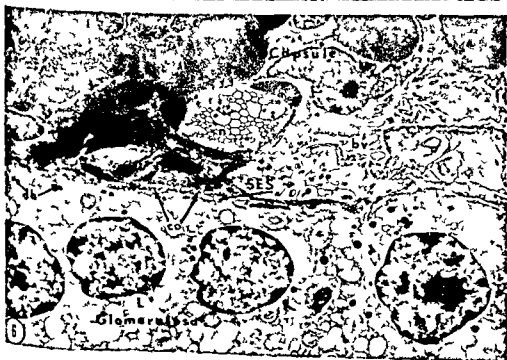
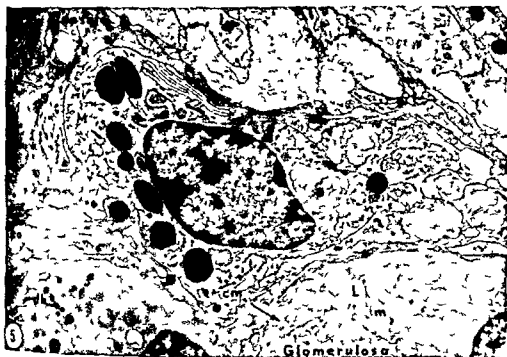


PLATE 2

EXPLANATION OF FIGURES

- 5 Capsule glomerulosa junction A large macrophage is present at the capsule glomerulosa junction The arrow points to the highly convoluted cell membrane of a glomerulosa cell Dense bodies are present in the cytoplasm of a glomerulosa cell $\times 8310$
- 6 Capsule-glomerulosa junction Collagen bundles nerve fibers and blood vessels typical of the capsule are shown here Note small dense bodies in glomerulosa cells $\times 4680$



PLATE 3

EXPLANATION OF FIGURES

- 7 Glomerulosa cell The cytoplasm is characterized by mitochondria granular reticulum and polysomes Note lack of agranular reticulum $\times 18\ 500$
- 8 Mitochondria in a glomerulosa cell Note lamellar cristae granular reticulum and small round dense bodies $\times 24\ 000$
- 9 Golgi region in a glomerulosa cell Golgi cisternae and Golgi vesicles are visible $\times 16\ 500$
- 10 Lobulated nucleus of a glomerulosa cell There is considerable variation in nuclear shape in the zona glomerulosa Most are round but many are deeply lobulated as illustrated here $\times 11\ 000$



PLATE 4

EXPLANATION OF FIGURE

- 11 Outer fasciculata cell Cytoplasm is characterized by a large number of lipid droplets. Note that the narrow subendothelial space is penetrated by microvilli. A portion of a macrophage is visible at the lower right of the micrograph. $\times 7400$



PLATE 5

EXPLANATION OF FIGURE

- 12 Inner fasciculata cell The subendothelial space is penetrated by numerous microvilli The cytoplasm is characterized by mitochondria with tubular cristae agranular reticulum lipid droplets and dense bodies $\times 7450$ Inset shows the tubules of the agranular reticulum at a higher magnification $\times 37600$



PLATE 6

EXPLANATION OF FIGURES

- 13 Inner fasciculata This micrograph illustrates the thin layer of endothelial cell cytoplasm which separates the subendothelial space of the cortex from the blood stream Portions of an erythrocyte and a leucocyte are visible in the lumen Microvilli are present in the subendothelial space The cortical cells show an abundance of agranular endoplasmic reticulum and polysomes $\times 22\ 220$
- 14 Inner fasciculata This micrograph illustrates the extensive intermingling of the microvilli from two cortical cells within the subendothelial space $\times 14\ 700$
- 15 Inner fasciculata A cytoplasmic fragment (cf) bounded by a unit membrane (um) is shown during the process of traversing an annular pore (ap) in an endothelial cell (ec) $\times 62\ 500$



PLATE 6

EXPLANATION OF FIGURES

- 13 Inner fasciculata This micrograph illustrates the thin layer of endothelial cell cytoplasm which separates the subendothelial space of the cortex from the blood stream Portions of an erythrocyte and a leucocyte are visible in the lumen Microvilli are present in the subendothelial space The cortical cells show an abundance of agranular endoplasmic reticulum and polysomes $\times 22\,220$
- 14 Inner fasciculata This micrograph illustrates the extensive intermingling of the microvilli from two cortical cells within the subendothelial space $\times 14\,700$
- 15 Inner fasciculata A cytoplasmic fragment (cf) bounded by a unit membrane (um) is shown during the process of traversing an annular pore (ap) in an endothelial cell (ec) $\times 62\,500$

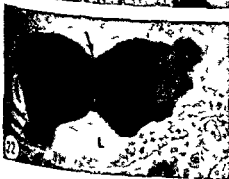
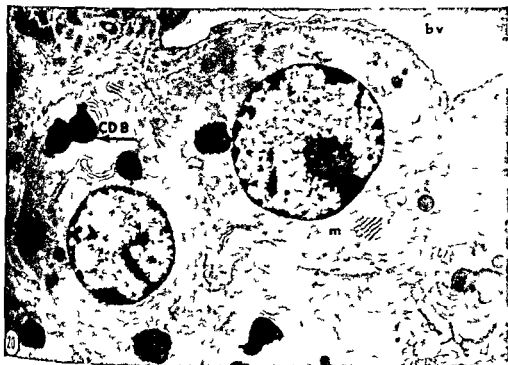


PLATE 8

EXPLANATION OF FIGURES

- 20 Reticularis Cells here are characterized by large and complex dense bodies. Arrow points to fusion between dense bodies. $\times 6930$
- 21 Reticularis An enlargement of part of figure 20. A single dense body. Note the characteristic granule which is usually found at the periphery of the dense body. The contents of the peripheral granule are more homogeneous than the rest of the body and the granule is always bounded by a very dense material. $\times 21900$
- 22 Reticularis An enlargement of the body labeled CDB in figure 20. Formation of a complex dense body by fusion. The arrow points to the membrane which surrounds both bodies. $\times 21000$
- 23 Reticularis An enlargement of the body labeled CDB in figure 24. Complex dense bodies. These are the largest and most complex dense bodies in the cortex. $\times 24700$



PLATE 9

EXPLANATION OF FIGURE

- 24 Reticularis medulla junction. An unmyelinated nerve within the subendothelial space separates the medulla from the cortex. The cytoplasm of a fibroblast is visible at the right. The cortical cell cytoplasm is characterized by complex dense bodies, presumably lipofuscin. The medullary cytoplasm is characterized by chromaffin granules (cg). $\times 16,580$



A Dynamic and Static Study of Hepatic Arterioles and Hepatic Sphincters^{1,2}

ROBERT S. McCUSKEY³

Department of Anatomy Western Reserve University Cleveland Ohio

ABSTRACT The purpose of this investigation was to demonstrate the cytology of the sphincters of hepatic sinusoids to elucidate further the pathway by which arterial blood is distributed to the sinusoids and to study the hormonal and local regulation of arterial and portal venous blood flow through the sinusoids.

The sphincters were found to consist of reticulo-endothelial cells and were the primary site for the regulation of blood flow through the sinusoids. By contracting in dependency or in unison the flow of blood was regulated through individual sinusoids through sinusoids supplying a portion of a lobule or through sinusoids supplying a whole lobule. When the sphincter cells contracted their nuclear region bulged into the lumen thereby occluding it.

Hepatic arterioles were found to wind around adjacent portal venules with an average curvature of 42° and communicated with sinusoids via arterio-sinus twigs. No structural arterio-portal anastomoses were observed however functional "arterio-portal anastomoses" were formed by short twigs which terminated in sinusoids near their origins. No branches were found to terminate near central venules.

The data suggest that the local regulation of blood flow through the hepatic sinusoids is mediated by vasodilator metabolites (adenosine and/or potassium) released from hypoxic hepatic cells as a result of the rapid glycogenolysis that accompanies hepatic cellular hypoxia.

The liver consists of many identical morphological units that fulfill its numerous functions. Each unit is microscopic in size and consists of a sinusoid with its afferent and efferent vascular connections and the surrounding hepatic tissue with its biliary lymphatic and nervous connections. As liver function is dependent upon the conveyance of substances to and from these functional units a knowledge of the dynamic anatomic and physiologic relationships of the vascular system with each unit is required for an understanding of liver function.

The current concept of the hepatic microvascular system is based primarily upon the investigation of the living liver of frogs by Knisely et al. (48) and in mammals by Irwin and MacDonald (53) and Enoch (55). Several structures seen in the living liver by these investigators however were seen infrequently were recorded incompletely or have not been seen by others. As a result the following problems have been answered only partially: (1) the reason for the closure of most of the hepatic arterioles during anesthesia is unknown; (2) the cytology of the afferent

and efferent sphincters of the sinusoids is almost unknown and (3) the local and hormonal regulation of blood flow through the sinusoids is understood poorly.

The purpose of this investigation was to demonstrate in life the cytology of the afferent and efferent sphincters and to elucidate the local and hormonal factors that acted on these structures to regulate the flow of portal and arterial blood through the sinusoids.

METHODS

Frogs (*Rana pipiens*) white rats (Sprague-Dawley) mice (Swiss-Webster) and rabbits (New Zealand albino) were used.

The frogs were fed with pieces of fresh rat liver and by injecting a sterile non pyrogenic 5% dextrose solution into the

¹Submitted to the Graduate School of Western Reserve University in partial fulfillment of the requirements for the degree of Doctor of Philosophy June 1965.

²Portions of this research were reported at the 13th Microcirculatory Conference Atlantic City April 9 1965 and at the 76th Meeting of the American Association of Anatomists Miami Beach April 21 1965.

³Present address: Department of Anatomy College of Medicine University of Cincinnati, Cincinnati, Ohio 45219.

subcutaneous lymphatic system, while the rats were fed a standard laboratory chow diet. When starved animals were required food was withheld from frogs for one week and from rats 48 hours prior to their use.

The frogs were anesthetized by injecting ethyl carbamate⁴ (Urethane, 25%) into the subcutaneous lymphatic system and the mammals by an intravenous (tail vein) injection of sodium pentobarbital⁵ (Nembutal, 10 mg/ml) or by an intraperitoneal injection of 25% ethyl carbamate. Anesthesia was maintained by injecting 10% of the initial dose as required.

The liver was exposed in frogs by making a paramedian thoraco-abdominal incision. The mammalian liver was exposed by making a L-shaped abdominal incision. The incision extended along the linea alba from just above the pubis to the xiphisternum and then continued laterally along the right subcostal margin to the tip of the twelfth rib. A tracheotomy was performed and a tracheal cannula was inserted for the administration of oxygen (see below).

Movement of the liver that was induced by the respiratory system, the heart and the gastrointestinal system was reduced by several methods. Those caused by the respiratory system in mammals were reduced by cutting the falciform ligament to partially free the liver from the diaphragm. Residual movements were eliminated by insufflating the lungs with oxygen introduced through a tracheal cannula using Irwin and MacDonald's (53) modification of the Meltzer and Auer technique or by paralyzing the diaphragm with an intravenous injection of succinylcholine chloride⁶ (Anectine, 0.2 mg/ml) while administering intratracheal oxygen. To reduce movements induced by the heart and gastrointestinal system the liver was immobilized on the mechanical stage of a modified compound binocular microscope. This was accomplished by positioning a lobe of the liver over a bay window covered with Saran Wrap⁷ and then immobilizing it with a movable clamp also covered with Saran Wrap. This clamp gently held the liver without interfering with its microcirculation. Gauze packing was placed between the liver and the intestines to eliminate the residual movements induced by the gastrointestinal tract.

Livers which were immobilized on the stage of the modified compound binocular microscope were transilluminated with white light supplied by a 150 watt projection bulb or with light from an Osram 100 watt mercury vapor lamp that was projected through a Leitz prism monochromator and reflected from the substage mirror through the substage condenser. Livers also were transilluminated with white or monochromatic light using the fused quartz rod technique of Knisely (36) as modified by Bloch (62).

The transilluminated liver was examined with a stereo-binocular microscope containing 4× 6× 8× or 12× objectives and 12.5× oculars, a monocular or a compound binocular microscope containing 10× 22×, 50× 55× 75× or 90× water immersion objectives and 10× or 25× oculars.

To obtain images of the liver on a television monitor a modified Dumont image orthicon television system was used (Bloch 63, 64, 65). The television camera contained an image orthicon tube (RCA 5820) on to whose face plate the optical image of the liver was projected. To secure maximum resolution (signal to image ratio) of a specific tissue component a magnification was selected which allowed the projected optical image to cover the largest possible area of the photocathode of the image orthicon tube (Bloch and McCuskey 66). Figure 1 is a block diagram of the optical and electronic system used.

The hepatic microvascular system of each animal was observed an average of four hours with observations ranging from 30 minutes to 18 hours. The hepatic microcirculation was considered healthy if the morphological criteria defined by Bloch (56) were fulfilled. Animals that did not fulfill these criteria were not used.

The dynamic events were recorded sequentially by the following methods: (1) the images were observed microscopically measured with a calibrated ocular scale.

⁴Ethyl carbamate (Urethane) Merck and Company Inc. Rahway New Jersey
⁵Sodium pentobarbital (Nembutal) Abbott Laboratories North Chicago Illinois
⁶Succinylcholine chloride (Anectine) Burroughs Wellcome and Company Tuckahoe New York
⁷Saran Wrap Dow Chemical Company Midland Michigan

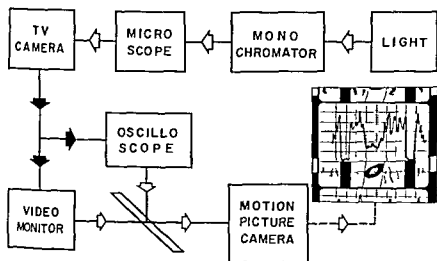


Fig 1 Block diagram of the optical and electronic equipment used for television microscopy of the living liver and scanning microspectrophotometry (from Bloch and Coys 63)

and the information transferred to scale onto graph paper (2) photographs were made directly from the microscope with a 35 mm camera (Praktina FX) without a lens* and to produce additional magnification a 5X or 10X compensating ocular was used (3) photographs were taken with a 16 mm motion picture camera (Kodak Cine Special I) without a lens at framing rates of 8 to 32 frames per second a good image to frame ratio being produced by using the following projection oculars 1.6X 3.2X or 4.0X and (4) the images from the video monitor were photographed at a framing rate of 24 frames per second with a 16 mm camera (Maurer) having a f 1.6 50 mm lens or with the 35 mm camera (Praktina FX) equipped with a f 2.0 58 mm lens.

The following pharmacodynamic substances salts and vital dyes were prepared and administered* Glucagon isopropyl norepinephrine epinephrine norepinephrine 5 ATP 5 ADP 5 AMP cyclic 3 5 AMP and adenosine were prepared in equivalent concentrations (1 μ M/L to 100 μ M/L) immediately before use Ionic salt solutions (NaCl Na₂SO₄ KCl and K₂SO₄) were prepared in equivalent solutions whose concentrations varied from 0.1 mEq/L to 100 mEq/L Glucose was administered as a 1% 5% 10% or 50% solution in isotonic saline Evans blue was

injected as a buffered stock solution (0.4%) and trypan blue was injected as a 1% or 2% buffered saline solution These solutions were administered in 0.1 ml doses by topical application to the liver surface with a micropipette or by intravascular injection

Dynamic blood pressures were recorded from portal and central venules of frogs using a modified Sanborn capacitance transducer system (Rappaport et al 59) A lobe of the liver was placed on a supporting frame which was covered with Saran Wrap Then a pyrex cannula with an orifice of 30 to 50 μ completely filled with degassed heparinized Ringer's solution and connected to the modified transducer system was positioned over the liver A portal or central venule was selected using the stereo-binocular microscope (at a magnification of 150X) and the cannula was inserted by means of a modified Chambers micromanipulator (Bloch et al 61) The pressure pulses were dis-

* Kodachrome II Professional Panatomic X, Plus X, Tri-X film were used.

Panatomic X, Plus X, or Tri-X film were used. These substances were obtained from the following sources: Glucagon and betadine glucose Eli Lilly and Company Indianapolis Indiana 11 propyl or epinephrine 1-epinephrine and 1-norepinephrine Winthrop Laboratories New York New York 5 ATP 5 ADP 5 AMP cyclic 3 5 AMP and adenosine Sigma Chemical Company St. Louis, Missouri Evans blue Wm. Warriner-Chilecot, Morris Plains New Jersey and trypan blue Allied Chemical and Dye Corporation, New York, New York.

played on an oscilloscope and recorded on thermosensitive paper with a Sanborn electrokymograph (Model 154-100B).

Serial sections were made of the livers that were observed *in vivo*. The livers were fixed *in situ* by perfusion through the thoracic aorta with Zenker's fluid, Helly's fluid, 10% neutral formalin, Carnoy's or Carnoy-Lebrun fluid (Humason, 62). Then the liver was excised, cut into 5 mm cubes and immersed in the fixative for 6 to 15 hours at 3°C. After dehydrating in ethanol and clearing in benzene, the pieces of liver were embedded in Paraplast[®] and serial sections (3 μ –40 μ) made with a Minot microtome. The sections were stained with one of the following stains: hematoxylin and eosin, Mallory's phosphotungstic acid hematin, Casson's Heidenhain or Heidenhain's iron hematoxylin, eosin orange G (Humason, 62).

The sections were examined by light microscopy and compared with the histology observed *in life*. The histology was recorded by camera lucida (Leitz) drawings and by 35 mm photomicrographs.

RESULTS

The transilluminated livers of 637 animals were examined (450 frogs, 150 rats, 25 mice and 12 rabbits). Qualitatively similar results were obtained from all species investigated.

Hepatic arterioles

Hepatic arterioles (and their branches) were seen in only 10% of the livers examined unless vasodilators were used to open them. The ability to observe this small number of arterioles was influenced further by the animal's nutrition, its anesthesia, the success in eliminating movements (induced by the heart, respiratory and gastrointestinal system) and the method of transillumination. Arterioles were seen more frequently in recently fed animals than in those which had been starved. Furthermore they were visible more often in animals anesthetized with ethyl carbamate than in those anesthetized with sodium pentobarbital. In animals lightly anesthetized with ethyl carbamate closure of hepatic arterioles was observed often when sodium pentobarbital was subsequently injected intravenously to maintain

anesthesia. Closure of these vessels was observed often when oxygen insufflation of the lungs was initiated to reduce movements induced by the respiratory system but no changes in arteriolar blood flow occurred when these movements were suppressed by immobilizing a lobe of the liver on the stage of the modified compound binocular microscope and the residual respiratory movements eliminated by paralyzing the diaphragm with succinylcholine chloride.

Hepatic arterioles were difficult to observe with white light transillumination due to their small size and the light color of the arterial blood which provided little contrast with the surrounding tissue. Observation of these vessels was facilitated however by transilluminating the liver with monochromatic light and using television microscopy which increased the contrast between its various tissue components. The following wavelengths of light were found particularly useful: 414, 430, 520, 560, 600 and 620 m μ . Contrast between the blood and its surrounding tissue was enhanced by wavelengths of blue light 407, 414 and 430 m μ permitting the patterns of blood flow to be observed easily. Good contrast between vascular and parenchymal components was obtained with wavelengths of green light 520, 540 and 560 m μ . Fluorescence was visualized best when wavelengths of red light 600 and 620 m μ were used. The best resolution of hepatic arterioles was obtained when the modified compound binocular microscope was used with 55 \times and 75 \times water immersion objectives.

The spatial relationship of hepatic arterioles with portal venules, sinusoids and central venules was investigated. These relationships were verified by injecting the dye Evans blue or trypan blue into the thoracic aorta which filled the hepatic arterial system prior to the filling of the portal venous system (fig. 10). The relationships which were observed are illustrated diagrammatically in figure 2.

Hepatic arterioles (and adjacent bile ducts) wound around adjacent distributing portal venules (portal venules from

¹ Paraplast, Aloe Scientific, St. Louis, Missouri.

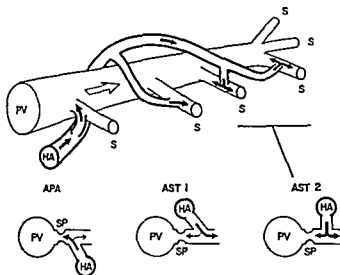


Fig 2 Schematic diagram of the relationships of the hepatic arteriole with its adjacent portal venule and sinusoids PV portal venule HA hepatic arteriole "APA" functional arterio-portal anastomoses AST arterio-sinus twigs S sinusoid SP inlet sphincter Solid arrows indicate direction of arterial blood flow Open arrows indicate direction of portal blood flow

which sinusoids originated) (figs 2 10-12) with an average curvature of 42°. The internal diameters of these arterioles varied from 4 to 10 μ in the mammals to 7 to 30 μ in the frog and they were always smaller than the adjacent portal venules (see table 1).

Branches of the arterioles communicated with sinusoids via arterio-sinus twigs (AST's). These terminated in sinusoids at or near the periphery of the lobule. None were found to terminate near the central venule. Three types of AST's were observed: (1) type 1 which terminated at acute angles to sinusoids directing arterial blood toward the central venule (figs 2 11 12); (2) type 2 which terminated at right angles to sinusoids (figs 2 11 12); and (3) short AST's which terminated near the origins of sinusoids from the portal venule (figs 2 11 12). All had an internal diameter equal to or less than a single red blood cell (3 to 10 μ for the mammals; 7 to 25 μ for the frogs).

Direct connections between hepatic arterioles and portal venules were never seen in livers transilluminated with monochromatic light and examined at high magnifications (220 \times - 900 \times) with the

modified compound binocular microscope. Functional "arterio-portal anastomoses" ("APAs") were observed however and these were composed of two segments: (1) a short arterio-sinus twig directed toward the portal venule and terminating in a sinusoid near its origin and (2) the short initial segment of the sinusoid with

TABLE 1
Dimensional relationships of hepatic arterioles with adjacent portal venules¹

Animal	PV μ	HA μ	A Curv degrees	R.B.C μ
Frog	65	28		
	50	28	42	15 \times 25
	30	24		
Rat	34	10		
	28	10	52	6
	21	7		
Mouse	30	9		
	21	6	48	6
	15	6		
Rabbit	50	10	26	6
	30	10		

¹ P.V., internal diameter of portal venule; H.A., internal diameter of hepatic arteriole; A Curv., average curvature of hepatic arteriole; see urements taken from scale draw logs and individual motion picture frames using a projector; R.B.C., average red blood cell dimensions.

its inlet sphincter which received the arterial blood (figs 2 11 12) Such APAs appeared to be direct connections between hepatic arterioles and portal venules however at low magnifications (100–150 \times) when white light quartz rod transillumination was used

The flow of arterial blood to the sinusoids was intermittent and lasted from a few seconds to several hours This was produced by arterioles, arterioportal anastomoses and arterio-sinus twigs which were independently contractile and opened and closed with no definable rhythm

Arterial blood flow modified the flow in portal venules sinusoids or both The various patterns of blood flow which were observed are illustrated in figures 2 11 and 12 When functional arterio-portal anastomoses (APAs) were wide open the arterial blood flow often reversed blood flow in the portal venule so that all sinusoids distal to the APA received only arterial blood (figs 2 11 12) If the APA was dilated partially a mixture of arterial and portal blood reached the distal sinusoids (fig 11) Closure of the inlet sphincter eliminated the flow of arterial blood in to the portal venule via the APA and resulted in the sinusoid being perfused with arterial blood Under these conditions the APA functioned as an AST A sinusoid with an open inlet sphincter and an open AST was perfused with a mixture of arterial and portal venous blood (figs 2 11 12) With the inlet sphincter closed only arterial blood flowed through the sinusoid Arterial blood entering a sinusoid from an AST often was observed to flow into the portal venule through an open inlet sphincter especially if the outlet sphincter of that sinusoid was narrowed or closed and the sinusoid was filled with blood (figs 11, 12) Under these conditions ASTs of type 1 and type 2 often behaved functionally as APAs even though they terminated in sinusoids 20–30 μ away from a portal venule When blood flow in hepatic arterioles or in individual ASTs and APAs ceased portal venous blood often was observed to flow into ASTs and APAs but rarely into hepatic arterioles Closure of the inlet sphincters eliminated this inflow of portal venous blood into APAs and ASTs

In fixed preparations, the distribution of the hepatic arteriole and its terminal branches was similar to that observed *in vivo* Often a muscular sphincter was observed at the origins of the ASTs from the hepatic arterioles, and although smooth muscle cells were seen occasionally in the more distal portion of these vessels not extended to the junction of the AST with the sinusoid

Sphincters of hepatic sinusoids

Good resolution of the sphincters of the hepatic sinusoids was obtained only with the modified compound binocular microscope and monochromatic light The best resolution of these structures was obtained at high magnifications (500–900 \times) with wavelengths of green light 520 540 and 560 m μ and with wavelengths of red light 600 and 620 m μ The lower wavelengths (green light) provided good contrast between the endothelial cells of the hepatic parenchymal cells and the cellular components of the blood The higher wavelengths (red light) accentuated the endothelial cell membranes

The sphincters consisted of endothelial cells which were located at (1) the junctions of sinusoids with portal venules (inlet sphincters) (2) the junctions of sinusoids with central venules (outlet sphincters) and (3) the junctions of intersinusoidal sinusoids with sinusoids (sphincters of intersinusoidal sinusoids) (fig 3) At magnifications between 500–900 \times the nuclear regions of the sphincter cells were seen to enlarge frequently and to bulge into the lumen thereby occluding it (figs 4 5 16) The resulting reduction in internal diameter was accompanied by a thickening of the endothelial cytoplasm and a smaller reduction in the outside diameter of the sinusoid (figs 4 5) In many instances two or more endothelial cells opposed each other and were capable of reducing the lumen almost to zero either individually or mutually (fig 15)

Sphincter cells in all locations were similar morphologically The sphincter cells of dilated sinusoids had flattened ovoid nuclei with single prominent nucleoli and occasional refractile granules in their attenuated cytoplasm The nuclei of sphincter cells which were bulging and occluding

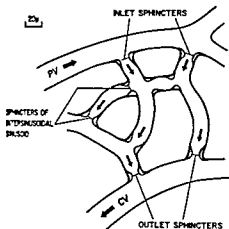


Fig. 3 Semischematic diagram of the location of hepatic sphincters. PV portal venule, CV central venule.

ing the sinusoid lumen were more rounded and their nucleoli more distinct (fig. 14). Such cells were demonstrated to be components of the hepatic reticulo-endothelial system (V. Kupffer cells) since they phagocytized particles of trypan blue or India ink that were injected intravascularly. Sphincter cells which were bulging and occluding the sinusoid lumen were still capable of removing foreign material from the blood stream. Furthermore, Kupffer cells containing phagocytized material continued to act as sphincters as demonstrated by their continued response to catecholamines.

The remainder of the sinusoid appeared to be a smooth continuously lined tube whose internal diameter varied as changes in the internal diameter of its sphincters occurred. A decrease in the internal diameter and a thickening of the endothelium as well as accompanied the contraction of its sphincter cells.

The sphincters regulated the flow of blood through the sinusoids by contracting independently or in unison. As a result the flow of blood through individual sinusoids, groups of sinusoids or the sinusoids comprising a whole lobule could be regulated independently of that in adjacent lobules or groups of sinusoids or those of other lobules. Open sphincters allowed normal or moderate rates of blood flow through the sinusoid with no deformation

of red or white blood cells. When the sphincters were closed partially, blood flow was slow and red blood cells squeezed through the narrowed sinusoid lumen (figs. 4B and 14). Often this flow was impeded by less plastic white blood cells which stuck in the incompletely closed sphincters (fig. 15). Complete closure of a sphincter prevented the flow of all cellular elements of the blood past that point (fig. 16).

Concomitant with constriction of the inlet and outlet sphincters there was usually a change in the internal diameter of the

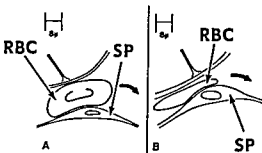


Fig. 4 Outlet sphincters in the living frog liver. Both A and B are tracings of single 16 mm motion picture frames photographed from the video monitor.

- A A non bulging outlet sphincter cell (SP) with red blood cell (RBC) passing through this sphincter.
- B A bulging outlet sphincter cell (SP) with red blood cell (RBC) being deformed as it passes through the sphincter.

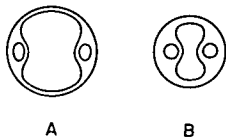


Fig. 5 Diagrammatic representation of how sphincters constrict. A is a cross-section of a relaxed non-bulging sphincter cell. B is a cross-section of two contracted bulging sphincter cells. Note the prominent bulging of the nuclear region, the rounding of the nucleus and the thickening of the attenuated portion of the cytoplasm. This results in a large reduction of the internal diameter of the sinusoid compared with a somewhat smaller reduction in its outside diameter.

its inlet sphincter which received the arterial blood (figs 2 11 12) Such APAs appeared to be direct connections between hepatic arterioles and portal venules however, at low magnifications (100–150 \times) when white light quartz rod transillumination was used

The flow of arterial blood to the sinusoids was intermittent and lasted from a few seconds to several hours This was produced by arterioles arterioportal anastomoses and arterio sinus twigs which were independently contractile and opened and closed with no definable rhythm

Arterial blood flow modified the flow in portal venules sinusoids or both The various patterns of blood flow which were observed are illustrated in figures 2 11, and 12 When functional arterio-portal anastomoses (APAs) were wide open the arterial blood flow often reversed blood flow in the portal venule so that all sinusoids distal to the APA received only arterial blood (figs 2 11 12) If the APA was dilated partially a mixture of arterial and portal blood reached the distal sinusoids (fig 11) Closure of the inlet sphincter eliminated the flow of arterial blood in to the portal venule via the APA and resulted in the sinusoid being perfused with arterial blood Under these conditions the APA functioned as an AST A sinusoid with an open inlet sphincter and an open AST was perfused with a mixture of arterial and portal venous blood (figs 2 11 12) With the inlet sphincter closed only arterial blood flowed through the sinusoid Arterial blood entering a sinusoid from an AST often was observed to flow into the portal venule through an open inlet sphincter especially if the outlet sphincter of that sinusoid was narrowed or closed and the sinusoid was filled with blood (figs 11 12) Under these conditions AST's of type 1 and type 2 often behaved functionally as APAs even though they terminated in sinusoids 20–30 μ away from a portal venule When blood flow in hepatic arterioles or in individual AST's and APAs ceased portal venous blood often was observed to flow into AST's and APAs but rarely into hepatic arterioles Closure of the inlet sphincters eliminated this inflow of portal venous blood into APAs and AST's

In fixed preparations, the of the hepatic arteriole and its branches was similar to that observed *in vivo* Often a muscular sphincter was observed at the origins of the AST's from hepatic arterioles and although muscle cells were seen occasionally in more distal portion of these vessels extended to the junction of the AST the sinusoid

Sphincters of hepatic sinusoids

Good resolution of the sphincters of hepatic sinusoids was obtained only with the modified compound binocular microscope and monochromatic light The resolution of these structures was at high magnifications (500–900 \times) with wavelengths of green light 520 540 560 m μ and with wavelengths of light 600 and 620 m μ The lower wavelengths (green light) provided good contrast between the endothelial cells hepatic parenchymal cells and the cellular components of the blood The longer wavelengths (red light) accentuated endothelial cell membranes

The sphincters consisted of cells which were located at (1) the junctions of sinusoids with portal venules (inlet sphincters) (2) the junctions of sinusoids with central venules (sphincters) and (3) the junctions of intersinusoidal sinusoids with (sphincters of intersinusoidal sinusoids) (fig 3) At magnifications between 500 900 \times the nuclear regions of the cells were seen to enlarge frequently to bulge into the lumen thereby increasing its internal diameter (figs 4 5 16) The resulting reduction in internal diameter was accompanied by a thickening of the endothelial lining and a smaller reduction in the outside diameter of the sinusoid (figs 4 5) In many instances two or more cells opposed each other and were capable of reducing the lumen almost to a point either individually or mutually (fig 15) Sphincter cells in all locations were similar morphologically The sphincter cells of dilated sinusoids had flattened nuclei with single prominent nucleoli and occasional refractile granules in their attenuated cytoplasm The nuclei of sphincter cells which were bulging and occlud-

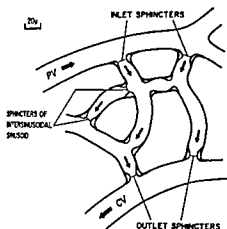


Fig 3 Semischematic diagram of the location of hepatic sphincters PV portal venule CV central venule

ing the sinusoid lumen were more rounded and their nucleoli more distinct (fig 14). Such cells were demonstrated to be components of the hepatic reticulo-endothelial system (V Kupffer cells) since they phagocytized particles of trypan blue or India ink that were injected intravascularly. Sphincter cells which were bulging and occluding the sinusoid lumen were still capable of removing foreign material from the blood stream. Furthermore Kupffer cells containing phagocytized material continued to act as sphincters as demonstrated by their continued response to catecholamines.

The remainder of the sinusoid appeared to be a smooth continuously lined tube whose internal diameter varied as changes in the internal diameter of its sphincters occurred. A decrease in the internal diameter and a thickening of the endothelium usually accompanied the contraction of its sphincter cells.

The sphincters regulated the flow of blood through the sinusoids by contracting independently or in unison. As a result the flow of blood through individual sinusoids groups of sinusoids or the sinusoids applying a whole lobule could be regulated independently of that in adjacent sinusoids groups of sinusoids or those of other lobules. Open sphincters allowed rapid or moderate rates of blood flow through the sinusoid with no deformation

of red or white blood cells. When the sphincters were closed partially blood flow was slow and red blood cells squeezed through the narrowed sinusoid lumen (figs 4B and 14). Often this flow was impeded by less plastic white blood cells which stuck in the incompletely closed sphincters (fig 15). Complete closure of a sphincter prevented the flow of all cellular elements of the blood past that point (fig 16).

Concomitant with constriction of the inlet and outlet sphincters there was usually a change in the internal diameter of the

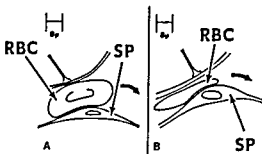


Fig 4 Outlet sphincters in the living frog liver. Both A and B are tracings of single 16 mm motion picture frames photographed from the video monitor.

- A A non-bulging outlet sphincter cell (SP) with red blood cell (RBC) passing through the sphincter.
- B A bulging outlet sphincter cell (SP) with red blood cell (RBC) being deformed as it passes through the sphincter.

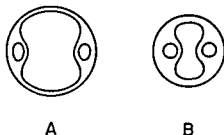


Fig 5 Diagrammatic representation of how sphincters constrict. A is a cross-section of two relaxed non-bulging sphincter cells. B is a cross-section of two contracted bulging sphincter cells. Note the prominent bulging of the nuclear region, the rounding of the nucleus and the thickening of the attenuated portion of the cytoplasm. This results in a large reduction of the internal diameter of the sinusoid compared with a somewhat smaller reduction in its outside diameter.

its inlet sphincter which received the arterial blood (figs 2, 11, 12) Such APAs appeared to be direct connections between hepatic arterioles and portal venules however, at low magnifications (100–150 \times) when white light quartz rod transillumination was used

The flow of arterial blood to the sinusoids was intermittent and lasted from a few seconds to several hours This was produced by arterioles, arterioportal anastomoses and arterio sinus twigs which were independently contractile and opened and closed with no definable rhythm

Arterial blood flow modified the flow in portal venules, sinusoids or both The various patterns of blood flow which were observed are illustrated in figures 2 11 and 12 When functional arterioportal anastomoses (APA's) were wide open, the arterial blood flow often reversed blood flow in the portal venule so that all sinusoids distal to the APA received only arterial blood (figs 2 11 12) If the APA was dilated partially a mixture of arterial and portal blood reached the distal sinusoids (fig 11) Closure of the inlet sphincter eliminated the flow of arterial blood in to the portal venule via the APA and resulted in the sinusoid being perfused with arterial blood Under these conditions the

APA functioned as an AST A sinusoid with an open inlet sphincter and an open AST was perfused with a mixture of arterial and portal venous blood (figs 2 11 12) With the inlet sphincter closed only arterial blood flowed through the sinusoid Arterial blood entering a sinusoid from an AST often was observed to flow into the portal venule through an open inlet sphincter especially if the outlet sphincter of that sinusoid was narrowed or closed and the sinusoid was filled with blood (figs 11 12) Under these conditions AST's of type 1 and type 2 often behaved functionally as APAs even though they terminated in sinusoids 20–30 μ away from a portal venule When blood flow in hepatic arterioles or in individual AST's and APAs ceased portal venous blood often was observed to flow into AST's and APAs but rarely into hepatic arterioles Closure of the inlet sphincters eliminated this inflow of portal venous blood into APAs and AST's

In fixed preparations the distribution of the hepatic arteriole and its branches was similar to that observed *in vivo* Often a muscular sphincter was served at the origins of the AST's from the hepatic arterioles and although muscle cells were seen occasionally in the more distal portion of these vessels none extended to the junction of the AST with the sinusoid

Sphincters of hepatic sinusoids

Good resolution of the sphincters of the hepatic sinusoids was obtained only with the modified compound binocular microscope and monochromatic light The resolution of these structures was at high magnifications (500–900 \times) wavelengths of green light 520 540 560 m μ and with wavelengths of light 600 and 620 m μ The lower wavelengths (green light) provided good contrast between the endothelial cells of hepatic parenchymal cells and the cellular components of the blood The wavelengths (red light) accentuated endothelial cell membranes

The sphincters consisted of cells which were located at (1) the junctions of sinusoids with portal venules (inlet sphincters), (2) the junctions of sinusoids with central venules (outlet sphincters) and (3) the junctions of intersinusoidal sinusoids with sinusoids (sphincters of intersinusoidal sinusoids (fig 3) At magnifications between 500 900 \times the nuclear regions of the sphincter cells were seen to enlarge frequently to bulge into the lumen thereby narrowing it (figs 4 5 16) The resulting reduction in internal diameter was accompanied by a thickening of the endothelial cells and a smaller reduction in the outside diameter of the sinusoid (figs 4 5) In many instances two or more endothelial cells opposed each other and were of reducing the lumen almost to occlusion either individually or mutually (fig 15)

Sphincter cells in all locations were similar morphologically The sphincter cells of dilated sinusoids had flattened nuclei with single prominent nucleoli and occasional refractile granules in their attenuated cytoplasm The nuclei of sphincter cells which were bulging and occluding

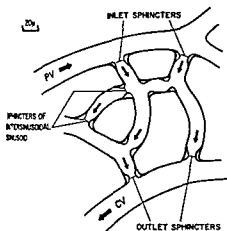


Fig. 3 Semischematic diagram of the location of hepatic sphincters PV portal venule CV central venule

ing the sinusoid lumen were more rounded and their nuclei more distinct (fig 14). Such cells were demonstrated to be components of the hepatic reticulo-endothelial system (V Kupffer cells) since they phagocytized particles of trypan blue or India ink that were injected intravascularly. Sphincter cells which were bulging and occluding the sinusoid lumen were still capable of removing foreign material from the blood stream. Furthermore Kupffer cells containing phagocytized material continued to act as sphincters as demonstrated by their continued response to catecholamines.

The remainder of the sinusoid appeared to be a smooth continuously lined tube whose internal diameter varied as changes in the internal diameter of its sphincters occurred. A decrease in the internal diameter and a thickening of the endothelium usually accompanied the contraction of its sphincter cells.

The sphincters regulated the flow of blood through the sinusoids by contracting independently or in unison. As a result the flow of blood through individual sinusoids, groups of sinusoids, or the sinusoids supplying a whole lobule could be regulated independently of that in adjacent sinusoids, groups of sinusoids or those of other lobules. Open sphincters allowed normal or moderate rates of blood flow through the sinusoid with no deformation

of red or white blood cells. When the sphincters were closed partially blood flow was slow and red blood cells squeezed through the narrowed sinusoid lumen (figs 4B and 14). Often this flow was impeded by less plastic white blood cells which stuck in the incompletely closed sphincters (fig 15). Complete closure of a sphincter prevented the flow of all cellular elements of the blood past that point (fig 16).

Concomitant with constriction of the inlet and outlet sphincters there was usually a change in the internal diameter of the

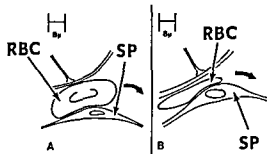


Fig. 4 Outlet sphincters in the living frog liver. Both A and B are tracings of single 16 mm motion picture frames photographed from the video monitor.

- A A non bulging outlet sphincter cell (SP) with red blood cell (RBC) passing through the sphincter.
- B A bulging outlet sphincter cell (SP) with red blood cell (RBC) being deformed as it passes through the sphincter.

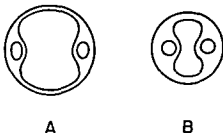


Fig. 5 Diagrammatic representation of how sphincters constrict. A is a cross-section of two relaxed non bulging sphincter cells. B is a cross section of two contracted bulging sphincter cells. Note the prominent bulging of the nuclear region, the rounding of the nucleus and the thickening of the attenuated portion of the cytoplasm. This results in a large reduction of the internal diameter of the sinusoid compared with a somewhat smaller reduction in its outside diameter.

remainder of the sinusoid lumen. Such a decrease in the internal diameter was noted when the inlet sphincter alone constricted but this decrease usually did not reduce the sinusoid lumen to zero. Sinusoids or segments of sinusoids which were devoid of blood cells appeared to be held open by the bulging nuclear regions of contracted sphincter cells located at the ends of intersinusoidal sinusoids. Sinusoids were observed occasionally, however, which contained no blood cells, had little lumen, and had a greatly reduced outside diameter. In such sinusoids no bulging endothelial cells were noted.

The sphincters were responsible for the storage of blood within sinusoids or segments of sinusoids and for the release or autotransfusion (Knisely et al, 48, Bloch 55) of this stored blood into the general circulation via the central venules, hepatic veins, inferior vena cava and right heart. Closure of the outlet sphincter alone caused the sinusoid to become distended with blood and with subsequent closure of the inlet sphincter this blood was isolated from the general circulation and stored. In addition blood could be stored in isolated segments of sinusoids by the independent action of the sphincters at the ends of intersinusoidal sinusoids. The blood stored in these intersinusoidal sinusoids could be released by the opening of their sphincters. An autotransfusion reaction occurred when the outlet sphincter of a sinusoid storing blood opened and a peristaltic wave of contraction along the sinusoid wall milked the sinusoid of its contained blood into the central venule. This reaction encompassed the many individual segments of a sinusoid and their respective sphincters.

In histologic preparations the nuclear region of endothelial cells lining the sinusoids often bulged into the lumen at the afferent and efferent ends of the sinusoid and at bifurcations of the anastomosing sinusoid network (ends of intersinusoidal sinusoids). Pairs of these cells often were wrapped around the sinusoid lumen much like a collar (fig 17). Bulging endothelial cells had oval vesicular nuclei usually with single prominent nucleoli. The cytoplasm was pale with a scant, dispersed basophilic granulation and occasionally

contained phagocytized particulate material. Non bulging endothelial cells had more compact, dense nuclei and nearly invisible cytoplasm. In sections stained with iron hematoxylin, structures suggestive of fibrillar contractile elements were observed occasionally in the cytoplasm of the cells lining the sinusoid.

Effect of glycogenolytic hormones, intermediates, and metabolites on the hepatic microvascular system

The hepatic microvascular system was affected significantly by glycogenolytic substances (glucagon, isopropyl norepinephrine, epinephrine, and norepinephrine), by adenine nucleotides (5 ATP, 5' ADP, cyclic 3', 5' AMP and 5' AMP) and by adenosine. The effectiveness of equimolar concentrations of the glycogenolytic substances in dilating intrahepatic blood vessels in decreasing order was glucagon > isopropyl norepinephrine > epinephrine > norepinephrine (fig 6). The effectiveness of equimolar concentrations of the adenine nucleotides and adenosine, in decreasing order was 5 ATP > 5' ADP > 5' AMP cyclic 3', 5' AMP and adenosine which were equivalent (fig 7). Other nucleotides or nucleotide derivatives, pyrophosphate, and phosphate were ineffective vasodilators (McCuskey 63b).

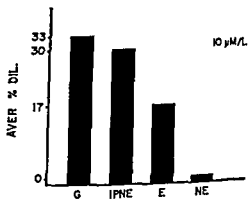


Fig 6 The effectiveness of equimolar concentrations of glycogenolytic substances in dilating intrahepatic blood vessels. AVER % DIL, average percentage of dilation of portal venules, hepatic arterioles, sinusoids, central venules and sphincters produced by glucagon (G), isopropyl norepinephrine (IPNE), epinephrine (E) and norepinephrine (NE).

¹² Average percentage increase in internal diameter of intrahepatic blood vessels obtained after the administration of the test substances.

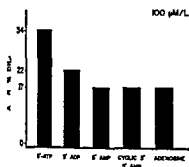


Fig. 7 The effectiveness of equimolar concentrations of adenine nucleotides and adenosine in causing intrahepatic blood vessels dilation. AVER. % is, average percentage of dilatation of portal venules, hepatic arterioles, sinusoids, central venules, and sphincters produced by adenosine-5-phosphate (5 ATP), adenosine-5-diphosphate (5 ADP), adenosine-5 monophosphate (5 AMP), adenosine-3,5-phosphate (cyclic-3,5 AMP) and adenosine.

Hepatic arterioles "APAs" and ASTs were opened quite often by glucagon, isopropyl norepinephrine and 5 ATP (tables 2 and 3). In addition these substances always caused dilatation of portal venules, sinusoids, sphincters and central venules with a corresponding increase in hepatic blood flow. Adenosine 5-diphosphate was slightly less effective than 5 ATP. Cyclic 3,5 AMP was a less effective vasodilator than glucagon, isopropyl norepinephrine, 5 ATP or 5 ADP. Cyclic 3,5 AMP was as effective as 5 AMP, adenosine or low concentrations of epinephrine.

The response to epinephrine was dose dependent. High concentrations (100 μ M/L) caused constriction of portal venules, hepatic arterioles, central venules and sphincters and a drastic reduction in blood flow through the sinusoids with a concomitant "autotransfusion" reaction. The duration of this vasoconstriction and reduced blood flow was 10 to 30 minutes. (Both the linear velocity and volume of blood flow were reduced.) Low concentrations of epinephrine (10 μ M/L) however produced a biphasic response characterized by a brief phase of vasoconstriction (2 to 5 minutes) followed by a longer phase of vasodilation (10 to 30 minutes) with increased blood flow through the hepatic sinusoids. In contrast norepinephrine generally produced effects similar to

those observed with high concentrations of epinephrine but did not produce the biphasic response seen with low concentrations of epinephrine. The vasoconstrictive effects of norepinephrine and high concentrations of epinephrine could be shortened by subsequent topical or intraportal administration of low concentrations of potassium as the chloride or sulfate salt, isopropyl norepinephrine, the adenine nucleotides and adenosine. In contrast glucagon was effective only when applied topically to the liver surface.

When potassium and sodium salts were parenterally injected or applied topically the following responses were observed. Low concentrations of potassium (0.1 mEq/L) as the chloride (KCl) or sulfate (K_2SO_4) salt were dilators of portal venules, sinusoids, sphincters and central venules. The hepatic arteriolar system was not affected significantly by these potassium salts. Higher concentrations (10 mEq/L) of potassium salts however were vasoconstrictors of all vessels of the hepatic microvascular system. No appreciable effect was observed when sodium as the chloride or sulfate salt was administered either topically or parenterally.

TABLE 2

Effect of glycogenolytic substances on the hepatic arteriolar system¹

Drug	N	H.A.
		%
Glucagon	36	33
Isopropyl norepinephrine	33	30
Epinephrine	20	14
Norepinephrine	20	0
Control	244	10

¹ N, number of experiments. H.A., percent go of N in which hepatic arterioles opened following the administration of the drug.

TABLE 3

Effect of adenine nucleotides and adenosine on the hepatic arteriolar system¹

Drug	N	H.A.
		%
5 ATP	80	44
5 ADP	10	25
5 AMP	10	18
Cyclic-3,5 AMP	15	16
Adenosine	20	18
Control	244	10

N., number of experiments. H.A., percent go of N in which hepatic arterioles opened following the administration of the drug.

Topical or parenteral beta d glucose (1%, 5%, and 10%) produced insignificant changes in intrahepatic blood vessel diameter or blood flow. The highest concentration (50%) however reduced blood flow through the sinusoids and increased whole blood storage with little change in the internal diameters of portal and central venules.

Dynamic blood pressures in intrahepatic blood vessels

Dynamic blood pressures from intrahepatic vessels were recorded only in frogs. These pressures were recorded from portal and central venules whose diameter varied from 45 to 90 μ and the duration of these recordings was 10 to 30 minutes. The range of blood pressures in these venules was considerable. In 11 portal venules the pressures varied from 16/0 to 108/0 mm Hg while in a similar number of central venules the pressures varied from 19/0 to 103/0 mm Hg. There was no correlation between their internal diameter and their dynamic blood pressures (table 4). However in three experiments the differences in dynamic blood pressures between a portal and central venule of the same lobule were secured. The average pressure in these portal venules was 94/0 mm Hg while the average pressure in the central venules was 50/0 mm Hg indicating an average pressure drop of 38 mm Hg across the sinusoid bed in these animals (table 5).¹³

DISCUSSION

The results of this investigation have been fruitful in further elucidating (1) the terminal distribution of hepatic arterioles (2) the dynamic cytology of hepatic sphincters, and (3) the local and hormonal factors that act on these structures to regulate the flow of arterial and portal blood through the sinusoids. The resultant concept of the dynamic anatomic and physiologic relationship of the hepatic microvascular system with the functional unit of the liver modified after Knisely et al (48) is illustrated in figure 8 and a theory for the metabolic regulation of blood flow through this unit is presented in figure 9. A discussion of these figures

follows based on the results of this investigation.

Examination of the hepatic arteriole in the living liver and those in fixed material generally reconfirmed the observations of Knisely et al (48), Irwin and MacDonald (53) and Bloch (55) that the mixing of arterial and portal blood occurred at or near the periphery of the lobule either in portal venules via arterioportal anastomoses or in sinusoids via arterio sinus twigs or both. In this study however the histology and distribution of these structures has been clarified further.

Arterio sinus twigs (ASTs) terminated in sinusoids near the periphery of the lobule in agreement with Kiernan (1833), Cameron and Mayes (30), Olds and Stafford (30), Wakim and Mann (42), Knisely et al (48), Senevirante (49), Andrews et al (49), Elias (49), Irwin

TABLE 4
Dynamic blood pressures in intrahepatic vessels of the frog¹

Portal venules		Central venules	
P	ID	P	ID
16/0	63	19/0	88
23/0	72	23/0	63
23/0	50	28/0	81
28/0	90	33/0	63
52/0	45	47/0	90
61/0	72	47/0	50
66/0	60	56/0	63
75/0	45	56/0	45
82/0	45	66/0	50
94/0	40	75/0	45
108/0	50	103/0	54

¹ P = blood pressure measured in millimeters of mercury ID = internal diameter measured in micra

TABLE 5
Dynamic blood pressures in portal and central venules of the same lobule¹

Portal venules		Central venules	
P	ID	P	ID
94/0	40	66/0	50
82/0	45	47/0	90
109/0	50	56/0	45
94/0	45	Average	56/0 62

¹ P = blood pressure measured in millimeters of mercury ID = internal diameter measured in micra

¹³ The data on the effect of glycogenolytic substances intermediaries and metabolites on intrahepatic blood pressures were insufficient to report quantitatively

HEPATIC LOBULE

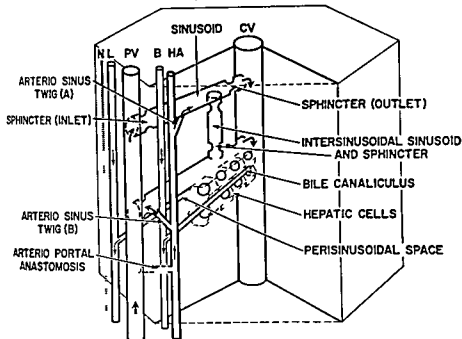


Fig 8 Schematic drawing of the functional unit of the liver and its relationship with the hepatic lobule (modified after Knisely et al 48) The functional unit of the liver consists of the sinusoid and its immediately adjacent hepatic tissue with their afferent and efferent vascular biliary lymphatic and nervous connections The anatomic components of this functional unit are (1) the sinusoid wall composed of reticulo-endothelial cells some of which function as sphincter cells and connective tissue elements (2) the hepatic cells among which are located the bile canaliculi (3) the perisinusoidal space and (4) nerves Many functional units form an hepatic lobule PV portal venule HA hepatic arteriole N nerves L lymphatic B bile duct CV central venule

and MacDonald (53) Bloch (55) Riedel and Moravec (59) Lee et al (60) and Tajiri (60) However no twigs terminated in sinusoids near the central venule as described by Wakim and Mann (41) Senevirante (49) Elias (49) Elias and Petty (53) and Lee et al (60) and their existence is doubted seriously The translobular capillaries observed by these investigators may have been sinusoids with closed inlet sphincters which were conducting only arterial blood Such vessels fill with India ink or latex injected into the hepatic artery and appear as continuous vessels originating from hepatic arterioles

In this study the presence of functional arterio-portal anastomoses ("APA's") in the periportal space was established These were short arterio-sinus twigs which

were directed toward portal venules and terminated in sinusoids near their origins (from portal venules) forming part of the peribiliary plexus Although arterio-portal anastomoses similar to those reported by Wakim and Mann (42) Knisely et al (48) Senevirante (49) Irwin and MacDonald (53) and Bloch (55) were seen at low magnifications using white light transillumination such direct connections were not confirmed at higher magnifications when monochromatic light and television microscopy were used nor were they seen in histologic preparations While direct connections between the hepatic arteriole and the portal venule may exist they probably are rare

The distribution of arterial blood to the periphery of the lobule and the control of arterial blood flow through each AST and

'APA by independently contractile pre capillary sphincters permits critical control of the amount of arterial blood flowing to each functional unit or each lobule. However, while the precapillary sphincters (composed of smooth muscle cells) regulate the flow of arterial blood to the sinusoids, endothelial sphincters in the sinusoids control the volume and rate of arterial and portal blood flow through each sinusoid. Thus, at any given moment each sinusoid is capable of conducting only portal blood, only arterial blood or any mixture of the two.

In this study the sphincters that regulate blood flow through the sinusoids were found at the afferent (inlet sphincter) and efferent (outlet sphincter) orifices of the sinusoids and in addition at the ends of intersinusoidal sinusoids (sphincters of intersinusoidal sinusoids). The endothelial cells forming the inlet and outlet sphincters were synonymous with the afferent and efferent sphincter mechanisms described by Knisely et al (48), Irwin and MacDonald (53), Bloch (55) and Knisely et al (57). These sphincter cells were present in all observed species and failure to observe them by others (Senevirante 49, Maegraith 58, Kratochvil et al, 59, Brauer, 63) is attributed to poor resolution due to the use of low magnifications or poor definition due to excessive movements of the liver. The demonstration of a significant difference of blood pressure between a portal venule and central venule of the same lobule of the frog (table 5) and in the rat by Nakata, Leong and Brauer (60) is compatible not only with the presence of these sphincters but also with the concept that these sphincters are the primary site for the regulation of blood flow through the sinusoids (especially since there is little difference in blood pressure between mesenteric venules and portal venules (McCuskey, 63b)).

All sphincters of hepatic sinusoids were similar morphologically and functionally. All were contractile endothelial cells which by bulging were capable of reducing the sinusoid lumen to zero or nearly zero and had the characteristics of the "gatekeeper" cells seen at bifurcations of alveolar capillaries in the living lung (Bloch and McCuskey, 64). That

endothelial cells might bulge into the sinusoid lumen and control blood flow has been suggested previously by Ruttner Vogel (60) in their electron microscopic studies, but the present investigation is the first demonstration of their structure and function in the living liver at high magnifications.

The mechanism of endothelial contraction however, is not clear but it may be accomplished by contractile fibrils structurally similar to myo- or fibrils. In this study structures suggestive of fibrils were seen occasionally and these were similar to those reported in the outlet sphincters of cevitic acid treated guinea pigs (Warner 40) and in the reticulo-endothelial cells of the spleen (Leblond et al, 60). It should be noted however that endothelial swelling might be due to a change in intracellular osmolarity causing the cell to imbibe extracellular water.

The sphincters are extremely to vasoactive substances circulating in the blood or released locally and in response to these substances, rapidly modify the volume and rate of blood flow through the sinusoids. While portal venules, hepatic arterioles and central venules also are affected by these substances and can reduce or increase the amount of blood delivered to or removed from the sinusoids, the sphincters are the structures responsible for the regulation of blood flow through the sinusoids.

The local and hormonal regulation of blood flow through the sinusoids is complex and understood poorly. Numerous physiological and biochemical data suggest that glycogenolytic substances, intermediaries and metabolites may play a role in the regulation of hepatic blood flow. Thus the regulation of blood flow through the sinusoids may be dependent upon glycogenolytic events in the hepatic cells. Investigations of the effect of catecholamines and glucagon (potent glycogenolytic substances) on the hepatic blood vascular system have shown that these vessels are affected significantly by the administration of these substances (Bloch 40, Wakim 44, Senevirante 49, Daniel and Prichard 51, Andrews et al 55, 56, Green et al, 59, Shoemaker et al 59).

'APA by independently contractile pre capillary sphincters permits critical control of the amount of arterial blood flowing to each functional unit or each lobule. However while the precapillary sphincters (composed of smooth muscle cells) regulate the flow of arterial blood to the sinusoids endothelial sphincters in the sinusoids control the volume and rate of arterial and portal blood flow through each sinusoid. Thus, at any given moment each sinusoid is capable of conducting only portal blood, only arterial blood or any mixture of the two.

In this study the sphincters that regulated blood flow through the sinusoids were found at the afferent (inlet sphincter) and efferent (outlet sphincter) orifices of the sinusoids and in addition at the ends of intersinusoidal sinusoids (sphincters of intersinusoidal sinusoids). The endothelial cells forming the inlet and outlet sphincters were synonymous with the afferent and efferent sphincter mechanisms described by Knisely et al (48) Irwin and MacDonald (53), Bloch (55), and Knisely et al (57). These sphincter cells were present in all observed species and failure to observe them by others (Senevirante, 49, Maegraith '58 Kratochvel et al, 59, Brauer, 63) is attributed to poor resolution due to the use of low magnifications or poor definition due to excessive movements of the liver. The demonstration of a significant difference of blood pressure between a portal venule and central venule of the same lobule of the frog (table 5) and in the rat by Nakata Leong and Brauer (60) is compatible not only with the presence of these sphincters but also with the concept that these sphincters are the primary site for the regulation of blood flow through the sinusoids (especially since there is little difference in blood pressure between mesenteric venules and portal venules (McCuskey '63b)).

All sphincters of hepatic sinusoids were similar morphologically and functionally. All were contractile endothelial cells which by bulging were capable of reducing the sinusoid lumen to zero or nearly zero and had the characteristics of the "gatekeeper" cells seen at bifurcations of alveolar capillaries in the living lung (Bloch and McCuskey, 64). That

endothelial cells might bulge into the sinusoid lumen and control blood flow has been suggested previously by Ruitner and Vogel (60) in their electron microscope studies, but the present investigator: the first demonstration of their structure and function in the living liver at high magnifications.

The mechanism of endothelial contraction, however is not clear but it may be accomplished by contractile intracellular fibrils structurally similar to myofibrils. In this study structures suggestive of fibrils were seen occasionally and they were similar to those reported in the outlet sphincters of cevitic acid treated guinea pigs (Warner, 40) and in reticulo-endothelial cells of the spleen (Leblond et al, 60). It should be noted, however, that endothelial swelling might be due to a change in intracellular osmolarity causing the cell to imbibe extracellular water.

The sphincters are extremely sensitive to vasoactive substances circulating in the blood or released locally and in response to these substances, rapidly modify the volume and rate of blood flow through the sinusoids. While portal venules, hepatic arterioles and central venules also are affected by these substances and can induce or increase the amount of blood delivered to or removed from the sinusoids, the sphincters are the structures responsible for the regulation of blood flow through the sinusoids.

The local and hormonal regulation of blood flow through the sinusoids is complex and understood poorly. Numerous physiological and biochemical data suggest that glycogenolytic substances, intermediaries and metabolites may play a role in the regulation of hepatic blood flow. Thus the regulation of blood flow through the sinusoids may be dependent upon glycogenolytic events in the hepatic cells. Investigations of the effect of catecholamines and glucagon (potent glycogenolytic substances) on the hepatic blood vascular system have shown that these vessels are affected significantly by the administration of these substances (Bloch 40 Wakim 44 Senevirante 49 Danforth and Prichard 51 Andrews et al 55 56 Green et al 59 Shoemaker et al 59).

U) In contrast frequent closure of these vessels was observed when intrahepatic oxygen (100%) was administered. It is obvious however that the hypothesis that blood flow through the sinusoids may be auto-regulated by oxygen lack requires further investigation under more controlled conditions (Ross et al 6) Currier et al 64) Rapid glycogenolysis is known to occur during hypoxia but whether the dilatation of intrahepatic blood vessels and especially hepatic arterioles during hepatic cellular hypoxia is mediated chemically by adenosine and/or potassium remains to be proven since the present evidence is circumstantial. Obviously adenosine needs to be identified in the effluent blood of the liver during hypoxia, glycogenolysis and periods of increased hepatic metabolic activity. In addition the role of potassium needs to be evaluated further since it did not significantly affect the hepatic arteriolar system which suggests that its role may not be important or may be secondary to that of adenosine.

ACKNOWLEDGMENTS

The author wishes to express his gratitude to Dr Edward H Bloch for his guidance and criticism during the course of this study and to Miss Joyce Mencin Mr Willard Holton Miss Lynn Yost and Miss Margaret Moonan for their technical assistance.

LITERATURE CITED

Adams W H H R Hecker B G Maegraith 1956 The action of adrenaline noradrenaline acetylcholine and histamine on the perfused liver of the monkey cat and rabbit *J Physiol* 132 509-521
Adams W H H R Hecker B G Maegraith and H D Ritchie 1955 The action of adrenaline noradrenaline acetylcholine and other substances on the blood vessels of the perfused canine liver *J Physiol* 128 413-424
Adams W H H B G Maegraith C E M Wren 1949 Studies on liver circulation. II. The microanatomy of the hepatic circulation *Ann Trop Med Parasit* 43 229-237
Mencin E S G T Evans B E Hallaway C Phillips and E F Freier 1961 Myocardial creatine phosphate and nucleotides in anoxic cardiac arrest and recovery *Amer J Physiol* 211 687-693

Berne R M 1963 Cardiac nucleotides in hypoxia Possible role in regulation of coronary blood flow *Amer J Physiol* 204 317-322
—— 1964a Regulation of coronary blood flow *Physiol Rev* 44 1-29
—— 1964b Personal communication
Bevan J A and J V Osher 1964 Effect of potassium on the resting length of vascular smooth muscle of the rabbit aorta and its response to 1 norepinephrine *Circulation Res.* 13 346-351
Blackman J R P J Klopfer and A Recourt 1960 Microangiographic investigation of the action of vasoconstrictor drugs on the liver vessels in rats In *X Ray Microscopy and X Ray Microanalysis* A Engstrom and V Cosslett (eds) Proc 2nd Internat Sym Stockholm Elsevier Publish Co Amsterdam 1960 pp 226-232
Bloch E H 1940 Some actions of adrenaline chloride and acetyl beta methyl choline chloride on finer vessels of living frog liver lobules *Anat Rec* 76 (Suppl) 7
—— 1955 The in vivo microscopic vascular anatomy and physiology of the liver as determined with the quartz rod method of transillumination *Angiology* 6 340-349
—— 1956 Microscopic observations of the circulating blood in the bulbar conjunctiva in man in health and disease *Ergebnisse d Anatomie u Entwicklungsgeschichte* 35 1-98
—— 1962 A quantitative study of hemodynamics in the living microvascular system *Am J Anat* 110 125-154
—— 1963 A method for studying the dynamics of transcapillary transfer quantitatively at the microscopic level in situ in living organs *Angiology* 14 97-106
—— 1964 The cytology of organs in living animals *Anat Rec* 148 423
—— 1965 The dynamic histology of organs in situ II The lung liver and kidney *Anat Rec* 151 498
Bloch E H and S I Coyas 1963 The transit of large molecules across individual endothelial cells analyzed in situ with absorption scanning microspectrophotometry *Anat Rec* 145 374
Bloch E H and R S McCuskey 1964 Unpublished observations
—— 1966 Sequential quantitative measurements in microsecond of living tissue *Anat. Rec* 154 507-508
Bloch E H R S McCuskey G Tucker and J Mencin 1961 The effect of cellular aggregation on pressure-flow relationships in the microvascular system *Angiology* 12 473-476
Bohr D F 1964 Electrolytes and smooth muscle contraction *Pharm Rev* 16 85-111
Brauer R W 1963 Liver circulation and function *Physiol Rev* 43 115-213
Butcher R W and E W Sutherland 1962 Adenosine-3' 5' phosphate in biological materials I Purification and properties of cyclic

Of interest is the recent identification of adenosine in the effluent of the coronary sinus in the isolated hypoxic heart (Berne 64b)

62) In brief the subsequent accumulation of cyclic 3', 5-AMP activates a kinase to convert inactive phosphorylase to active phosphorylase resulting in the breakdown of glycogen to glucose in the hepatic cell. Most of this glucose is released into the blood stream and can raise the level of blood sugar in the hepatic vein several hundred per cent (Ellis, 56 Craig, 58 Shoemaker et al, 59 Craig and Honig 63). Although glucose is released in large amounts it does not produce any significant change in the blood flow and thus does not appear to play a role in regulating blood flow through the hepatic sinusoids.

The cyclic 3', 5' AMP produced during glycogenolysis does not accumulate in large amounts since it is degraded continuously to 5' AMP by phosphodiesterase (Sutherland and Rall, 60 Sutherland, 62, Butcher and Sutherland '62). Since the liver contains small concentrations of adenylic acid deaminase dephosphorylation of 5 AMP quite likely precedes deamination with the result that adenosine and not inosine is produced (Conway and Cooke 39). Adenosine and adenine nucleotides are potent dilators of intrahepatic vessels and sphincters (fig 7 table 3) as well as other vessels (Drury 36 Folkow 49 Winbury et al, 53 Duff et al 54 Furchgott 55, Wolf and Berne 56 McCuskey '63a '65a,b) and therefore their role in the local regulation of blood flow through the sinusoids must be considered. Of interest is the recent proposal of Berne (63 '64a) for the regulation of coronary blood flow. Berne postulates that adenosine which is able to penetrate the cell membrane diffuses out of hypoxic myocardial cells and produces arteriolar dilatation. This adenosine may arise from the intracellular breakdown of adenine nucleotides during hypoxia (Michal et al 59 Benson et al, 61) as a result of low blood pO_2 or an increase in myocardial metabolism. A similar breakdown of adenine nucleotides has been observed in the hypoxic liver (Kayne et al '64). Although the adenine nucleotides (5 ATP 5 ADP and 5 AMP) are potent vasodilators they are thought not to be involved since these charged nucleotides do not penetrate cell membranes (Lowy et al 52 58 Wil-

liams and Lepage, 58, Whittam, '6 Jacob and Berne 60 '61). That purinergic dilators than 5 AMP cyclic 3', 5 AMP = adenosine (fig 7, table 3) is presumed to be due to the more rapid inactivation of adenosine and AMP in the blood (Conway and Cooke 39).

Concomitant with glycogenolysis a large efflux of potassium ion is observed in the hepatic venous blood prior to the elevation of the blood glucose concentration. The efflux of potassium is large enough to double or even triple the normal serum potassium levels in hepatic venous blood (Ellis 56 Shoemaker and Funder 60 Ellis and Beckett '63, Craig and Honig 63 Funder et al 64). Potassium is a potent vasodilator of intrahepatic vessels and sphincters and is released along with glucose in large quantities from the hypoxic liver (Ellis, 56 Cahill et al '57 Ellis and Beckett 63). This suggests that potassium might be an important factor in the regulation of blood flow through the sinusoids especially since potassium also has been demonstrated to cause vasodilation in other vessels (Dawes 41 Scott et al 59 Waugh 62 Frohlich et al, 62) and a number of studies suggest that the muscular tone of blood vessels and their sensitivity to neural and hormonal stimuli are determined partly by local changes in the concentrations of cations (Jang 40 Furchgott 55 Emanuel et al 59 Scott et al 61 Frohlich et al 62 Hanenson 62 Bevan and Osher 64 Bohr 64).

Taken together the available data suggest that the regulation of blood flow through the sinusoids of anesthetized animals depends to a large extent upon the metabolic demands for oxygen by the hepatic parenchyma. Hepatic cellular hypoxia resulting from increased metabolism or from lowered sinusoid blood pO_2 causes a concomitant opening of hepatic arterioles which increases the oxygenation of the blood perfusing the sinusoids. Gross physiological studies of the changes in hepatic arterial and portal blood flow following the administration of glycogenolytic substances and during hypoxia indicate similar increases in arterial blood flow (Grabner et al 58, Cohn and Kountz 63 Fischer 63 Craig and Honig

- Le Y B H Elias and I Davidsohn 1960 Vascular pattern in the liver of the mouse *Proc. Animal Care Panel* 10 25-32
- Low B A J Davoll and G B Brown 1952 The utilization of purine nucleosides for nucleic acid synthesis in the rat *J Biol Chem* 197 591-600
- Low B A E R Jaffe G A Vanderhoff L Cook and I M London 1958 The metabolism of purine nucleosides by the human erythrocyte *in vitro* *J Biol Chem* 230 409-413
- Marguth B G 1958 Sinusoids and sinusoidal flow in liver function *R W Brauer* (ed.) *Amer Inst Biol Sci Wash D C* pp 130-139
- Muskey R S 1963a Effect of ATP on the microscopic arterial system in the living liver *Anat. Rec* 14 259
- 1963b Unpublished results
- 1963a The effect of glycogenolytic substances on the hepatic microvascular system (Film) Thirteenth Microcirculatory Conference Atlantic City April 9 1965
- 1963b An *in vivo* and histologic study of the distribution of the hepatic arteriole *Anat. Rec* 151 384
- Mohal G S Naegle W H Dauforth F B Ballard and R J Bing 1959 Metabolic changes in heart muscle during anoxia *Amer J Physiol* 197 1147-1150
- Mund F Y M Chi T W Rall and E W Sutherland 1962 Adenyl cyclase III The effect of catechol amines and choline esters on the formation of adenosine-3' 5' phosphate by preparations from cardiac muscle and liver *J Biol Chem* 237 1233-1238
- Nakata K C F Leong and R W Brauer 1960 Direct measurement of blood pressures in minute vessels of the liver *Amer J Physiol* 199 1181-1188
- Old J K and E S Stafford 1930 On the manner of anastomoses of the hepatic and portal circulations *Johns Hopkins Hosp Bull* 4 16-185
- Li-paport M B E H Bloch and J W Irwin 1959 A manometer for measuring dynamic pressures in the microvascular system *J Appl Physiol* 14 651-655
- Medel V J and R Moravec 1959 Das System der Pfortader und der Leberarterie in der Leber *Arch Anat Anz* 107 99-110
- Low J M H M Falcchid J Weldy and A C G non 1962 Autoregulation of blood flow by oxygen lack *Amer J Physiol* 202 21-24
- Ermer J and M Vogel 1960 Quoted by Y B Lee et al. as a personal communication *Proc Animal Care Panel* 10 25-32
- Seitz D Emanuel and F Haddy 1959 Effect of potassium on renal vascular resistance and urine flow rate *Amer J Physiol* 197 305-313
- Scott J E Frohlich R Hardin and F Haddy 1961 Na⁺ K⁺ Ca⁺⁺ and Mg⁺⁺ action on coronary vascular resistance in the dog heart *Amer J Physiol* 201 1095-1100
- Senevirante R D 1949 Physiological and pathological responses in blood vessels of liver *Quart J Exp Physiol* 35 77-110
- Shoemaker W C and A G Finder 1961 Relation of potassium and glucose release from the liver in the unanesthetized dog *Proc Soc Exp Biol Med* 108 248-252
- Shoemaker W C L N Turk III and F D Moore 1961 Hepatic vascular response to epinephrine *Amer J Physiol* 201 58-62
- Shoemaker W C T B Van Itallie and W F Walker 1959 Measurement of hepatic glucose output and hepatic blood flow in response to glucagon *Amer J Physiol* 196 315-318
- Sutherland E W 1962 The biological role of adenosine 3' 5' phosphate *Harvey Lectures* 1961-62 Academic Press New York pp 17-33
- Sutherland E W and T W Rall 1960 The relation of adenosine 3' 5' phosphate and phosphorylase to the actions of catechol amines and other hormones *Pharm Rev* 12 265-299
- Tajiri S 1960 The terminal distribution of the hepatic artery *Acta Med Okayama* 14 215-225
- Wakim K G 1944 The effect of certain substances on the intrahepatic circulation of blood in the intact animal *Amer Heart J* 27 289-300
- Wakim K G and F C Mann 1942 The intrahepatic circulation of blood *Anat Rec* 82 233-253
- Warner L 1940 Morphological changes in liver and spleen following intraperitoneal injection of cevitic acid *Anat Rec* 76 (Suppl.) 57
- Waugh W 1962 Role of calcium in contractile excitation of vascular smooth muscle by epinephrine and potassium *Circulation Res* 11 927-940
- Whittam R 1960 The high permeability of human red cells to adenosine and hypoxanthine and their ribosides *J Physiol* 154 614-623
- Williams A M and G A Lepage 1958 Purine metabolism in mouse ascites tumor cells II *In vitro* incorporation of preformed purines into nucleotides and polynucleotides *Cancer Res* 18 548-553
- Winbury M M D H Papierski M L Hemmer and W E Hambourger 1953 Coronary dilatation action of the adenine ATP series *J Pharmacol* 109 255-260
- Wolf M M and R M Berne 1956 Coronary vasodilator properties of purine and pyrimidine derivatives *Circulation Res* 4 343-348

- 3, 5 nucleotide phosphodiesterase and use of this enzyme to characterize adenosine-3, 5 phosphate in human urine *J Biol Chem* 237 1244-1250
- Cahill G F Jr J Ashmore S Zottu and A B Hastings 1957 Studies on carbohydrate metabolism in rat liver slices *J Biol Chem* 224 237-250
- Cameron G R and B T Mayes 1930 Ligation of the hepatic artery *J Path Bact*, 332 799-831
- Carrier O Jr J R Walker and A C Guyton 1964 Role of oxygen in autoregulation of blood flow in isolated vessels *Amer J Physiol* 206 951-954
- Cohn R and S Kountz 1963 Factors in influencing control of arterial circulation in the liver of the dog *Amer J Physiol* 205 1260-1264
- Conway E J and R Cooke 1939 The deaminases of adenosine and adenylic acid in blood and tissue *Biochem J* 33 479-492
- Craig A B Jr 1958 Observations on epinephrine and glucagon induced glycogenolysis and potassium loss in the isolated perfused frog liver *Amer J Physiol* 193 425-430
- Craig A B and C R Honig 1963 Hepatic metabolic and vascular responses to epinephrine: a unifying hypothesis *Amer J Physiol* 205 1132-1138
- Daniel P M and M M L Prichard 1951 Effects of stimulation of the hepatic nerves and of adrenaline upon the circulation of the portal venous blood within the liver *J Physiol* 114 538-548
- Dawes G S 1941 The vaso-dilator action of potassium *J Physiol* 99 224-238
- Drury A N 1936 The physiological activity of nucleic acid and its derivatives *Physiol Rev* 16 292-325
- Duff F G C Patterson and J T Sheppard 1954 A quantitative study of the response to adenosine triphosphate of the blood vessels of the human hand and forearm *J Physiol* 125 581-589
- Elias H 1949 A re-examination of the structure of the mammalian liver II The hepatic lobule and its relation to the vascular and biliary systems *Am J Anat* 85 379-456
- Elias H and D Petty 1953 The terminal distribution of the hepatic artery *Anat Rec* 116 9-17
- Ellis S 1956 The metabolic effects of epinephrine and related amines *Pharm Rev* 8 485-562
- Ellis S and S B Beckett 1963 Mechanisms of the potassium mobilizing action of epinephrine and glucagon *J Pharm Exp Therap* 142 318-326
- Emanuel D J Scott and F Haddy 1959 Effect of potassium upon small and large blood vessels of the dog forelimb *Amer J Physiol* 197 637-642
- Flinder A G T Boyne and W C Shoemaker 1964 Relationship of hepatic potassium efflux to phosphorylase activation induced by glucagon *Amer J Physiol* 206 738-742
- Fischer A 1963 Dynamics of the circulation in the liver *In The Liver* Vol I C Roulet (ed) Academic Press New York pp
- Folkow B 1949 The vasodilator action of enosine triphosphate *Acta Physiol Scand*, 4 311-316
- Froehlich E J Scott and F Haddy 1962 of cations on resistance and responsiveness of renal and forelimb vascular beds *Amer J Physiol* 203 583-587
- Furchgott R F 1955 Pharmacology of lar smooth muscle *Pharm Rev* 7 183-263
- Grabner G F Kalndi P Kohn and A N mayer 1958 Das Verhalten der blutung während Sauer-Stoffman Z Kreisforsch 47 798
- Green H D L S Hall J Sexton and C P 1959 Autonomic vasomotor responses in canine hepatic arterial and venous beds *J Physiol* 196 196-202
- Hanenson I B 1962 Effects of electrical and hormones on contraction of arterial smooth muscle *Circulation* 26 727
- Humason G L 1962 *Animal Tissue Technique* W H Freeman and Company Francisco 468 pp
- Irwin J W and J MacDonald III 1953 microscopic observations of the intrahepatic circulation of living guinea pigs *Anat Rec* 111 1-15
- Jacob M I and R M Berne 1960 olism of purine derivatives by the isolated heart *Amer J Physiol* 198 322-326
- 1961 Metabolism of adenosine by isolated anoxic cat heart *Proc Soc Exptl Med* 107 738-739
- Jang C 1940 Ions and adrenergic sion in the rabbit's ear *J Physiol* 99 126
- Kayne H L N Taylor and N R Alpert Regulation of oxygen consumption in rat slices *Amer J Physiol* 206 1091-1094
- Kiernan F 1833 The anatomy and of the liver *Trans Roy Soc London* 711-770
- Knisely M H 1936 A method of living structure for microscopic study *Rec* 64 499-524
- Knisely M H E H Bloch and L Warner Selective phagocytosis I Microscopic tions concerning the regulation of the flow through the liver and other organs and the mechanism and rate of phagocytosis of particles from the blood *Kgl Danske skab Selskab Biol Skrifter* 4 1-93
- Knisely M H F Harding and H 1957 Hepatic sphincters *Science* 125 1026
- Kratohvil V M J Riedel and R 1959 Der Subterminale und terminale schnitt der Pfortader und Leberarterie in Leber des Frosches und einige Bemerk zur Regulation des Blutdurchflusses durch sinusoiden Kapillaren der Leber *Anat* 106 265-270
- Leblond C P H Puchter and Y 1960 Structures corresponding to bars and terminal web in many types of Nature 186 764-768

- Y B H Elias and I Davidsohn 1960 Vascular pattern in the liver of the mouse *Proc Animal Care Panel* 10 25-32
- Y B H Elias and G B Brown 1952 The utilization of purine nucleosides for nucleic acid synthesis in the rat *J Biol Chem* 197 591-600
- Y B H Elias, R Jaffe, G A Vanderhoff, L Crook and I M London 1958 The metabolism of purine nucleosides by the human erythrocyte *in vitro* *J Biol Chem* 230 409-413
- Grath B G 1958 Sinusoids and sinusoidal flow. In *Liver Function* R W Brauer (ed) Amer Inst Biol Sci Wash D C pp 133-139
- Cuskey R S 1963a Effect of ATP on the microscopic arterial system in the living liver *Anat Rec* 145 2-9
- 1963b Unpublished results
- 1965a The effect of glycogenolytic substances on the hepatic microvascular system (Film) Thirteenth Microcirculatory Conference Atlantic City April 9 1965
- 1965b An *in vivo* and histologic study of the distribution of the hepatic arteriole *Anat Rec* 151 384
- Chal, G S Naegle, W H Dauforth, F B Ballard and R J Bing 1959 Metabolic changes in heart muscle during anoxia *Amer J Physiol* 197 1147-1150
- Urad F Y M Chu, T W Rall and E W Sutherland 1962 Adenyl cyclase III. The effect of catechol amines and choline esters on the formation of adenosine 3, 5 phosphate by preparations from cardiac muscle and liver *J Biol Chem* 237 1233-1238
- Ikata K, C F Leong and R W Brauer 1960 Direct measurement of blood pressures in minute vessels of the liver *Amer J Physiol* 199 1181-1188
- di J K and E S Stafford 1930 On the manner of anastomoses of the hepatic and portal circulations *Johns Hopkins Hosp Bull* 4 16-185
- Report M, B E H Bloch and J W Irwin 1959 A manometer for measuring dynamic pressures in the microvascular system *J Appl Physiol* 14 651-655
- Edel, J J and R. Moravec 1959 Das System der Pfortader und der Leberarterie in der Leber der Ratte *Anat Anz* 107 99-110
- as, J M H, V Fairchild, J Weldy and A C Guyton 196 Autoregulation of blood flow by vertebrate lack. *Amer J Physiol* 202 21-24
- and M Vogel 1960 Quoted by Y B Lee et al as a personal communication *Proc. Animal Care Panel* 10 25-32
- et, J D Emanuel and F Haddy 1959 Effect of potassium on renal vascular resistance and urine flow rate *Amer J Physiol* 197 305-308
- Scott J E, Frohlich R, Hardin and F Haddy 1961 Na^+ , K^+ , Ca^{++} and Mg^{++} action on coronary vascular resistance in the dog heart *Amer J Physiol* 201 1095-1100
- Senevirante R D 1949 Physiological and pathological responses in blood vessels of liver *Quart J Exp Physiol* 35 77-110
- Shoemaker W C and A G Finder 1961 Relation of potassium and glucose release from the liver in the unanesthetized dog *Proc Soc Exp Biol Med* 108 248-252
- Shoemaker W C, L N Turk III and F D Moore 1961 Hepatic vascular response to epinephrine *Amer J Physiol* 201 58-62
- Shoemaker W C, T B Van Itallie and W F Walker 1959 Measurement of hepatic glucose output and hepatic blood flow in response to glucagon *Amer J Physiol* 196 315-318
- Sutherland E W 1962 The biological role of adenosine-3, 5 phosphate. Harvey Lectures 1961-62 Academic Press New York pp 17-33
- Sutherland E W and T W Rall 1960 The relation of adenosine-3, 5 phosphate and phosphorylase to the actions of catechol amines and other hormones *Pharm Rev* 12 265-299
- Tajiri S 1960 The terminal distribution of the hepatic artery *Acta Med Okayama* 14 215-225
- Wakim K G 1944 The effect of certain substances on the intrahepatic circulation of blood in the intact animal *Amer Heart J* 27 289-300
- Wakim K G and F C Mann 1942 The intrahepatic circulation of blood *Anat Rec* 82 233-253
- Warner L 1940 Morphological changes in liver and spleen following intraperitoneal injection of cevitic acid *Anat Rec* 76 (Suppl.) 57
- Waugh W 1962 Role of calcium in contractile excitation of vascular smooth muscle by epinephrine and potassium *Circulation Res* 11 927-940
- Whittam R 1960 The high permeability of human red cells to adenosine and hypoxanthine and their ribosides *J Physiol* 154 614-623
- Williams A M and G A Lepage 1958 Purine metabolism in mouse ascites tumor cells II. *In vitro* incorporation of preformed purines into nucleotides and polynucleotides *Cancer Res* 18 548-553
- Winbury M M, D H Papierski, M L Hemmer and W E Hambourger 1953 Coronary dilator action of the adenine-ATP series *J Pharmacol* 109 255-260
- Wolf M M and R M Berne 1956 Coronary vasodilator properties of purine and pyrimidine derivatives *Circulation Res* 4 343-348

- 3 5 nucleotide phosphodiesterase and use of this enzyme to characterize adenosine-3, 5 phosphate in human urine *J Biol Chem* 237 1244-1250
- Cahill G F Jr J Ashmore S Zottu and A B Hastings 1957 Studies on carbohydrate metabolism in rat liver slices *J Biol Chem* 224 237-250
- Cameron G R and B T Mayes 1930 Ligation of the hepatic artery *J Path Bact* 332 799-831
- Carrier O Jr J R Walker and A C Guyton 1964 Role of oxygen in autoregulation of blood flow in isolated vessels *Amer J Physiol* 206 951-954
- Cohn R, and S Kountz 1963 Factors in influencing control of arterial circulation in the liver of the dog *Amer J Physiol* 205 1260-1264
- Conway E J and R Cooke 1939 The deaminases of adenosine and adenylic acid in blood and tissue *Biochem J* 33 479-492
- Craig A B Jr 1958 Observations on epinephrine and glucagon induced glycogenolysis and potassium loss in the isolated perfused frog liver *Amer J Physiol* 193 425-430
- Craig A B and C R Honig 1963 Hepatic metabolic and vascular responses to epinephrine a unifying hypothesis *Amer J Physiol* 205 1132-1138
- Daniel P M and M M L Prichard 1951 Effects of stimulation of the hepatic nerves and of adrenaline upon the circulation of the portal venous blood within the liver *J Physiol* 114 538-548
- Dawes G S 1941 The vaso-dilator action of potassium *J Physiol* 99 224-238
- Drury A N 1936 The physiological activity of nucleic acid and its derivatives *Physiol Rev* 16 292-325
- Duff F G C Patterson and J T Sheppard 1954 A quantitative study of the response to adenosine triphosphate of the blood vessels of the human hand and forearm *J Physiol* 125 581-589
- Elias H 1949 A re-examination of the structure of the mammalian liver II The hepatic lobule and its relation to the vascular and biliary systems *Am J Anat* 85 379-456
- Elias H and D Petty 1953 The terminal distribution of the hepatic artery *Anat Rec* 116 9-17
- Ellis S 1956 The metabolic effects of epinephrine and related amines *Pharm Rev* 8 485-562
- Ellis S and S B Beckett 1963 Mechanisms of the potassium mobilizing action of epinephrine and glucagon *J Pharm Exp Therap* 142 318-326
- Emanuel D J Scott and F Haddy 1959 Effect of potassium upon small and large blood vessels of the dog forelimb *Amer J Physiol* 197 637-642
- Finder A G T Boyne and W C Shoemaker 1964 Relationship of hepatic potassium efflux to phosphorylase activation induced by glucagon *Amer J Physiol* 206 738-742
- Fischer A 1963 Dynamics of the in the liver In *The Liver* Vol I C Rouill (ed.) Academic Press New York pp 329-37
- Folkow B 1949 The vasodilator action of an enzyme triphosphate *Acta Physiol Scand* 1 311-316
- Frohlich E J Scott and F Haddy 1962 Effect of cations on resistance and responsiveness renal and forelimb vascular beds *Amer J Physiol* 203 583-587
- Furchgott R F 1955 Pharmacology of vascular smooth muscle *Pharm Rev* 7 183-265
- Grabner G F Kaindl P Kohn and A Neumayer 1958 Das Verhalten der Leberdurchblutung während Sauerstoffmangel *Z Kreisf Forsch* 47 798
- Green H D L S Hall J Sexton and C P De 1959 Autonomic vasomotor responses in the canine hepatic arterial and venous beds *Amer J Physiol* 196 196-202
- Hanenson I B 1962 Effects of electrolyte and hormones on contraction of arterial smooth muscle *Circulation* 26 727
- Humason G L 1962 *Animal Tissue Technique* W H Freeman and Company San Francisco 468 pp
- Irwin J W and J MacDonald III 1953 A microscopic observations of the intrahepatic circulation of living guinea pigs *Anat Rec* 111 1-15
- Jacob M I and R M Berne 1960 Metabolism of purine derivatives by the isolated heart *Amer J Physiol* 198 322-326
- 1961 Metabolism of adenosine by the isolated anoxic cat heart *Proc Soc Exptl Med* 107 738-739
- Jang C 1940 Ions and adrenergic stimulation in the rabbit's ear *J Physiol* 99 1126
- Kayne H L N Taylor and N R Alpert 1961 Regulation of oxygen consumption in rat liver slices *Amer J Physiol* 206 1091-1094
- Kiernan F 1933 The anatomy and function of the liver *Trans Roy Soc London* 10 711-770
- Knisely M H 1936 A method of living structure for microscopic study *Anat Rec* 64 499-524
- Knisely M H E H Bloch and L Warner 1959 Selective phagocytosis I Microscopic observations concerning the regulation of the blood flow through the liver and other organs as to the mechanism and rate of phagocytosis of particles from the blood *Acta Danica Selskab Biol Skrifter* 4 1-93
- Knisely M H F Harding and H 1957 Hepatic sphincters *Science* 125 102-1026
- Kratochvil V M J Riedel and R 1959 Der Subterminale und terminale Abschnitt der Pfortader und Leberarterie in Leber des Frosches und einige Bemerkungen zur Regulation des Blutdurchflusses durch sinusoiden Kapillaren der Leber *Anat* 106 265-270
- Leblond C P H Puchtler and Y 1960 Structures corresponding to bars and terminal web in many types of cell *Nature* 186 784-788

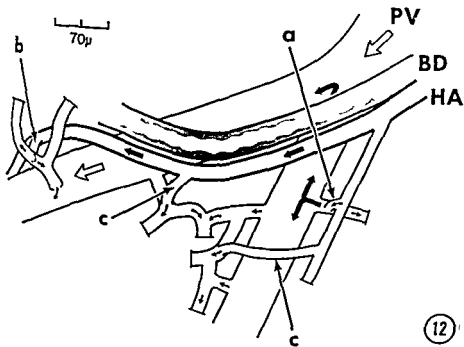
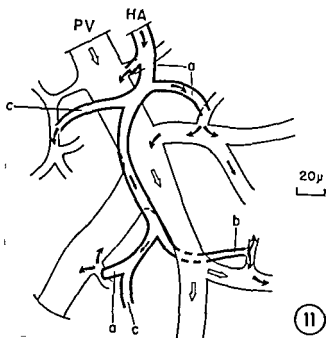


PLATE 1

EXPLANATION OF FIGURES

- 10 An hepatic arteriole (HA) and an arterio sinus twig (AST) selectively filled with Evans blue dye injected into the arterial system and adjacent to a portal venule (PV) Photographed from the living frog liver transilluminated with the white light using the quartz rod
- 11 Relationship of an hepatic arteriole (HA) with its adjacent portal venule (PV) and sinusoids (a arterio portal anastomosis b arterio sinus twig type 2 c arterio sinus twig type 1) Drawn to scale from the liver of a living rat transilluminated with monochromatic light (560 m μ)
- 12 Relationship of an hepatic arteriole (HA) and bile duct (BD) with their adjacent portal venule (PV) and with the sinusoids (a arterio portal anastomosis b arterio sinus twig type 2 c arterio sinus twig type 1) Drawn to scale from the liver of living frog transilluminated with monochromatic light (560 m μ)

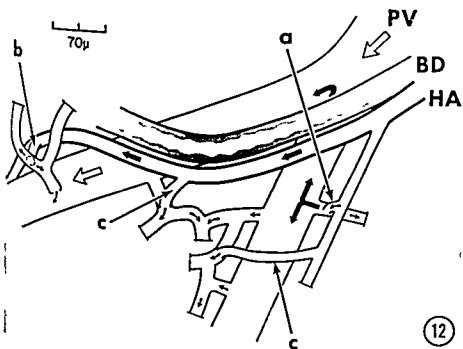
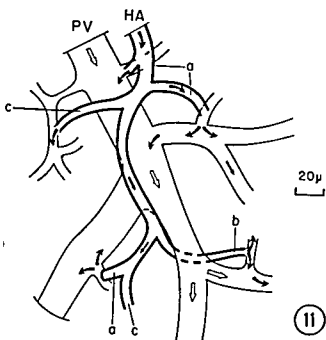


PLATE 1

EXPLANATION OF FIGURES

- 10 An hepatic arteriole (HA) and an arterio sinus twig (AST) selectively filled with Evans blue dye injected into the arterial system and adjacent to a portal venule (PV) Photographed from the living frog liver transilluminated with the white light using the quartz rod
- 11 Relationship of an hepatic arteriole (HA) with its adjacent portal venule (PV) and sinusoids (a arterioportal anastomosis b arterio sinus twig type 2 c arterio sinus twig type 1) Drawn to scale from the liver of a living rat transilluminated with monochromatic light (560 m μ)
- 12 Relationship of an hepatic arteriole (HA) and bile duct (BD) with their adjacent portal venule (PV) and with the sinusoids (a arterioportal anastomosis b arterio sinus twig type 2 c arterio sinus twig type 1) Drawn to scale from the liver of living frog transilluminated with monochromatic light (560 m μ)

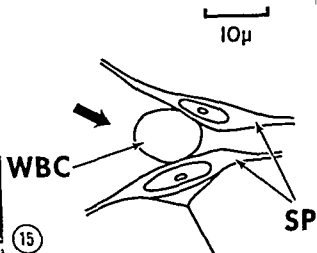
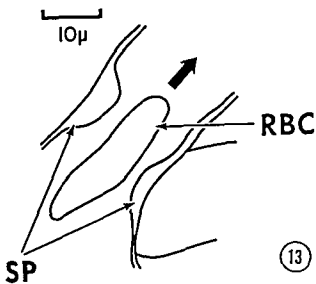


PLATE 2

EXPLANATION OF FIGURES

- 13 Inlet sphincter (SP) in the living frog liver transilluminated with monochromatic light ($414\text{ m}\mu$) The sphincter is dilated allowing red blood cells (RBC) to pass through it without deformation
- 14 Sphincter (SP) of an intersinusoidal sinusoid in the living frog liver transilluminated with monochromatic light ($550\text{ m}\mu$) The sphincter is constricted partially and its nucleus and nucleolus (n) are prominent
- 15 Inlet sphincter (SP) in the living frog liver transilluminated with monochromatic light ($560\text{ m}\mu$) A white blood cell (WBC) has stuck in the partially closed sphincter

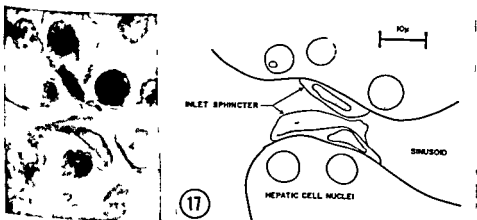
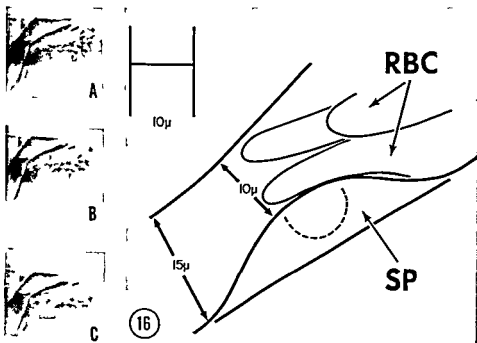


PLATE 3

EXPLANATION OF FIGURES

- 16 Outlet sphincter (SP) in the living frog liver transilluminated with monochromatic light (560 m μ) The sphincter is closed impeding the flow of red blood cells (RBC) through it Only one cell of the sphincter was in focus A second cell on the opposite side of the sinusoid also was bulging into the lumen and the two cells working together completely blocked the flow of blood from the sinusoid into the central venule A B and C are frames from a motion picture of this sphincter These were taken to illustrate its sustained closure for 10 minutes (A) 20 minutes (B) and 30 minutes (C)
- 17 Histology of an inlet sphincter in the frog This is a composite camera lucida drawing of two 10 μ serial sections stained with hematoxylin and eosin one of which is illustrated in the photograph

The Fine Structure of Ependymal Processes in the Teleost Optic Tectum¹

LAWRENCE KRUGER AND DAVID S. MAXWELL

Department of Anatomy and Brain Research Institute
Center for Health Sciences University of California Los Angeles

ABSTRACT Ependymal cell processes in the optic tectum of the adult sand bass *Paralabrax nebulifer* extend across the neural tube to the pial surface of the brain and exhibit several unique cytoplasmic features which readily distinguish these cells from other elements in the brain when examined in the electron microscope. These include large perpendicularly oriented bundles of filaments cross striated by a series of irregular membranous structures ("ependymal reticulum"), glycogen granules and dense-core vesicles in the outer portions and lateral protuberances of the main ependymal shaft, large clear vacuoles more numerous near the pial surface, large mitochondria with a distinctive pattern of tubular cristae and a flocculent matrix and fasciae occludentes at sub-pial endfoot contacts. These morphological findings suggest that ependymal cells do not simply constitute a primitive source for new cells or merely serve as structural support but rather are highly specialized and may display secretory activity.

Early investigations of neuroglial elements primarily based on metallic impregnation methods in the brains of cyclostomes, elasmobranchs and teleosts revealed long ependymal processes (Nansen 1886, Miró 1895, Müller 1900, Retzius 1893, Studnička 1900, Cajal 1911, Achucarro 1915). In some regions of the brain in several lower vertebrate classes these long processes extend perpendicularly from the perventricular lining across the neural tube and expand into end feet below the pial surface. This relationship of the ependymal processes (sometimes referred to as "tanyocyte processes") to both surfaces of the neural tube appears to persist in adult specimens in some regions of the nervous system in most vertebrates. Cajal (1911) believed that the ependymal cells or "neuroepithelial" elements of most submammalian vertebrates constituted the sole non neuronal or neuroglial component of the brain parenchyma although his student Achucarro (1915) recognized the existence of independent dendritic glial cells (*neuroglia autotoma*) in some regions of teleost brains. The presence of fibrillar material, the extensive distribution of ependymal processes throughout the neuropil and the relative paucity of neuroglial elements in the teleost brain was interpreted by earlier workers as an indication that these cells

are principally concerned with a supportive and nutritive function similar to that of mammalian neuroglia. In addition many early workers (Achucarro 1915, Agduhr 1932) regarded the ependymal cell as a secretory or "glandular" element.

The basal or perinuclear portion of ependymal cell has been studied recently in a number of vertebrates (Brightman and Palay 1963, Olsch 1958, Duncan 1957, Bellairs 1959, Schultz, Berkowitz and Pease 1956, Tennyson and Pappas 1962, Klinkerfuss 1964) but the fine structure of the long processes extending to the pial surface in lower vertebrate brains has not been described. The present report is concerned with the fine structural characteristics of ependymal processes in the optic tectum of the adult marine teleost brain and especially with the description of some unique cytoplasmic features which distinguish these processes from all other nervous system elements.

MATERIAL AND METHOD

Material was obtained from seven teleosts (all Serranidae) of over 15 cm body length. Animals were perfused by inserting a needle with flexible polyethylene tubing on the tip through the ventricle into the truncus arteriosus. A variety of alde-

¹Supported by United States Public Health Service grants NB-3604, NB-04578 and NB 06594.

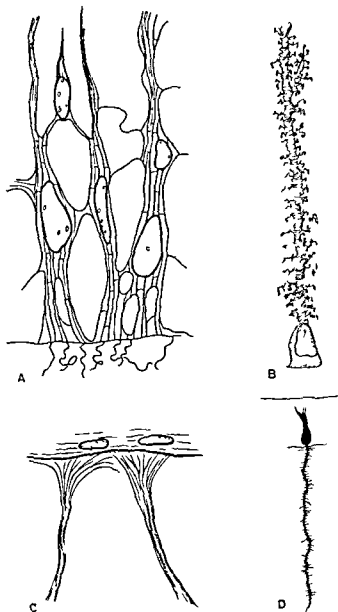


Fig. 1 Drawings of the ependymal processes of lower vertebrates seen with light microscopic techniques by earlier workers. The ventricular surface is below and the pia above in all drawings

- A. Iron hematoxylin preparation of the arrangement of ependymal processes in *Petromyzon*. Note the orientation of processes and cross-striations (after Studnička '00)
- B. Methylene blue preparation of the basal ependyma ("neuroepithelial cells") and their processes in the frog (after Cajal '11)
- C. Iron hematoxylin preparation of ependymal processes with their sub-pial end feet in *Scyllium* (after Studnička '00)
- D. Golgi preparation of ependymal processes with their sub-pial end-feet in the teleost (*Clupea sardina*) optic tectum (after Mirto 1893)

hyde fixatives and combinations with different buffers was studied and our most satisfactory material was obtained with a combination of 2% formaldehyde, 2% glutaraldehyde in a 0.1 molar cacodylate buffer and fish saline consisting of (in gm/l), NaCl 10.23, CaCl₂ 0.11, MgCl₂ 0.20, NaHCO₃ 0.024 and NaH₂PO₄ 0.002. The micrographs in this paper were all obtained from a single specimen of the sand bass, *Paralabrax nebulifer*, perfused with the above described mixture. We are indebted to Sea World, San Diego and the Scripps Institution of Oceanography La Jolla California for providing fish and facilities.

Immediately following perfusion the optic tectum was cut into strips of 1 mm or less extending to the ventricle (optocoele). These were rapidly transferred to cold cacodylate buffered 1% osmium tetroxide for 1 to 2 hours the tissue was rapidly dehydrated in ethanol and embedded in Araldite. Thick plastic sections (0.5 μ) were cut on a Porter Blum microtome with glass knives and stained by several methods for examination in the light microscope. Some thin sections were mounted on Formvar films over slotted grids for initial orientation but all of the illustrative material was obtained with thin unsupported sections. Sections were stained with lead citrate and photographed in the Hitachi HU 11A electron microscope.

RESULTS

Ependymal processes in the optic tectum of adult teleost brains extend from the ventricular to the pial surface and constitute the majority of the extensively branched glial cells in metallic impregnation preparations. The long processes which can be traced upward from each ependymal cell have been studied recently with various staining methods by Horstmann (54) and Fleischhauer (57). These elements have also been called neuroepithelial cells (Cajal '11) ependymal spongioblasts (Penfield, 32) and some what similar elements in the developing mammalian neural tube have been identified in the electron microscope as "ependymal astroblasts" (Tennyson and Pappas 62, Klunkerfuss 64).

A striking feature of the long ependymal processes which persist in lower vertebrate brains is a series of grape like tuberosities (fig 1b) extending laterally along the course of the entire process (Cajal '11). The nuclei occur at varying depths but tend to concentrate at the ventricular surface (Studnicka, 00 Agduhr, 32). At the surface the ependymal processes expand into broad end feet (fig 1) beneath the external limiting membrane (basal lamina) constituting a substantial portion of the brain surface (Studnicka 00, Retzius 1893, Mirto 1895, Horstmann, '54, Fleischhauer, 57). Early observations with iron hematoxylin preparations (Studnicka 00) revealed large longitudinal fibrillar bundles, vacuoles and some cross striations (figs 1a, c).

In the electron microscope profiles of the shaft of the ependymal processes rarely exceed 1-2 μ in diameter, but their distinctive features render them readily recognizable. The central portion of each process contains a dense cytoplasm matrix filled with numerous fine filaments and surrounded by a less dense cytoplasmic periphery which is continuous with the lateral expansions. As the processes approach the surface they expand as subpial end feet abutting with adjacent ependymal end feet or subpial astrocyte processes. The distinctive organelles of the ependymal processes include unique mitochondria longitudinally oriented fine filaments, large clear cytoplasmic vacuoles, dense core vesicles reminiscent of secretory granules or catecholamine containing vesicles, glycogen and an unusual array of smooth endoplasmic reticulum.

An electron micrograph of a typical ependymal process approaching the surface of the optic tectum is shown in figure 2. The cell can be distinguished readily from adjacent neuropil by the foamy appearance imparted by numerous large clear vacuoles of up to 0.6 μ in diameter. These vacuoles display irregular contours and tend to be larger and more numerous near the pial extremity of the process where they are generally arranged in longitudinal rows. At the surface, the process abuts the basal lamina and some vacuoles appear to fuse with the plasma membrane (fig 3 arrow). Another striking feature

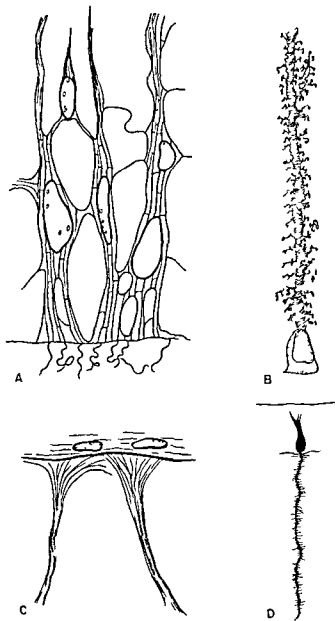


Fig. 1 Drawings of the ependymal processes of lower vertebrates seen with light microscopic techniques by earlier workers. The ventricular surface is below and the pia above in all drawings.

- A. Iron hematoxylin preparation showing the arrangement of ependymal processes in *Petromyzon*. Note the orientation of processes and cross-striations (after Studnička '00)
- B. Methylene blue preparation of the basal ependyma ("neuroepithelial cells") and their processes in the frog (after Cajal '11)
- C. Iron hematoxylin preparation of ependymal processes with their sub-pial end feet in *Scyllium* (after Studnička '00)
- D. Golgi preparation of ependymal processes with their sub-pial end feet in the teleost (*Clupea sardina*) optic tectum (after Mirto 1895)

is the presence of distinctive mitochondria of unusual configuration and large diameter predominantly oriented along the long axis in the outer portion of the process, and containing sparse irregularly disposed tubular cristae in a flocculent matrix of moderate electron opacity (figs 4, 5, 6, 11). With the present method of tissue preparation the cytoplasmic matrix density of the central region of the ependymal processes is usually distinctly greater than that of most of the surrounding neuropil.

Numerous fine filaments of less than 100 Å in diameter are aggregated in the central region of the process. These bundles presumably correspond to the fine fibrils originally described by Muller (00) and Studnička (00). Similar filaments have been seen with the electron microscope in the perikaryal region of mammalian ependymal cells (Tennyson and Pappas 62, Brightman and Palay 63, Klunkerfuss 64). Following the ependymal process to a depth of approximately 50 μ from the surface the filaments are seen to be densely packed and oriented in the longitudinal axis of the main process with few if any extending into lateral branches (figs 6, 11). Complex tortuous lateral expansions often can be traced for several microns and become interspersed between all elements of the neuropil. Contained within these tuberous processes are large quantities of glycogen like granules, large vacuoles and occasional accumulations of vesicles with an electron-opaque core (figs 2-13) but all of these organelles appear to be most concentrated in the subpial end feet. The small free granules of approximately 200-400 Å display a marked electron opacity. Because of their resemblance to glycogen in other tissues (Revel, Napolitano and Fawcett 60) including astrocytes in mammalian brain (Maxwell and Kruger 65) we shall refer to these as glycogen although this has not been demonstrated experimentally in this tissue.

The dense core vesicles consist of a cytoplasmic vesicle bounded by a single layered membrane, with a rounded central core matched only by glycogen in its electron opacity. Many larger irregular vesicles are observed containing double or

complex cores (figs 6-10). The range of vesicle size is 650 to 1600 Å in outer diameter for vesicles with less complex cores. Some profiles display small lateral membranous buds or retain attachment to vacuoles or to the flat tubular endoplasmic reticulum (figs 6-9). Although these dense-core vesicles are predominantly distributed within ependymal cells similar organelles usually of about the size of the smaller ependymal vesicles have been seen occasionally in axonal endings.

A series of irregular membranous structures distributed in a plate like manner perpendicular to the long axis of the process appear in micrographs as cross-striations with an irregular repeat period of approximately 0.2-0.35 μ (fig 11). These membranes are essentially planar, tubular arrays displaying numerous anastomoses and a few lateral dilatations. This tubular system might appropriately be designated the ependymal reticulum. Specialized junctions or fusions of the plasma membrane similar to the fascia occludens described between ependymal cells lining the cerebral ventricle in mammals (Tennyson and Pappas 62, Brightman and Palay 63, Klunkerfuss 64, Brightman 65) have frequently been noted (figs 2, 12, 13) and similar junctional complexes can be seen to occur with astrocyte processes. At these junctional regions between astrocyte or ependymal end feet the contours of the processes become complicated by irregular interdigitating processes united in extensive lengths of tight junctional complexes (fig 13). These tight junctions appear to be invariably present at the contacts of adjacent subpial end foot expansions of ependymal cells but are rare or absent along the main shaft of the process. The frequent association of tight junctions with electrical transmission (Robertson et al 63, Furshpan 64) may be indicative of a subpial specialization for rapid ionic exchange in the teleost brain.

DISCUSSION

The ependymal cells of adult teleosts differ markedly from those of adult mammals (Tennyson and Pappas 62, Brightman and Palay 63, Klunkerfuss 64) in that they possess an unusually broad proc-

es of specialized cytoplasm extending across the width of the neural tube. The sub-pial expansions of these processes comprise a substantial portion of the surface area of the optic tectum. The bundles of fine filaments or gliafibrils have been noted in the perikaryal region in mammals (Tennyson and Pappas 62, Brightman and Palay 63, Klinkerfuss 64) and reptiles (Fleischhauer 57). Although it is virtually impossible to trace a single ependymal cell through its entire course, the width of the processes, their orientation, and their specialized organelles simplifies the identification of most well preserved portions of ependyma.

The designation of the long ependymal cells that traverse the neural tube in fishes as supportive spongioblasts (Penfield 30) seems less than appropriate in the light of present-day knowledge. It is also doubtful that these cells are transitional between primitive ependyma and astrocytes because of the more specialized nature of the cytoplasmic organelles in the tanycyte variety of ependyma.

Ependymal cells display some features which are common to astrocytes. These include the fine filaments and glycogen granules which are characteristic of all mammalian astrocytes (Maxwell and Kruger 65). In fishes (cyclostomes and teleosts) glial elements which have migrated from the ependymal layer possess these two organelles in quantities dependent upon their distribution and quality of preservation (Horstmann 54, Robertson and Stage 63, Mugnani and Walberg 65, Nakajima, Bennett and Pappas 60, Kruger and Maxwell in press) and these cells would appear to be homologous of mammalian astrocytes. The astrocyte may be regarded as the most direct derivative of spongioblasts which have migrated from the ependymal layer. The ependymal cells which extend processes to the external limiting membrane of the brain might appropriately be called "ependymal astrocytes" (Tennyson and Pappas 62, Klinkerfuss 64) but these cells are clearly more specialized in terms of their component organelles than the astrocytes in the teleost central nervous system.

A supportive function for ependymal cells in submammalian forms was suggested on the basis of the broad, relatively straight fibrillar processes and their orientation across the neural tube (e.g. Muller 00, Studnicka 00, Agduhr 32, Cajal 11). The ependymal reticulum oriented perpendicular to the longitudinal filaments may be related to the supportive function of ependymal processes, but there is no direct evidence concerning their functional significance. The striking resemblance of ependymal reticulum and filaments to the arrangement of myofibrils and sarcoplasmic reticulum is noteworthy although there is no evidence to suggest that these cells possess contractile properties.

Numerous early workers (Studnicka 00, Cajal 11, Achucarro 15) also emphasized that ependyma play a glandular or secretory role in the brain as well as subserving special metabolic functions. The choroid plexus epithelium may be regarded as a specialization of the ependyma and it is clear that its principal function involves secretory activity. The contact of teleost ependymal cells with the ventricular and pial surfaces provides an unusual situation for exchange between the fluids bathing both surfaces. Evidence of pinocytosis was observed in the ventricular portion of mammalian ependyma (Brightman 65). The extensive distribution of vacuoles in the sub-pial processes may reflect transport in the direction of exchange of materials with the subarachnoid space.

The extensive distribution of glycogen and the occasional contacts with capillary walls *en passage* as noted earlier by Achucarro (15) suggests that ependyma may parallel some of the functional properties of astrocytes which are the principal perivascular and glycogen-laden elements in mammalian brain (Maxwell and Kruger 65). Distinct ependymal processes with vascular end feet have been demonstrated in fishes (Horstmann 54), amphibians (Bairati and Tripoli 54) and reptiles (Fleischhauer 57). It has been argued that gliovascular architecture is predominantly formed by ependymal processes in urodeles and anurans (Bairati and Tripoli 54) but electron microscopic evidence in

is the presence of distinctive mitochondria of unusual configuration and large diameter predominantly oriented along the long axis in the outer portion of the process, and containing sparse, irregularly disposed tubular cristae in a flocculent matrix of moderate electron opacity (figs 4 5 6 11). With the present method of tissue preparation the cytoplasmic matrix density of the central region of the ependymal processes is usually distinctly greater than that of most of the surrounding neuropil.

Numerous fine filaments of less than 100 Å in diameter are aggregated in the central region of the process. These bundles presumably correspond to the fine fibrils originally described by Muller (60) and Studnicka (60). Similar filaments have been seen with the electron microscope in the perikaryal region of mammalian ependymal cells (Tennyson and Pappas 62, Brightman and Palay 63, Klinkerfuss 64). Following the ependymal process to a depth of approximately 50 μ from the surface the filaments are seen to be densely packed and oriented in the longitudinal axis of the main process with few if any extending into lateral branches (figs 6 11). Complex tortuous lateral expansions often can be traced for several microns and become interspersed between all elements of the neuropil. Contained within these tuberous processes are large quantities of glycogen like granules, large vacuoles and occasional accumulations of vesicles with an electron-opaque core (figs 2-13) but all of these organelles appear to be most concentrated in the subpial end feet. The small free granules of approximately 200-400 Å display a marked electron opacity. Because of their resemblance to glycogen in other tissues (Revel, Napolitano and Fawcett 60) including astrocytes in mammalian brain (Maxwell and Kruger 65), we shall refer to these as glycogen although this has not been demonstrated experimentally in this tissue.

The dense core vesicles consist of a cytoplasmic vesicle bounded by a single layered membrane with a rounded central core matched only by glycogen in its electron opacity. Many larger irregular vesicles are observed containing double or

complex cores (figs 6-10). The range of vesicle size is 650 to 1600 Å in outer diameter for vesicles with less complex cores. Some profiles display small membranous buds or retain attachment to vacuoles or to the flat tubular endoplasmic reticulum (figs 6-9). Although dense core vesicles are predominantly distributed within ependymal cells similar organelles usually of about the size of the smaller ependymal vesicles have been seen occasionally in axonal endings.

A series of irregular membranous structures distributed in a plate like manner perpendicular to the long axis of the process appear in micrographs as cross striations with an irregular repeat period of approximately 0.2-0.35 μ (fig 11). These membranes are essentially planar tubular arrays displaying numerous anastomoses and a few lateral dilatations. This tubular system might appropriately be designated the *ependymal reticulum*. Specialized junctions or fusions of the plasma membrane similar to the *fascia occludens* described between ependymal cells lining the cerebral ventricle in mammals (Tennyson and Pappas 62, Brightman and Palay 63, Klinkerfuss 64, Brightman 65) have frequently been noted (figs 2 12 13), and similar junctional complexes can be seen to occur with astrocyte processes. At these junctional regions between astrocyte or ependymal end feet the contours of the processes become complicated by irregular interdigitating processes united in extensive lengths of tight junctional complexes (fig 13). These tight junctions appear to be invariably present at the contacts of adjacent subpial end foot expansions of ependymal cells but are rare or absent along the main shaft of the process. The frequent association of tight junctions with electrical transmission (Robertson et al 63, Furshpan 64) may be indicative of a subpial specialization for rapid ionic exchange in the teleost brain.

DISCUSSION

The ependymal cells of adult teleosts differ markedly from those of adult mammals (Tennyson and Pappas 62, Brightman and Palay 63, Klinkerfuss 64) in that they possess an unusually broad pro-

- Ceballos G H. 1964 An electron microscopic study of the ependyma and subependyma of the lateral ventricle of the cat. *Ann J Anat.* 115 71-100
- Eger L, and D S Maxwell. Comparative fine structure of vertebrate neuroglia Teleosts and reptiles. *J Comp Neur* in press
- Kawell, D S and L. Kruger. 1965 The fine structure of astrocytes in the cerebral cortex and their response to focal injury produced by heavy ionizing particles. *J Cell Biol* 25 141-157
- M. J. D. 1895 Sulla fina Anatomia del tetto cranio del Pesci teleostei e sull origine reale del nervo ottico. *Riv Sper Freniat* 21 136-148
- Kyriani, E., and F Walberg. 1964 Ultrastructure of neuroglia. *Ergebn Anat Entwickl Gesch* 37 193-236
- 1965 The fine structure of the capillaries and their surroundings in the cerebral hemispheres of *Myxine glutinosa* (L) *Z. Zellforsch* 66 333-351
- M. J. E. 1900 Studien uber Neuroglia. *Arch Mikr Anat.* 55 11-62
- Nakama, Y G D Pappas and M V L Bennett. 1963 The fine structure of the supramedullary neurons of the puffer with special reference to endocellular and pericellular capillaries. *Ann J Anat.* 116 471-477
- Nissen, F. 1886 Preliminary communication on some investigations upon the histological structure of the central nervous system in the *Acrida* and in *Myxine glutinosa*. *Ann Mag Natur Hist.* 18 (Fifth Series) 209-226
- Oehme A. 1958 Histologische Untersuchungen über die Bedeutung des Ependyms der Glia und der Plexus Chorioidei für der Kohlenhydratstoffwechsel des ZNS. *Z Zellforsch* 48 74-129
- Penfield W. 1932 Neuroglia normal and pathological in Cytology and Cellular Pathology of the Nervous System ed. W Penfield vol 11 421-479
- Pesetsky I. 1965 Thyroxine stimulated oxidative enzyme activity associated with precocious brain maturation in Anurans a histochemical study. *Gen Comp Endocrin* 5 411-417
- 1966 Thyroxine-stimulated thiamine pyrophosphatase activity in ependymal cells of anuran amphibians. *Anat Rec* 154 401
- Retzius G. 1893 Studien über Ependym und Neuroglia. in *Biol Untersuch Neue Folge* Stockholm Samson & Wallin 1890-1921 Vol 5 p 9-26
- Revel J P L Napolitano and D W Fawcett. 1960 Identification of glycogen in electron micrographs of thin tissue sections. *J Biophys and Biochem Cytol.* 8 575-589
- Richardson K. 1962 The fine structure of autonomic nerve endings in smooth muscle of the rat vas deferens. *J Anat* 96 427-442
- Robertson J D T S Bodenheimer and D E. Stage. 1963 The ultrastructure of Mauthner cell synapses and nodes in goldfish brains. *J Cell Biol* 19 159-199
- Schultz R E C Berkowitz and D C Pease. 1956 The electron microscopy of the lamprey spinal cord. *J Morph* 98 251-273
- Studnicka F K. 1900 Untersuchungen über den Bau des Ependyms der Nervosen centralorgane. *Anat Hefte* 15 301-431
- Tennyson V A and G D Pappas. 1962 An electron microscope study of ependymal cells of the fetal early postnatal and adult rabbit. *Z. Zellforsch* 56 595-618

even more primitive vertebrates (e.g. cyclostomes) indicates that migrated neuroglial elements similar to mammalian astrocytes form most of the glial investment of capillaries (Mugnaini and Walberg 65)

The most remarkable morphological features suggestive of a specialized metabolic role for ependyma are the large quantities of glycogen and the mitochondria of unusual size and distinctive cristal pattern. Earlier suggestions of a glandular function (Achucarro, 15) based on the presence of secretory granules may find some support in the present study if the dense core vesicles could be interpreted as structural counterparts of secretory processes. A variety of similar, but not identical granular or dense core vesicles have been noted in several portions of the nervous system especially in axonal endings. The largest vesicles with dense cores range from less than 1000 Å to 4000 Å diameter and are generally referred to as neurosecretory vesicles or granules (Richardson, 62). Many but not all of the smaller granular vesicles of less than 1000 Å diameter appear to be related to catecholamines in axonal endings (Gray and Guillery 66). The presence of this broad class of vesicles with internal granular structure in axonal knobs in autonomic endings and in neurohypophysis has led to the interpretation that they are related to neurosecretory phenomena. The dense core vesicles of somewhat similar morphology in non-neuronal elements (i.e. ependymal cells) may be an expression of secretory phenomena unrelated to transmitter release at synapses. The apparent origin of these vesicles from membranes of the smooth endoplasmic reticulum (most commonly seen in relation to the ependymal reticulum or the vacuoles that appear to arise from them) is consistent with the interpretation of these vesicles as a secretory product.

The extensive Golgi apparatus in the basal portions (Horstmann 54, Fleischhauer 57, Brightman and Palay 63, Tennyson and Pappas 62, Klinkerfuss '64) and the ependymal reticulum would also appear to suggest that these elements might subserve significant synthetic function. Pesetsky ('65) has demonstrated that

thyroidectomy or thyroxine stimulation, accompanied by alterations in size and number of ependymal cells as well as in number of histochemical changes in the developing anuran brain. The recent demonstration of thyroid regulation of thymine pyrophosphatase activity (Tennyson '66) suggests phasic activity in the Golgi apparatus of ependymal cells. The of distinctive organelles present in teleost ependymal cells would appear to indicate that these cells are not simple primitive supportive elements.

ACKNOWLEDGMENTS

We are indebted to Mrs. Olga Fiorelli, Mrs. Sharon Sampogna and Dr. Horst Schwassmann for assistance to Mr. Krista Osterberg for the drawing and Mrs. Diana Brinton for typing the manuscript.

LITERATURE CITED

- Achucarro N. 1915. De l'évolution de la neuroglie et spécialement de ses relations avec le plexus vasculaire. *Trab. Lab. Invest. Biol. (Madrid)* 13: 169-212.
- Agduhr E. 1932. Choroid plexus and ependyma in cytology and cellular pathology of the nervous system. ed. W. Penfield. vol. 11. pp. 53-573.
- Bairati A. and G. Tripoli. 1954. Ricerche morfologiche ed istochimiche sulla glia del nervasso di vertebrati. *Z. Zellforsch.* 39: 392-413.
- Bellairs R. 1959. The development of the nervous system in chick embryos studied by electron microscopy. *J. Embryol. exp. Morph.* 9: 94-115.
- Brightman M. W. The distribution within the brain of ferretin injected into cerebrospinal fluid compartments. 1. Ependymal distribution. *J. Cell Biol.* 26: 99-123.
- Brightman M. W. and S. L. Palay. 1963. The fine structure of ependyma in the brain of the rat. *J. Cell Biol.* 19: 415-439.
- Cajal S. Ramon y. 1911. *Histologie du système nerveux de l'homme et des vertébrés*. Paris: A. Maloine.
- Duncan D. 1957. Electron microscope study of the embryonic neural tube and notochord. *Tex. Rep. Biol. Med.* 15: 367-377.
- Fleischhauer K. 1957. Untersuchungen an Ependym des Zwischen- und Mittelhirns der Landschildkröte (*Testudo graeca*). *Z. Zellforsch.* 46: 729-767.
- Furshpan E. J. 1964. Electrical transmission at an excitatory synapse in a vertebrate brain. *Science* 144: 878-880.
- Gray E. G. and R. W. Guillery. 1966. Synaptic morphology in the normal and degenerating nervous system. *Int. Rev. Cytol.* 19: 111-182.
- Horstmann E. 1954. Die Fasergröße des Selachiergehirns. *Z. Zellforsch.* 39: 588-617.

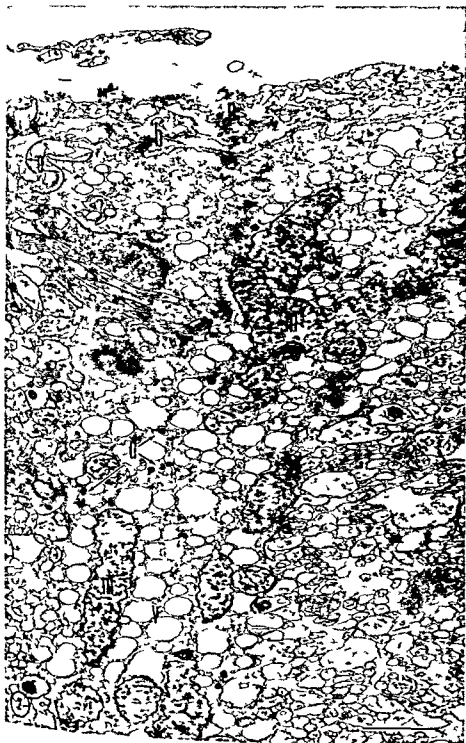


PLATE 1

EXPLANATION OF FIGURE

- 2 Electron micrograph of an ependymal process expanding into a sub-pial end foot. Note the characteristic dense cytoplasmic matrix, large clear vacuoles (V), dense-core vesicles (d) and large mitochondria (m) with a flocculent matrix and tubular cristae. Numerous glycogen granules can be seen in the ependymal cytoplasm beneath the basal lamina (b) separating the brain from the overlying pial processes (p). Near the surface an interdigitating process of an adjacent ependymal end foot forms a "tight junction" of the fascia occludens variety (o). Bar in this and all subsequent figures represents one micron.

FISH EPENDYMA
Lawrence Kruger and David S. Maxwell II

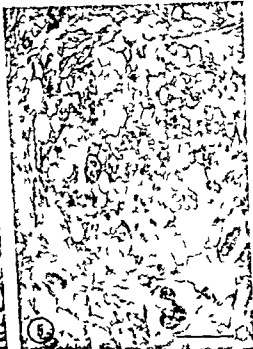
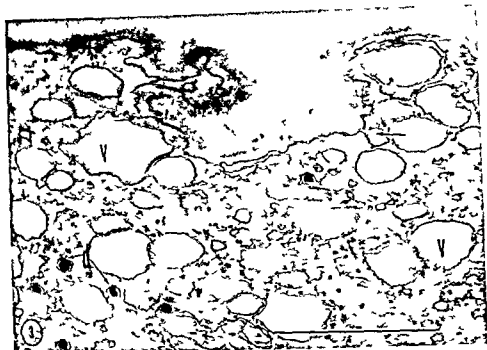


PLATE 2

EXPLANATION OF FIGURES

- 3 A sub pial ependymal end foot containing numerous large clear vacuoles (V) one of which opens onto the surface (arrow) Typical organelles of ependymal cytoplasm present include glycogen filaments and dense core vesicles (d)
- 4 A deep ependymal process cut perpendicular to its long axis The central core contains numerous filaments cut transversely and a cluster of membranes forming the ependymal reticulum The outer portions of the process contain mitochondria and large clear vacuoles
- 5 Transverse section of an ependymal process near the level of expansion to form a sub-pial end foot An increase in the number of large vacuoles and dense-core vesicles can be seen in the outermost (sub pial) portion of the ependymal process and they display a tendency to cluster into the lateral portion and side branches

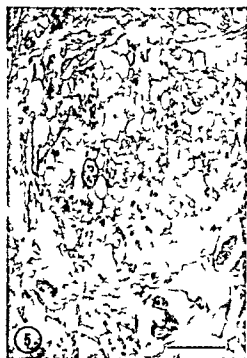
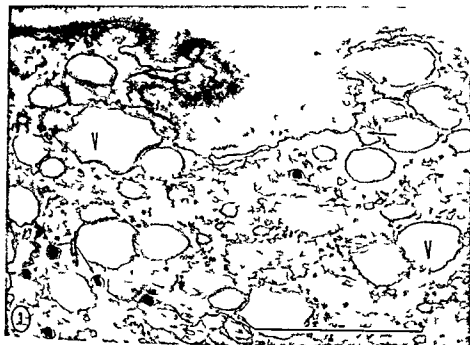


PLATE 3

EXPLANATION OF FIGURE

- 6 Ependymal process oriented perpendicular to the pial surface. The central core contains large bundles of longitudinal filaments (f) irregularly striated by tubules or vesicles of the ependymal reticulum (er). The outer portions of the process contain large long mitochondria (m) clear vacuoles (V) glycogen granules (g) and dense core vesicles (d).

FISH EPENDYMA

Lawrence Krug and David S. Maxwell

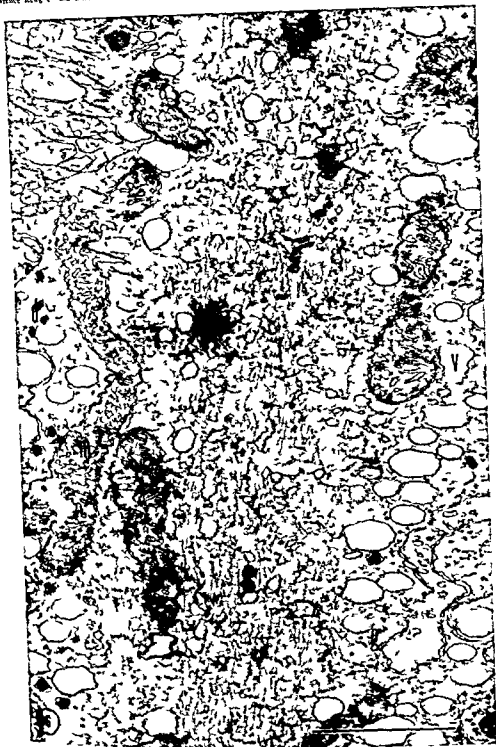


PLATE 3

EXPLANATION OF FIGURE

- 6 Ependymal process oriented perpendicular to the pial surface. The central core contains large bundles of longitudinal filaments (f) irregularly striated by tubules or vesicles of the ependymal reticulum (er). The outer portions of the process contain large long mitochondria (m), clear vacuoles (V), glycogen granules (g) and dense core vesicles (d).

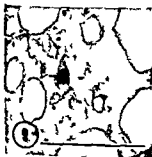
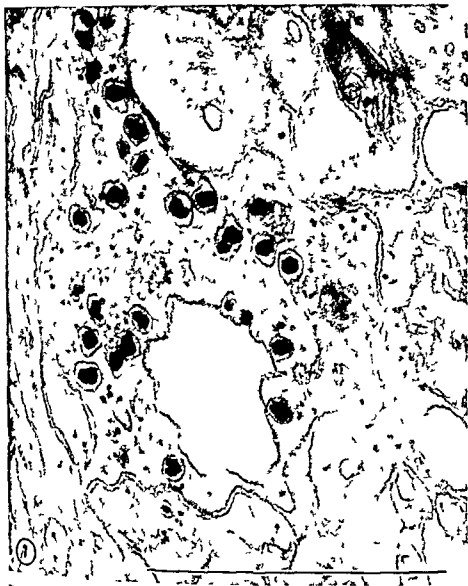


PLATE 4

EXPLANATION OF FIGURES

- 7 A lateral protuberance of an ependymal process containing a variety of dense core vesicles. Note that some of the cores appear to consist of two or more granules
- 8 A dense-core vesicle continuous with a large clear vacuole
- 9 A dense-core vesicle with lateral tubular expansions of its membrane
- 10 Two attached dense-core vesicles with complex cores

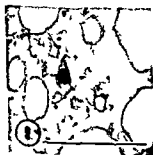


PLATE 5

EXPLANATION OF FIGURE

- 11 Ependymal process displaying a typical central core with bundles of longitudinal filaments and an irregular series of cross striations consisting of membranous plates and vesicular expansions—the ependymal reticulum (er arrows) Large vacuoles (V) display attachments to the ependymal reticulum Glycogen granules (g) and dense core vesicles (d) are irregularly scattered and extend into small lateral protuberances

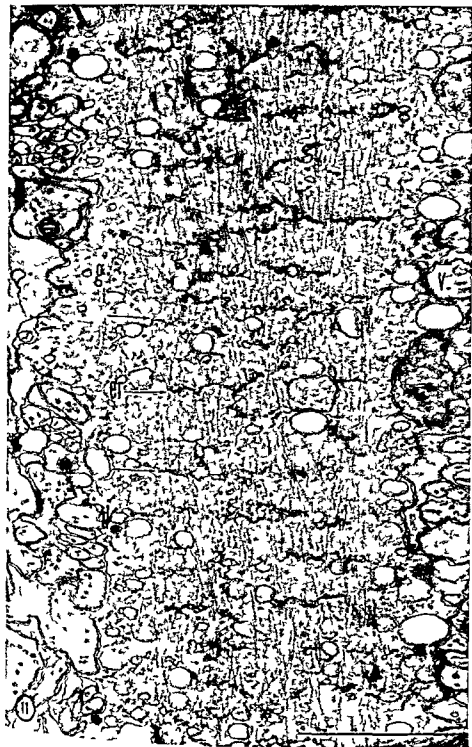


PLATE 6

EXPLANATION OF FIGURES

- 12 Interdigitating finger like processes between a subpial ependymal end foot (ep) and an adjacent astrocyte process (a) displaying *fasciae occludentes* junctions (o) near the surface of the brain
- 13 Ependymal tight junctions of the *fascia occludens* variety

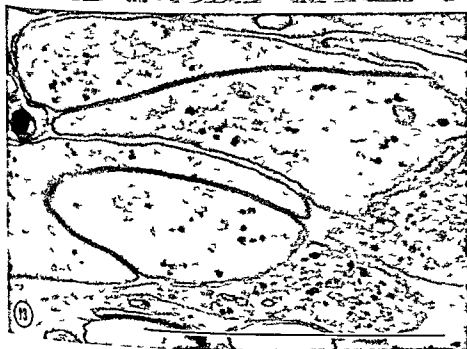


PLATE 6

EXPLANATION OF FIGURES

- 12 Interdigitating finger like processes between a sub pial ependymal end foot (ep) and an adjacent astrocyte process (a) displaying *fasciae occludentes* junctions (o) near the surface of the brain
- 13 Ependymal tight junctions of the *fascia occludens* variety

An Evaluation of Possible Intracellular Nucleic Acid Quenching of Carcinogenic Hydrocarbon Fluorescence¹

THOMAS K. SHIRES

Departments of Anatomy and Urology University of Oklahoma
Oklahoma City Oklahoma²

ABSTRACT An investigation was made to evaluate the role of intranuclear nucleic acids on the reported lack of accumulation of fluorescent polycyclic carcinogenic hydrocarbons (CH) within the nucleus of the live cell. Analysis of CH distribution with integrated phase-contrast and u.v. fluorescent microscopy was performed on whole cells and subcellular nuclear fractions from which nucleic acids had been removed and on ultracentrifuged live cells whose nuclei were stratified into nucleic acid rich and nucleic acid poor regions. No intranuclear fluorescence was found in any experimentally treated material or in the live cell controls after their exposure to CH. The absence of any evidence for the quenching of CH fluorescence by intranuclear nucleic acids supports the u.v. fluorescence microscopists' contention that little or no CH enters live cell nuclei.

The general applicability of the u.v. fluorescence microscopic technique to the tracing of exogenous polycyclic carcinogenic hydrocarbons (CH) into live cells was first demonstrated by Graffi (39). Subsequent u.v. fluorescence microscopic studies have shown that the intracellular distribution of CH follows a pattern common to a wide variety of live nucleated vertebrate and invertebrate cell types (Graffi and Mass 38; Gunther 41; Leber and Saini 60; Shires 62; Jones 70; Harvey et al. 63). This pattern shows hydrocarbon accumulation in the general cytoplasmic matrix and a relatively higher accumulation in elements of the Golgi complex and lipid droplets. With one possible exception there is no apparent accumulation of CH in the intranuclear area. Graffi (39-40) reported the accumulation of CH in the nucleus of live tumor cells but this has not been confirmed by later studies (Richter and Saini 61).

It is not clear why there is no karyoplasmic localization of CH as assayed by u.v. fluorescence microscopy both *in vivo* and *in vitro*. Purely biochemical studies have shown that bonding of CH with RNA and DNA in aqueous solutions is accompanied by quenching of the CH fluorescence (Boyland and Green 62-64). This would suggest that the apparent ab-

sence of CH accumulation by the karyoplasm in living cells is a quenching effect and thus a limiting defect in the u.v. fluorescence microscopic method. However, Giovanella et al. (64) and Heidelberger (64) have questioned the occurrence of nucleic acid binding with CH both *in vivo* and *in vitro*. In this report data are presented which bear on the question of whether the apparent lack of karyoplasmic accumulation of CH is real or whether it is due to the quenching of CH fluorescence by intranuclear RNA and DNA.

MATERIALS AND METHODS

Study of the influence of nucleic acids on the u.v. fluorescence of intracellular CH involved (1) a depletion of nucleic acids by (a) nuclease digestion of whole fixed cells, (b) nuclease digestion and saline extraction of subcellular nuclear fractions, and (c) ultracentrifugal displacement and stratification of nucleic acids in live whole cells; (2) exposure of this treated material to 3,4-benzo(a)pyrene (BP) (Hoffman, LeRoche); (3) examination of intracellular BP patterns and their comparison with those in untreated control material.

¹Supported by a National Institute of Health Pre-Doctoral Fellowship.

This report comprises part of a dissertation submitted to the Graduate Faculty of the University of Oklahoma in partial fulfillment of the requirements for the degree of Doctor of Philosophy.

which the enzymes had been omitted. In the case of DNAase an additional control preparation was made in which the enzyme and magnesium cofactor were jointly omitted. In any one preparation control or experimental several coverslips were processed together, part to be used for histochemical assay for the extent of nucleic acid removal effected by the phosphodiesterase and part for examination with the carcinogen.

Liver nuclear fractions Nucleic acids were removed from rat liver nuclei by a modification of the method of Georgiev and Chensov (62). (1) Nuclear fractions were prepared in 0.25 M sucrose as described above. (2) washed three times in McIlvaine's pH 6 buffer. (3) digested six hours in 1 mg/ml DNase with 0.005 M NaCl in pH 6 McIlvaine's buffer. (4) extracted in 1 M NaCl for 30 minutes in a cold room — the extraction being repeated 9 to 11 times.

At steps no 2 no 3 and no 4 samples were withdrawn from the fractions and subdivided for the following procedures: (a) observation of nuclei on crystalline beds of BP. (b) histochemical tests for nucleic acids. (c) measurement of nuclear sizes with a Leitz Ojeckmikrometer and (d) a test of the polymeric state of nucleoprotein in the nuclear fraction by its capacity to form gels in 1 M NaCl (Dounce '55). Nucleoprotein which did not flow down the side of an inverted test tube was designated a strong gel that which showed some flow was arbitrarily considered weak and that which was watery in consistency was designated as not capable of gel formation.

Methods of BP introduction and observation

BP was introduced from crystalline beds on glass coverslips or slides formed by evaporation of a saturated ethanol BP stock solution applied by wire loop 20 mm in diameter. The various biological materials were exposed to CH as follows: (1) Centrifuged or uncentrifuged liver cell suspensions in Eagle's MEM or BME and liver nuclear fractions in sucrose McIlvaine's buffer. DNAase solutions or 1 M NaCl were pipetted onto crystalline beds of BP prepared on glass slides. (2) Glass cover

slips bearing living or experimentally treated L-929 fibroblasts in growth medium or distilled water respectively were inverted and applied to BP crystalline beds on glass slides. (3) Crystalline BP beds were prepared on sterile glass coverslips in culture vessels and L-cells suspended in BME or MEM were pipetted into the vessels and cultured for 36-72 hours.

Two histochemical procedures were used to assess the presence and location of nucleic acids in experimental and control preparations: (a) the Feulgen reaction (Feulgen and Rossenbeck '24; Bauer '32) using Schiff's reagent prepared by the method of Coleman ('38) from Hartman and Leddon Basic Fuchsin. (b) Galloycin Chrom Alum prepared and used according to Einarson ('51) with RNAase or DNAase treated controls (Galloycin from Matheson, Coleman and Bell).

The equipment and methods of the integrated phase-contrast and ultrafluorescence microscopic technique were similar to those described in detail by Richter and Saini ('60).

OBSERVATIONS

L 929 fibroblasts

The form of L-cells on glass substrates was predominantly stellate with spindle shaped cells less common. The mitochondria were usually rod shaped or granular and occurred at random in the cytoplasm or oriented with the long axis of cell processes (figs 1-3). The Golgi material occurred in two forms: a condensed juxtanuclear zone (Bensch et al '64) appearing in approximately 33% of the cells (figs 19-25) and a dispersed form composed of small angular structures (Hayward '61). The Golgi granules (figs 1-3) located throughout the cytoplasm. L-cells contained a single oval to round nucleus although bi- or multinucleate cells and cells with micronuclear fragments were common (figs 1-3) as reported for many other strains of cultured cells (Lewis '47; '51; Bucher and Gattiker '53; Ludford '54; Hsu and Moorhead '55; '56; Nagata '60; Longwell and Yerganian '65). Nucleoli occurred either as large irregular structures numbering 1 to 3 per nucleus (figs 1-3) or as small compact entities numbering four or more per nucleus (figs

Preparation of biological material

Biological test material consisted of monolayers of Earle's L 929 mouse fibroblasts (Microbiological Associates) dissociated but intact liver cells in suspension and subcellular nuclear fractions from rat liver.

Routine stocks of strain L 929 fibroblasts were carried in Eagle's MEM or BME with 10% horse serum and a penicillin streptomycin mixture (Microbiological Associates or Flow Labs). Experimental studies were carried out on coverslip cultures grown in disposable petri dishes (Falcon Plastics). Cells were seeded at approximately 200 000 per ml and allowed to grow 2 to 4 days.

Whole liver cells were obtained from King Holtzman rats sacrificed by cervical dislocation. Small fragments of liver were quickly excised and immersed in Eagle's MEM or BME in a physiologically clean petri dish. Fragments were minced with no. 15 Bard Parker knives fitted with scissor type strokes of knives fitted with no. 15 Bard Parker knives until a turbid suspension of dissociated cells was obtained.

Subcellular nuclear fractions of King Holtzman rat livers were isolated in 0.25 M sucrose by a procedure similar to those described by Hogeboom et al. (62) and Allfrey et al. (57). Homogenization was done in 0.25 M sucrose with 0.0018 M CaCl_2 made up in triple distilled water (Cutter). Ten milliliters of medium was used per gram of tissue. The homogenate was filtered through 4 to 6 layers of sterile surgical gauze and the filtrate centrifuged at $150 \times G$ for ten minutes in an International Clinical Centrifuge Model CL to sediment the unbroken cells. The supernatant was then spun at approximately $380 \times G$ for ten minutes; the sediment represented the nuclear fraction. Resuspension and resedimentation of the nuclear fractions were done several times to remove as much non nuclear material as possible. All steps were carried out either in a cold room (2°) or in an ice bath.

Removal or displacement of nucleic acids

Ultracentrifugation Ultracentrifugation of liver tissue was accomplished with a

Beams air turbine centrifuge (J W Bear '30). Constant pressure air supply provided by a Quincy air-compressor (Model 325) rated at 22 cubic feet per minute and driven by a five hp motor.

Clean aluminum rotors were loaded with 0.5–0.8 cm³ of Eagle's BME or MEM and 3 to 5 liver fragments freshly excised and reduced to dimensions of approximately 0.3–0.5 cm by 1 to 2 cm. Centrifugal forces of 300 000 or 400 000 \times were maintained on the tissue for one and a half or two hours. Calculation of centrifugal forces was based on pressure rotational speed curves prepared for the rotors by Fritz Linke of the Physical Laboratory, University of Virginia.

In vitro preparations of centrifuged liver were prepared by mincing the fragments in the same manner as was described above for the uncentrifuged liver. Portions of the centrifuged tissue were fixed in formalin and sectioned in paraffin for histochemical tests.

L 929 fibroblasts Removal of nucleic acids from L-cells was carried out after fixation in Zenker's fluid (one hour) and conventional removal of mercuric chloride with Lugol's solution and sodium thiosulfate (Cowdry 48).

Deoxyribonuclease (DNAase) (Worthington, 1X crystallized) was used in M. Haines buffer (0.1 M citrate and 0.2 M phosphate) at pH 6.0 (Kunitz 50, Korsos 51, Daoust and Clermont 55) with 0.01 M MgCl_2 (Kunitz 50). The enzyme concentrations employed were 0.2–0.6 U/ml and 2.0 mg/ml. One mg% chloramphenicol (Parke Davis) was added to incubation media when the enzyme concentration exceeded 1 mg/ml. Incubation lasted 3 to 6 hours at 37° . The cells were fixed and digested directly on their original coverslip substrates.

For removal of RNA monolayers of Zenker's fluid fixed L-cells were incubated in RNAase (Cal Biochem 5X crystallized) for 30 minutes one or two hours at 37° or 60° after Brachet (51). 0.1 mg/ml enzyme was dissolved in triple distilled water (Cutter) whose pH was adjusted to 6.0 with 0.1 N NaOH.

Control preparations for both DNAase and RNAase were incubated in media for

which the enzymes had been omitted in the case of DNAase an additional control preparation was made in which the enzyme and magnesium cofactor were omitted. In any one preparation control or experimental several coverslips were processed together part to be used for histochemical assay for the extent of nucleic acid removal effected by the phosphodiesterase and part for examination with the carcinogen.

Liver nuclear fractions Nucleic acids were removed from rat liver nuclei by a modification of the method of Georgiev and Gentsov (62). (1) Nuclear fractions were prepared in 0.25 M sucrose as described above. (2) washed three times in 0.1 M Tris pH 6 buffer. (3) digested six hours in 1 mg/ml DNase with 0.005 M MgCl_2 in pH 6 McIlvaine's buffer. (4) extracted in 1 M NaCl for 30 minutes in a cold room — the extraction being repeated 9 to 11 times.

At steps no 2 no 3 and no 4 samples were withdrawn from the fractions and subdivided for the following procedures: (a) observation of nuclei on crystalline beds of BP. (b) histochemical tests for nucleic acids. (c) measurement of nuclear sizes with a Leitz Ojeckmikrometer and (d) a test of the polymeric state of nucleoprotein in the nuclear fraction by its tendency to form gels in 1 M NaCl (Dounce).

(1) Nucleoprotein which did not flow down the side of an inverted test tube was designated a strong gel that which showed some flow was arbitrarily considered weak and that which was watery in consistency was designated as not capable of gel formation.

Methods of BP introduction and observation

BP was introduced from crystalline beds on glass coverslips or slides formed by evaporation of a saturated ethanol BP stock solution applied by wire loop 20 mm in diameter. The various biological materials were exposed to CII as follows: (1) centrifuged or uncentrifuged liver cell suspensions in Eagle's MEM or BME and liver nuclear fractions in sucrose McIlvaine's buffer. DNAase solutions or 1 M NaCl were pipetted onto crystalline beds of BP prepared on glass slides. (2) Glass cover

slips bearing living or experimentally treated L-929 fibroblasts in growth medium or distilled water respectively were inverted and applied to BP crystalline beds on glass slides. (3) Crystalline BP beds were prepared on sterile glass coverslips in culture vessels and L-cells suspended in BME or MEM were pipetted into the vessels and cultured for 36–72 hours.

Two histochemical procedures were used to assess the presence and location of nucleic acids in experimental and control preparations: (a) the Feulgen reaction (Feulgen and Rossenbeck 24 Bauer 32) using Schiff's reagent prepared by the method of Coleman (38) from Hartman and Leddon Basic Fuchsin. (b) Gallocyanin Chrom Alum prepared and used according to Einarson (51) with RNAase or DNAase treated controls (Gallocyanin from Matheson Coleman and Bell).

The equipment and methods of the integrated phase-contrast and u.v. fluorescence microscopic technique were similar to those described in detail by Richter and Sami (60).

OBSERVATIONS

L 929 fibroblasts

The form of L-cells on glass substrates was predominantly stellate with spindle shaped cells less common. The mitochondria were usually rod shaped or granular and occurred at random in the cytoplasm or oriented with the long axis of cell processes (figs 1–3). The Golgi material occurred in two forms: a condensed juxtaposed clear zone (Bensch et al 64) appearing in approximately 33% of the cells (figs 19–25) and a dispersed form composed of small angular structures (Hayward 61) the Golgi granules (figs 1–3) located throughout the cytoplasm. L-cells contained a single oval to round nucleus although bi or multinucleate cells and cells with micronuclear fragments were common (figs 1–3) as reported for many other strains of cultured cells (Lewis 47 51 Bucher and Gattiker 53 Ludford 54 Hsu and Moorhead 55 56 Nagata 60 Longwell and Yerganian 65). Nucleoli occurred either as large irregular structures numbering 1 to 3 per nucleus (figs 1–3) or as small compact entities numbering four or more per nucleus (figs

Preparation of biological material

Biological test material consisted of monolayers of Earle's L-929 mouse fibroblasts (Microbiological Associates) dissociated but intact liver cells in suspension and subcellular nuclear fractions from rat liver.

Routine stocks of strain L-929 fibroblasts were carried in Eagle's MEM or BME with 10% horse serum and a penicillin streptomycin mixture (Microbiological Associates or Flow Labs). Experimental studies were carried out on coverslip cultures grown in disposable petri dishes (Falcon Plastics). Cells were seeded at approximately 200 000 per ml and allowed to grow 2 to 4 days.

Whole liver cells were obtained from King Holtzman rats sacrificed by cervical dislocation. Small fragments of liver were quickly excised and immersed in Eagle's MLM or BME in a physiologically clean petri dish. Fragments were minced with scissor type strokes of knives fitted with no. 15 Bard Parker knives until a turbid suspension of dissociated cells was obtained.

Subcellular nuclear fractions of King Holtzman rat livers were isolated in 0.25 M sucrose by a procedure similar to those described by Hogeboom et al. (62) and Allfrey et al. (57). Homogenization was done in 0.25 M sucrose with 0.0018 M CaCl_2 made up in triple distilled water (Cutter). Ten milliliters of medium was used per gram of tissue. The homogenate was filtered through 4 to 6 layers of sterile surgical gauze and the filtrate centrifuged at $150 \times G$ for ten minutes in an International Clinical Centrifuge Model CL to sediment the unbroken cells. The supernatant was then spun at approximately $380 \times G$ for ten minutes; the sediment represented the nuclear fraction. Resuspension and resedimentation of the nuclear fractions were done several times to remove as much non-nuclear material as possible. All steps were carried out either in a cold room (2°) or in an ice bath.

Removal or displacement of nucleic acids

Ultracentrifugation Ultracentrifugation of liver tissue was accomplished with a

Beam's air turbine centrifuge (J. W. Be. 30). Constant pressure air supply provided by a Quincy air compressor (Model 325) rated at 22 cubic feet per minute and driven by a five hp motor.

Clean aluminum rotors were loaded with 0.5–0.8 cm³ of Eagle's BME or MLM and 3 to 5 liver fragments freshly excised and reduced to dimensions of approximately 0.3–0.5 cm by 1 to 2 cm. Centrifugal forces of 300 000 or 400 000 $\times G$ were maintained on the tissue for one and a half, or two hours. Calculation of centrifugal forces was based on pressure rotational speed curves prepared for rotors by Fritz Lanke of the Physical Laboratory, University of Virginia.

In vitro preparations of centrifuged liver were prepared by mincing the fragments in the same manner as was described above for the uncentrifuged liver. Portions of the centrifuged tissue were fixed in formalin and sectioned in parallel for histochemical tests.

L-929 fibroblasts Removal of nucleic acids from L-cells was carried out as follows: fixation in Zenker's fluid (one hour), conventional removal of mercuric chloride with Lugol's solution and sodium thiosulfate (Cowdry 48).

Deoxyribonuclease (DNAase) (Worthington 1X crystallized) was used in 1 M ilvaines buffer (0.1 M citrate and 0.2 M phosphate) at pH 6.0 (Kunitz 50 kers 51 Daoust and Clermont 55) with 0.01 M MgCl_2 (Kunitz 50). The enzyme concentrations employed were 0.2, 0.6, and 2.0 mg/ml. One mg% chloramphenicol (Parke Davis) was added to incubation media when the enzyme concentration exceeded 1 mg/ml. Incubation lasted 3 to 6 hours at 37° . The cells were fixed and digested directly on their original coverslip substrates.

For removal of RNA monolayers Zenker's fluid fixed L-cells were incubated in RNAase (Cal Biochem 5X crystallized for 30 minutes, one or two hours at 37° , 60 after Brachet (51)) 0.1 mg/ml. The enzyme was dissolved in triple distilled water (Cutter) whose pH was adjusted to 6.0 with 0.1 N NaOH.

Control preparations for both DNAase and RNAase were incubated in media from

living preparations (Beams and King 43, Claude 43, Lagerstedt 49, Brenner 51, Bernhard et al 54, Kopac 55). Gallo-cyanin-Chrom Alum staining after DNAase treatment and Feulgen staining demonstrated that RNA and DNA occurred in the chromatin (figs 33-34). In agreement with Brenner (53), some nuclear membrane associated chromatin did not sediment even under forces of $200,000 \times G$ for two hours (figs 33-34). Interchromatin regions, especially in the centripetal portions of the nucleus, appeared to be free of histochemically demonstrable nucleic acid.

The distribution of BP in ultracentrifuged cells in comparison with uncentrifuged controls suggested that the displacement of cell organelles had no effect on their affinity for BP. Lipid droplets and the small granule component showed high concentrations of the CH and mitochondria relatively little uptake of BP (figs 36-38). Displacement of nuclear chromatin also had no effect in altering the lack of affinity of all intranuclear structures for CH (figs 36-38).

Liver cell nuclei

Pellets of liver nuclei fractionated in 0.25 M sucrose-0.0018 M CaCl₂ were always contaminated with cytoplasmic material. The nuclei resembled those prepared by Roodyn (63) in being circumscribed by a dark nuclear rim and containing one to several dark compact nucleoli in nearly featureless non-nucleolar karyoplasm (figs 39-41). Resuspension of the nuclei in pH 6.0 bicarbonate buffer and incubation for six hours at 37° produced (a) coalescence of the non-nucleolar karyoplasm (b) the appearance of blebs on the nuclear rim and

(c) the agglutination of cytoplasmic debris on the nuclear rim (fig 43). These characteristics were also found when MgCl₂ was added to the incubation buffer (figs 45-47). Weak nucleoprotein gels were formed by nuclear fractions incubated in buffer whereas strong gels having little or no flow were formed by the fresh sucrose preparations (table 1).

Resuspension and incubation of sucrose isolated nuclei in DNAase caused the loss of all Feulgen stainable material and the appearance of clear areas in the non-nucleolar karyoplasm as found by Anderson (53b) (figs 49-51). Sequential treatment with DNAase and 1M NaCl produced poor yields of shrunken, distorted nuclei. In these nuclei the nuclear rim was connected to the residual nucleolus by a few strands of dark material (figs 53-56-58). The average nuclear size was less than one third that of the untreated nuclei in sucrose (table 1). Staining with the Feulgen procedure or Gallo-cyanin-Chrom Alum was not observed in any of the exhaustively extracted nuclei (table 1).

BP accumulations in liver nuclei prepared in 0.25 M sucrose were limited to the nuclear rim (figs 40-42) confirming the findings of Norden (57). No demonstrable BP occurred within the confines of the nuclear rim in Feulgen negative nuclei incubated in DNAase (figs 50-52) or in buffer with or without magnesium (figs 44-46-48). No apparent CH concentration occurred in nuclear blebs except in their rims (figs 44-46-50). Fluorescence occurring over the dark central non-fluorescent intranuclear region appeared referable to localizations of BP in cytoplasmic

TABLE 1
Characteristics of treated liver nuclei¹

Treatment	Feulgen	Gel	Nuclear dimensions ²
1. In 0.25 M sucrose and 0.0018 M CaCl ₂	yes	strong	11.0 (±2.55) × 8.7 (±2.26)
2. In McDermott's B six hours without Mg	yes	weak	5.7 (±1.36) × 5.2 (±0.85)
3. In McDermott's B six hours with Mg	yes	weak	5.3 (±1.04) × 5.0 (±0.92)
4. In DNAase solution	no	none	5.6 (±1.26) × 5.5 (±0.64)
5. In DNAase followed by 1 M NaCl	no	none	3.8 (±0.11) × 3.6 (±0.05)

¹Observations were carried out on more than 600 nuclei per procedure except those in the DNAase-1M NaCl preparation where only 53 nuclei in 8 preparations were found.
²The size dimensions and standard deviations are all in mic.

5 7) Vacuolation (Lewis 43) occurred in the large nucleoli (figs 5 9)

The distribution of BP in living L cells was similar in cells exposed to the CH crystals for a few moments or cultured on BP several days. Accumulations of CH were relatively greatest in components of the Golgi apparatus (figs 2 4). Mitochondria displayed lower apparent BP concentrations than occurred throughout the general cytoplasmic matrix (fig 2). All nuclear structures including nuclear membrane nucleoli chromatin and micronuclei showed no demonstrable accumulation of BP.

Fixation of L cells with Zenker's fluid produced a coarsely precipitated cytoplasm in which no mitochondria were observed (Strangeways and Canti 28). Lipid droplets and vacuoles appeared much more commonly in the fixed cells than in the living (figs 5 7). Golgi material preservation was apparently variable (cf figs 11 13 vs figs 5 7). The chromatin material was finely precipitated and more discrete than in living cells both chromatin and nucleoli tended to be relatively more refractile than in life (figs 5 7). A dense precipitation of cytoplasmic and nucleoplasmic material in the nuclear membrane region was characteristic of Zenker's fluid fixation (figs 5 7).

No alteration in the phase contrast microscopic morphology of Zenker's fluid fixed cells was incurred when mercuric chloride was removed with Lugol's solution and thiosulfate (fig 9). No apparent changes in Zenker's fluid fixed cytology occurred when cells were (a) incubated in Mellvaine's buffer six hours (fig 11) (b) digested with DNAase with or without the magnesium cofactor (figs 13 15 17 19) so that Feulgen staining was totally abolished (c) digested with RNAase so that Gallocyanin Chrom Alum staining of the cytoplasm was absent and nuclear staining reduced (figs 21 23) or (d) sequentially incubated with both phosphodiesterases until Feulgen and Gallocyanin Chrom Alum staining were absent or greatly reduced (figs 25 27). No depletion in the amount of precipitated chromatin material was noticed although a substantial diminution of histochemically demonstrable nucleic

acid was obtained (figs 13 15 17 19 21 23).

The pattern of intracellular BP appeared similar in the enzyme treated and untreated Zenker's fluid fixed cells. Golgi material and lipid droplets demonstrated the relatively highest BP accumulation while lower CH concentrations were localized in the cytoplasmic vacuoles in cells digested with DNAase (with or without magnesium — figs 14 16 18 20) with RNAase (figs 22 24) with RNAase and DNAase (figs 26 28) or in cells simplified in Zenker's fluid with or without removal of mercuric chloride (figs 6 8 10). No demonstrable BP was localized in any nuclear structure in cells depleted of DNA (figs 14 16 18 20) RNA (figs 22 24) DNA and RNA (figs 26 28) or in cells in which the nucleic acid complement was intact (figs 6 8 10 12).

Hepatic paraenchymal cells

In living rat hepatic parenchymal cells, the nuclei contained discrete nuclear membranes, one to several irregular shaped dark nucleoli and irregular strands of chromatin (Zollinger 48, Bucciolini and Marsili 60, Colosi and Marsili 60) (figs 29 31). In the cytoplasm mitochondria lipid droplets and a fine granular component of uncertain nature were distinguishable (figs 29 31). Intracellular BP was not localized in any nuclear structure or in the mitochondria accumulations of the CH occurred in lipid droplets and the small granule component in relatively greater concentrations than those in the general cytoplasmic matrix (figs 30 32).

Living ultracentrifuged liver cells observed in slide preparations failed to consistently show discrete cytoplasmic strata in contrast to three or four strata found on fixed sections of the same material and as reported by Beams and King (34), Claude (43), Lagerstedt (49), Bernhard et al (54) and Kopac (55). The distinctness of the cytoplasmic strata was probably due to relocation of components during the preparation after centrifugation (Matejko and Kopac, 63).

Most nuclear chromatin in ultracentrifuged liver cells was found sedimented against the centrifugal nuclear pole (figs 33 34) as previously described for fixed

or lung preparations (Beams and King 34 Claude 43 Lagerstedt 49 Brenner 53 Bernhard et al 54 Kopac 55) Gallo-cyanin-Chrom Alum staining after DNAase hydrolysis and Feulgen staining demonstrated that RNA and DNA occurred in the chromatin (figs 33 34) In agreement with Brenner (53) some nuclear membrane associated chromatin did not sediment, even under forces of $200\,000 \times G$ for two hours (figs 33 34) Interchromatin regions especially in the centripetal portions of the nucleus appeared to be free of histochemically demonstrable nucleic acid.

The distribution of BP in ultracentrifugal cells in comparison with uncentrifuged controls suggested that the displacement of cell organelles had no effect on their affinity for BP Lipid droplets and the small granule component showed high concentrations of the CH and mitochondria relatively little uptake of BP (figs 36 38) Displacement of nuclear chromatin also had no effect in altering the lack of affinity of all intranuclear structures for CH (figs 36 38)

Liver cell nuclei

Pellets of liver nuclei fractionated in 0.25 M sucrose-0.0018 M CaCl_2 were always contaminated with cytoplasmic material. The nuclei resembled those prepared by Roodyn (63) in being circumscribed by a dark nuclear rim and containing one to several dark compact nucleoli in nearly hyaline non nucleolar karyoplasm (figs 39 41) Resuspension of the nuclei in pH 6.0 McIlwaine's buffer and incubation for six hours at 37 produced (a) coalescence of the non nucleolar karyoplasm (b) the ap-

pearance of blebs on the nuclear rim and (c) the agglutination of cytoplasmic debris on the nuclear rim (fig 43) These characteristics were also found when MgCl_2 was added to the incubation buffer (figs 45 47) Weak nucleoprotein gels were formed by nuclear fractions incubated in buffer whereas strong gels having little or no flow were formed by the fresh sucrose preparations (table 1)

Resuspension and incubation of sucrose isolated nuclei in DNAase caused the loss of all Feulgen-stainable material and the appearance of clear areas in the non nucleolar karyoplasm as found by Anderson (53b) (figs 49 51) Sequential treatment with DNAase and 1M NaCl produced poor yields of shrunken distorted nuclei In these nuclei the nuclear rim was connected to the residual nucleolus by a few strands of dark material (figs 53 56 58) The average nuclear size was less than one third that of the untreated nuclei in sucrose (table 1) Staining with the Feulgen procedure or Gallo-cyanin-Chrom Alum was not observed in any of the exhaustively extracted nuclei (table 1)

BP accumulations in liver nuclei prepared in 0.25 M sucrose were limited to the nuclear rim (figs 40 42) confirming the findings of Nordin (57) No demonstrable BP occurred within the confines of the nuclear rim in Feulgen negative nuclei incubated in DNAase (figs 50 52) or in buffer with or without magnesium (figs 44 46 48) No apparent CH concentration occurred in nuclear blebs except in their rims (figs 44 46 50) Fluorescence occurring over the dark central non fluorescent intranuclear region appeared referable to localizations of BP in cytoplas-

TABLE 1
Characteristics of treated liver nuclei¹

Treatment	Feulgen	Gel	Nuclear dimensions ²
1. In 0.25 M sucrose and 0.0018 M CaCl_2	yes	strong	$11.0 (\pm 2.5) \times 8.7 (\pm 2.26)$
2. In McIlwaine's B six hours without Mg	yes	weak	$5.7 (\pm 1.36) \times 5.2 (\pm 0.85)$
3. In McIlwaine's B six hours with Mg	yes	weak	$5.3 (\pm 1.04) \times 5.0 (\pm 0.92)$
4. In DNAase solution	no	none	$5.6 (\pm 1.26) \times 5.5 (\pm 0.64)$
5. In DNAase followed by 1 M NaCl	no	none	$3.8 (\pm 0.11) \times 3.6 (\pm 0.05)$

¹Observations were carried out on more than 600 nuclei per procedure except those in the DNAase-1M NaCl preparations where only 53 nuclei in five preparations were found.
²The nuclear dimensions and standard deviation are all in microns.

5 7) Vacuolation (Lewis 43) occurred in the large nucleoli (figs 5 9)

The distribution of BP in living L cells was similar in cells exposed to the CH crystals for a few moments or cultured on BP several days. Accumulations of CH were relatively greatest in components of the Golgi apparatus (figs 2 4). Mitochondria displayed lower apparent BP concentrations than occurred throughout the general cytoplasmic matrix (fig 2). All nuclear structures including nuclear membrane nucleoli chromatin and micronuclei showed no demonstrable accumulation of BP.

Fixation of L-cells with Zenker's fluid produced a coarsely precipitated cytoplasm in which no mitochondria were observed (Strangeways and Cantu 28). Lipid droplets and vacuoles appeared much more commonly in the fixed cells than in the living (figs 5 7). Golgi material preservation was apparently variable (cf figs 11 13 vs figs 5 7). The chromatin material was finely precipitated and more discrete than in living cells both chromatin and nucleoli tended to be relatively more refractile than in life (figs 5 7). A dense precipitation of cytoplasmic and nucleoplasmic material in the nuclear membrane region was characteristic of Zenker's fluid fixation (figs 5 7).

No alteration in the phase contrast microscopic morphology of Zenker's fluid fixed cells was incurred when mercuric chloride was removed with Lugol's solution and thiosulfate (fig 9). No apparent changes in Zenker's fluid fixed cytology occurred when cells were (a) incubated in McIlvaine's buffer six hours (fig 11) (b) digested with DNAase with or without the magnesium cofactor (figs 13 15 17 19) so that Feulgen staining was totally abolished (c) digested with RNAase so that Gallocyanin Chrom Alum staining of the cytoplasm was absent and nuclear staining reduced (figs 21 23) or (d) sequentially incubated with both phosphodiesterases until Feulgen and Gallocyanin Chrom Alum staining were absent or greatly reduced (figs 25 27). No depletion in the amount of precipitated chromatin material was noticed although a substantial diminution of histochemically demonstrable nucleic

acid was obtained (figs 13 15 17 19 21 23).

The pattern of intracellular BP appeared similar in the enzyme treated and untreated Zenker's fluid fixed cells. Golgi material and lipid droplets demonstrated the relatively highest BP accumulation while lower CH concentrations were localized in the cytoplasmic vacuoles in cells digested with DNAase (with or without magnesium—figs 14 16 18 20) with RNAase (figs 22 24) with RNAase and DNAase (figs 26 28) or in cells simply fixed in Zenker's fluid with or without removal of mercuric chloride (figs 6 8 10). No demonstrable BP was localized in any nuclear structure in cells depleted of DNA (figs 14 16 18 20) RNA (figs 22 24) DNA and RNA (figs 26 28) or in cells in which the nucleic acid complement was intact (figs 6 8 10 12).

Hepatic parenchymal cells

In living rat hepatic parenchymal cells the nuclei contained discrete nuclear membranes one to several irregular shaped dark nucleoli and irregular strands of chromatin (Zollinger 48 Bucciolini and Marsili 60 Colosi and Marsili 60) (figs 29 31). In the cytoplasm mitochondria lipid droplets and a fine granular component of uncertain nature were distinguishable (figs 29 31). Intracellular BP was not localized in any nuclear structure or in the mitochondria accumulations of the CH occurred in lipid droplets and the small granule component in relatively greater concentrations than those in the general cytoplasmic matrix (figs 30 32).

Living ultracentrifuged liver cells observed in slide preparations failed to consistently show discrete cytoplasmic strata in contrast to three or four strata found on fixed sections of the same material and as reported by Beams and King (34) Claude (43) Lagerstedt (49) Bernhard et al (54) and Kopac (55). The indistinctness of the cytoplasmic strata was probably due to relocation of components during the preparation after centrifugation (Mateyko and Kopac 63).

Most nuclear chromatin in ultracentrifuged liver cells was found sedimented against the centrifugal nuclear pole (figs 33 34) as previously described for fixed

The retention and assay of nucleic acids

Existing literature suggests complete removal of nucleic acids from cells is not achieved with either nuclease or salt extraction. DNA reportedly remains in liver sections fixed in any of several fluids including Zenkers after DNAase hydrolysis (Fixq and Errera 58). Isolated unfixed tissue nucleic acids have variously been reported to retain about one fourth of their total DNA content after DNAase treatment (Allfrey et al 57; Allfrey and Mirsky 58; Naora et al 61). Some RNA remains in unfixed nuclei after exhaustive enzymatic and salt extractions (Georgiev 58; Zbarski and Georgiev 59; Smetana et al 63; Steele and Busch 63).

The Feulgen reaction as a method for assessing DNA reportedly has a high threshold of sensitivity (Widstrom 28; Caspersson 32; Ris and Mirsky 49; Dische 55). The binding of Gallocyanin Chrom Alum with either DNA or RNA occurs stoichiometrically but apparently to precise data on the nucleic acid concentration range demonstrable with the Emisson technique has been presented (Sandritter et al 63).

The limitations in histochemical sensitivity as well as the incomplete extractability of nucleic acids mean that nuclei totally free of nucleic acids probably have not been obtained in the present study. Presumably if CH fluorescence is quenched by intranuclear nucleic acids a reduction in the nucleic acid concentrations to or below the sensitivity thresholds for the Feulgen and Gallocyanin Chrom Alum tests would result in the appearance of a faint intranuclear fluorescence.

CONCLUSIONS

Cells and their nuclei submitted to three different experimental procedures for assaying nucleic acid content at specific cell sites consistently showed no apparent BP accumulations in intranuclear material. This invariable pattern of BP compartmentalization is similar to that observed in living cells relative to the nucleus. The evident lack of dependence of the BP pattern on nucleic acid content or distribution suggests that the nucleic acid associated quenching of BP fluorescence found

by Boyland and Green (62) using biochemical techniques may not occur in biological structures such as the nucleus.

Berg (51-52) hypothesized the lack of intranuclear accumulation of BP was related to the absence of lipid in the nucleus. There are however numerous biochemical and histochemical reports of lipid in the nucleus in chromosomes — both mitotic and interphase (Claude and Potter 43; Ris and Mirsky 49; Cohen 49; Brock et al 52; Idelman 57; 58a, b; Chayen et al 57; 59; LaCour et al 58) in nucleoli (Brock et al 52; Zagury 57; Barer and Dick 57; Georgiev 58; Zbarski et al 62; Georgiev and Chentsov 62) in the nuclear membrane (Schmitt 38) and in whole nuclei (Stoneburg 39; Hack 48; Engbring and Laskowski 53; Wang et al 53; Dounce 55; Chauveau et al 56; Levin and Thomas 61). Experimental lipid extraction of cells generally supports Berg's position that lipid determines the distribution of CH in the cytoplasm (Shires 65b) but at present there is no data on which to base an explanation for the lack of affinity for BP by cell sites which apparently contain lipid.

The lack of intranuclear fluorescence in live cells exposed to BP may indicate low levels of BP but not its total absence from the nucleus. While concentrations near those in serum (60-70 µg/ml in calf serum — Morimura et al 64) are perceptible with u.v. fluorescence microscopy (Richter and Saini 60) lower concentrations perhaps would be indiscernible in the nucleus. Reactions between CH and cell constituents would seem more likely in sites where apparently high CH concentrations occur e.g. the cytoplasm than in regions where at most very low concentrations are suspected. Of the various proposed mechanisms of chemical carcinogenesis, u.v. fluorescence microscopic data is not consistent with direct interaction between CH and chromosomal material (e.g. Hadlow 58) but does support theories which allow primary CH reactions to occur at the edge of the nucleus or in the cytoplasm (e.g. Pitot and Heidelberger 63).

ACKNOWLEDGMENTS

The author wishes to express his gratitude to Dr K. M. Richter for his guidance.

mlic debris on the nuclear rim Liver nuclei sequentially treated with DNAase and 1 M NaCl displayed high accumulations of CH in the nuclear rim but no demonstrable BP in the nuclear interior (figs 54 55, 57 59) The pattern of BP distribution in all experimentally treated isolated liver nuclei was similar to the pattern of BP relative to the nucleus in live hepatic parenchymal cells

DISCUSSION

No demonstrable intranuclear BP was found in live fibroblasts and hepatic cells or in nuclear fractions from which nucleic acids had been removed or displaced These results were obtained despite the cytologic alterations resulting from the side effects of the procedures for nucleic acid removal

Fixation of fibroblasts was necessary for the long enzymatic hydrolysis and was achieved using Zenker's fluid fixation which was compatible with nuclease activity (cf Brachet 53, Pearse 60) and caused little alteration in the live cell pattern of intracellular BP Its selection was made after preliminary studies previously reported in part (Shires, 65a) The effect of Zenker's fluid fixation in agglutinating material to the nuclear membrane and in precipitating the karyoplasm also seen by Strangeways and Canti (28) probably led to the common incidence of CH fluorescence imposed on the nuclear profile by highly BP rich cytoplasmic structures above or below the nuclear rim No noticeable change in the appearance of Zenker's fluid fixed protoplasm was found after incubation with RNAase DNAase or the buffer without enzyme

The DNAase incubation medium used on rat liver nuclear fractions contained constituents in addition to the enzyme which altered the appearance of nuclei isolated in sucrose solutions Suspension and incubation of nuclei in McIlvaine's buffer with or without Mg led to changes described by others for Mg phosphate or citrate ions at concentrations similar to those in the incubation medium (1) condensation of the nucleoplasm (Bernstein and Mazia 53, Philpott and Stanier, 56

57 Schneider 55 Roodyn, 63) (2) promotion of the appearance of blebs from the nuclear rim (Anderson 53a) (3) decrease in nuclear volume (Anderson and Wilbur 52) The incubation mixture also contained cytoplasmic contaminants of the nuclear fraction which probably contributed some DNAase activity (Dounce et al 57)

Exhaustive nucleic acid extraction by the sequential treatments of isolated nuclei with phosphodiesterase and 1 M NaCl entails removal of chromosomal and peripheral chromosomal globulins DNA, histones and the tryptophane rich proteins (Mirsky and Pollister, 46 Mirsky and Ris 50 51 Georgiev, 58 Zbarski and Georgiev 59 Zbarski et al 62 Georgiev and Chentsov 62 Steele and Busch 63 Busch et al 63) The removal of these substances probably leaves some unextractable ribonucleoprotein uncharacterized lipid and an acidic protein (Mirsky and Pollister, 46 Wang et al 53 Georgiev 58 Zbarski and Georgiev 59 Zbarski and Ermolaeva 60 Zbarski et al 62 Georgiev and Chentsov 62 Steele and Busch, 63 Busch et al 63) in which BP could accumulate The phase contrast photomicrographs of the present study and the electron micrographs of Zbarski et al (62) and Georgiev and Chentsov (62) suggest that most of this residual material is located in the nuclear rim

In contrast to the nucleic acid removal procedures ultracentrifugal dislocation of chromatin represents an alteration not harmful even to highly differentiated cell types (Guyer and Claus 36a b MacDougald et al 37 Dornfeld 36 37 Mateyko and Kopac 63) The results of this mild procedure on the intracellular distribution of BP confirm those of Waddington and Goodhart (49) on oocytes and gastrular cells of *Triturus alpestris*, using BP solubilized with caffeine The similarity of the nuclear BP patterns in centrifuged rat liver cells with those in nucleic acid depleted L-cells and nuclear fractions suggests that the technical alterations involved in the nuclease or extraction procedures did not influence the distribution of BP

The retention and assay of nucleic acids

Existing literature suggests complete removal of nucleic acids from cells is not achieved with either nuclease or salt extraction. DNA reportedly remains in liver sections fixed in any of several fluids including Zenker's after DNAase hydrolysis (Ficq and Errera 58). Isolated unfixed thymic nucleic acids have variously been reported to retain about one fourth of their total DNA content after DNAase treatment (Allfrey et al 57, Allfrey and Mirsky 58, Naora et al 61). Some RNA remains in unfixed nuclei after exhaustive enzymatic and salt extractions (Georgiev 58, Zbarski and Georgiev 59, Smetana et al 63, Steele and Busch 63).

The Feulgen reaction as a method for assessing DNA reportedly has a high threshold of sensitivity (Widstrom 28, Cispersson 32, Ris and Mirsky 49, Dische 55). The binding of Galloyanin Chrom Alum with either DNA or RNA occurs stoichiometrically but apparently no precise data on the nucleic acid concentration range demonstrable with the Emerson technique has been presented (Sandritter et al 63).

The limitations in histochemical sensitivity as well as the incomplete extractability of nucleic acids mean that nuclei totally free of nucleic acids probably have not been obtained in the present study. Presumably if CH fluorescence is quenched by intranuclear nucleic acids a reduction in the nucleic acid concentrations to or below the sensitivity thresholds for the Feulgen and Galloyanin Chrom Alum tests would result in the appearance of a faint intranuclear fluorescence.

CONCLUSIONS

Cells and their nuclei submitted to three different experimental procedures for altering nucleic acid content at specific cell sites consistently showed no apparent BP accumulations in intranuclear material. This unvariable pattern of BP compartmentalization is similar to that observed in liver cells relative to the nucleus. The evident lack of dependence of the BP pattern on nucleic acid content or distribution suggests that the nucleic acid associated quenching of BP fluorescence found

by Boyland and Green (62) using biochemical techniques may not occur in biologic structures such as the nucleus.

Berg (51, 52) hypothesized the lack of intranuclear accumulation of BP was related to the absence of lipid in the nucleus. There are however numerous biochemical and histochemical reports of lipid in the nucleus in chromosomes — both mitotic and interphase (Claude and Potter 43, Ris and Mirsky 49, Cohen 49, Brock et al 52, Idelman 57, 58a, b, Chayen et al 57, 59, LaCour et al 58) in nucleoli (Brock et al 52, Zagury 57, Barer and Dick 57, Georgiev 58, Zbarski et al 62, Georgiev and Chentsov 62) in the nuclear membrane (Schmitt 38) and in whole nuclei (Stoneburg 39, Hack 48, Engbring and Laskowski 53, Wang et al 53, Dounce 55, Chauveau et al 56, Levin and Thomas 61). Experimental lipid extraction of cells generally supports Berg's position that lipid determines the distribution of CH in the cytoplasm (Shires 65b) but at present there is no data on which to base an explanation for the lack of affinity for BP by cell sites which apparently contain lipid.

The lack of intranuclear fluorescence in live cells exposed to BP may indicate low levels of BP but not its total absence from the nucleus. While concentrations near those in serum (60–70 µg/ml in calf serum — Morimura et al 64) are perceptible with *uv* fluorescence microscopy (Richter and Saini 60), lower concentrations perhaps would be indiscernible in the nucleus. Reactions between CH and cell constituents would seem more likely in sites where apparently high CH concentrations occur, e.g. the cytoplasm than in regions where at most very low concentrations are suspected. Of the various proposed mechanisms of chemical carcinogenesis, *uv* fluorescence microscopic data is not consistent with direct interaction between CH and chromosomal material (e.g. Hadlow 58) but does support theories which allow primary CH reactions to occur at the edge of the nucleus or in the cytoplasm (e.g. Pitot and Heidelberger 63).

ACKNOWLEDGMENTS

The author wishes to express his gratitude to Dr K. M. Richter for his guidance.

during the course of this work and for his help in the preparation of this manuscript. The helpful suggestions of Dr J F Lhotka are also gratefully acknowledged.

LITERATURE CITED

- Allfrey V G and A E Mirsky 1958 Some effects of substituting desoxyribonucleic acid of isolated nuclei with other polyelectrolytes Proc Nat Acad Sci 44 981-991
- Allfrey V G S Osawa and A E Mirsky 1957 Protein synthesis in isolated cell nuclei J Gen Physiol 40 451-490
- Anderson N G 1943a Studies of isolated cell components V The effects of various solutions on the nuclear envelope of the isolated rat liver nucleus Exp Cell Res 4 306-315
- 1953b Studies of isolated cell components VI The effects of nucleases and proteases on rat liver nuclei Exp Cell Res 5 361-374
- Anderson N G and K M Wilbur 1952 Studies of isolated cell components IV The effects of various solutions on the isolated rat liver nucleus J Gen Physiol 35 781-797
- Barer, D and D A T Dick 1957 Interferometry and refractometry of cells in tissue culture Exp Cell Res Suppl 13 103-135
- Bauer, H 1932 Die Feulgensche Nuklealfärbung in Ihrer Anwendung auf Cytologische Untersuchungen Ztschr Zellforsch 15 225-247
- Beams J W 1930 An apparatus for obtaining high speeds of rotation Rev Sci Instr 1 667-671
- Beams H W and R. L. King 1934 Effect of ultracentrifugation on the mitochondria of the hepatic cells of the rat Anat Rec 59 395-401
- Bensch K, G Gordon and L Miller 1964 The fate of DNA-containing particles phagocytized by mammalian cells J Cell Biol 21 105-114
- Berg N O 1951-52 A histological study of masked lipid stainability, distribution and functional variations Acta Path Microbiol Scand Suppl 90 1-192
- Bernhard W A Gautier and C Roullier 1954 La notion de *microsomes* et la problem de la basophile cytoplasmique. Etude critique et experimentale Arch d'Anat 43 236-275
- Bernstein M H and D Mazia 1953 The desoxyribonucleoprotein of sea urchin sperm II Properties Blochem Biophys Acta 11 59-68
- Boydland, E and B Green 1962 The interaction of polycyclic hydrocarbons and nucleic acids Brit J Canc 16 507-517
- 1964 On the reported sedimentation of polycyclic hydrocarbons from aqueous solutions of DNA J Mol Biol 9 589-597
- Brachet J 1953 The use of basic dyes and ribonuclease for the cytochemical detection of ribonucleic acid Quart J Micr Sci 94 1-10
- Brenner S 1953 The chromatic nuclear membrane Exp Cell Res 5 257-260
- Brock B R E Stowell and K. Couch 195 Staining of intranuclear lipids of mouse liver under different conditions of growth Lab Invest 1 439-446
- Bucciolini M G and G Marsili 1960 La morfologia della cellule epatiche isolate e ratto osservate al microscopio elettronico Sperimentale 110 177-190
- Bucher O and R Gattiker 1953 Contribution a l'etude des cellules binuclees dans les cultures de fibroblasts Exp Cell Res 5 461-477
- Busch H P Byvoet and K Smetana 1963 The nucleolus of the cancer cell a review Cancer Res 23 313-339
- Caspersson T O 1932 Die quantitative Bestimmung von Thymonucleinsäure mittels fuchsin-schwefeliger Säure Blochem Ztschr 253 97-111
- Chauveau J T Moulé and C Roullier 1956 Isolation of pure and unaltered nuclei morphology and biochemical composition Exp Cell Res 11 317-321
- Chayen J L F LaCour and P B Gahan 1956 Uptake of benzpyrene by a chromosomal phospholipid Nature 180 652-653
- Chayen J P B Gahan and L F LaCour 1956 The nature of a chromosomal phospholipid Quart J Micr Sci 100 279-284
- Claude A 1943 Distribution of nucleic acids in the cell and the morphological constitution of cytoplasm Biol Symp 10 111-129
- Claude A and J S Potter 1943 Isolation of chromatin threads from the resting nucleus of leukemic cells J Exp Med 77 345-354
- Cohen I 1949 Sudan Black B — a new stain for chromosome smear preparations Stain Tech 24 177-184
- Coleman L C 1938 Preparation of leuco basic fuchsin for use in the Feulgen reaction Stain Tech 13 123-124
- Colosi G and G Marsili 1960 Aspetti istochimici di cellule epatiche isolate in sopravvivenza Boll Soc Ital Biol Sperim 36 1137-1140
- Cowdry E V 1948 Laboratory Technique in Biology and Medicine Williams and Wilkins, Co Baltimore Md
- Daoust R and Y Clermont 1955 Distribution of nucleic acids in germ cells during the cycle of the seminiferous epithelium in the rat Am J Anat 96 255-284
- Dusche Z 1955 Color reactions of nucleic acid components In The Nucleic Acids E Chargaff and J N Davidson ed Academic Press, Inc N Y, pp 285-305
- Dornfeld E J 1936 Nuclear and cytoplasmic phenomena in the centrifuged adrenal glands of the albino rat Anat Rec 65 403-416
- 1937 Structural and functional reconstruction of ultracentrifuged rat adrenal cells in autoplasmic grafts Anat Rec 69 229-246
- Dounce A 1955 The isolation and composition of cell nuclei and nucleoli In The Nucleic Acids Vol II E. Chargaff and J N Davidson ed Academic Press Inc N Y pp 93-153

- Demet A. L. M. P. O'Connell and K. J. Monty 1957 Action of mitochondrial DNAase I in destroying the capacity of isolated nuclei to form gels. *J. Biophys. Biochem. Cytol.* 3: 649-662
- Enson L. 1951 On the theory of Galloy chromochrom Alum staining and its application for quantitative estimation of basophilia. A selective staining of exquisite progressivity. *Acta Path. Microbiol. Scand.* 28: 82-102
- Eichberg V. K. and M. Laskowski 1953 Protein components of chicken erythrocyte nuclei. *Biochem. Biophys. Acta* 11: 244-251
- Folger, R. and H. Rosenbeck 1924 Mikroskopisch-chemischer Nachweis einer Nukleinsäure von Typus der Thyminnukleinsäure und die darauf beruhende elektive Färbung von Zellkern in mikroskopischen Präparaten. *Zeit. Physiol. Chem.* 135: 203-248
- Fox A. and M. Errera 1958 Analyse autoradiographique de l'incorporation de la phénylalanine-2-C dans les noyaux isolés. *Exp. Cell Res.* 14: 182-192
- Geoprey G. P. 1958 A histochemical study of nucleoprotein fractions of cell nuclei. *Biochemistry* 23: 657-662
- Geoprey G. P. and J. S. Chentsov 1962 On the structural organization of nucleochromosomal ribonucleoproteins. *Exp. Cell Res.* 27: 50-572
- Gonzalez, B. P. L. E. McKinney and C. Heidelberg 1964 On the reported solubilization of carcinogenic hydrocarbons in aqueous solutions of DNA. *J. Mol. Biol.* 8: 20-27
- Graff, A. 1939 Zelluläre Speicherung cancerogener Kohlenwasserstoffe. *Ztschr. Krebsforsch.* 49: 477-495
- 1940 Intrazelluläre Benzpyrenspeicherung in lebenden Normal- und Tumorzellen. *Ztschr. Krebsforsch.* 50: 196-219
- Graff, A. and H. Maas 1938 Über die Eigenschaften des Benzpyrens zur Fluoreszenzmikroskopischen Untersuchung Fett- und Lipidreicher Strukturen in lebenden Zellen und Mikroorganismen. *Arbeiten Staatl. Inst. f. Exp. Therapie* Frankfurt 3: 21-34
- Gurber W. H. 1941-42 Über den histologischen Nachweis des Benzpyrens. *Ztschr. Krebsforsch.* 52: 57-60
- Gveti M. F. and P. I. Claus 1936a Recovery changes in transplanted anterior pituitary cells stratified in the ultracentrifuge. *Biol. Bull.* 71: 462-468
- 1936b Growth of cancerous and of embryonic tissues stratified in the ultracentrifuge. *Proc. Soc. Exp. Biol. Med.* 35: 468-473
- Hack M. H. 1948 Distribution of the phospholipids in rat liver nuclei and cytoplasmic particulates. *Amer. J. Physiol.* 155: 441
- Haddow A. 1958 Chemical carcinogens and their modes of action. *Brit. Med. Bull.* 14: 79-92
- Harvey G. I., Sloan and C. N. Loeser 1963 Spectroscopic analysis of carcinogenic hydrocarbons in biologic interactions *in vivo* and *in vitro*. *Canc. Res.* 23: 1555-1565
- Hayward A. F. 1961 Increase in the dense cytoplasmic bodies in radiation induced giant cells of the cultured fibroblast. *Nature* 192: 891-892
- Heidelberg C. 1964 Studies on the molecular mechanism of hydrocarbon carcinogenesis. *J. Cell and Comp. Physiol. Suppl.* 64: 129-148
- Hogeboom G. H. W. C. Schneider and M. S. Striebeck 1952 Cytochemical studies. II On the isolation and biochemical properties of liver cell nuclei. *J. Biol. Chem.* 196: 111-120
- Hsu T. C. and P. S. Moorhead 1955-56 Chromosome anomalies in human neoplasms with special reference to the mechanisms of polyploidization and aneuploidization in the HeLa strain. *Ann. N. Y. Acad. Sci.* 63: 1083-1094
- Idelman S. 1957 Existence d'un complexe lipides-nucléoprotéines à groupements sulphydrilés au niveau du chromosome. *C. R. Acad. Sci.* 244: 1827-1828
- 1958a Localisation du complexe lipides-protéines à groupements sulphydrilés au sein du chromosome. *C. R. Acad. Sci.* 248: 1098-1100
- 1958b Démasquage des lipides du chromosome géant des glandes salivaires de chironome par digestion enzymatique des protéines. *C. R. Acad. Sci.* 246: 3283-3284
- Jones J. L. 1962 UV fluorescence studies on the intracellular accumulation of carcinogenic hydrocarbons by developing mammalian erythrocytes *in vitro*. *Anat. Rec.* 142: 310-311
- Kopac M. J. 1955 Chemical micrurgy. *Internat. Rev. Cytol.* 4: 1-30
- Korson R. 1951 A differential stain for nucleic acids. *Stain Tech.* 26: 265-270
- Kunitz, M. 1950 Crystalline desoxyribonuclease. I. Isolation and general properties. *J. Gen. Physiol.* 33: 349-362
- LaCour L. F. J. Chayen and F. B. Gahan 1958 Evidence for lipid material in chromosomes. *Exp. Cell Res.* 14: 469-485
- Lagerstedt S. 1949 Cytological studies on the protein metabolism of the liver in rat. *Acta Anat. Suppl.* 9: 1-116
- Levin E. and L. E. Thomas 1961 Cellular lipoproteins. III. The insoluble material of rat liver cell fractions. *Exp. Cell Res.* 22: 363-369
- Lewis W. H. 1943 Nucleolar vacuoles in living normal and malignant fibroblasts. *Canc. Res.* 3: 531-536
- 1947 Interphase (resting) nuclei chromosomal vesicles and amitosis. *Anat. Rec.* 97: 433-445
- 1951 Cell division with special reference to cells in tissue culture. *Ann. N. Y. Acad. Sci.* 51: 1281-1294
- Longwell A. C. and G. Yerganian 1965 Some observations on nuclear budding and nuclear extrusions in a Chinese hamster cell culture. *J. Nat. Canc. Inst.* 34: 53-69
- Ludford R. J. 1954 Nuclear structure and its modification in tumors. *Brit. J. Canc.* 8: 112-131
- MacDougald T. J. H. W. Beams and R. L. King 1937 Growth of ultracentrifuged cells in tissue culture. *Proc. Soc. Exp. Biol. Med.* 37: 234-235
- Matejko G. M. and M. D. Kopac 1963 Cytophysical studies on living normal and neo-

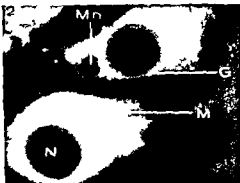
- plastic cells *Ann N Y Acad Sci* 105 183-286
- Mirsky A E and A W Pollister 1946 Chromosomatin a desoxyribose nucleoprotein complex of the cell nucleus *J Gen Physiol* 30 117-148
- Mirsky A E and H Ris 1950-51 The composition and structure of isolated chromosomes *J Gen Physiol* 34 475-491
- Morimura Y P Kotin and H L Falk 1964 Photodynamic toxicity of polycyclic aromatic hydrocarbons in tissue culture *Canc Res* 24 1249-1260
- Nagata T 1960 Observations on the nuclear transformations of chick fibroblasts in tissue culture as revealed by time-lapse cinematography *Med J Shinshu Univ* 5 265-285
- Naora H A E Mirsky and V G Allfrey 1961 Magnesium and calcium in isolated cell nuclei *J Gen Physiol* 44 713-742
- Norden G 1957 Benzpyrene and cell nuclei *Acta Path Microbiol Scand* 40 181-187
- Pearse A G E 1960 Histochemistry Little Brown and Co Boston Mass p 916
- Philpott J S L and J E Stanier 1956 The choice of suspension medium for rat liver cell nuclei *Biochem J* 63 214-223
- 1957 Comparison of interphase and prophase isolated rat liver nuclei *Nature* 179 102-103
- Pitot H E and C Heidelberger 1963 Metabolic regulatory circuits and carcinogenesis *Canc Res* 23 1694-1700
- Richter K M and V K Saini 1960 UV fluorescence studies on the in vitro intracellular accumulation of carcinogenic hydrocarbon *Am J Anat* 107 209-235
- Ris H and A E Mirsky 1949 The state of the chromosomes in the interphase nucleus *J Gen Physiol* 32 489-502
- Roodyn D B 1963 A comparative account of methods for isolation of nuclei *Biochem Soc Symp*, 23 21-36
- Schmitt F O 1938 Optical studies of the molecular organization of living systems *J Appl Phys* 9 109-117
- Schneider R M 1955 The effect of anions on the optical properties of rat liver nuclei isolated in glycerol solutions *Exp Cell Res* 8 24-34
- Shires T K 1962 The intracellular distribution of carcinogenic hydrocarbons in glandular cells *Anat Rec* 142 326
- 1965a Studies on the effects of conventional fixatives on the post fixation accumulation of carcinogenic hydrocarbon in Stain I fibroblasts *Amer Zool* 4 316
- 1965b Unpublished
- Smetana K W J Steele and H Busch 1963 A nuclear ribonucleoprotein network *Exp Cell Res* 31 198-201
- Steele W J and H Busch 1963 Studies on acidic nuclear proteins of Walker tumor and liver *Canc Res* 23 1153-1163
- Stoneburg C A 1939 Lipids of the cell nucleus *J Biol Chem* 129 189-196
- Strangeways T S P and R G Canti 1958 The living cell in vitro as shown by dark ground illumination and the changes induced in such cells by fixing reagents *Quart J Micro Sci* 71 1-14
- Waddington C H and C B Goodhart 1949 Localization of absorbed carcinogens within the amphibian cell *Quart J Micro Sci* 90 209-219
- Wang T Y D T Mayer and L E Thomas 1953 A lipoprotein of rat liver nuclei *Exp Cell Res* 4 102-106
- Widstrom G 1928 Über die Verwendbarkeit der Schiff'schen Fuchsin-schwefelgssäurereaktion zur quantitativen Bestimmung von Thymonucleinsäure *Biochem Ztschr* 199 298-306
- Zbarski I B N F Dimetrieva and L P Yermolayeva 1962 On the structure of tumor cell nuclei *Biochemistry* 27 573-576
- Zbarski I B and L Ermolaeva 1960 The characteristics of nuclear nucleoproteins of some tissues *Biochemistry* 25 80-85
- Zbarski I B and G P Georgiev 1959 New data on the fractionation of cell nuclei of rat livers and the chemical composition of nuclear structures *Biochemistry* 24 177-184
- Zagury D 1957 Existence d'un complexe liporibonucleoprotidique à groupements sulfhydrylés au sien du nucléole *C R Acad Sci* 244 1825-1827
- Zollinger H U 1948 Cytologic studies with phase microscopy II Mitochondria and other cytoplasmic constituents under various experimental conditions *Amer J Path* 24 569-584

All the figures are ordinary light (LPM) dark-contrast medium phase (PCM) or uv fluorescence (UVPM) photomicrographs taken with a 35 mm Leica camera with a Micro-Ibso attachment and a 1/3dx conical extension tube. All figures are 1700X magnification.

PLATE 1

EXPLANATION OF FIGURES

- 1 Two live L-cells approximately five minutes after contact with BP crystals displaying Golgi granules (G) and mitochondria (M) in the cytoplasm and nucleoli (nc) chromatin (Ch) and nuclear membrane (Nm) as parts of the nucleus. A micronuclear fragment (Mn) is seen in the upper cell. PCPM
- 2 Same cells as in figure 1 in which BP concentrations are highest in Golgi granules (G) but absent in mitochondria (M) and nuclei (N). UVPM
- 3 Two L-cells grown on BP crystals for about 60 hours showing Golgi granules (G) a micronucleus (Mn) and nuclear detail including nucleoli (nc). PCPM
- 4 The same cells as in figure 3 showing no BP uptake by any nuclear structure (N) or the micronucleus (Mn) but relatively high uptake by the Golgi granules (G). UVPM
- 5 Portions of two L-cells fixed in Zenker's fluid before exposure to BP. Nucleoli (nc) are refractile. A protoplasmic precipitate has aggregated in the region of the nuclear membrane (nm). Vacuoles occur in the cytoplasm (V). PCPM
- 6 The same cells as in figure 5 displaying no discrete BP accumulations in the whole nuclear region (N) or in cytoplasmic vacuoles (V). UVPM
- 7 L-cells from a culture grown on BP for 48 hours fixed in Zenker's fluid showing fine chromatin in the nucleus (Ch) and a heavy deposit of material in the vicinity of the nuclear membrane (nm). PCPM
- 8 The same cells as in figure 7 in which no BP accumulation is apparent within the nucleus (N). UVPM
- 9 A large spindle shaped cell grown on BP crystals *in vitro* fixed in Zenker's fluid and treated with Lugol's solution and thiosulfate. Highly refractile nucleoli (nc) fine chromatin precipitate (Ch) and cytoplasmic vacuoles (V) are indicated. PCPM
- 10 The same cell as in figure 9 in which no intranuclear accumulation of BP is demonstrable (N). Cytoplasmic vacuoles (V) also appear free of the CH. UVPM



All the figures are ordinary light (LPM) dark-contrast medium phase (PCM) or u v fluorescence (UVP) photomicrographs taken with a 35 mm Leica camera with a Micro-Ibso attachment and a 1/3dx conical extension tube. All figures are 1700 X magnification.

PLATE 1

EXPLANATION OF FIGURES

- 1 Two live L-cells approximately five minutes after contact with BP crystals, displaying Golgi granules (G) and mitochondria (M) in the cytoplasm and nucleoli (nc), chromatin (Ch) and nuclear membrane (Nm) as parts of the nucleus. A micronuclear fragment (Mn) is seen in the upper cell. PCPM
- 2 Same cells as in figure 1 in which BP concentrations are highest in Golgi granules (G) but absent in mitochondria (M) and nuclei (N). UVP
- 3 Two L-cells grown on BP crystals for about 60 hours showing Golgi granules (G), a micronucleus (Mn) and nuclear detail including nucleoli (nc). PCPM
- 4 The same cells as in figure 3 showing no BP uptake by any nuclear structure (N) or the micronucleus (Mn) but relatively high uptake by the Golgi granules (G). UVP
- 5 Portions of two L-cells fixed in Zenker's fluid before exposure to BP. Nucleoli (nc) are refractile. A protoplasmic precipitate has aggregated in the region of the nuclear membrane (nm). Vacuoles occur in the cytoplasm (V). PCPM
- 6 The same cells as in figure 5 displaying no discrete BP accumulations in the whole nuclear region (N) or in cytoplasmic vacuoles (V). UVP
- 7 L-cells from a culture grown on BP for 48 hours fixed in Zenker's fluid showing fine chromatin in the nucleus (Ch) and a heavy deposit of material in the vicinity of the nuclear membrane (nm). PCPM
- 8 The same cells as in figure 7 in which no BP accumulation is apparent within the nucleus (N). UVP
- 9 A large spindle shaped cell grown on BP crystals *in vitro* fixed in Zenker's fluid and treated with Lugol's solution and thiosulfate. Highly refractile nucleoli (nc), fine chromatin precipitate (Ch) and cytoplasmic vacuoles (V) are indicated. PCPM
- 10 The same cell as in figure 9 in which no intranuclear accumulation of BP is demonstrable (N). Cytoplasmic vacuoles (V) also appear free of the Ch. UVP



PLATE 3

EXPLANATION OF FIGURES

- 21 A flattened L fibroblast exposed to BP after incubation in RNAase. The residue of several nucleoli (nc) are seen in the nucleus. PCPM
- 22 The same cell as in figure 21. No BP uptake is associated with any specific intranuclear structure (N). UVPM
- 23 Several L-cells digested in RNAase after growing on crystalline BP for approximately 48 hours. Nucleolar (nc) and chromatin (Ch) residues are visible within the nucleus. PCPM
- 24 The same cells as in figure 23. No BP accumulations appear localized in any intranuclear structure. Fluorescence over the nuclear region appears referable to cytoplasmic structures above or below the nucleus. UVPM
- 25 Two L-cells exposed to a crystalline bed of BP after successive digestions in DNAase and RNAase. A Golgi zone (Gz) is seen in the cytoplasm of one cell and the remnants of nucleoli (nc) and chromatin (Ch) are seen within both nuclei. PCPM
- 26 The same cells as in figure 25 showing relatively high BP concentrations in the Golgi zone (Gz) but no BP localization in any discrete intranuclear structure (N). UVPM
- 27 Several L-cells grown approximately 48 hours on BP prior to consecutive digestions in DNAase and RNAase. No Feulgen stainable material was present in the chromatin residue (Ch) and only a faint diffuse staining with Gallocyanin Chrom Alum was present in the nucleus. ICPM
- 28 The same cells as in figure 27 showing no apparent BP uptake by any intranuclear structure (N). UVPM

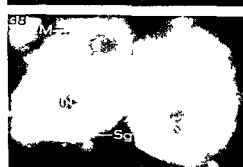
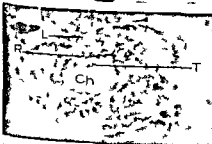
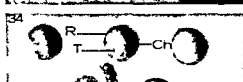
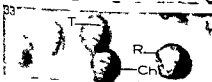
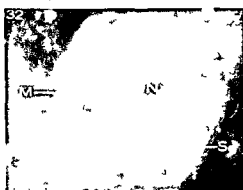
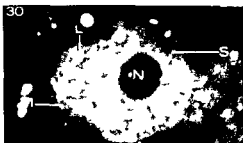


PLATE 4

EXPLANATION OF FIGURES

- 29 A dissociated heptic parenchymal cell showing lipid droplets (L) swollen mitochondria (M) the small granular component (Sg) and nuclear chromatin (Ch) PCPM
- 30 Same cell as in figure 29 with demonstrable BP accumulated in lipid droplets (L) and the small granule component (Sg) but no fluorescence within the nucleus (N) or mitochondria (M) UVPM
- 31 A dissociated binucleate rat liver cell *in vitro* with mitochondria (M) and the small granule component (Sg) discernible in the cytoplasm and nucleoli (nc) in the nucleus PCPM
- 32 Same cell as in figure 31 demonstrating BP uptake in the small granule component (Sg) and relatively no BP localization in nuclei (N) or mitochondria (M) UVPM
- 33 Paraffin section of ultracentrifuged liver stained with the Feulgen reaction Most chromatin (Ch) is in the centrifuged nuclear region connected by chromatin threads (T) with unsedimented DNA (R) LPM
- 34 Paraffin section of ultracentrifuged rat liver stained with Gallocyanin Chrom Alum after treatment with DNAase RNA is demonstrated in the sedimented chromatin (Ch) connecting threads (T) and the unsedimented rim (R) LPM
- 35 A dissociated ultracentrifuged liver cell *in vitro* showing the centrifugal accumulation of chromatin (Ch) the connecting threads (T) and the centripetal undisplaced chromatin (R) PCPM
- 36 Same cell as in figure 35 displaying high BP concentrations in lipid droplets (L) but little in the whole nuclear region (N) UVPM
- 37 A pair of binuclear ultracentrifuged liver cells with mitochondria (M) the small granule component (Sg) and centrifugally displaced chromatin (Ch) PCPM
- 38 Same cells as in figure 37 showing no apparent BP accumulation in the nucleus (N) or mitochondria (M) but relatively high BP concentrations in the small granule component (Sg) UVPM

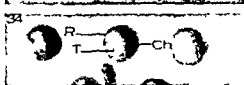
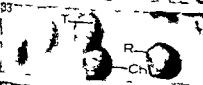
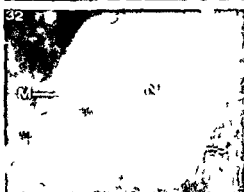
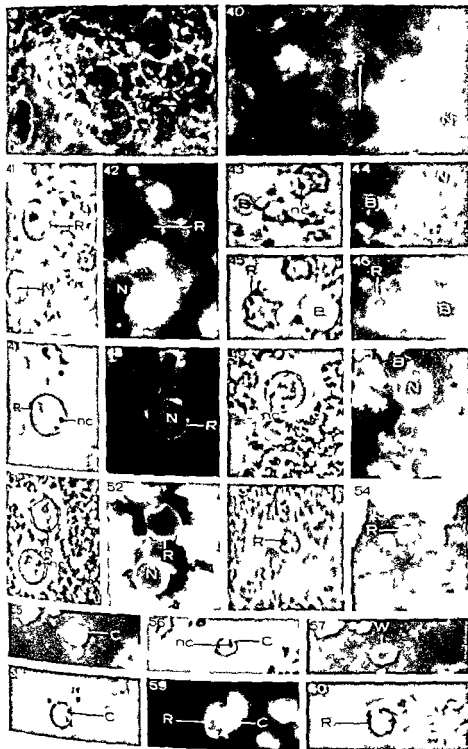


PLATE 5

EXPLANATION OF FIGURES

- 39 Several rat liver nuclei in 0.25 M sucrose 0.0014 M CaCl_2 . The nuclear rims (R) and nucleoli (nc) are discernible PCPM
- 40 The same nuclei as in figure 39 showing localization of BP only in the nuclear rim (R). BP uptake is also seen in the non nuclear debris UVPM
- 41 Rat liver nuclei viewed in 0.25 M sucrose on crystalline BP. Some condensation of the karyoplasmic material (Ky) is evident UVPM
- 42 The same nuclei as in figure 41 showing the apparent absence of BP in all nuclear structures (N) except the nuclear rim (R) PCPM
- 43 A single nucleus with nucleoli (nc) and a number of nuclear blebs (B) from a preparation incubated at 37° for six hours in McIlvaine's buffer PCPM
- 44 The same nucleus as in figure 43 showing no BP localization by nuclei (N) or blebs (B) except in their rims (R) UVPM
- 45 A rat liver nucleus and its blebs (B) from a preparation incubated in pH 6 McIlvaine's buffer with magnesium for six hours prior to exposure to BP PCPM
- 46 The same nucleus as in figure 45 showing no fluorescence in the nucleus (NO) or its blebs (B) except in their rims (R) UVPM
- 47 A single rat liver nucleus from a preparation similar to that of figure 45
- 48 The same nucleus as in figure 47 showing no apparent intranuclear BP (N). The nuclear rim and adherent cytoplasmic debris accumulate BP (R)
- 49 A Feulgen negative nucleus after digestion with DNAase and exposure to BP. Nucleoli (nc), blebs and clear spaces in the non nucleolar karyoplasm are demonstrated PCPM
- 50 The same nucleus as in figure 49 showing no BP accumulation within the nucleus (N) and BP uptake by the rim UVPM
- 51 Two Feulgen negative nuclei after DNAase treatments with discernible nucleoli (nc) PCPM
- 52 The same cells as in figure 51 showing no BP uptake by material within the confines of the rim (R) UVPM
- 53 A rat liver nucleus after both DNAase and 1 M NaCl extraction. The rim (R) has much adherent debris PCPM
- 54 The same nucleus as in figure 53 showing BP uptake only in the rim (R) UVPM
- 55 A nucleus from a similar preparation to that in figure 53. Apparent BP localization is limited to the nuclear rim and adherent debris (C) UVPM
- 56 The same nucleus as in figure 55 showing the presence of a residual nucleolus (nc) PCPM
- 57 The same cell as in figures 55 and 56 showing BP uptake in a wrinkle of the nuclear rim (W) UVPM
- 58 A liver nucleus after DNAase and exhaustive 1 M NaCl extraction. A thick rim with adherent debris (C) surrounds the nucleus PCPM
- 59 The same nucleus as in figure 58 displaying BP accumulation only in the rim (R) and cytoplasmic debris (C) UVPM
- 60 The same nucleus as in figure 58 as a lower focal plane PCPM



Placentation of the Sea Otter¹

AKHOURI A. SINHA AND H. W. MOSSMAN

Department of Anatomy University of Wisconsin Madison Wisconsin

ABSTRACT Development of the sea otter placenta is described from implantation to term. It is a typical carnivore placenta labyrinthine endothelochorial and zonary (sometimes incomplete mesometrially). The annulus has 4 to 8 lobes and is widest antimesometrially. Maternal capillaries of the labyrinth have very thick almost columnar endothelium and thick diastase resistant, heavily PAS positive basement membranes. They are surrounded by syntrophoblast and a few cytotrophoblast cells. Instances of intratrophoblastic fetal capillaries increase with age thus maternal and fetal blood are in greater proximity in late gestation. The hematoma arises during the hump-bud period at the center of the antimesometrial portion of the developing chorio-allantoic placenta as small isolated pouches of vascular chorio-allantoic membrane filled with maternal blood. Each pouch is lined by columnar cytotrophoblast which phagocytoses maternal erythrocytes and no doubt also absorbs histiotrophic products of the endometrial glands at its base. These early pouches grow and coalesce to form larger ones. The definitive hematoma consists of one large often bilobed sac (diam. 5 to 7 cm) surrounded at the base of its stalk by several smaller sacs. Elaborate villous folds subdivide the sacs and stalk. The whole hematomatous mass invaginates the allantoic vesicle the endoderm of which thus becomes its outer covering. The hematoma remains very large to term. The uterine glands of the placental base are highly active throughout gestation.

The sea otter *Enhydra lutris* (Linnaeus) inhabits the coastal waters of the North Pacific Ocean and is the only living marine mustelid. They have been exploited for fur since the Bering Expedition of 1741-42 yet until recently little has been known of their reproductive phenomena. Burabash-Nikiforov (47) noted the ovarian shape. Lensink (62) gave field observations on sea otter reproduction. Sinha (63) described the morphology of the female genital tract based on 140 animals. Sinha (63) gave a brief description of the ovarian morphology and Sinha Conroy and Kenyon (66) described its reproduction. Pearson (52) described the ovarian and placental morphology from a single gravid decaying frozen female recovered from the beach at China Cove, California. It had a zonary chorio-allantoic placenta with an antimesometrial bilobed sac-like hematoma. The placental structure described for the European river otter *Lutra vulgaris* by Bischoff (1865a) and for the American form *Lutra canadensis* by Creed and Biggers (64) seems to be essentially like that of the sea otter. The reviews of placentation in carnivores by Rau (25), Mossman (37), Amoroso (52) and Starck (59) show that

limited observations have been made on several carnivore genera but that the complete morphogenesis of the fetal membranes has been recorded only for the dog, cat and ferret. The description of the latter by Strahl and Ballmann (15) gives much useful detail on several stages from the blastocyst to full term. Hamilton (34 and 37) made very careful studies of the period from fertilization to mesoblast and notochord formation. More limited observations on mustelid placentation have been made on the ferret *Mustela furo* (Robinson 04, Lawn and Chiquoine 65), mink *Mustela vison* (Hansson 47, Enders 57), martens *Martes martes* and foina (Bischoff 1865b), weasel *Mustela vulgaris* (Bischoff 1865b), zorilla *Zorilla striata* (Rau 25), wolverine *Gulo luscus* (Wislocki and Amoroso 56), European badger *Meles meles* (Fleischmann 1891), Strahl 06, Amoroso 54), American

¹ This research was supported by grant 86-5027, a General Research Support Grant to the University of Wisconsin in Medicine from the National Institutes of Health, Division of Research Facilities and Resources, Bethesda, Maryland, and in part by Public Health Service grant HD 00277-09. The specimens for this study were gathered under the supervision of M. K. El W. Kenyon in cooperation with the Alaska Department of Game, a part of the Bureau of Sport, Fisheries and Wildlife study of the life history of the sea otter.

badger *Taxidea taxus* (Hamlett 32) and the skunks *Mephitis mephitis* and *macro-ura* and *Spilogale putorius* (Creed and Biggers 64)

It is apparent from the above literature that our knowledge of carnivore placentation and that of mustelids in particular is based upon relatively few species and usually upon a limited stage of gestation in a limited number of specimens. Because nearly 40 pregnant sea otter uteri at most stages from blastocyst to very near term were available it seemed worthwhile to record the development of their fetal membranes in detail.

MATERIALS AND METHODS

The material consists of 39 gravid sea otter uteri collected around Amchitka Simeonof Little Konijui Amak Shumagin, and the Aleutian Islands by Mr Karl W Kenyon of the Fish and Wildlife Service of the United States Department of Interior. Most of the animals were killed by Fish and Wildlife Service personnel; however a few were found dead on the beaches. The tracts of the latter were often somewhat decomposed. Reproductive tracts were excised and fixed in AFA (alcohol formalin and acetic acid) or 10% formalin and stored in 70% ethyl or isopropyl alcohol. The material was made available to Dr Clinton H Conaway University of Missouri. We are therefore greatly indebted to Mr Karl W Kenyon and Prof Clinton H Conaway.

Macroscopic observations and measurements of fetuses placentae umbilical cords and hematomas were made on 19 animals (table 1). Appropriate pieces from these uteri were embedded cut at 6 to 10 μ and stained in Groat's tetrachrome stain. Sample sections were also stained in periodic acid Schiff (PAS) Heidenhain's iron and hematoxylin and eosin. Representative portions of hematomas were embedded in celloidin and stained in hematoxylin and eosin. Twenty smaller gestation sacs were sectioned entire at 6 to 10 μ . Ten of these were serially mounted where is only every tenth section of the others was mounted. The same staining procedures were used as for the older specimens. Unimplanted blastocysts were

measured at their greatest diameter using an ocular micrometer.

OBSERVATIONS

Uterus and gestation sac

In sea otter uteri with unimplanted embryos the endometrium usually has 4 to 5 asymmetrical rugae and is packed with coiled glands which form three distinct zones: the luminal compact zone, the middle spongy zone, and the deep glandular zone (figs 14 15). However these zones are greatly modified at the implantation site so that each gestation sac has asymmetrical endometrial lobes consisting of one major lobe and 3 to 6 minor ones. The major lobe occupies the antimesometrial portion and extends a variable distance toward one or both sides of the horn. Histologically structures in both major and minor lobes are alike. The grooves or depressions between the lobes are spanned by the smooth chorion and the unmodified glands of their deep glandular zones are continuous with those of the deep glandular zones of the major and minor lobes. The spongy zone is lacking at the groove (figs 16 17 19).

Blastocyst

One unimplanted blastocyst was recovered from each of 11 sea otters. Two of these were near implantation. Most were shrunken and had broken zona pellucidae but there were three normal oval ones with intact zonae. These three range from 97 to 202 μ in diameter which suggests considerable growth before implantation. Like most other mammals the sea otter blastocyst has a single layer of flattened trophoblastic cells closely adherent to the zona and an inner mass of cells (fig 13). Usually the zona pellucida is 4 to 6 μ in thickness and is composed of an outer thin more densely stained layer and inner thick homogeneous layer. Blastocysts near implantation have approximately 500 cells in the inner cell mass. Implantation is central (fig 1) essentially the entire circumference of the trophoblastic layer coming into contact with the uterine endometrium as in other carnivores (Mossman 37 and Amoroso 52).

TABLE

A. im t n mbe	T. f in mm	CH h m	Cho lo- li b d	O. l. h in lon	O. c n	W. n. f. m	W. n. f. m	L. n. id	b. n. d. l. m	A. n. m. l.	N. L. n. h	N. m. n. of m. n. h	W. n. h.
62-53	40	31	complete	caud d	antrn on trl l	25	28/30	38	—	—	—	—	—
62-23	45	35	incomplete	caud d	antimesom trl	25	30/30	40	10	—	—	—	—
62-136	50	45	complete	caudad	antimesometrial	20	18/20	40	0	—	—	—	—
62-27	55	48	incomplete	cranial	antime ometrial	30	42/45	50	14	10	—	—	—
62-147	70	60	complete	caudad	antime ometrial	30	32/45	40	15	10	—	—	—
62-31	142	120	incomplete	caudad	cranial	35	38/40	57	55	25	—	—	—
62-29	190	160	complete	caudad	cranial	40	45/50	60	70	30	—	—	—
62-135	190	160	incomplete	caudad	cranial	50	65/65	80	100	35	—	—	—
62-8	225	190	complete	cranial	cranial	47	55/57	60	92	57	—	—	—
62-47	240	200	complete	cranial	cranial	53	67/65	72	84	65	—	—	—
62-109	280	230	complete	cranial	cranial	50	55/45	70	110	50	—	—	—
62-176	280	235	complete	cranial	cranial	55	70/70	80	75	40	—	—	—
62-33	320	270	incomplete	caudad	caudad	55	60/62	75	100	70	—	—	—
62-35	360	300	complete	cranial	cranial	55	80/80	85	105	15	—	—	—
62-37	370	315	complete	cranial	caudad	55	70/70	85	110	50	—	—	—
62-39	370	300	complete	cranial	cranial	60	70/75	85	70	70	—	—	—
60-4	370	300	complete	cranial	cranial	—	—	—	—	—	—	—	—
62-141	440	360	incomplete	caudad	cranial	0	65/75	85	165	60	—	—	—
62-119	440	370	incomplete	caudad	lateral	0	80/80	95	105	65	—	—	—

badger *Taxidea taxus* (Hamlett 32) and the skunks *Mephitis mephitis* and *Macrotis* and *Spilogale putorius* (Creed and Biggers 64)

It is apparent from the above literature that our knowledge of carnivore placentation and that of mustelids in particular is based upon relatively few species and usually upon a limited stage of gestation in a limited number of specimens. Because nearly 40 pregnant sea otter uteri at most stages from blastocyst to very near term were available it seemed worthwhile to record the development of their fetal membranes in detail.

MATERIALS AND METHODS

The material consists of 39 gravid sea otter uteri collected around Amchitka Simeonof, Little Konij, Amak Shumagin and the Aleutian Islands by Mr. Karl W. Kenyon of the Fish and Wildlife Service of the United States Department of Interior. Most of the animals were killed by Fish and Wildlife Service personnel; however a few were found dead on the beaches. The tracts of the latter were often somewhat decomposed. Reproductive tracts were excised and fixed in AFA (alcohol, formalin and acetic acid) or 10% formalin and stored in 70% ethyl or isopropyl alcohol. The material was made available to Dr. Clinton H. Conaway, University of Missouri. We are therefore greatly indebted to Mr. Karl W. Kenyon and Prof. Clinton H. Conaway.

Macroscopic observations and measurements of fetuses, placentae, umbilical cords and hematomas were made on 19 animals (table 1). Appropriate pieces from these uteri were embedded, cut at 6 to 10 μ and stained in Groat's tetrachrome stain. Simple sections were also stained in periodic acid Schiff (PAS). Heidenhain's azan and hematoxylin and eosin. Representative portions of hematomas were embedded in celloidin and stained in hematoxylin and eosin. Twenty smaller gestation sacs were sectioned entire at 6 to 10 μ . Ten of these were serially mounted, whereas only every tenth section of the others was mounted. The same staining procedures were used as for the older specimens. Unimplanted blastocysts were

measured at their greatest diameter using an ocular micrometer.

OBSERVATIONS

Uterus and gestation sac

In sea otter uteri with unimplanted embryos the endometrium usually has 4 to 5 asymmetrical rugae and is packed with coiled glands which form three distinct zones: the luminal compact zone, the middle spongy zone and the deep glandular zone (figs 14-15). However these zones are greatly modified at the implantation site so that each gestation sac has asymmetrical endometrial lobes consisting of one major lobe and 3 to 6 minor ones. The major lobe occupies the antimesometrial portion and extends a variable distance toward one or both sides of the horn. Histologically structures in both major and minor lobes are alike. The grooves or clefts between the lobes are spanned by the smooth chorion and the unmodified glands of their deep glandular zones are continuous with those of the deep glandular zones of the major and minor lobes. The spongy zone is lacking at the groove (figs 16-17-19).

Blastocyst

One unimplanted blastocyst was recovered from each of 11 sea otters. Ten of these were near implantation. Most were shrunken and had broken zona pellucida but there were three normal ones with intact zona. These three ranged from 97 to 202 μ in diameter which suggests considerable growth before implantation. Like most other mammals the sea otter blastocyst has a single layer of flattened trophoblastic cells closely adherent to the zona and an inner mass of cells (fig 13). Usually the zona pellucida is 4 to 6 μ in thickness and is composed of an outer thin more densely stained layer and inner thick homogeneous layer. Blastocysts near implantation have approximately 500 cells in the inner cell mass. Implantation is central (fig 1) essentially the entire circumference of the trophoblastic layer coming into contact with the uterine endometrium as in other carnivores (Mossman 37 and Amoroso 52).

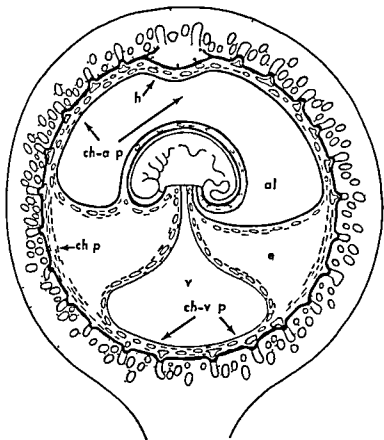


Fig. 2 Diagram of a cross section of the uterus at a very early stage of attachment showing allantoic vesicle al exocoelom e vitelline cavity v chorionic placenta ch p chorio-allantoic placenta ch a p chorio-vitelline placenta ch v p hematome h

Nonvascular chorionic placenta The area of nonvascular chorionic placenta in the sea otter depends upon the extent of exocoelom formation in the area vasculosa. It is located on the lateral sides of the gestation sac (figs 2 16) and appears to be a functional portion of the placental mechanism as in the cat (Amoroso 52)

Chorio-allantoic placenta The chorio-allantoic placenta of the sea otter is typical of that of other carnivores. Its development starts just before the limb buds appear but the zonary band is completed somewhat later. The allantoic vesicle is large (fig 16). Except for its antimesometrial location and vascularization by allantoic vessels the chorio-allantoic placenta (fig. 22) at this stage is strikingly similar to the chorio-vitelline placenta (fig

21). It is from the first endotheliochorial. Distinct giant cells are absent as in the zorilla ferret and dog.

Fetal membranes from the early fetal period to term

Once the chorio-allantoic placenta is established further changes are essentially elaboration of the pre-existing structures. At each of the stages described below the placenta consists of a typical zonary band which may be complete or incomplete because of a narrow gap mesometrially. Each annulus is narrower in width mesometrially than antimesometrially and has 4 to 8 lobes of different size (fig 9). The hematome is located antimesometrially on the zonary band. It will be described separately. The fetus may face either cranially or caudally in the uterus and there



Fig 1 Diagram of a cross section of the uterus showing the central location of the blastocyst and the relatively antimesometrial orientation of the embryonic disc. Asymmetrically located grooves *g* divide the endometrium into irregular lobes. Mesoderm dashed lines.

Early fetal membranes through the limb bud stage

Only one embryo of this group of nine has nonvascular bilaminar omphalopleure. The other eight have three distinct regions in the gestation sac: the chorio-vitelline placenta, the nonvascular chorionic placenta, and the chorio-allantoic placenta (figs 2-16). The relative size and position of these placental areas varies from animal to animal. Each embryo is antimesometrial but somewhat lateral to the midline. Placental differentiation and relative embryo growth are probably rapid after implantation begins, especially up through the limb bud period.

Bilaminar omphalopleure In the one sea otter with a nonvascular bilaminar omphalopleure, the trophoblastic villi are straight and solid (fig 20). They are mostly cellular but a syncytial mantle is frequently observed on those villi penetrating the glandular symplasma and blocking the lumina of hypertrophied spongy zone glands. Occasionally a villus has a mesodermal core and is branched. Glands usually have cuboidal cells with centrally located nuclei. However, those glandular

cells near the villi hypertrophy to form columnar cells which often fragment and become pycnotic followed by shrinkage and symplasma formation.

Chorio-vitelline placenta In eight specimens the area of chorio-vitelline placenta has been restricted by the extension of the exocoelom into the area vasculosa, thus splitting the chorio-vitelline placenta to form two new structures: the outer non-vascular chorionic placenta and the inner free splanchnopleuric yolk sac wall (fig 16). The chorio-vitelline placenta becomes more and more restricted on the mesometrial side; however, it is better developed than in the cat and dog (Amoroso '52). Although less massive and elaborate than the chorio-allantoic placenta, it has the same regions: the labyrinth, junctional zone, and the spongy and deep glandular zones.

The chorio-vitelline placental labyrinth is established just before the limb buds appear, and persists through the limb bud period. No hematome is formed in the region of the chorio-vitelline placenta. The labyrinth occupies roughly a third of the placental depth (figs 19-21). The trophoblastic villi have mesodermal cores and a few very delicate fetal capillaries. The villi are branched and usually tortuous and form networks enclosing maternal capillaries. The maternal capillary endothelium is thickened as in the ferret, mink, wolverine, and raccoon but unlike that of the dog and cat which is more squamous. Its PAS positive and diastase resistant basement membrane is relatively thin. Thus an endothelicochorial condition is well established in this chorio-vitelline placenta.

Villi usually occupy the glands in the junctional zone and the adjacent portion of the spongy glandular zone. They apparently absorb histiotrophic material. The spongy zone glands are hypertrophied, greatly dilated, and irregularly folded and branched. Their adjacent walls form septa (figs 19-20). Each septum is bounded on either side by cuboidal or low columnar epithelial cells which enclose its core of maternal connective tissue and vessels. Maternal vessels enter and leave the labyrinth through these septa. In the deep glandular zone the glands are unmodified and their bases reach the myometrium.

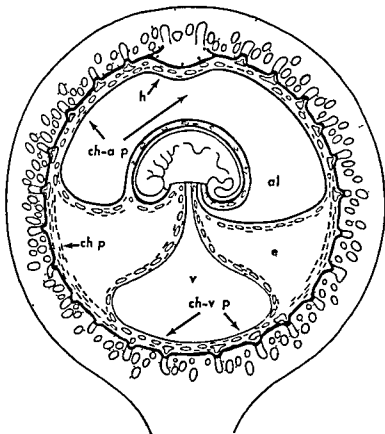


Fig 2 Diagram of a cross section of the uterus at a very early stage of attachment showing allantoic vesicle al exocoelom e vitelline cavity v chorionic placenta ch p chorio-allantoic placenta ch-a p chorio-vitelline placenta ch-v p hematoma h

Nonvascular chorionic placenta The area of nonvascular chorionic placenta in the sea otter depends upon the extent of exocoelom formation in the area vasculosa. It is located on the lateral sides of the gestation sac (figs 2 16) and appears to be a functional portion of the placental mechanism as in the cat (Amoroso 52).

Chorio-allantoic placenta The chorio-allantoic placenta of the sea otter is typical of that of other carnivores. Its development starts just before the limb buds appear but the zonary band is completed somewhat later. The allantoic vesicle is large (fig. 16). Except for its antimesometrial location and vascularization by allantoic vessels the chorio-allantoic placenta (fig 22) at this stage is strikingly similar to the chorio-vitelline placenta (fig

21). It is from the first endotheliochorial. Distinct giant cells are absent as in the zorilla ferret and dog.

Fetal membranes from the early fetal period to term

Once the chorio-allantoic placenta is established further changes are essentially elaboration of the pre-existing structures. At each of the stages described below the placenta consists of a typical zonary band which may be complete or incomplete because of a narrow gap mesometrially. Each annulus is narrower in width mesometrially than antimesometrially and has 4 to 8 lobes of different size (fig 9). The hematoma is located antimesometrially on the zonary band. It will be described separately. The fetus may face either cranially or caudally in the uterus and there



Fig 1 Diagram of a cross section of the uterus showing the central location of the blastocyst and the relatively antimesometrial orientation of the embryonic disc. Asymmetrically located grooves g divide the endometrium into irregular lobes. Mesoderm dashed lines

Early fetal membranes through the limb bud stage

Only one embryo of this group of nine has nonvascular bilaminar omphalopleure. The other eight have three distinct regions in the gestation sac: the chorio vitelline placenta, the nonvascular chorionic placenta, and the chorio allantoic placenta (figs 2-16). The relative size and position of these placental areas varies from animal to animal. Each embryo is antimesometrial but somewhat lateral to the midline. Placental differentiation and relative embryo growth are probably rapid after implantation begins, especially up through the limb bud period.

Bilaminar omphalopleure In the one sea otter with a nonvascular bilaminar omphalopleure the trophoblastic villi are straight and solid (fig 20). They are mostly cellular but a syncytial mantle is frequently observed on those villi penetrating the glandular symplasma and blocking the lumina of hypertrophied spongy zone glands. Occasionally a villus has a mesodermal core and is branched. Glands usually have cuboidal cells with centrally located nuclei. However, those glandular

cells near the villi hypertrophy to form columnar cells which often fragment and become pycnotic followed by shrinkage and symplasma formation.

Chorio-vitelline placenta In eight specimens the area of chorio vitelline placenta has been restricted by the extension of the exocoelom into the area vasculosa thus splitting the chorio vitelline placenta to form two new structures: the outer non-vascular chorionic placenta and the inner free splanchnopleuric yolk sac wall (fig 16). The chorio-vitelline placenta becomes more and more restricted on the mesometrial side; however, it is better developed than in the cat and dog (Amoroso '52). Although less massive and elaborate than the chorio-allantoic placenta, it has the same regions: the labyrinth junctional zone and the spongy and deep glandular zones.

The chorio-vitelline placental labyrinth is established just before the limb buds appear, and persists through the limb bud period. No hematome is formed in the region of the chorio vitelline placenta. The labyrinth occupies roughly a third of the placental depth (figs 19-21). The trophoblastic villi have mesodermal cores and a few very delicate fetal capillaries. The villi are branched and usually tortuous and form networks enclosing maternal capillaries. The maternal capillary endothelium is thickened as in the ferret, mink, wolverine, and raccoon but unlike that of the dog and cat which is more squamous. Its PAS positive and diastase resistant basement membrane is relatively thin. Thus an endothelicochorial condition is well established in this chorio vitelline placenta.

Villi usually occupy the glands in the junctional zone and the adjacent portion of the spongy glandular zone. They apparently absorb histiotrophic material. The spongy zone glands are hypertrophied, greatly dilated, and irregularly folded and branched. Their adjacent walls form septa (figs 19-20). Each septum is bounded on either side by cuboidal or low columnar epithelial cells which enclose its core of maternal connective tissue and vessels. Maternal vessels enter and leave the labyrinth through these septa. In the deep glandular zone the glands are unmodified and their bases reach the myometrium.

Definitive yolk sac

The splanchnopleuric yolk sac of the sea otter is a large permanent structure as in other carnivores (Mossman 37) and is restricted to the mesometrial side (fig 3). The sac is elongated in the direction of the uterine axis and is free except for a thread like mesodermal attachment at each of these ends. It remains vascularized throughout gestation.

Hematome

Placental hematomas are characteristic of many carnivores and of a few insectivores (Strauss 43) and bats (Wimsatt and Gopalakrishna 58). They consist of a mass of extravasated maternal blood lying between the vascular chorio-allantoic membrane lined by phagocytic cytotrophoblast and a glandular area of the endometrium. The accumulation of blood may be

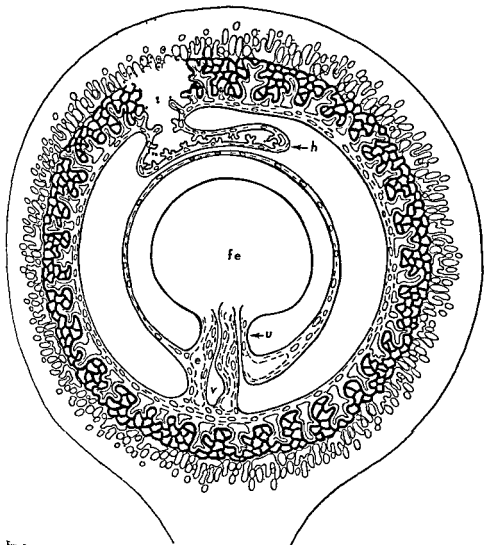


Fig 3 Diagram of a cross section of the uterus in late pregnancy. The chorio-allantoic placenta is now annular. The chorio-vitelline placenta has disappeared. Fetus fe, umbilical cord u, other abbreviations as in figure 2.

is no correlation between its orientation and the position of the hematome (table 1)

Intermediate stage of the chorio allantoic placenta In the five animals having fetuses between 40 and 70 mm in length the placental labyrinth occupies roughly two-thirds of the placental depth (figs 23-25). In stained sections it appears less compact than the labyrinth of the mature placenta (fig 28). It has a series of lamellate fetal villi between which are the branched and tortuous maternal capillaries intimately enclosed by the syntrophoblast (fig 24). Instances of intratrophoblastic fetal capillaries are frequent thus maternal and fetal blood are brought into greater proximity. Basement membranes of the maternal capillaries are relatively thinner near the junctional zone than at the fetal surface. This indicates that the increase in the thickness of the basement membrane is a later acquisition probably produced by the deposition of argyrophilic fibers of maternal endothelial cell origin as in the zorilla (Rau 25) and wolverine (Wislocki and Amoroso 56). This difference in the thickness of basement membrane is not noticeable in the mature placenta.

Most of the villi have not yet penetrated beyond the central ends of the spongy zone glands however a few have entered deeper into their lumina (figs 23-25). Those portions of the villi which project into the lumina have tall columnar phagocytic cytotrophoblastic cells with more or less basal nuclei and usually are devoid of syncytial cells. The glands are more dilated hence the septa are thin at this stage. Usually the basal ends of the dilated portions are smooth (figs 23-25).

At the margin of the placenta the zony band is deeply undercut (fig 25) by a fold of chorio allantois. The annulus gradually thins towards its margins. The folds in the undercut margin have tall columnar cytotrophoblastic cells with more or less basal nuclei (fig 40). These cells are phagocytic and apparently absorb histiotrophic material from the partially degenerate spongy zone glands of the area. Normally there is no extravasated blood in the marginal phagocytic region contrary to

the condition in the dog where the marginal region is a hematome.

Beyond the placental margin the chorio allantois and the uterine epithelium are separated only by a thin space usually under 1 mm in thickness which contains variable amounts of histiotrophic material. The chorio allantois is a smooth membrane whose cuboidal trophoblastic cells appear to be absorptive. The uterine epithelium is also cuboidal (fig 40).

Definitive chorio allantoic placenta In the 14 animals having 142 to 440 mm fetuses the placenta has reached its definitive structure but does of course increase in size during this period. The labyrinth occupies roughly four fifths of the placental depth (fig 28). It is still endotheliochorial however the complexity of the maternal and fetal capillaries has greatly increased and instances of intratrophoblastic fetal capillaries are much more numerous (fig 42). By light microscopy these appear to be apposed to the basement membrane of the maternal endothelium (fig 42). Thus maternal and fetal blood are in even greater proximity and if the trophoblast has actually disappeared from these areas they would be endothelio endothelial in nature. The fetal capillaries usually have flattened endothelial cells and thin PAS positive basement membranes.

Both the junctional and spongy zones are greatly compressed and the villi penetrate into the spongy gland lumina as in the raccoon (Creed and Biggers 63). These villi are often branched inside the lumina. Instead of syncytium their intraglandular portions are covered by tall columnar phagocytic cytotrophoblastic cells with basal nuclei (fig 34). These are obviously histiotrophic absorptive areas and their trophoblast is very similar to that lining the hematome. The deep glandular zone is greatly reduced.

Amnion

During early pregnancy the amnion is a thin membrane separated from the allantois by the voluminous extra-embryonic coelom but by the time the embryo has reached about 70 mm the amnion is well vascularized by the allantoic vessels except for a small area adjacent to the umbilical cord (figs 2-3).

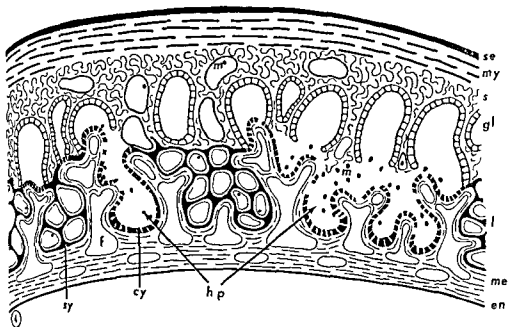


Fig 4 Early labyrinth and hematoma pouches

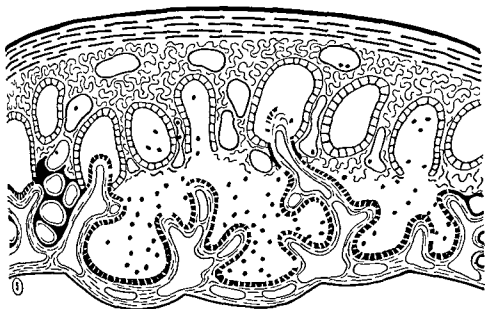


Fig 5 Coalescence of the pouches initiates the formation of a central major hematoma pouch

so massive that the chorioallantois is bulged inward to form one or more large sacs which are sometimes pedunculated. In such cases the blood appears at first sight, to be entirely enclosed by the chorioallantois because the only contact with endometrium is the relatively small area at the base of the stalk (or stalks in the case of multiple sacs). At the other extreme are absorptive areas ranging in size from relatively large to microscopic in which there is no grossly visible extravasate yet in which microscopical examination shows active phagocytosis of maternal erythrocytes by the lining cytotrophoblast. In some species there is little or no erosion of the epithelium of the basal endometrium, but in others the septal ridges between the glands lose all or most of their epithelium as in the sea otter. In the definitive larger hematomas the inner vascular layer is almost always elaborately folded or villous or both. Its cytotrophoblastic lining is columnar and obviously absorptive and phagocytic. Where placental labyrinth borders a hematoma a single chorio-allantoic fold or villus may serve the hematoma on one side and the labyrinth on the other side (fig. 39). Besides being areas for contact with and absorption of maternal blood hematomas contain at least some glandular secretion and therefore are functionally both "hemotrophic" and "histiotrophic". Structurally they are homologous to such absorptive areas as chorionic vesicles, areolae, and rosettes known in the placentae of many mammalian groups including the carnivores themselves, moles (*Talpidae*), lemurs, galagos, lorises, perissodactyls and artiodactyls (Mossman 37, Amoroso 52).

Placental absorptive areas including hematomas are clearly significant structures both from the standpoint of the light they may throw on the phylogenetic development of the placenta and the interrelationships of placental mammals and also from that of placental function. Unfortunately we still know very little for certain about either of these aspects. Are they primitive or specialized placental mechanisms? Is the contained blood mass of a hematoma truly an extravasate or does it slowly circulate through the hematoma?

What brings about the extravasation? Does some form of digestion of the blood and glandular secretions take place in the hematoma as Creed and Biggers (63) suggested? Are the red blood cells phagocytosed entire and still alive? or are they dead or fragmented? What is the nature of the lining trophoblast cells which allows them to function in these ways and how and in what form are the absorbed substances transferred to the fetal blood? What is the developmental history of a placental hematoma?

Our sea otter material can contribute very little toward the solution of most of these problems but we have been able to follow some features of the development of the hematoma from its first appearance at the limb bud stage to term.

Early development of the hematoma. The hematoma first appears during the limb bud period on the antimesometrial side of the chorioallantoic placenta usually on the major endometrial lobe and somewhat laterally (figs. 2-18). This is at the time when the early vascular chorioallantoic villi have begun to penetrate into the mouths of the endometrial glands and when labyrinth in beginning to form between them through the erosion of the epithelium covering the interglandular area followed by engulfment of the maternal capillaries by the syntrophoblast. In the area of the hematoma maternal blood appears as an extravasate between the villi. It is not clear in our material whether the maternal vascular rupture is brought about by syntrophoblastic erosion or whether syntrophoblast is actually lacking at these points. The endometrial surface epithelium between the gland mouths is missing in the areas where the first extravasations appear and the villi extend into the gland necks but blood first appears between the villi and the gland walls.

Figs. 4-8 Diagrams of vertical sections through the antimesometrial area of the chorioallantoic placenta and uterine wall to show the development of the labyrinth *l* and hematoma *h*. Uterine serosa *sc*, myometrium *my*, endometrial stroma *s*, gland epithelium *gl*, maternal blood in early hematoma pouches *h p*, syntrophoblast (heavy black) *sy*, phagocytic cytotrophoblast (heavy black cross hatched) *cy*, fetal blood vessels *f*, allantoic mesenchyme *me*, allantoic endoderm *en*.

chorio-allantoic membrane between the villi is pulled inward toward the allantoic cavity (figs 4-8). The villi become progressively detached from the endometrium allowing enlargement of the pouches. As this process continues smaller pouches are incorporated into their larger neighbors while at the same time newer ones may be forming peripheral to the earlier ones (figs 4 5 6 29 30). All this is happening when the whole hematoma may be only 1 to 5 mm in diameter. How

ever this process probably stops rather early as where labyrinth has once formed it is difficult to see how new hematomas could develop and also the hematomas of later stages although as wide or wider than the zonary labyrinth always have a narrow peduncular base 5 to 10 mm in diameter (figs 10 11 31 32).

In each pouch the cytotrophoblast becomes a tall columnar epithelium with basal nuclei (fig 37). The cytoplasm of many of these cells is soon filled with

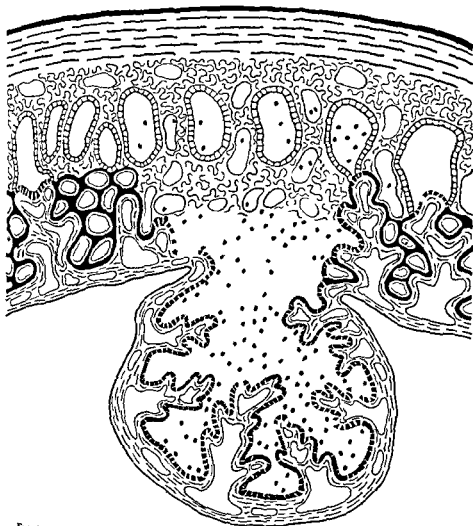


Fig 7 Beginning formation of the hematoma stalk. The basal fibrous zone is shown as it appears in a section slightly lateral to the central axis of the stalk. Connections of the gland lumina to the stalk cavity are not shown because they are present only at the center of the base of the stalk.

not deep in the glands (figs 4 5) The trophoblast lining these areas is high columnar and phagocytic If syntrophoblast is initially present, it must separate completely from the cellular layer but since none is identifiable on the endometrial side when the plane of section is vertical through the base of the hematome we think it either disappears very early or has always been absent from these potential hematome areas Neither does our material tell us for certain whether extravasation takes place by leakage from ruptured capillaries or by diapedesis However, two observations make diapedesis seem unlikely first there is no infiltra-

tion of erythrocytes into the stroma as one would expect unless diapedesis were confined strictly to those vessels directly bordering the potential hematome space and second the massive amount of blood that soon accumulates in the hematome as well as the pressure which it must exert to produce the bulging sac like shape suggests leaking open vessels No open vessels have been observed but the capillaries of the fibrous capsular area are shrunken and have degenerate endothelial cells (fig 35)

In the sea otter the first extravasations are near one another but not necessarily contiguous As blood accumulates the

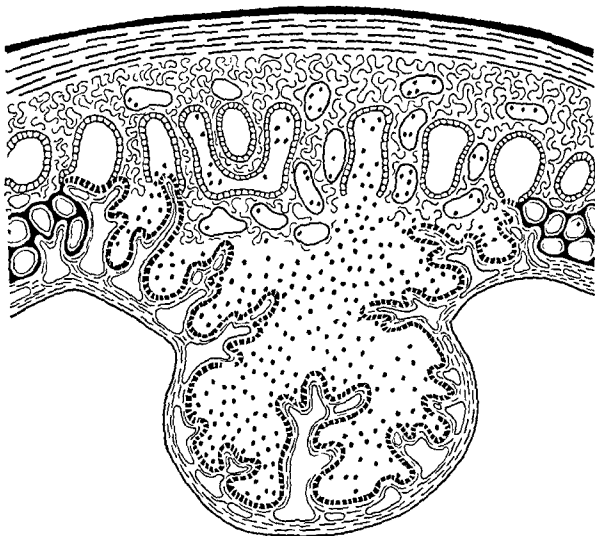


Fig 6 Increasing extravasation of maternal blood and additional coalescence of immediately adjacent pouches results in a prominent central hematoma sac Much of its base consists of fibrous endometrial stroma with many maternal capillaries but in a few places underlying gland lumina are continuous with the hematoma blood spaces and are themselves filled with maternal blood

chorio-allantoic membrane between the villi is bulged inward toward the allantoic cavity (figs 4-8). The villi become progressively detached from the endometrium above, enlargement of the pouches. As this process continues smaller pouches are incorporated into their larger neighbors while at the same time newer ones may be forming peripheral to the earlier ones (figs 4 5 6 29 30). All this is happening when the whole hematome may be only 1 to 5 mm in diameter. How

ever this process probably stops rather early as where labyrinth has once formed it is difficult to see how new hematomas could develop and also the hematomas of later stages although as wide or wider than the zonary labyrinth always have a narrow peduncular base 5 to 10 mm in diameter (figs 10 11 31 32).

In each pouch the cytotrophoblast becomes a tall columnar epithelium with basal nuclei (fig 37). The cytoplasm of many of these cells is soon filled with

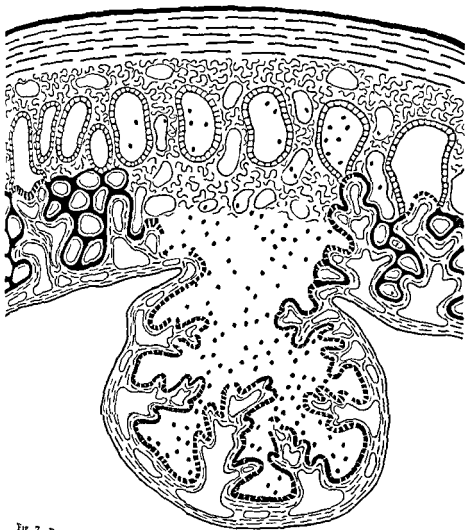


FIG 7 Beginning formation of the hematome stalk. The basal fibrous zone is shown as it appears in a section slightly lateral to the central axis of the stalk. Connections of the gland lumina to the stalk cavity are not shown because they are present only at the inner of the base of the stalk.

phagocytosed maternal erythrocytes. Degenerating multinucleate masses presumably of epithelial origin but possibly syntrophoblastic are often seen in the contents of the pouches (cf Wimsatt and Gopalakrishna 58). As the pouches increase in size, numerous large complexly branched lamellate and villous folds differentiate and subdivide the blood masses in their lumina.

At the time the hematoma pouches first form the underlying endometrium is like that already described for the labyrinthine area but when the pouches begin to coalesce changes occur especially in the junctional zone. Instead of being invaded by syntrophoblast to form labyrinth the stroma becomes more fibrous the capillaries become narrower their epithelium shows degenerative changes and

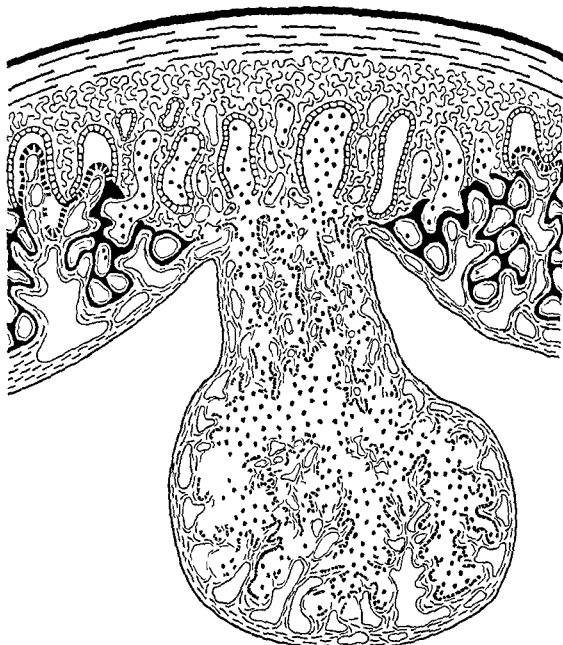


Fig 8 This shows the basic structure of the definitive chorioallantoic placental labyrinth and the hematoma i.e. the numerous richly vascular laminae and villi of the major sac and stalk the maternal blood in the dilated basal glands the endothelochorial labyrinth and the phagocytic cytotrophoblast covering the tips of the allantoic villi which occupy the open ends of the basal glands

their diastase resistant basement membranes become thicker and more strongly PAS positive (fig 35) This somewhat E.ous capsule like zone separates the hematomaic pouches from the dilated spongy gland zone (figs 7 8 32 35) except for central perforations left by the necks of the glands It is continuous at its margins with the surrounding labyrinth where of course syntrophoblast becomes conspicuous Leakage from maternal vessels of this zone seems to be the most likely source of the blood filling the hematoma Deeper in the septa of the spongy zone the maternal capillaries are normal

Definitive hematoma From the early fetal period onward the hematoma increases markedly in size and complexity but does not change otherwise except that the central portion becomes more and more prominent and definitely stalked while the peripheral pouches become less prominent and tend to disappear presumably by incorporation into one another or into the main one Unlike that of the mink and raccoon the hematoma maintains its large size to term (table 1) As shown in figures 3 7 8 32 33 it invaginates the chorioallantois toward the allantoic cavity and so is covered to the base of its stalk by the allantoic endoderm It is so large and so closely pressed against

the amnion and fetus that in preserved specimens each bears imprints of the other (figs 10 11 12) No doubt in the living the hematoma is a semi turgid sac but because of the variety of positions it may take with reference to the fetus the preserved organ may be compressed oval pear shaped saucer like or ball shaped (figs 10 11 12) It is composed of one or two large central lobes attached to the junctional zone by a long narrow stalk There are several small accessory pouches at its base In one animal (62-39) both the hematoma and placental annulus were cephalic to the fetus which had an umbilical cord about 70 mm long instead of the normal 10 to 30 mm In this case the body of the hematoma was ball shaped

Microscopically there are three regions of the main central lobe of the definitive hematoma the body the stalk and the junctional and spongy zone or base (fig 8) The body is a thick walled vascular chorio-allantoic sac much like that of the wolverine badger and raccoon It contains 75 to 95% of the extravasated blood It is covered by low cuboidal or squamous allantoic endoderm and is lined by tall phagocytic and absorptive cytotrophoblast Numerous profusely branched villus like folds divide the main sac into smaller yet confluent compartments (figs 8 32 33) These folds actually appear to take up

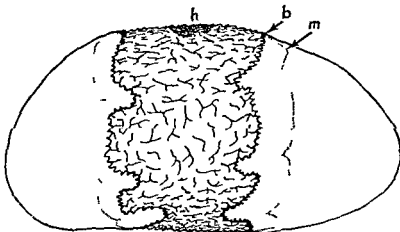


Fig 9 Diagram of a whole conceptus removed from the uterus to show the lobed zonary band and the area of attachment (internally) of the hematoma h on the antimesometrial portion of the zone Free margin of annular placenta m border of basal attached

almost as much space as the maternal blood does. The folds are fewer and simpler near the stalk. They are highly vascular and their capillaries have distinct basement membranes. The distal cytoplasm of most of the cytotrophoblast cells is packed with maternal erythrocytes or fragments of them and with orange red crystals. No doubt other materials originating from the blood or glandular secretions are phagocytosed but our material was unsuitable for identification of such elements. The intensity of pigmentation of the extravasated blood still occupying the hematoma at full term suggests that the trophoblast rejects large amounts of blood pigment while it presumably selects and absorbs the iron.

The stalk is distinctly demarcated from the placental labyrinth by a deep groove lined by the chorioallantoic (figs 7 8 32 33 34). Its structure like that of the main body except that the vascular folds clearly parallel its long axis and thus divide it into 15 to 30 narrow channels through which the maternal blood enters the body of the organ. These folds are the pathways for the fetal vessels supplying the entire sac and are continuous with those of the main body. They are also covered by phagocytic epithelium (figs 36 39).

The junctional and spongy zone glands at the base of the definitive hematoma are much more complex than earlier (figs 31 32). The lumina are filled with ma-



Fig 10. Gestation sac with fetus (total length 115 mm) with one side of gestation sac and membranes removed to show the major sac of the hematoma with several smaller basal pouches. Note the narrow stalk of the major sac. Note also the narrowness of the mesometrial portion of the zonary placental band compared to the antimesometrial portion (above in the fig). (Photo by H. W. Kenyon of JEB 63-40 which is not included in our tables.)



Fig 11 Gestation sac with fetus (total length 118 mm) showing the very large stalked hematoma. The placenta is cut almost at the center of the hematoma stalk. The mesometrial portion of the placental band (below in fig) is relatively broad in this specimen. (Photo by K W Kenyon of JEB 63-63 which is not included in our tables)

terial blood and occasionally villi arising from the folds of the stalk penetrate into them. The junctional zone remains fibrous and retains its degenerate maternal capillaries to term.

DISCUSSION

There is paleontological evidence of a close phylogenetic relationship between the sea otter and the river otter (Taylor 14). Relatively little is known of the fetal membranes of the river otters *Lutra vulgaris* (Bischoff 1865a) and *Lutra canadensis* (Creed and Biggers 64) but grossly they are very similar to those of *Enhydra*. All three have somewhat lobate usually completely zonary endothelial placentae with a large bag like antimesometrial hematoma attached by a

stalk surrounded by smaller hematoma pouches.

The placenta of the wolverine *Gulo gulo* also has a somewhat lobed zonary form with a large antimesometrial hematoma (Wislocki and Amoroso 56). The ferret *Mustela furo* during the early fetal period has a zonary placenta which is however incomplete at the mesometrial side. Its antimesometrial hematoma is composed of several small sac like diverticula none of which have the distinct stalk characteristic of the otters and wolverine. In late gestation (Strahl and Ballmann 15) the ferret labyrinth becomes divided into two lateral discoid areas while the hematoma remains antimesometrial its base separated by several millimeters from one or both discs. Our speci-

almost as much space as the maternal blood does. The folds are fewer and simpler near the stalk. They are highly vascular and their capillaries have distinct basement membranes. The distal cytoplasm of most of the cytotrophoblast cells is packed with maternal erythrocytes or fragments of them and with orange red crystals. No doubt other materials originating from the blood or glandular secretions are phagocytosed but our material was unsuitable for identification of such elements. The intensity of pigmentation of the extravasated blood still occupying the hematoma at full term suggests that the trophoblast rejects large amounts of blood pigment while it presumably selects and absorbs the iron.

The stalk is distinctly demarcated from the placental labyrinth by a deep groove lined by the chorioallantoic membrane (figs 7 8 32 33 34). Its structure is like that of the main body except that the vascular folds clearly parallel its long axis and thus divide it into 15 to 30 narrow channels through which the maternal blood enters the body of the organ. These folds are the pathways for the fetal vessels supplying the entire sac and are continuous with those of the main body. They are also covered by phagocytic epithelium (figs 36 39).

The junctional and spongy zone glands at the base of the definitive hematoma are much more complex than earlier (figs 31 32). The lumina are filled with ma-



Fig 10 Gestation sac with fetus (total length 115 mm) with one side of gestation sac and membranes removed to show the major sac of the hematoma with several smaller basal pouches. Note the narrow stalk of the major sac. Note also the narrowness of the mesometrial portion of the zonary placental band compared to the antimesometrial portion (above in the fig). (Photo by K W Kenyon of JEB 63-40 which is not included in our tables.)

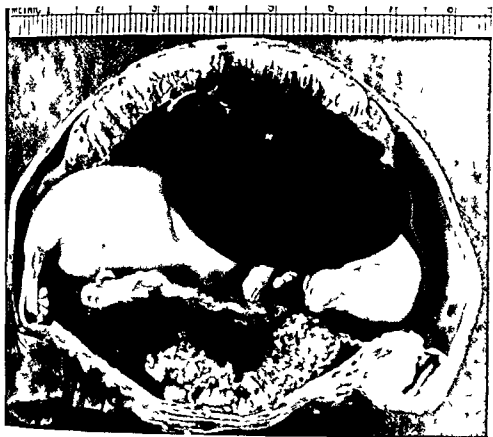


Fig 11 Gestation sac with fetus (total length 118 mm) showing the very large stalked hematoma. The placenta is cut almost at the center of the hematoma stalk. The mesometrial portion of the placental band (below in fig) is relatively broad in this specimen (Photo by A. W. Kenyon of JEB 63-83 which is not included in our tables)

terial blood and occasionally villi arising from the folds of the stalk penetrate into them. The junctional zone remains fibrous and retains its degenerate maternal capillaries to term.

DISCUSSION

There is paleontological evidence of a close phylogenetic relationship between the sea otter and the river otter (Taylor '74). Relatively little is known of the fetal membranes of the river otters *Lutra vulgens* (Bischoff 1865a) and *Lutra cana densis* (Creed and Biggers '64) but grossly they are very similar to those of *Enhydra*. All three have somewhat lobate usually completely zonary endothelial chorionic placentae with a large bag like antimesometrial hematoma attached by a

stalk surrounded by smaller hematomal pouches.

The placenta of the wolverine *Gulo gulo* also has a somewhat lobed zonary form with a large antimesometrial hematoma (Wislocki and Amoroso '56). The ferret *Mustela furo* during the early fetal period has a zonary placenta which is however incomplete at the mesometrial side. Its antimesometrial hematoma is composed of several small sac like diverticula none of which have the distinct stalk characteristic of the otters and wolverine. In late gestation (Strahl and Ballmann '15) the ferret labyrinth becomes divided into two lateral discoid areas while the hematoma remains antimesometrial its base separated by several millimeters from one or both discs. Our speci-

almost as much space as the maternal blood does. The folds are fewer and simpler near the stalk. They are highly vascular and their capillaries have distinct basement membranes. The distal cytoplasm of most of the cytotrophoblast cells is packed with maternal erythrocytes or fragments of them and with orange red crystals. No doubt other materials originating from the blood or glandular secretions are phagocytosed but our material was unsuitable for identification of such elements. The intensity of pigmentation of the extravasated blood still occupying the hematoma at full term suggests that the trophoblast rejects large amounts of blood pigment while it presumably selects and absorbs the iron.

The stalk is distinctly demarcated from the placental labyrinth by a deep groove lined by the chorioallantoic membrane (figs 7, 8 32 33 34). Its structure is like that of the main body except that its vascular folds clearly parallel its long axis and thus divide it into 15 to 30 narrow channels through which the maternal blood enters the body of the organ. The folds are the pathways for the fetal vessels supplying the entire sac and are continuous with those of the main body. They are also covered by phagocytic epithelium (figs 36 39).

The junctional and spongy zone gland at the base of the definitive hematoma is much more complex than earlier (fig 31 32). The lumina are filled with m-



Fig. 10 Gestation sac with fetus (total length 115 mm) with one side of gestation sac and membranes removed to show the major sac of the hematoma with several smaller basal pouches. Note the narrow stalk of the major sac. Note also the narrowness of the mesometrial portion of the zonary placental band compared to the antimesometrial portion (above in the fig). (Photo by K. W. Kenyon of JEB 63-40 which is not included in our tables.)



Fig. 11 Gestation sac with fetus (total length 118 mm) showing the very large stalked hematoma. The placenta is cut almost at the center of the hematoma stalk. The mesometrial portion of the placental band (below in fig.) is relatively broad in this specimen (Photo by K. W. Kenyon #12 63-63 which is not included in our tables)

lental blood and occasionally villi arising from the folds of the stalk penetrate into the junctional zone remains fibrous and retains its degenerate maternal capillaries to term.

DISCUSSION

There is paleontological evidence of a close phylogenetic relationship between the sea otter and the river otter (Taylor 1914). Relatively little is known of the fetal membranes of the river otters *Lutra vulgaris* (Bischoff 1865a) and *Lutra canadensis* (Creed and Biggers 61) but possibly they are very similar to those of the hydra. All three have somewhat like usually completely zonary endothelial placentae with a large bag like mesometrial hematoma attached by a

stalk surrounded by smaller hematoma pouches.

The placenta of the wolverine *Gulo gulo* also has a somewhat lobed zonary form with a large antimesometrial hematoma (Wislocki and Amoroso 56). The ferret *Mustela furo* during the early fetal period has a zonary placenta which is however incomplete at the mesometrial side. Its antimesometrial hematoma is composed of several small sac like diverticula none of which have the distinct stalk characteristic of the otters and wolverine. In late gestation (Strahl and Ballmann 15) the ferret labyrinth becomes divided into two lateral discoid areas while the hematoma remains antimesometrial its base separated by several millimeters from one or both discs. Our speci-

almost as much space as the maternal blood does. The folds are fewer and simpler near the stalk. They are highly vascular and their capillaries have distinct basement membranes. The distal cytoplasm of most of the cytotrophoblast cells is packed with maternal erythrocytes or fragments of them and with orange red crystals. No doubt other materials originating from the blood or glandular secretions are phagocytosed but our material was unsuitable for identification of such elements. The intensity of pigmentation of the extravasated blood still occupying the hematoma at full term suggests that the trophoblast rejects large amounts of blood pigment while it presumably selects and absorbs the iron.

The stalk is distinctly demarcated from the placental labyrinth by a deep groove lined by the chorion allantoic (figs 7 8 32 33 34). Its structure like that of the main body except that its vascular folds clearly parallel its long axis and thus divide it into 15 to 30 narrow channels through which the maternal blood enters the body of the organ. The folds are the pathways for the fetal vessels supplying the entire sac and are continuous with those of the main body. They are also covered by phagocytic epithelium (figs 36 39).

The junctional and spongy zone glands at the base of the definitive hematoma are much more complex than earlier (fig. 31 32). The lumina are filled with m-



Fig 10 Gestation sac with fetus (total length 115 mm) with one side of gestation sac and membranes removed to show the major sac of the hematoma with several smaller basal pouches. Note the narrow stalk of the major sac. Note also the narrowness of the mesometrial portion of the zonary placental band compared to the antimesometrial portion (above in the fig) (Photo by K W Kenyon of JEB 63-40 which is not included in our tables)



Fig. 11 Gestation sac with fetus (total length 118 mm) showing the very large stalked hematoma. The placenta is cut almost at the center of the hematoma stalk. The mesometrial portion of the placental band (below in fig) is relatively broad in this specimen. (Photo by K. W. Kenyon #153 63-63 which is not included in our tables.)

tral blood and occasionally villi arising from the folds of the stalk penetrate into them. The junctional zone remains fibrous and retains its degenerate maternal capillaries to term.

DISCUSSION

There is paleontological evidence of a close phylogenetic relationship between the sea otter and the river otter (Taylor 14). Relatively little is known of the fetal membranes of the river otters *Lutra vulgaris* (Buschhoff 1865a) and *Lutra canadensis* (Creed and Biggers 64) but possibly they are very similar to those of fishydra. All three have somewhat lobate usually completely zonary endothelial placenta with a large bag like antimesometrial hematoma attached by a

stalk surrounded by smaller hematoma pouches.

The placenta of the wolverine *Gulo gulo* also has a somewhat lobed zonary form with a large antimesometrial hematoma (Wislocki and Amoroso 56). The ferret *Mustela furo* during the early fetal period has a zonary placenta which is however incomplete at the mesometrial side. Its antimesometrial hematoma is composed of several small sac like diverticula none of which have the distinct stalk characteristic of the otters and wolverine. In late gestation (Strahl and Ballmann 15) the ferret labyrinth becomes divided into two lateral discoid areas while the hematoma remains antimesometrial its base separated by several millimeters from one or both discs. Our speci-



Fig 12 Gestation sac with fetus (total length 186 mm) showing lobation of zonary band (upper portion in fig) and the large hematoma pouch dorsal to the forward half of the fetus (Photo by K W Kenyon of ADFG 520 which is not included in our tables)

mens of the mink *Mustela vison* and long tailed weasel *Mustela frenata* all in the mid to late fetal period also have incomplete zonary placenta with anti mesometrial non stalked hematomas. The skunks *Mephitis mephitis* *Mephitis macroura* and *Spilogale putorius* based on one uterus each with embryos of 32 35 and 7 mm respectively all have complete zonary placentae with broad antimesometrial hematomas (Creed and Biggers 64). Whether or not some or all of these Amer-

ican mustelids arrive at a double discoid shape or some other variation in gross placental form late in gestation is uncertain. Such changes in form would not be unlikely due to rapid increase in uterine girth possibly accompanied by pressure atrophy of labyrinth adjacent to the bulging hematoma which is presumably turgid with extravasated maternal blood.

From the above it is clear that closely related mustelids do have placentae of similar external form although their form

may change much during development. It might therefore be argued that gross placental characters indicate closer relationship between *Enhydra lutra* and *Gulo* than with the other mustelids studied. This may be true but one must remember that Creed and Biggers (63) have shown that the placenta of the raccoon *Procyon lotor*, a member of the family *Procyonidae*, also has an irregular zonary shape with a large stalked antimesometrial hematoma. Furthermore the dog and sea lion members of different suborders have zonary placentae which differ from each other only in very minor details. So while it is generally true that members of the same genus or even of the same family have like placental shapes, the converse—that placentae of the same shape within such a group indicate close relationship—is not a safe deduction. (For further discussion of the fetal membranes and physiology see Mossman 37, 53; Amoroso 50.)

One encounters an equally confusing and even more speculative set of concepts when one seeks to trace the evolution of a specific placental characteristic or type within the mammalian group. Rau (25) for example attempted to show the origin in carnivores of the double discoid placenta with an isolated hematoma such as that of the mustelids from the zonary placenta with the more extensive yet less complex green border hematoma such as that of the canids. He placed much weight on the fact that some mustelid placentae start out as zonary but later become double discoid. Rau was handicapped by incomplete information especially regarding raccoon placentation. Considerably more is now known about carnivore placentation but far too little to allow one to produce convincing evidence of its evolutionary course. We are however inclined to a view somewhat opposite to that of Rau partly because the mustelids, procyonids and ursids are considered to be relatively primitive groups and the canids, felids and pinnipeds relatively specialized. Also it seems reasonable to us to assume that the first mammalian placentation would have been epitheliochorial and diffuse (i.e. broadly zonary). However when more intimate

relationships between the endometrium and chorio-allantois developed there is no reason to assume that it involved the whole zonary area. Since extravasation of maternal blood is a common occurrence in the endometrium during and even before implantation an easily imagined first step in supplementation of the epitheliochorial and uterine secretion stage of fetal nutrition would be formation of hematomatous masses of noncirculating maternal blood confined between the endometrium and the vascular absorptive chorio-allantois. Phagocytosis of extravasated maternal blood along with absorption of glandular secretions would seem a far simpler mechanism to evolve than a labyrinth with circulating maternal blood whether of the hemochorial or endotheliochorial type. Also placentation of this sort could easily be adequate for short gestation periods with young being born as most marsupials are in a very immature state. As intra uterine development was carried further there would have been more and more need for the elaboration of a structure permitting rapid and efficient interchange especially of respiratory gases and it is in response to this need that zones of intimate contact between the fetal and maternal capillaries would have evolved. We are therefore inclined to think that isolated hematomas may be as old or older phylogenetically than labyrinths. Although hematomas and labyrinths are both formed primarily of chorioallantois we think it likely that they arose independently in time. Perhaps the best argument against our view is the fact that hematomas are relatively rare as such in mammalian placentae and in fact are unknown in the placentation of marsupials and reptiles where simple labyrinths have however been evolved. Yet one must recognize that absorptive areas, areolae and the like are common in mammalian placentae and areas functioning in a similar fashion do no doubt exist in marsupials and reptiles and since we believe that hematomas are essentially specialized areolae or chorionic vesicles the absence of blood in absorptive areas may not be very significant.

Such speculations as Rau's and our own are probably of most value in drawing

attention to the paucity of information with which all of us are working. It is remarkable that the paper by Strahl and Ballmann on the ferret and this one on the sea otter are the only ones attempting to describe the full developmental history of the fetal membranes of a mustelid group represented by at least 29 recognized living genera. In fact of the well over 100 genera of Carnivora the only others for which the morphogenesis of the fetal membranes has been adequately described are the domestic dog and cat. At present even granting an enormously greater knowledge of comparative placentology, it is difficult to believe that such questions of placental evolution can ever be answered with complete scientific certainty. However future advances in our understanding of the mechanisms of heredity and differentiation may give us in sight far beyond our present capacity.

The ultrastructure and specific function of hematomas and other phagocytic absorptive areas are also matters of uncertainty. There is the somewhat academic question as to whether a hematoma is an example of epitheliochorial or hemochorial placentation. In the dog and especially in the cat where accumulation of extravasated maternal blood is minimal the blood clearly lies between relatively intact uterine epithelium and the phagocytic trophoblast of the chorio allantois. Such a hematoma is an area of the chorio allantois which is designed to absorb uterine contents composed of glandular secretions (uterine milk) and extravasated maternal blood. It is obviously homologous structurally with the absorptive areas or areolae well known in the pig placenta but also present in the moles, lemurs, galagos, lorises, cetaceans, perisodactyls, non-ruminant artiodactyls and camels. The placentae of all of these are largely epitheliochorial and the absorptive areas can also be considered epitheliochorial as Wislocki and Padykula (61) did. But what of the large stalked hematoma characteristic of the sea otter and raccoon (Creed and Biggers 63)? Here a large mass of maternal blood is enclosed in a complexly partitioned bag of absorptive vascular chorio allantois and the only connection with the uterine epithelium is

at the narrow base of the stalk. If maternal blood is so characteristically in contact with trophoblast while maternal epithelium occurs only at the base of the stalk and because there is also some fusion of uterine epithelium between the glands Creed and Biggers consider the raccoon hemophagous organ a form of hemochorial placentation. Strictly on the basis of the criteria used one can make a case for interpreting placental hematomas as either epitheliochorial or hemochorial. However Grosser applied his system of classification to the zone of the chorio allantoic and chorio vitelline placenta characterized by fetal capillaries in close apposition to channels containing actively circulating maternal blood to what might be called the zone of double circulation or vascular intimacy in other words the labyrinthine zone or the villous zone. This application of the Grosser system of terminology has been generally but not universally followed. To us it seems best to continue this application. In that case since the maternal blood of a hematoma is almost certainly not circulating and since it occupies a space along with uterine histiotrophs we prefer to regard such structures as supplementary placentae if they are large and clearly demarcated and simply as phagocytic absorptive areas if they are small and scattered in close association with the villous or labyrinthine zones. Enough confusion exists in the application of the still very useful Grosser terminology when one confines it to the areas of dual circulation or zones of intimacy of chorio allantoic and chorio vitelline placentae. The larger absorptive areas in carnivores almost always contain maternal blood and can be adequately distinguished by the term placental hematoma or hemophagous organ. Nothing is gained by applying the Grosser terminology to them as they are all essentially alike. In fact the histiotrophic absorptive areas of the carnivores and the many other groups mentioned above are of the same fundamental structure as the hematomas and hence do not need specific designation by Grosser's terminology.

The problem of hematoma function is well discussed by Creed and Biggers (63) yet somewhat futilely because of the lack

of experimental evidence. It is certain that the placental hematoma unlike the pathological one is a functional organ. Wislocki and Dempsey (46a, b) clearly demonstrated the absorption of iron by the columnar cytotrophoblastic cells of the hematoma and junctional zones of the cat and dog and by the areolae and chorionic vesicles of the pig. The highly developed columnar cytotrophoblastic cells are clearly specialized for phagocytic purposes. Yet the exact manner of utilization of the blood is unknown. No doubt many elements of the plasma are also absorbed in conventional manner but even this awaits proof. Certainly there is as yet no evidence of active digestive processes in absorptive areas but there is no doubt that in some cases whole erythrocytes are phagocytosed by the trophoblastic cells and that in others there is much breakdown of corpuscles and of hemoglobin itself in the cavity of the hematoma. The green pigment in the dog hematoma and similar rich pigmentation in hematomas of other species is direct proof of this cellular and chemical breakdown. Observation of apparently entire erythrocytes in the cytoplasm of the lining trophoblast cells in many forms including the sea otter black bear, dog, cat and bobcat (*Lynx rufa*) is good evidence for phagocytosis before erythrocyte breakdown. Apparently both processes usually occur together but perhaps in certain species only one prevails. For instance cats including the bobcat show relatively little pigmentary or other gross evidence of a marginal hematoma but sections of the area disclose large numbers of maternal erythrocytes being phagocytosed by the trophoblast lining a zone entirely comparable otherwise to the dog's green border. Apparently in such cases phagocytosis occurs as fast as extravasation hence there is little accumulation of maternal blood and most hemoglobin breakdown must occur intracellularly after phagocytosis and possibly during further transport to the fetal blood stream. In such hematomas as those of the mustelids the black bear and dog extravasation rate exceeds phagocytosis rate and therefore large masses of blood accumulate with resulting large scale hemolysis and hemoglobin breakdown in the hematoma. On

the face of it this latter situation seems less efficient and well adapted than the situation in the cats. This accords with our idea that the placentae of mustelids are relatively primitive and those of the felids more advanced.

The similarity of the fetal membranes of *Enhydra* to those of other mustelids is another example of the relative conservatism of fetal membrane characters within a major mammalian group of fairly certain phylogenetic interrelationships. Although the series of ontogenetic stages of the sea otter membranes is not as closely graded as could be desired it is complete enough to demonstrate that there is no significant variation from that of the ferret, dog or cat the only others as well known. In fact we have noted such complete similarity to these others in character of blastocyst, yolk sac, amnion, allantoic vesicle and umbilical cord that it has been unnecessary to describe these features other than to point out that they are typical of carnivore membranes so far studied. It seems probable in view of the known similarities between the later stages of the fetal membranes of representatives of the pinnipeds and of the seven families of fissipeds that there are no major divergences of membrane type within the order Carnivora although the detailed morphology of the hyaena placenta is certainly somewhat unusual (Morton 57, Wynn and Amoroso 64) and more information is needed to understand just how far it differs from the type. If differences of fundamental nature are found they will probably be in the most primitive or the most specialized or aberrant genera.

Synopsis of basic data on the fetal membranes of the sea otter

Implantation

Orientation (disc) Antimesometrial

Orientation (first attachment) Antimesometrial and mesometrial becoming zonary

Depth Superficial

Decidua None Great hypertrophy and dilation of uterine glands

Amniogenesis Folding

Chorion Present early but all eventually converted to chorio-allantois

Yolk sac

Bilaminar omphalopleure Temporary
Chorio-vitelline placenta Well developed and persists through limb bud stage

Vascular splanchnopleure Medium sized collapsed permanent bilobed or T shaped sac attached by a strand at each arm of the T to the chorion

Chorio-allantoic placenta

Shape Annular lobed (sometimes in complete) Type Labrynthine

Finer morphology Endotheliochorial (appears by light microscopy to be endothelio-endothelial at many points late in gestation)

Accessory placenta Antimesometrial pedunculated sac like hematoma surrounded by smaller hematoma pouches

Location Annular

Allantoic vesicle Large and permanent

Authorities Authors

LITERATURE CITED

- Amoroso E C 1952 Placentation In Marshall's Physiology of Reproduction A S Parkes ed Longmans London Vol 2 Ch 15
- 1954 The comparative anatomy and histology of the placental barrier In Gestation L B Flexner ed The Josiah Macy Jr Foundation by Corlies Macy and Company Inc New York 119-224
- Barabash Nikiforov I I 1947 The sea otter (*Enhydra lutris* L.) Translated from Russian by A Burton and Z S Cole Published for the National Science Foundation Washington D C by the Israel Program for Scientific Translations Jerusalem 1962
- Bischoff T L W 1865a Ueber das Vorkommen eines eigenthümliches Blut und Hämoglobin enthaltenden Beutels an der Placenta der Fischotter (*Lutra vulgaris*) Sitzungsber Akad Wissensch München 1 214-255
- 1865b Ueber die Ei und Placenta Bildung des Hehn und Edel Marders (*Mustela foina* und *martes*) und des Wiesels (*M. vulgaris*) Sitzungsber Akad Wissensch München 1 339-348
- Creed R F S and J D Biggers 1963 Development of the raccoon placenta Am J Anat 113 417-445
- 1964 Placental hemophagous organs in the Procyonidae and Mustelidae J Reprod Fertil 8 133-137
- Enders A C 1957 Histological observations on the chorio-allantoic placenta of the mink Anat Rec 127 231-245
- Fleischmann A 1891 Entwicklung und Struktur der Placenta bei Raubtieren Sitzungsber d k Preuss Akad d Wissensch Berlin 661-670
- Hamilton W J 1934 The early stages in the development of the ferret Fertilization to the formation of the prochorial plate Trans Roy Soc Edin 58 251-278
- 1937 The early stages in the development of the ferret The formation of the mesoblast and notochord Trans Roy Soc Edin 59 165-193
- Hamlett G W D 1932 Observations on the embryology of the badger Anat Rec 53 283-303
- Hansson A 1947 The physiology of reproduction in mink (*Mustela vison* Schreb) with special reference to delayed implantation Acta Zool 28 1-136
- Lawn A M and A D Chiquoine 1965 The ultrastructure of the placental labyrinth of the ferret (*Mustela putorius furo*) J Anat 99 47-69
- Lensink C J 1962 The history and status of sea otters in Alaska Dissertation Abstract 22 5 (chapter on reproduction seen)
- Morton W R M 1957 Placentation in the spotted hyena (*Crocuta crocuta*) J Anat 91 374-382
- Mossman H W 1937 Comparative morphogenesis of the fetal membranes and accessory uterine structures Contrib Embryol Carnegie Inst Wash 26 129-246
- 1953 The genital system and the fetal membranes as criteria for mammalian phylogeny and taxonomy J Mammal 34 289-298
- Pearson O P 1952 Notes on pregnant sea otter J Mammal 33 387
- Rau A Subba 1925 Contributions to our knowledge of the structure of the placenta of Mustelidae Ursidae and Sciuridae Proc Zool Soc London 1027-1070
- Robinson A 1904 Lectures on the early stages in the development of mammalian ova and on the differentiation of the placenta in the different group of mammals J Anat 38 186-204 325-340 and 485-502
- Sinha Akhouri A 1965 Morphology of the female reproductive organs of sea otters (*Enhydra lutris* L.) Dissertation University of Missouri Columbia Missouri
- 1965 Ovary of the sea otter *Enhydra lutris* L Am Zoologist 5 668
- Sinha Akhouri A C H Conaway and A W Kenyon 1966 Reproduction in the female sea otter J Wildlife Management 30 121-130
- Starck D 1959 Ontogenie und Entwicklungsphysiologie der Säugetiere Walter de Gruyter and Company Berlin 9 1-276
- Strahl H 1906 Die Embryonalhüllen der Säugetiere und die Placenta In Handbuch der vergleichenden und experimentellen Entwicklungslehre der Wirbeltiere O Hertwig ed Jena 1 (2) 235-268
- Strahl H and E Ballmann 1915 Embryonalhüllen und Placenta von *Putorius furo* Abhandl d k Preuss Akad der Wissensch Berlin (Phys Math Cl) 1-69

- Strass, F 1943 Die placentation von *Erinaceus artemus* Rev Suisse Zool 50 17-87
- Tobler W P 1914 The problem of aquatic adaptation in the carnivora as illustrated in the osteology and evolution of the sea otter Calif Publ Bull Dept of Geol 7 465-493
- Vincent, W A and A Gopalakrishna 1958 Occurrence of a placental hematoma in the sensitive streath tailed bats (*Emballonuridae*) with observations on its structure development and histochemistry Am J Anat 103 35-67
- Wislocki G B and E W Dempsey 1946(a) Histochemical reactions in the placenta of the cat Am J Anat 78 1-45
- 1946b Histochemical reactions of the placenta of the pig Am J Anat 78 181-226
- Wislocki G B and E C Amoroso 1956 The placenta of the wolverine (*Gulo gulo luscus*) Bull Mus Comp Zool Harvard Univ 114 91-100
- Wynn R M and E C Amoroso 1964 Placentation in the spotted hyena (*Crocuta crocuta* Erxleben) with particular reference to the circulation Am J Anat 115 327-362

Yolk sac

Bilaminar omphalopleure Temporary
Chorio-vitelline placenta Well developed and persists through limb bud stage

Vascular splanchnopleure Medium sized collapsed permanent bilobed or T shaped sac attached by a strand at each arm of the T to the chorion

Chorio-allantoic placenta

Shrpe Annular lobed (sometimes in complete) Type Labyrinthine

Finer morphology Endotheliochorial (appears by light microscopy to be endothelio endothelial at many points late in gestation)

Accessory placentae Antimesometrial pedunculated sac like hematome surrounded by smaller hematoma pouches

Location Annular

Allantoic vesicle Large and permanent

Authorities Authors

LITERATURE CITED

- Amoroso E C 1952 Placentation In Marshall's Physiology of Reproduction A S Parkes ed Longmans London Vol 2 Ch 15
- 1954 The comparative anatomy and histology of the placental barrier In Gestation L B Flexner ed The Josiah Macy Jr Foundation by Corlies Macy and Company Inc New York 119-224
- Barabash Nikiforov I I 1947 The sea otter (*Enhydra lutris* L.) Translated from Russian by A Birron and Z S Cole Published for the National Science Foundation Washington D C by the Israel Program for Scientific Translations Jerusalem 1962
- Bischoff T L W 1865a Ueber das Vorkommen eines eigenthümlichen Blut und Harnstoffin enthaltenden Beutels an der Placenta der Fischotter (*Lutra vulgaris*) Sitzungsab Akad Wissensch München 1 214-255
- 1865b Ueber die Ei und Placenta Bildung des Heim und Edel Marders (*Mustela foina* und *martes*) und des Wiesels (*M. putorius*) Sitzungsab Akad Wissensch München 1 339-348
- Creed R F S and J D Biggers 1963 Development of the raccoon placenta Am J Anat 113 417-445
- 1964 Placental hemophagous organs in the Procyonidae and Mustelidae J Reprod Fert 8 133-137
- Enders A C 1957 Histological observations on the chorio allantoic placenta of the mink Anat Rec 127 231-245
- Fleischmann A 1891 Entwicklung und Struktur der Placenta bei Raubtieren Sitzungsab Akad Wissensch Berlin 661-670
- Hamilton W J 1934 The early stages in the development of the ferret Fertilization to the formation of the prochordal plate Trans Roy Soc Edin 58 251-278
- 1937 The early stages in the development of the ferret The formation of the mesoblast and notochord Trans Roy Soc Edin 59 165-193
- Hamlett G W D 1932 Observations on the embryology of the badger Anat Rec 53 283-303
- Hansson A 1947 The physiology of reproduction in mink (*Mustela vison* Schreb) with special reference to delayed implantation Acta Zool 28 1-136
- Lawn A M and A D Chiquoine 1965 The ultrastructure of the placental labyrinth of the ferret (*Mustela putorius furo*) J Anat 99 47-69
- Lensink C J 1962 The history and status of sea otters in Alaska Dissertation Abstract 22 5 (chapter on reproduction seen)
- Morton W R M 1957 Placentation in the spotted hyena (*Crocuta crocuta*) J Anat 91 374-382
- Mossman H W 1937 Comparative morphogenesis of the fetal membranes and accessory uterine structures Contrib Embryol Carnegie Inst Wash 26 129-246
- 1953 The genital system and the fetal membranes as criteria for mammalian phylogeny and taxonomy J Mammal 34 289-298
- Pearson O P 1952 Notes on pregnant sea otter J Mammal 33 387
- Rau A Subba 1925 Contributions to our knowledge of the structure of the placenta of Mustelidae Ursidae and Sciuridae Proc Zool Soc London 1027-1070
- Robinson A 1904 Lectures on the early stages in the development of mammalian ova and on the differentiation of the placenta in the different group of mammals J Anat 38 166-204 325-340 and 485-502
- Sinha Akhouri A 1965 Morphology of the female reproductive organs of sea otters (*Enhydra lutris* L.) Dissertation University of Missouri Columbia Missouri
- 1965 Ovary of the sea otter *Enhydra lutris* L Am Zoologist 5 668
- Sinha Akhouri A C H Conaway and H W Kenyon 1966 Reproduction in the female sea otter J Wildlife Management 30 121-130
- Starck D 1959 Ontogenie und Entwicklungsphysiologie der Säugetiere Walter de Gruyter and Company Berlin 9 1-276
- Strahl H 1906 Die Embryonalhüllen der Säugetiere und die Placenta In Handbuch der vergleichenden und experimentellen Entwicklungslehre der Wirbeltiere O Hertwig ed Jena 1 (2) 235-268
- Strahl H and E Ballmann 1915 Embryonalhüllen und Placenta von *Putorius furo* Abhandl d k Preuss Akad der Wissensch Berlin (Phys Math Cl) 1-69

- Schiff F 1943 Die placentation von *Ericulus*
gliscus Rev Suisse Zool 50 17-87
- Inter W P 1914 The problem of aquatic
adaptation in the carnivora as illustrated in
the osteology and evolution of the sea otter
Law Calif Publ Bull Dept of Geol 7
455-495
- Kinsitt, W A and A Gopalakrishna 1958
Occurrence of a placental hematoma in the
fruit-eating striped tailed bats (*Emballonuridae*)
with observations on its structure development
and histochemistry Am J Anat 103 35-67
- Wislocki G B and E W Dempsey 1946(a)
Histochemical reactions in the placenta of the
cat Am J Anat 78 1-45
- 1946b Histochemical reactions of the
placenta of the pig Am J Anat 78 181-226
- Wislocki G B and E C Amoroso 1956 The
placenta of the wolverine (*Gulo gulo luscus*)
Bull Mus Comp Zool Harvard Univ 111
91-100
- Wynn R M and E C Amoroso 1964 Pla-
centation in the spotted hyena (*Crocuta cro-
cuta* Ertleben) with particular reference to
the circulation Am J Anat 115 327-362

PLATE 1

EXPLANATION OF FIGURES

- 13 Unimplanted blastocyst in the uterine lumen. The irregular scattering of the cells is probably an artifact. Note the large number of uterine glands characteristic of carnivores. 107-55 \times 80
- 14 Cross section of uterus showing asymmetrical endometrial lobes and large collapsed blastocyst probably near time of implantation. 62-41 \times 11
- 15 Higher magnification of uterine wall of figure 14 showing the luminal compact zone, the still thin middle spongy zone where the gland lumina are just beginning to dilate, and the relatively thick deep glandular zone. 62-41 \times 52
- 16 Cross section of gestation sac showing endometrial lobes and grooves spanned by smooth chorion. Note the lack of spongy zone at the grooves. Between the antimesometrial allantoic sac (above in fig.) and the mesometrial yolk sac is the large exocoelom. 42-40 \times 8
- 17 Another section of the gestation sac shown in figure 16 showing the allantoic stalk (arrow). 42-40 \times 8
- 18 Another section of the gestation sac shown in figure 16 showing the antimesometrial hematoma just starting to bulge toward the allantoic vesicle. It is on the major endometrial lobe. 42-40 \times 8

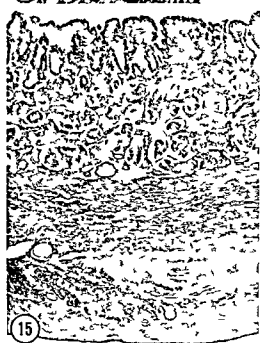
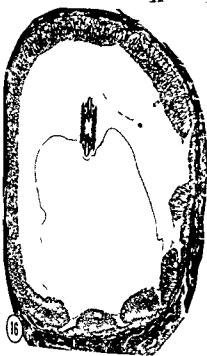


PLATE 2

EXPLANATION OF FIGURES

- 19 Detail of a portion of the mesometrial region of figure 16 showing the chorio vitelline placental labyrinth (above) the spongy zone and the unmodified glands of the deep glandular zone. The spongy zone glands are hypertrophied greatly dilated and their walls folded. Note the splanchnopleuric yolk sac (arrow) and just outside it the smooth chorion spanning an endometrial groove where the spongy zone is lacking. The uterine lumen undercuts the margin of the chorio vitelline placenta 62-40 \times 32
- 20 Detail of beginning chorio-vitelline placenta (earlier than fig 19) showing relatively straight and solid trophoblastic villi penetrating the gland lumina 62-168 \times 200
- 21 Detail of figure 19 showing the chorio-vitelline labyrinth which is endotheliochorial in type. The villi have vascular mesodermal cores (arrow) and are branched and tortuous. Note the dark masses of gland symplasma at the tips of the villi 62-10 \times 100
- 22 Detail of the chorio-allantoic labyrinth in the antimesometrial region shown in figure 16. Note the similarity to the chorio-vitelline placenta shown in figure 21 both are endotheliochorial 62-40 \times 100

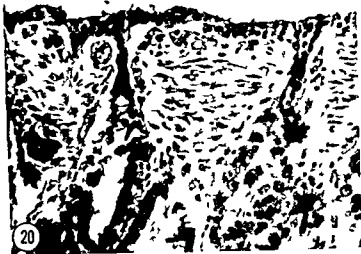


PLATE 2

EXPLANATION OF FIGURES

- 19 Detail of a portion of the mesometrial region of figure 16 showing the chorio vitelline placental labyrinth (above) the spongy zone and the unmodified glands of the deep glandular zone. The spongy zone glands are hypertrophied greatly dilated and their walls folded. Note the splanchnopleuric yolk sac (arrow) and just outside it the smooth chorion spanning an endometrial groove where the spongy zone is lacking. The uterine lumen undercuts the margin of the chorio vitelline placenta 62-40 \times 32
- 20 Detail of beginning chorio-vitelline placenta (earlier than fig 19) showing relatively straight and solid trophoblastic villi penetrating the gland lumina 62-168 \times 200
- 21 Detail of figure 19 showing the chorio vitelline labyrinth which is endotheliochorial in type. The villi have vascular mesodermal cores (arrow) and are branched and tortuous. Note the dark masses of gland symplasma at the tips of the villi 62-10 \times 100
- 22 Detail of the chorio-allantoic labyrinth in the antimesometrial region shown in figure 16. Note the similarity to the chorio-vitelline placenta shown in figure 21 both are endotheliochorial 62-40 \times 100



PLATE 3

EXPLANATION OF FIGURES

- 23 An intermediate stage of the chorio-allantoic placenta showing the labyrinth the spongy zone glands and a few glands (arrow) of the deep zone *Note the maternal vessel in a septum* 62-53 $\times 28$
- 24 Detail of placenta shown in figure 23 showing the endotheliochorial labyrinth The maternal capillary endothelium is noticeably thick 62-53 $\times 100$
- 25 Margin of the antimesometrial portion of the zonary band of an intermediate stage placenta showing the deep undercut (arrow) and the slanting direction of the dilated glands 62-136 $\times 32$
- 26 Detail of labyrinth of definitive stage of the chorio-allantoic placenta showing the well developed villi and the sharply delineated zones of intimacy between them 62-29 $\times 20$
- 27 Intermediate placenta showing spongy zone glands diverging fanlike from a small area This borders a deep interlobular groove (arrow) on the fetal surface of the placenta 62-147 $\times 20$
- 28 Definitive placenta showing the relatively thick labyrinth and the greatly compressed junctional and spongy zones Maternal vessels are prominent in the septa at the base and in the myometrium 62-47 $\times 11$

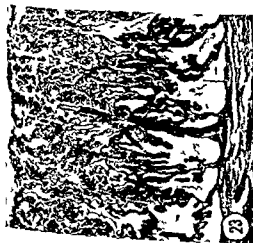


PLATE 4

EXPLANATION OF FIGURES

- 29 Portion of antimesometrial region of specimen shown in figures 16-18 showing early hematoma pouches coalescing to form larger ones 62-40 \times 32
- 30 More marginal portion of hematoma area shown in figure 29 showing separate small developing hematoma pouches with their closely apposed chorio allantoic vessels 62-40 \times 32
- 31 Section of a definitive placenta through the hematoma showing its folds or septa extending into its stalk and the dilatation with blood of the glands to which the stalk attaches ADFG 518 \times 68
- 32 Section through part of the hematoma and stalk of a late placenta showing the complicated folding of its lining and the connections of its cavity with those of the basal glands 62-135 \times 65
- 33 Portion from figure 32 enlarged to show continuity of chorio allantois of labyrinth (upper margin) with that of hematoma. The tall epithelium and the brown pigment (black in illustration) of the highly folded absorptive lining of the hematoma are obvious 62-135 \times 16



PLATE 5

EXPLANATION OF FIGURES

- 34 Detail of the base of the definitive placenta showing an interglandular septum with its vessels complex folds and columnar epithelium. In the gland lumen at the right is a characteristic villous tip covered by columnar phagocytic epithelium 62-47 $\times 100$
- 35 Detail at the base of the hematome stalk of a late placenta (same as fig 32) showing the fibrous zone surrounding the area where the stalk connects to the spongy gland zone. Here the maternal capillaries and other small vessels are shrunken and their endothelium is degenerating. They are strongly PAS positive and hence appear black in the photomicrograph. Apparently maternal blood leaks from these vessels into the dilated glands and into the stalk of the hematome 62-135 $\times 32$
- 36 Detail of a portion of the stalk of the late hematome in figure 32 showing a narrow channel between two folds of chorionic allantoic membrane. The tall columnar trophoblastic epithelium is packed with phagocytosed maternal erythrocytes. Note the rich fetal capillary plexus at its base 62-135 $\times 200$
- 37 Detail of a portion of the early hematome shown in figure 18. The trophoblastic epithelium is already tall columnar and actively phagocytic 62-40 $\times 200$
- 38 Detail of a branched fold in a late hematome. The tall phagocytic cells are full of maternal erythrocytes. Although not shown here in most places the lumen would be completely occupied by mostly degenerating maternal erythrocytes and much pigment often in crystalline form. The detached cells and degenerating cell fragments shown here are probably the result of postmortem changes before fixation of the tissue 62-37 $\times 200$



PLATE 6

EXPLANATION OF FIGURES

- 39 Detail of a portion of the junction of the hematome stalk and adjacent labyrinth of the late placenta shown in figure 32. The connective tissue strip to the right of center is the core of a chorio-allantoic villus. Note that the trophoblast on its left side forms the epithelial lining of the stalk of the hematome while that on its right side forms the labyrinthine trophoblast enclosing the vessels lined by maternal endothelium. 62-135 \times 112
- 40 Detail of the margin of the placenta shown in figure 25. The central portion of the figure is occupied by a villus-like fold of the chorio-allantoic membrane just lateral to the endotheliochorial labyrinth. At the right is the low columnar epithelium of the uterine wall and at the left a portion of the outer wall of one of the most lateral glands of the spongy zone. The absence of uterine epithelium from this latter portion may be due to postmortem sloughing. The trophoblastic epithelium of these marginal folds appears to be as actively phagocytic as it is at the tips of the villi throughout the placental base. 62-136 \times 200
- 41 Labyrinth of a late placenta. 62-135 \times 80
- 42 Detail of the labyrinth of the definitive stage of the placenta shown in figure 28. Note the thick maternal endothelium *c* lining the broad maternal tubules and the adjacent trophoblastic layer often deeply indented toward the tubules by fetal capillaries *c*. 62-47 \times 384



The Production of Congenital Malformations Using Tissue Antisera

IV EVALUATION OF THE MECHANISM OF TERATOGENESIS BY VARYING THE ROUTE AND TIME OF ADMINISTRATION OF ANTI RAT KIDNEY ANTISERUM¹

ROBERT L BRENT

*Departments of Radiology Pediatrics and the Eleanor Roosevelt
Cancer Research Laboratories of the Jefferson Medical College
Philadelphia Pennsylvania*

ABSTRACT Sheep anti rat kidney serum and rabbit anti rat kidney serum were utilized in a number of biological studies in order to clarify some of the qualitative and quantitative effects of this antiserum. The teratogenic factor or factors present in these antisera can be characterized as follows. The antiserum is (1) ineffective when administered by the oral route (2) the antiserum is teratogenic when administered by the intravenous intraperitoneal subcutaneous or intrauterine route (3) more effective by the intravenous and intraperitoneal route than by the subcutaneous route and (4) no more effective when injected into the uterine lumen of a pregnant rat than when given intravenously (5) uterine vascular clamping experiments and injection of the antiserum during the preimplantation period indicate that the teratogenic milieu persists for days following the administration of the antiserum (6) the antiserum can be considered a classical teratogenic agent because it produces a different spectrum of malformations on different days of gestation and concomitant fetal mortality and growth retardation although stage specificity is not as dramatic with the antiserum as with irradiation (7) although the exact mechanism of teratogenesis is not understood it was pointed out that fluorescent localization data and the experiments reported herein indicate a similarity between teratogenic antiserum and trypan blue (8) the importance of yolk sac pathology during the period of differentiation is discussed as it pertains to normal embryology teratogenesis and the utilization of animals in drug testing programs for the evaluation of teratogenic effects

The teratogenicity of rat kidney anti serum has previously been reported (Brent Averch and Drapiewski 61) and corroborated (David Mercier and Tuchman-Duplessis 63). Furthermore rat placental antiserum has also been demonstrated to be teratogenic (Brent 64a b 65 66a). Both these antisera produce a similar spectrum of congenital malformations in rat embryos exposed to the antisera during the early periods of differentiation (Brent 64a 65). As yet we cannot confidently state the exact series of events that result in congenitally malformed offspring. In fact we are not certain of the primary site of action of the antiserum (embryo maternal organism placenta or extraembryonic membranes).

The purpose of this presentation is to further characterize the biologic aspects of antiserum induced teratogenesis by varying the route and time of injection of

the antiserum. It would be beneficial to know the similarities and differences between these antisera and other well known teratogenic agents. Finally further characterization of the quantitative and qualitative properties of teratogenic serum may provide valuable direction to the necessary biochemical and immunologic studies.

MATERIALS AND METHODS

The method of obtaining timed pregnancies in our strain of Wistar rats has been described in previous publications (Brent 64a). The pregnant rat was anesthetized with sodium pentobarbital (30 mg/kg subcutaneously) on the day that the antiserum was injected. If the maternal rat was pregnant for five or more days a laparotomy was performed and the number and condition of the embryonic sites

¹ Supported by N.I.H. grant HD 630 and 1 T1 HD 141

TABLE 1

The teratogenic lethal and growth retarding effects of rabbit anti rat kidney serum when administered by the intravenous intraperitoneal subcutaneous or oral route to rats eight days pregnant

Route of administration	Dose in ml/100 g pregnant rat	Number of embryos (Pre-injection)	Per cent mortality	Term number	Fetuses weight \pm S D	Per cent fetuses malformed
Intravenous	0.125	58	10.5	52	4.51 \pm 0.37	42.3
	0.25	65	24.2	52	4.15 \pm 0.52	75.0
	0.50	80	48.9	41	4.19 \pm 0.67	95.2
Intraperitoneal	0.25	68	19.0	55	4.06 \pm 0.17	85.6
	0.50	87	49.4	44	4.04 \pm 0.21	79.6
	0.75	68	97.1	2	1.55	100.0
	1.0	71	100.0	0	—	—
Subcutaneous	0.25	79	5.1	75	5.21 \pm 0.502	5.3
	—	—	—	—	—	—
	0.75	68	20.5	53	4.12 \pm 0.60	81.2
Oral	1.00	63	31.8	43	3.87 \pm 0.62	86.3
	1.00	74	0.0	74	4.44 \pm 0.36	0.0
	2.00	59	5.1	56	4.93 \pm 0.41	1.9
Control	3.00	24	4.1	23	5.05 \pm 0.31	0.0
	—	97	8.2	89	4.80 \pm 0.31	1.7

TABLE 2

The spectrum and incidence of malformations produced by intravenous intraperitoneal and subcutaneous administration of rabbit anti rat kidney antiserum to rat eight days pregnant

	Route of administration		
	I V	I P	S C
Total live term fetuses from all dosage groups	145	101	171
Total live term fetuses with one or more malformations	103	84	85
Per cent live term fetuses malformed	71.2	83.2	50.0
	Per cent malformed fetuses with a particular malformation		
Situs inversus totalis	13	24	23
Omphalocele and evisceration	27	83	—
Anencephaly	—	24	—
Meningocele	—	12	—
Encephalocele	27	155	39
Hydrocephaly	59.7	75.0	67.4
All eye malformations	76.3	96.5	81.3
Cleft palate	—	47	46
Facial clefts	—	24	—
Jaw and tongue malformation	18.0	83	46
Aortic arch malformation (total)	69	25.0	98
Diaphragm anomalies	13	24	69
Right renal agenesis	—	—	23
Left renal agenesis	13	155	186
Bilateral renal agenesis	69	107	162
Left ovarian agenesis	—	12	—
Left uterine agenesis	—	23	—
Bilateral testicular agenesis	41	—	23
Right sided cryptorchidism	—	—	—
Left sided cryptorchidism	27	24	46
Bilateral cryptorchidism	69	131	69
Bilateral absent or low set ears	—	24	—
Syndactyly	—	—	—
Limb hypoplasia	—	—	—
Recto vesical fistula	—	12	—

were observed and recorded. The incision was closed with silk sutures and metal wound clamps and the animal was injected or administered teratogenic kidney antiserum and allowed to go until the twenty first day of gestation at which time the maternal organism was sacrificed and the fetuses were delivered by cesarean section. The fetuses were weighed, fixed in Bouin's solution and dissected. The mortality, mean weight, standard deviation of the fetal weights and the incidence of malformations were determined.

There were three separate experiments dealing with modifications of route and time of administration of the teratogenic antiserum. The first series of experiments consisted of the administration of teratogenic doses of antiserum to anesthetized eight day pregnant rats via the oral, subcutaneous, intraperitoneal or intravenous route (tables 1-2). The intravenous injection

was administered via the tail vein. The oral administration of the antisera was carried out with the aid of a small polyethylene catheter which was placed in the animal's stomach.

In the second series of experiments the teratogenic antiserum was injected into the lumen of a pregnant rat uterus (fig. 1, table 3). In order to make certain that the antiserum once placed in the uterine cavity did not leak out via the vagina or fallopian tube, a ligature was placed at both the vaginal and ovarian ends of the uterus without interfering with the blood supply to that uterine horn (fig. 1). Following the placement of the ligatures, a small volume of highly concentrated antiserum was injected into the uterine lumen with a 30 gauge stainless steel needle. The other uterine horn was similarly prepared and injected with saline rather than teratogenic serum (table 3).

TABLE 3

Comparison of the effect of an intravenous injection of teratogenic sheep anti-rat kidney serum and a comparable dose injected intraluminally into the isolated right uterine horn of an eight day pregnant rat

Agent injected	Route	Dose	Mortality		Term fetal weight		Malformation	
			Right horn	Left horn	Right horn	Left horn	Right horn	Left horn
Saline	intrauterine	0.5 ml	14.2	0	4.239 gm	4.240 gm	0	0
Sheep anti-rat kidney serum	intrauterine	140 mg (0.25 ml)	100	100	—	—	—	—
Sheep anti-rat kidney serum	intrauterine	70 mg (0.25 ml)	100	100	—	—	—	—
Sheep anti-rat kidney serum	intrauterine	35 mg (0.25 ml)	95.2	52.9	2.998	3.212	100	100
Sheep anti-rat kidney serum	intravenous	35 mg	88.2	82.8	2.457	2.467	100	100
Sheep anti-rat kidney serum	intrauterine	26.5 mg	80.0	77.7	3.690	2.948	100	100
Sheep anti-rat kidney serum	intrauterine	87.5 mg/kg approx 20 mg/rat	34.7	14.2	4.128	4.252	86.6	75
Sheep anti-rat kidney serum	intravenous	87.5 mg/kg approx 20 mg/rat	11.7	16.7	4.006	4.099	53.5	60

¹ Ligature was placed at ovarian and cervical ends without interfering with blood supply to prevent injected material from leaking out via the fallopian tube and/or vagina.

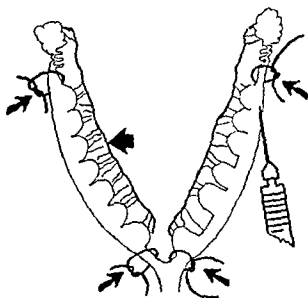


Fig 1 The intrauterine injection of either saline or teratogenic serum was accomplished with a number 30 needle. The cervical and ovarian ends of both uterine horns were ligated prior to the injection without interfering with the uterine blood supply. The small arrows point to the ligatures and the large arrow points to the intact uterine vascular supply. By concentrating the serum effective amounts could be administered in small volumes.

The third series of experiments consisted of administering teratogenic anti-serum by the intraperitoneal route on various days of gestation prior to the time of differentiation (table 4). It was previously reported that congenital malformations could be produced by injecting teratogenic antiserum on the seventh, eighth, ninth or tenth day of rat gestation (Brent, 64a). In these studies teratogenic kidney anti-serum was administered after zero, three and five days of rat gestation.

The fourth series of experiments consisted of combining the uterine vascular clamping procedure with the intravenous injection of teratogenic rabbit anti-rat kidney antiserum. In previous reports we demonstrated that 30 minutes of uterine vascular clamping on the eighth day of gestation did not appreciably interfere with embryonic growth or produce excessive fetal mortality or malformations (Brent and Franklin '60, Franklin and Brent '64). Therefore, following the application of clamps to both the cervical and ovarian ends of one uterine horn an intravenous injection of teratogenic anti-serum was administered to a pregnant rat on the eighth day of gestation. Thirty minutes later the clamp was removed and the pregnant rat was allowed to go to term. There were 54 pregnant rats who underwent the combined clamping procedure and injection of the teratogenic antiserum (table 5).

RESULTS

The teratogenic lethal and gross retardation effect of rabbit anti-rat kidney anti-sera administered by various routes is summarized in table 1. The operative control group had a malformation rate of 1.7% and a resorption rate of 8.2%. The administration of massive doses of teratogenic serum via the oral route did not interfere with the embryonic development of the rat. The intravenous, intraperitoneal and subcutaneous routes of administration all had some deleterious effect upon the embryo. The subcutaneous route was the least effective of the three for

TABLE 4

The teratogenic lethal and growth retarding effectiveness of a single administration of rabbit anti-rat kidney serum on various days of gestation in the rat

Day	Dose of antiserum ml/100 g of rat	Number of embryos after 8 days of pregnancy	Number of term fetuses	Mortality %	Term fetal weight g	Malformations %
0	1.0	31	29	6.4	4.660 ± 0.37 ¹	6.8
3	0.5	51	48	5.8	4.762 ± 0.41	16.6
5	0.5	36	34	5.5	4.285 ± 0.52	47.0
7	0.5	66	36	45.4	3.990 ± 0.61	38.9
8	0.5	87	44	49.4	4.191 ± 0.44	95.6
9	0.5	87	54	38.0	4.110 ± 0.43	55.6
10	0.5	80	69	23.6	3.801 ± 0.57	42.0

TABLE 5

The effect of combining the technique of uterine vascular clamping and the intravenous injection of teratogenic antiserum into eight-day pregnant rats

	Length of clamping	Dose of antiserum	Number of embryos	Mortality	Term fetal weight	Mal formations
	minutes	ml		%	g	%
Clamping alone	30	0	74	6.7	4.59	3.9
Clamping plus antiserum	30	0.25	191	29.8	4.475	16.4
Antiserum alone	0	0.25	234	27.8	4.507	18.8

the embryos could receive over twice the amount of the antisera that was equivalent to the intravenous or intraperitoneal LD/50 dose and yet have only a 30% mortality. In spite of this there was a dose of antiserum that could be given by any of these three routes that would result in malformations lethality and growth retardation. Although the intravenous and intraperitoneal routes were fairly comparable at the high dose levels it was possible to produce malformations with significantly smaller intravenous doses than were listed in table 1 while these same small doses given by the intraperitoneal route were not teratogenic.

The spectrum and incidence of malformations following the injection of teratogenic serum by various routes are summarized in table 2. The incidence and type of malformations are not too different following the administration of teratogenic antiserum by the three parenteral routes. Those organ systems which are heavily involved following the administration of the antiserum by one route are similarly involved when the antiserum is administered by the other routes. There was a lower incidence of malformations in the group administered the teratogenic serum subcutaneously probably because all groups of animals in this category received less than the embryonic LD/50 dose (table 1).

A comparison of the effectiveness of the intrauterine and intravenous route of administration yielded some very interesting results (table 3). When saline was injected into the ligatured uterine horn it was not surprising to find a slightly increased mortality in the embryos in the injected uterine horn although the incidence of malformations was no greater

than in the control group. If the intrauterine injection of concentrated teratogenic serum contained more than 70 mg of lyophilized teratogenic serum there was a 100% mortality in both uterine horns. In the experimental groups in which some embryos survived it was apparent that the intrauterine method of administering the antiserum was no more effective than the intravenous route. Furthermore the fetuses from the intrauterine group that were in the uninjected uterine horn were just as severely affected as were those fetuses in the horn that received the intraluminal injection of antisera (table 3).

Thus the embryos in the uninjected or control uterine horn had the same incidence of malformations, resorptions and growth retardation as the embryos in the tied and injected uterine horn. Furthermore the mortality and incidence of malformations are quantitatively the same following either the intraluminal or intravenous injection of the same dose of antiserum.

The administration of teratogenic antiserum prior to and during the period of implantation yielded the most unpredictable results since malformations were observed in term fetuses whose mothers were injected with antiserum on the third and fifth day after conception (table 4). It is even more interesting to note that in the five-day group the term mortality was only 5.5% although the incidence of malformations was 47%. Furthermore there was no evidence of increased mortality or growth retardation in the three-day group and yet there was a significant increase in the incidence of malformations. Thus it is apparent that the injection of teratogenic antiserum from the third day post conception to at least the tenth day post

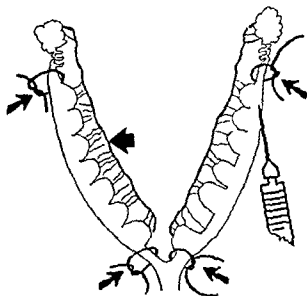


Fig 1 The intrauterine injection of either saline or teratogenic serum was accomplished with a number 30 needle. The cervical and ovarian ends of both uterine horns were ligated prior to the injection without interfering with the uterine blood supply. The small arrows point to the ligatures and the large arrow points to the intact uterine vascular supply. By concentrating the serum effective amounts could be administered in small volumes.

The third series of experiments consisted of administering teratogenic anti serum by the intraperitoneal route on various days of gestation prior to the time of differentiation (table 4). It was previously reported that congenital malformations could be produced by injecting teratogenic antiserum on the seventh, eighth, ninth or tenth day of rat gestation (Brent '64a). In these studies teratogenic kidney anti serum was administered after zero, three and five days of rat gestation.

The fourth series of experiments consisted of combining the uterine vascular clamping procedure with the intravenous injection of teratogenic rabbit anti rat kidney antiserum. In previous reports we demonstrated that 30 minutes of uterine vascular clamping on the eighth day of gestation did not appreciably interfere with embryonic growth or produce excessive fetal mortality or malformations (Brent and Franklin '60, Franklin and Brent '64). Therefore, following the application of clamps to both the cervical and ovarian ends of one uterine horn an intravenous injection of teratogenic anti serum was administered to a pregnant rat on the eighth day of gestation. Thirty minutes later the clamp was removed and the pregnant rat was allowed to go to term. There were 54 pregnant rats who underwent the combined clamping procedure and injection of the teratogenic antiserum (table 5).

RESULTS

The teratogenic lethal and gross retarding effect of rabbit anti rat kidney anti sera administered by various routes is summarized in table 1. The operative control group had a malformation rate of 1.7% and a resorption rate of 8.2%. The administration of massive doses of teratogenic serum via the oral route did not interfere with the embryonic development of the rat. The intravenous, intraperitoneal and subcutaneous route of administration all had some deleterious effect upon the embryo. The subcutaneous route was the least effective of the three for

TABLE 4

The teratogenic, lethal and growth retarding effectiveness of a single administration of rabbit anti rat kidney serum on various days of gestation in the rat

Day	Dose of antiserum ml/100 g of rat	Number of embryos after 8 days of pregnancy	Number of term fetuses	Mortality	Term fetal weight	Malformations
0	1.0	31	29	6.4	4.680 ± 0.37 ¹	6.8
3	0.5	51	48	5.8	4.762 ± 0.41	16.6
5	0.5	36	34	5.5	4.285 ± 0.52	47.0
7	0.5	66	36	45.4	3.990 ± 0.61	38.9
8	0.5	87	44	49.4	4.191 ± 0.44	95.6
9	0.5	87	54	38.0	4.110 ± 0.43	55.6
10	0.5	80	69	13.6	3.801 ± 0.57	42.0

fetal death growth retardation and malformations Early injection of the anti serum practically eliminates the lethal effect while fetal growth retardation and malformation appear to be modified to a similar extent (table 4) Does this mean that the growth retarding and malforming factor or factors in the antiserum are the same or more closely allied than the factor which produces lethality? Until the pathologic immunoglobulins can be isolated in pure form one cannot determine whether all three pathologic effects are properties of one or more molecules

If one believes that the teratogenic milieu persists for several days then the vascular isolation of one uterine horn for 30 minutes following the administration of antiserum should not protect against malformations Thus failure to protect with the technique of uterine vascular clamping and malformation production follow in the injection of teratogenic serum during the preimplantation period are results that are in agreement

The purpose of injecting teratogenic serum directly into one pregnant uterine horn was to determine whether pathologic effects could be limited to the injected horn If this occurred then the mechanism of action of the antiserum would be partially clarified since it would eliminate the possibility that teratogenesis was the indirect effect of induced maternal metabolic disease and the result of a direct effect upon either the trophoblast uterus extra embryonic membranes or embryo The fact that the embryos in both uterine horns were equally affected indicates that the induction of maternal metabolic or physiologic disease cannot be eliminated by this experiment One explanation for this result is that the antiserum could not diffuse from the uterine lumen to the implantation site and therefore the antiserum was absorbed into the circulation just as if it had been injected intravenously or intraperitoneally thus affecting both uterine horns to the same extent

3 Do these biologic experiments give any indication that the antiserum is teratogenic because it contains teratogenic immunoproteins? Although we have evidence that the teratogenic factor is present in the gamma globulin fraction of the

serum is non dialyzable and is inactivated by antiserum made against the gamma globulin from the teratogenic serum (Brent 66d) there is only minimal evidence from these biologic experiments to support the data obtained from immunochemical studies Although the ineffectiveness of oral administration of teratogenic antiserum is presumptive evidence that the teratogenic factor is a protein which is destroyed in the gastrointestinal tract it also could be a small molecule that is labile or not able to be absorbed from the intestine Thus although the immunologic data strongly supports the existence of a teratogenic immunoglobulin these biologic experiments were only of minimal help

4 Are there important similarities and differences between teratogenic antiserum and other classical teratogenic agents? Teratogenic antiserum can be considered a classical teratogenic agent which produces a wide spectrum of malformations during the period of rapid differentiation It is unusual in one respect in that it is harvested from mammals following the injection of mammalian tissue The type of malformations vary somewhat with the day of administration although the variation Growth retardation and embryonic mortality are intimately related to the teratogenic process The fact that injections as early as the third post-conception day in the rat result in malformations and that the immunoprotein localizes in the yolk sac membrane (Slotnick and Brent 66) are properties that characterize trypan blue which is a chemical teratogenic agent (Wislocki '20 Fox 58 Wilson Shepard and Gennar 63 Beck Spencer and Baxter 60) This is an instance where the biologic experiment and immunologic experiment reinforce an interesting similarity between a teratogenic agent prepared immunologically in a mammal and a chemical dye prepared in the laboratory If events prove that both these agents produce teratogenesis via yolk sac pathology we may have to reconsider the relative importance of this mechanism of teratogenesis If yolk sac pathology proves to be an important factor in teratogenesis then drug testing programs

conception results in an increased incidence of malformations in the term fetuses. Although the incidence of malformations in the zero day group is three times greater than the control group there were only three malformed embryos in a term group of 29 embryos. This incidence is not significantly different from the incidence in the control embryos at the 5% level of significance.

The combination of uterine vascular clamping and the injection of teratogenic antiserum is summarized in table 5. It is apparent that the isolation of one uterine horn from circulating teratogenic serum for 30 minutes does not protect the isolated embryos from the effects of the circulating antiserum since the growth retarding lethal and malforming effects were similar in the clamped and non clamped embryos.

DISCUSSION

Biochemical and immunologic techniques will undoubtedly encompass the final steps in clarifying the mechanism of action of teratogenic antisera. We have reported that fluorescent labeled teratogenic sheep anti rat kidney gamma globulin localizes in the glomerular basement membrane, adrenal and to a lesser extent in the spleen and liver of the maternal rat (Slotnick and Brent '66). Furthermore this same labeled antiserum localizes very heavily in the developing yolk sac basement membrane during the period of early embryonic differentiation but does not localize in the tissues of the very young embryos *in vivo*. Thus the fluorescent localization data support the latter two of the three possible mechanisms of teratogenesis: (1) direct effect upon the embryos, (2) direct effect on the trophoblast or extra embryonic membranes or (3) indirect effect on the embryos via induced maternal metabolic disease.

The biological experiments reported in this manuscript can yield some information which is difficult to obtain from biochemical and immunologic experiments.

1 *Does the route and rate of administration of the antiserum influence the quantitative and qualitative effects of teratogenic serum?* The experiments reported here indicate that the route of adminis-

tration can modify the pathologic effects of the antiserum. While oral administration was shown to be ineffective teratogenesis resulted when the antiserum was administered by any parenteral route. When low doses of antiserum were administered parentally the intravenous route was the most effective and the subcutaneous route least effective. At higher doses the intravenous and intraperitoneal routes were comparable and the subcutaneous route was still the least effective. These data indicate that local inactivation or local adsorption can modify the effectiveness of injected antiserum. These same phenomena could also be explained on the basis of variation in dose rate since it is likely that the subcutaneous administration of antiserum results in a lower peak serum level which is attained at a later time after administration. With the subcutaneous injection or low doses administered by other routes there was unequal attenuation of the rate of fetal death, growth retardation and malformations. The significance of this will be discussed later.

2 *How long after injecting the antiserum does the teratogenic milieu persist?* Malformations were produced by the administration of teratogenic antiserum as early as three days post conception. Since the types of malformations produced by injections on three and five days post conception were qualitatively similar to those produced in seven and eight-day old embryos it seems likely that the teratogenic effect is functioning during the period of differentiation (8½ to 12 days) and therefore the teratogenic milieu can last for four to six days following injection of the antiserum in the rat. This is further substantiated by the fact that although the malformation types are the same, the incidence progressively declines as one administers the antiserum further from the period of differentiation and closer to the time of conception. The same dose of antiserum produces a malformation rate of 16.6%, 47.0% and 95% when injected on three, five and eight days post conception respectively. Furthermore attenuation of pathologic effects of the antiserum by earlier injection causes a disproportionate change in the incidence of

Index

A

- ADAMS ELEANOR C ARTHUR T HERTIG AND
SUSANNE FOSTER Studies on guinea pig
oocytes II. Histochemical observations
on some phosphatases and lipid in devel-
oping and in atretic oocytes and follicles 303
- Adrenocortical cells in adult male rhesus
monkeys fine structure of 429
- Anatomy of the muscles nerves and arteries
of the bovine female perineum the topo-
graphic 79
- Ani muscles constant cell populations in
normal testosterone-deprived and testos-
terone-stimulated levator 263
- Ani muscles morphology of the cells of nor-
mal testosterone-deprived and testoste-
rone-stimulated 271
- Anti rat kidney antiserum IV evaluation of
the mechanism of teratogenesis by vary-
ing the route and time of administra-
tion of the production of congenital mal-
formations using tissue antisera 555
- Antisera the production of congenital mal-
formations using tissue IV Evaluation
of the mechanism of teratogenesis by
varying the route and time of administra-
tion of anti rat kidney antiserum 555
- Antiserum IV evaluation of the mechanism
of teratogenesis by varying the route and
time of administration of anti rat kidney
the production of congenital malforma-
tions using tissue antisera 555
- Arteries of the bovine female perineum the
topographic anatomy of the muscles
nerves and 79
- Arterioles and hepatic sphincters a dynamic
and static study of hepatic 455
- Autoradiography with the electron micro-
scope the synthesis and storage of protein
by isolated lymphoid cells examined by 375

B

- Basophilia in the mouse uterus from mating
through implantation the changing pat-
tern of 1
- Bats studies on sperm survival mechanisms
in the female reproductive tract of hiber-
nating I. Cytology and ultra structure
of intra uterine spermatozoa in *Myotis*
lucifugus 25
- Bladder dual innervation of the mammalian
urinary A histochemical study of the
distribution of cholinergic and adrenergic
nerves 405
- Bovine female perineum the topographic
anatomy of the muscles nerves and
arteries of the 79
- BRENT ROBERT M Fine structure of
adrenocortical cells in adult male rhesus
monkeys 429

- BRENT ROBERT L The production of con-
genital malformations using tissue anti-
sera IV Evaluation of the mechanism
of teratogenesis by varying the route and
time of administration of anti rat kidney
antiserum 555

C

- Carcinogenic hydrocarbon fluorescence an
evaluation of possible intracellular nu-
cleic acid quenching of 499
- Cell populations in normal testosterone-de-
prived and testosterone stimulated levator
ani muscles constant 263
- Cells examined by autoradiography with
the electron microscope the synthesis and
storage of protein by isolated lymphoid
Cells fine structure of the surface of mouse
hepatic 97
- Cells in adult male rhesus monkeys fine
structure of adrenocortical 429
- Cells in the mouse uterus following mating
and through implantation of the embryo
metrial gland and other glycogen contain-
ing 15
- Cells of normal testosterone-deprived and
testosterone stimulated levator ani mus-
cles morphology of the 271
- Cells of vertebrates on the occurrence of a
fibrous lamina on the inner aspect of the
nuclear envelope in certain 129
- Changing pattern of basophilia in the
mouse uterus from mating through im-
plantation the 1
- Cholinergic and adrenergic nerves a histo-
chemical study of the distribution of dual
innervation of the mammalian urinary
bladder 405

- CLARK SAM L JR The synthesis and stor-
age of protein by isolated lymphoid cells
examined by autoradiography with the
electron microscope 375
- Congenital malformations using tissue anti-
sera the production of IV Evaluation
of the mechanism of teratogenesis by
varying the route and time of administra-
tion of anti rat kidney antiserum 555
- Constant cell populations in normal testos-
terone-deprived and testosterone stimu-
lated levator ani muscles 263
- Cytology and ultra structure of intra uterine
spermatozoa in *Myotis lucifugus* I studies
on sperm survival mechanisms in the
female reproductive tract of hibernating
bats 25

D

- DALLENBACH HELLWEG C A B DAWSON
AND F L HISAW The effect of relaxin
on the endometrium of monkeys Histo-
logical and histochemical studies 61

will have to consider this possibility when choosing appropriate experimental animals (Brent, 64c). This would indicate that more must be learned about yolk sac function in mammals during the period of differentiation in order to add to our understanding of the variable importance of yolk sac function in various mammalian species.

ACKNOWLEDGMENTS

This work was supported by a research grant from the National Institute of Child Health and Human Development. Many helpful suggestions were made by Drs F. Dixon and J. Feldman of the Department of Experimental Pathology, Scripps Research Foundation, La Jolla, California. The author was ably assisted by Misses J. Garaguso, M. Spoerl and Messrs J. Hefton and A. Johnson. Appreciation is extended to Mrs. E. Ward and Miss M. DuRant for typing the manuscript.

LITERATURE CITED

- Beck F. B. Spencer and J. S. Baxter 1960 Effect of trypan blue on rat embryos. *Nature* (4737) 605-607.
- Brent R. L. 1964a The production of congenital malformations with tissue antibodies II. The spectrum and incidence of malformations following the administration of kidney antiserum to the pregnant rat. *Am J Anat*, 115: 525-542.
- 1964b The production of congenital malformations using tissue antisera III. Placental antiserum. *J Pediatr* 65: 1053 (abstract).
- 1964c Drug testing in animals for teratogenic effects. Thalidomide in the pregnant rat. *J Pediatr* 64: 762-770.
- 1965 Effect of proteins, antibodies and autoimmune phenomena upon conception and embryogenesis. Chapter 9, pp. 215-233 in *Teratology: Principles and Techniques*, edited by J. G. Wilson and J. Warkany. University of Chicago Press, Chicago.
- 1966a Immunologic aspects of developmental biology. Chapter 4, pp. 81-129 in *Advances in Teratology*, edited by D. M. H. Woollam. Logos Press, London.
- 1966a b Unpublished data.
- Brent R. L., E. Averich and V. A. Draplewski 1961 Production of congenital malformations using tissue antibodies I. Kidney antiserum. *Proc Soc Exp Biol Med* 106: 523-526.
- Brent R. L. and J. B. Franklin 1960 Uterine vascular clamping. New procedure for the study of congenital malformations. *Science* 132: 89-91, 1960.
- David G. L. Mercier, Parot and H. Tuchmann-Duplessis 1963 Action teratogene d'hetero-anticorps tissulaires I. Production de malformations chez le rat par action d'un serum antirein. *Comptes rendus des seances de la Societe de Biologie* 165: 939, 1963.
- Fox M. H., C. M. Goss and L. F. Bordeau 1958 The effect of trypan blue injections at different stages of pregnancy upon the fetus. *Anat Rec* 130: 302-303.
- Franklin J. B. and R. L. Brent 1964 The effect of uterine vascular clamping on the development of rat embryos three to fourteen days old. *J Morph* 115: 273-290.
- Slotnick V. and R. L. Brent 1966 The production of congenital malformations using tissue antiserum V. Fluorescent localization of teratogenic antisera in the maternal and fetal tissue of the rat. *J Immunol* 96: 606-610.
- Wilson J. G. 1958 Time of teratogenic action of trypan blue in the rat. *Anat Rec* 130: 358-389.
- Wilson J. G., T. H. Shepard and J. F. Gennar 1963 Studies on the site of teratogenic action of C^{14} labeled trypan blue. *Anat Rec* 145: 300.
- Wislocki G. B. 1920 Experimental studies on fetal absorption. *Contributions to embryology*. Carnegie Institute, Wash. 11: 47-59.

- Histochemical study of the esterases of the rat heart 235
- Histochemical studies histological and the effect of relaxin on the endometrium of monkeys 61
- Histological and histochemical studies the effect of relaxin on the endometrium of monkeys 61
- Hydrocarbon fluorescence an evaluation of possible intracellular nucleic acid quenching of carcinogenic 499

I

- Implantation of the embryo metrial gland and other glycogen containing cells in the mouse uterus following mating and through 15
- Implantation the changing pattern of basophilia in the mouse uterus from mating through 1
- Innervation of the mammalian urinary bladder dual a histochemical study of the distribution of cholinergic and adrenergic nerves 405
- Intracellular nucleic acid quenching of carcinogenic hydrocarbon fluorescence an evaluation of possible 499
- Intra uterine spermatozoa in *Myotis lucifugus* cytology and ultra structures of I studies on sperm survival mechanisms in the female reproductive tract of hibernating bats 25

K

- KRUGER LAWRENCE AND DAVID S MAXWELL The fine structure of ependymal processes in the teleost optic tectum 479
- KADTSCHEK PHILIP H See Wimsatt William A 25

L

- Lamina on the inner aspect of the nuclear envelope in certain cells of vertebrates on the occurrence of a fibrous 129
- Levator ani muscles constant cell populations in normal testosterone-deprived and testosterone-stimulated 263
- Levator ani muscles morphology of the cells of normal testosterone-deprived and testosterone-stimulated 271
- Lipid in developing and in atretic oocytes and follicles II histochemical observations on some phosphatases and studies on guinea pig oocytes 303
- LITGARTEN MAX A Electron microscopic study of the gingivo-dental junction of man 147
- Lymphatic drainage suprarenal gland 359
- Lymphoid cells examined by autoradiography with the electron microscope the synthesis and storage of protein by isolated 375

M

- Malformations using tissue antisera the production of congenital IV Evaluation of the mechanism of teratogenesis by varying the route and time of administration of anti rat kidney antiserum 555
- Mammalian urinary bladder dual innervation of the A histochemical study of the distribution of cholinergic and adrenergic nerves 405
- Man electron microscopic study of the gingivo-dental junction of 147
- Mating and through implantation of the embryo metrial gland and other glycogen containing cells in the mouse uterus following 15
- Mating through implantation the changing pattern of basophilia in the mouse uterus from 1
- MAXWELL DAVID S See Kruger Lawrence 479
- MCCUSKEY ROBERT S A dynamic and static study of hepatic arterioles and hepatic sphincters 455
- MERKLIN ROBERT J Suprarenal gland lymphatic drainage 359
- Metrial gland and other glycogen containing cells in the mouse uterus following mating and through implantation of the embryo 15
- Microscope the synthesis and storage of protein by isolated lymphoid cells examined by autoradiography with the electron 375
- Microscopic study of the gingivo-dental junction of man electron 147
- Monkeys the effect of relaxin on the endometrium of Histological and histochemical studies 61
- Morphology of the cells of normal testosterone deprived and testosterone stimulated levator ani muscles 271
- MOSSMAN H W See Sinha Akhouri A 521
- Mouse hepatic cells fine structure of the surface of 97
- Mouse thymus cultured in diffusion chambers differentiation of 341
- Mouse uterus following mating and through implantation of the embryo metrial gland and other glycogen containing cells in the Mouse uterus from mating through implantation the changing pattern of basophilia in the 1
- Muscles constant cell populations in normal testosterone-deprived and testosterone stimulated levator ani 263
- Muscles morphology of the cells of normal testosterone-deprived and testosterone stimulated levator ani 271
- Muscles nerves and arteries of the bovine female perineum the topographic anatomy of the 79
- Myelinated tissue cultures of rat trigeminal ganglion the development and maintenance of 179
- Myotis lucifugus* cytology and ultra-structure of intra uterine spermatozoa in I studies on sperm survival mechanisms in the female reproductive tract of hibernating bats 25

- DAWSON A B See Dallenbach Hellweg G
Development and maintenance of myelin
ated tissue cultures of rat trigeminal gan-
glion the 429
Differentiation of mouse thymus cultured
in diffusion chambers 479
Diffusion chambers differentiation of mouse
thymus cultured in 97
Dual innervation of the mammalian urinary
bladder A histochemical study of the
distribution of cholinergic and adrenergic
nerves 499
Dynamic and static study of hepatic arte-
rioles and hepatic sphincters a 303
455 FOSTER SUSANNE See Adams, Eleanor C 303

E

- Effect of relaxin on the endometrium of
monkeys the Histological and histo-
chemical studies 61
Effects of triton WR 1339 on the rat yolk
sac placenta 199
EL BADAWI AHMAD AND ERIC A SCHENK
Dual innervation of the mammalian uri-
nary bladder A histochemical study of
the distribution of cholinergic and adre-
nergic nerves 405
Electron microscope the synthesis and stor-
age of protein by isolated lymphoid cells
examined by autoradiography with the
Electron microscopic study of the gingivo-
dental junction of man 375
Embryo metrial gland and other glycogen
containing cells in the mouse uterus fol-
lowing mating and through implantation
of the 147
Endometrium of monkeys the effect of
relaxin on the Histological and histo-
chemical studies 15
Ependymal processes in the teleost optic
tectum the fine structure of 61
Esterases of the rat heart a histochemical
study of the 479
Evaluation of possible intracellular nucleic
acid quenching of carcinogenic hydrocar-
bon fluorescence an 235
Evaluation of the mechanism of teratogen-
esis by varying the route and time of ad-
ministration of anti rat kidney antiserum
IV the production of congenital mal-
formations using tissue antisera 499
555

F

- FAWCETT DON W On the occurrence of a
fibrous lamina on the inner aspect of the
nuclear envelope in certain cells of verte-
brates 129
Female reproductive tract of hibernating
bats studies on sperm survival mecha-
nisms in the I Cytology and ultra-
structure of intra uterine spermatozoa in
Myotis lucifugus 25
FERRANS VICTOR J See Hegab El Sayad
H H 235
Fibrous lamina on the inner aspect of the
nuclear envelope in certain cells of verte-
brates on the occurrence of a 129

G

- Ganglion the development and maintenance
of myelinated tissue cultures of rat tri-
geminal 179
Gingivo dental junction of man electron
microscopic study of the 147
Gland lymphatic drainage suprarenal 359
Glycogen containing cells in the mouse
uterus following mating and through im-
plantation of the embryo metrial gland
and other 15
Guinea pig oocytes studies on II Histo-
chemical observations on some phospho-
tases and lipid in developing and in
atretic oocytes and follicles 303

H

- HABEL, ROBERT E The topographic anatomy
of the muscles nerves and arteries of the
bovine female perineum 79
Heart a histochemical study of the ester-
ases of the rat 235
HEATH TREVOR AND STEVEN L WISSIG
Fine structure of the surface of mouse
hepatic cells 97
HEGAB EL SAYED H H AND VICTOR J
FERRANS A histochemical study of the
esterases of the rat heart 235
Hepatic arterioles and hepatic sphincters
a dynamic and static study of 455
Hepatic cells fine structure of the surface
of mouse 97
Hepatic sphincters a dynamic and static
study of hepatic arterioles and 455
HERTIG ARTHUR T See Adams Eleanor C 303
Hibernating bats studies on sperm survival
mechanisms in the female reproductive
tract of I Cytology and ultra structure
of intra uterine spermatozoa in *Myotis
lucifugus* 25
HISAW F L See Dallenbach Hellweg G 61
Histochemical observations on some phos-
phatases and lipid in developing and in
atretic oocytes and follicles II studies
on guinea pig oocytes 303
Histochemical study of the distribution of
cholinergic and adrenergic nerves a dual
innervation of the mammalian urinary
bladder 403

- Histochemical study of the esterases of the rat heart a 235
- Histochemical studies histological and the effect of relaxin on the endometrium of monkeys 61
- Histological and histochemical studies the effect of relaxin on the endometrium of monkeys 61
- Hydrocarbon fluorescence an evaluation of possible intracellular nucleic acid quenching of carcinogenic 499
- I**
- Implantation of the embryo metrial gland and other glycogen containing cells in the mouse uterus following mating and through 15
- Implantation the changing pattern of basophilia in the mouse uterus from mating through 1
- Inservation of the mammalian urinary bladder dual a histochemical study of the distribution of cholinergic and adrenergic nerves 405
- Intracellular nucleic acid quenching of carcinogenic hydrocarbon fluorescence an evaluation of possible 499
- Intra uterine spermatozoa in *Myotis lucifugus* cytology and ultra-structures of I studies on sperm survival mechanisms in the female reproductive tract of hibernating bats 25
- K**
- KRUGER LAWRENCE AND DAVID S MAXWELL The fine structure of ependymal processes in the teleost optic tectum 479
- KAUTZSCH PHILIP H See Wimsatt William A 25
- L**
- Lamina on the inner aspect of the nuclear envelope in certain cells of vertebrates on the occurrence of a fibrous 129
- Levator ani muscles constant cell populations in normal testosterone-deprived and testosterone-stimulated 263
- Levator ani muscles morphology of the cells of normal testosterone-deprived and testosterone-stimulated 271
- Lipid in developing and in atretic oocytes and follicles II histochemical observations on some phosphatases and studies on guinea pig oocytes 303
- LITGABTEN MAX A Electron microscopic study of the gingivo-dental junction of man 147
- Lymphatic drainage suprarenal gland 359
- Lymphoid cells examined by autoradiography with the electron microscope the synthesis and storage of protein by isolated 375
- M**
- Malformations using tissue antisera the production of congenital IV Evaluation of the mechanism of teratogenesis by varying the route and time of administration of anti rat kidney antiserum 555
- Mammalian urinary bladder dual innervation of the A histochemical study of the distribution of cholinergic and adrenergic nerves 405
- Man electron microscopic study of the gingivo-dental junction of 147
- Mating and through implantation of the embryo metrial gland and other glycogen containing cells in the mouse uterus following 15
- Mating through implantation the changing pattern of basophilia in the mouse uterus from 1
- MAXWELL DAVID S See Kruger Lawrence 479
- McCUSKEY ROBERT S A dynamic and static study of hepatic arterioles and hepatic sphincters 455
- MERKLIN ROBERT J Suprarenal gland lymphatic drainage 359
- Metrial gland and other glycogen containing cells in the mouse uterus following mating and through implantation of the embryo 15
- Microscope the synthesis and storage of protein by isolated lymphoid cells examined by autoradiography with the electron 375
- Microscopic study of the gingivo-dental junction of man electron 147
- Monkeys the effect of relaxin on the endometrium of Histological and histochemical studies 61
- Morphology of the cells of normal testosterone deprived and testosterone-stimulated levator ani muscles 271
- MOSSMAN H W See Sinha Akhouri A 521
- Mouse hepatic cells fine structure of the surface of 97
- Mouse thymus cultured in diffusion chambers differentiation of 341
- Mouse uterus following mating and through implantation of the embryo metrial gland and other glycogen containing cells in the 15
- Mouse uterus from mating through implantation the changing pattern of basophilia in the 1
- Muscles constant cell populations in normal testosterone-deprived and testosterone stimulated levator ani 263
- Muscles morphology of the cells of normal testosterone-deprived and testosterone stimulated levator ani 271
- Muscles nerves and arteries of the bovine female perineum the topographic anatomy of the 79
- Myelinated tissue cultures of rat trigeminal ganglion the development and maintenance of 179
- Myotis lucifugus* cytology and ultra-structure of intra uterine spermatozoa in I studies on sperm survival mechanisms in the female reproductive tract of hibernating bats 25

N

- NAPOLITANO LEONARD See Wimsatt, William A
- Nerves and arteries of the bovine female perineum the topographic anatomy of the muscles 25
- Nuclear envelope in certain cells of vertebrates on the occurrence of a fibrous lamina on the inner aspect of the 79
- Nucleic acid quenching of carcinogenic hydrocarbon fluorescence an evaluation of possible intracellular 129
- 499

O

- On the occurrence of a fibrous lamina on the inner aspect of the nuclear envelope in certain cells of vertebrates 129
- Oocytes and follicles II histochemical observations on some phosphatases and lipid in developing and in atretic studies on guinea pig oocytes 303
- Oocytes studies on guinea II Histochemical observations on some phosphatases and lipid in developing and in atretic oocytes and follicles 303
- Optic tectum the fine structure of ependymal processes in the teleost 479

P

- Perineum the topographic anatomy of the muscles nerves and arteries of the bovine female 79
- Pig oocytes studies on guinea II Histochemical observations on some phosphatases and lipid in developing and in atretic oocytes and follicles 303
- Phosphatases and lipid in developing and in atretic oocytes and follicles II histochemical observations on some studies on guinea pig oocytes 303
- Placenta effects of triton WR 1339 on the rat yolk sac 199
- Placentation of the sea otter 521
- Production of congenital malformations using tissue antisera the IV Evaluation of the mechanism of teratogenesis by varying the route and time of administration of anti rat kidney antiserum 555
- Protein by isolated lymphoid cells examined by autoradiography with the electron microscope the synthesis and storage of 375

R

- Rat heart, a histochemical study of the esterases of the 235
- Rat trigeminal ganglion the development and maintenance of myelinated tissue cultures of 179
- Rat yolk sac placenta effects of triton WR 1339 on the 199
- REGER JAMES F See Schultz Phyllis W 199
- Relaxin on the endometrium of monkeys, the effect of Histological and histochemical studies 61

- Reproductive tract of hibernating bats studies on sperm survival mechanisms in the female I Cytology and ultra structure of intra uterine spermatozoa in *Myotis lucifugus* 25
- Rhesus monkeys fine structure of adrenocortical cells in adult male 429

S

- SCHENK ERIC A See El Badawi Ahmad 405
- SCHULTZ PHYLLIS W JAMES F REGER AND RICHARD L SCHULTZ Effects of triton WR 1339 on the rat yolk sac placenta 199
- SCHULTZ RICHARD L See Schultz Phyllis W 199
- Sea otter placentation of the 521
- SKELTON EMMA Differentiation of mouse thymus cultured in diffusion chambers 341
- SHIRES THOMAS A An evaluation of possible intracellular nucleic acid quenching of carcinogenic hydrocarbon fluorescence 499
- SINHA AKOURI A AND H W MOSSMAN Placentation of the sea otter 521
- SMITH LOIS JEAN Metrial gland and other glycogen containing cells in the mouse uterus following mating and through implantation of the embryo 15
- SMITH LOIS JEAN The changing pattern of basophils in the mouse uterus from mating through implantation 1
- Spermatozoa in *Myotis lucifugus* cytology and ultra structure of intra uterine I studies on sperm survival mechanisms in the female reproductive tract of hibernating bats 25
- Sperm survival mechanisms in the female reproductive tract of hibernating bats studies on I Cytology and ultra structure of intra uterine spermatozoa in *Myotis lucifugus* 25
- Sphincters a dynamic and static study of hepatic arterioles and hepatic 455
- Studies on guinea pig oocytes II Histochemical observations on some phosphatases and lipid in developing and in atretic oocytes and follicles 303
- Studies on sperm survival mechanisms in the female reproductive tract of hibernating bats I Cytology and ultra structure of intra uterine spermatozoa in *Myotis lucifugus* 25
- Suprarenal gland lymphatic drainage 359
- Surface of mouse hepatic cells fine structure of the 97
- Synthesis and storage of protein by isolated lymphoid cells examined by autoradiography with the electron microscope the 375

T

- Tectum the fine structure of ependymal processes in the teleost optic 479
- Teleost optic tectum the fine structure of ependymal processes in the 479
- Teratogenesis by varying the route and time of administration of anti rat kidney antiserum evaluation of the mechanism of IV the production of congenital malformations using tissue antisera 553

- Testosterone-deprived and testosterone-stimulated levator ani muscles morphology of the cells of normal
271
- Testosterone-stimulated levator ani muscles constant cell populations in normal
263
- Testosterone-stimulated levator ani muscles morphology of the cells of normal testosterone-deprived and
271
- Thymus cultured in diffusion chambers diff retention of mouse
341
- Tissue antisera the production of congenital malformations using IV evaluation of the mechanism of teratogenesis by varying the route and time of administration of antiratal kidney antiserum
505
- Tissue cultures of rat trigeminal ganglion the development and maintenance of myelinated
179
- Topographic anatomy of the muscles nerves and arteries of the bovine female perineum the
79
- Trigeminal ganglion the development and maintenance of myelinated tissue cultures of rat
179
- Triton WR 1339 on the rat yolk sac placenta effects of
199

U

- Urinary bladder dual innervation of the mammalian a histochemical study of the distribution of cholinergic and adrenergic nerves
405
- Uterus following mating and through implantation of the embryo metrial gland and other glycogen containing cells in the mouse
15

- Uterus from mating through implantation the changing pattern of basophilia in the mouse
1

V

- VENABLE JOHN H Constant cell populations in normal testosterone-deprived and testosterone-stimulated levator ani muscles
263
- VENABLE JOHN H Morphology of the cells of normal testosterone-deprived and testosterone-stimulated levator ani muscles
271
- Vertebrates on the occurrence of a fibrous lamina on the inner aspect of the nuclear envelope in certain cells of
129

W

- WIMSATT WILLIAM A PHILIP H KRUTZSCH AND LEONARD NAPOLITANO Studies on sperm survival mechanisms in the female reproductive tract of hibernating bats I Cytology and ultra-structure of intra-uterine spermatozoa in *Myotis lucifugus*
25
- WINKLER GERALD F AND MERRILL K WOLF The development and maintenance of myelinated tissue cultures of rat trigeminal ganglion
179
- WISSIG STEVEN L See Heath Trevor
97
- WOLF MERRILL K See Winkler Gerald F
179

Y

- Yolk sac placenta effects of triton WR 1339 on the rat
199

